



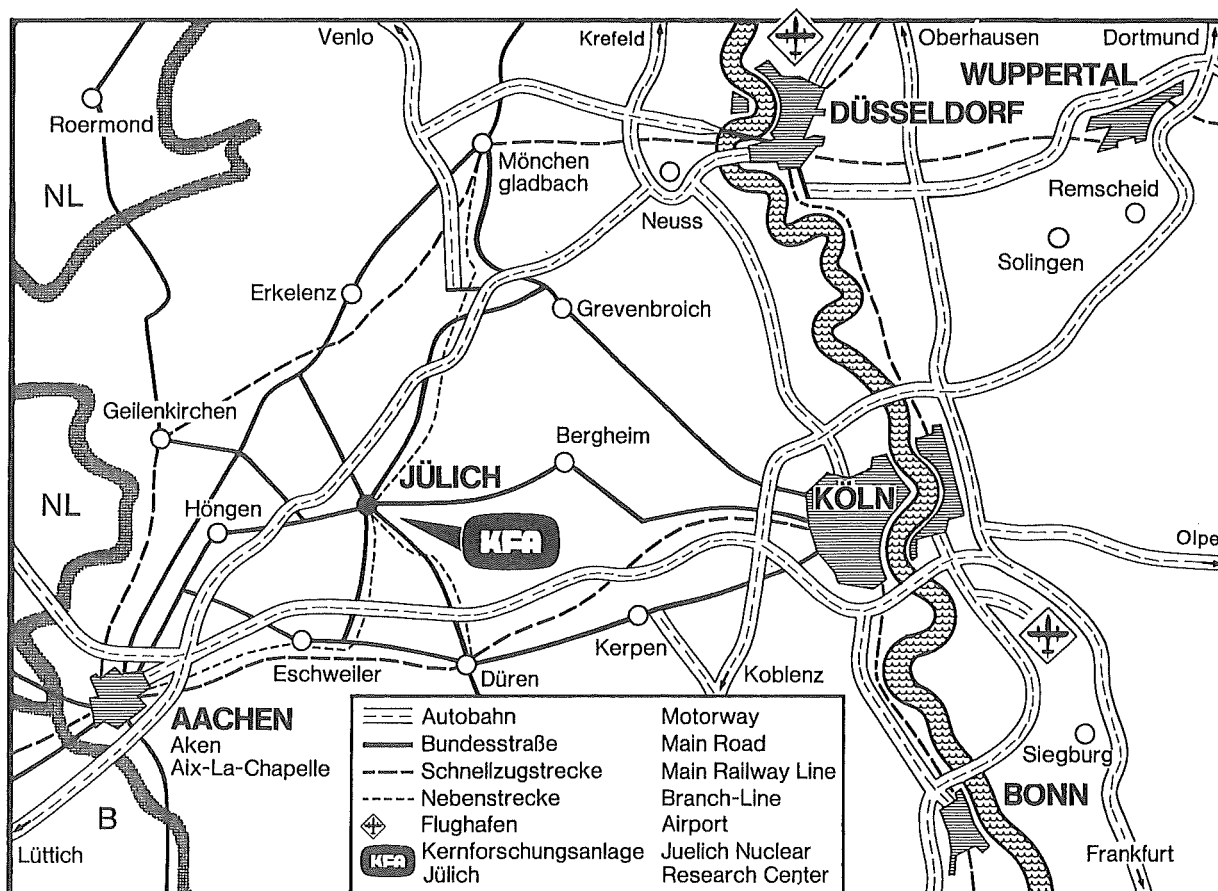
KERNFORSCHUNGSANLAGE JÜLICH GmbH

**Proceedings of the First Workshop
of Particulate Control**

16th / 17th March 1978

Kernforschungsanlage Jülich GmbH

**JÜL - Conf - 28
Januar 1979
ISSN 0344-5798**



Als Manuskript gedruckt

Berichte der Kernforschungsanlage Jülich - Jül - Conf - 28

Zu beziehen durch: ZENTRALBIBLIOTHEK der Kernforschungsanlage Jülich GmbH,
Jülich, Bundesrepublik Deutschland

Proceedings of the First Workshop of Particulate Control

16th / 17th March 1978

Kernforschungsanlage Jülich GmbH

Prepared by

U.S. Environmental Protection Agency,

Office of Research and Development, Washington, D.C. 20460

and

Energy Research Project Management,

Nuclear Research Establishment Jülich GmbH,

Box 1913, 5170 Jülich



P R E F A C E

The workshop was opened by Dr. Engelmann (member of the KFA, Board of Directors), who welcomed the participants and briefly outlined the objectives of the work performed at the KFA. He pointed out that although this research center is renowned for its nuclear program, considerable developments are being made in the non-nuclear field. This description was followed by an introduction by Dr. Holighaus (Project Management for Energy Research) to the workshop's theme: particulate control in coal-fired power stations. He stressed the need, because of increased use of coal to find solutions for protecting the environment and public from the pollution.

Dr. Holighaus then asked Dr. Gage, who represented the American members of the workshop, and Dr. Ziegler, representing the federal ministry, to give short opening statements.

Welcome

- Stephen J. Gage -

I am pleased to have this opportunity to welcome you to this "Joint Workshop on Particulate Control". It is very enjoyable to return here to Jülich which we visited last July during the initiation of this important exchange.

This workshop is being carried out under the umbrella of the US-FRG program for cooperation in the field of pollution control for coal-fired powerplants. I should say that our mutual experience with these cooperative efforts has been an outstanding success in the past year. In fact, it has been a stunning victory over the normal bureaucratic barriers which typically confront and delay such international efforts.

On both sides of the Atlantic Ocean, governmental activities for energy and environmental research is located in several agencies. This fact alone could have resulted in inaction. However, through sincere efforts by both sides -- and I should take special note of the outstanding assistance given by Dr. Alois Ziegler of BMFT and Dr. Rolf Holighaus of KFA in this regard -- we have launched information exchange in numerous areas.

The subject of particulate control is quite important in the United States at this time. First, the U.S. Congress is now considering legislation which will greatly accelerate use of coal, especially by combustion in industrial and utility boilers. However, the increased use of coal will not result in degraded air quality in the U.S. since both the President and Congress have agreed upon stringent air pollution controls. To carry out this objective, the U.S. Environmental Protection Agency will soon propose New Source Performance Standards for Particulate Control in large power plants. Consequently we are very interested in learning from the experience here in Germany relating to the control of Particulates.

The fourteen U.S. papers to be presented here present a good summary of the state-of-the-art of conventional particulate control, high temperature/high pressure Particulate Control and particulate measurement Technology in the U.S. As you will see, these papers will be presented by a combination of EPA and private sector engineer scientists. This is typical of the approaches we have to use to conduct our research and development. I notice in the program that you also are involving researchers from your universities and private companies. The broad spectrum of interests and experiences should result in a very productive meeting.

I am looking forward to participation in this conference. I am also looking forward to housing you in the United States when we again review progress in this important area of cooperation.

Opening address
to the Workshop on Particulate Control

by Dr. Alois Ziegler,
Federal Ministry for Research and Technology

Ladies and Gentlemen,

I am glad to have the opportunity to be with you during the opening session of this workshop. My task here is to put this workshop into the perspective of government-to-government co-operation. We have to consider this workshop as an element of cooperation under the Agreement for Cooperation on Environment Protection Policy between the governments of the United States and of the Federal Republic of Germany.

EPA and BMFT started their cooperation under the aforesaid agreement only 11 months ago. In March 77, Dr. Holighaus and myself had a short discussion with Dr. Stephan Gage at the ERDA offices about the new programme issue of the Federal Government: environmentally acceptable coal-fired power stations. This meeting was followed by two days of discussion at Bonn about the possibilities of cooperation between the two agencies in July 1977. After that meeting several cooperative tasks could already be executed. This workshop is now another step forward.

I have been asked to say a few words about my position at the Federal Ministry for Research and Technology. I manage the section for non-nuclear energy research and technology. We have two sections with that title. I am responsible for the development of technologies for prospection, exploitation, mining, preparation and conversion of primary energy carriers, (this means of coal, oil, gas), geothermal energy, wind energy, etc.) Solar energy and the technologies for the distribution, storage and application of secondary energy carriers are allocated to the second section.

As I am not an expert on environment protection technologies, I will say only a few words on the subject of 'Particulate Control' which you are dealing with and I will not stop you from starting to work. I will do this in a rather personal way. When I went to school late in the forties and in the beginning of the fifties, I was taught that in our contry the Ruhr area, and in your country the Pittsburgh area, were the most dirty regions of the world. But when I came to the Ruhr area first in 1969 and to the Pittsburgh area in 1975, I found in both cases a lovely and rather clean landscape. In that context I remember the election slogan of one of our great political parties in 1958 - 1960 : blue sky over the Ruhr area.

What do I want to say with these indications: Particulate control is not a new subject. During the last twenty years there has been tremendous progress in the technology for particulate control and especially in the extended application of this technology. Much has already been achieved, but some work remains to be done. The emission of fine particulates especially still gives grounds for concern with regard to the health of people living in areas with higher immission rates. I am sure that this workshop will deal at least to some extent with the problems of fine particulate control.

I wish you a fruitful exchange of information and views during the workshop, the initiation of one or the other scientific relationship and finally a few hours of relaxation and recreation at Jülich.

THE WORKSHOP CONSISTED OF FIVE SESSIONS:

- SESSION I: CONTROL TECHNOLOGY PERFORMANCE
DR. STEVEN GAGE, SESSION CHAIRMAN

- SESSION II: ADVANCED SYSTEMS FOR DUST REMOVAL
DR. STEVEN GAGE, SESSION CHAIRMAN

- SESSION III: CONCURRENT REMOVAL OF DUST AND GASEOUS CONSTITUENTS
DR. ROLF HOLIGHAUS, SESSION CHAIRMAN

- SESSION IV: HIGH TEMPERATURE AND PRESSURE PARTICULATE CONTROL
DR. PETER DAVIDS, SESSION CHAIRMAN

- SESSION V: MEASUREMENT TECHNOLOGY
DALE L. HARMON, SESSION CHAIRMAN

T A B L E O F C O N T E N T S

| | Page |
|---|------|
| S E S S I O N I: Control Technology Performance | |
| "EPA Studies in Fabric Filtration" R.P. Donovan ----- | 12 |
| "A.P.T. Field Evaluation of Fine Particles Scrubbers" Dr. S. Calvert----- | 33 |
| "Elektrostatic Precipitator Performance" J. Gooch ----- | 58 |
| S E S S I O N II: Advanced Systems for Dust Removal | |
| "Electrostatically Augmented Particulate Collection Devices" D.L. Harmon ----- | 100 |
| "How to Raise the Efficiency of Dry Elektrostatic Precipitators by means of Gas Conditioning" Dr. H. Reißmann ----- | 125 |
| "Improved Design Method for F/C Scrubbing" Dr. S. Calvert ----- | 140 |
| "Application of High Gradient Magnetic Separation to Fine Particle Control" C.H. Gooding ----- | 158 |
| "Advanced Dust Collection Techniques in the Federal Republic of Germany: Selected Examples and Research Priorities" G. Güthner ----- | 175 |

.....

Page

S E S S I O N III: Concurrent Removal of Dust and Gaseous
 Constituents

"SO₂ Removal by a Fabric Filter Using Nahcolite Injection"
R.P. Donovan ----- 188

"Performance Tests of the Montana Power Company Colstrip
Station Flue Gas Cleaning System"
J.D. McCain ----- 210

"Simultaneous Separation of Dust and Gaseous Constituents at
High Gas Temperature by the Use of Molten Metals and Salts"
Dr. K. Hübner, Prof. Dr. E. Weber ----- 239

"Optimization of Wet and Dry Processes for Simultaneous
Removal of Particulates and Gaseous Air Pollution from
Coal Fired Power Stations"
Dr. P. Davids ----- 252

S E S S I O N IV: High Temperature and Pressure Particulate
 Removal

"Fundamentals of Particle Collection at High Temperatures and
Pressure"
Dr. S. Calvert, Dr. R. Parker ----- 269

"Granular Bed Filters and Dry Scrubbers"
Dr. R. Parker, Dr. S. Calvert ----- 297

"Application and Efficiency of Dry Elektrostatic Precipitators"
H.-G. Pape, Prof. Dr. E. Weber ----- 324

.....

Page

"Range of Use for Filtering Dust Collectors"

R. Schulz, Prof. Dr. E. Weber ----- 335

"High-Temperature Filtration"

M.A. Shackelton, Dr. D.C. Drehmel ----- 348

"Problems on the Application of Centrifugal Separators,
Especially of Rotary Flow Collectors"

Dr. P. Walzel, Prof. Dr. P. Schmidt ----- 376

S E S S I O N V: Measurement Technology

"Experience with Continuously Recording Dust Measuring
Instruments"

Dr. D.W. Laufhütte ----- 383

"Continuous Control of the Dust Content in Stack Gases with
Laser Devices"

H. Wiggers, Prof. Dr. E. Weber ----- 395

"Manual Methods for the Determination of Particulate Concen-
tration, Resistivity and Particle Size Distribution in In-
dustrial Flue Gases"

J.D. McCain ----- 403

"Instrumental Techniques for Sizing Industrial Source Parti-
culate"

W.B. Kuykendal ----- 425

.....

Page

"Evaluation of Particle Size Distribution by Means of
Particle Counters"

C. Helsper, Prof. Dr. H.J. Fißan ----- 448

"A Particulate Sampling System for Pressurized Fluidized
Bed Combustion"

L. Cooper, W. Masters, B. Larkin ----- 463

SESSION I: CONTROL TECHNOLOGY PERFORMANCE

EPA STUDIES IN FABRIC FILTRATION

by

R. P. Donovan
Research Triangle Institute
Energy & Environmental Research Division
Process Engineering Department
P. O. Box 12194
Research Triangle Park, N. C. 27709

(Draft text for presentation to be made to the Particulate Workshop,
Jülich, Federal Republic of Germany, March 16-17, 1978)

March 1978

EPA STUDIES IN FABRIC FILTRATION

R. P. Donovan
Research Triangle Institute
Energy & Environmental Research Division
Process Engineering Department
P. O. Box 12194
Research Triangle Park, N. C. 27709

The long term goals of EPA's research and development work in fabric filtration are to ensure that the full potential of fabric filtration as a particulate control technology is realized in the United States and that the United States environment receives the full benefit of the control capability inherent in this technology. To achieve these goals EPA sponsors basic studies in fabric filtration, hoping thereby to acquire better process understanding and subsequently more efficient, lower cost equipment. EPA also sponsors selected applications of fabric filters (or, more commonly, documentation of applications) so that the experiences of the early users of this technology in a given application area will be readily available to the general public and particularly to other potential users in that same application area. This paper describes some ongoing or recent EPA projects from each of these two R&D activities.

Most of these projects relate to the removal of particulates from the flue gas of coal-fired boilers, an application area of high EPA interest at present.

1.0 BASIC STUDIES: MATHEMATICAL MODELING

Although fabric filters (baghouses) have been used to control industrial particulate emissions for over a century, the details of their operation remain inadequately understood. Much of today's baghouse design is still empirical, since mathematical models are not yet able to predict fabric filtration performance satisfactorily.

EPA now conducts both internal and contractor/grantee research and development work with the goal of improved understanding of the fabric filtration process. The hope here is to eventually develop mathematical models that will be capable of reliable baghouse design. Such models will take account of variables not generally recognized at present. Some illustrative examples follow.

1.1 Modeling of Filter Performance

GCA Corporation's (Dennis, et al. [Ref.1]) description of the discontinuous, two-state condition of a flyash-coated, woven glass fabric during reverse cleaning is a basic insight not previously recognized widely. Their analysis breaks the bag into two parallel subdivisions: a bag area from which no dust has been removed and a bag area from which effectively all dust (except a permanent residual dust component) has been removed (Figure 1). Variation of cleaning times and cleaning energies simply transfers bag area from one subdivision to the other. Total gas flow through the filter is viewed as the sum of the flows through two parallel paths--one through the cleaned area, the other through the uncleaned area. This concept enables the GCA researchers to mathematically model the pressure/time characteristics of woven glass fabrics filtering flyash more accurately than previously, as has been demonstrated in both laboratory filtration experiments and in field installations at Sunbury and Nucla [Ref.1]. The complete filtration modeling problem is far from solved, however, and the GCA model, as it exists today, still requires numerous empirical inputs for satisfactory predictions and then only over a narrow range.

1.2 Particle Penetration Through A Fabric

Mechanisms of particle penetration through a fabric filter are not adequately modeled by the classical single fiber interactions of interception, impaction and diffusion. Defect processes such as non-uniformities in the fabric (a quality control problem) and pinhole plugs in the dust cake (dust cake collapse or bursting in a discrete region) clearly dominate under certain operating conditions, as shown by EPA-sponsored work at the Harvard School of Public Health.

Several such penetration mechanisms are schematically illustrated in Figure 2. Assuming that both the seepage and pinhole plug mechanisms of particle penetration are nonfractionating mechanisms (straight-through penetration is a fractionating process) and by use of chemically tagged flyash, the particle penetration mechanisms through the fabrics studied at Harvard have been shown to vary with deposit thickness as illustrated in Figure 3. The key penetration properties of each mechanism were assumed to be as follows:

1. Straight-through -- The outlet flyash is of the same chemical composition as the inlet and changes immediately with inlet changes.
2. Seepage -- Only the initially deposited flyash penetrates so that the chemical composition of the outlet flyash is the same as that originally deposited and is independent of subsequent changes in inlet chemical composition.
3. Pinhole plugs -- The outlet chemical composition represents the cumulation of all previous inlet dust compositions and changes continually with time, following any change in the inlet chemical composition.

The Harvard work shows that the size distribution of the outlet dust is, within experimental error, the same as that of the inlet dust and hence reinforces the process model wherein such nonfractionating penetration mechanisms as pinhole plugs and seepage dominate. (The face velocity of the Harvard investigations was between 5 cm/sec and 15 cm/sec--well above the velocities used in most field applications.)

Methods and operating modes for minimizing particle penetration by these, at present, non-modeled mechanisms are also part of the EPA sponsored program at Harvard. For example the Harvard researchers have found that modifying the valve sequence of their pulse jet so as to stretch its closing time over several hundred milliseconds reduces particle penetration (and probably lengthens bag life). The pulse modification is simply the isolation of the main air pressure source after the cleaning pulse has been initiated at the bags. The line pressure therefore decreases after the initial pulse and when the bag valve closes it does so against a much lower line pressure than in an unmodified pulse. This simple change produces dramatic reduction in filter penetration [Ref.3].

1.3 Electrostatic Effects

The importance of electrostatic forces during fabric filtration continues to be an elusive concept to quantify. Dust/fabric systems exist for which electrostatic interactions are of first-order importance and yet general recognition of the need to consider electrical/electrostatic properties during fabric filtration does not yet exist, as evidenced by the omission of such information from the specifications of most users and manufacturers of fabric filters.

What evidence exists to indicate that electrical/electrostatic forces are significant? Work at Carnegie-Mellon [Ref.4] provides some answers as plotted in Figure 4. This figure shows the collection efficiency of a clean woven glass fabric, filtering smoke generated by an electric arc. Three cases are contrasted: externally charged particles with an applied field; applied field only; and the nonelectrified case (no external charge, no field). The influence of external charge and field shown here are typical of Professor Penney's observations on a variety of dust/fabric systems--just an applied field enhances collection efficiency and when the dust particles are in addition charged, the improvement is enhanced further.

Even more important, perhaps, is the concurrent reduction in pressure drop. Comparisons of the pressure drops between conventional, nonelectrified

operation and that in which the dust passes through a corona charger and is filtered with an external electric field applied perpendicular to the filter surface invariably show that the pressure drop under this electrified operation is less than under nonelectrified operation. Professor Penney attributes this desirable consequence to a clustering of the dust on the fabric surface brought about by the electric forces. The details of how this clustering comes about are not as well understood as the practical advantages of being able to capitalize upon this effect.

Complementing work at Carnegie-Mellon University under the direction of E. R. Frederick shows that even under nonelectrified operation electrostatic properties can be significant [Ref. 5]. These effects are those that are observed in operation with no dust charger and no applied electric field. Charging effects still occur because of triboelectric interactions between the dust and the fabric (and probably other surfaces of the baghouse). Frederick was one of the early investigators of electrostatic interactions [Ref. 6]. His approach has been to attempt to classify both fabrics and dusts according to their triboelectric interaction. Two different materials when brought into intimate contact (or rubbed together to form this contact--the tribo [frictional] aspect of the interaction) undergo a charge exchange in order to establish electronic equilibrium across the interface (to equalize the Fermi level across the interface). When subsequently separated, one material has an excess of electrons; the other, a deficiency. Consequently, the first material is charged negatively with respect to the latter and to ground. The triboelectric series is an attempt to classify materials with respect to charge exchange with each other. Ranking one material above another in this series means that it will become positively charged when rubbed with that other material. A drastically abbreviated version of Frederick's triboelectric series appears in Figure 5. This series was prepared by pressing a test fabric against a spinning wheel of a reference fabric for a short (1-2 seconds) fixed time. Upon separation the electrostatic voltage is measured by pressing a probe against the test fabric and reading with a high impedance electrometer.

The scale in Figure 5 is normalized by Frederick and reflects some average of the magnitude of the electrostatic voltages generated on the test fabric after rubbing against two different reference fabrics. Unfortunately the voltages are not additive--the test fabric voltage after rubbing against reference fabric A does not equal the test fabric voltage after rubbing against test fabric B plus or minus the electrostatic voltage between reference fabrics A and B. Other factors such as surface texture and coatings or contamination complicate this simple picture. This complexity can also be seen by the varying location on the scale of nominally identical materials so it is easy to understand why different researchers often prepare differently ordered triboelectric series. Indeed any given researcher is hard pressed to reproduce his own ordering. Consequently the scale is only qualitative and cannot be used to predict the magnitude of electrostatic voltages between materials. It represents only a broad, general classification.

Perhaps the points to remember from a triboelectric series are that certain materials are electropositive (wool, nylon, glass) and other electronegative (teflon). Electrostatically these materials look different to a dust and choosing fabrics from different locations of the triboelectric series could be expected to change the electrostatic interactions between a given dust and the fabric filter. Photomicrographs of a dust-laden fabric composed of wool and acrylic fibers shows dust particles (charged by a corona, but no field) packed densely around the wool fiber while the acrylic fibers are bare (see cover of J.A.P.C.A., Jan. 1976).

Frederick has explored the use of triboelectric classification in industrial applications [Ref.5]. A brief sampling of results are reproduced in Table 1. This industrial dust was matched against fabrics of varying triboelectrical properties. The preferred fabric turned out to be a high permeability wool, not an especially obvious choice. Its electropositive triboelectric position conceivably favored the formation of an effective dust cake which enabled it to outperform the much more costly teflon fabric.

Variables other than composition, such as surface texture, nap, finish and coatings, influence electrostatic properties. Accounting for all these different influences promises to be a long term activity but evidence is slowly accumulating to suggest that such activity will be worthwhile.

In pulse jet filtration of room temperature flyash, too, filtration performance appears to correlate with electrostatic properties [Ref. 7]. Tables 2 and 3 show that certain fabrics treated so as to favor charge dissipation perform better than identical fabrics not so treated (Table 2); similarly, fabrics treated so as to retard charge dissipation can fare poorer than those not so treated (Table 3).

1.4 Fiber Geometry

Research at the Textile Research Institute (TRI) shows that trilobal or rough fibers can produce practical fabric filters with improved efficiencies at no increase in pressure drop [Ref.8]. After a dust cake is formed, efficiency increases in the following order of fiber geometries: bilobal < round < pentalobal < trilobal. Before cake forms, however, no differences exist. The effect apparently depends upon the interaction between the dust cake and the fiber structure--perhaps like the electrostatic effects just discussed. TRI continues research to classify dust cake structure and to relate it to its critical variables of formation and to measure its influence upon filtration performance.

2.0 FIELD DOCUMENTATION

Supplementing the basic studies outlined in Section 1.0 are careful examination and analysis of certain fabric filters in utility and industrial service. The utility applications best known in the U. S. are those at Sunbury, Pa. and Nucla, Col. largely because of EPA support of extensive documentation of these experiences [Ref. 9,10]. The reports issued [Ref. 9,10] describe the installation specifications, the costs (both capital and operating), the performance over more than a two year period (Figure 6, for example) and a log of maintenance and troubleshooting. Both Reference 9 and Reference 10 contain many particle size distribution curves and differential size distribution curves which compare the properties of the inlet and outlet dusts and lead to fractional efficiency curves. Many raw data records are also part of the reports, including the properties of the input coal and, in the Sunbury report, flue gas analysis.

The impact of EPA support of these activities goes beyond the issuance of reports. Workers and management at both installations responded to their "showcase" status by hosting countless visitors and responding to the many inquiries. Such courtesies were not part of the EPA program, of course, but reflected recognition of the spirit and significance of the venture. Because of EPA's interest and the utilities' pride in their leading edge position, these two installations are acknowledged pivotal demonstrations of the contribution fabric filters can make in helping utilities meet environmental standards.

A similar exercise has been performed on a small industrial boiler at Kerr Industries in Concord, N.C. [Ref. 11]. This activity has resulted in an expansion of the fabric filter installation to full size and to its use as a field test site for different fabrics and/or at higher than standard air-to-cloth ratio.

A similar program is just beginning at Southwest Public Service, Amarillo, TX. The Harrington Station there consists of three units totalling 1,050 to 1,100 MW generating capability. Harrington No. 2 boiler, a 350 MW unit, will have a Wheelabrator-Frye (WF) baghouse come

on line during 1978. This boiler burns low sulfur western coal rated at 19.6 MJ/kg (8,425 Btu/lb); its ash content is 5.5 percent; sulfur, 0.3 percent. The WF baghouse consists of 28 compartments capable, all total, of handling $757.5 \text{ m}^3/\text{sec}$ (1,605,000 acfm) of flue gas at 156°C (313°F) and an air cloth ratio of 1.7 cm/sec (3.4 fpm). Under their EPA-sponsored test plan Southwest Public Service will monitor and report all solids and gases entering and leaving the boiler. Five sampling ports will be used and the particulate information to be recorded includes: mass, size-distribution, total carbon in the ash, elemental analyses and sulfate, sulfite and nitrate analyses.

The collection and dissemination of reliable field measurements has become even more important now that baghouses have become "acceptable" as particulate control devices for boilers. The region of greatest growth may well be the Western U.S. where Southwest Public Services and Nucla are located so operating information from this region is of special importance.

Initial results from Harrington are expected in about a year and, coupled with the WF installation at Texas Utilities' Monticello Station, (a retrofit, independent of EPA sponsorship) should provide valuable guidance in regard to future research and applications for furthering the capability of fabric filters in performing the particulate control function.

REFERENCES

1. Dennis, R. et al., "Filtration Model for Coal Fly Ash with Glass Fabrics," EPA-600/7-77-084, (NTIS No. PB 276-489/AS), August 1977, GCA Corp., Bedford, MA 01730.
2. Leith, D., S. N. Rudnick and M. W. First, "High Velocity, High-Efficiency Aerosol Filtration," EPA-600/2-76-020, (PB 249-457/AS), January 1976, Harvard School of Public Health, 665 Huntington Ave., Boston, MA 02115.
3. Leith, D., M. W. First and D. D. Gibson, "Effect of Modified Cleaning Pulses on Pulse Jet Filter Performance" (presentation to the Third Symposium on Fabric Filters for Particle Collection, Tucson, Arizona, Decemeber 5-6, 1977).
4. Penney, G. A., "Electrostatic Effects in Fabric Filtration: Vol. 1. Fields, Fabrics and Particles, An Annotated Data Book", Final Report, Grant R803020 (in press).
5. Frederick, E. R., "Electrostatic Effects in Fabric Filtration: Vol. 2. Triboelectric Measurements and Bag Performance, An Annotated Data Book", Final Report, Grant R803020 (in press).
6. Frederick, E. R., "How Dust Filter Selection Depends on Electrostatics," Chemical Engineering, June 26, 1961, pp. 107-114.
7. Donovan, R. P., R. L. Ogan and J. H. Turner, "The Influence of Electrostatically-Induced Cage Voltage Upon Bag Collection Efficiency During the Pulse-Jet Fabric Filtration of Room Temperature Flyash" (presentation to the Third Symposium on Fabric Filters for Particle Collection, Tucson, AZ, December 5-6, 1977).
8. Miller, B., G. Lamb, P. Costanza and J. Craig, "Nonwoven Fabric Filters for Particulate Removal in Respirable Dust Range", EPA-600/7-77-115, October 1977, Textile Research Institute, P. O. Box 625, Princeton, N. J. 08540.
9. Cass, R. W. and R. M. Bradway, "Fractional Efficiency of a Utility Boiler Baghouse: Sunbury Steam-Electric Station", EPA-600/2-76-077b, (NTIS No. PB 253-943/AS), March 1976, GCA Corp., Bedford, MA 01730.
10. Bradway, R. M. and R. W. Cass, "Fractional Efficiency of a Utility Boiler Baghouse: Nucla Generating Plant", EPA-600/2-75-013a, (NTIS PB 246-641/AS), August 1975, GCA Corp., Bedford, MA 01730.
11. McKenna, J. D., J. C. Mycock and W. O. Lipscomb, "Applying Fabric Filtration to Coal Fired Industrial Boilers, A Pilot Scale Investigation," EPA-650/2-74-058a, (NTIS PB 245-186/AS), August 1975, Enviro- Systems and Research Inc., P. O. Box 658, Roanoke, VA 24004.

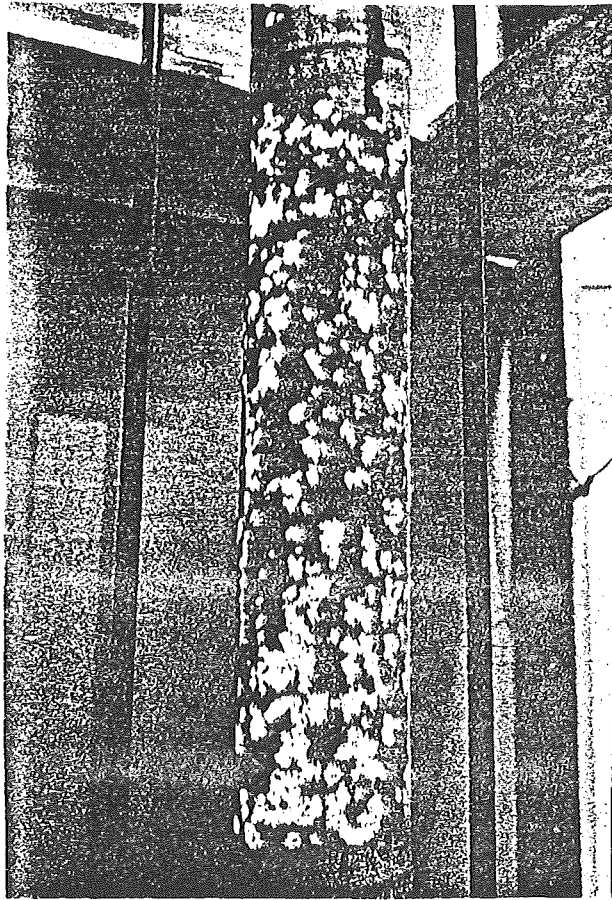


Figure 1. Partially cleaned, woven glass bag under inside illumination [Ref.1].

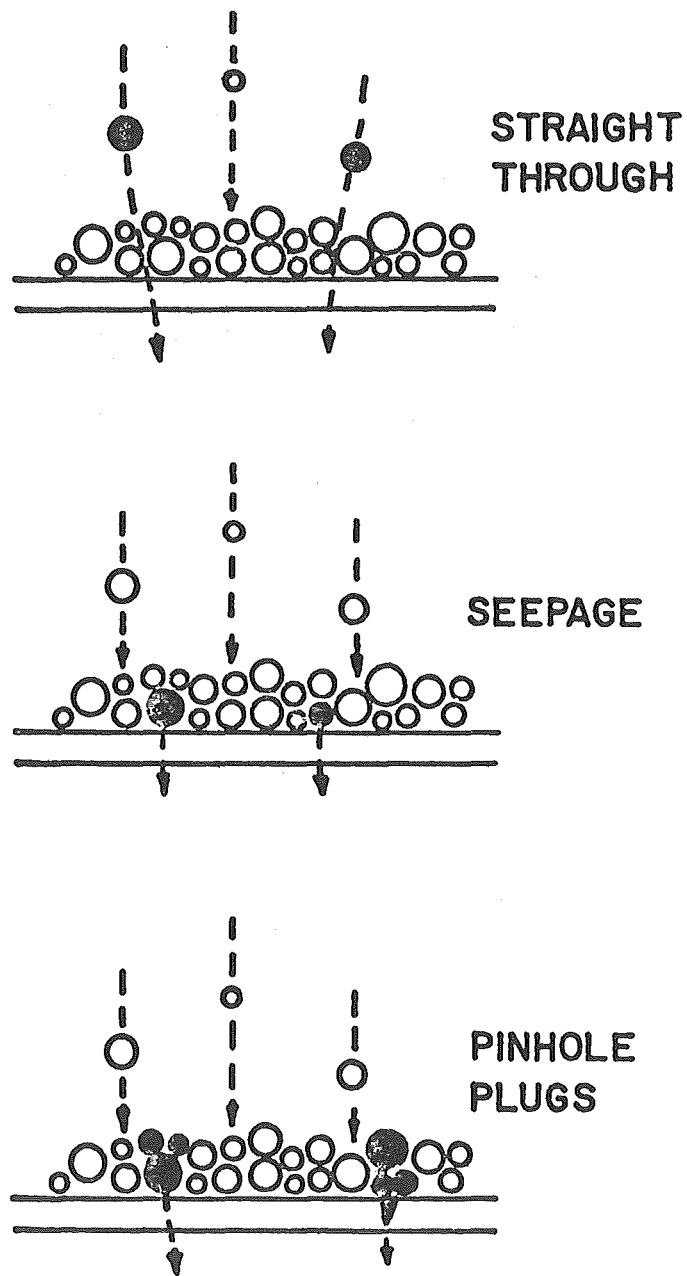


Figure 2. Schematic representation of flyash emission mechanisms [Ref.2].

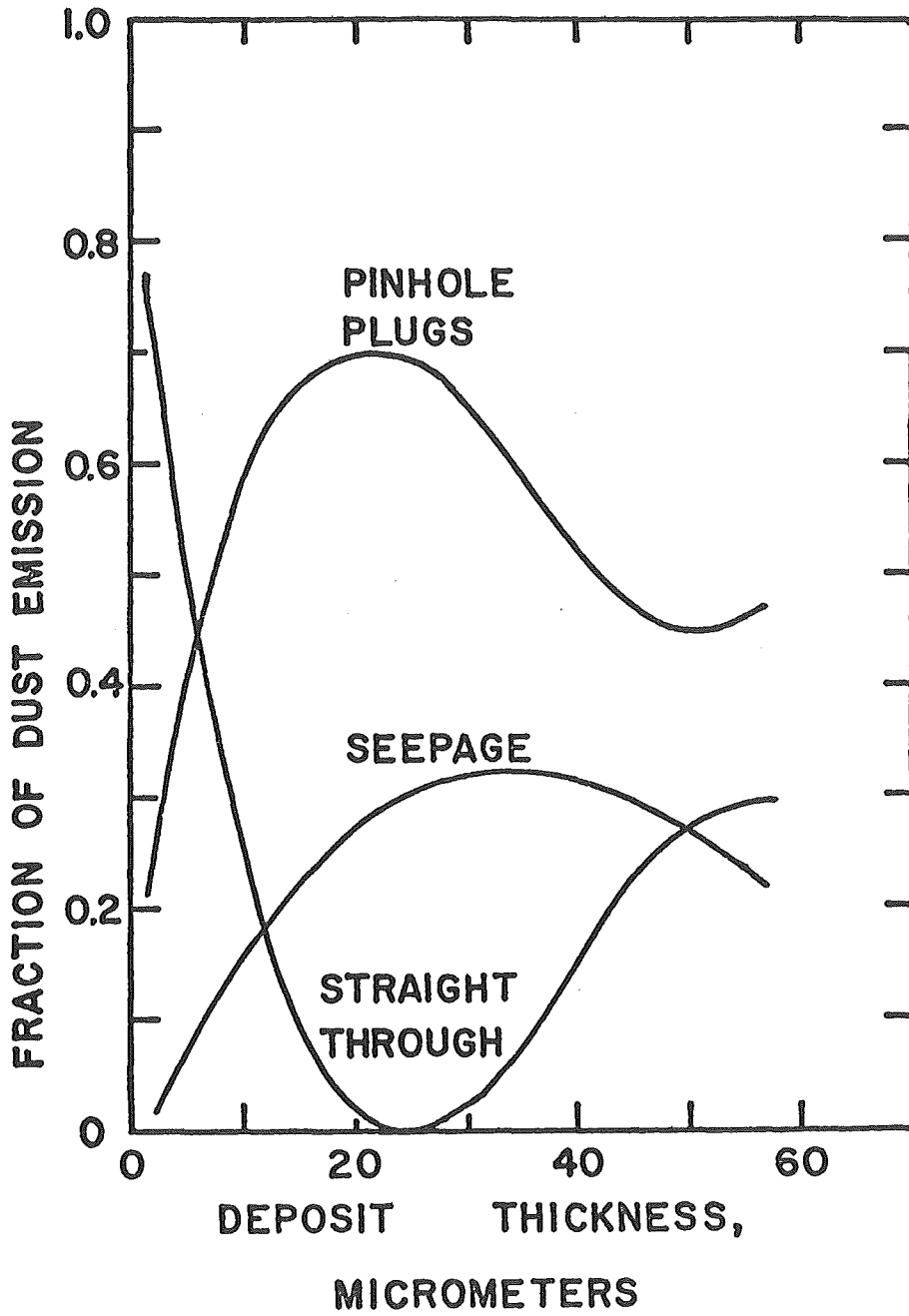


Figure 3. Fractional flyash emission according to mechanism of penetration [Ref.2].

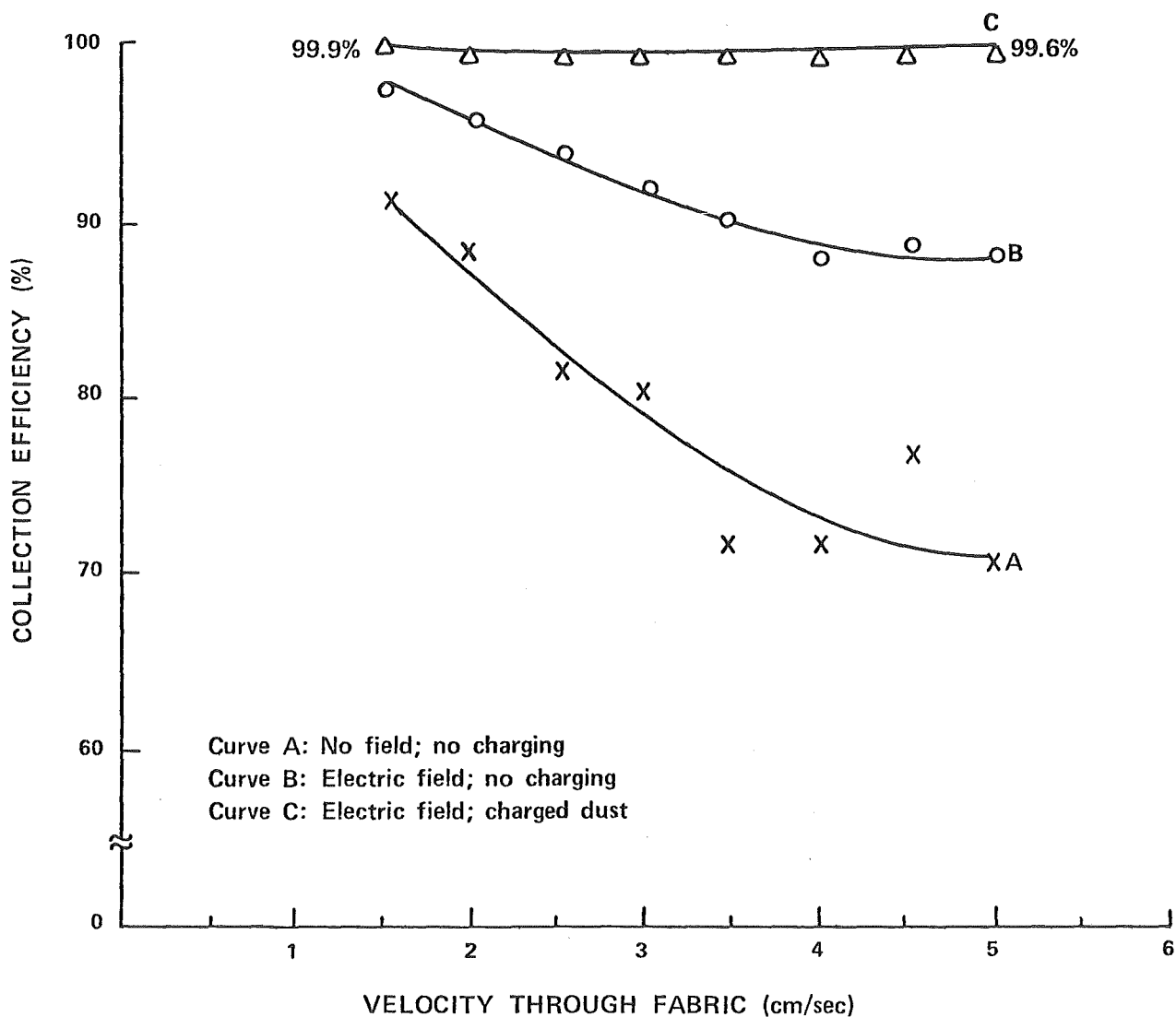


Figure 4: Electrostatic augmentation of the collection efficiency of a clean woven glass fabric filtering smoke from an electric arc [Ref. 4].

- WOOL/NYLON 1 [20%]
- WOOL 1 [80%]
- WOOL/NYLON 2 [80%]

- + 6 -- NYLON 800 B (REFERENCE)
 - WOOL 2 [85%]

- + 5 • DACRON 1 [50%]

- + 4 • WOOL 3 [80%]
 - POLYESTER 1 [90%]

- + 3 • ACRYLIC, ZC [90%]

- + 2 • DACRON 2 [40%]
 - DRALON T [30%]

- + 1 • GLASS [77%]
 - POLYESTER 2 [70%]

- 0 • ACRYLIC, Z [25%]
 - ORLON [30%]

- 1 • DRALON T [30%]

- 2 • POLYPROPYLENE [50%]

- 3 •

- 4 -- DARLAN S546 (REFERENCE)
 - TEFLON [0%]

[] = RELATIVE CHARGE RATE [LOSS (%) IN 2 MINUTES] AT 50% RH

Figure 5. Frederick's triboelectric series of selected filter fabrics [Ref. 5].

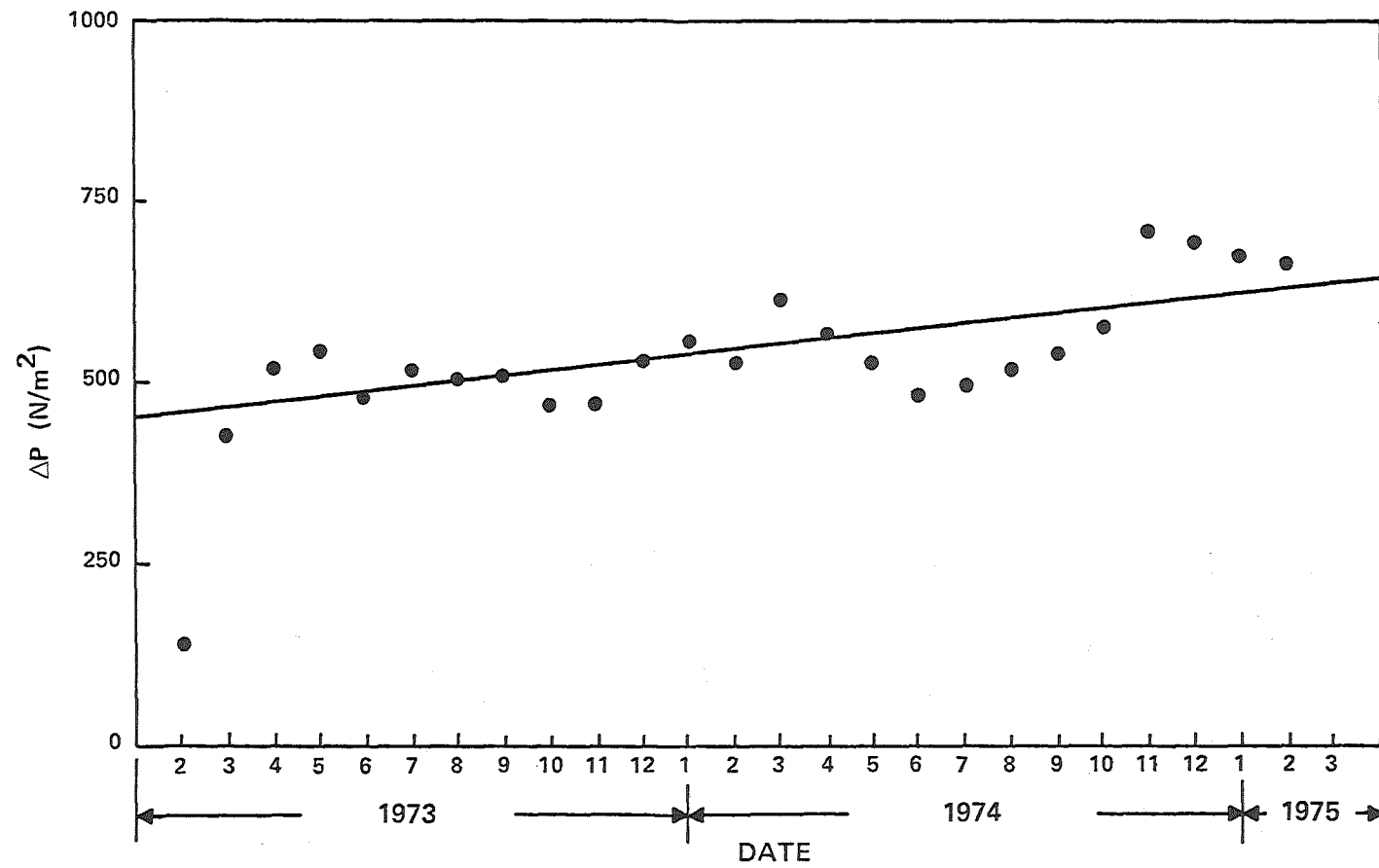


Figure 6. Pressure differential history of Sunbury baghouse.

TABLE 1
EXPERIMENTAL FILTRATION OF A FERROMOLYBDENUM BY-PRODUCT DUST [Ref 5]

| | Permeability, $\frac{N}{cm \cdot sec}$ at $0.125 \frac{N}{m^2}$ (fpm at 0.5") | | Triboelectric Properties | | Cake | | | | |
|---|--|--------|-------------------------------|--|-----------------------|--|-------|---------------|---------------------|
| | | | Position (Frederick Scale) | Rate of Charge Loss (% in 2 min) | Collected mass (g) | Pressure drop, N/cm^2 (in. H_2O) | | Weight (g) | Relative Leakage |
| woven staple acrylic (napped surface) | 0.25 | (50) | -1.1 | 75 | 16 | 56 | (1.1) | ~ 76 | low |
| woven staple acrylic (TFE finish) | 0.11 | (21) | -2.4 | 75 | 12 | 71 | (1.4) | ~ 56 | low |
| woven filament polypropylene | 0.10 | (20) | -2.7 | 10 | 23 | 40 | (0.7) | 4.5 | very high |
| woven filament Teflon | 0.11 | (21) | ~-8.0 | 0 | 12 | 50 | (0.9) | 4.6 | very high |
| woven staple wool | 0.26 | (50.5) | + 5.5 | 85 | 16 | 30 | (0.6) | ~ 45 | low |

TABLE 2
PERFORMANCE SERIES
WITH EXPERIMENTAL NOMEX FELTS [Ref 7]

| RUN NO. | FABRIC | COLLECT. EFF. (%) |
|---------|---|-------------------|
| 1 | CONTROL WITH ANTI-STATIC COATING (50% RELATIVE HUMIDITY) | 98.7* |
| 2 | CONTROL ALONE (50% RELATIVE HUMIDITY) | 97.1 |
| 3 | CONTROL ALONE (70% RELATIVE HUMIDITY) | 99.3 |
| 4 | CONTROL ALONE (50% RELATIVE HUMIDITY) | 96.8 |

*Average of two runs, 2 days apart

TABLE 3
FILTRATION PERFORMANCE
OF TEST POLYESTER FELTS [Ref 7]

| FABRIC TESTED | ELECTRICAL RESISTANCE OF MOUNTED BAGS (ohms) | COLLECT. EFF. (%) |
|---|---|----------------------|
| STANDARD POLYESTER FELT | $10^8 - 10^9$ | 99.8 |
| STANDARD POLYESTER FELT AFTER MULTIPLE SOAKS IN PERCHLOROETHYLENE | $\geq 10^{10}$ | 97.2 |

Discussion

The discussions which followed were opened by a question raised by Dr. Guthner as to the difference between electrostatic precipitators and fabric filters in economic terms. Mr. Donovan replied that in at least two recent analyses by major utilities total baghouse costs (initial plus operating) were found to be cheaper and hence baghouses were selected as the preferred control technology. Two important points were raised: 1) the efficiency of an electrostatic precipitator depends on the coal properties (the flyash from low sulfur coals is more costly to remove); 2) performance predictability and especially performance stability seems to be better for the baghouse than for the electrostatic precipitator when burning low sulfur coal or coals with variable sulfur content. In reply to Dr. Kastner's query about the cost of baghouse maintenance work, Mr. Donovan stated that although baghouse maintenance costs are typically estimated on the assumption that the bags will be changed at least every two years, field experience shows that four or five year bag life can be achieved. His comment that the argument for fabric filters was very strong was seconded by Mr. Princiotta. Dr. Davids wished to know which filter materials were preferred in coal fired power stations, upon which Mr. Donovan replied that the temperature requirements generally dictated the use of fiberglass.

A.P.T. FIELD EVALUATION
OF FINE PARTICLE SCRUBBERS

by

Seymour Calvert

Air Pollution Technology, Inc.
4901 Morena Blvd., Suite 402
San Diego, California 92117
USA

INTRODUCTION

The need for more reliable data on the fine particle collection efficiency of air pollution control scrubbers has become increasingly apparent as control requirements have grown more demanding. Design methods, including mathematical models, have been developed from basic theory plus whatever good data were available, but to a large extent they were untested.

To compare predictions with scrubber performances in different situations one needs to know efficiency as a function of particle size, commonly called "grade efficiency."

The program reported here was supported by the US Environmental Protection Agency over the past 5 years in response to the need for additional reliable performance data on fine particle collection efficiency as a function of particle size for scrubbers operating on representative industrial emission sources and to reconcile the performance data with existing mathematical models.

FIELD SAMPLING METHOD

The method of approach to the program objectives involved a number of experimental determinations to obtain collection efficiency data, the acquisition of information on system characteristics and behavior, and computations which utilized the performance data and mathematical models.

In the beginning of the program the particle size range of primary interest was from a few tenths to a few microns diameter, which is within the measurement range of a cascade

impactor. Later the size range was extended downward by an order of magnitude and it was necessary to use a diffusion battery in addition to the cascade impactor. The apparatus and methods used are outlined below:

1. Gas velocity distribution and parameters had to be measured at the inlet and outlet of the scrubber in order to define the following:
 - a. conditions for isokinetic sampling,
 - b. particle concentration per unit volume of dry gas, and
 - c. gas flow rate.
2. Particle size distribution and concentration (loading) in the inlet and outlet of the scrubber were always made with cascade impactors and sometimes with diffusion batteries. In some tests, a "pre-cutter" was used to remove either the heavy particle loading from inlet samples or the entrained liquid from outlet samples. A cyclone separator with about a 3 μ m cut diameter was first used but a round jet impactor with about an 8 μ m cut diameter was found to have better characteristics and was adopted for use for both inlet and outlet sampling.

Simultaneous inlet and outlet measurements minimize the effects of particle size distribution changes caused by fluctuations in the operation parameters. Since the program objective was to investigate scrubber performance on fine particles, the sampler was held at one location in the duct for the duration of each sampling run. This is an adequate technique for obtaining good samples of particles smaller

than a few microns in diameter because they generally are well distributed across the duct.

RESULTS

A summary of the scrubbers tested is given in Table I. The first ten scrubbers in Table I are classified as conventional scrubbers. The last three are novel devices because they are different in some manner from conventional technology.

The dashed lines in Figures 1 through 10 are experimental grade penetration curves. They were computed from simultaneous inlet and outlet particle size/concentration data. We use the symbol " μmA " for aerodynamic diameter, which is defined by:

$$d_{pa} = d_p (C' \rho_p)^{\frac{1}{2}}, \mu\text{mA} \quad (1)$$

DISCUSSION

Comparison of the experimental results with mathematical models was done wherever models were available. Table II is a list of the design equations taken from the "Scrubber Handbook" (Calvert et al. 1972). All of these equations are based on particle collection by inertial impaction.

The predicted grade penetration curves are represented by the solid lines in Figures 1 through 10. By comparing the predicted and the measured grade penetration curves, we can either verify or reject the design equations. The results of this comparison are summarized as follow:

1. Valve tray on urea prilling tower - We used the particle collection model for sieve plates because the gas jets emerging from the slots between the valve cap and the tray impinge on a liquid froth similar to the round gas on a sieve plate. The model compared well with the data after accounting for particle growth due to water vapor condensation.
2. Vaned centrifugal on KCl dryer - The collection efficiency of this scrubber could not be accounted for simply by centrifugal deposition caused by the internal vanes. A gas atomized spray model gave predictions which agreed with the data.
3. Mobile bed on coal-fired boiler - No satisfactory model is available. Subsequent work in a carefully controlled pilot plant has yielded much lower efficiency than obtained on the boiler flue gas scrubber. Particle growth due to plant conditions is suspected.
4. Venturi on coal-fired boiler - The model for a venturi in terms of particle cut diameter correlated with pressure drop agrees well with the experimental results.
5. Wetted fiber on NaCl dryer - Heated impactors were used in the field sampling. Thus, the measured particle size is that of a dry particle. In the scrubber the particles are wet and therefore larger than the dry particles. We did not measure the wet particle size in the field so wet particle diameter was calculated from dry particle diameter with the theoretical prediction that its physical diameter should double. Calculation results are shown

in Figure 5. The fibers in the filter pad were ellipsoidal in shape with the longer axis normal to the direction of gas flow. Therefore, the collection efficiency should lie somewhere between those of a ribbon and a cylinder.

6. Impingement plate on NaCl dryer - A model based on impingement from round jets gives good agreement with the data after allowing for particle growth due to condensation.
7. Venturi rod on cupola - The venturi model gives a good prediction for particles larger than about $1.0 \mu\text{m}$ but does not account for low penetration for the sub-micron particles.
8. Venturi on asphalt dryer - The venturi model prediction agrees with the performance data.
9. Venturi on borax fusing furnace - The model agrees with data for particles with diameter larger than $1 \mu\text{m}$. For particles smaller than $1 \mu\text{m}$ diameter, the model predicted penetration a few percent higher than measured.
10. Variable rod on cupola - The model predicted penetration higher than that measured.

CUT/POWER RELATIONSHIP

When scrubbers are operated at different pressure drops it is very difficult to evaluate and to compare their performances based only on grade penetration curves. We have developed a useful correlation called the cut/power relationship

for this purpose and others. The cut/power relationship is a plot of the cut diameter given by the scrubber against pressure drop or power input, as illustrated in Figure 11. Cut diameter is the particle diameter whose collection efficiency is 50%. The solid lines in this graph were calculated theoretically from the design equations presented in the "Scrubber Handbook."

The performance cut diameters determined experimentally in this program were plotted against measured pressure drop in Figure 11. (In cases where penetration curves do not reach 50%, the reported cut diameters were equivalent cut diameters calculated by the method presented by Calvert, 1974). As can be seen, predictions for impingement and sieve plates agree with the experimental data. The solid line for venturi scrubber from the previous correlation slightly overestimates the pressure drop. The dashed line fits the experimental data determined in this study and is based on a revised method for predicting pressure drop (Ref: Yung et al. 1976).

NOVEL DEVICES

Under the novel device test program, we have tested a CHEAF, an electrostatic scrubber, and a charged droplet scrubber.

Electrostatically Augmented Scrubber

The electrostatic scrubber by Air Pollution Systems is essentially a venturi scrubber with a particle charging electrode placed ahead of the throat. The unit we tested is a pilot scale unit with a capacity of about 28 m³/min (1,000 CFM). The experimental data are shown in Figure 12 for the

scrubber system with the charger off and with the charger on.

In a venturi scrubber the most important mechanism responsible for particle collection is by inertial impaction on drops. When particles are charged, electrostatic deposition forces augment the inertial force and increase the collection efficiency of the drop.

Calvert et al. (1973) calculated the theoretical total collection efficiency due to particle deposition caused by flux forces plus inertial force. A plot of single drop collection efficiency against inertial impaction parameter with flux deposition number, N_{FD} , as the parameter is presented in Figure 13. Flux deposition number is defined as:

$$N_{FD} = \frac{u_F}{u_o} = \frac{\text{Particle deposition velocity}}{\text{Gas velocity past drop}} \quad (2)$$

Assuming Stokes' law holds, the particle deposition velocity is given by:

$$u_F = \frac{C' Q_p E}{3 \pi \mu_G d_p} \quad (3)$$

Single drop collection efficiency, η_d , is related to scrubber penetration by an equation given by Calvert for a venturi:

$$(Pt)_d = \frac{2 Q_L \rho_L d_d u_{Gt}}{55 Q_G \mu_G} \int_{f_a}^o \eta_d df \quad (4)$$

Equation (4) with " η_d " obtained from Figure 13 was used to predict the collection efficiency of the A.P.S. scrubber both with the charger on and with the charger off. Figure 12 shows the

predicted A.P.S. scrubber performance along with experimental curves. As can be seen the design equations predict a higher penetration than actually measured in the sub-mircon region.

Wetted Fibrous Bed

The CHEAF system is primarily a wetted fibrous bed scrubber system. It consists of water sprays to wet and clean the filter medium, a rotary drum containing a fibrous "sponge" filter medium, and a water reservoir.

The CHEAF unit we tested was on a diatomaceous earth dryer exhaust. The experimental results are shown in Figure 14. The grade penetration curve for wet particles in the figure was calculated from the penetration curve for dry particles (containing NaCl) and particle growth data.

We can mathematically represent the filter as an array of equally spaced cylinders. The "Scrubber Handbook" gave the following equation for the prediction of particle penetration of a clean fibrous bed:

$$(Pt)_d = \exp \left[- S \eta_f \right] = \exp \left[- \frac{4 \ell (1-\epsilon)}{\pi d_f} \eta_f \right] \quad (5)$$

where " η_f " is the effective collection efficiency of a single fiber in the bed which was assumed to be the collection efficiency of an isolated fiber.

The pressure drop across the fiber bed is the sum of the drag losses of all fibers. We used the drag coefficient for an isolated cylinder.

$$\Delta P = 6.5 \times 10^{-4} \frac{\lambda(1-\epsilon) \rho_G C_D u_G^2}{d_f} \quad (6)$$

Equations (5) and (6) were used to predict the performance of the CHEAF. The result is shown in Figure 15, a cut/power plot for various fiber diameters. The cut/power relation is highly dependent on the diameter of the fiber, but not much on the solidity factor. The circle in the figure represents the data we determined experimentally. The fiber diameter and filter porosity were not disclosed to us so we could not check the model.

It is possible to compare our model with the data of Rei and Cooper (1976) for tests on a pilot scale unit of the CHEAF. They reported the volume fraction void of the filter medium to be 97% and the fiber diameters to be 64 μm , 44 μm , and 36 μm for foams with 18, 26, and 33 pores per cum. They also reported the measured cut diameter was somewhere below 0.5 μm A for pressure drops ranging from 40 to 90 cm W.C. The dashed line in Figure 15 shows their data, which are consistent with our predictions.

Charged Droplet Scrubber

The charged droplet scrubber by TRW Systems does not charge the particles but charges the water drops. The water flows out of small diameter tubes, which also act as electrodes, and is atomized. Particle collection of this scrubber

is due to inertial impaction and the electrostatic deposition. The 680 m³/min (24,000 CFM) unit we tested was used to control emissions from a coke oven.

Figure 16 shows the experimental data. We did not compare a model prediction with data in this case.

CONCLUSIONS

Except for the design equation for the mobile bed scrubber, design equations for the scrubber types tested in this program give reasonable performance predictions. In cases where $(Pt)_d$ was lower than predicted it could be accounted for by particle growth due to water condensation.

The cut/power relationship has many useful applications. It can be used to compare and evaluate scrubbers, to make preliminary scrubber selections, and to estimate the minimum pressure drop of a scrubber for it to attain the required performance. We have verified and extended this relationship in this study.

ACKNOWLEDGEMENT

The work upon which this paper is based was performed pursuant to Contracts 68-02-0285, 68-02-1328, 68-02-1496, and 68-02-1869 with the Environmental Protection Agency.

NOMENCLATURE

- C_D = drag coefficient, dimensionless
- C_p = particle concentration, g/cm³
- C_{pt} = total particle concentration, g/cm³
- C' = Cunningham slip factor, dimensionless
- d_c = collector diameter, cm
- d_d = drop diameter, cm
- d_f = fiber diameter, cm
- d_h = diameter of perforation, cm
- d_p = particle diameter, μm
- d_{pa} = aerodynamic particle diameter, μm
- d_{pa50} = cut diameter, μm
- d_{pg} = mass median particle diameter, μm
- E = field strength, kV/cm
- F = foam density, dimensionless
- f = empirical constant, dimensionless
- f_a = empirical constant = 0.5
- $f(d_p)$ = frequency distribution of particles
- K_p = inertial impaction parameter, dimensionless
- K_{pt} = inertial parameter in the venturi throat, dimensionless
- l = thickness of filter pad, cm
- N_{FD} = flux force deposition number, dimensionless
- n = number of stages, dimensionless
- \overline{Pt} = overall penetration, fraction or percent
- $(Pt)_d$ = penetration for particles with diameter d_p , fraction

NOMENCLATURE (continued)

- Q_G = gas volumetric flow rate, m^3/s
 Q_L = liquid volumetric flow rate, m^3/s or l/s
 Q_p = electrical charge carried by the particle,
coulomb
 S = solidity factor, dimensionless
 T_G = gas temperature, $^{\circ}C$
 u_F = particle drift velocity, cm/s
 u_G = gas velocity, cm/s
 u_{Gi} = interstitial gas velocity, cm/s
 u_{Gt} = gas velocity in the venturi throat, cm/s
 u_h = velocity of gas through perforation, cm/s
 u_o = gas velocity, past drop, cm/s
 z = static bed height, cm

Greek

- ϵ = porosity, fraction
 l = filter pad thickness, cm
 η = single drop (η_d) or single fiber (η_f) collection
efficiency, fraction
 μ_G = gas viscosity, poise
 ρ_G = gas density, g/cm^3
 ρ_L = liquid density, g/cm^3
 ρ_p = particle density, g/cm^3
 σ_g = geometric standard deviation
 Δp = pressure drop, cm W.C.

Table 1. SUMMARY OF SCRUBBERS TESTED

| No. ^a | Control Device | Source | Q _G Am ³ /min | Q _L /Q _G ℓ/m ³ | T _G , °C | | Pres- sure Drop cm W.C. | Inlet Size Distri- bution | | Perfor- mance Cut Dia- meter (μm) | |
|------------------|--|-------------------------------------|--|--|---------------------|-----|----------------------------------|------------------------------------|----------------|---|------|
| | | | | | In | Out | | d _{pg} , μm | σ _g | | |
| 1 | Valve tray (Koch Flexitray) | Urea prilling tower | 86 | 0.7 | 27 | 17 | 30 | 1.1 | 1.5 | 54 | 1.0 |
| 2 | Vaned centrifugal (Ducon) | KCl dryer | 465 | 0.26 | 196 | 78 | 8 | >100 | - | 3 | 1.3 |
| 3 | Mobile bed (UOP/TCA) | Coal fired utility boiler | 18,000 | 6.6 | 143 | 85 | 30 | 3 | 2.5 | 6 | 0.48 |
| 4 | Venturi (Chemico) | Coal fired utility boiler | 13,400 | 1.8 | 163 | 54 | 25 | 3.8 | 5 | 2.7 | 0.67 |
| 5 | Wetted fiber filter (Encort Corp) | Salt dryer | 1,590 | 0.24 | 38 | 32 | 19 | 10 | 4.8 | 2.7 | 0.64 |
| 6 | Impingement plate (Sly Impinjet) | Salt dryer | 238 | 0.15 | 85 | 38 | 30 | >100 | - | 10 | 1.3 |
| 7 | Venturi rod (Enviro-engineering) | Foundry cupola | 1,274 | 2.4 | 88 | 65 | 273 | 1 | 2 | 0.4 | 0.25 |
| 8 | Venturi (AAF) | Asphalt batch plant | 800 | 1.3 | 149 | 57 | 66 | 10 | 3 | 0.3 | 0.37 |
| 9 | Venturi (AAF) | Borax calciner & fusing furnace | 1,200 | 1.7 | 80 | 55 | 110 | 1 | 3 | 2.5 | 0.2 |
| 10 | Variable-rod venturi (National Dust Collector) | Foundry cupola | 1,010 | 2.1 | 35 | 20 | 180 | 0.75 | 1.8 | 1.5 | 0.18 |
| 11 | CHEAF (Johns-Manville) | Diatomaceous earth calciner & dryer | 710 | 0.75 | 63 | 60 | 48-53 | 0.85 | 4 | 5 | 0.8 |
| 12 | Electrostatic scrubber (Air Pollution Systems) | TiO ₂ test dust | 23 | 1.8 | 16 | 16 | 40 | 1 | 2.1 | 8.5 | 0.35 |
| 13 | Charged droplet (TRW) | Coke oven | 680 | 0.05 | 120 | 60 | 10 | 1.4 | 2.1 | 88-94 | 0.35 |

a. Numbers cited in Figure 11.

Table 2. DESIGN EQUATIONS FOR VARIOUS SCRUBBER TYPES

| SCRUBBER TYPE | DESIGN EQUATIONS |
|--------------------------------|--|
| Sieve and valve tray | $(Pt)_{d_p} = \exp \left[-40F^2 K_p \right], \quad K_p = \frac{d_{pa}^2 u_h}{9 \mu_G d_h}$ $0.38 < F < 0.65$ |
| Mobile bed | $(Pt)_{d_p} = \exp \left[-9.5 \times 10^6 \left(\frac{Q_L}{Q_G} \right)^{3.3} (u_G \rho_G)^{3.66} K_p \frac{z}{d_c} \right]$ $K_p = \frac{d_{pa}^2 u_{Gi}}{9 \mu_G d_c}$ |
| Venturi and gas atomized spray | $(Pt)_{d_p} = \exp \left[\frac{2 Q_L u_{Gt} \rho_L d_d}{55 Q_G \mu_G} F(K_{Pt}, f) \right]$ $F(K_{Pt}, f) = \frac{1}{K_{Pt}} \left[1.4 \ln \left(\frac{K_{Pt} f + 0.7}{0.7} \right) + \frac{0.49}{0.7 + K_{Pt} f} - (K_{Pt} f + 0.7) \right]$ |
| Wetted fiber filter | $(Pt)_{d_p} = \exp (-\eta_f S)$ $S = \frac{4 \ell (1-\epsilon)}{\pi d_f}$ |
| Impingement | $d_{pa_{50}} = \left(\frac{1.37 \mu_G n d_h^3}{Q_G} \right)^{0.5}$ |

REFERENCES

1. Calvert, S., J. Goldshmid, D. Leith, and D. Mehta. "Wet Scrubber System Study, Volume I, Scrubber Handbook." EPA-R2-72-118a (NTIS PB 213-016), August 1972.
2. Calvert, S., J. Goldshmid, D. Leith, and N.C. Jhaveri, "Feasibility of Flux Force/Condensation Scrubbing for Fine Particulate Collection," EPA 650/2-73-036 (NTIS PB 227-307), October 1973.
3. Calvert, S., "Engineering Design of Fine Particle Scrubbers," J. of A.P.C.A., 24, No. 10, p. 929, October 1974.
4. Yung, S., S. Calvert, and H. Barbarika, "Venturi Scrubber Performance Model," Final report to EPA, EPA 650/2-75-021b (NTIS PB 271-515) August 1977.
5. Junge, C.E., "Air Chemistry and Radioactivity," Academic Press, 1963.
6. Pei, M.T., and D.W. Cooper, "Laboratory Evaluation of the Cleanable High Efficiency Air Filter (CHEAF)", EPA-600/2-76-202 (NTIS PB 256-698/AS), July 1976.

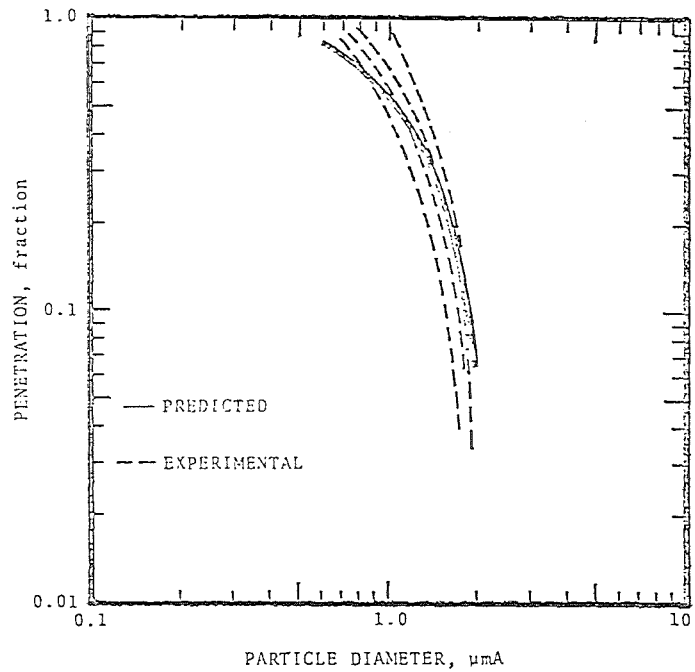


Figure 1. Predicted and experimental penetrations for Koch Flexitray.

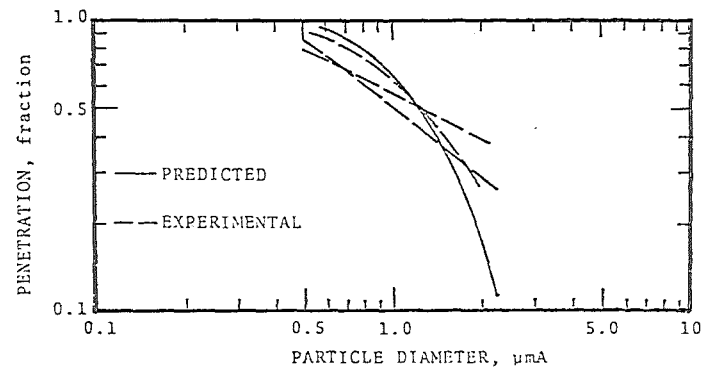


Figure 2. Predicted and experimental penetrations for Ducon Multivane scrubber.

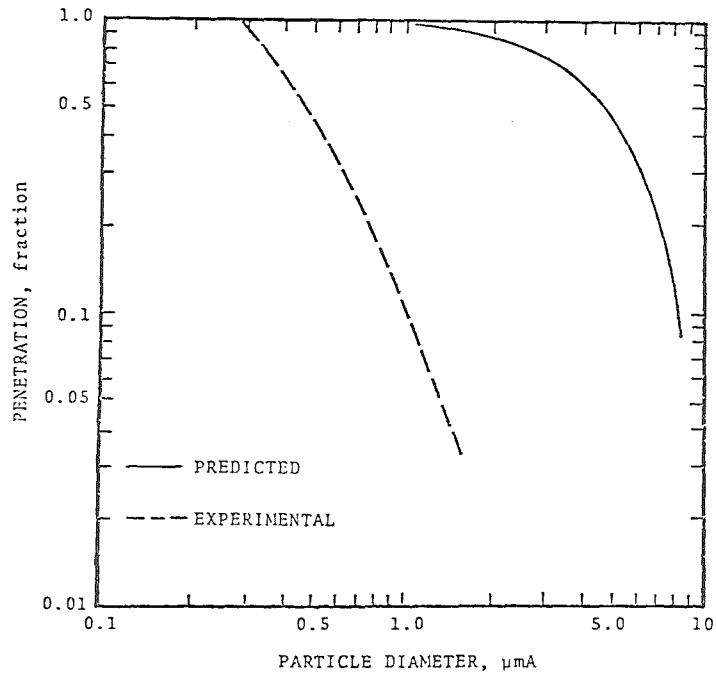


Figure 3. Predicted and experimental penetration for mobile bed scrubber.

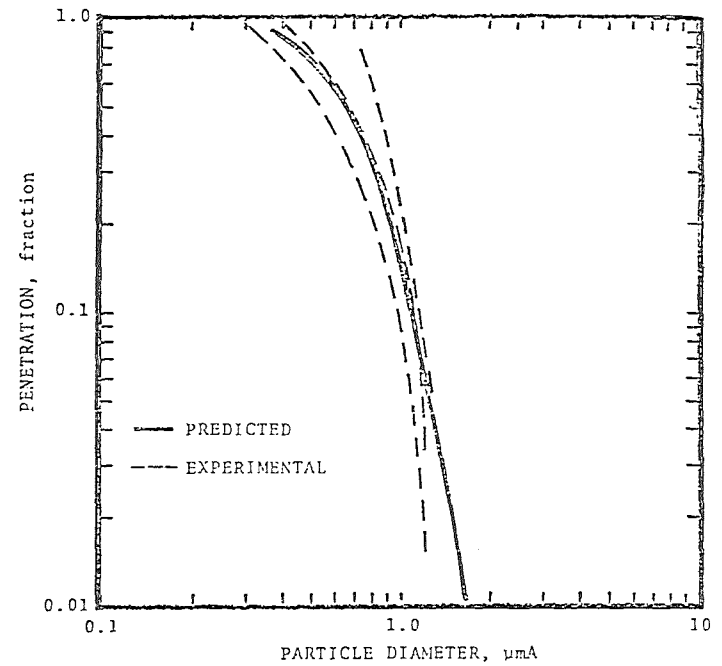


Figure 4. Predicted and experimental penetrations for Chemico venturi.

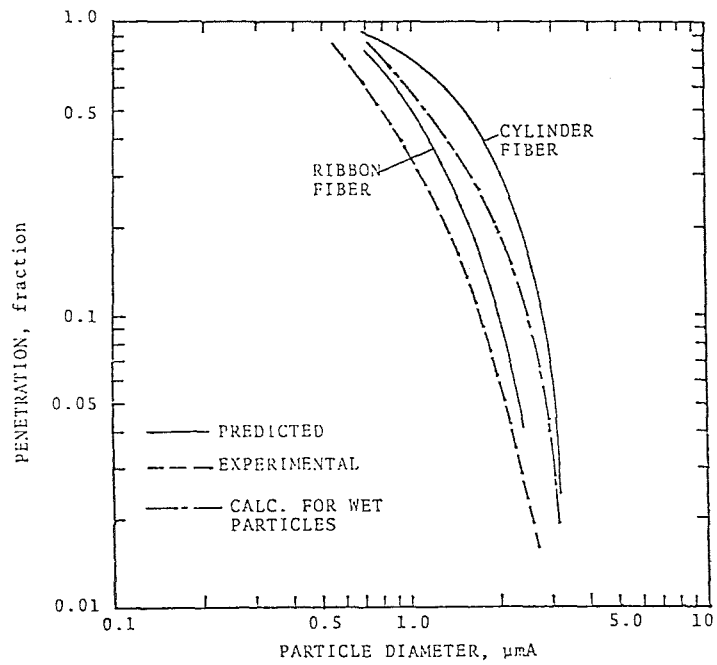


Figure 5. Predicted and experimental penetrations for Encort wetted fiber scrubber.

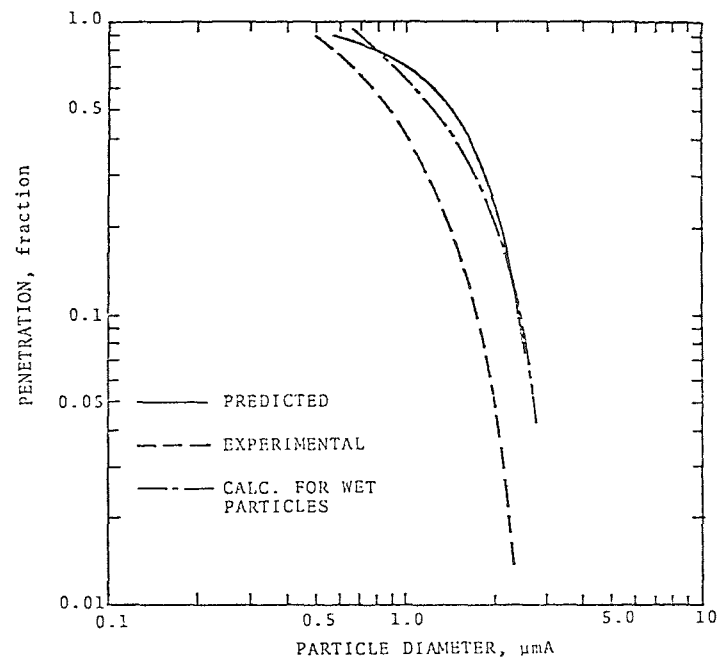


Figure 6. Predicted and experimental penetration for Sly Impinjet.

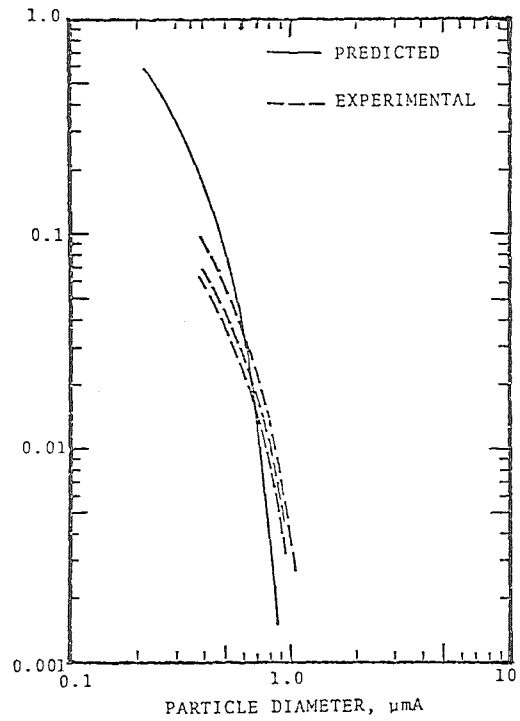


Figure 7. Predicted and experimental grade penetration curves for venturi rod scrubber.

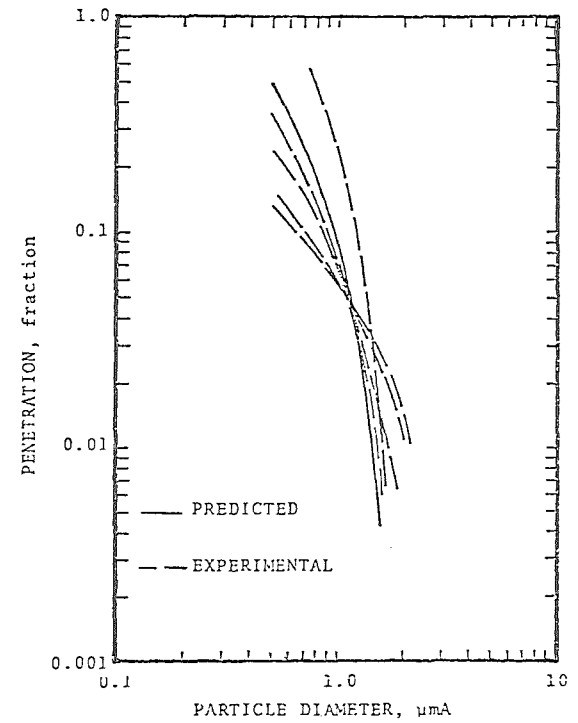


Figure 8. Predicted and experimental penetrations for AAF Kincofactor 32.

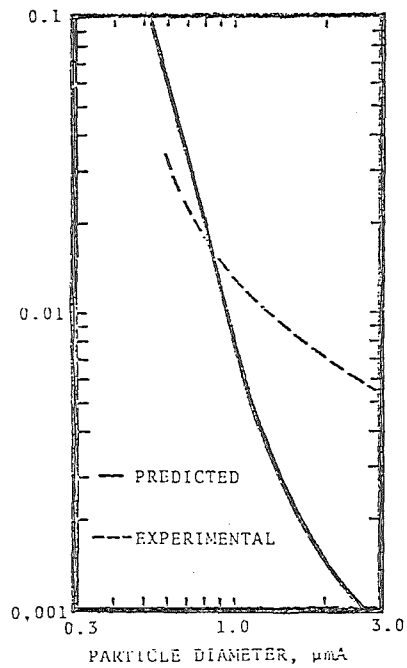


Figure 9. Predicted and experimental grade penetration curves for AAF Kine-pactor 56.

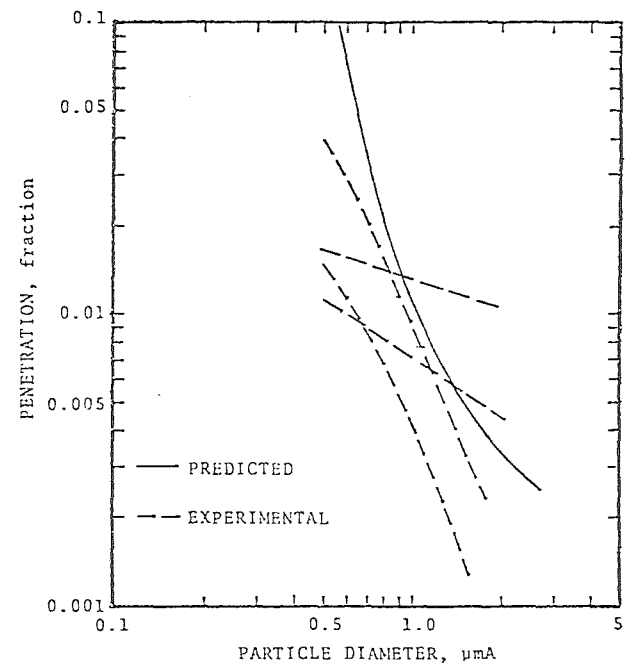


Figure 10. Predicted and experimental penetrations for variable rod scrubber.

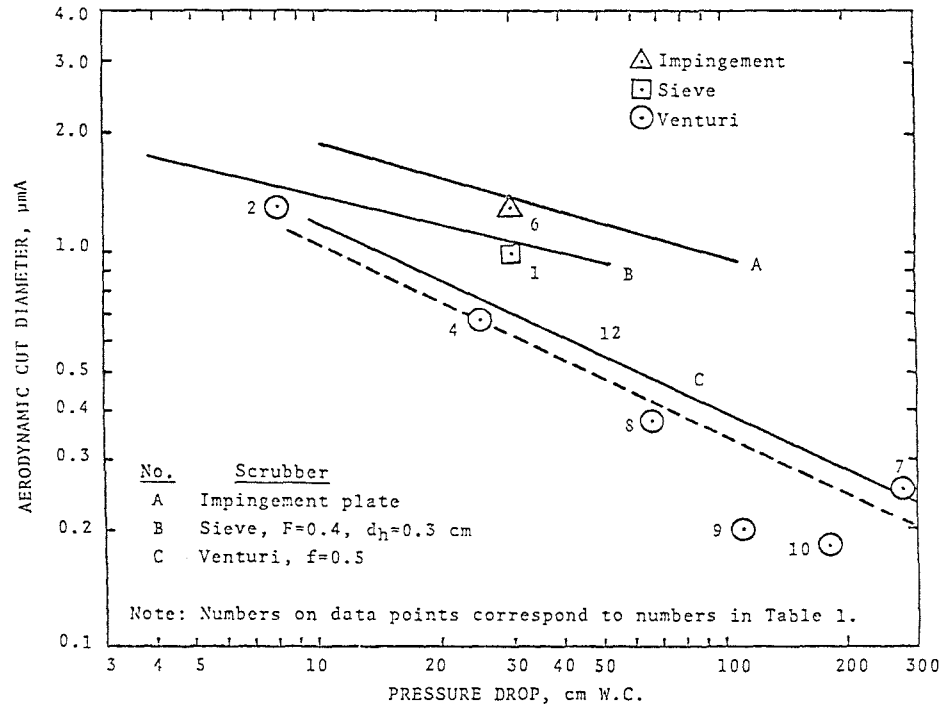


Figure 11. Theoretical and experimental cut diameters as a function of pressure drop for several scrubber types.

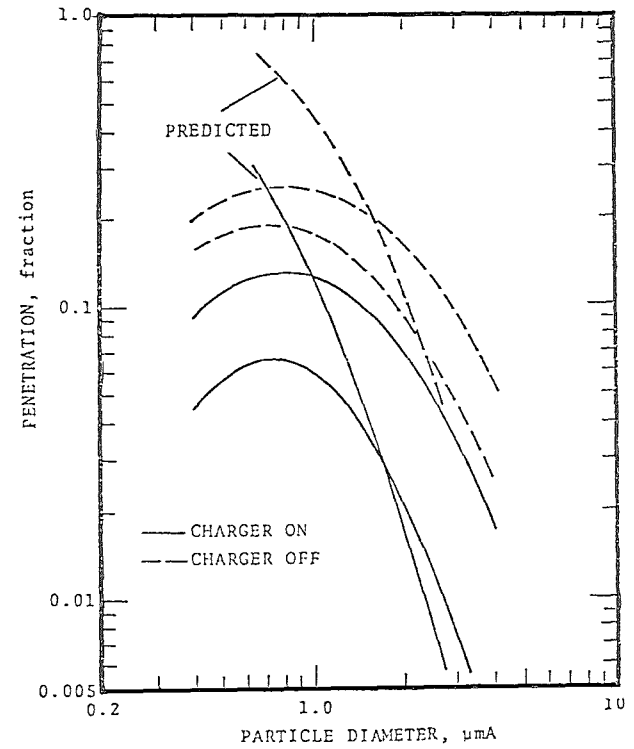


Figure 12. Predicted and experimental penetrations for APS electrostatic scrubber.

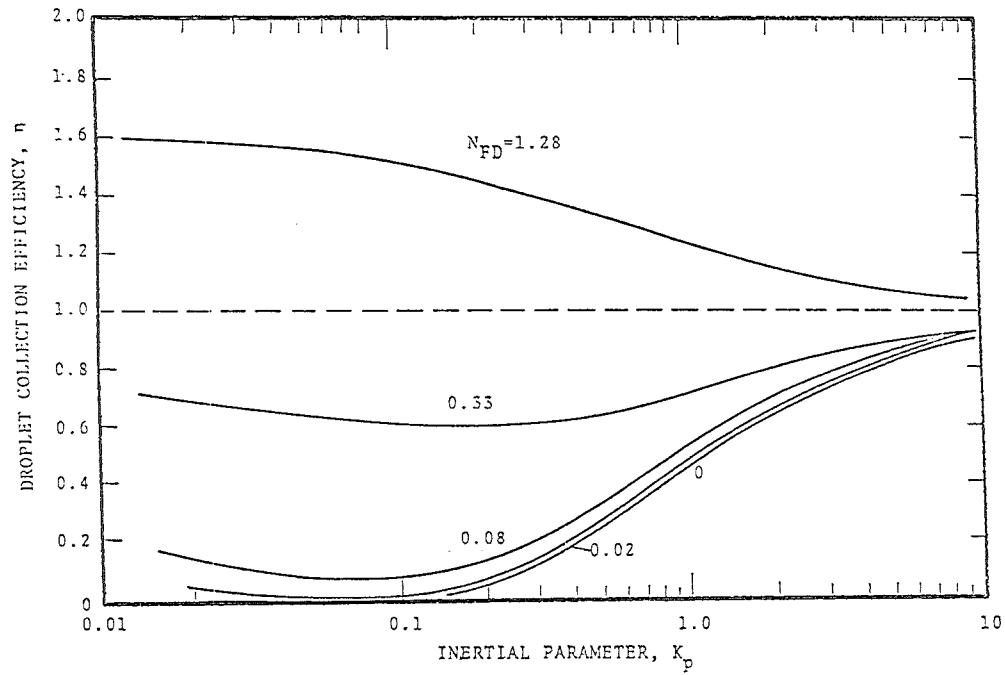


Figure 13. Collection efficiency of single drop versus inertia parameter at $N_{Re_d}=9.6$ with N_{FD} as parameter.

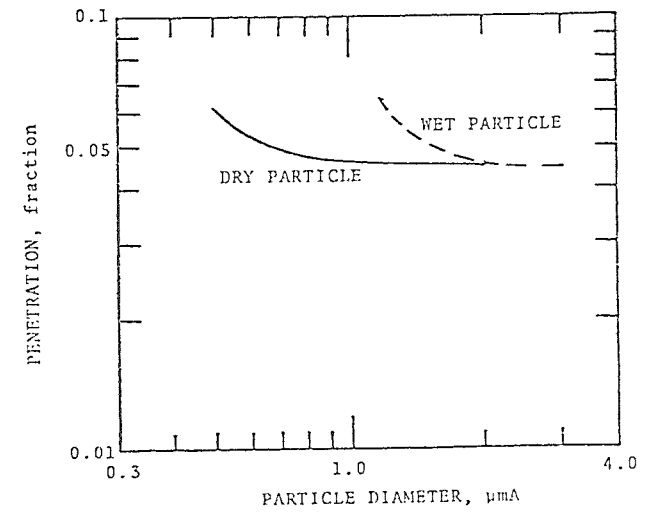


Figure 14. Experimental grade penetration curve for CHEAF.

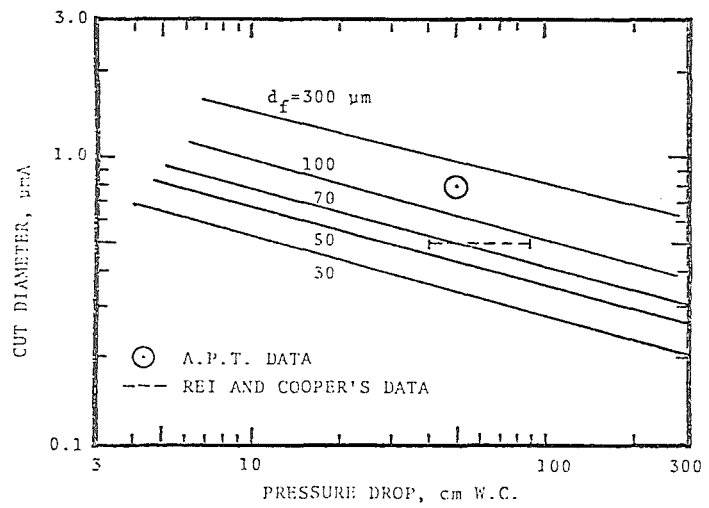


Figure 15. Cut diameter versus pressure drop for fibrous bed.

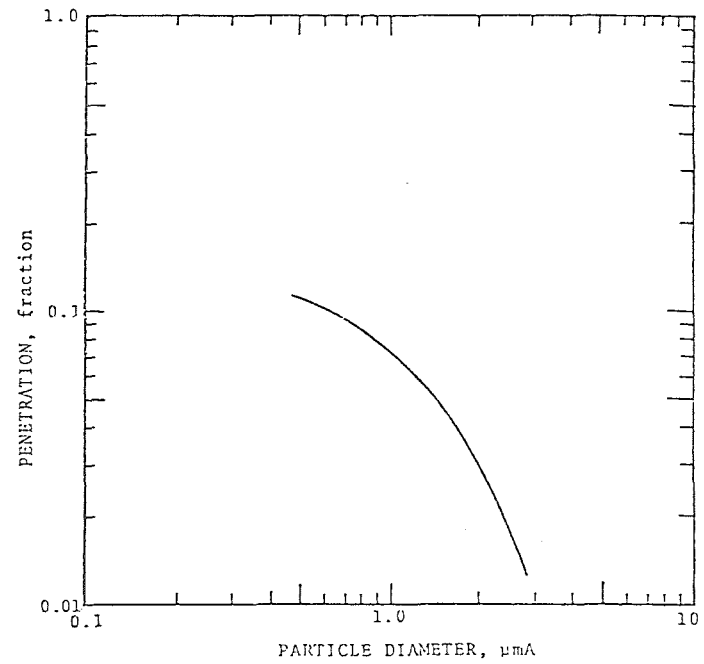


Figure 16. Experimental penetration curve for charged droplet scrubber

Discussion

Mr. GÜthner drew Dr. Calvert's attention to three omissions in table 1: the dust concentration, the solids load and a list of gas inlet and outlet temperatures. Dr. Calvert explained that the reason for the first two omissions was that neither the mist eliminator nor the entrainment separator were functioning adequately, while the last was missing only owing to lack of space. In reply to Prof. Weber's request for information on measuring drop diameters and the relationship between these and the theoretical values, Dr. Calvert mentioned the work of Richard Ball, Nuki Yama Tanasawa (whose investigations form the basis of APT's measurements) and Howard Hesketh, which deals with cloud-type atomization. Atomization varies according to the length of the scrubber.

ELECTROSTATIC PRECIPITATOR PERFORMANCE

by

John P. Gooch
Southern Research Institute
2000 Ninth Avenue, South
Birmingham, Alabama 35205
U. S. A.

DRAFT

prepared for

A Particulate Workshop
conducted by
The Federal Republic of Germany

March 16-17, 1978

ACKNOWLEDGMENTS

The principal financial support for the work discussed in this paper was provided by the Electric Power Research Institute. The cooperation and financial assistance of the Industrial Environmental Research Laboratory, Research Triangle Park, N.C., of the Environmental Protection Agency is also gratefully acknowledged.

The field measurements were performed by members of the Environmental Engineering Group at Southern Research Institute.

ABSTRACT

Studies of the performance of electrostatic precipitators were conducted at six coal-fired power plant sites. Overall collection efficiency and collection efficiency as a function of particle size were measured with the collecting electrode rappers energized and deenergized. Chemical analyses were obtained on samples of coal, fly ash, and flue gas. In situ and/or laboratory measurements of dust resistivity were performed, and secondary voltage-current relationships were obtained from the precipitator transformer-rectifier sets. The measurements of fractional efficiency with and without electrode rapping indicated that rapping efficiency losses occur primarily for particle diameters greater than 2.0 μm diameter. The performance of the electrostatic precipitators was analyzed using a mathematical model based on the physical principles of the electrostatic precipitation process.

SECTION I

INTRODUCTION

As emission control requirements become more stringent, the detailed analysis of existing particulate control device installations assumes more importance in developing more accurate design techniques and in improving the performance capabilities of existing designs. This paper summarizes the techniques employed and the results obtained from studies of the performance of electrostatic precipitators at six coal-fired power plant sites.¹ The basic objectives of the study were threefold: (1) determination of fractional and overall collection efficiency with and without collection electrode rapping for electrostatic precipitators collecting fly ash under various conditions (2) utilization of the data in an existing mathematical model of the electrostatic precipitation process (3) enlargement of the data base concerning electrostatic precipitator usage on coal-fired boilers.

The test programs were designed to provide the data necessary to differentiate between previously collected but reentrained particles resulting from electrode rapping and uncollected particles. Measurements with and without electrode rapping were performed with mass trains, inertial impactor systems, an ultrafine extractive system for particle diameters less than 0.20 μm , and a large particle sizing system based on a size selective diluter and an optical particle counter. The installations selected for study were in relatively good mechanical condition and were characterized by high

collection efficiencies (at least 99%). Boilers using fuels producing high and low resistivity dusts were selected so that the effect of widely varying dust properties could be examined. Two hot-side units were tested to examine the variations in performance that may occur for precipitators located upstream of the air preheater.

SECTION II

MEASUREMENT TECHNIQUES

Figure 1 illustrates the measurements performed at the six installations. The major portion of the effort was directed toward particulate characterization at the precipitator inlet and outlet using cascade impactors for in situ size determination and mass trains with in-stack filters for total mass loading measurements. A point to plane resistivity probe was used for in situ resistivity measurement at the inlet sampling locations. Since SO_x concentrations in flue gases influence dust resistivity, emphasis was placed on obtaining SO_3 - SO_2 concentrations at the operating conditions of the precipitators. The accurate determination of SO_3 concentration requires extreme care because of the potential interference of the relatively large concentrations of SO_2 which accompany the SO_3 . The technique employed for this determination is similar to one described by Lisle and Sensenbaugh², and it involves the use of a condenser maintained below the sulfuric acid dewpoint, but above the water dewpoint.

Cascade impactor sampling procedures as outlined by Harris³ were followed during the measurement programs to obtain size distribution data from 0.2 to 10 μm particle diameter. Glass fiber substrates, which were preconditioned in the flue using filtered flue gas to minimize weight gains caused by chemical reaction with the gas, were employed for all outlet impactor runs. Blank impactor runs were conducted using the preconditioned substrate material

simultaneously with the real runs to determine a correction factor for weight gain attributable to reaction between the flue gas and the preconditioned substrate material.

Data reduction procedures for the impactor stage weights consisted of the following steps:

- (1) Stage weights were corrected for blank weight gains.
- (2) Cut points for the individual stages for each impactor were based on calibration studies conducted in the laboratory using polystyrene latex beads for sizes smaller than 2.0 μm diameter and ammonium fluorescein particles for particle diameters from 2.0 to 8.0 μm diameter. Glass fiber substrates were in place for the calibration studies.
- (3) Impactor runs are arranged in groups in an appropriate manner for the individual test series.
- (4) The data are supplied as input to a computer program which calculates size distributions and fractional efficiencies. (see reference 4)

A Thermo-Systems, Inc. Model 3050 Electrical Aerosol Analyzer (EAA) was used sequentially at single sampling points at the inlet and outlet sampling location to determine concentration vs size information in the diameter range of 0.01 to 0.30 μm . The operating principle of the EAA is based on placing a known charge on the particles and then precipitating the particles under closely controlled conditions. Size selectivity is obtained by varying the electric field in the precipitator section of the instrument. Charged particle mobility is monotonically related to particle size in the operating

regime of the mobility analyzer. A dilution system is required because the instrumentation cannot tolerate raw flue gases as sampling streams nor cope with particle concentrations encountered in flue gases. A detailed discussion of the dilution system and data reduction techniques for the mobility analyzer-dilution system is available in reference 5.

Conventional sampling methods with mass trains and impactor systems require long integration times which are unsuited for examining 1 to 5 second duration transient events, such as rapping puffs, on a real time basis. In order to more clearly define the mechanisms by which reentrained dust emissions occur, time resolved data are required on the particulate concentrations and size distributions across typical portions of precipitator exit planes. Therefore, a decision was made to construct and employ a real-time optical particle sizing system to obtain supporting data for the inertial systems. The optical system consists of a modified ambient air particle counter and a size selective diluter. The diluter, as a result of the steep gradient in the fly ash size distributions on a number basis, dilutes small particles in the sample gas streams by large factors, but a relatively confined and undiluted stream containing the lower concentration of large particles is passed directly to the particle sensor. This system has been designated the Large Particle Sizing System (LPSS).¹

Under ideal sampling conditions, the LPSS would be used as illustrated in Figure 2, with the aerosol sample extracted through a vertical probe from below the outlet duct with a single 90° bend between the sampling point and the particle sensor. In this

configuration, the system could conceivably be calibrated to give absolute concentrations. For most of the plant locations discussed in this paper, the ideal configuration was not practical, and a secondary extractive system as illustrated in Figure 3 was constructed. This sampling system provided information on relative concentrations of various particle sizes between and during rapping puffs, but it did not provide quantitative concentration data because of the uncertainties in the probe losses and in the degree to which the secondary sample represented the average concentration in the high flow rate probe.

The use of inertial sampling systems (mass trains and impactors) for the measurement of rapping reentrainment requires a sampling strategy which will differentiate between steady-state particulate emissions and those which result from electrode rapping. At the first installation tested in this research program, the strategy employed consisted of sampling on subsequent days with the rapping system energized and subsequently deenergized while an attempt was made to maintain boiler operating parameters as constant as was practical. The precipitator was characterized by high collection efficiency (99.9%), which required extended sampling times to obtain meaningful mass measurements. However, it was found that the sensitivity of the electrostatic precipitator to changes in resistivity and other process variables could mask the differences in total emissions caused by energizing and deenergizing the rappers.

In order to minimize this difficulty, a revised sampling strategy was adopted for the remaining installations. The revised strategy consisted of sampling with mass trains and impactors dedicated to designated "rap" and "no-rap" periods. Data with a rapping system

energized and deenergized were obtained by traversing selected ports with dedicated sampling systems in subsequent periods on the same day. This procedure, while necessarily distorting the frequency of the rapping program being examined, minimized the effects of resistivity and other process variable changes.

The use of the alternating sampling strategy leads to at least three possible procedures for calculating the fraction of losses attributable to rapping reentrainment. The first procedure consists of the calculation of the ratio of emissions obtained with rappers off to rappers on and subtracting from unity. The emissions data utilized in this procedure were obtained during the time in which alternating sampling periods for rap and no rap sampling trains were employed. The second procedure consists of subtracting the mass emissions obtained with the rappers deenergized from those of the previous day with normal rapping, and dividing by the emissions obtained with the rappers operating normally. The data obtained from the "rap" period will be approximately equal to that obtained during other test periods in which the rappers are operating in a normal fashion if: (1) the distortion of the rapping frequency does not significantly influence emissions during the "rap" period and (2) there are no other variations in parameters affecting the precipitator performance.

A third possible procedure consists of the use of a weighted time average emission during the rap-no rap periods as an approximation to the normal emission rates, subtracting the no rap emission from the weighted time average, and dividing the difference by the weighted time average to obtain the fraction of emissions attributable

to rapping. This procedure provides an estimate of rapping reentrainment with the effective intervals which result from the alternating sampling periods. All of the above calculation procedures are used when applicable to analyze emissions data from the six installations tested.

SECTION III

RESULTS

In terms of location in the power plant system and type of fuel burned in the boiler, the installations studied in this program may be classified as follows:

Plants 1 and 5 - Cold-side ESP's collecting ash from low-sulfur
Western coals

Plant 6 Hot-side ESP collecting ash from low sulfur
Western coal

Plant 4 Hot-side ESP collecting ash from low sulfur
Eastern coal

Plant 2 and 3 - Cold-side ESP's collecting ash from high sulfur
Eastern coals

Figure 4 through 10 illustrate the configuration and electrical sectionalization of the precipitator installations. A mechanical collector precedes the ESP at Plant 1. Table 1 summarizes the important design parameters and the results obtained for the six installations. The installations were characterized by relatively high overall mass efficiency. Rapping losses as a percentage of total mass emission ranged from over 80% for one of the hot-side units to 30% for the cold-side units. The high rapping losses at Plant 4 are probably due both to reduced dust adhesivity at high temperatures and the relatively short rapping intervals.

Table 2 lists the rapping intervals for each field at the various installations. Also shown are the effective rapping intervals resulting from the alternating sampling schedules which were used to obtain the rap-no rap data. To the extent allowed by process variations, the range of emissions attributable to rapping should be established by the calculations using (rap-no rap) and (normal-no rap) data sets. However, the time weighted average (TWA) calculation is of interest in that it indicates the change in rapping emissions caused by the effective increase in time intervals between raps. With the exception of the normal current density data set at Plant 2, the time weighted average calculation gives the lowest percentage emissions due to rapping of the three calculation methods. Table 3 provides typical flue gas and fly ash compositions obtained at the test sites.

Figure 11 shows the time variations over the test period at Plant 1 in boiler load, precipitator power, dust resistivity and relative particle concentrations in two size bands (0.6 to 1.8 μm and 1.5 to 3 μm). August 5 and 6 were "normal" rapper operation test periods, whereas August 7 and 8 were "no-rap" test periods. It is readily apparent that, on August 7, changes in variables other than rapper energization caused exit particulate concentration changes which masked the effect of rapping system deenergization. The LPSS system, however, was able to detect rapping puffs, as described below.

Figures 12 and 13 show the number of 6-12 and 12-24 μm diameter particles counted in 10 minute intervals through one day of testing with rapping and one day of testing without rapping, respectively. Cyclic concentration variations with a period of one hour were expected when the rappers were on and are fairly apparent in the data shown in Figure 12. No such cyclic pattern is apparent in the data shown

in Figure 13 which were obtained with the rappers deenergized. Note the obvious effect of losing power to one of the T.R. sets. The average counting rate was much reduced in the 6-12 and 12-24 μm channels with the rappers turned off as can be seen by comparison of Figures 12 and 13.

As indicated previously, the attempt to determine rapping losses at Plant 1 by comparison of mass train and impactor data sets from normal and no rap periods was not successful due to other factors influencing outlet emissions. However, an estimate of the contribution of rapping losses to total mass emission was made from data from the LPSS and outlet impactor systems. The estimate is that 30% of total outlet mass emission during normal rapper operation can be attributed to rapping reentrainment. Figure V-10 shows the rap-no rap data for the EAA system and the rap and no-rap impactor derived efficiencies. The estimated no-rap efficiencies are based on the data from the LPSS system and these are subject to large uncertainties because of the poor counting statistics for the larger particles coupled with the limited time span over which the data were taken. Fifty percent confidence intervals are shown for the impactor and EAA data. Even with the existence of the indicated uncertainties, it is apparent that very high collection efficiencies are achieved in the particle diameter range 0.05 to 20.0 μm . The minimum collection efficiency is approximately 99.2% at 0.20 μm diameter.

The alternating sampling strategy with impactors and mass trains was successfully employed at Plant 2 and subsequent test sites to differentiate between reentrainment resulting from rapping and steady-state emissions. Figure 15 presents rap and no rap data from Plant 2 from the EAA and the impactor sampling system. The large error

bars (50% confidence intervals) on data obtained from the ultrafine particle system are a reflection of difficulties encountered with condensation of sulfuric acid, which created an interfering aerosol in the ultrafine size range. The data were screened and those results which were felt to be non-representative were discarded. It is apparent that rapping losses become significant only for particle diameters larger than 1 to 2 μm . The presence of significant large particle emissions in the absence of rapping is also indicated by Figure 15, and was confirmed by data obtained from the LPSS. These emissions apparently resulted from sparking or voluntary reentrainment. Plant 2 was operating with a high sulfur Eastern coal which produced a fly ash with low electrical resistivity.

Figure 16 illustrates the large particle losses (on a relative basis) measured at Plant 4, which is a hot-side installation, using the impactor and ultrafine sampling systems with the rap-no rap sampling sequence. The data obtained with normal rapper operation (not shown) show reasonable agreement for sizes greater than 1.0 μm diameter, indicating the alternating sampling strategy did not significantly distort the results obtained. As with the previously discussed data, the results indicate that rapping reentrainment does not cause a significant change in fine particle emissions.

Comparisons were made between measured collection efficiencies as a function of particle size and those obtained from a mathematical simulation of the precipitators using a model developed at Southern Research Institute under the sponsorship of the Environmental Protection Agency.⁶ The model predicted with reasonable accuracy the relative changes in fine particle collection efficiency resulting from resistivity changes and the resultant input power

SECTION IV

CONCLUSION

Measurements of fractional efficiency with and without electrode rapping at full scale precipitator installations show that rapping efficiency losses occur primarily for particle diameters greater than 2.0 μm diameter. The largest rapping losses were measured on hot-side installations. Mass emission data suggest a correlation, for the installations tested in this research program, between the dust removal rate in the last field of the precipitator and the emissions due to rapping. The electrostatic precipitator with the highest overall mass efficiency exhibited a minimum collection efficiency of 99.2% at 0.20 μm diameter.

Comparisons were made between measured and calculated fractional and overall collection efficiencies using a theoretical model augmented by empirical relationships based on the field test data. The comparisons indicated that the empirical factors improved the capability of the model to simulate the operation of full-scale electrostatic precipitators under field conditions.

variations. The comparisons indicated that the theoretically calculated collection efficiencies in the fine particle size range were lower than the measured values as a result of certain unmodeled effects. Significant large particle penetrations resulting from sporadic events in the absence of rapping which exceeded theoretical predictions of penetration were also observed. Empirical correction factors were incorporated into the model to account for the under-prediction of fine particle collection efficiencies and to increase the value of the model for design purposes until adequate theoretical modeling of fine particle collection efficiencies under field conditions is accomplished.

Rapping reentrainment losses were represented in the model using an average apparent size distribution of a rapping puff and an empirical relationship between the dust removal rate in the last field and emissions attributable to rapping. Figure 11 contains rapping emissions for the six installations as a function of the dust calculated to have been removed in the last field of the precipitator. Note the effect of current reduction at Plant 2. These data suggest a correlation between rapping losses and dust removal rate in the last field. Data for the two hot-side installations tested show higher rapping losses, which is consistent with the reduced dust adhesivity which is expected at higher temperatures. Obviously, additional data under various conditions are required to determine if this approach or a variation thereof may be used to estimate rapping losses under a range of operating conditions.¹

Figure 18 illustrates the manner in which the empirical correction factors and the representation of rapping change the fractional

efficiency prediction of the model for the normal current density test series at Plant 2. The solid line illustrates the model's prediction of efficiency as a function of particle size using only theoretical relationships, the operating parameters for the test conditions, and the precipitator geometry as input data. The open circles give the model prediction with the same input data, but with the inclusion of empirical relationships concerning fine particle collection, gas velocity non uniformity, gas by-passage, and rapping reentrainment. It is apparent that the agreement between measured and predicted results under field conditions is improved by the use of the empirical relationships. In general, it is expected that the rapping puff correlation will tend to under predict large particle emission because the correlation does not represent the large particle penetrations which were observed due to sporadic events other than rapping.

Section V

REFERENCES

1. Gooch, John P., and Guillaume H. Marchant, Jr. "Electrostatic Precipitator Rapping Reentrainment and Computer Model Studies." Final Draft Report by Southern Research Institute to the Electric Power Research Institute under EPRI Contract RP413-1. August 1977.
2. Lisle, E. S., and J. D. Sensenbaugh. Combustion 36(1), 12 (1965).
3. Harris, D. Bruce. "Procedures for Cascade Impactor Calibration and Operation in Process Streams." Environmental Protection Technology Series, EPA-600/2-77-004. January 1977.
4. Johnson, J., G. I. Clinard, L. G. Felix, and J. D. McCain. "A Computer-Based Cascade Impactor Data Reduction System." U. S. Environmental Protection Agency, Research Triangle Park, N. C. February 1978.
5. Smith, W. B., K. M. Cushing, and J. D. McCain. "Procedures Manual for Electrostatic Precipitator Evaluation." EPA-600/7-77-059. June 1977.
6. Gooch, John P., J. R. McDonald, and S. Oglesby, Jr. "A Mathematical Model of Electrostatic Precipitation." EPA-650/2-75-037, U. S. Environmental Protection Agency, Research Triangle Park, N. C. 1975.

| MEASUREMENTS | PLANT 1 | PLANT 2 | PLANT 3 | PLANT 4 | PLANT 5 | PLANT 6 |
|----------------------------|---------|---------|----------------|----------------|----------------|----------------|
| MASS TRAIN | ▲ | ▲ | ▲ ¹ | ▲ | ▲ | ▲ |
| IMPACTORS | ▲ | ▲ | ▲ | ▲ | ▲ | ▲ |
| ULTRAFINE SYSTEM | ▲ | ▲ | ▲ | ▲ | ▲ | ▲ |
| LARGE PARTICLE SYSTEM | ▲ | ▲ | ▲ | ▲ | ▲ | ▲ |
| V-I CURVES | ▲ | ▲ | ▲ | ▲ ² | ▲ | ▲ |
| ACCELEROMETER | | ▲ | ▲ | | ▲ | |
| <u>IN SITU</u> RESISTIVITY | ▲ | ▲ | ▲ | ▲ | ▲ | |
| GAS ANALYSIS | ▲ | ▲ | ▲ | ▲ | ▲ | ▲ |
| VELOCITY DISTRIBUTION | | ▲ | ▲ | | ▲ ³ | ▲ ⁴ |
| LEAR SIEGLER | ▲ | ▲ | ▲ | ▲ | ▲ | |
| COAL ANALYSIS | ▲ | ▲ | ▲ | ▲ | ▲ | ▲ |
| ASH ANALYSIS | ▲ | ▲ | ▲ | ▲ | ▲ | ▲ |

1. MASS TRAIN MEASUREMENT AT OUTLET ONLY
2. V-I CURVES OBTAINED ONE MONTH PRIOR TO EPRI TEST
3. OBTAINED BY SF-CARBORUNDUM BEFORE START UP
4. OBTAINED BY SALT RIVER PROJECT PERSONNEL

Figure 1. Types of Data Obtained

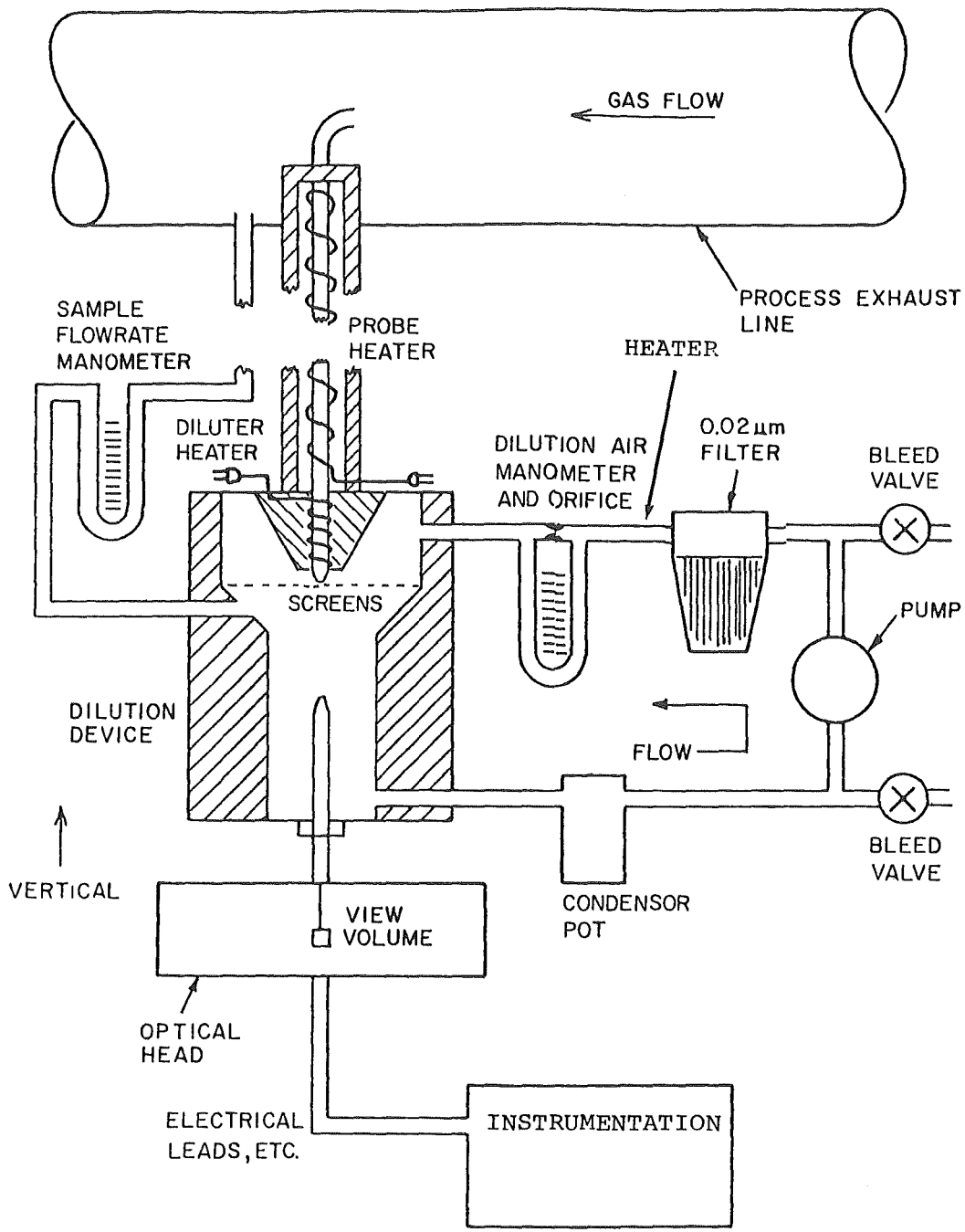


Figure 2. Large Particle Sizing System

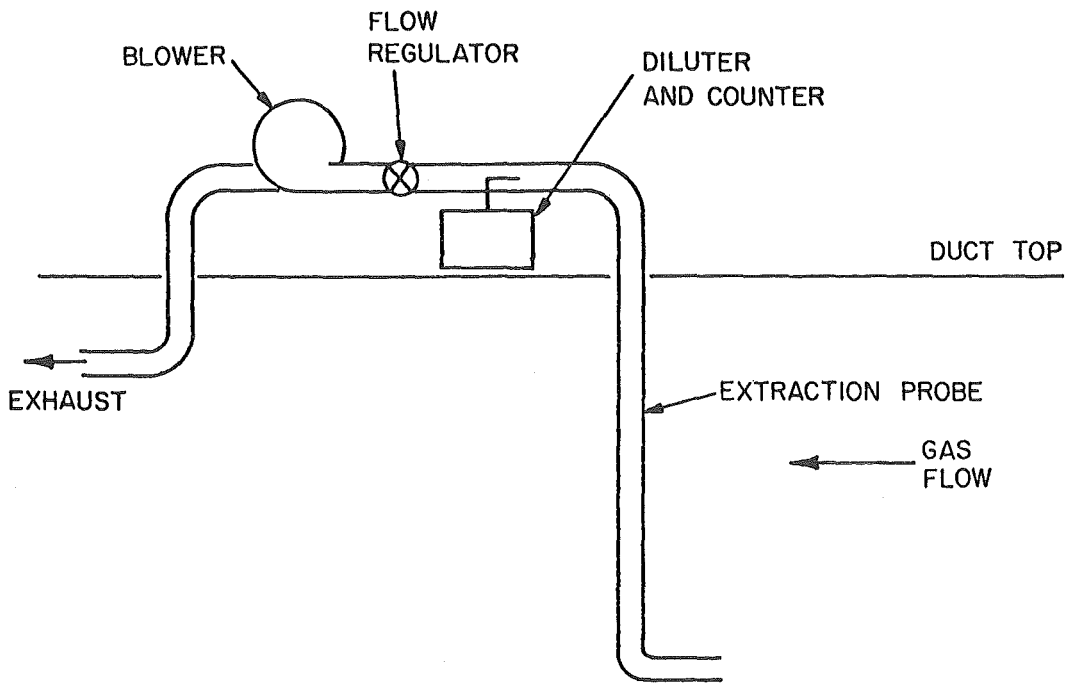
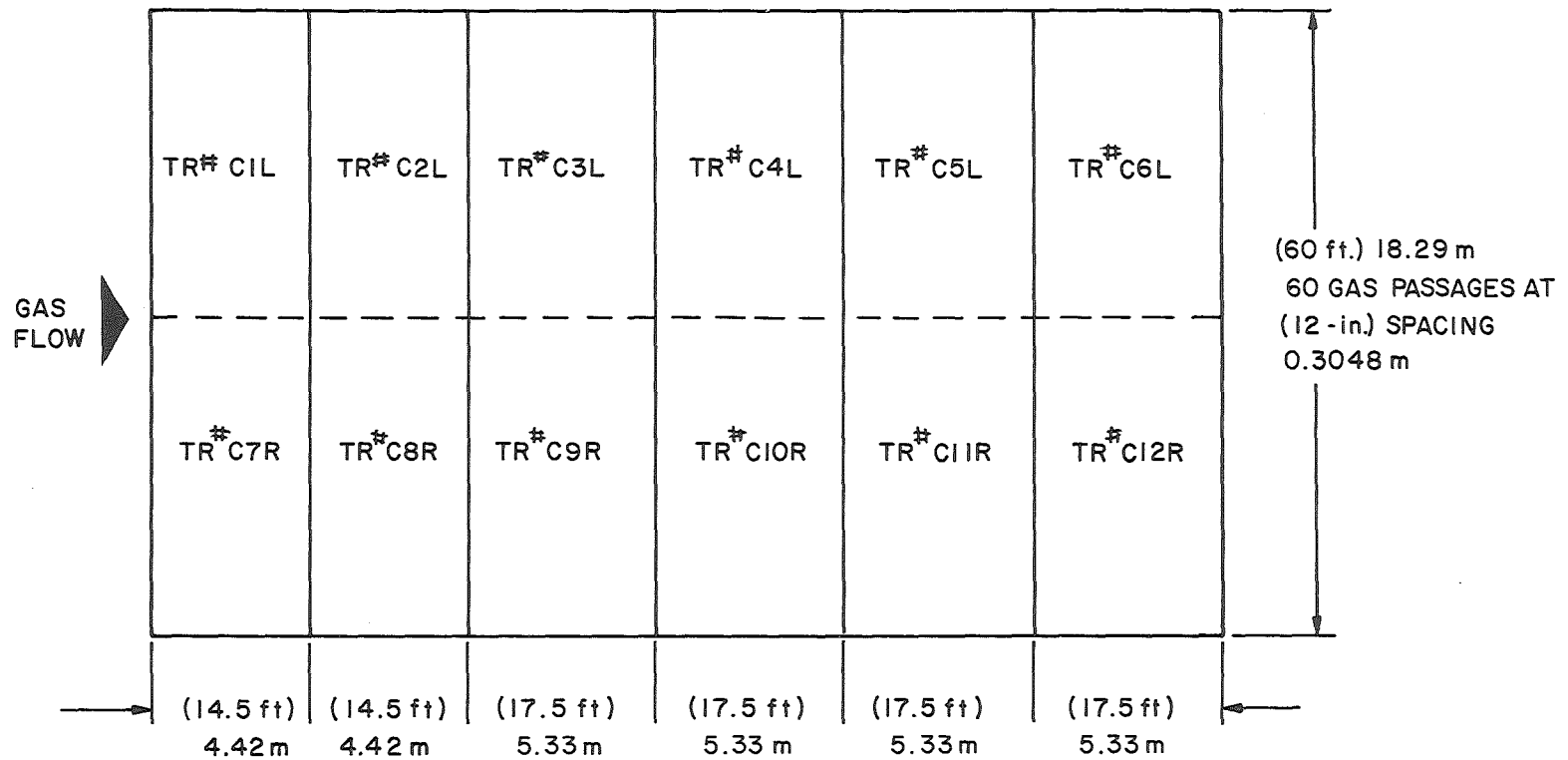


Figure 3. Extractive Sampling System



1
08
1

NOTE DISTANCE BETWEEN EACH FIELD - (2.5 ft) 0.762 m
COLLECTING PLATES IN 1 AND 2 FIELDS ARE (12 ft) 3.66 m DEEP
FIELDS 3 THRU 6 ARE (15 ft) 4.57 m DEEP
ALL COLLECTION PLATES ARE (40 ft) 12.19 m HIGH

Figure 4. Precipitator layout for Plant 1

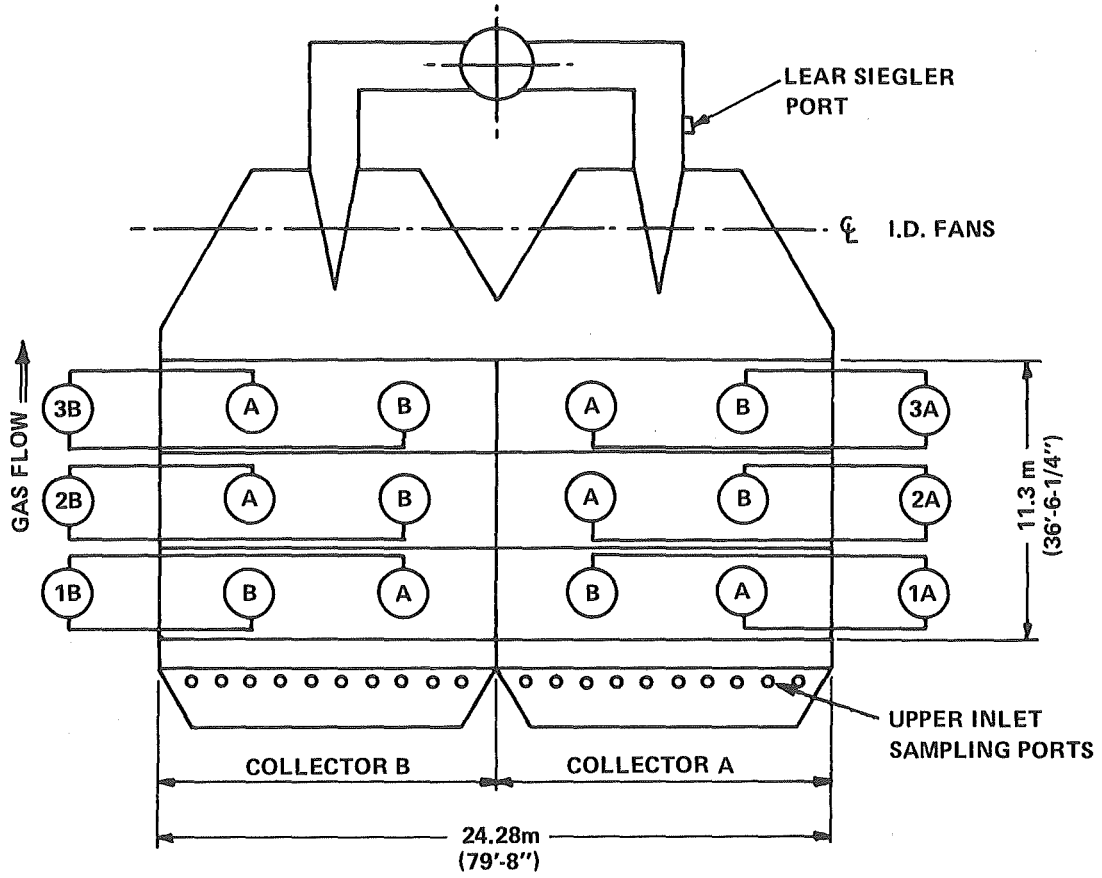


Figure 5. Precipitator layout for Plant 2

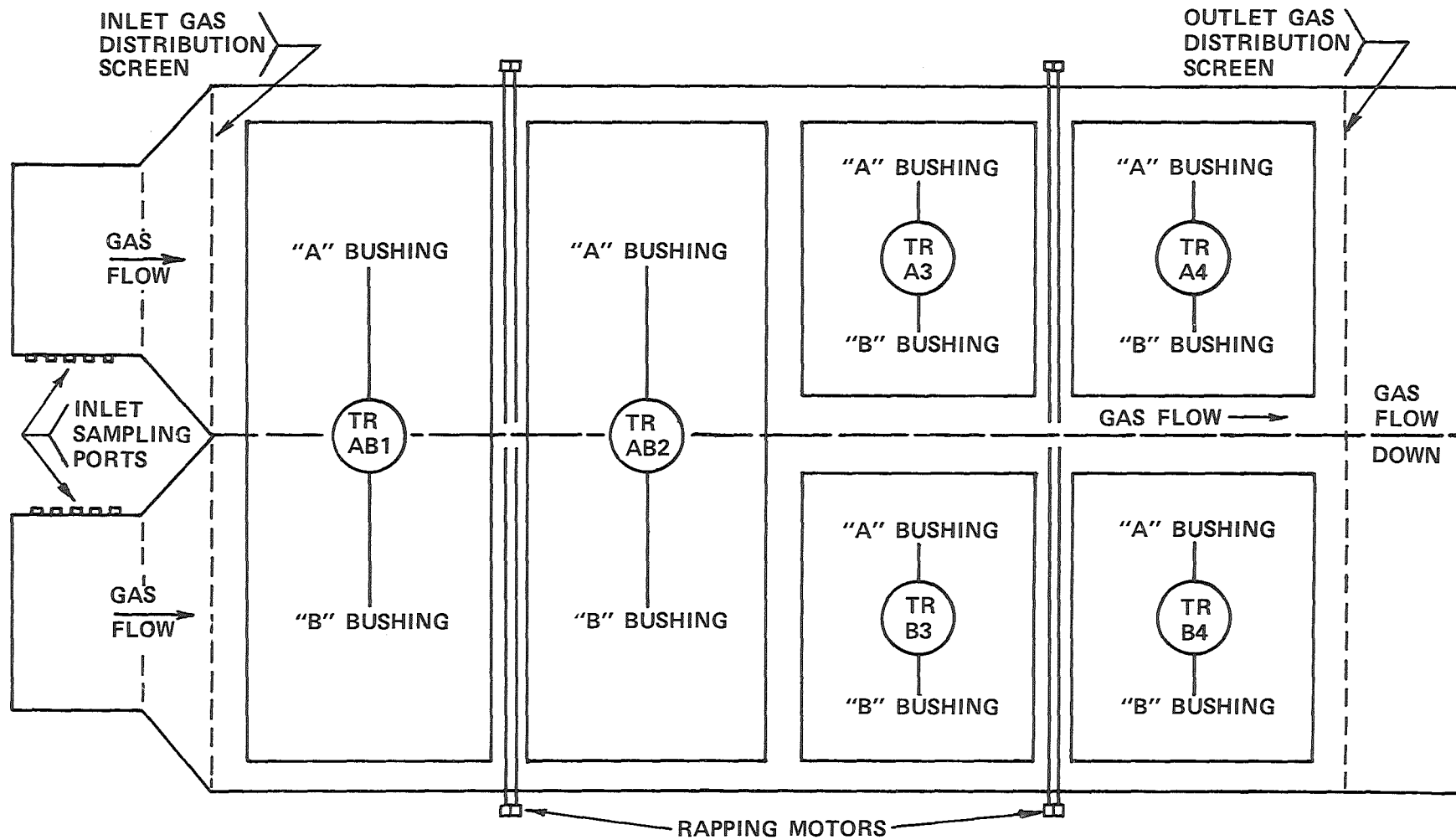


Figure 6. Plant 3 precipitator layout

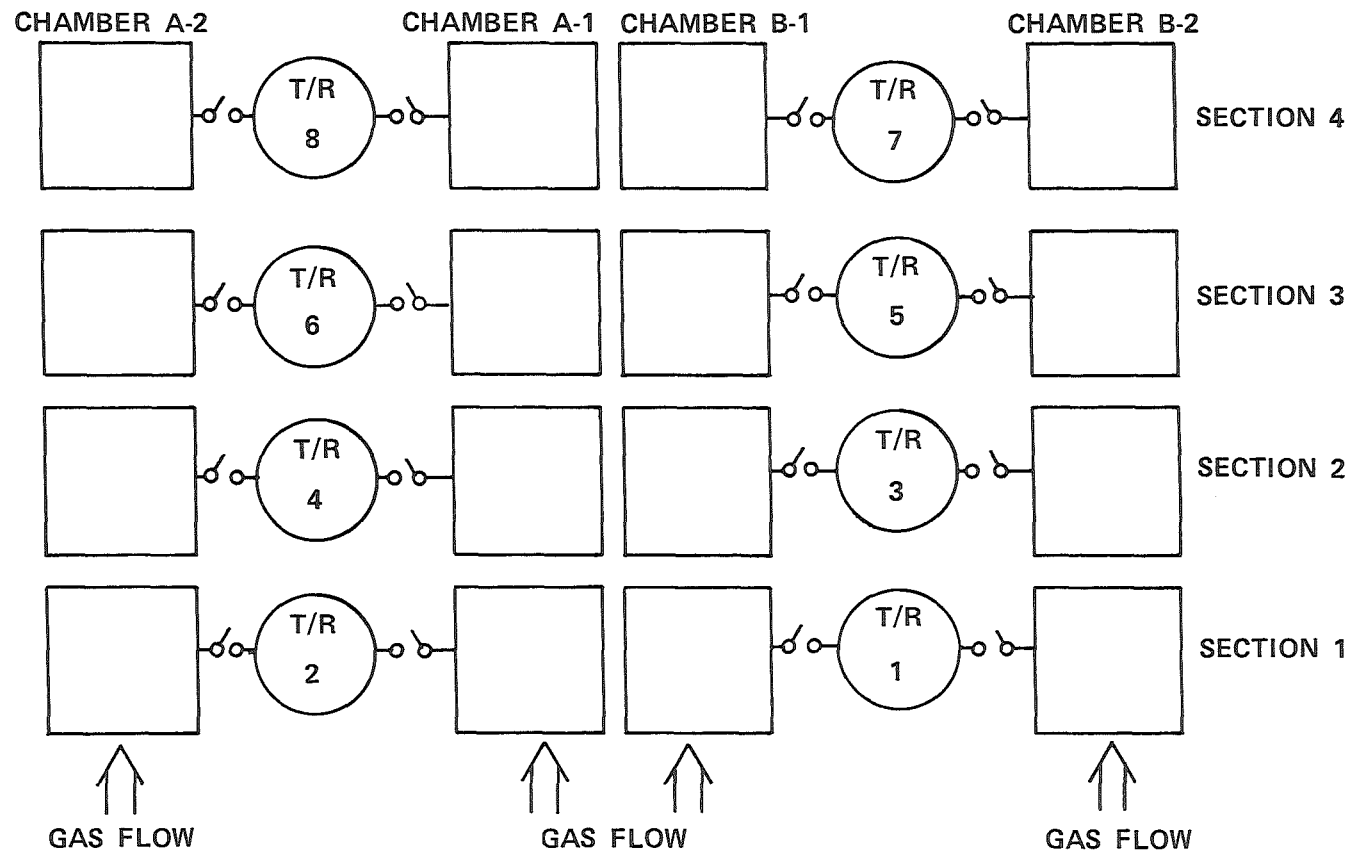


Figure 7. Plant 4 precipitator configuration

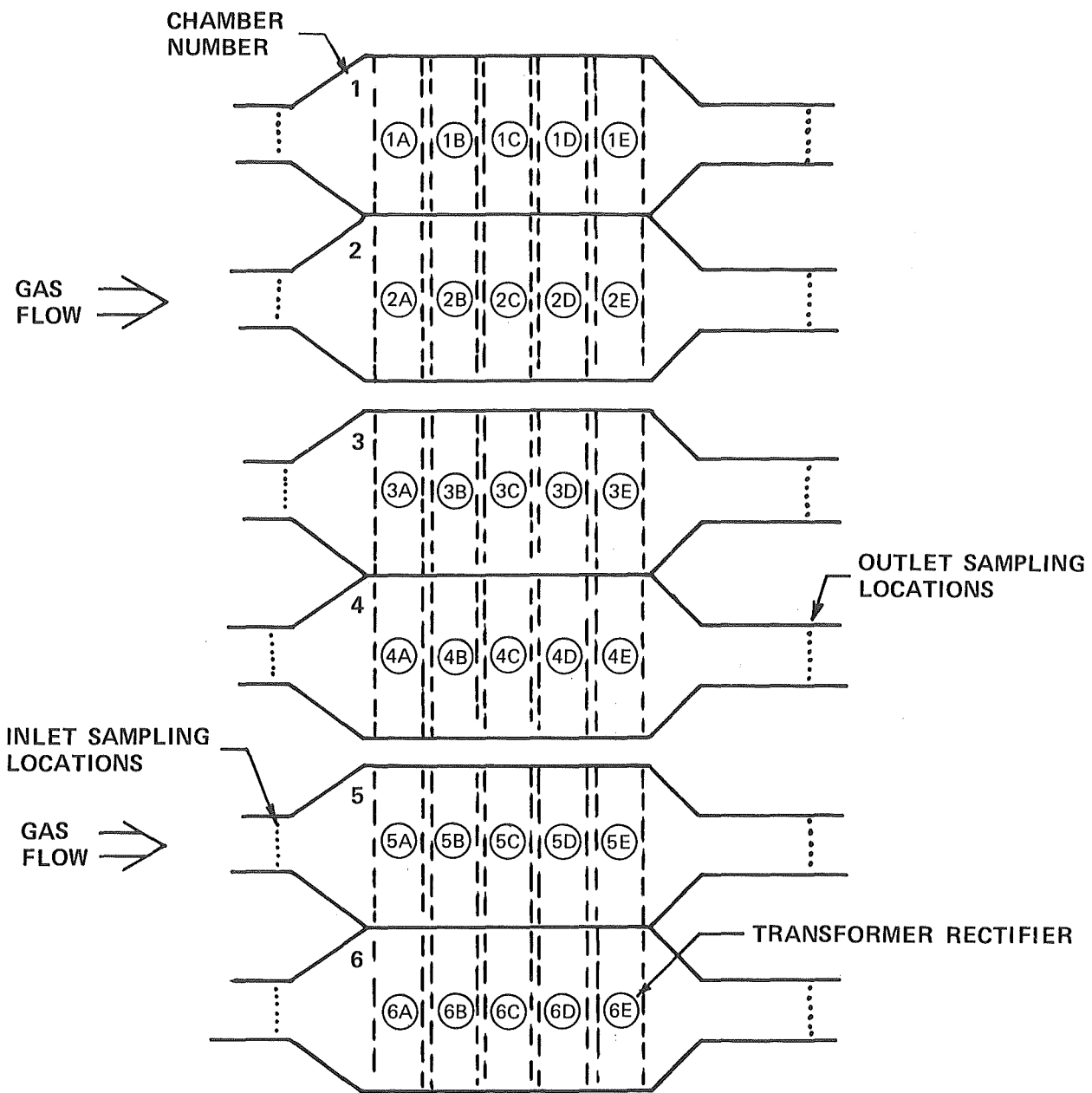


Figure 8. Plant 5 precipitator layout

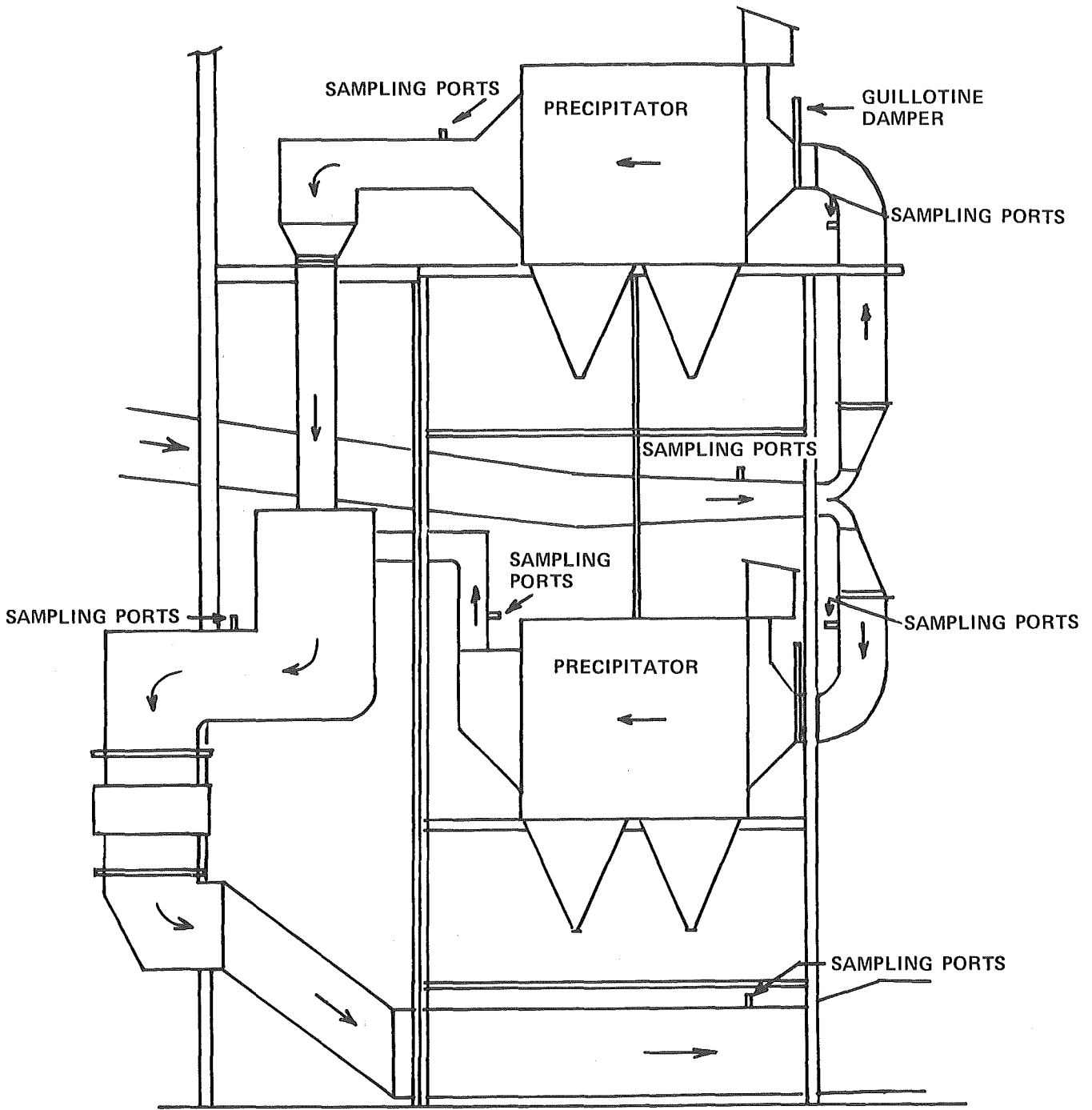


Figure 9. Ductwork arrangement for Plant 6

Figure 10. Chamber arrangement for Plant 6

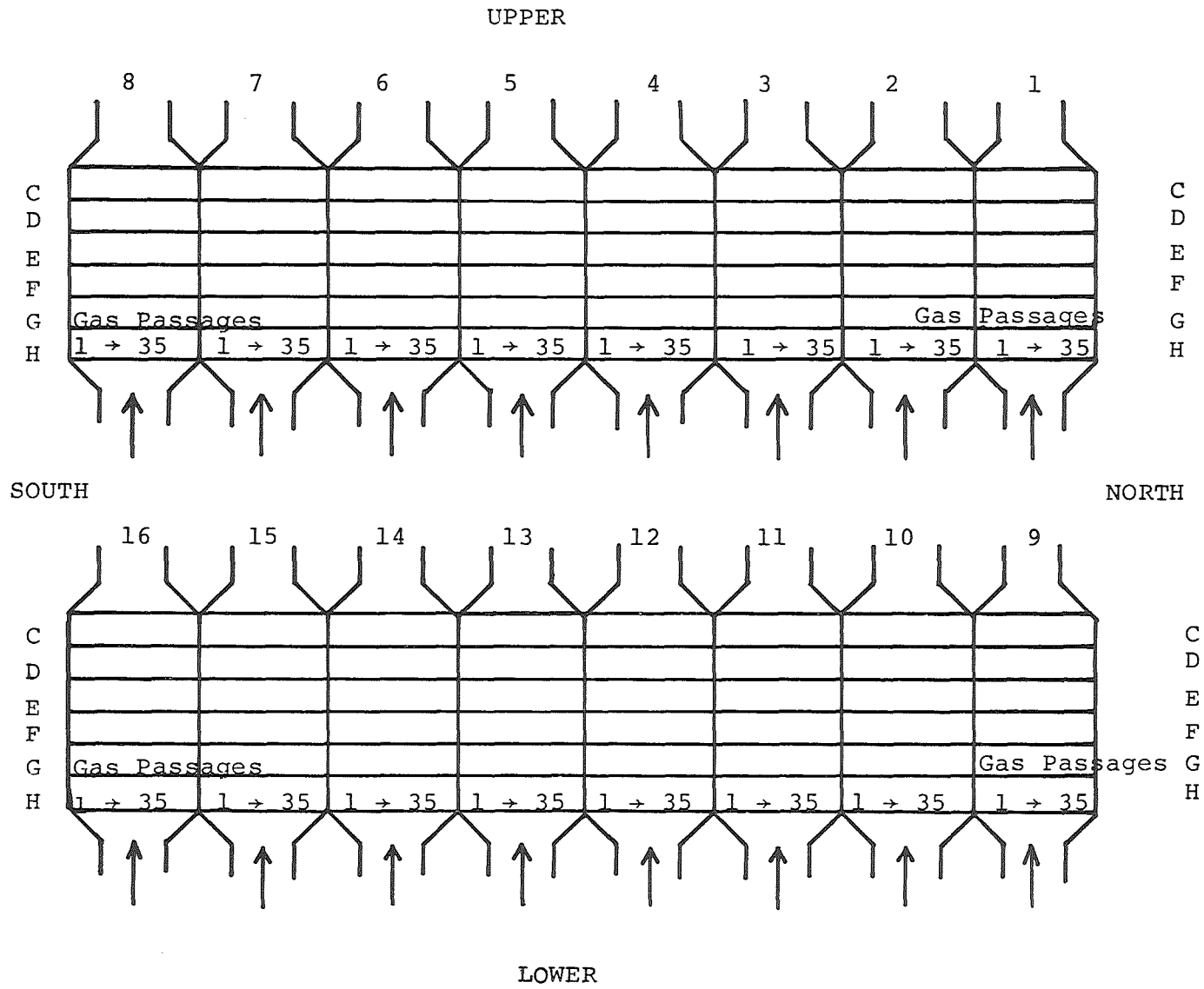


Table 1. SUMMARY OF RESULTS FROM EPRI TESTS

| | | | | | | |
|--|--------------------------------|--------------------------------|--------------------|----------------------|-----------------------------------|--------------------------|
| Plant | 1 | 2 | 3 | 4 | 5 | 6 |
| Number of Electrical Fields in Direction of Gas Flow | 6 | 3 | 4 | 4 | 5 | 6 |
| Plate-to-Plate Spacing, cm | 30.48 | 27.94 | 25.4 | 22.86 | 24.76 | 22.86 |
| Emitting Electrode Design | Mast with Square Twisted Wires | Mast with Square Twisted Wires | Rigid Barbed Wires | Hanging Round Wires | Electrode Frame With Spiral Wires | Hanging Round Wires |
| Rapper Design | Drop Hammer | Drop Hammer | Tumbling Hammers | Magnetic Drop Hammer | Tumbling Hammers | Magnetic Impulse Hammers |
| Portion of ESP Tested | Total | 1/2 | 1/2 | 1/2 | 1/6 | 1/16 |
| Boiler Load During Test, MW | 128 | 160 | 122 | 271 | 508 | 800 |
| Gas Flow During Test, am ³ /sec | 330.2 | 155.2 | 117.2 | 203.9 | 149.4 | 126.8 |
| Temperature During Test, °C | 152.2 | 155 | 157.2 | 321.1 | 106.1 | 358.9 |
| SCA During Test, m ² /(m ³ /sec) | 113.5 | 47.6 | 50.4 | 76.8 | 117.9 | 55.4 |
| Measured Efficiency,% | 99.92 | 99.55 | 99.80 | 99.64 | 99.85 | 98.98 |
| Dust Resistivity at Operating Temp, Ω-cm | 1.4x10 ¹¹ | 1.7x10 ¹⁰ | 2x10 ¹⁰ | 3.2x10 ¹⁰ | 4.6x10 ¹¹ | 1.5x10 ^{9b} |
| % of Mass Emissions Attributed to Rapping ^a | 31 | 65-33 | 30 | 85 | 36-29 | 63-44 |

^aIndicating range of values from two methods of calculation.

^bLaboratory measurement.

PENETRATION-EFFICIENCY

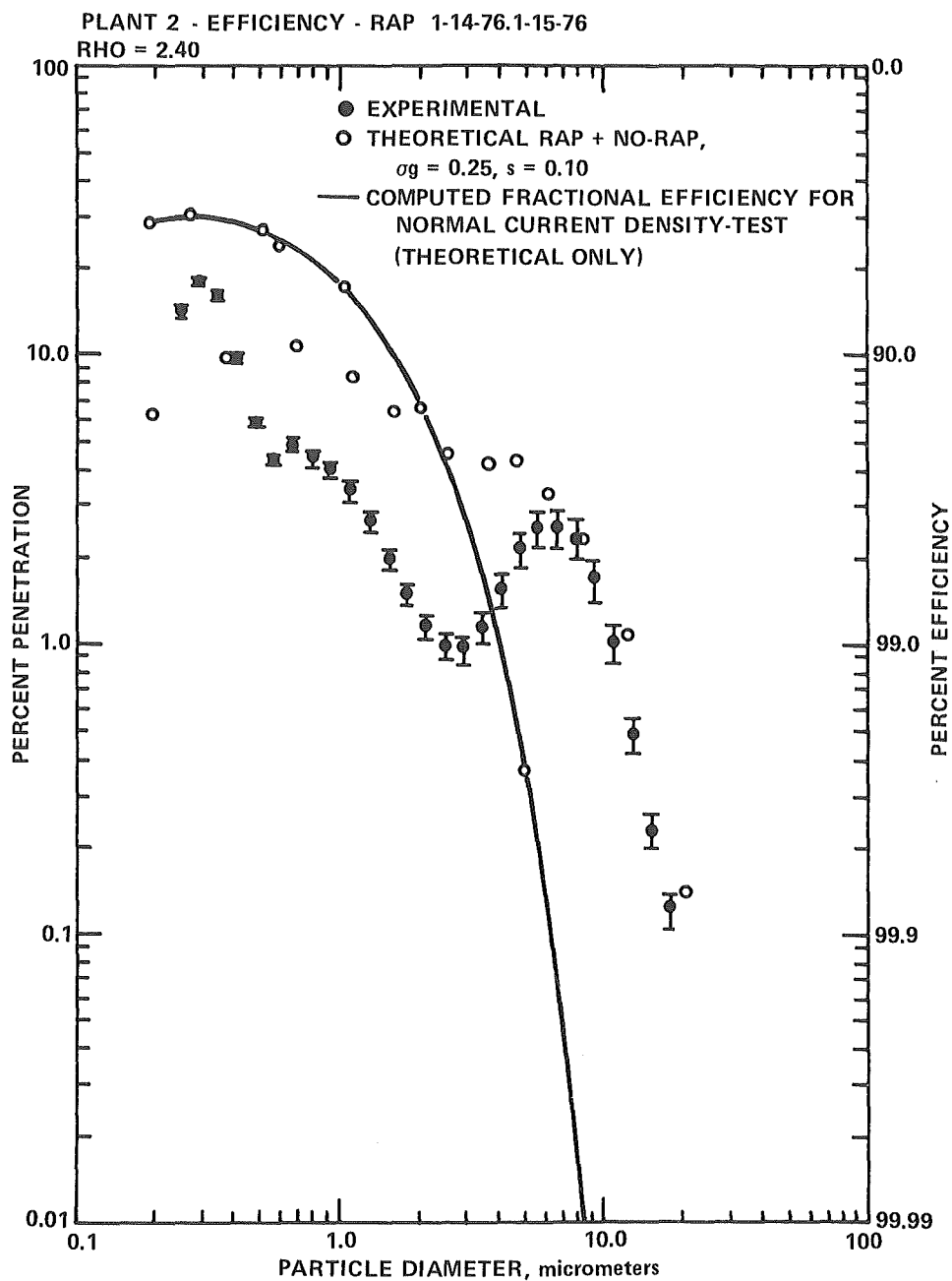


Figure 18. Comparison of measured and computed efficiencies from Plant 2 normal current density series.

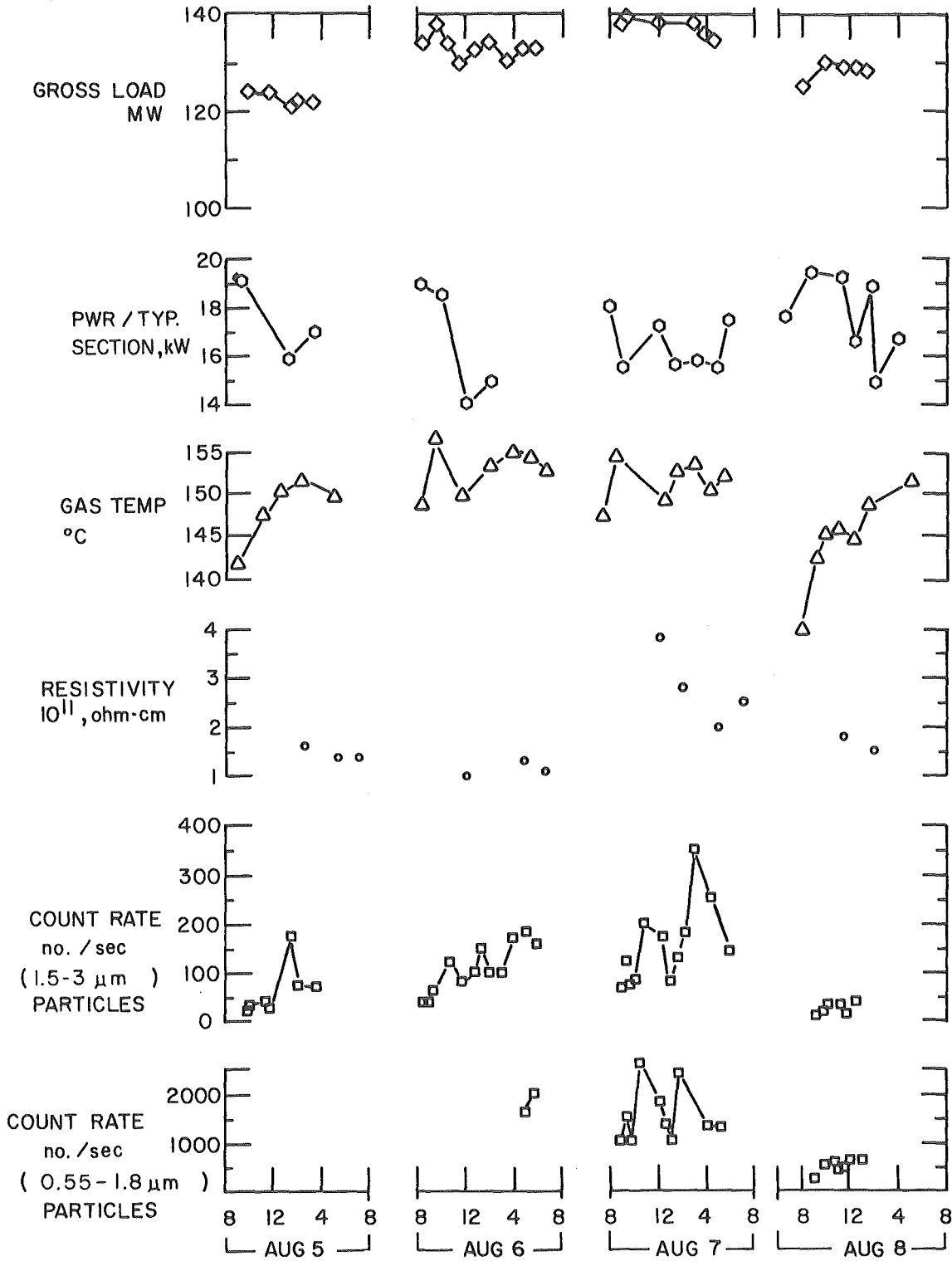


Figure 11. Events for test period Plant 1

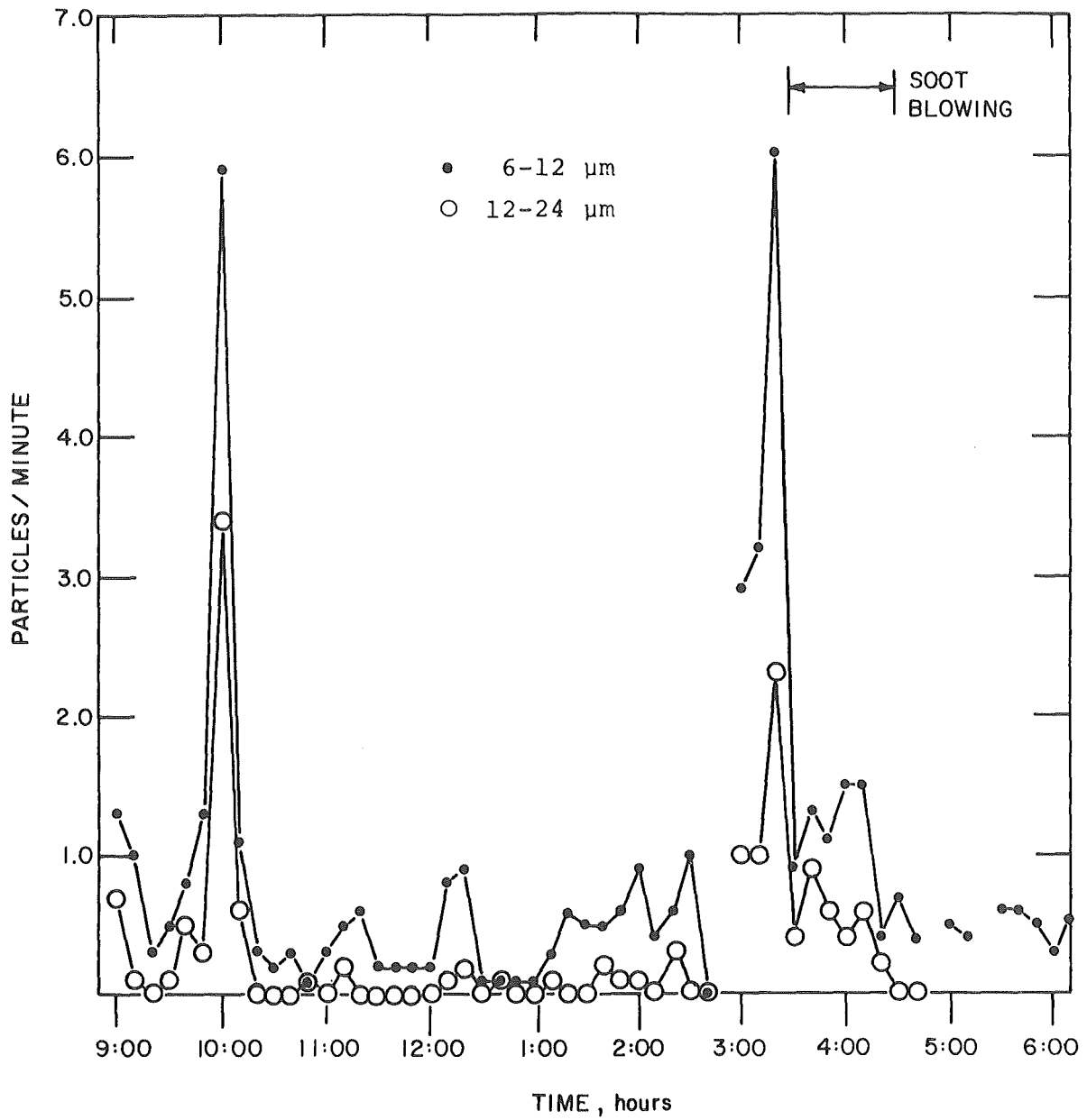


Figure 12. Particles per minute vs. time for large particle system on August 6, 1975. Rappers on. (Plant 1)

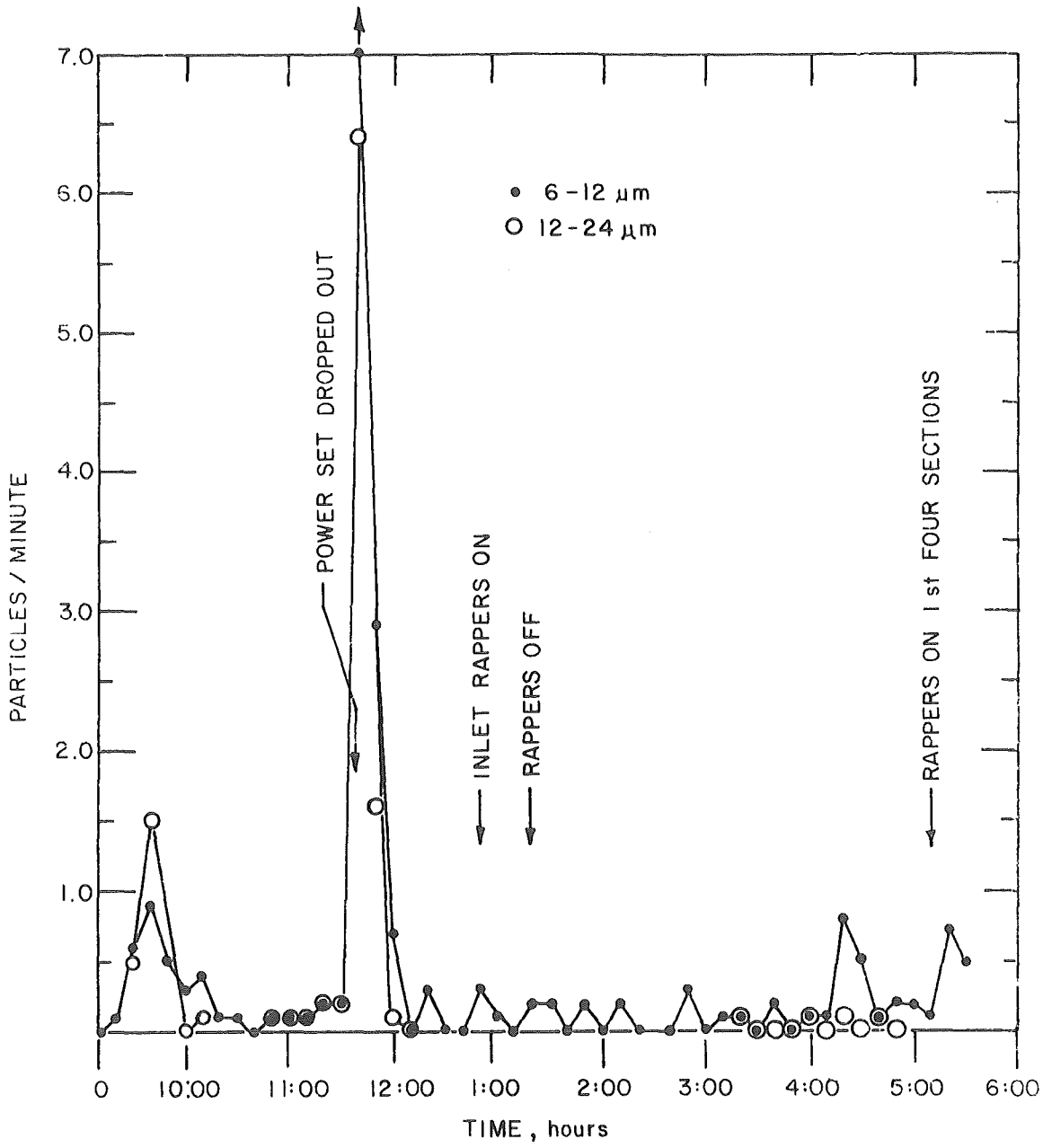


Figure 13. Particles per minute vs. time for large particle system on August 7, 1975. Rappers off. (Plant 1)

PENETRATION-EFFICIENCY

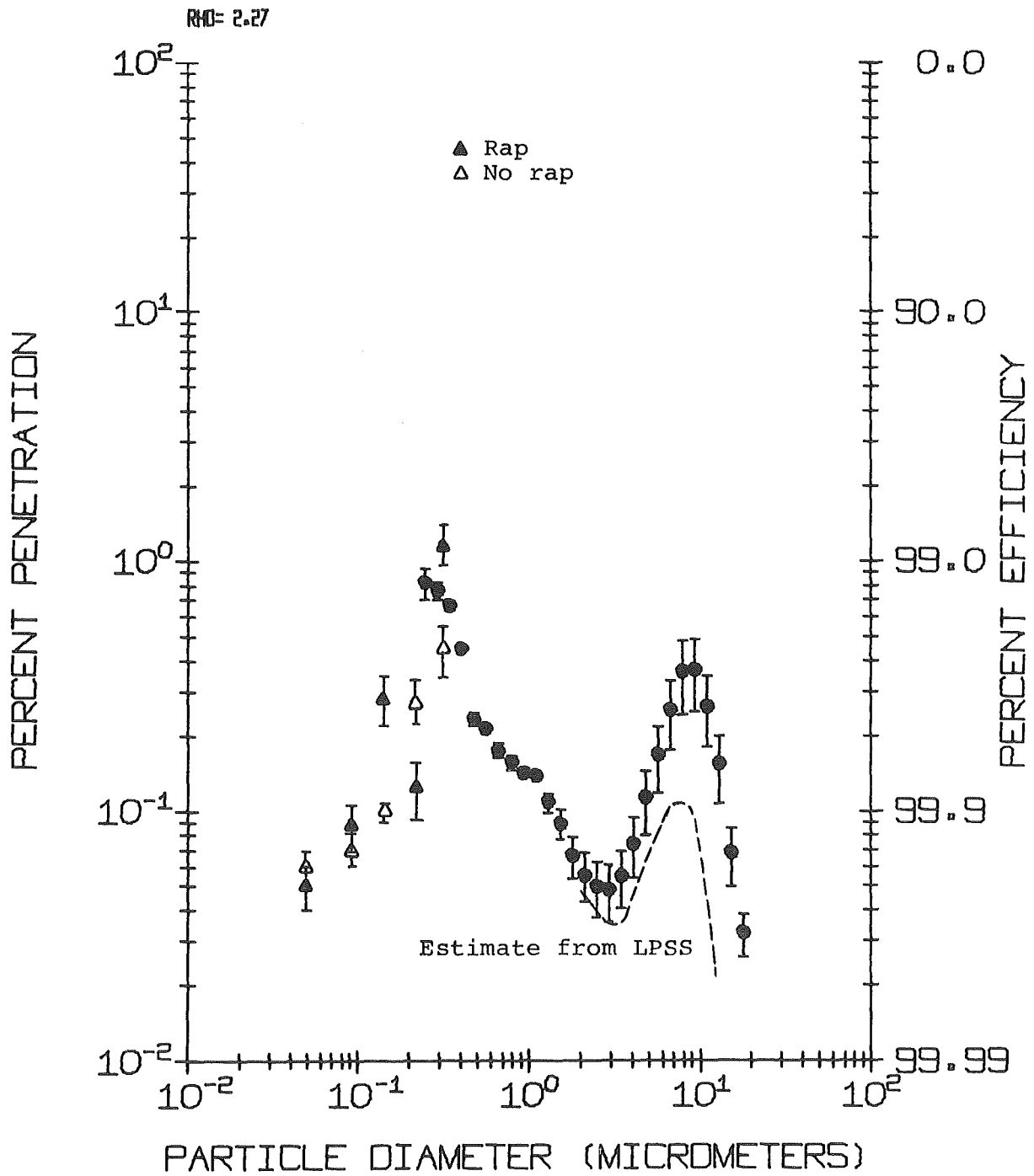


Figure 14. Plant 1 rap-no rap fractional efficiency including ultrafine and impactor measurements.

PENETRATION-EFFICIENCY

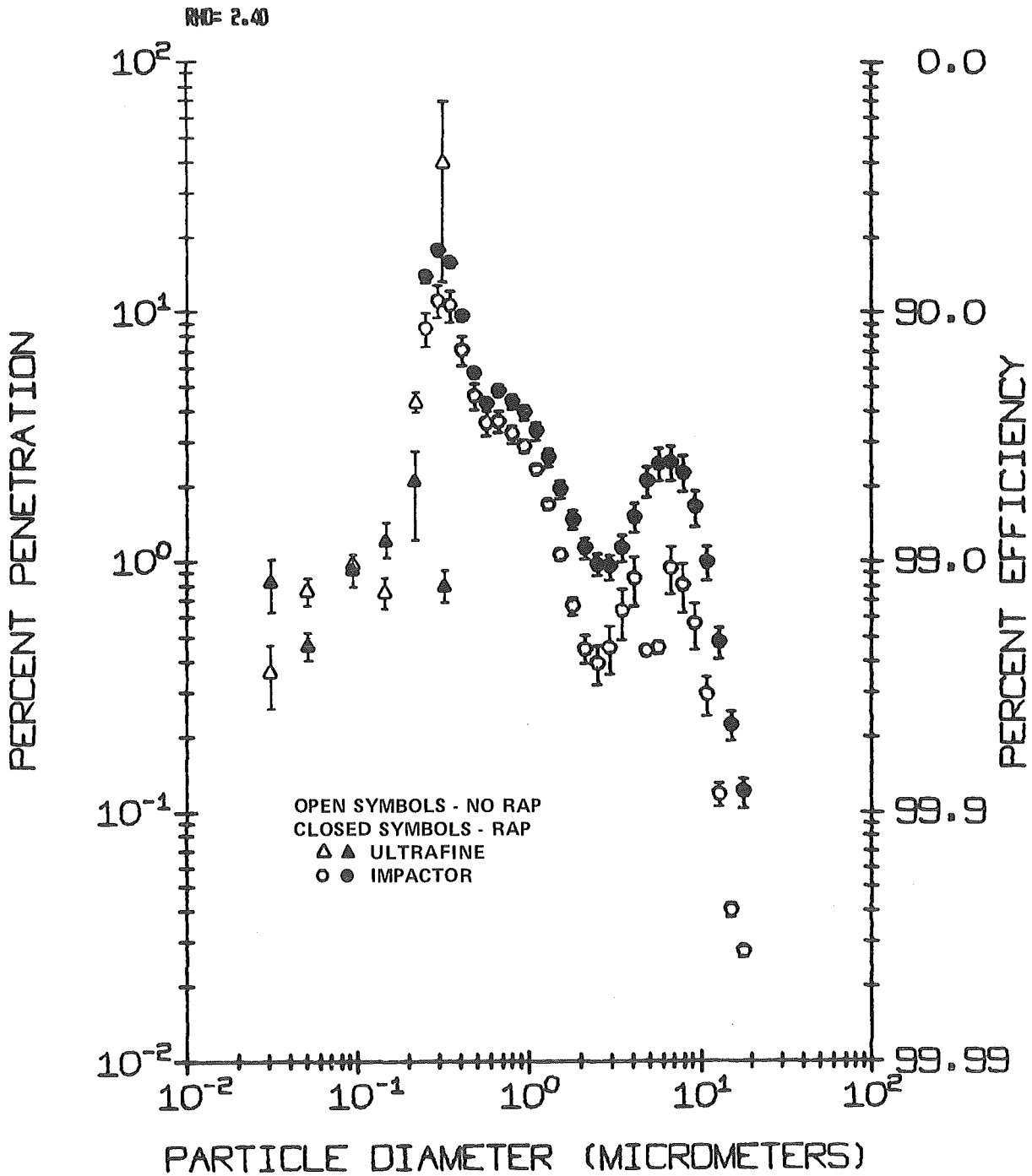


Figure 15. Rap no-rap ultrafine and impactor fractional efficiency. Normal current density, Plant 2.

PENETRATION-EFFICIENCY

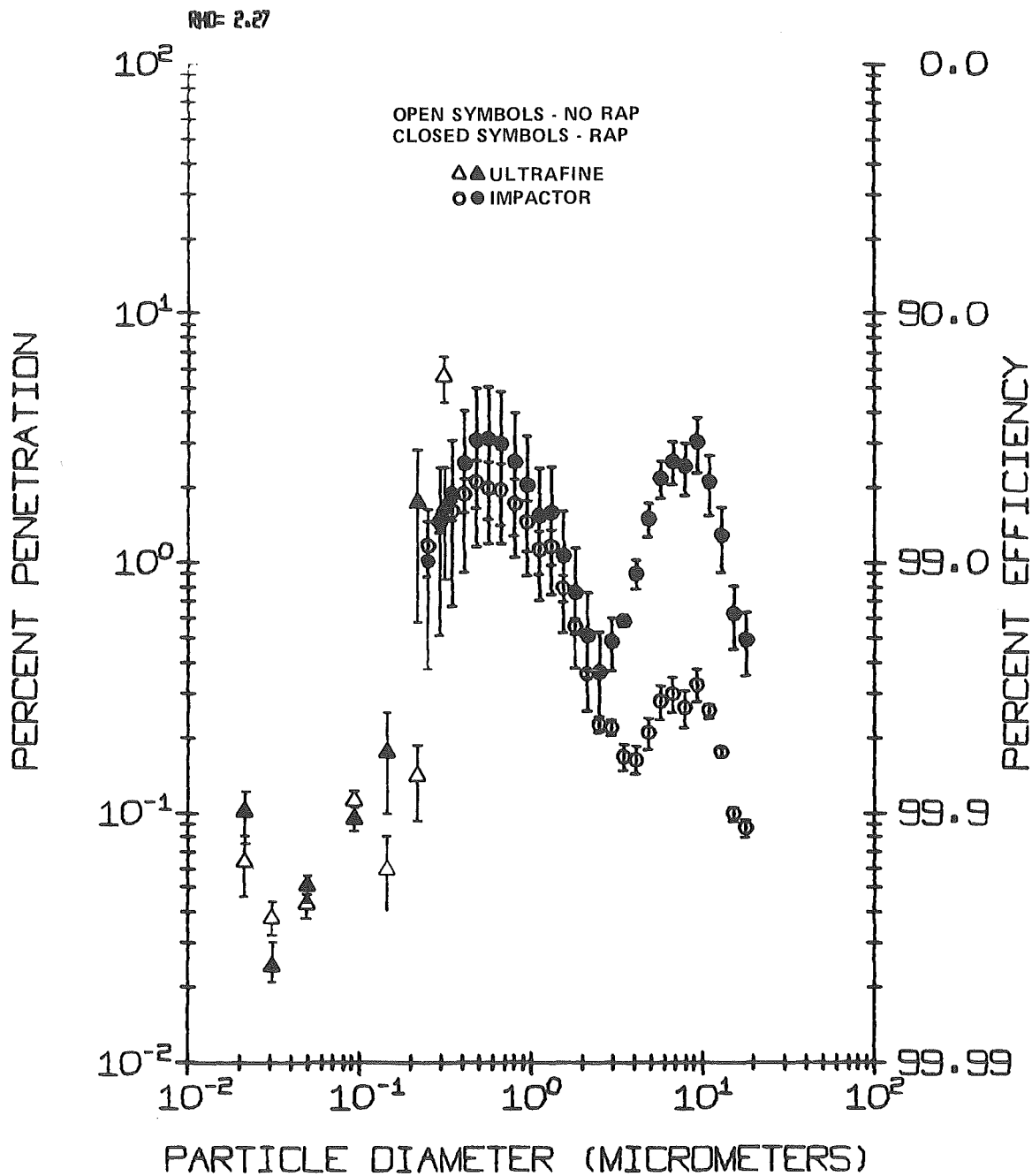


Figure 16. Ultrafine and impactor rap-no rap fractional efficiencies, Duct Bl., Plant No. 4, with 50% confidence intervals.

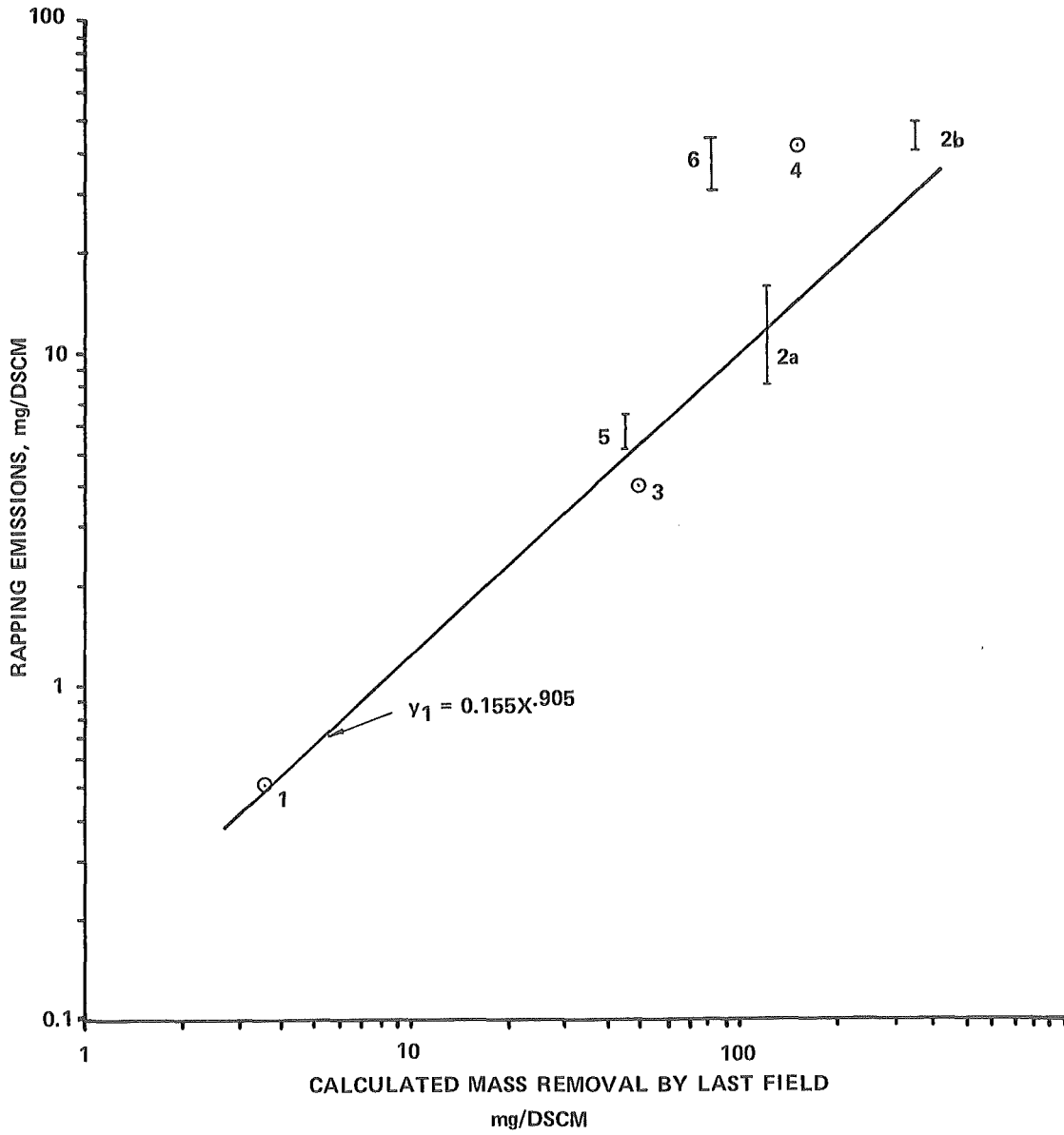


Figure 17. Rapping emissions vs. dust removal by last field (Plant 6 and Plant 4 are hot-side installations)

Table 2. SUMMARY OF REENTRAINMENT RESULTS

| Plant | 1 | 2 | | 3 | 4 | | 5 | 6 | | | | |
|------------------------|----------------|---------------------|----------------|-----------------|----------------|----------------|----------------|----------------|---------------|----------------|----|------|
| | | <u>Raps/Hr</u> | | | | <u>Raps/Hr</u> | | | | | | |
| | | <u>Rap - No-Rap</u> | | | | | | | | | | |
| | | | <u>Normal</u> | <u>One-Half</u> | | | | | | | | |
| | | | <u>Current</u> | <u>Current</u> | | | | | | | | |
| | | | <u>Density</u> | <u>Density</u> | | | | | | | | |
| <u>Field</u> | <u>Raps/Hr</u> | <u>Normal</u> | <u>Normal</u> | <u>Normal</u> | <u>Raps/Hr</u> | <u>Raps/Hr</u> | <u>Raps/Hr</u> | <u>Raps/Hr</u> | <u>Raps</u> | <u>Raps/Hr</u> | | |
| | <u>Normal</u> | | <u>Density</u> | <u>Density</u> | <u>Normal</u> | <u>Rap-</u> | <u>Normal</u> | <u>Normal</u> | <u>Min</u> | <u>Normal</u> | | |
| | | | | | <u>No-Rap</u> | <u>No-Rap</u> | <u>No-Rap</u> | <u>No-Rap</u> | <u>Normal</u> | <u>No-Rap</u> | | |
| 1 | 6 | 10 | 4.29 | 3.75 | 10 | 1.67 | 30-60 | 12.5-25 | 10 | 4.17 | 8 | 2.74 |
| 2 | 6 | 6 | 2.57 | 2.25 | 10 | 1.67 | 30-60 | 12.5-25 | 5 | 2.08 | 8 | 2.74 |
| 3 | 3 | 1 | 0.43 | 0.38 | 5 | 0.83 | 30 | 12.5 | 5 | 2.08 | 3 | 1.03 |
| 4 | 3 | - | | | 5 | 0.83 | 30 | 12.5 | 2 | 0.83 | 3 | 1.03 |
| 5 | 1 | - | | | - | | - | - | 1 | 0.42 | 1 | 0.34 |
| 6 | 1 | - | | | - | | - | - | - | | 1 | 0.34 |
| <u>Rapping Losses,</u> | | | | | | | | | | | | |
| <u>% of Emissions</u> | | | | | | | | | | | | |
| Rap-No Rap/Rap | - | | 65 | 55 | 30 | | 85 | | 29 | | 44 | |
| Normal-No Rap/Normal | 31 | | 33 | 82 | - | | 85 | | 36 | | 63 | |
| T.W.A.-No Rap/T.W.A. | - | | 45 | 38 | 18 | | 71 | | 15 | | 24 | |

Table 3. TYPICAL FLUE GAS AND ASH COMPOSITIONS

| Plant | 1 | 2 | 3 | 4 | 5 | 6 |
|--------------------------------|----------|------------------|------------------|------------------|------------------|------------------|
| Date | 8/7/75 | 1/16/76 | 2/25/76 | 4/28/76 | 10/6/76 | 1/31/77 |
| Flue Gas | | | | | | |
| Temp., °C | 164 | 154 | 155 | 333 | 106 | 346 |
| SO ₂ , ppm by vol. | 282 | 3200 | 2430 | 750 | 470 | 355 |
| SO ₃ , ppm by vol. | 0.3 | 12 | 8.3 | 2.7 | <0.5 | <0.5 |
| H ₂ O, vol. % | 8.2 | 7.2 | 8.2 | 7.4 | 8.7 | 9.6 |
| Fly Ash | | | | | | |
| Ash Source | Hopper 1 | High Vol. Sample | High Vol. Sample | High Vol. Sample | High Vol. Sample | High Vol. Sample |
| Date | 8/7/75 | 1/15/76 | 3/2/76 | 4/27/76 | 10/5 & 10/6/76 | 1/31/77 |
| Wt. % of ¹ | | | | | | |
| Li ₂ O | 0.02 | 0.02 | 0.03 | 0.04 | 0.02 | 0.013 |
| Na ₂ O | 0.26 | 0.54 | 0.67 | 0.43 | 1.38 | 1.52 |
| K ₂ O | 1.72 | 2.49 | 2.12 | 3.5 | 0.54 | 1.4 |
| MgO | 3.61 | 0.95 | 1.00 | 1.3 | 1.1 | 1.8 |
| CaO | 8.71 | 4.73 | 4.95 | 1.1 | 5.8 | 6.0 |
| Fe ₂ O ₃ | 5.49 | 22.72 | 13.13 | 7.2 | 6.1 | 5.0 |
| Al ₂ O ₃ | 24.64 | 18.52 | 21.76 | 28.4 | 13.2 | 24.3 |
| SiO ₂ | 50.55 | 45.69 | 50.23 | 53.8 | 70.8 | 57.6 |
| TiO ₂ | 1.22 | 1.45 | 1.96 | 1.8 | 0.87 | 2.1 |
| P ₂ O ₅ | 0.50 | 0.30 | 0.78 | 0.23 | 0.05 | 0.32 |
| SO ₃ | 0.75 | 2.77 | 2.29 | 0.50 | 0.50 | 0.54 |
| LOI ² | 0.61 | 5.72 | 10.92 | 3.5 | 1.0 | 0.11 |

¹ Chemical analyses obtained from ignited samples

² Loss on ignition

Discussion

Mr. Gdthner mentioned a rapping loss of up to 85% of the total emissions (not only of fine particulate) and wondered how this could be reduced, as minimization of losses is essential for the improvement of precipitators. Dr. Gooch answered that this value (85%) was from a hot side installation, which has frequent rapping and was not typical of rapping reentrainment emissions in general. Emissions below 2 microns are not affected by a rapping optimization program; to reduce fine particle emissions, more plates are needed. An optimization program can however reduce overall mass emissions.

Mr. Gdthner asked how many particles in the stack gas were larger than 5 microns; the answer was not many, and that information regarding size distribution was available, on a cumulative basis. A decrease in efficiency in the 6 micron diameter region occurs even without rapping due to sporadic reentrainment possibly as a result of sparking in the ESP.

The theoretical calculations used for constructing the ESP model were the subject of a question posed by Prof. Weber. Mr. Gooch said that the model was referenced in his paper and then described steps in the calculation of the migration velocity at Prof. Weber's request: the precipitator uses a mapping technique to calculate field distribution for incremental lengths through the ESP. Mr. Wiggers asked what assumptions were made in the calculations of migration velocity. The reply was that particles are uniformly mixed, and that problems arise because of the following assumptions:

- 1) The non-uniform particle concentration gradients.
- 2) An average electric field was used in calculating the particle charge in spite of the non-uniform field distribution.

Additional work should be performed in modeling the collection of particles in the diameter range of 0.5 to 4 microns. Dr. Kastner raised the problem of rapping losses and of cleaning collecting electrodes (which cannot always be cleaned by rapping), but Mr. Gooch replied that the Southern Research Institute had made no investigations of rapping system effectiveness to date. Mr. Gage added that optimization was required to minimize rapping losses.

SESSION II: ADVANCED SYSTEMS FOR DUST REMOVAL

ELECTROSTATICALLY AUGMENTED PARTICULATE COLLECTION DEVICES

Dale L. Harmon
Industrial Environmental Research Laboratory
Environmental Protection Agency
Research Triangle Park, N. C.

INTRODUCTION

EPA is placing increased emphasis on the control of fine particulates which persist in the atmosphere, comprise a variety of known toxic substances, and are a major contributor to atmospheric haze and visibility problems. The Particulate Technology Branch of IERL-RTP under the direction of James H. Abbott has the objective of developing and demonstrating control systems capable of effectively removing large fractions of the under three micron size dust particles from smoke stack effluents. The conventional systems have been demonstrated to have this capability for some sources however, the cost of high efficiency collection is generally high, in large part because the efficiency of most dust collectors decreases for fine particle size. This performance loss must therefore be offset by large size or high energy input.

Devices or dust collection systems based on new collection principles or on radical redesign of conventional collectors are sometimes offered by private developers. In the fall of 1973 a novel device evaluation program was initiated to identify, evaluate and develop, where necessary, those devices or systems which showed the most promise for high efficiency collection of fine particulate. A novel particulate collection device is a device or a dust collection system based on new collection principles or on radical redesign of conventional collectors which is available for testing as a pilot scale or full scale unit. Dale L. Harmon of the Particulate Technology Branch has had the primary responsibility for this program since it was started.

More than 40 novel particulate collectors have been identified. About half of the devices identified have been of sufficient interest to justify a technical evaluation. To date 13 devices have been either field or laboratory tested. These are:

Braxton-Sonic Agglomerator
Lone Star Steel - Steam Hydro Scrubber
R. P. Industries - Dynactor Scrubber
Aronetics - Two-Phase Wet Scrubber
Purity Corporation - Pentapure Impinger
Entoleter - Centrifield Scrubber
Andersen 2000 - CHEAF
Rexnord - Granular Filter Bed
Air Pollution Systems - Electrostatic Scrubber
Air Pollution Systems - Electro-Tube
Century Industrial Products - FRP-100 Low Energy Wet Scrubber
American Precision Industries - Apitron
Particulate Control Systems - EFB-Electrified Bed

In addition to these evaluations, a pilot scale TRW Charged Droplet Scrubber was designed, built and demonstrated on a steel mill coke oven and a mobile University of Washington electrostatic scrubber has been built for tests on a variety of industrial sources.

Future plans include testing of the following devices if satisfactory test sites can be located:

Combustion Power - Dry Scrubber
United McGill - NAFCO ESP
Dart Industries - "Hydro-Precipitrol" wetted wall ESP
Ceilcote Company - Ionizing Wet Scrubber
DuPont Company - DuPont Scrubber

Most of the novel devices which have been tested are scrubber types. The only scrubber types tested which have demonstrated a major improvement over conventional scrubbers are the electrostatically augmented scrubbers. Two of the other non-scrubber types of novel devices tested have also been electrostatically augmented. This paper will present results of the electrostatically augmented novel particulate collection devices which have been tested by EPA.

NOVEL DEVICE TEST RESULTS

TRW Charged Droplet Scrubber

The TRW Charged Droplet Scrubber (CDS) applies electrohydrodynamically sprayed water droplets to remove particulate material from a gas stream. The droplets have a size in the range of 60 to 250 μm in diameter and have a surface charge density near that allowed by surface tension forces. The charged droplets are accelerated through the gas stream by an applied electrostatic field. EPA's involvement with the CDS began with laboratory and bench scale studies for the application of the CDS to fine particle control. These studies included an analysis of the particle removal interactions between particulate material and charged droplets. The laboratory scale studies included the determination of charged droplet characteristics under system operating conditions. The results of these studies were used to verify some of the models used in the fine particle removal analysis. The particle removal efficiencies of a small size CDS operating under simulated process conditions were measured during the bench scale studies. The results of these tests indicated that the CDS should be effective for fine particle control and was sufficiently developed for a pilot demonstration test.

Following the laboratory and bench scale tests, a pilot scale demonstration was funded by EPA. The objectives of the pilot demonstration were to verify the applicability for removing fine particles from an industrial effluent stack, to determine the influence of CDS operating variables on performance and behavior of the CDS under long term operation. The demonstration unit was to be of sufficient size to adequately describe the behavior of a full size unit. The emission source was to be characteristic of those requiring control with a relatively large fraction of particulate material in the submicron range.

The source selected for the demonstration was the flue gas emissions from a coke oven battery. Heretofore, it was the general concensus of the industry that there was no suitable control technology for this process because of the wide process fluctuations. Emissions consisted of varying relative concentrations of submicron sticky hydrocarbon and micron sized high conductivity carbon black.

The CDS unit used in the demonstration had a capacity of 51,000 m³/hr at 1.83 m/s gas flow rate. An isometric sketch of the CDS is shown in Figure I. A design summary is shown in Table I.

The scrubber contained three electrostatic spraying stages arranged in series with parallel collecting plates on 0.127 m centers. It had 19 collecting modules. The scrubber structural members and collector plates were fabricated from mild steel. Although the compatibility problem of mild steel in the stack gas environment was recognized, it was felt that the material would maintain its integrity during the test period. The electrodes which distribute high voltage and water were fabricated from type 316 stainless steel tubing.

Table I. CDS Design Summary

- Three high voltage scrubbing stages with 0.127 m collector plate spacing.
 - Flow cross sectional area, 7.36 m²
 - High voltage electrode, type 316 stainless steel tubing 19 mm diameter, flattened to 12.7 mm.
 - High voltage electrodes contained 67 spray tubes each on 44.5 mm centers.
 - Spray tubes, titanium with a 1.27 mm O.D. by 0.15 mm wall and protruding 25.4 mm from the electrode.
 - Collector plates 3.05 m long by 1.83 m high by 2.0 mm thick mild steel.
 - Wall wash system covering each collecting surface.
-

The CDS demonstrated effective control of the emissions from the coke oven battery over widely fluctuating process conditions. Particle removal efficiencies up to 95% were measured and were an increasing function of the time averaged particle loading. Improvements in the gas distribution internal to the equipment should result in additional improvements in collecting efficiency.

The average inlet particulate load varied between 155 and 755 mg/Nm³, associated aerodynamic mean diameters varied between 0.4 μm (hydrocarbon aerosol) and 1.5 μm (carbon black). The most sensitive design variable affecting efficiency was the gas volume flow rate through the equipment. Low total energy and water consumptions, 0.7 - 1 watts/hr/Nm³ and 0.11-0.3 l/Nm³, respectively, were demonstrated over most of the test conditions. Operation of the CDS with intermittent (8 hour cycle) collector plate over sprays was adequate for deposit control.

Since the pilot scale demonstration funded by EPA was completed a full scale CDS unit was purchased and installed on this source. Collection efficiency has been equal or better than that observed during the pilot demonstration but severe corrosion problems have developed. EPA is supporting work to solve these problems.

Air Pollution Systems Scrub-E

The Air Pollution Systems (A.P.S.) electrostatic scrubber (Scrub-E) is basically an electrostatic charger (or ionizer) followed by a venturi scrubber. Figure II is a schematic diagram of the pilot system. An electrode is placed upstream of the venturi to charge the inlet particles, which then enter the venturi throat. The gas stream atomizes the central water spray in the venturi throat and the charged particles, according to A.P.S., are then attracted and collected by the highly polarized water molecules. The charged particles are also collected on the walls of the ionizer section prior to the throat of the venturi. A thin film of water is run down the inclined surfaces to keep the walls clear and prevent high voltage arcing. The particle laden water droplets are then collected by a cyclonic separator and sent into a settling tank (clarifier). The water can then be recycled back into the scrubber system. However, during the test program, fresh water was used.

The ionizer consists of an electrode supported in the inlet of the venturi section. According to A.P.S., a stable electrical discharge of high intensity is maintained across the venturi throat between the center electrode and the wall. A.P.S. claims that the average field

that can be maintained across the electrode gap (space between the electrode probe and the wall) is substantially higher, 14-16 kV/cm, than that of a standard electrostatic precipitator, 4 kV/cm.

The pilot scale laboratory test of the Scrub-E showed this system to be equal to a conventional venturi scrubber with a power requirement 1-1/2 to 2-1/2 times as great.

Last year a competitive procurement was issued to demonstrate at pilot or small full scale the technical and economic feasibility for the most promising existing novel particulate collection system for control of fine particulate emissions from industrial sources. This competitive procurement was won by A.P.S. for demonstration of the Scrub-E. A contract was funded in September, 1977 with A.P.S. to demonstrate a 300 to 600 m³/min Scrub-E on a fine particulate source. A.P.S. is now looking for a site for this demonstration. Emphasis is being placed on locating a primary smelter. Final site selection will be made and equipment design will be underway within the next few days.

Air Pollution Systems Electro-Tube

The pilot scale A.P.S. Electro-Tube is basically a tube electrostatic precipitator with a central rod electrode and wetted wall collector. Figure III is a schematic diagram of the pilot system. The inlet particles are charged in a high energy field (12 kV/cm) by a high intensity ionizer at the base of the electrode. The charged particles then migrate to the wetted wall in the body of the device in a field of 5-10 kV/cm. A.P.S. indicates that initial saturation charge on the particles is higher than the usual 4-5 kV/cm for a conventional ESP and facilitates increased migration in the collecting electric field.

The A.P.S. Electro-Tube, which is similar to a wet wall electrostatic precipitator, gave some very high efficiencies on fine particulates--as high as 98.9% on 0.5 micron particles. This performance is similar to that which can be achieved in small wet electrostatic precipitators with the same ratio of plate area to volumetric flow rate.

University of Washington Electrostatic Scrubber

The University of Washington (UW) Electrostatic Scrubber involves the use of electrostatically charged water droplets to collect air pollutant particles electrostatically charged to a polarity opposite to that of the droplets. A schematic illustration of the UW Electrostatic Scrubber system is presented in Figure IV. The particles are electrostatically charged (negative polarity) in the corona section.

From the corona section the gases and charged particles flow into a scrubber chamber into which electrostatically charged water droplets (positive polarity) are sprayed. The gases and some entrained water droplets flow out of the spray chamber into a mist eliminator consisting of a positively charged corona section in which the positively charged water droplets are removed from the gaseous stream.

The Particulate Technology Branch has funded construction of a mobile UW Electrostatic Scrubber for tests on a variety of industrial sources. Tests have been completed with the unit on the emissions from an electric arc steel furnace. The tests illustrated the system's capability for high efficiency fine particle collection at a relatively low energy consumption. Measured overall particle collection efficiencies ranged from 79.7% to 99.6% depending on electrostatic scrubber operating conditions and upon the inlet particle size distribution. Figure V illustrates the effect of specific plate area (SCA) and liquid/gas ratio (L/G) on the particle collection efficiency as a function of particle size.

The mobile unit is now installed on a coal-fired power plant and preliminary tests showed collection efficiencies as high as 98% for a 0.5 micron diameter particle.

Apitron Electrostatically Augmented Fabric Filter

American Precisions Industries, Inc. has developed the Apitron unit which is an electrostatically augmented fabric filter. Figure VI provides a cutaway view of the pilot plant unit which was tested by EPA.

The device is divided into two separate compartments, which share a common inlet, hopper, and power supply but each has its own exit duct and flow metering capability. Only one of the two compartments was used in these tests. Pertinent dimensions and operating data are given in Table II.

Table II. Apitron Operating Data

| | |
|------------------------------------|--------------------------|
| Precipitator tube inside diameter | 12.7 cm |
| Precipitator tube length | 83.8 cm |
| Number of tubes per compartment | 3 |
| Number of independent compartments | 2 |
| Number of bags per tube | 4 |
| Filter area per bag | 0.293 m ² |
| Operating voltage | 30 kv |
| Operating current per compartment | 7.5 mA |
| Cleaning pulse duration | 50 msec |
| Cleaning interval | 6 minutes |
| Nominal air flow per compartment | 0.118 am ³ /s |
| Operating pressure drop | 3.3 cm w.c. |
| Bag material | Teflon or Nomex |

Incoming air flow enters the precipitator section from below with the upper portion of the hopper serving as an inlet plenum. The flow then passes upward, through the tubes of a set of parallel wire-pipe type precipitators in which the particulate is charged and much is precipitated. Flow continues upward, past the tubes, into and through the bags where the final filtration takes place. Clean air exits the unit at an exhaust located in the side of the bag housing section. In the pilot plant operation each tube (and associated set of bags) is cleaned one at a time with a six minute interval between successive cleaning of any one tube and bag set. In the full scale system, six bag and tube sets are cleaned at a time. Cleaning is initiated by an electrical

pulse from the control system which opens a diaphragm valve for several tens of milliseconds. A blow pipe connected to the valve is then pressurized which results in a compressed air jet downward from a nozzle directly above and concentric with the corona wire of the tube being cleaned. The jet of air flowing downward through the tube entrains and mixes with a secondary air flow sweeping the tube clean of deposited dust by the mixture of high velocity air. The secondary air flow, passing from the outside to the inside of the bags, snaps the bags inward and dislodges the dust deposits from the bags. Vertical height constraints in the mobile pilot plant required the use of four short bags in parallel over each precipitator tube rather than one longer bag over each tube as would be used in full scale systems.

The operating conditions for the Apitron device during the seven test days are given in Table III. The first two days of testing of the Apitron system was done with relatively old Nomex bags in use. These bags had been subjected to sulfuric acid attack during an earlier test program and were tested only because a new set of Teflon bag which were scheduled to be used were not immediately available. After two days of testing with the Nomex bags the Teflon bags arrived and were installed. One day of tests were performed with the new, unconditioned Teflon material, after which the bags were run continuously for two more days over a weekend for conditioning before testing was resumed.

After testing was resumed two days of data were obtained with electrostatic augmentation at a face velocity of about 35 mm/sec, followed by two days of testing without electrostatic augmentation. One of the tests without electrostatic augmentation was run at a face velocity of 33 mm/sec and the other at a face velocity of 14 mm/sec.

The results of the total particulate tests are given in Table IV. The power consumption figures do not include the required compressor power for the cleaning pulses nor any conversion efficiencies for fans, motors, power supplies, etc. The estimated total energy usage including losses in the latter items is approximately 40% greater.

Table III. Apitron Operating Conditions

| Date | Bag Material | Outlet gas flow | | Outlet temp. °C | Bag face mm/sec | Velocity fpm | ESP conditions | | | | | Apitron pressure drop cm w.c. | Energy usage, air moving joules/m ³ | |
|----------|---------------------|----------------------|------|-----------------|-----------------|--------------|----------------|------------|--------------------------|------|------------------------------------|-------------------------------|--|------------------------------------|
| | | am ³ /min | acfm | | | | Voltage kv | Current mA | Specific collecting area | | Current density nA/cm ² | | | Energy usage joules/m ³ |
| 11/30/77 | Nomex | 7.31 | 258 | 74 | 34.7 | 6.83 | 31 | 7.5 | 8.25 | 41.9 | 750 | 1910 | 5.3 | 530 |
| 12/1/77 | Nomex | 7.00 | 247 | 77 | 33.2 | 6.53 | 31 | 7.5 | 8.60 | 43.7 | 750 | 2000 | 5.3 | 520 |
| 12/2/77 | Teflon ^a | 8.47 | 299 | 71 | 40.2 | 7.91 | 30.5 | 7.5 | 7.11 | 36.1 | 750 | 1620 | 0.5 | 50 |
| 12/5/77 | Teflon | 7.42 | 262 | 74 | 35.2 | 6.93 | 30 | 8.0 | 8.11 | 41.2 | 800 | 1940 | 3.0 | 300 |
| 12/6/77 | Teflon | 7.00 | 247 | 74 | 33.2 | 6.53 | 29 | 8.5 | 8.60 | 43.7 | 850 | 2120 | 3.8 | 380 |
| 12/7/77 | Teflon | 6.91 | 244 | 74 | 32.8 | 6.46 | 0 | 0 | 0 | 0 | 0 | 0 | 8.9 | 868 |
| 12/8/77 | Teflon | 2.92 | 103 | 54 | 13.8 | 2.72 | 0 | 0 | 0 | 0 | 0 | 0 | 3.3 | 323 |

^a New, clean Teflon bags installed overnight of 12/1 - 12/2

Table IV. Apitron Efficiency Results

| <u>Date</u> | <u>Collection Efficiency, %</u> | <u>Energy Usage, joules/am³</u> |
|-------------|---------------------------------|--|
| 12/1/77 | 99.59 | 2520 |
| 12/2/77 | 99.84 | 1670 |
| 12/5/77 | 99.90 | 2240 |
| 12/6/77 | 99.94 | 2500 |
| 12/7/77 | 99.905 | 868 |
| 12/8/77 | 99.93 | 323 |

Inertial sizing of the inlet and outlet particulates was accomplished using modified Brink impactors and University of Washington impactors. Collection efficiencies in excess of 99% were consistently obtained in the fine particle size range ($<3 \mu\text{m}$) when either the Teflon or Nomex bags were used. The efficiency curves for both materials showed efficiency minima near a diameter of $7 \mu\text{m}$ which may have resulted from agglomerates bleeding through the fabric of the bags. The efficiencies were higher on the two days of testing with the ESP section de-energized than during the tests with power on. The highest efficiencies during the entire test series were obtained on December 8 when the device was operated as a conventional baghouse at a low face velocity. There is some uncertainty in the significance of the differences among the results for the various test conditions with the Teflon bags because the bags were being tested immediately after installation and for a few days thereafter. The efficiency of the device showed a constant improvement with each day of testing after the new bags were installed. Thus, the efficiencies which were obtained during the last two days of testing with the ESP de-energized may have been obtained had it been on as well. Fractional efficiencies are shown on an aerodynamic diameter basis for two days in Figures VII and VIII.

Particulate Control Systems Electrified Bed

Particulate Control Systems, EFB, Inc., has developed an electrified granular bed (EFB). A schematic diagram of the EFB is shown in Figure IX.

A corona charging section charges the particulate before collection in a charged granular bed. A pilot scale unit installed on an asphalt roofing plant asphalt saturator is currently being tested by EPA. In this application, rather than clean the dirty granular material, it is used in the process on the asphalt shingles.

Ceilcote Ionizing Wet Scrubber

The Ceilcote Company is marketing an Ionizing Wet Scrubber. A schematic diagram of this device is shown in Figure X. In operation, contaminated gases pass through a high-voltage ionizer section that houses negative-polarity discharge electrodes and wetted plates that act as positively grounded electrodes. Electric corona discharge from the electrodes produces ions that intercept the fine contaminants and relinquish their charge to the particles. Then, the charged particles enter the crossflow wet scrubber section that is packed with Tellerettes where the larger particles (3-5 μ and larger) collect through inertial impaction. If the smaller particles (less than 3-5 μ) do not impact at some point along their journey, the probability is high that they will be captured by electrostatic attraction.

An EPA sponsored test of this device is planned in the near future.

R. P. Industries Electro-Dynactor

The Electro-Dynactor System (EDS) is marketed by R. P. Industries, Inc. In the EDS, the influent gas is ionized and particulate contaminants are electrically charged by an electrostatic ionizer prior to each stage of aspiration and wet scrubbing. The ionizers use about 15,000 volts and are self-protected against short circuits due to sparks that occasionally jump the ionizers components.

A three-stage EDS is shown schematically in Figure XI. Particulate-laden gas is aspirated through the EDS by the diffusion of the scrubbing water as shown in each of the three scrubbing stages. As the gas passes through each ionizer, the sub-micron particulate is charged negatively.

by a combination of diffusion and field charging. Upon being aspirated into each scrubbing section, the gas mixes intimately with a dense cloud of water droplets. The negatively charged particles induce positive charges called "image charges" in nearby neutral water droplets. The electrostatic force of attraction between the charged particle and its image in a water droplet causes the particle to be attracted and collected by the droplet. The liquid is separated from the gas in the reservoir/separator. The gas passes through a mist eliminator, and then is recharged in the succeeding ionizer. Normally three similar units (stages) are used in series; thus, the process is repeated three times, after which the gas passes to the stack through a final mist eliminator.

The EDS is being considered for an EPA sponsored test.

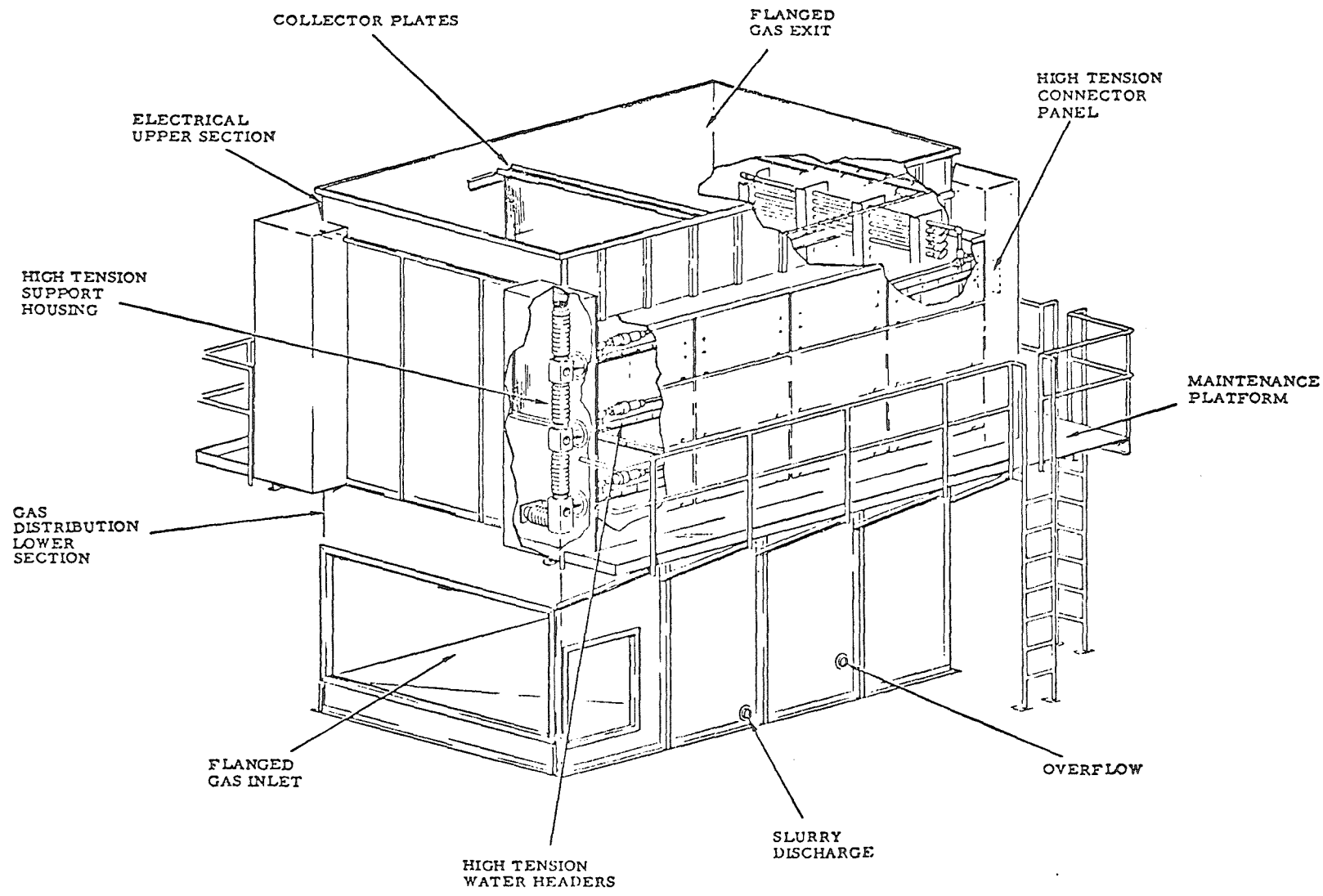


Figure I. TRW charged droplet scrubber.

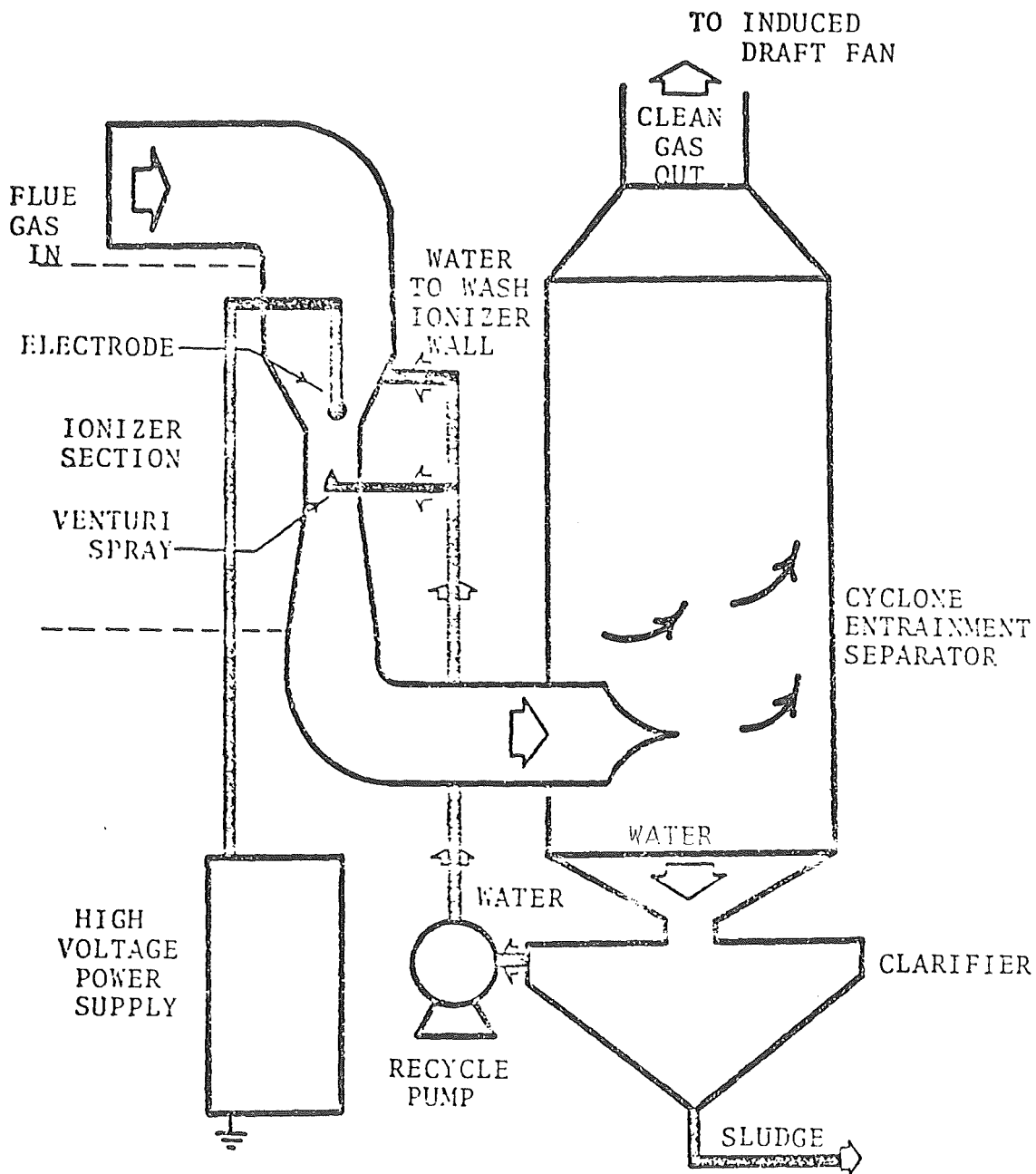


Figure II. Air Pollution Systems Scrub-E

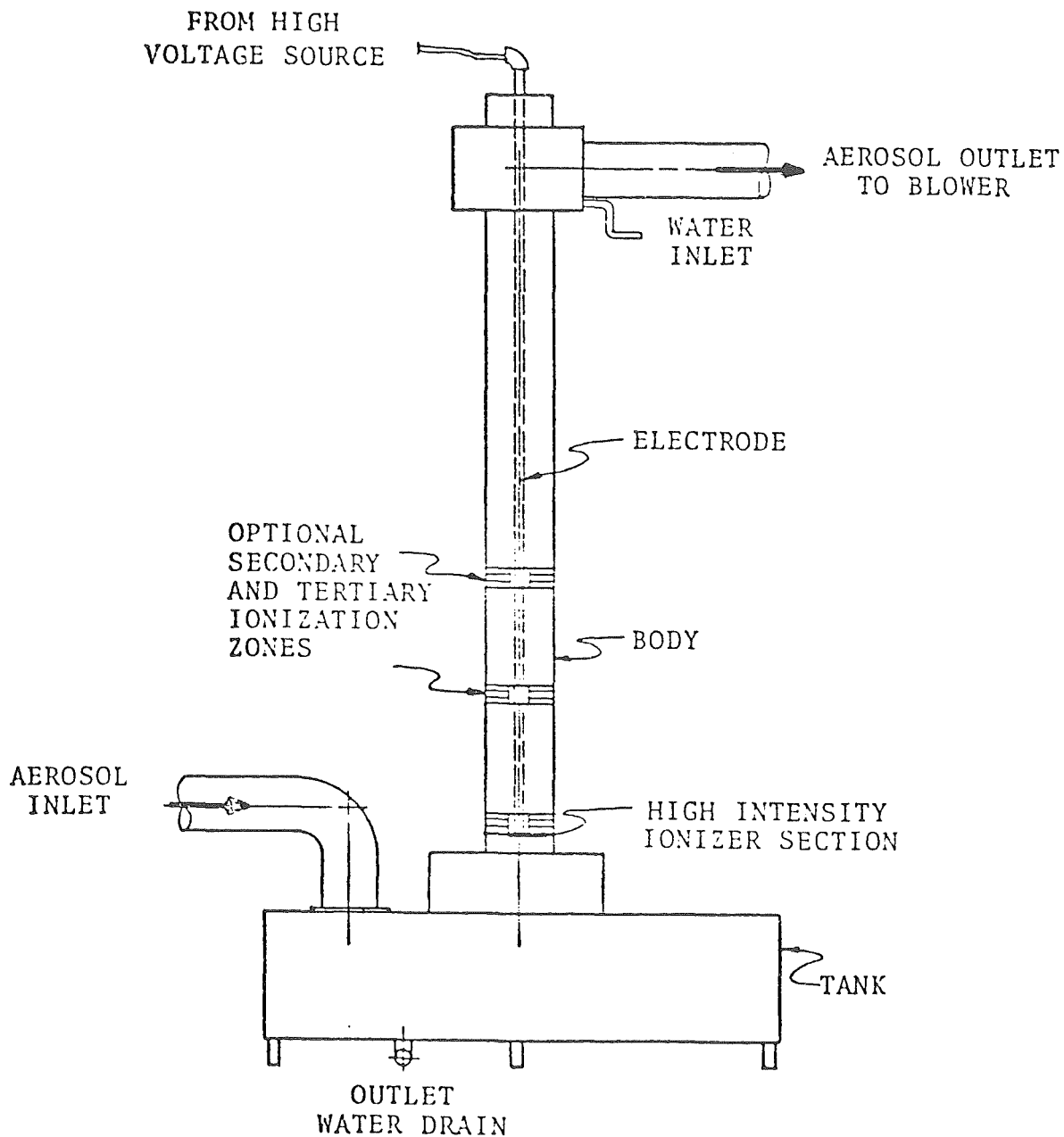


Figure III. Air Pollution Systems Electro-Tube

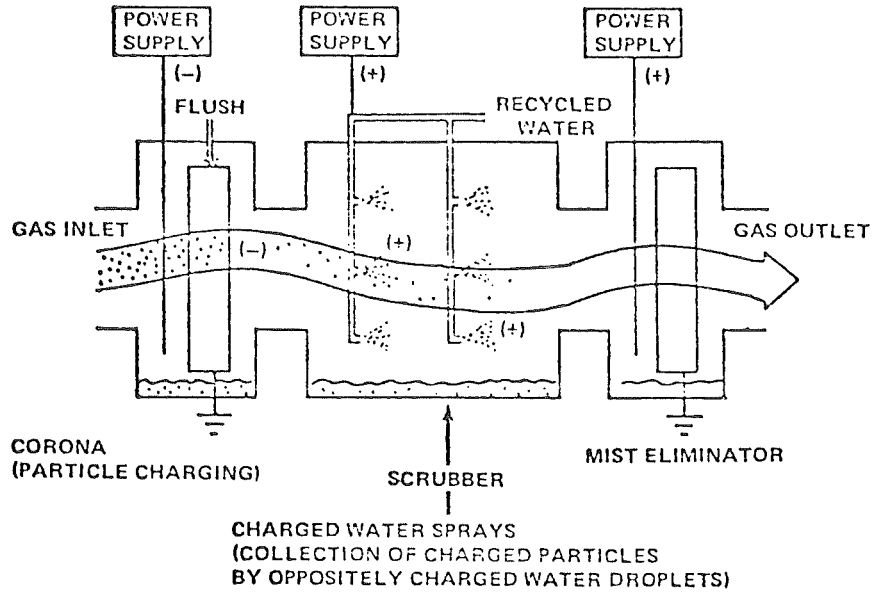


Figure IV. University of Washington Electrostatic Scrubber

| Test No. | Corona V, kV | Spray V, kV | Overall Coll Eff, % | SCA, ft ² /cfm | L/G, gal./1000 cf |
|----------|--------------|-------------|---------------------|---------------------------|-------------------|
| 22 | 70 | 10 | 98.6 | 0.047 | 17.2 |
| 23 | 70 | 10 | 96.4 | 0.045 | 16.8 |
| 26 | 65 | 10 | 99.0 | 0.072 | 23.2 |
| 27 | 65 | 10 | 98.9 | 0.071 | 22.0 |
| 28 | 70 | 10 | 86.5 | 0.038 | 16.0 |
| 29 | 70 | 10 | 87.3 | 0.038 | 15.7 |

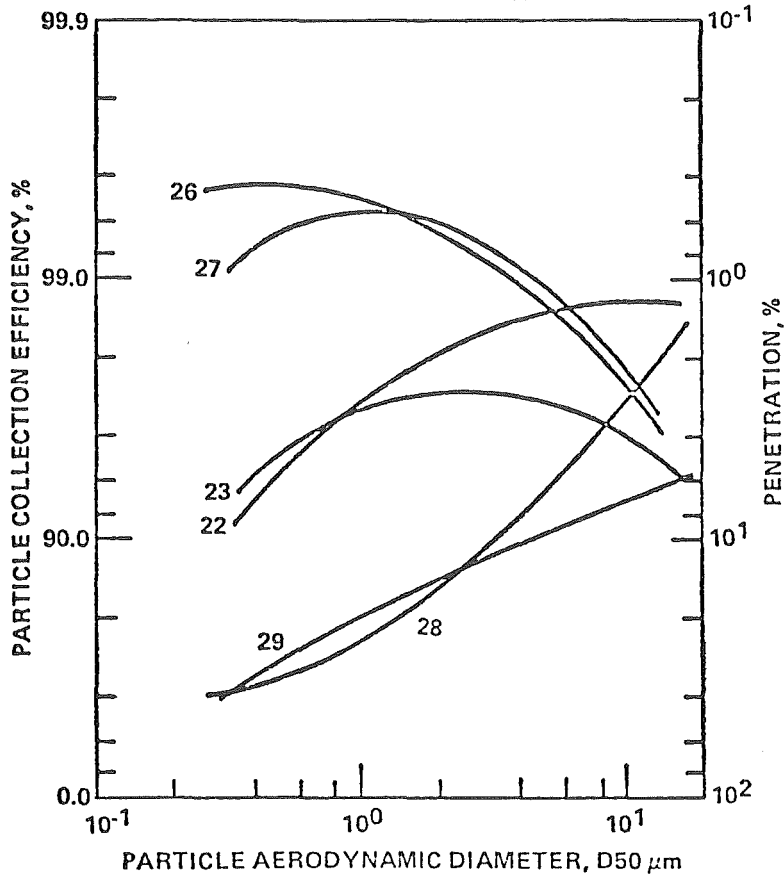


Figure V. Influence of SCA and L/G on Particle Collection Efficiencies.

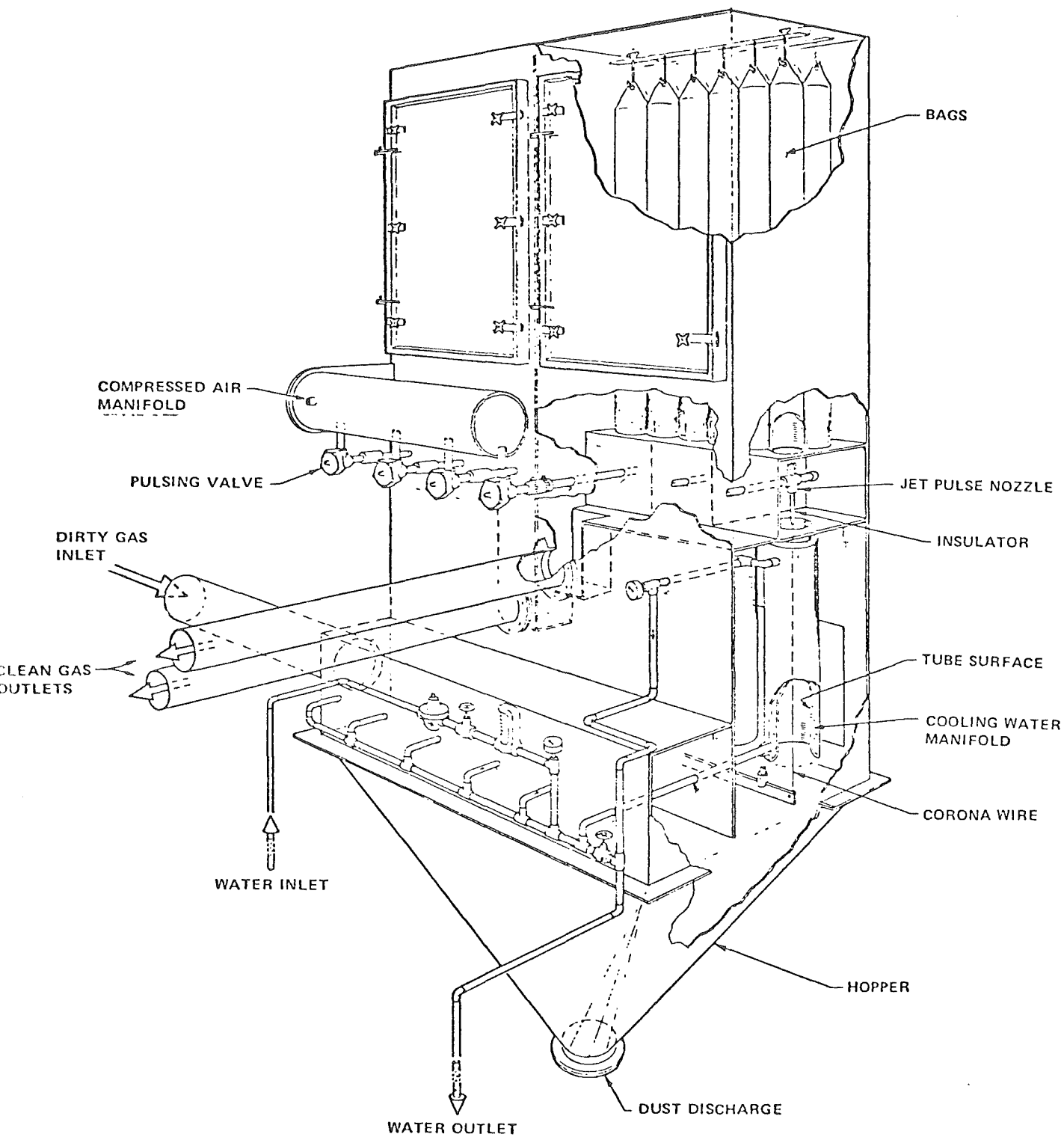


Figure VI. Electrostatically Augmented Fabric Filter

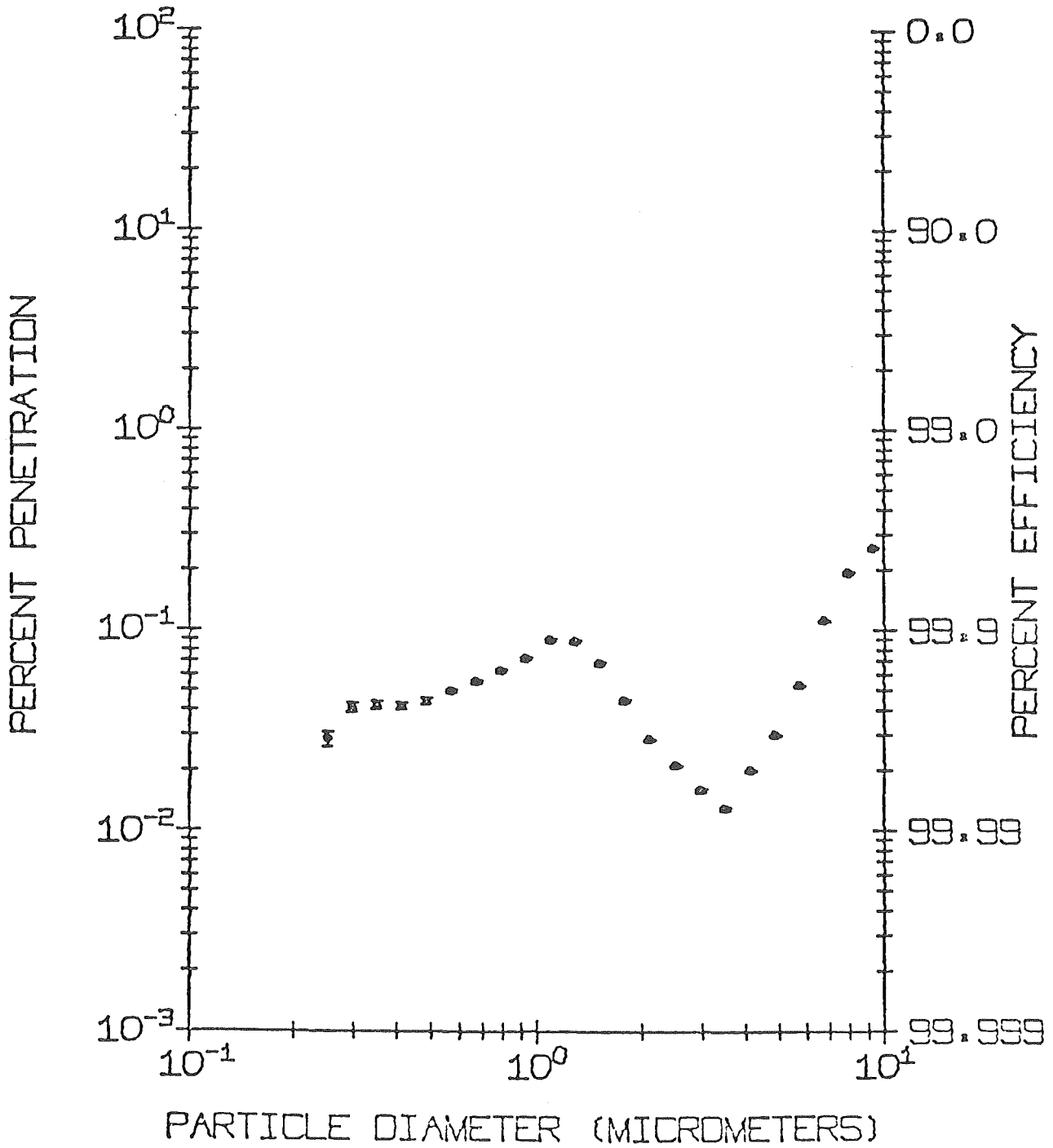


Figure VII. Apitron Fractional Efficiency - 12/6/77

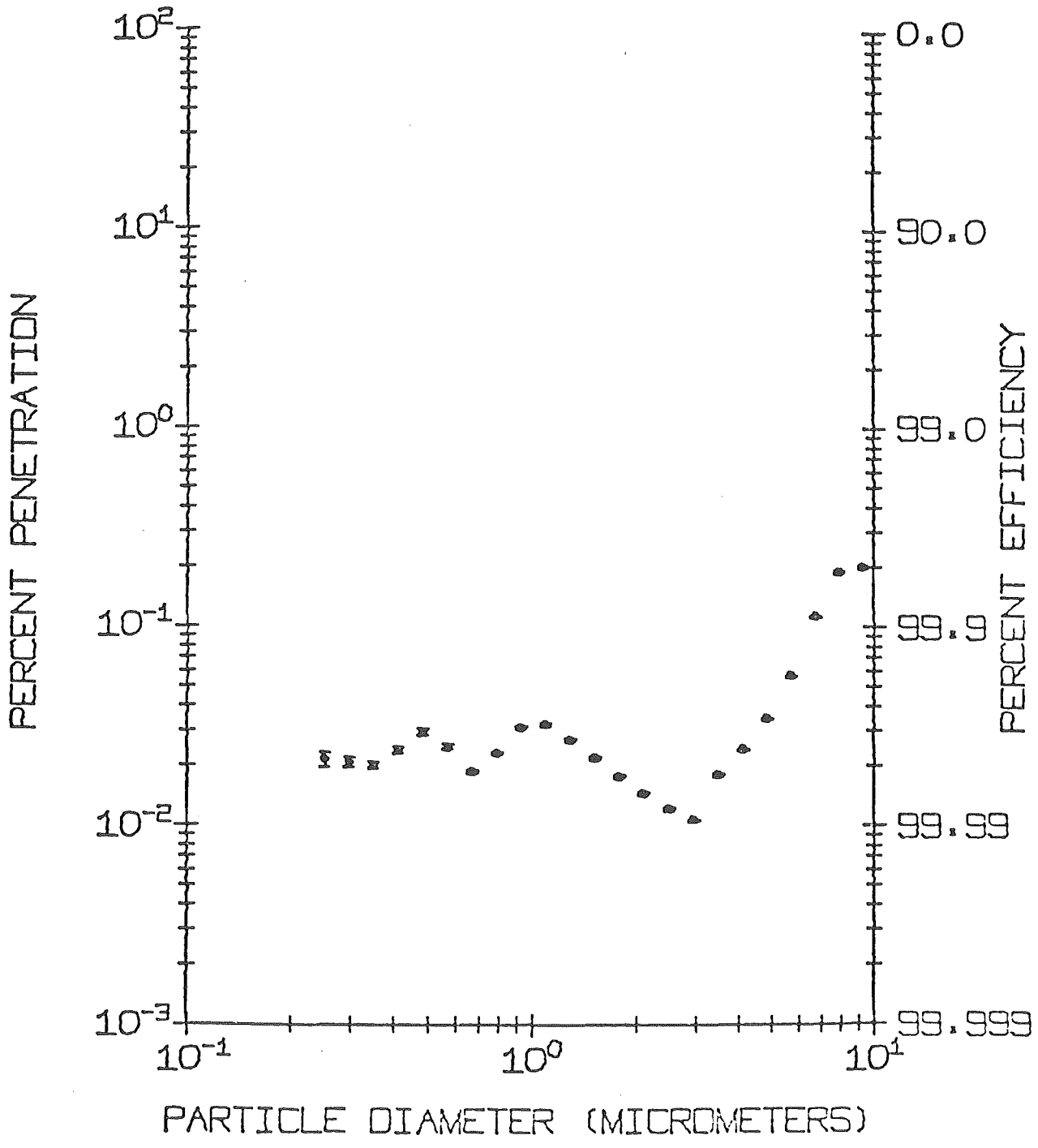


Figure VIII. Apitron Fractional Efficiency - 12/7/77

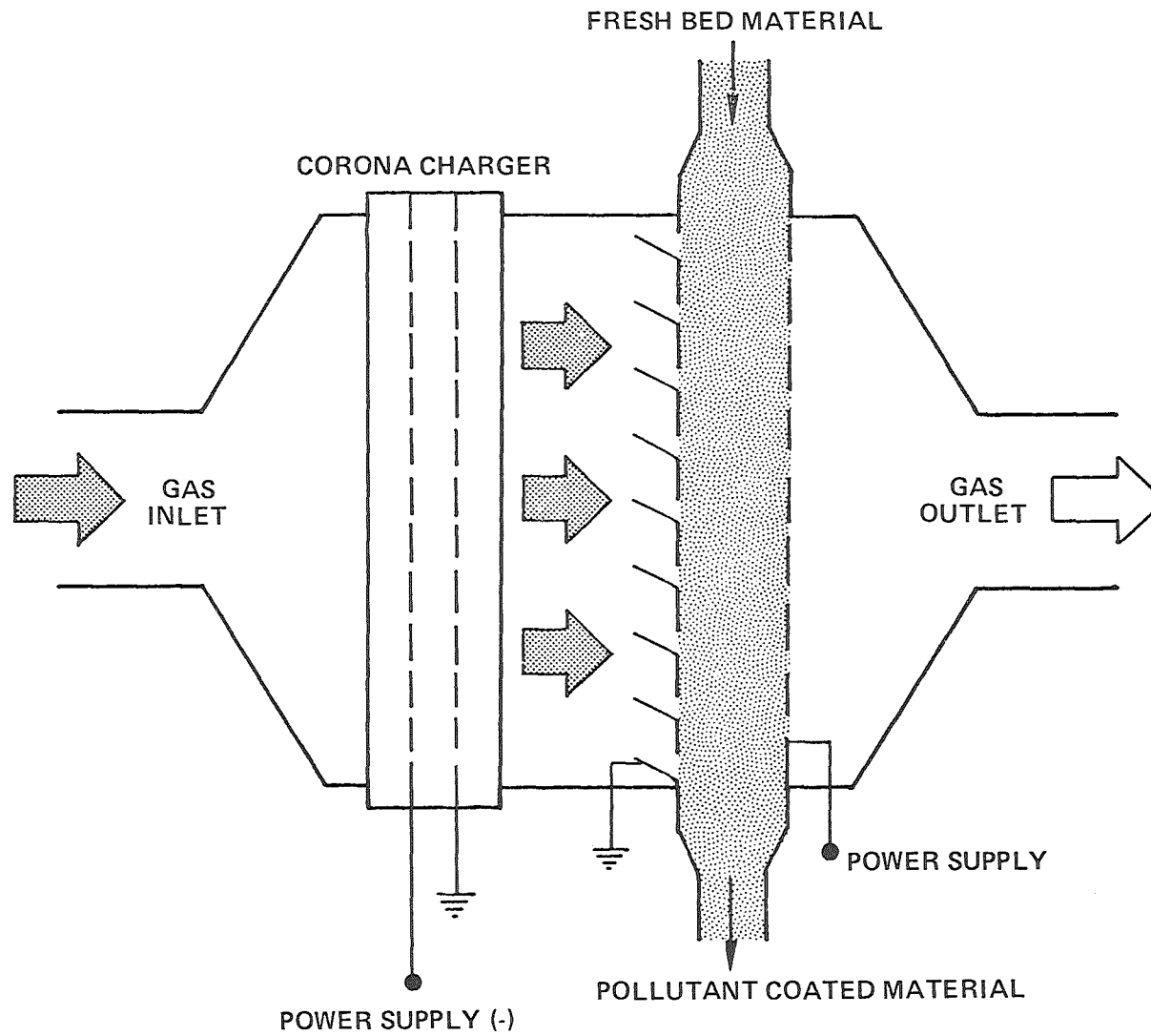


Figure IX. Particulate Control Systems electrified bed.

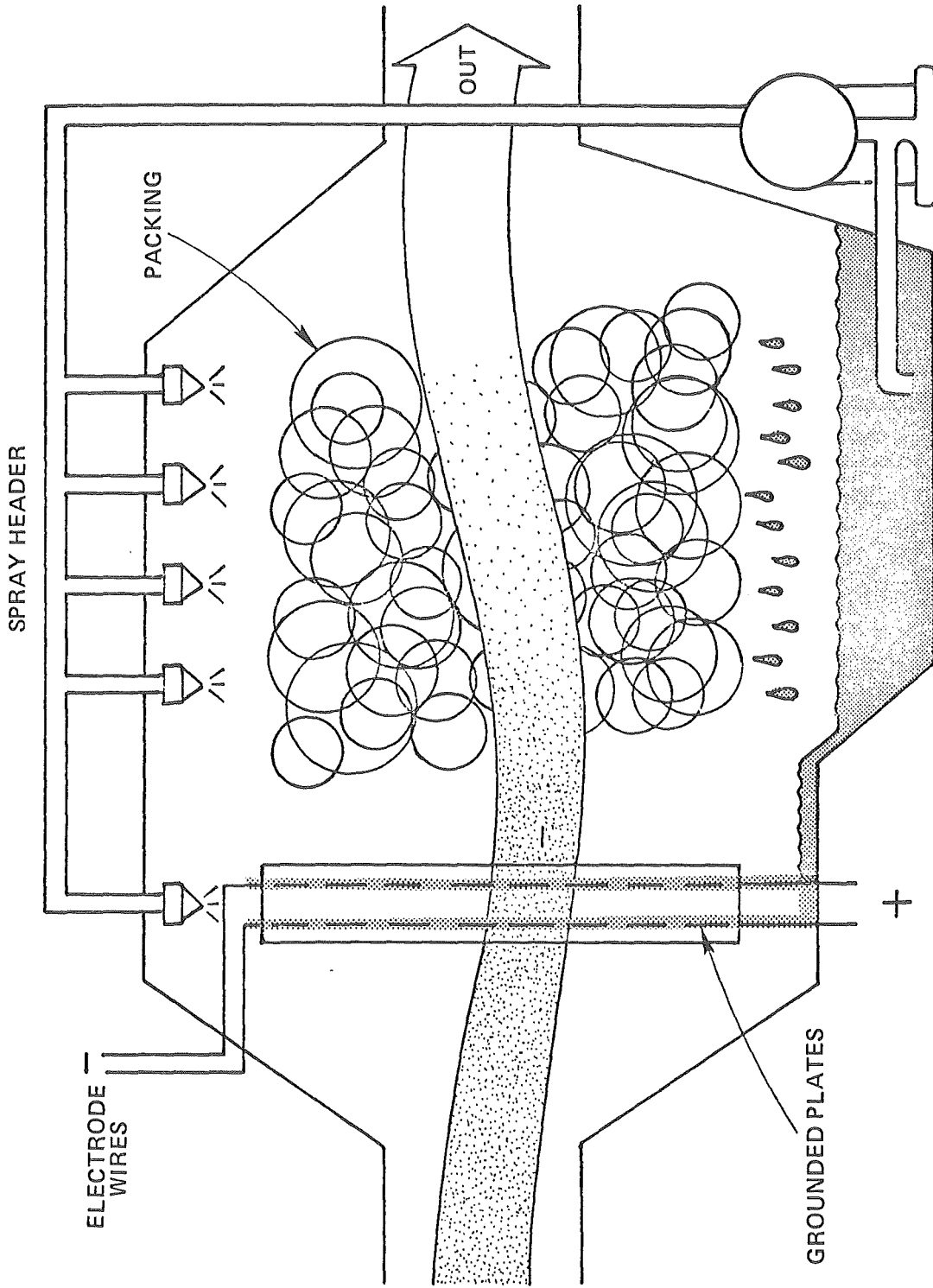
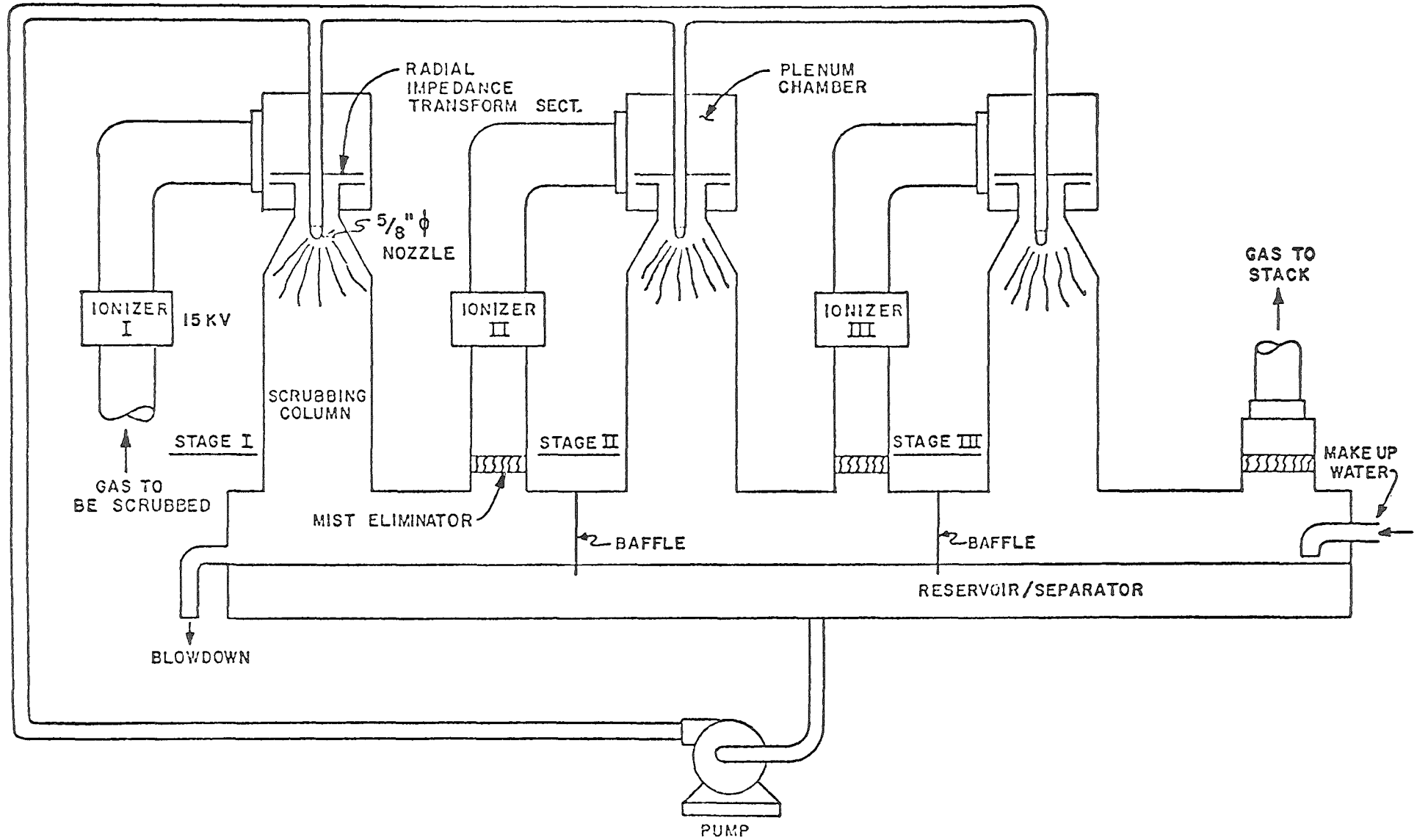


Figure X. Ceilcote ionizing wet scrubber.

FIGURE XI
A SCHEMATIC VIEW OF A 3 STAGE
ELECTRODYNACTOR SYSTEM



Discussion

Dr. G thner asked which of the new techniques described in the talk was the most promising when compared with conventional techniques in term of energy consumption. Mr. Harmon replied that the API Electrostatic Scrubber which had been demonstrated showed great promise although other units were comparable.

How to raise the efficiency of dry electrostatic precipitators
by means of gas conditioning

Dr. H. Reißmann

Lurgi Umwelt und Chemotechnik GmbH

Frankfurt/Main

Gentlemen,

1. Introduction

The dust properties have a great influence on the collection efficiency or, in the case of equal efficiency, on the required precipitator size. Depending on the different conditions, the precipitator size can vary according to the relation 1 : 6.

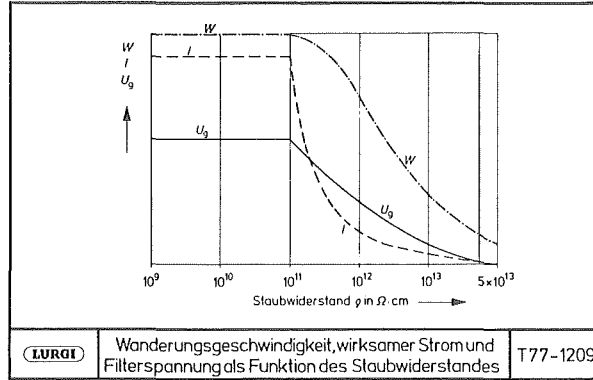
The dust collection conditions must be regarded as a complex of many factors such as fuel properties, combustion mechanisms, gas composition, dust quantity, chemical properties of the dust, grain size and surface characteristics of the dust particles.

Many of these influences cannot be measured nor calculated. The only factor that can be represented is the electrical dust resistivity, which is determined by the majority of the other factors, thus forming the most important criterion for the assessment of precipitator conditions.

...

The following figure

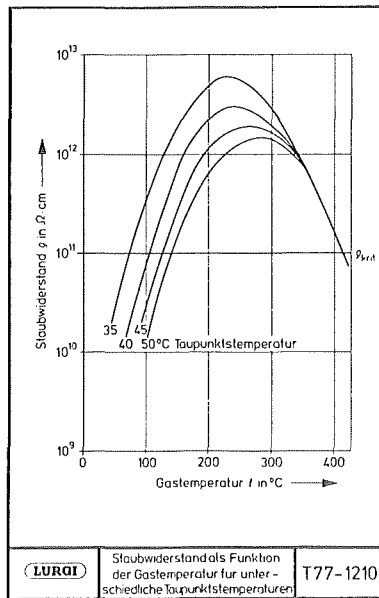
Figure 1



shows the dependence of the flash-over voltage U_g , the possible discharge current I and the attainable migration velocity w on the dust resistivity; it has to be pointed out in this connection that, with equal efficiency, the collection area is proportional to the w value.

By far the greatest problems arise in large pit coal fired blocks. The following figure

Figure 2



shows the electrical resistivity of a pit coal fly ash as a function of the gas temperature and the water vapour content at constant SO_3 content of the flue gas.

It can be seen that the resistivity passes, at normal operating temperatures and moisture contents, through a range far beyond 10^{11} ohms x cm, which is the approximate critical limit for trouble-free precipitator operation. Below the maximum, the resistivity is reduced by the condensation of electrolytes - primarily sulphuric acid - on dust particles, preferably on the rugged surfaces and in the recesses of the agglomerates.

Above the maximum, the dust resistivity decreases due to the increasing conductivity of the material. A surface condensation at temperatures which are considerably above the acid dew point is no longer possible. It is at this point that the dust resistivity curves corresponding to the different water vapour contents meet. In the majority of modern pit coal fired boilers, we find many of these unfavourable factors, such as:

low sulphur content of the coal,

low conversion rates of SO_2 and SO_3 due to high combustion chamber temperatures and to the small amount of air in excess,

flue gas temperatures which are mostly in the range of the maximum dust resistivity after the air preheaters,

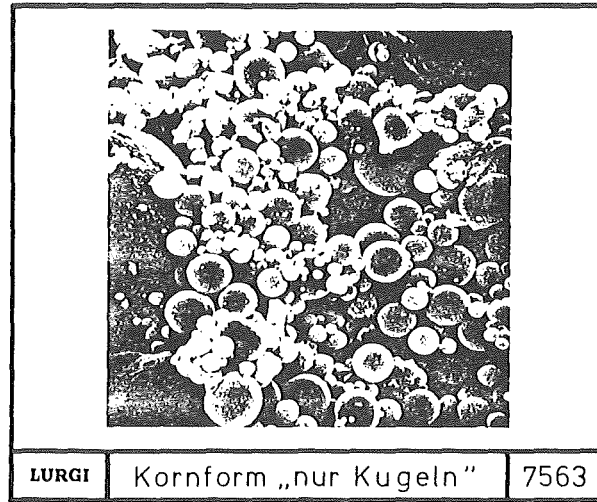
low content of unburnt particles, i.e. of conductive dust particles,

fine, spherical particles as shown in the following electron micrograph.

The dust shown comes from a 340 MW boiler with dry ash removal; the magnification ratio is 1 : 2000.

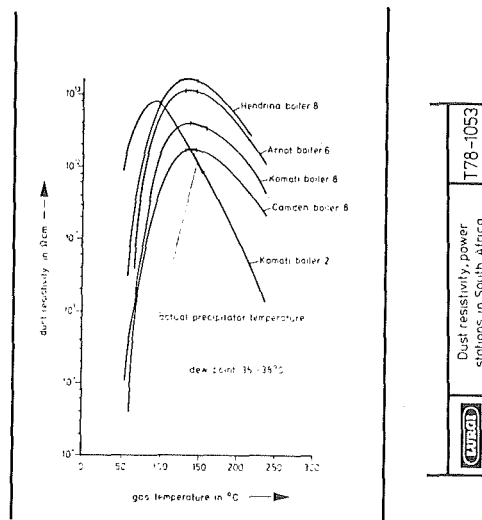
...

Figure 3



The following figure shows dust resistivities in several South African power plants. We find highly differing dust resistivities, although the coal analyses are almost identical. This means that the dust resistivity is very much influenced by the processes taking place in the boiler. Therefore the dust resistivity cannot be precalculated on the basis of the coal analysis alone, but it has to be measured in the plant itself.

Figure 4



With a view to coping with these unfavourable factors which, in extreme cases, cannot be controlled without influencing them, we investigated the possibilities of improving the operating conditions. Flue gas conditioning, that means

influencing of the dust resistivity by improving the surface conductivity, is a solution to this problem. Flue gas conditioning can be carried out by increasing the water vapour or SO_3 content in the flue gas, by reducing the gas temperature or by adding other chemicals such as ammonia or triethylamine.

2. Conditioning by the addition of SO_3

By adding SO_3 or sulphuric acid vapours, the conductivity of high resistivity dusts can easily be improved. The tests carried out on a precipitator plant working under unfavourable conditions in a German 300 MW block show the following results:

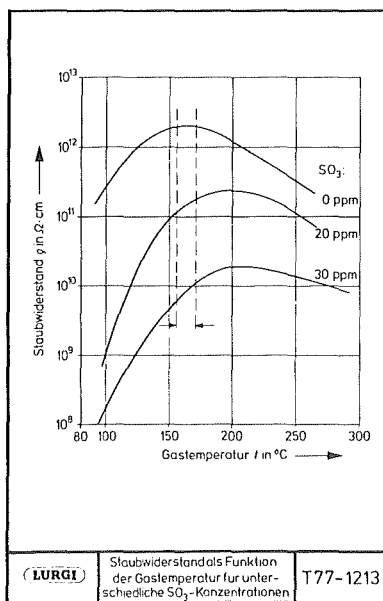


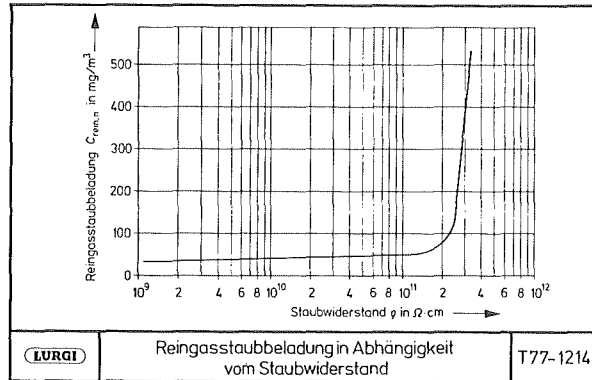
Figure 5

From the diagram it can be seen that the addition of 20 ppm by volume of SO_3 would suffice for reducing the dust resistivity to a more favourable value.

...

The following figure

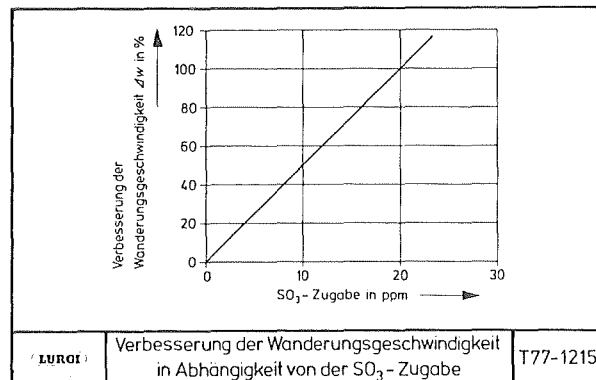
Figure 6



shows the dependence of the clean gas content on the dust resistivity and thus on the SO_3 content for the case mentioned. I should like to point out again that, according to the diagram shown, a dust resistivity of 10^{11} ohms x cm can already be achieved by adding approximately 20 ppm of SO_3 . As can be seen, the clean gas dust content is reduced by 8% of the initial value, that means from $500 \text{ mg}/\text{m}^3$ to approximately $40 \text{ mg}/\text{m}^3$.

Tests carried out in an Australian power station showed the following relative increase in the migration velocity as a function of the SO_3 addition.

Figure 7



With an addition of 20 ppm of SO_3 the increase amounts to 100%, that means that the collection area necessary is only 50% of the area required in systems without conditioning.

...

Naturally, such vital improvements can only be expected in cases where the flue gas at the boiler outlet contains virtually no free SO_3 ; this may be the case with coal having a very low sulphur content so that no SO_3 , or only a small amount, is formed in the firing system, and that almost complete absorption of the SO_3 by the alkaline dust particles is ensured.

SO_3 conditioning is already carried out on an industrial scale in a few power stations in the United States of America, in Australia and in Great Britain. Due to the fact that the handling of ready-made SO_3 involves problems, it is advisable to produce the gas on the spot.

The following figure

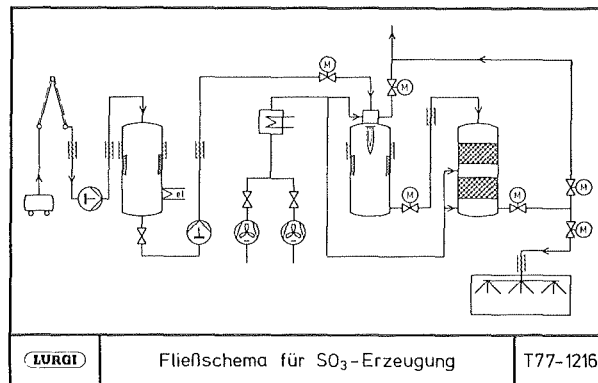


Figure 8

shows the flow diagram of an SO_3 production plant. Liquid sulphur is burned to form SO_2 , which is oxidized to SO_3 with the help of a catalyst. The SO_3 is mixed with air and injected into the flue gas flow. SO_3 production plants working according to this principle are frequently used in the chemical industry. A flue gas conditioning plant in a German power station with 1 x 500 MW and 2 x 150 MW blocks will go into operation about the middle of this year.

...

There is no reason to fear that conditioning of the flue gas by means of SO₃ will cause an additional impact on the environment due to the higher sulphur dioxide emission. The SO₃ injected is almost completely absorbed by the dust. A higher SO₃ concentration in the flue gas after the electrostatic precipitator could not be ascertained. It is only in the case of slag tap firing systems with dust recirculation that the sulphur compounds are decomposed again in the firing system, so that additional SO₂ is set free. However, for a 750 MW block, the quantity involved by the addition of 20 ppm of SO₃ is only approximately 140 kg/h, which corresponds to an increase in the sulphur content of the coal by 0.02%.

When comparing 600 MW block dust collection plants with and without SO₃ conditioning for operation conditions with dust resistivities as shown for the South African power stations at the beginning, we obtain the following values:

| | without | | with |
|------------------------------|---------|------------------------------|------|
| | | SO ₃ conditioning | |
| Gas volume m ³ /s | | 913 | |
| Collection efficiency % | | 99.2 | |
| Precipitator size % | 100 | | 60 |
| Investment costs % | 100 | | 83 |

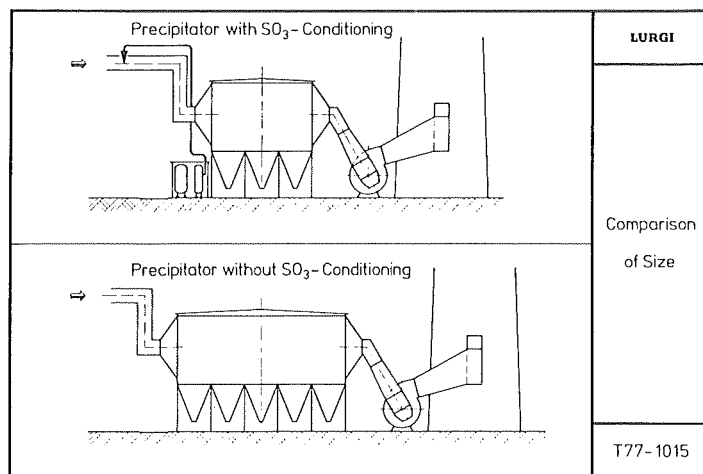
The additional operating costs amount only to \$40,000 for 8,000 operating hours per year.

...

Apart from considerable cost savings, the electrostatic precipitator plant with SO₃ conditioning system has the advantage of operating with constant collection efficiencies even in the case of fluctuating operating conditions and therefore varying dust resistivities.

The sizes of precipitator plants with and without SO₃ conditioning are compared in the following figure:

Figure 9



3. Conditioning by means of water

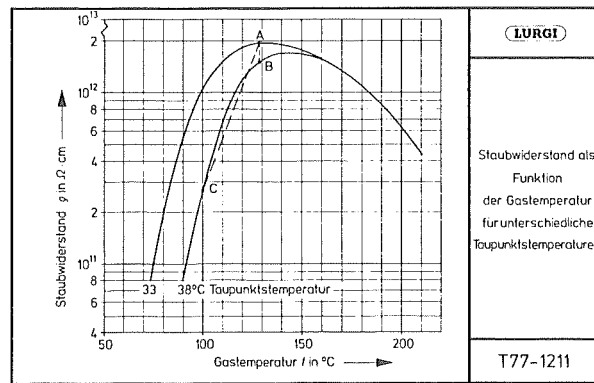
A relatively simple way of conditioning, which is occasionally used also for the improvement of existing plants, is the injection and evaporation of water in the boiler in order to increase the moisture content of the gas. However, if a high dust resistivity is to be considerably reduced, the water vapour content has to be raised to at least 10% by volume. In the case of a 750 MW block, this

...

corresponds to an injection water volume of approximately 95 tonnes/hour. The evaporation of this volume is, like the addition of steam, unfeasible for economical reasons.

But there is another solution available and that is the injection of water after the air preheaters. In this way the flue gas is cooled and at the same time the dust resistivity is reduced by the two components, namely the higher water content and the lower gas temperature. The following figure

Figure 10



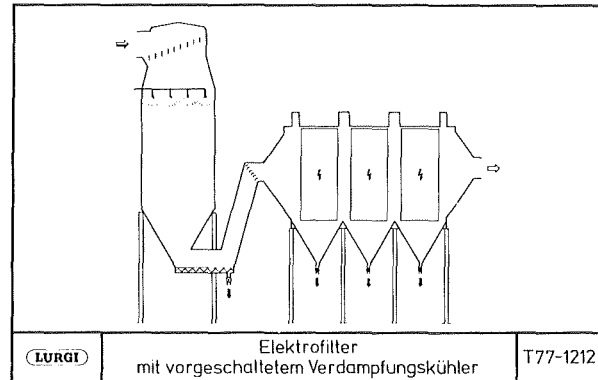
shows the test results obtained in a 350 MW block with pit coal slag tap firing system. While the influence of the higher water dew point alone is still small at operating temperature (Line A-B), it is considerably increased as the temperature drops (Line A-C). By simultaneous cooling and moistening, the dust resistivity can be reduced by approximately one power of ten. The reduction of the gas temperature is the more important factor in this connection. In this special case, the injection of only 8 g water / m³ gas brought about a decrease of the clean gas dust content from 180 to 60 mg/m³.

...

With this type of conditioning, the water volumes are comparatively small. In order to reduce the flue gas temperature by 20°C while having a simultaneous increase of the dew point by approximately 4°C, approximately 25 tonnes/h water are required for a 750 MW block.

Water injection constitutes a relatively simple way for improving the collection conditions. However, complete evaporation of the liquid injected must be ensured in order to avoid accretions of the moistened dust. In spite of the fine atomization, this demands, at the low temperature level involved, relatively long retention times so that the use of special evaporation coolers becomes necessary.

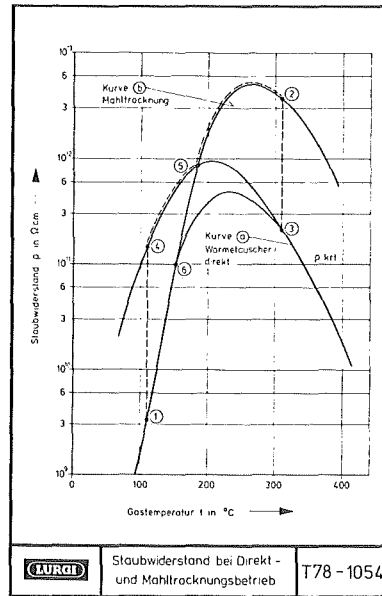
Figure 11



This method of conditioning the gas by means of water in an evaporation cooler has been applied in the cement sector before electrostatic precipitators arranged after suspension preheater kilns for many years.

...

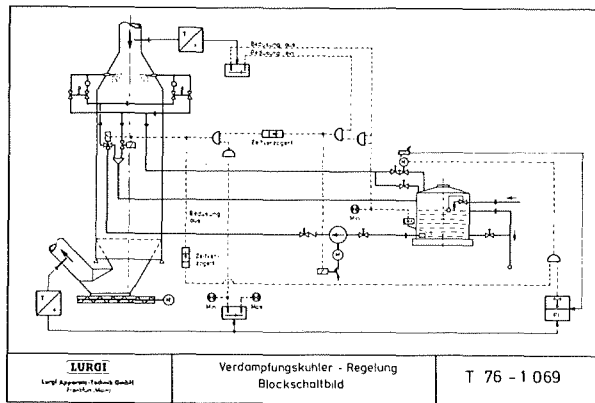
Figure 12



Here we have two types of dust with extremely different resistivity curves, namely curve a, which corresponds to the so-called direct operation, and curve b, which corresponds to the operation with a raw material grinding and drying unit. If either method is applied in continuous operation, the dust resistivities will not be super critical (Items 1 and 3). However, in the majority of cases, a change-over from direct to compound operation is carried out once a week, and the dust resistivity resulting for the electrostatic precipitator operation will follow items 1 - 4 - 5 - 2. It will only be after an extended continuous operation that the resistivity will drop to 3. In this case, it is advisable to use an evaporation cooler before the precipitator and thus to change the operating temperature prevailing during direct operation from 310°C to approximately 150°C. Due to the simultaneous increase of the dew point, the dust resistivity will always remain below the critical value. (Item 6)

...

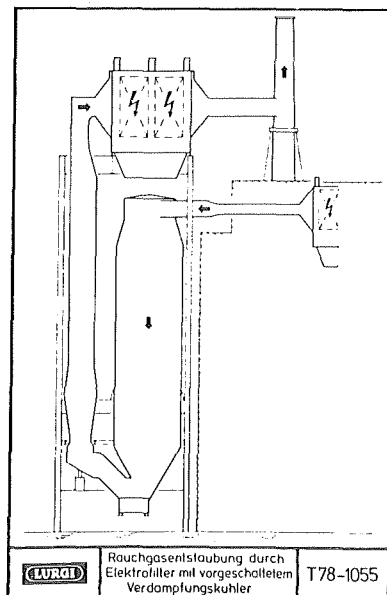
Figure 13



The water to be evaporated is injected into the cooler head. The volume is controlled in dependence on the precipitator inlet temperature. Since the cooler volume required for complete evaporation is proportional to the square of the maximum droplet diameter, greatest importance has to be attached to the finest possible atomization. The so-called return flow nozzles have proved to be the best design for this application.

While there are many evaporation coolers in operation in the cement sector, in the steel industry, after waste incinerators and in other industrial fields, the application of evaporation coolers for the collection of dust from power station waste gases is new. Therefore, an industrial scale pilot plant is being constructed at the moment in a German power station.

Figure 14



...

The power station concerned is a 150 MW block. The evaporation cooler has been designed to lower the temperature from 150°C to less than 100°C. The evaporation cooler is followed by the fan, the electrostatic precipitator and the stack. By cutting in or cutting out one of the preceding electrostatic precipitators, the dust content of the raw gas reaching the pilot plant can be altered in order to allow testing of the separation of very fine dusts with and without conditioning by water. It is expected that very low clean gas dust contents, such as achieved after bag filters, will be reached. The first results will be available in about a year. Preliminary tests which have already been carried out give us grounds to be optimistic.

Other conditioning means

Conditioning by means of the admission of ammonia is also carried out in some plants. Its effect on the collection conditions however is differing and rather small compared to SO₃. Tests were carried out and it was found that, although equal quantities had been added, the ammonia raised the migration velocity by 30%, whereas the SO₃ increased the migration velocity in the plant by 100%.

Tests which were primarily carried out in Australia have shown that triethylamine is, in principle, a good conditioning agent. Application of triethylamine in practical operation is, however, unfeasible at the moment due to the high purchase costs.

DrRm/Shdt/Bltt
7th March 1978

Discussion

Mr. McCain asked whether SO_3 was created during the electrostatic process. Dr. Reissmann replied that there is, whether conversion from SO_2 to SO_3 in the boiler or in the precipitator (this was confirmed by Mr. Gooch).^{*} He added that it is difficult to differentiate SO_3 from SO_2 by measurement. Mr. Parker inquired as to the effect of conditioning on particle size; unfortunately it was not yet possible for Dr. Reissman to answer this type of question. Mr. Princiotta raised the question of the economic viability of SO_3 when compared with humidification and water addition. The answer was that the actual running costs at a plant were low and could vary according to conditions. Mr. Gage then wished to know whether possibilities existed for cooperation between the U.S. and W. Germany in humification studies. Dr. Reissmann said that this was not feasible at the time; however, at Mannheim a plant was under construction which would test a considerable variety of coals including overseas. He expressed the hope that future cooperation would take place, and was supported by Dr. Holighaus. Dr. Laufhutte pointed out that conversion of SO_2 to SO_3 is minimized in coals having a low sulphur content. Dr. Reissmann stated that normally all boilers were fired with coal; the German boilers however, were of a slag hole type and produced only small quantities of SO_3 . He added that SO_3 contents less than 1% were sufficient for the conditioning process.

The question of sulphur trioxide content in fly ash was raised by Dr. Davids, who was informed that there was no increase at the stack of SO_3 in the gas. SO_3 passed into the dust (which was recycled into the furnace) and split into SO_2 .

^{*}Mr. Gooch does not recall what he "confirmed" but he would not expect significant amounts of oxidation of SO_2 in the ESP.

IMPROVED DESIGN METHOD FOR F/C SCRUBBING

by

Seymour Calvert

Air Pollution Technology, Inc.
4901 Morena Blvd., Suite 402
San Diego, California 92117
USA

IMPROVED DESIGN METHOD FOR F/C SCRUBBING

Flux force/condensation (F/C) scrubbing provides a means for the enhancement of fine particle collection efficiency through the effects of condensing water vapor. Several phenomena are simultaneously involved and a detailed mathematical model is complex. In a series of previous studies ^{1,2,3,4} we have developed a design method (i.e., performance prediction) based on a model which required the simultaneous solution of several differential equations. While it produced useful results, it was a time-consuming procedure, even with the aid of an electronic computer.

In the course of refining our design method we arrived at the conclusion that the flux force effects could be treated separately from the condensation effects in many scrubber situations. While the condensation-induced improvement in inertial impaction efficiency could be handled conveniently, the flux force deposition prediction remained cumbersome. Recently the senior author became aware of a concept developed by Whitmore⁵ which provided the key to simplifying the prediction of the flux force effects in F/C scrubbing. By incorporating Whitmore's concept into our model we have developed a much simpler design method which is convenient to use. This revised model will be described below.

BASIC CONCEPTS - Before proceeding to the details of the mathematical model the basic concepts and outline of the approach will be discussed. If we consider a typical F/C scrubbing system, it might have the features shown in Figure 1. The gas leaving the source is hot and has a water vapor content which depends on the source process. The first step is to saturate the gas by quenching it with water. This will cause no condensation if the

particles are insoluble, but will if they are soluble. There will be a diffusiophoretic force directed away from the liquid surface.

Condensation is required in order to have diffusiophoretic deposition, any growth on insoluble particles, and extensive growth on soluble particles. Contacting with cold water or a cold solid surface is done next to cause condensation. While condensation occurs there will be diffusiophoretic and thermophoretic deposition as well as some inertial impaction (and, perhaps, Brownian diffusion). The particles in the gas leaving the condenser will have grown in mass due to the layer of water they carry.

Subsequent scrubbing of the gas will result in more particle collection by inertial impaction. This will be more efficient than impaction before particle growth because of the greater inertia of the particles. There may be additional condensation, depending on water and gas temperatures, and its effects can be accounted for as discussed above.

One can apply this general outline of F/C scrubbing to a variety of scrubber types and Figure 2 shows a multi-plate F/C scrubber system. It can be seen that the gas is saturated before entering the plate column, although this is not always necessary. The first plate can serve as the saturator and partial condenser. Generally, the efficiency of heat and mass transfer is so high (say, 80%+) on a well designed plate that most of the condensation occurs on the first plate.

In subsequent plates the gas is scrubbed by inertial impaction and there will be a minor amount of additional condensation. We have shown a simple counter-current column but other variations are possible.

The mathematical model is based on the process just described for a plate-type F/C scrubber. It is outlined on the following page.

- I. Saturate the gas before plate 1
 - A. Particles are collected at size " d_{p1} ".
 - B. No condensation occurs on the particles (they are assumed insoluble).
- II. Contact on plate 1
 - A. Particles are collected by impaction in the bubble formation zone, still at size " d_{p1} ".
 - B. Condensation occurs and particles grow to " d_{p2} ".
 - C. Diffusiophoretic deposition removes some particles from the gas in the froth layer on the plate. Thermophoresis and centrifugal deposition are neglected.
- III. Contact on plate 2
 - A. Particles are collected by impaction in the bubble formation zone at size " d_{p2} ".
 - B. Negligible condensation occurs.
- IV. Contact on subsequent plates has same characteristics as plate 2.

Although the model is somewhat idealized, it is well within the bounds of engineering accuracy and the precision of experimental measurements. One can always revise any stage of the model with a closer approximation of parameters if he wishes to examine the sensitivity of the method to parametric values. In our evaluations of the model we found that further refinements did not produce significant changes in predictions.

DIFFUSIOPHORETIC DEPOSITION

Particle deposition by diffusiophoresis was described by the following equation in our previous models ^{2,3,4}:

$$u_{pD} = \frac{\sqrt{M_1} D_G}{\left[y\sqrt{M_1} + (1-y)\sqrt{M_2} \right] (1-y)} \left(\frac{dy}{dr} \right), \text{ cm/s} \quad (1)$$

or,

$$u_{pD} = C_1 D_G \left(\frac{1}{1-y} \right) \frac{dy}{dr} \quad (2)$$

where D_G = diffusivity of water vapor in carrier gas, cm^2/s
 M_1 = molecular weight of water, g/mol
 M_2 = molecular weight of non-transferring gas, g/mol
 y = mole fraction water vapor, dimensionless
 r = distance in the direction of diffusion, cm

The molecular weight and composition function represented by " C_1 ", describes the effect of molecular weight gradient on the deposition velocity corresponding to the net motion of the gas due to diffusion (the "sweep velocity"). For water mole fraction in air ranging from 0.1 to 0.5, " C_1 ", varies from 0.8 to 0.88. We used a rough average of 0.85 for " C_1 ", for computing " u_{pD} " and consequent particle collection efficiency by integrating over the period of condensation.

Whitmore⁵ concludes that the fraction of particles removed from the gas by diffusiophoresis is equal to either the mass fraction or the mole fraction condensing, depending on what theory is used for deposition velocity. In other words, it is not necessary to follow the detailed course of the condensation process, computing instantaneous values of deposition velocity, and integrating over the entire time to compute the fraction of particles collected. One can simply observe that if some fraction of the gas is transferred to the liquid phase it will carry along its load of suspended particles.

We have used Whitmore's general concept but with two modifications. First, one can see from equation (1) that Whitmore's theory would be comparable to assuming that the particles move with the same velocity as the gas phase. We have chosen to retain the correction for molecular weight gradient, which means that we will compute the particle collection efficiency as 85% of the volume fraction of gas condensing on the cold surface.

The second modification concerns how to compute the proper value of the volume fraction of gas condensing. The problem is that not all of the condensate goes to the heat transfer surface; some of it goes to the suspended particles. As will be shown in detail later, the fraction of the condensate which causes particle growth depends on several factors and ranged from about 0.1 to 0.4 of the total condensate for the range of parameters we explored.

If one is concerned only with diffusiphoretic deposition the particle collection efficiency would, therefore, be 60% to 90% of that computed without accounting for condensation on particles. In the case of a scrubber which also employs inertial impaction the particles would be agglomerated to some extent by the diffusional sweep, so they would have higher mass and be easier to collect.

Without going into a detailed model of this phenomenon one could use either of two simplifying assumptions:

1. Assume that the condensation on particles causes no agglomeration.
2. Assume that the condensation on particles causes agglomeration and that the inertial impaction efficiency is sufficiently high that all of the particles swept to other particles will be collected by impaction.

The first assumption will lead to too low an efficiency and the second to too high an efficiency. However, the maximum difference between the two for a representative case of 25% of the volume condensing and 25% of that going to the particles would

be 5.3% (i.e., $0.25 \times 0.85 \times 0.25 \times 100$). This is a relatively small effect compared to the other uncertainties.

PARTICLE GROWTH

Particle growth is dependent on how well the particles can compete with the cold surface for the condensing water. There are several transport processes at work simultaneously in the condenser section of an F/C scrubber:

1. Heat transfer
 - a. From the gas to the cold surface
 - b. From the particles to the gas
2. Mass transfer
 - a. From the gas to the cold surface
 - b. From the gas to the particles

A mathematical model which accounted for these transport processes in addition to particle deposition has been described in EPA reports ^{2,3,4}. The portions of that model relating to particle deposition were deleted to provide a model which would describe particle growth in the absence of deposition. The basic relationships involved are as follow:

The rate of change of particle radius is given by a mass balance,

$$\frac{dr_p}{dt} = \frac{k'_{pG} (p_G - p_{pi})}{\rho_M}, \text{ cm/s} \quad (3)$$

where:

$$k'_{pG} = \frac{2 D_G P}{RT_G d_p p_{BM}} = \text{particle to gas mass transfer coefficient, gmol/cm}^2\text{-s-atm} \quad (4)$$

p_G = water vapor partial pressure in bulk of gas bubble, atm

p_{BM} = mean partial pressure to non-transferring gas, atm

r_p = particle radius, cm

T_G = gas bulk temperature, °K

ρ_M = molar density of water, gmol/cm³

p_{pi} = water vapor partial pressure at vapor-liquid interface, atm

Particle temperature can be computed from an energy balance:

$$h_{pG} (T_{pi} - T_G) + \left(\frac{\rho_p C_{pp} r_p}{3} \right) \frac{dT_{pi}}{dt} = k'_{pG} L_M (P_G - P_{pi}) \quad (5)$$

where:

$$h_{pG} = \frac{2k}{d_p} = \text{particle to gas heat transfer coefficient,} \quad (6)$$

cal/cm²-s-°K

where C_{pp} = heat capacity of particle, cal/g-°K
 k = thermal conductivity of gas, cal/cm²-s-°K/cm
 L_M = latent heat of vaporization for water, cal/gmol
 t = time, s

The overall energy balance for the gas-liquid interface is given by :

$$k'_G a_t L_M (P_G - P_{Li}) A_p dZ = h_L a_t (T_{Li} - T_L) A_p dZ + h_G a_t (T_{Li} - T_G) A_p dZ \quad (7)$$

where k'_G = mass transfer coefficient, gas to liquid, gmol/cm²-s-atm
 a_t = interfacial area for transfer volume of scrubber, cm²/cm³
 A_p = cross-sectional area of scrubber, cm²
 h_G = heat transfer coefficient, gas to liquid, cal/cm²-s-°K
 T_L = temperature of liquid bulk, °K

The equations given above are used along with enthalpy and material balances for the total system of gas, liquid, and suspended particles to form a mathematical model for condensation and growth. The model was solved through a finite difference method on an electronic computer for several situations which are discussed below.

PREDICTION OF CONDENSATION

The condensation model was used to predict the particle condensation ratio, f_p , (which is the fraction of the total condensate which goes to the particles) as a function of several parameters. The conditions investigated are as follow:

1. Scrubber type - one sieve plate
2. Inlet gas - saturated from 310°K to 350°K
3. Water - uniform bulk temperature from 310°K to 325°K
4. Particle number concentration - 10^7 to 10^9 /cm³
5. Particle diameter - 0.1 to 1.0 μ m
6. Liquid phase heat transfer coefficient - 0.01 to 0.1 cal/cm²-s-°K
7. Condensation can occur when the gas is saturated

The computed values are plotted on Figures 3 through 7. As can be seen, the figures show the following:

- (Figure)
3. " f_p " does not depend much on " d_p "
 4. " f_p " decreases significantly with " T_L "
 5. " f_p " decreases with " T_G " to an extent which depends on " T_L "
 6. " f_p " increases slightly with " n_p " above 10^7 /cm³
 7. " f_p " increases with " h_L " up to " h_L "
 ≈ 0.1 cal/s-cm²-°K

It was found in computations not reported here that " f_p " decreases significantly with " n_p " below about 10^6 particles/cm³. Industrial emissions generally have particle number concentrations on the order of 10^7 , and greater. The liquid phase heat transfer coefficient is an important parameter but unfortunately, predictions of its magnitude vary considerably depending on which correlation is used. The value of 0.1 appears to be the best supported by the literature for mass transfer on perforated plates.

For a combination of parameters such as might be encountered in a practical situation a value of " f_p " ≈ 0.25 appears to be reasonable. Given this one can compute the amount of particle growth that will result from a given condensation ratio (i.e., g water condensed/g dry gas = q = condensation ratio). If the particle size distribution and the scrubber characteristics are known one can predict the overall penetration that will be achieved in the scrubber.

INERTIAL IMPACTION DURING BUBBLE FORMATION

During the formation of bubbles on a sieve plate the jets of gas emerging from the perforations impact on the liquid. Particles are thus deposited on the liquid surface by inertial impaction. Particle collection can be determined from:

$$Pt_i = \exp \left(- \frac{40 F^2 d_p^2 \rho_p C' u_h}{9 \mu_G d_h} \right) \quad (8)$$

where F = foam density, volume fraction liquid

d_p = particle diameter, cm

ρ_p = particle density, g/cm³

C' = Cunningham slip correction factor, dimensionless

u_h = gas velocity in the perforation, cm/s

μ_G = gas viscosity, poise

d_h = diameter of perforation, cm

Pt_i = penetration of particles of diameter d_p , fraction

PERFORMANCE PREDICTION METHOD

The sequence of steps to be followed in predicting the performance of an F/C scrubber system involving a sieve plate column is as follow:

1. Determine the initial particle size distribution.
2. Compute particle penetration from the saturator based on the saturator collection efficiency characteristics and the initial particle size distribution. No growth occurs in the saturator.
3. Compute particle penetration due to inertial impaction during bubble formation on the first plate. Use the particle size distribution leaving the saturator and the collection efficiency relationship for sieve plate given in equation (8).
4. Calculate the condensation ratio corresponding to the scrubber operating conditions, from this compute " f_v ", the volume fraction of gas condensing, and then calculate the penetration due to diffusiophoresis according to equation (9)

for a conservative estimate or equation (10) for an optimistic estimate

$$1 - Pt_D = 0.85 (f_v) (1 - f_p) \quad (9)$$

$$1 - Pt_D = 0.85 f_v \quad (10)$$

The diffusiphoretic penetration applies equally to all particle sizes so it will not change the size distribution but will decrease the particle concentration.

5. Determine the particle size distribution leaving the condenser from the values of "q'" and "f_p". Figure 8 is a size distribution plot showing lines for the particles before and after condensation. The conditions used for this plot were:

$$\begin{aligned} \text{Initial } d_{pg} &= 0.75 \text{ } \mu\text{m} = \text{dry mass median diameter} \\ \sigma_g &= 2.5 = \text{geometric std. deviation} \\ n_p &= 10^9 / \text{DNcm}^3 \text{ (Dry Normal cm}^3, @ 0^\circ\text{C)} \\ q' &= 0.3 \text{ g/g} \\ f_p &= 0.25 \end{aligned}$$

6. Compute the particle penetration function for the remaining stages of the scrubber, based on the penetration for one stage given by equation (8). The penetration for a given particle diameter on one stage is "Pt_i". For "N" stages of equal efficiency the penetration for a given particle diameter is "Pt_i^N".

7. Use the relationship between "Pt_i^N" and "d_p" from step 5 and the grown size distribution from step 5 to compute the overall penetration due to inertial impaction after growth.

8. To summarize, the total overall penetration for the F/C scrubber \overline{Pt} will be the product of the following:

- a. " \overline{Pt}_a " due to impaction in the saturator
- b. " \overline{Pt}_b " due to impaction in the condenser
- c. " \overline{Pt}_c " due to diffusiphoresis in the condenser
- d. " \overline{Pt}_d " due to impaction in stages after the condenser.

Thus,

$$\overline{Pt} = \overline{Pt}_a \times \overline{Pt}_b \times \overline{Pt}_c \times \overline{Pt}_d \quad (11)$$

COMPARISON WITH DATA

Predictions based on the model described above were made for a number of experimental determinations on a 100 m³/min sieve plate F/C scrubber. Some examples of comparisons of predictions with experimental results are shown in Figures 9 and 10. The correlation shown in Figure 9 is the best obtained and that in Figure 10 is representative of the average case.

CONCLUSIONS

The revised model is much simpler to use than our previous version and it appears to give very good predictions. It also offers the opportunity for easy modification to suit specific situations. The fraction condensing on the particles is a key quantity and it needs more study for plates and other contacting systems.

REFERENCES

1. Calvert, S., J. Goldshmid, D. Leith, and D. Mehta. Scrubber Handbook. A.P.T., Inc., EPA Contract No. CPA-70-95. NTIS No. PB 213-016. August, 1972.
2. Calvert, S., J. Goldshmid, D. Leith, and N. Jhaveri. Feasibility of Flux Force/Condensation Scrubbing for Fine Particulate Collection. A.P.T., Inc., EPA Contract No. 68-02-0256, NTIS No. PB 227-307. October, 1973.
3. Calvert, S., and N. Jhaveri, and T. Husking. Study of Flux Force/Condensation Scrubbing of Fine Particles. A.P.T., Inc., EPA Contract No. 68-02-1082. August, 1975.
4. Calvert, S., and S. Yung. Study of Horizontal Spray Flux Force/Condensation Scrubber. A.P.T., Inc., EPA Contract No. 68-02-1328, Task No. 10. July, 1976.
5. Whitmore, P.J. Diffusiophoretic Under Turbulent Conditions, Ph.D. Thesis, University of British Columbia, 1976.

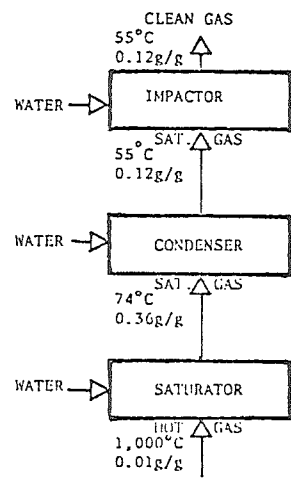


Figure 1. Generalized F/C Scrubber System.

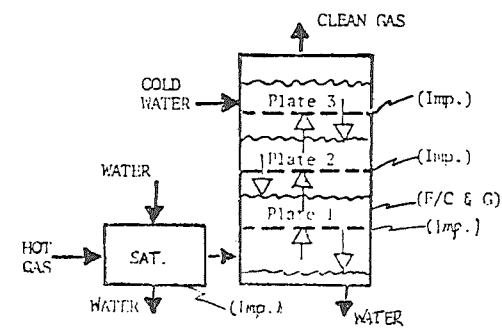


Figure 2. Multiple plate F/C scrubber system.

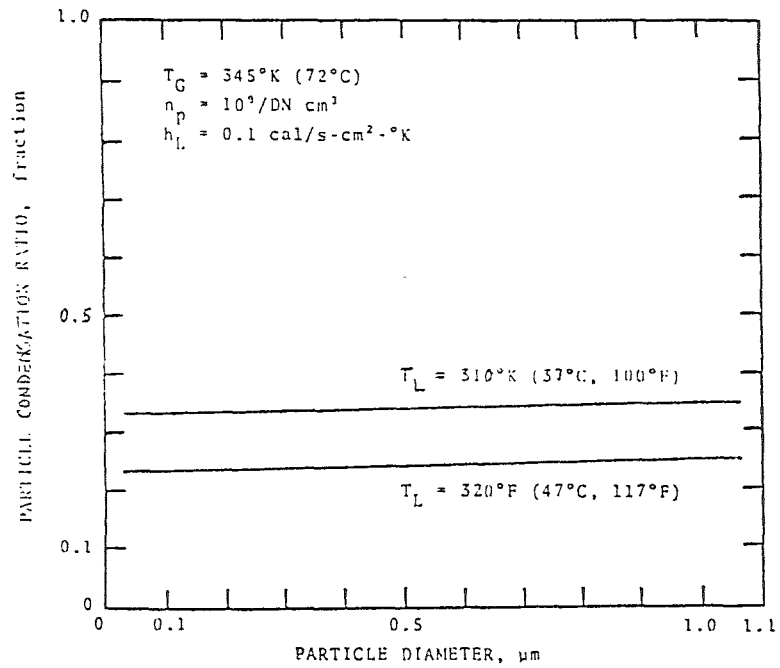


Figure 3. Effect of particle diameter on condensation ratio.

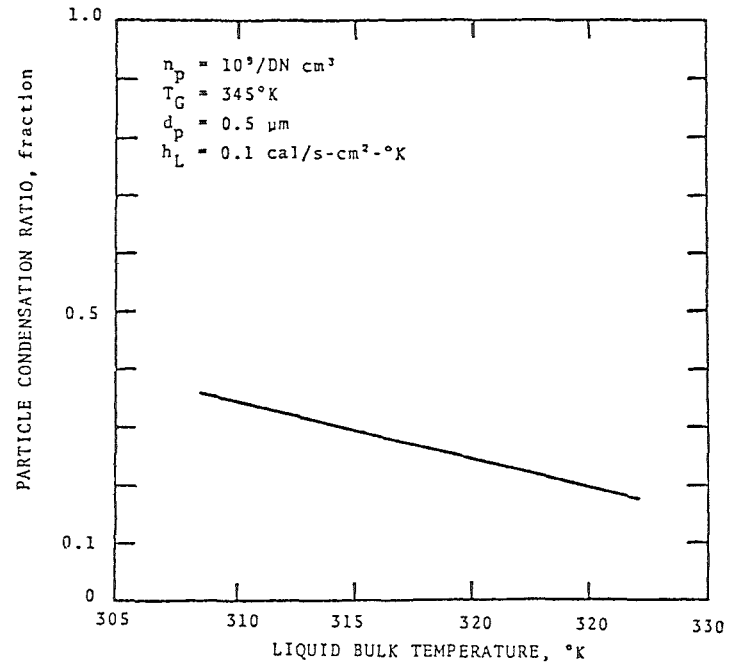


Figure 4. Effect of liquid bulk temperature on condensation ratio.

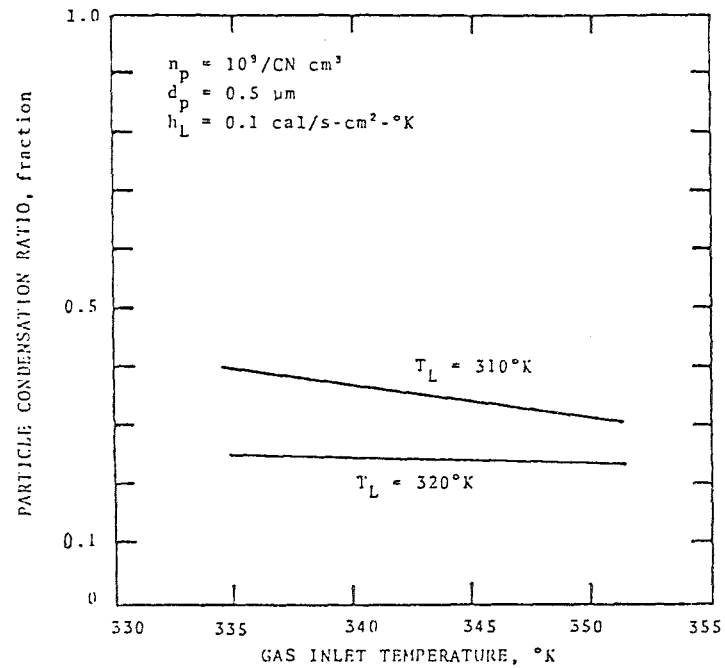


Figure 5. Effect of gas inlet temperature on condensation ratio.

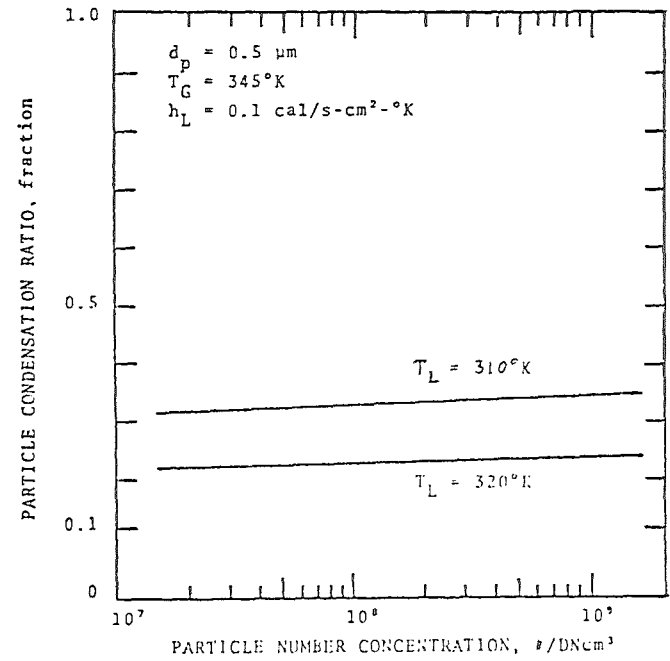


Figure 6. Effect of particle number concentration on condensation ratio.

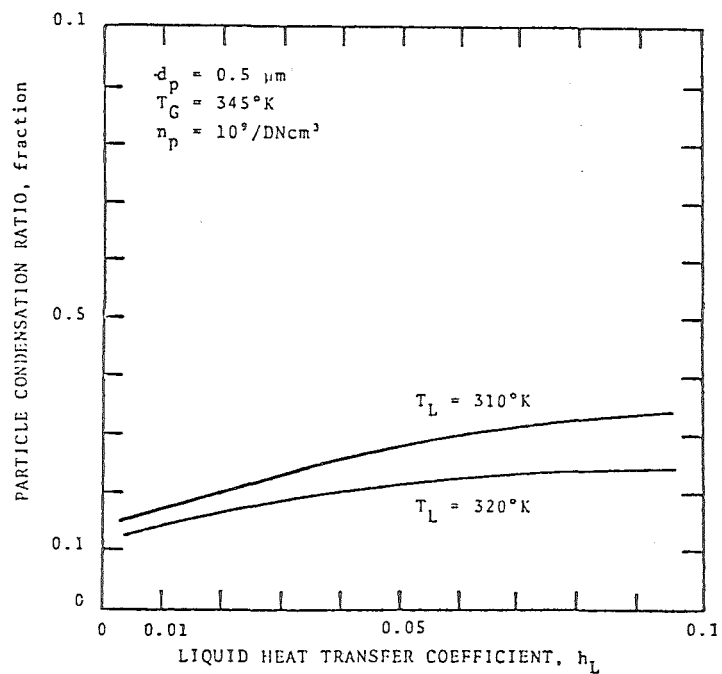


Figure 7. Effect of liquid heat transfer coefficient on condensation ratio.

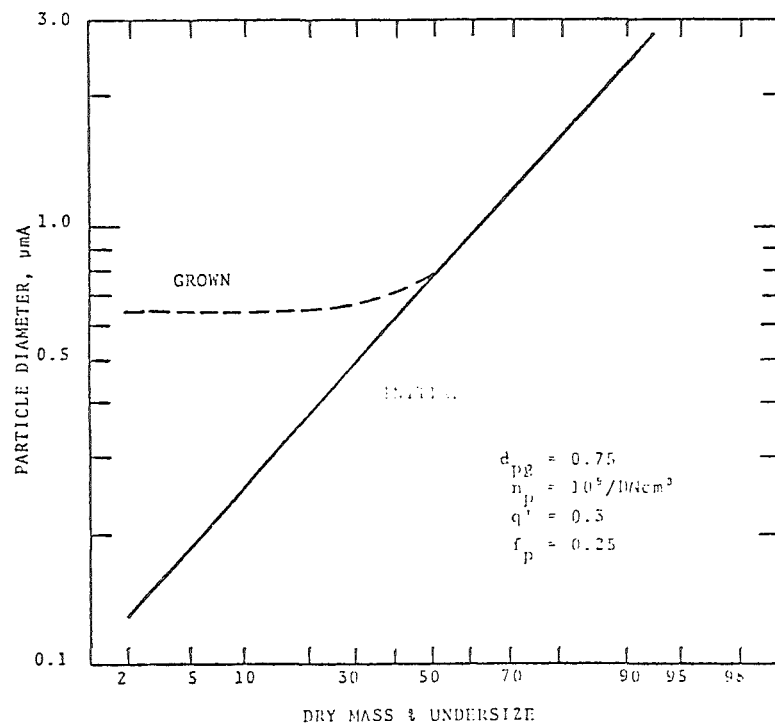


Figure 8. Particle size distribution before and after condensation.

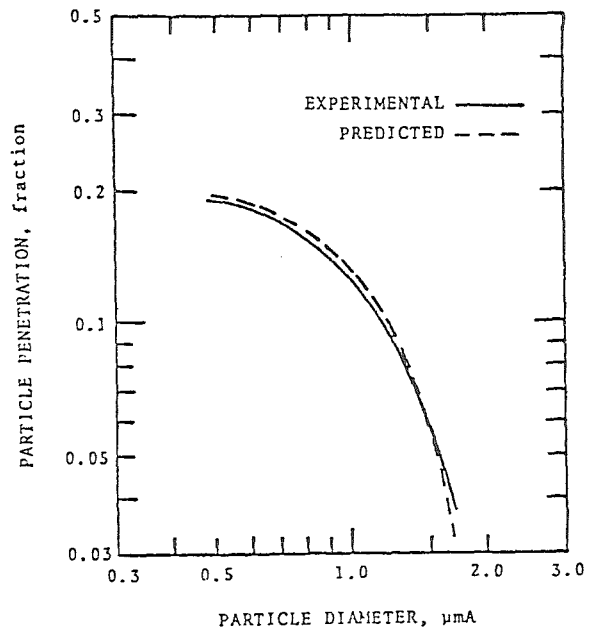


Figure 9. Particle penetration versus aerodynamic diameter for Run 64.

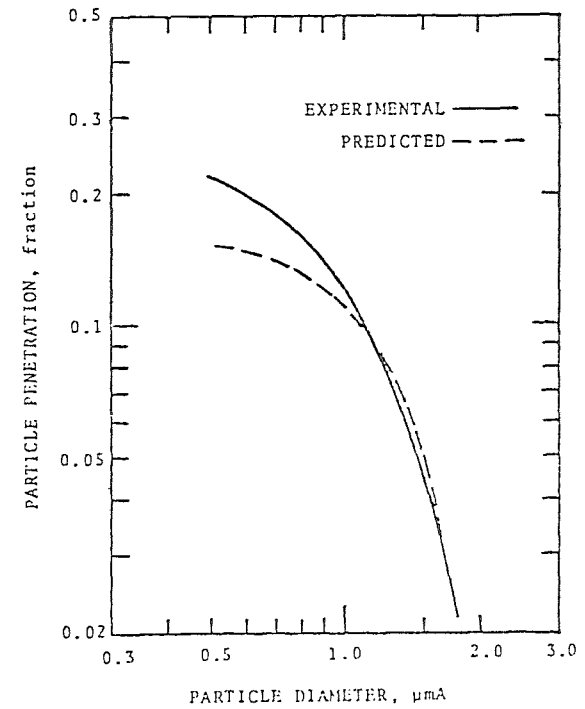


Figure 10. Particle penetration versus aerodynamic diameter for Run 69.

Discussion

Prof. Weber said experience indicated that a few particles were used as a condensation nucleus. Hot and cold streams of air were mixed after which spontaneous condensation, a disadvantageous process, occurred. The experiments reported in the paper were not, according to Dr. Calvert, with hot and cold air. Instead, hot gas came into contact with water, thus producing a gradual temperature gradient and a liquid film.

Experimental data on condensation scrubbing was consistent with the high concentration of particles. The model fitted with the data from pilot studies and laboratory experiments. Dr. Holighaus inquired whether condensation occurred at all outside the water surface. Dr. Calvert replied that cold drops of water were vaporized into saturated gas, each water drop having the same heat capacity. Super-saturation and condensation of the particles took place and air mixed with a boundary layer. Dr. Holighaus pointed out that this layer consisted of heat and mass.

Mr. Calvert said that the contrary had been proved by laboratory experiments with plate columns and sprays: condensation was present, and an important mass transfer coefficient in gas to heat occurred.

APPLICATION OF HIGH GRADIENT MAGNETIC SEPARATION
TO FINE PARTICLE CONTROL

Charles H. Gooding
Research Triangle Institute
Energy and Environmental Research Division
P. O. Box 12194
Research Triangle Park, NC 27709

Presentation for the
USA/FRG Particulate Workshop
Jülich, West Germany
March 16-17, 1978

INTRODUCTION

Several widely-used industrial processes, primarily in the iron and steel and ferroalloy industries, emit large quantities of waste gas containing magnetic particles. Particulate emissions from these processes are presently controlled with varying degrees of success by conventional technologies such as electrostatic precipitation, wet scrubbing, and fabric filtration. In the last decade research and commercial applications have demonstrated that high gradient magnetic separation (HGMS) is an effective and economical method of removing small, weakly-magnetic particles from selected liquid streams[1], and generalized theory indicates that the process should also be applicable to the control of fine, magnetic particle emissions from industrial stacks.

BASIC CONCEPT OF THE PROCESS

In essence HGMS is an enhanced filtration process. The fundamental concept is the collection of small particles on ferromagnetic fibers that are immersed in a uniformly applied magnetic field. The ferromagnetic fibers induce regions of highly non-uniform magnetic field intensity, and the particles are attracted to the fibers' surface by magnetic force.

In its most simple practical form, the high gradient magnetic separator consists of a canister packed with a fibrous, ferromagnetic material such as steel wool (Figure 1). The canister is located in a magnetic field that is normally generated by a solenoid, and the magnetic traction force provides high-efficiency collection of particles as the gas passes through the canister. When the collection matrix becomes fully loaded, the magnetic force is removed and the particles may be flushed from the matrix with a pulse of pressurized air. This can be accomplished by using a system of several modules such as the one depicted in Figure 1 in a parallel-flow, cyclic mode of operation. That is, each module undergoes a period of filtration. Then the flow is diverted to other modules; the magnetic field of the loaded module is

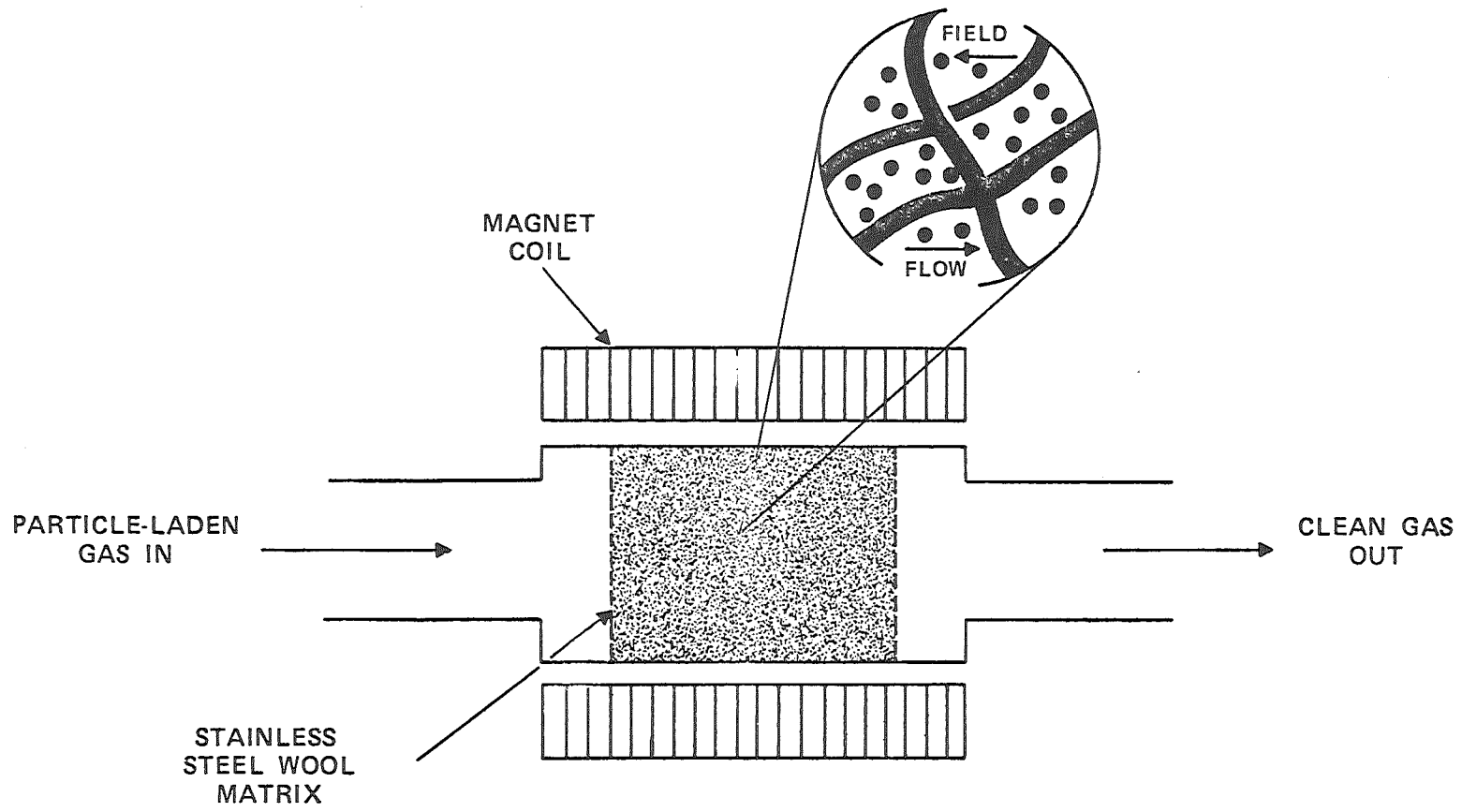


Figure 1. Schematic representation of a high gradient magnetic separator.

deenergized; the matrix is cleaned; the field is reenergized; and filtration resumes. An alternate continuous scheme, which results in better utilization of the magnetized volume, is to construct the magnet and matrix so that the dirty matrix can be removed from the magnetized region into a non-magnetized cleaning region and continuously replaced by clean matrix material without interrupting the filtration process.

High gradient magnetic separation is widely used on a commercial scale in the clay industry to remove fine paramagnetic color bodies from slurries of kaolin[1]. Laboratory and pilot-scale investigations have been conducted to assess other liquid system applications in mineral processing[2,3], wastewater treatment[3], and coal cleaning[4,5,6]. Several of these programs are current, and other commercial applications of HGMS seem likely to occur over the next few years.

POTENTIAL APPLICATIONS FOR FINE PARTICLE CONTROL

With current magnet technology the capital costs and power requirements of large, iron-bound solenoids make HGMS potentially competitive with other particulate control methods. Since the filtration process is enhanced by the magnetic force, the void volume of the collection matrix can be much larger than in a conventional filter, allowing very high gas velocities at a relatively low pressure drop. This combination translates into a potential reduction in energy requirements compared to conventional particulate control techniques, even though production of the magnetic field requires some energy. High operating velocities help to reduce both the capital costs and space requirements of the equipment. Furthermore, the process as developed up to this stage is completely dry so it should avoid the water pollution problems associated with some scrubber installations. Magnetic stainless steels of the 400 series can be used as a collection matrix to make the process compatible with high temperature and corrosive environments, and the absence of any sparking mechanism in the collection process should allow its application in combustible gas streams.

The magnetic susceptibility and size distribution of the dust particles are the key parameters that will determine the practicality of fine particle emission control applications although other gas characteristics could affect economics to a lesser extent. Magnetic susceptibility of particulate matter cannot be predicted quantitatively from composition data alone, but the percentage of iron is a qualitative indicator. With relatively high iron concentrations even submicron particles should be collected efficiently and economically. Reported data on the particle size distribution and composition of dusts emitted from several processes in the iron and steel are shown in Table I. Emissions from ferroalloy processes are much more diverse, but the production of several alloys including silico-manganese, ferromanganese, and ferrochrome, results in the emission of particulate containing significant quantities of iron as well as other strongly magnetic species. All of these processes should be considered potential candidates for HGMS fine particle control.

DESCRIPTION OF COMPLETED EXPERIMENTAL WORK

The competitive methods of particulate emission control delineate practical constraints on the design of an HGMS device for stack gas applications. Technology is currently available to control particulate emissions from most industrial sources with a capital investment for uninstalled primary equipment no greater than \$8500 per cubic meter of gas flow per second (\$4/cfm). Power consumption is normally less than 3.2 kw/m³/s (2.0 hp/1000cfm) in precipitators and fabric filters, but can be many times greater in difficult applications where high-energy wet scrubbers must be employed. One can deduce from these general criteria and the cost and power requirements of conventional HGMS equipment that an HGMS control device would have to operate satisfactorily with a superficial gas velocity of at least 5 m/s (1000 ft/min), a pressure drop of less than 2.0 kPa (20 cm H₂O), and an applied magnetic field of less than 1.0 T in order to be competitive with other control methods in most applications.

At the beginning of this study bench-scale experiments were conducted to gain a preliminary evaluation of the practicality of the process.

TABLE I. EXPECTED CHARACTERISTICS OF UNCONTROLLED GAS STREAMS FROM SEVERAL PROCESSES

| Process | Dust Concentration g/m ³ | Mass Median Diameter μm | Iron Composition % Total Fe | Noteworthy Gas Characteristics |
|-----------------------------|--|----------------------------|--------------------------------|---|
| <u>Sinter Machine</u> | | | | |
| Windbox | 1-2 | 10 | 25-50 | 5-15% H ₂ O, hydrocarbons,, flourides, SO _x , 120-180 ^o C |
| Discharge End | 5-12 | 10 | 25-50 | 120-180 ^o C |
| <u>Blast Furnace</u> | | | | |
| | 10-25 | 100 | 35-50 | 20-40% CO, 2-6% H ₂ , 200-300 ^o C |
| <u>Basic Oxygen Furnace</u> | | | | |
| Open System | 10-25 | 1 | 55-70 | 250-300 ^o C |
| Closed System | 40-70 | 15 | 55-70 | 75% CO, 250-300 ^o C |
| <u>Electric Arc Furnace</u> | | | | |
| | 0.2-7 | 1 | 15-40 | 40-120 ^o C |
| <u>Open Hearth Furnace</u> | | | | |
| | 4-7 | 5 | 55-70 | 7-15% H ₂ O, 250-350 ^o C |
| <u>Scarfig Machine</u> | | | | |
| | 0.5-1 | 0.5 | 50-70 | H ₂ O saturated, 50-60 ^o C |

Dust from an industrial basic oxygen steelmaking furnace (BOF) was dispersed in an air stream and passed through a loosely-packed steel wool matrix contained in an 8.9 cm canister, which was positioned in the bore of an iron-bound solenoid. The unit was operated with superficial gas velocities up to 10.6 m/s (2100 ft/min), and high efficiency collection of dust was achieved with applied fields of 0.3 T or lower. Pressure drop through the matrix was normally less than 2.5 kPa (25 cm. H₂O). Figure 2 shows the dramatic reduction in the penetration of particles through the matrix that was achieved when relatively low magnetic fields were applied. These preliminary experiments confirmed that the HGMS process could be successfully applied to collect gas-borne particles and provided data from which a larger unit and a more systematic experiment were designed.

The layout of the second-phase, pilot-scale HGMS system is depicted schematically in Figure 3. Dusts from a BOF as well as an electric arc steelmaking furnace (EAF) were dispersed into a wind tunnel, and a 0.8 m³/s (1700cfm) slipstream was drawn off and processed through the HGMS pilot plant. A low efficiency cyclone was placed upstream of the HGMS to remove uncharacteristically large agglomerates that were not adequately broken up by the dispersion system. The magnetic separator consisted of a 30-cm diameter iron-bound solenoid surrounding a canister of loosely-packed 430 stainless steel wool. The ranges of the experimental operating parameters are given in Table II. The experiments were systematically designed so that the effects of individual parameters could

TABLE II. RANGES OF OPERATING PARAMETERS
IN HGMS EXPERIMENTS.

| | |
|--------------------------|--|
| Applied Field | 0 - 0.4 T |
| Matrix Packing Density | 0.005 - 0.010 |
| Matrix Length | 15 - 30 cm |
| Superficial Gas Velocity | 5.2 - 11.1 m/s (1020 - 2185 ft/min) |
| Gas Temperature | 25 - 110°C |

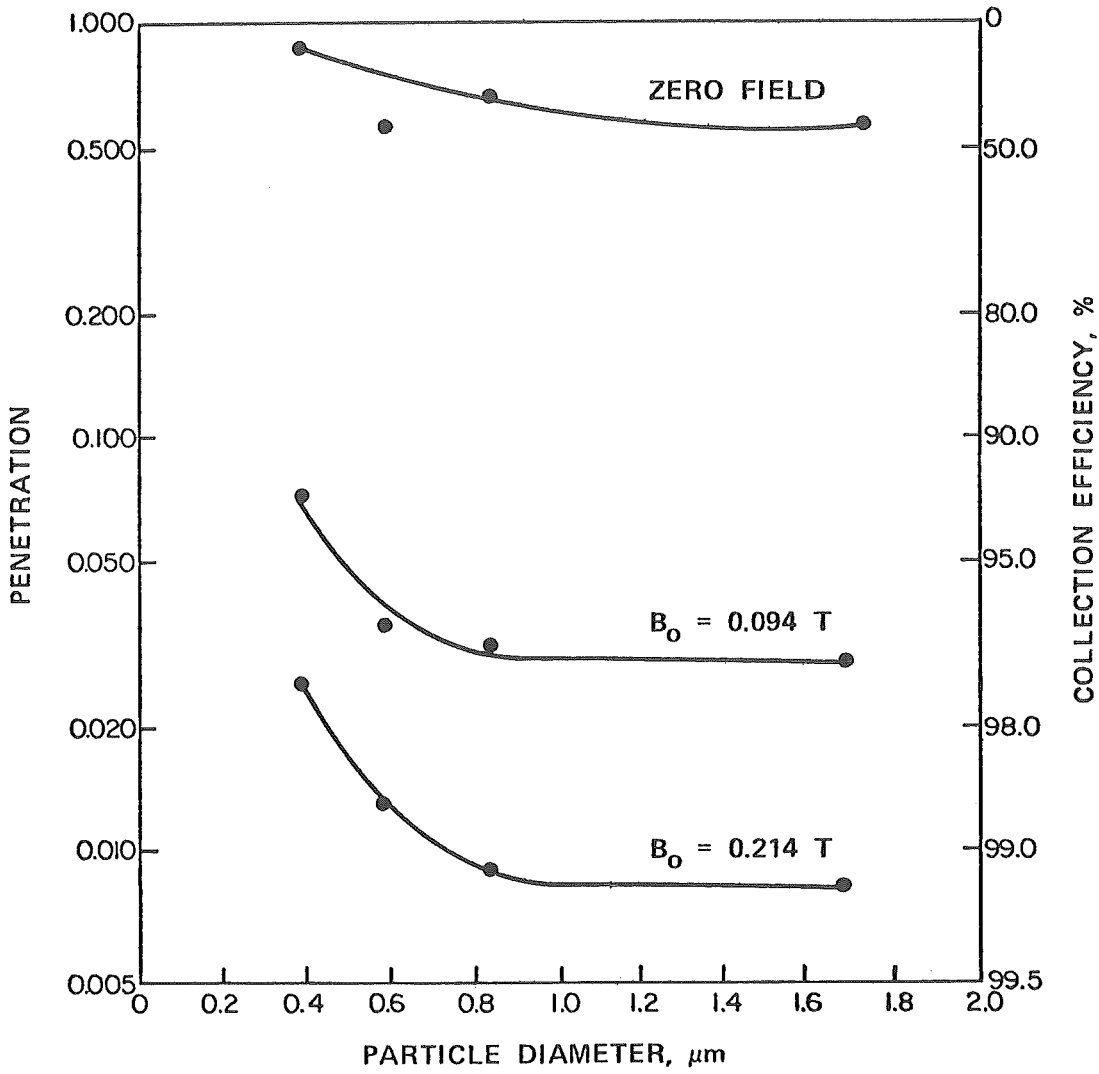


Figure 2. Bench-scale collection of B0F dust with a gas velocity of 8.4 m/s (1650 ft/min) and a pressure drop of 1.7 kPa (17 cm water).

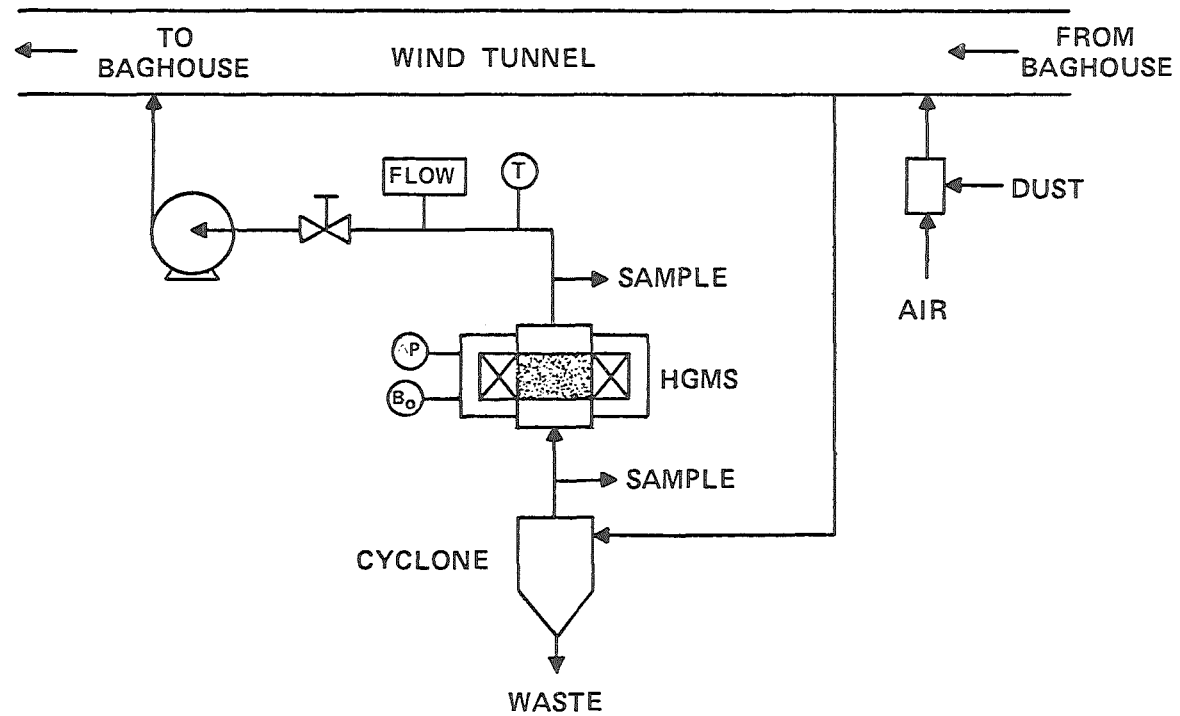


Figure 3. Schematic representation of pilot-scale HGMS facility.

be studied. Experimentally determined magnetization curves for the two dusts are shown in Figure 4.

After the operating conditions were established for a particular run, the fractional penetration of dust particles through the HGMS was determined as a function of particle size by using cascade inertial impactors to measure the concentration and size distribution of the dust upstream and downstream of the matrix. Since the impactors required approximately 90 minutes to collect an adequate sample, an optical (light-scattering) particle sizing device was also used to ensure that no significant upsets or transients occurred during the impactor sampling period.

PILOT-PLANT EXPERIMENTAL RESULTS FOR TWO DUSTS

The experimental efficiency with which the two dusts were collected under identical operating conditions is shown in Figure 5. As expected, the more strongly magnetic BOF dust was collected more efficiently than the EAF dust. The curves drawn in Figure 5 are predictions of a theoretical model. Basically the model predicts single-fiber collection efficiencies from a solution of the equations of motion that yields particle trajectories. The single-fiber efficiencies, R_c , are then extended to predictions of total matrix penetration, P , using the equation

$$P = \exp[-EFLR_c/a(1-F)]. \quad (1)$$

F is the matrix packing density; L is the matrix length; a is the fiber radius; and E is an "effectiveness factor," which was included to allow for deviations from the idealized assumptions of the model. Reasonable assumptions and geometric arguments predict the value of E to be $4/\pi^2$, but reduction of experimental data from all of the runs showed the BOF and EAF data to be better fit by E values of 0.09 and 0.07, respectively. It should be noted that the single-fiber collection efficiency can be

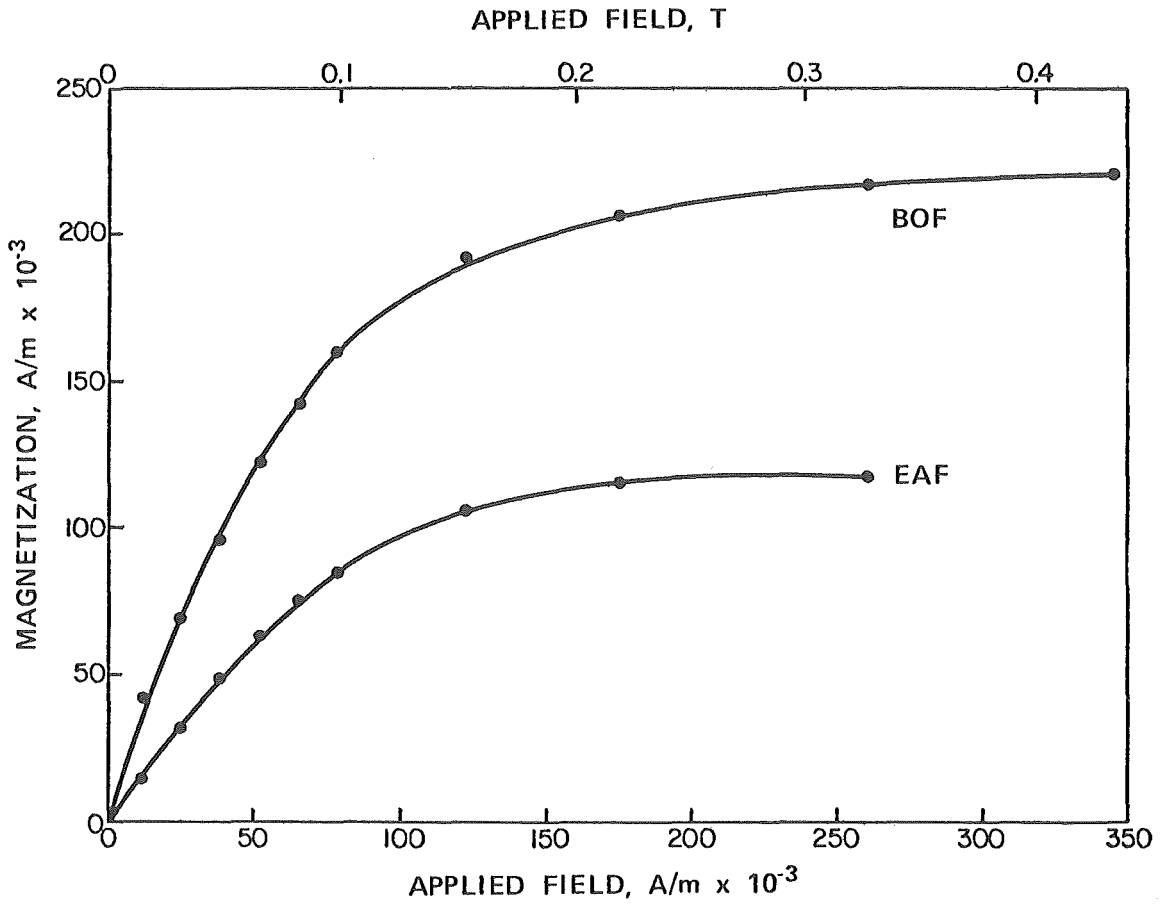


Figure 4. Magnetization curves of two steel industry dusts.

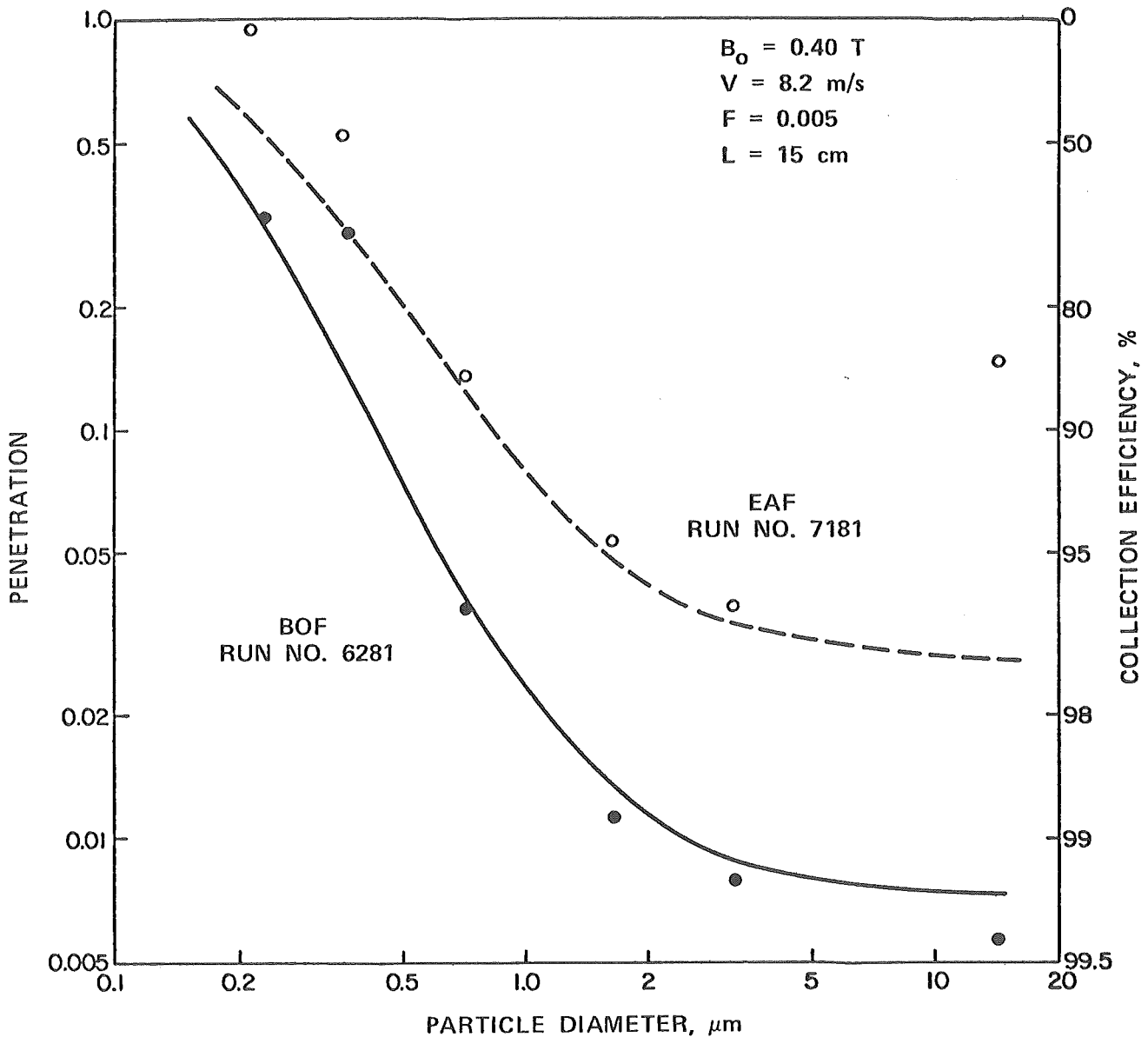


Figure 5. Experimental data and theoretical predictions of HGMS collection of two dusts under identical conditions.

greater than one because of the magnetic traction force. The development of the model is described in more detail elsewhere[7,8].

The effects of individual parameters on particle collection were found to be in reasonable agreement with theoretical expectations. The particle size and magnetic susceptibility dependence are illustrated in Figure 5. At lower fields and higher velocities, the penetration of larger particles tends to be greater than predicted. The reason for this observation is not yet fully understood, but it may be due to detrimental inertial effects that contribute to particle bounce and reentrainment. Gas velocity has a relatively small effect on the collection of submicron particles, and higher velocities may actually be beneficial by enhancing inertial impaction in those cases in which the single-fiber collection efficiency is less than one.

Higher magnetic fields enhance the collection of particles, but the effect is diminished as both the particles and matrix approach magnetic saturation. With dusts exhibiting magnetic properties similar to those shown in Figure 4, collection efficiency can probably be improved more economically by increasing the density or length of the collection matrix rather than increasing the applied field beyond 0.4 to 0.5 T. The experimental data confirm the effects of matrix density and length expressed in Equation (1).

Increasing the operating temperature could adversely affect particle collection since the gas viscosity (and hence the drag force on the particles) would be increased, and magnetization of the particles and matrix may be diminished. However, no significant effect of temperature could be discerned from a few experimental runs that were made at the higher temperature level used in this study.

Figure 6 demonstrates that both of the dusts studied in this work can be collected with high efficiency. The collection efficiency of the larger particles was not as high as the present model predicts (particularly the high-velocity BOF run) but was still greater than 99 percent. Based on currently available, continuous-cleaning HGMS equipment, projections

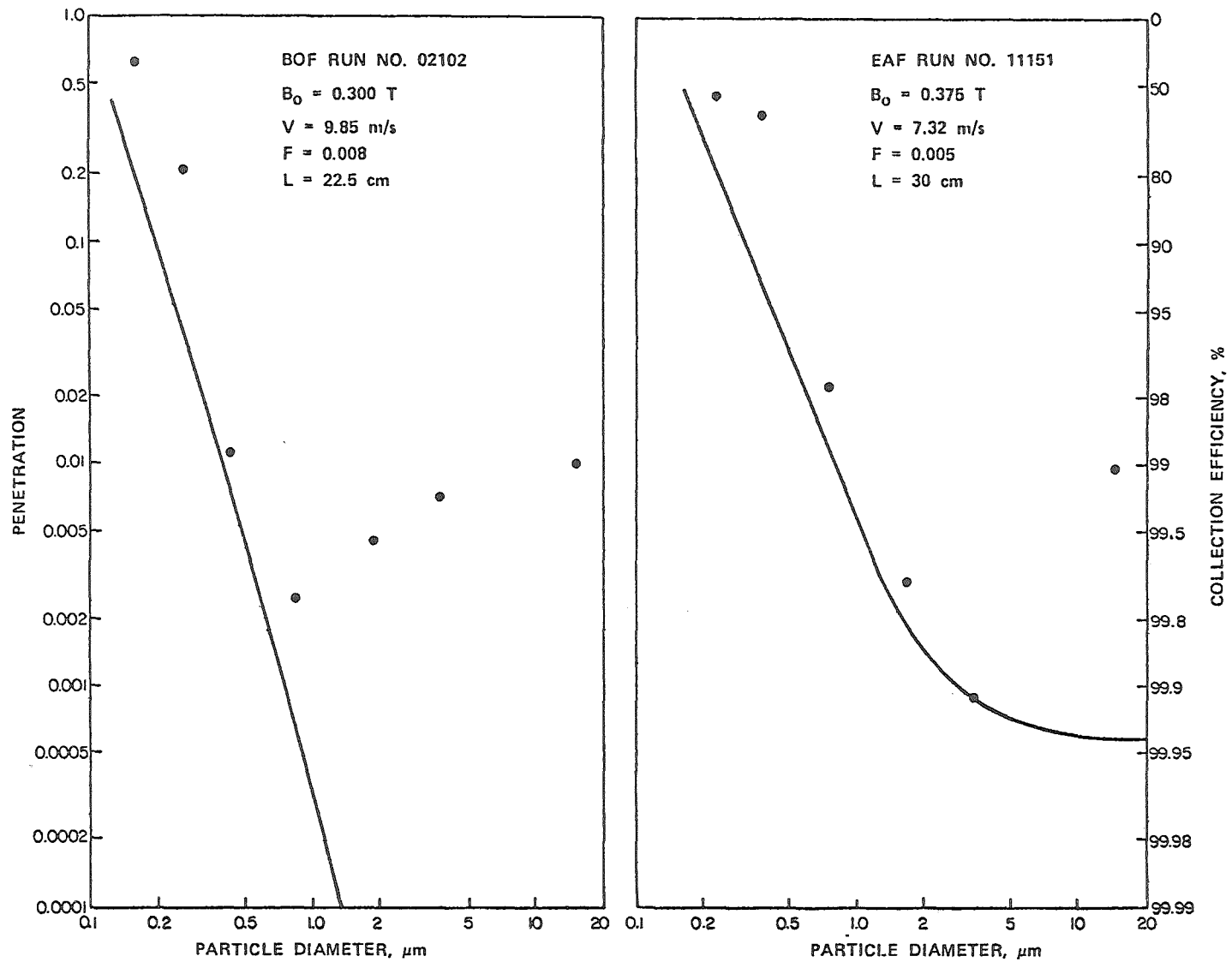


Figure 6. High-efficiency collection of BOF and EAF dusts: theory and experimental data.

for a full-scale, high-efficiency BOF dust collection device predict an uninstalled capital cost of \$8200/m³/s (\$3.86/cfm) and power requirements of 3.2 kW/m³/s (2.0 hp/1000cfm). Collection of the EAF dust would be slightly more expensive. These costs estimates were projected from a singular design and could possibly be lowered by optimization techniques.

CONCLUSIONS AND CONTINUING WORK

The results of this investigation indicate that HGMS may be an efficient and economical method of particulate emission control in selected applications in which relatively high susceptibility dust must be collected. Several processes in the iron and steel and ferroalloy industries are potential candidates for fine particle control by HGMS. The theoretical model provides a valuable tool to screen potential applications, to evaluate alternative designs, to plan experiments, to analyze data, and to conduct economic analyses.

Additional pilot plant data are being obtained to broaden current experience with the process and to quantify requirements for matrix cleaning. Refinement of the theoretical model is also continuing. A mobile pilot plant is being designed so that experiments can be conducted at industrial sites.

REFERENCES

1. Oder, R. R., High Gradient Magnetic Separation Theory and Applications, IEEE Trans. Magn., Vol. MAG-12(5), Sept., 1976, pp. 436-443.
2. Murray, H. H., Beneficiation of Selected Industrial Minerals and Coal by High Intensity Magnetic Separation, IEEE Trans. Magn., Vol. MAG-12(5), Sept., 1976, pp. 498-502.
3. Oberteuffer, J. A., Engineering Development of High Gradient Magnetic Separators, IEEE Trans. Magn., Vol. MAG-12(5), Sept., 1976, pp. 444-449.
4. Oder, R. R., Magnetic Desulfurization of Liquefied Coals: Conceptual Process Design and Cost Estimation, IEEE Trans. Magn., Vol. MAG-12(5), Sept., 1976, pp. 532-537.
5. Liu, Y. A., and C. J. Lin, Assessment of Sulfur and Ash Removal from Coals by Magnetic Separation, IEEE Trans. Magn., Vol. MAG-12(5), Sept., 1976, pp. 538-550.
6. Maxwell, E., D. R. Kelland, and I. Y Akoto, High Gradient Magnetic Separation of Mineral Particulates from Solvent Refined Coal, IEEE Trans. Magn., Vol. MAG-12(5), Sept., 1976, pp. 507-510.
7. Lawson, W. F., W. H. Simons, and R. P. Treat, The Dynamics of a Particle Attracted by a Magnetized Wire, J. Appl. Phys., Vol. 48(8), pp. 3213-3224, August, 1977.
8. Gooding, C. H., T. W. Sigmon, and L. K. Monteith, Application of High Gradient Magnetic Separation to Fine Particle Control, EPA-600/2-77-230. National Technical Information Service, Springfield, Va., 1978.

Discussion

In answer to Mr. McCain's question regarding methods of cleaning HGMS filters, Mr. Gooding replied that particles could be blown off the fibers by pulses of air. This method has been demonstrated in the laboratory, and work is being undertaken to design a unit to do this in a practical way. With high concentrations of dust in the gas the frequency of cleaning might be excessive. However, in the case of lower dust concentration gas streams, prospects are good.

Dr. Wiggers asked whether the number of cleanings was limited; Mr. Gooding said that although long term evaluation was needed, it appeared that the durability of the matrix against corrosion would be good. He clarified, at the request of Dr. Wiggers, that the matrix is made of inexpensive stainless steel wool.

Mr. Parker inquired whether fly ash from coal-fired boilers could be controlled. A few tests had been performed on eastern low sulfur coal, whose iron content was significant, replied Mr. Gooding. The results were not as good as those in the case of a steel mill dusts for which the process described in the paper was more suitable.

Mr. Donovan wondered if adhering magnetic particles could function like the collection matrix and enhance magnetic collection, or whether it were essential to remove all particles frequently. Mr. Gooding said that with weakly adhering magnetic particles the particles will begin to blow off as the matrix is loaded, resulting in inefficient collection. However, longterm tests with more strongly magnetic particles indicated constant collection efficiency: the wire grew and remained strongly magnetic. However, the pressure drop increased making cleaning necessary eventually.

Advanced Dust Collection Techniques in the Federal Republic of Germany: Selected Examples and Research Priorities.

Dipl.-Ing. G. GÜthner
Umweltbundesamt
Bismarckplatz
D-1000 Berlin 33

Within the scope of the First General Administrative Regulation under the Federal Immission Control Law (TA Luft 74) the particulate emissions of 35 stationary sources are restricted to values ranging from 20 to 300 mg/m³. In addition to the source-related standards for 55 hazardous materials limitations are provided; these materials are classified into three categories ranging from 20 to 75 mg/m³, respectively (table 1). This material related provision favours the application of those collection techniques which yield high collection efficiencies in the fine particulate range at modest energy consumptions; those techniques are mainly fabric filters and electrostatic precipitators, not at least wet electrostatic precipitators (WEP's). The new ruling should have its major impact in the metallurgical and chemical industry.

The following example, a Wet-EP application in a Tin-refining process might be typical: The refining facility consists of crucible furnaces in which the molten tin is treated with gaseous Chlorine. The flue gas which escapes from the furnaces contains Chlorides and Oxides of the impurities (mainly Lead and Zink) and trace of Chlorine; it used to be blended with the flue gases from a Tin scap melting furnace containing organic aerosols. The TA Luft restricts emissions of Lead compounds to 20 mg/m³, of Zink compounds to 50 mg/m³ and of gaseous inorganic chlorine compounds to 30 mg/m³ (calculated as CL⁻). It has been decided to install a WEP because pilot-Venturi scrubbers and pilot Dry electrostatic precipitators have not performed satisfactory. It can be gathered from table 2 that the dean gas dust concentration of the full size unit is only 2 to 5 mg/m³ and far below the design value of 20 mg/m³. The concentration of gaseous chlorine has been determined at 10 - 15 mg/m³, but this value seems arbitrary, because it has been measured only once at a ph-value of some 2,5 (instead of 6 to 8 at regular conditions). The precipitator

is of the parallel plate type with stainless steel internals and casing. A major design feature is the possibility to remove the electrodes easily, because their life time should not exceed two years, due to corrosion attack by the Chlorides.

Explanation of Slides. Emission control of an anode baking furnace in a primary Aluminum plant is another successful application of the WEP's. The flue gas characteristics of such a furnace are listed in table 3 (column one for the raw gas and column 5 for the clean gas). The design requirements have been 90 % collection efficiency for SO_2 , 95 % for HF and 97 % for tar. Two precipitators in line, one operating dry for tar collection only, and the second equipped with continuously spraying nozzles to remove gases and tar simultaneously have been installed. Both precipitators are of the parallel plate type, with plane collection plates and rigid discharge frames. The specific collection area is some $70 \text{ m}^2/(\text{m}^3/\text{sec})$ in both precipitators. SO_2 - and HF removal is achieved by a double alkaline absorption process; i.e. the primary (scrubbing) circuit is operating with Na OH, which is being recovered by $\text{Ca}(\text{OH})_2$ in the secondary (water treatment) circuit.

Heavy built up and corrosion problems have been encountered during start up of the plant. The built up problem has been solved by treating the recovered NaOH with CO_2 -containing flue gas, thus lowering its Ca-ion contents. To cope with corrosion it has been necessary to line the casing with fiber glass coating and to replace the mild steel internals by those from stainless steel. The actual price for such an installation should be some DM 70/ (Nm^3/h) for conditioning tower, precipitators, fans and ducts. Inclusion of the water treatment system will raise the price to DM 100/ (m^3/h). Energy consumption without water treatment system is some 2,8 kWh/1000 m^3 . The water treatment system will add some 0,5 kWh/1000 m^3 . The benefits of such an installation are - besides from air pollution control - that no waste water has to be drained, that the sludge can be dumped and the tar be reused for anode making after some additional treatment by the tar supplier.

Explanation:

Slide 3 + 4 Anode Baking installation.

Application of fabric filters for control of gaseous and particulate

emission by use of dry agents is a well known technique for Aluminum reduction furnaces. The use of additives not for gaseous emission control but to render possible bag cleaning has been successfully tested with the emission control system of a glass melting furnace. The need to develop the new technology has arisen when dedusting of flue gases from a Lead-Boron-Silicone glass furnace turned out to be impossible because the bags of a conventionally operated fabric filter have been clogging rapidly. The suitability of Dolomite, Calciumhydroxide and Alumina ($\text{Al}_2\text{O}_3 \times \text{H}_2\text{O}$) for additives has been tested with a pilot plant. Each of these materials serve as raw material for the glass furnace. It turned out that only Alumina could be used, because with Calciumhydroxide the dosing screws have been plugged and Dolomite has caused rapid wear of the bags.

The operation data of the full size unit are listed in table 4. Major components of the installation are the plate cooler (to reduce the gas temperature from 700°C to 200°C), two pulse jet filters with fans in parallel and the additive-dosing system. Each filter and fan are capable to handle the total gas flow. The additive is fed into the system before the cooler by a metering screw. Whilst dust concentration of the raw gas is some $0,5$ to $0,7 \text{ g/m}^3$ it is increased by the additive feed to 4 to 6 g/m^3 . The clean gas dust concentration is less than 5 mg/m^3 . This result should be compared with the TA-Luft standards of 20 mg/m^3 and 75 mg/m^3 for Lead and Boron, respectively.

An explanation for the excellent dust cake removal may be given by electron microscope photographs, which reveal that the submicron Lead-Boron sublimates are aggregated to the large 10 to 30 Alumina particles in thin uniform layers, but they do not stick to each other. It is another advantage of this process that the dust from the hoppers can be reused for feed of the furnace, which has not been possible at comparable installations without additives.

Explanation.

Some TA Luft provisions have strongly influenced the design of electrostatic precipitators for power stations, too. The TA Luft rules that Particulate emission from coal fired water tube boilers

be restricted to 150 mg/m^3 , even if one field of each chamber (i.e. parallel section) is out of service. So far there are two operating 600 - 700 MW utility power stations in the Federal Republic whose precipitators have been designed by consideration of these requirements. Some design and operation data are presented in table 5. The most outstanding design features are large specific collection areas, a far-going sectionalization (No. of HV-groups) and collection plate heights with up to 14,7 m. What is not mentioned in the table are the very tough warranty requirements in terms of corrosion prevention, rigidity of electrode frames and plates and on life time of electrodes; e.g.: no more than 8 wire ruptures during the first year of operation are accepted with installation I and no more than 10 ruptures for 2 years with installation II. (0.012 % and 0.01 %, respectively). But the performance is remarkable too, because the average clean gas dust concentrations are less than one third of the TA-Luft standard with both installations.

It should be mentioned that the present 700 MW dry bottom boilers have been preceded in the early 70 ties, by 350 MW wet bottom boilers. The precipitators to those installations have also been designed to meet the 150 mg/m^3 standard but with two fields and specific collection areas of $75 \text{ m}^2/(\text{m}^3/\text{sec})$ only. As the emission of such an installation proved to be considerably higher than anticipated a third field had been retrofitted, thus increasing the collection area to $100 \text{ m}^2(\text{m}^3/\text{sec})$;

Explanation

The R&D activities on dust collection technology - under funding by the Umweltbundesamt - are strongly application related. The major objectives of any of these projects are extension of the respective technology to new applications and minimization of overall expenditure related to efficiency.

On electrostatic precipitators a pilot study is being conducted to evaluate whether further sectionalization could be a means to increase overall migration velocity. For this purpose the sparkover voltage distribution will be measured in a pilot precipitator and in a full size unit and the feasibility of appropriate design modifications be studied.

Within the scope of a second project on precipitators the influence of passage width on migration velocity shall be studied. This investigation has mainly been initiated to prove findings of some researchers and a precipitator manufacturer predicting an increase of migration velocity with passage width (at constant field strength). Confirmation of these anticipations would offer an interesting approach to lower the overall expenditure of precipitators.

Scrubbers, in particular Venturis shall be optimized by means of pilot tests at various sources, mainly in the metallurgical industry. The major design features to be varied will be throat shape and water supply configuration. Collection efficiency and power requirement in dependence upon operation mode and design will be studied. In addition criteria for the transfer of pilot results to full size units shall be developed.

Another pilot investigation is being conducted with fabric filters. This project has mainly been conceived to extend the application range to new sources, in particular in the metallurgical and chemical industry and to industrial coal- and Oil-fired boilers. Another objective is the evaluation of collection efficiency in dependence of bag deterioration and mode of bag cleaning.

Any of these projects has been conceived not only to improve the technology but also to produce data on fine particle emission by means of particle size distribution measurements.

Table 1:

Emission Standards for Hazardous Materials in the Federal Republic of Germany

| | | | | | | | |
|----------|-----|----|----------------|----|---|---|----------------------|
| Category | I | -- | (m > 0.1 kg/h) | -- | c | ≤ | 20 mg/m ³ |
| Category | II | -- | (m > 1 kg/h) | -- | c | ≤ | 50 mg/m ³ |
| Category | III | -- | (m > 3 kg/h) | -- | c | ≤ | 75 mg/m ³ |

m = raw gas mass-flow

c = clean gas dust concentration

| <u>M a t e r i a l:</u> | <u>Category:</u> |
|---|------------------|
| Aluminum carbide | III |
| Aluminum nitride | III |
| Ammonium compounds | III |
| Antimony and its soluble compounds *) | II |
| Arsenic and its soluble compounds *) | I |
| Asbestos | I |
| Barium sulfate | III |
| Barium compounds if soluble *) | II |
| Beryllium and its soluble compounds *) | I |
| Bitumen | III |
| Boron trifluoride | II |
| Boron compounds, if soluble *) | III |
| Lead and its soluble compounds *) | I |
| Cadmium and its soluble compounds *) | I |
| Calcium arsenate | I |
| Calcium cyanamide | III |
| Calcium fluoride | II |
| Calcium hydroxide | III |
| Calcium oxide | III |
| Chromium compounds, if hexavalent | I |
| Cristobalite with particles smaller than 5 μm | II |
| Fluorine compounds, if soluble *) | I |
| Fluorspar | II |

| <u>M a t e r i a l :</u> | <u>Category :</u> |
|--|-------------------|
| Iodine and its compounds | II |
| Diatomaceous earth | II |
| Cobalt and its compounds | II |
| Copper and its soluble compounds *) | III |
| Copper fume | I |
| Magnesium hydroxide | III |
| Magnesium oxide | III |
| Molybdenum and its soluble compounds *) | III |
| Nickel | I |
| Nickel carbonate | I |
| Nickel oxide | I |
| Nickel sulfide | I |
| Phosphates | III |
| Phosphorus pentoxide | I |
| Quartz with particles smaller than 5 μ m | II |
| Mercury and its compounds, except cinnabar | I |
| Soot | II |
| Selenium and its soluble compounds *) | I |
| Silver compounds, very soluble, e.g. silver nitrate*) | II |
| Ferrosilicon | III |
| Silicon carbide | III |
| Strontium and its compounds | II |
| Tar | II |
| Cutback pitch | II |
| Tellurium and its soluble compounds *) | I |
| Thallium and its compounds | I |
| Tridymite with particles smaller than 5 μ m | II |
| Uranium and its compounds | I |
| Vanadium and its compounds | I |
| Bismuth | III |
| Tungsten and its compounds, except tungsten carbide | III |
| Zinc and its compounds | II |
| Dusts of organic compounds, e.g. anthracenes, aromatic amines, 1,4-Benzoquinone, naphthalene | II |

*) Soluble compounds are those materials which are soluble in the respiratory and digestive tracts, on the surface of the skin or in the absorbing organs of plants to such a degree that they can cause hazardous effects.

| | WEP Inlet | WEP Outlet |
|---|-----------|------------|
| Gas Flow [m ³ /h] | 10.000 | 10.000 |
| Gas Temperature [°C] | ~60 | ~30 |
| Dust Concentration [mg/m ³] | 2.000 | < 5 |

| | | |
|--------------------------|---|-----------|
| Spec. collection area | [m ² /(m ³ /sec)] : | 75 |
| Spec. filter current | [mA/m ²] : | 0,2 - 0,5 |
| N ^o of fields | [-] : | 2 |
| Liquid to gas ratio | [dm ³ /m ³] : | 1,5 |
| Energy consumption | [kWh/1000m ³] : | 1,8 |
| Capital expenditure | [DM/(m ³ /h)] : | 50 |

pH-control by Ca(OH)₂

| | | |
|-------------|---|--|
| UBA 1978 | Wet Electrostatic Precipitator to a Tin Refining Process | |
|-------------|---|--|

| | <u>Design Data</u> | | | <u>Operation Data</u> | |
|--------------------------------------|--------------------|----------------|-------------------|-----------------------|----------|
| | Inlet (Tar Prec.) | Outlet WEP | | Outlet | |
| | | Existing inst. | New inst. | Tar prec. | WEP |
| Gas flow [m ³ /h] | 40.000 | | | ~ 35.000 | ~ 35.000 |
| Gas temperature [°C] | 110 | ~ 40 | ~ 40 | 75 | 40 |
| SO ₂ [mg/m ³] | 1.000 | 100 | 50 | - | 40-60 |
| HF [mg/m ³] | 100 | 5 | 1,3 (gas + solid) | - | < 3 |
| Tar [mg/m ³] | 1.500 | 50 | 50 | - | ~ 25 |
| Dust [mg/m ³] | 150 | 50 | 1 | - | ~ 15 |

Liquid to gas ratio of wet electrostatic precipitator [dm³/m³]: 1,25

| | |
|-------------|--|
| UBA 1978 | Emission Control of Flue Gas from an Anode-Baking Furnace by Combined Dry (Tar) and Wet Electrostatic Precipitators |
|-------------|--|

Table 3

Gas flow $[Am^3/h]$: 2820
 Temperature before cooler $[^{\circ}C]$: max. 700
 Temperature before filter $[^{\circ}C]$: 200
 Dust concentration before filter $[mg/Am^3]$: 500
 Dust concentration after filter $[mg/Am^3]$: ≤ 5
 Differential pressure $[Pa/mmWG]$: 1.900 / $\sim 4,4$
 Pulse air consumption $[Nm^3/h]$: 10
 Pulse air pressure $[bar/psig]$: 4 / ~ 60
 Energy consumption (total) $[kWh/1000Am^3]$: 3,9
 Energy consumption main fan $[kWh/1000Am^3]$: 1,3
 Energy consumption pulse air $[kWh/1000Am^3]$: 1,0
 Energy consumption cooler fans $[kWh/1000Am^3]$: 1,6
 Filter rate $[m^3/(m^2 \cdot min)]$: 1,8
 Bag material TEFLON needle felt
 Adsorbent (for additive) : Alumina ($Al_2O_3 \cdot H_2O$)
 Adsorbent concentration before cooler/filter $[g/Am^3]$: 3,5 - 5,3
 Adsorbent flow (recirculated) $[kg/h]$: 10 - 15
 Adsorbent feed $[kg/h]$: 1 - 3

| | | |
|-------------|--|--|
| UBA 1978 | Fabric Filter for Lead-Boron Glass Furnace Emission Control | |
|-------------|--|--|

Table 4

| | Installation I | Installation II |
|---|----------------|-----------------|
| Capacity [MW] | 650 | 720 |
| Sulfur content of coal [%] | 1.0 | 0.6 |
| Spec. collection area [m ² /(m ³ /sec)] | 155 | 135 |
| N ^o of "streets" in parallel | 4 | 8 |
| N ^o of fields in line | 4 | 4 |
| N ^o of high Voltage groups | 16 | 32 |
| Dust conc. before ESP [g/m ³] | 5* | 15** |
| Dust conc. after ESP [mg/m ³] | | |
| 4 fields — guaranteed | 45 | — |
| measured | < 45 | 10-50 |
| 3 fields — guaranteed | 112 | 76 |
| measured | — | — |
| Plate height [m] | 14.7 | 13 |
| Passage width [m] | 0.3 | 0.3 |

* measured

** designed

| | | |
|-------------|--|--|
| UBA 1978 | Electrostatic Precipitator for Utility Power Station Emission Control | |
|-------------|--|--|

Table 5

Discussion

Dr. Donovan asked whether the alumina was added after the cooler, or if it was added where the gas temperature was 700 °C. Mr. Gütner replied that it was advantageous to add the alumina before the cooler, and said (in reply to a second question by Mr. Donovan) that the adhering dust is recycled. Statistically, every particle is recycled 10 times. The fate of the recycled particles was queried by Mr. Donovan, who was informed that they are fed into the furnace, and that the alumina additive becomes part of the glass product.

Mr. Gooch wished to know how SO₂ removal was accomplished in wet precipitators. Dr. Gütner answered that this was achieved by means of sophisticated, continuously-spraying inlet nozzles, which ensured saturation of the gas as it entered the electric field.

Mr. Princiotta wondered whether workers had encountered any sulphur-scaling or plugging problems, and was told that the calcium ion contents of the recovered sodium hydroxide was up to 2 grams per liter. Mr. Princiotta added that excess oxygen led to too much sodium sulphate and drew attention to double alkali technology which helps eliminate scaling. Dr. Gütner referred to the pH factor (5 - 6) in de-scaling, and said that chlorine ion had been proved to be equally satisfactory.

SESSION III: CONCURRENT REMOVAL OF DUST AND GASEOUS CONSTITUENTS

SO₂ REMOVAL BY A FABRIC FILTER USING NAHCOLITE INJECTION

by

R. P. Donovan
Research Triangle Institute
Energy & Environmental Research Division
Process Engineering Department
P. O. Box 12194
Research Triangle Park, N. C. 27709

(Draft text for presentation to be made to the Particulate Workshop,
Jülich, Federal Republic of Germany, March 16-17, 1978)

March 1978

SO₂ REMOVAL BY A FABRIC FILTER USING NAHCOLITE INJECTION

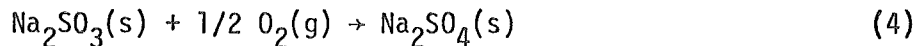
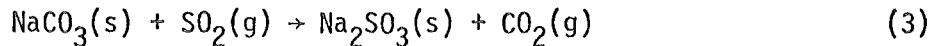
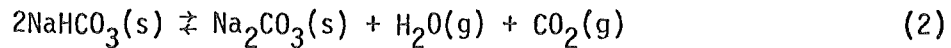
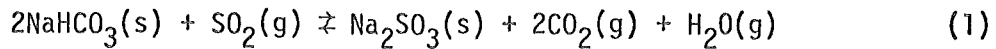
R. P. Donovan
Research Triangle Institute
Energy & Environmental Research Division
Process Engineering Department
P. O. Box 12194
Research Triangle Park, N. C. 27709

Reagent injection is the name applied to the technique whereby a reagent is injected into a gas flow for the purpose of converting a gaseous species in that flow into a solid product that can be removed along with other particulate matter by a downstream fabric filter. The application of highest EPA interest is the removal of SO₂ from flue gas in a dry scrubbing process.

While a variety of reagents have been investigated for this function, (Table 1), the most promising system now is that based on nahcolite injection. Nahcolite is a naturally occurring mineral consisting of 60 to 90 percent sodium bicarbonate. In the Piceance Basin of Colorado it exists in quantities measured in the billions of tons. However, present production is zero [Ref.1]. Most nahcolite must be recovered by underground deep mining and will involve large startup expenses. Before undertaking these costs, mine owners are seeking to obtain purchase commitments from users (primarily utilities) who at present are uncertain of the value of the product in their process. Given these uncertainties neither the utilities nor the miners are willing to risk the sizable investment required for production and it is this impasse that EPA is now seeking to break by sponsoring both analytic and pilot scale evaluations of the nahcolite injection process.

PROCESS OUTLINE

The chemical reactions between injected nahcolite and SO₂ in the flue gas are thought to consist of the following reactions occurring simultaneously [Ref.2]:



In the typical process the nahcolite ore is crushed and ground to a fine mesh (say, -200 mesh on the Tyler scale [material passes through a sieve whose openings are 75 μm]). This fine powder is then injected into the gas flow upstream of the fabric filter. The ground nahcolite reacts according to the chemistry outlined above, the solid products (Na_2SO_3 , Na_2SO_4 plus unreacted NaHCO_3 and Na_2CO_3) being caught by the fabric filter. The reactions take place anytime after injection including after being collected by the fabric filter since the gas flow passes through the filter cake on the bags.

Reaction 1 represents a direct interaction between NaHCO_3 and SO_2 . Note that two moles of NaHCO_3 are required to chemically balance one mole of SO_2 . These relative quantities define a stoichiometric ratio of one; i.e., a stoichiometric ratio = 1 implies that two moles of NaHCO_3 have been injected for every mole of SO_2 in the gas flow.

An alternative reaction sequence for SO_2 removal is given by Reactions (2) and (3). An equilibrium is established between NaHCO_3 and Na_2CO_3 (Reaction 2) and a reaction of SO_2 with Na_2CO_3 takes place to again produce the Na_2SO_3 product (Reaction 3). Again two moles of NaHCO_3 are required for every mole of SO_2 reacted by this sequence.

BACKGROUND

EPA (actually N.C.A.P.C., a predecessor government agency) involvement with reagent injection began nearly 10 years ago with field experiments at the Mercer Generating Station of New Jersey Public Service Co. [Ref.3].

These tests consisted of feeding a slipstream from a coal-fired boiler into a four compartment pilot baghouse. Sodium bicarbonate was added to the flow at various points upstream of the baghouse. Among the variables investigated, in addition to point of NaHCO_3 addition, were

- (1) stoichiometric ratio $[\text{NaHCO}_3/\text{SO}_2]$,
- (2) temperature,
- (3) flow rate,

plus various operating modes (batch feed versus continuous feed, various cycling times). The primary measures of performance were the percent of

SO_2 removed from the gas $\left(\frac{\text{inlet } \text{SO}_2 \text{ concentration}}{\text{outlet } \text{SO}_2 \text{ concentration}} \times 100 \right)$ and the percent of NaHCO_3 utilized in the reaction $\left(\left[1 - \frac{\text{NaHCO}_3 \text{ in spent additive}}{\text{total NaHCO}_3 \text{ added}} \right] \times 100 \right)$.

Temperature and stoichiometric ratio proved to have the most significant impact on SO_2 removal efficiency (Figure 1) and NaHCO_3 utilization (Figure 2). Some dependencies on nahcolite feed mode (continuous feed or batch feed-- either periodically to coincide with the resumption of filtering after bag cleaning or one shot at the beginning of a test run) may exist; these dependencies were not as strong as those on temperature or stoichiometric ratio.

While moving the feed point upstream (and thereby increasing the time the nahcolite is in the gas stream) did produce increased SO_2 removal and nahcolite utilization, these gains were also small and based on analysis of fallout before the bags and the dust cake on the bags, much of the reaction between NaHCO_3 and SO_2 (88 percent in this case, although this value varies widely among different investigators) took place while the gas passed through the filter cake on the bags. One of the conclusions of this early work was that increased efficiency and utilization would be favored by a system that increased the deposition of additive on the bag. Subsequent experience shows the interaction to be more complex than just precoating the bags, however. Common practice is to precoat with part of the additive load and feed the rest into the upstream gas flow.

A second EPA-sponsored study in reagent injection was performed by researchers at Owens-Corning Fiberglas Corp. [Ref.4]. Most of the reagents studied required high temperature for optimum reaction (Table 1). The low temperature reagents, alkalyzed alumina and nahcolite, both were assumed to be impractical without reagent regeneration. American Air Filter Co. has independently followed up this approach by developing a regenerative process for nahcolite [Ref.5]. During regeneration slaked lime is used to recover the sodium salts, the calcium being disposed of as waste. Figure 3 summarizes the chemical reactions. The regeneration step reduces the nahcolite consumption by over two orders of magnitude. It is replaced by the lime and CO₂ requirements of the regeneration but lime is cheap and CO₂ is readily available from the scrubber flue gas. Economic feasibility of the overall regeneration cycle is not yet demonstrated, however.

This American Air Filter work also showed the important influences of temperature and stoichiometric ratio upon SO₂ removal efficiency. Moreover a dependence upon water concentration was documented by them as shown in Figure 4. Increases in water vapor concentration above 5 percent seem unimportant but as the Figure 4 data show, SO₂ removal efficiency suffers at say 2 percent water vapor concentration. Happily the flue gas of interest typically has water vapor concentration above 5 percent.

EPA-SPONSORED STUDY AT TRW, INC. [Ref.6]

The regenerative process is not the approach currently being sponsored by EPA. EPA is investigating the economics of a nahcolite throwaway process. The reacted nahcolite is discarded along with the flyash. Because these sodium salts are highly soluble, their disposal constitutes an additional environmental problem. Conceivably adequate environmental safeguards may require insolubilization of the sodium sulfate product prior to disposal. Coprecipitation with acidic ferric ion to form insoluble double salts $\text{NaFe}_3(\text{SO}_4)_2(\text{OH})_6$ and $\text{Na}_2\text{Fe}(\text{SO}_4)_2\text{OH} \cdot 3\text{H}_2\text{O}$ is one candidate process [Ref.7]. Such environmental considerations depend heavily on the locale and while clearly important in determining process feasibility, cannot be specifically assessed independently of a specific site.

The conditions defined for assessment in the EPA-sponsored study at TRW are given in Table 2 [Ref.6].

Flue gas at the boiler exit is assumed to consist of the following constituents and proportions, which are typical for western coal-firing:

| | | |
|------------------|---|-----------------------------------|
| N ₂ | - | 74% |
| O ₂ | - | 4.8% |
| CO ₂ | - | 12.3% |
| SO ₂ | - | variable |
| SO ₃ | - | 1.0% of the SO ₂ value |
| NO | - | 0.06% |
| HCl | - | 0.01% |
| H ₂ O | - | 8.8% |

The limitation of distance from the coal source (Table 2) immediately confines the applicability of the process evaluated to the Western United States as shown in Figure 5. Also listed in this Figure are the major coal deposits within that area. Coal properties of each of these sources are tabulated in Table 3.

The state in which each of these deposits lie makes a difference because the standards governing emissions vary from state to state (Table 4). By matching the coal sulfur content with the appropriate state regulations, the required SO₂ removal for legally burning the coal in the state in which it is found can be deduced. With 70 percent SO₂ removal (Table 2) half of the 10 sources would be legal. The highest required SO₂ removal is for the Sheridan deposit which needs 91 percent SO₂ removal in order to be combusted within the state of its location.

An additional uncertainty of the evaluation is a pending Federal SO₂ standard calling for 90 percent SO₂ removal regardless of absolute value but in no cases to exceed the already existing standard. Table 4 lists only

the existing Federal standard. The impact of this anticipated Federal change is not yet clear. A 90 percent removal efficiency would require more nahcolite or a higher reaction temperature or a combination of both.

Assuming the conditions of Table 2 and estimating the cost of delivered nahcolite to be \$32.50/ton and that of disposing of the flyash/spent nahcolite in a landfill to be \$6/ton, cost comparisons of the nahcolite injection process with the lowest cost, wet scrubbing technologies are given in Table 5. These estimates are for conditions favorable for the nahcolite process. They are for 1 percent sulfur coal. At higher sulfur concentrations both capital (Figure 6) and operating (Figure 7) costs rise rapidly. Nahcolite injection is unlikely to compete favorably with lime or limestone scrubbing on boilers fired with high sulfur eastern coals. Western coals also typically have higher ash content than eastern coals so that the added spent nahcolite, while significant, is not as great an increase in disposal burden. If a landfill is employed, as in this assessment, having a low water table lowers the costs of isolating the highly soluble sodium salts from the environment. Again in the Eastern United States one would not be so favored.

The estimates in Table 5 ignore the particulate removal requirements. The fabric filter is primarily a particulate removal device and no added costs are anticipated. The wet scrubbing process may entail additional costs for particulate control that are not reflected in Table 5. When this is true, the dual pollutant control functions of the fabric filter would become a major economic advantage.

Even without adjustment for particulate control the dry scrubbing process appears to be competitive in the Western United States. The economic advantage is not great but EPA now plans to jointly sponsor a field assessment of the process with the City of Colorado Springs. This assessment will begin before the end of the year and some preliminary data should be available in early 1979.

In addition both the ongoing fabric filter evaluations at Kerr Industries and Southwest Public Services (both sponsored by EPA) include options to pursue nahcolite injection for SO₂ control. That these options will be exercised by the contractors is not yet known and may depend in part upon the experiences at Colorado Springs and at Arapahoe/EPRI and Wheelabrator-Frye/Superior Oil where similar work is being sponsored by other groups.

REFERENCES

1. McIlvaine, R.W., "SO₂ Removal with Fabric Filters," pp.8-1 to 8-31 in the Proceedings of the Second International Fabric Alternatives Forum, Denver, CO, July 27-28, 1977, American Air Filter Co., Inc., 215 Central Avenue, Louisville, KY 40277.
2. Genco, J.M. and H.S. Rosenberg, "Sorption of SO₂ on Ground Nahcolite Ore," J. Air Pollution Control Assn. 26, No.10, October 1976, pp. 989-990.
3. Chaffee, R.L. and H. Liu, "Evaluation of Fabric Filter as Chemical Contactor for Control of Sulfur Dioxide from Flue Gas," Final Report-Part 1, HEW Contract No. PH 22-68-51 (NTIS PB 194-196), 28 August 28, 1969, the Air Preheater Co., Inc., Wellsville, NY 14895.
4. Veazie, F.M. and W.H. Kielmeyer, "Feasibility of Fabric Filter as Gas-Solid Contactor to Control Gaseous Pollutants," Final Report, Contract No. PH-22-68-64 (NTIS PB 195 884), August 1970, Owens-Corning Fiberglas Corp., Granville, OH 43023.
5. Doyle, D.J., "Fabric and Additive Remove SO₂," Electrical World, February 15, 1977, pp. 32-34.
6. Christman, R.C., et al., "Evaluation of Dry Sorbents and Fabric Filtration for FGD," Final Report, Contract No. 68-02-2165, in preparation, trw Environmental Engineering Division, 800 Follin Lane, S.E., Vienna, VA 22180.
7. Genco, J.M., et al., "The Use of Nahcolite Ore and Bag Filters for Sulfur Dioxide Emissions Control," J. Air Pollution Control Assn. 25, No.12, December 1975, pp. 1244-1253.

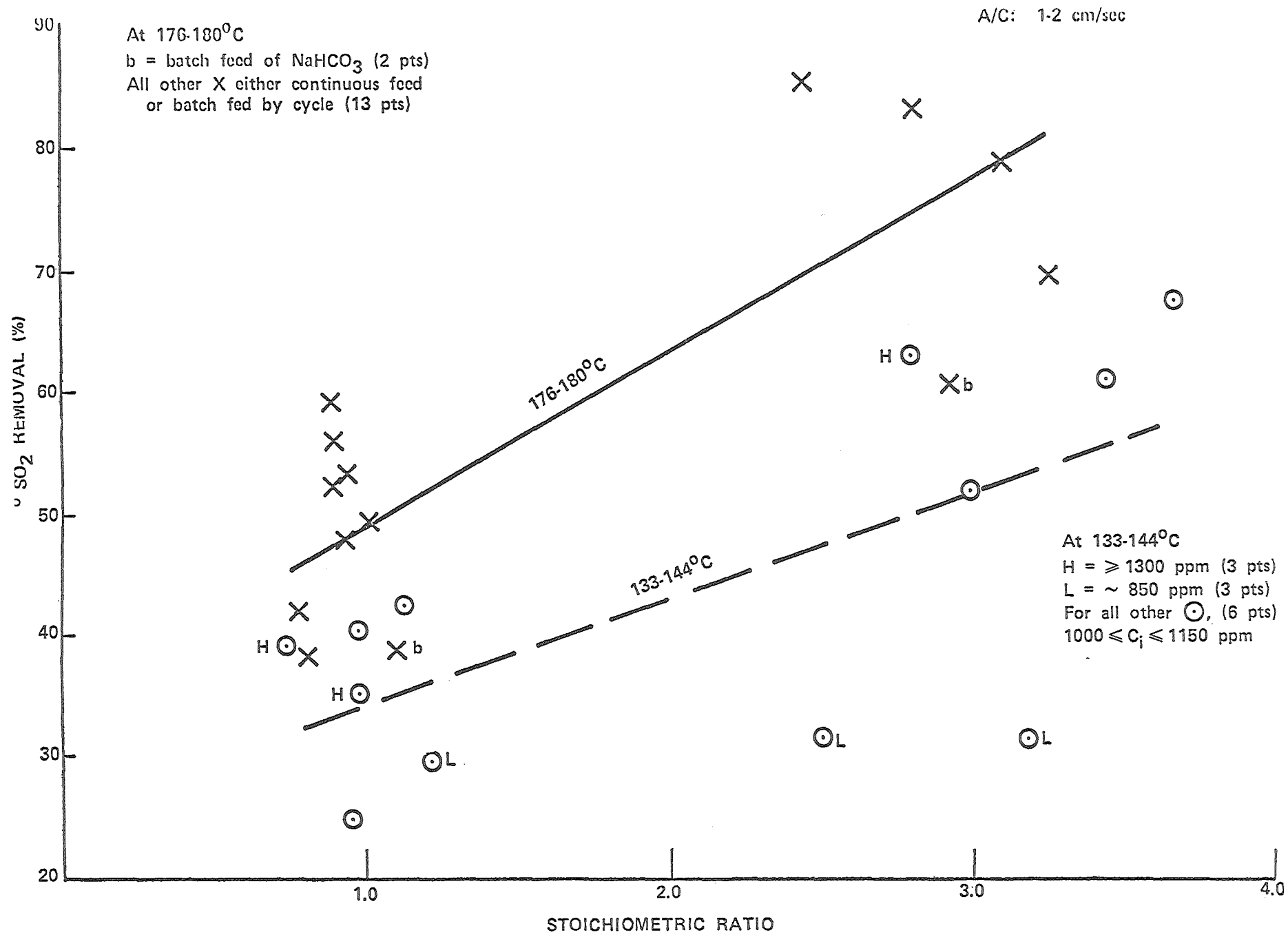


Figure 1. SO₂ removal efficiency [Ref 3].

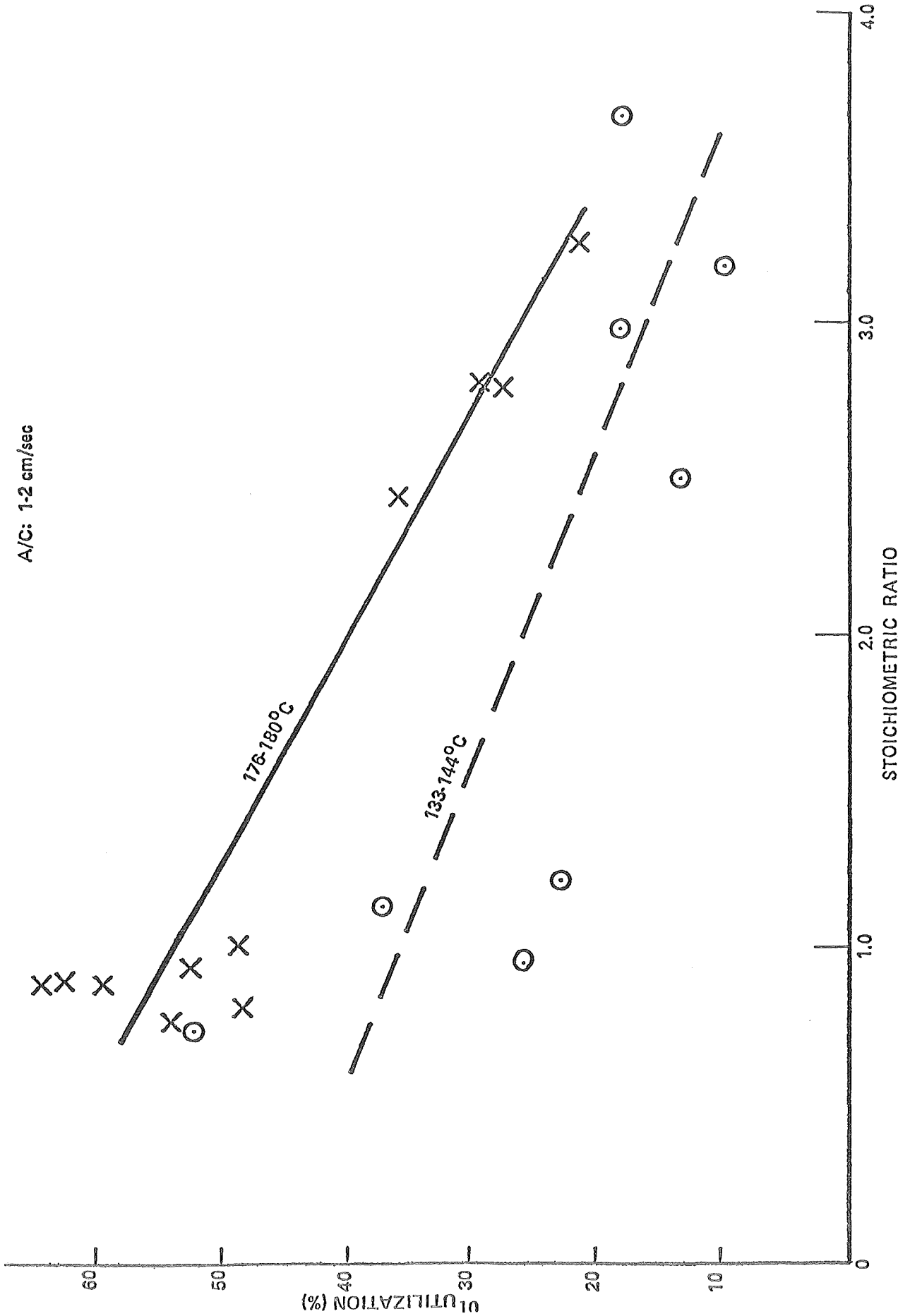


Figure 2. NaHCO₃ utilization rate [Ref 3].

CANDIDATE REGENERATION CHEMISTRY [REF 5]

- (1) $2\text{NaHCO}_3 + \text{SO}_2 \rightarrow \text{Na}_2\text{SO}_3 + 2\text{CO}_2 + \text{H}_2\text{O}$
- (3) $\text{Na}_2\text{CO}_3 + \text{SO}_2 \rightarrow \text{Na}_2\text{SO}_3 + \text{CO}_2$
- (4) $\text{Na}_2\text{SO}_3 + \text{Ca}(\text{OH})_2 \rightarrow 2\text{NaOH} + \text{CaSO}_4$
- (5) $\text{Na}_2\text{CO}_3 + \text{Ca}(\text{OH})_2 \rightarrow 2\text{NaOH} + \text{CaCO}_3$
- (6) $\text{NaHCO}_3 + \text{Ca}(\text{OH})_2 \rightarrow \text{NaOH} + \text{CaCO}_3 + \text{H}_2\text{O}$
- (7) $\text{NaOH} + \text{CO}_2 \rightarrow \text{NaHCO}_3$
- (8) $2\text{NaOH} + \text{CO}_2 \rightarrow \text{Na}_2\text{CO}_3 + \text{H}_2\text{O}$

Figure 3.

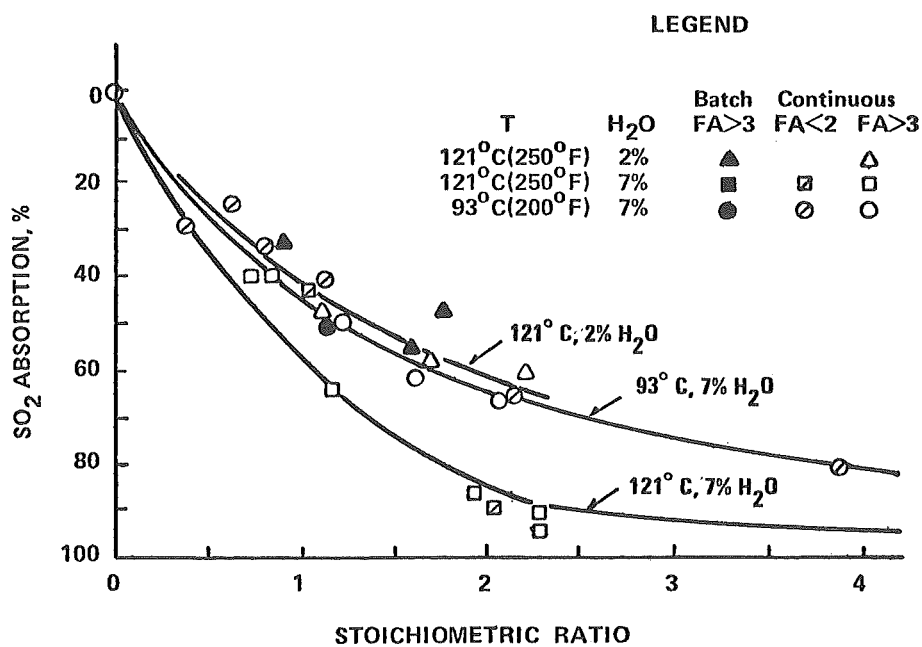
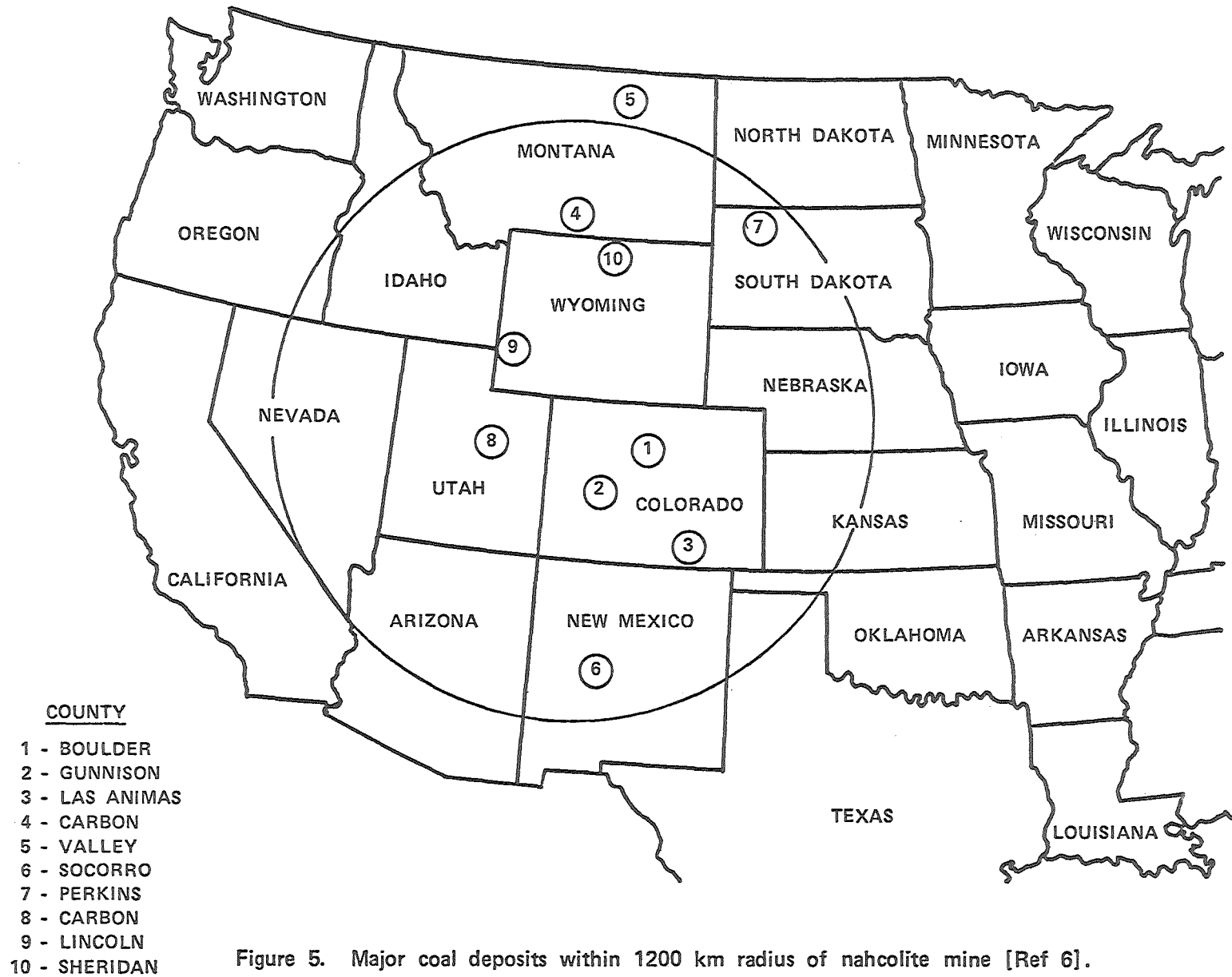


Figure 4. SO₂ removal efficiency [Ref. 5].



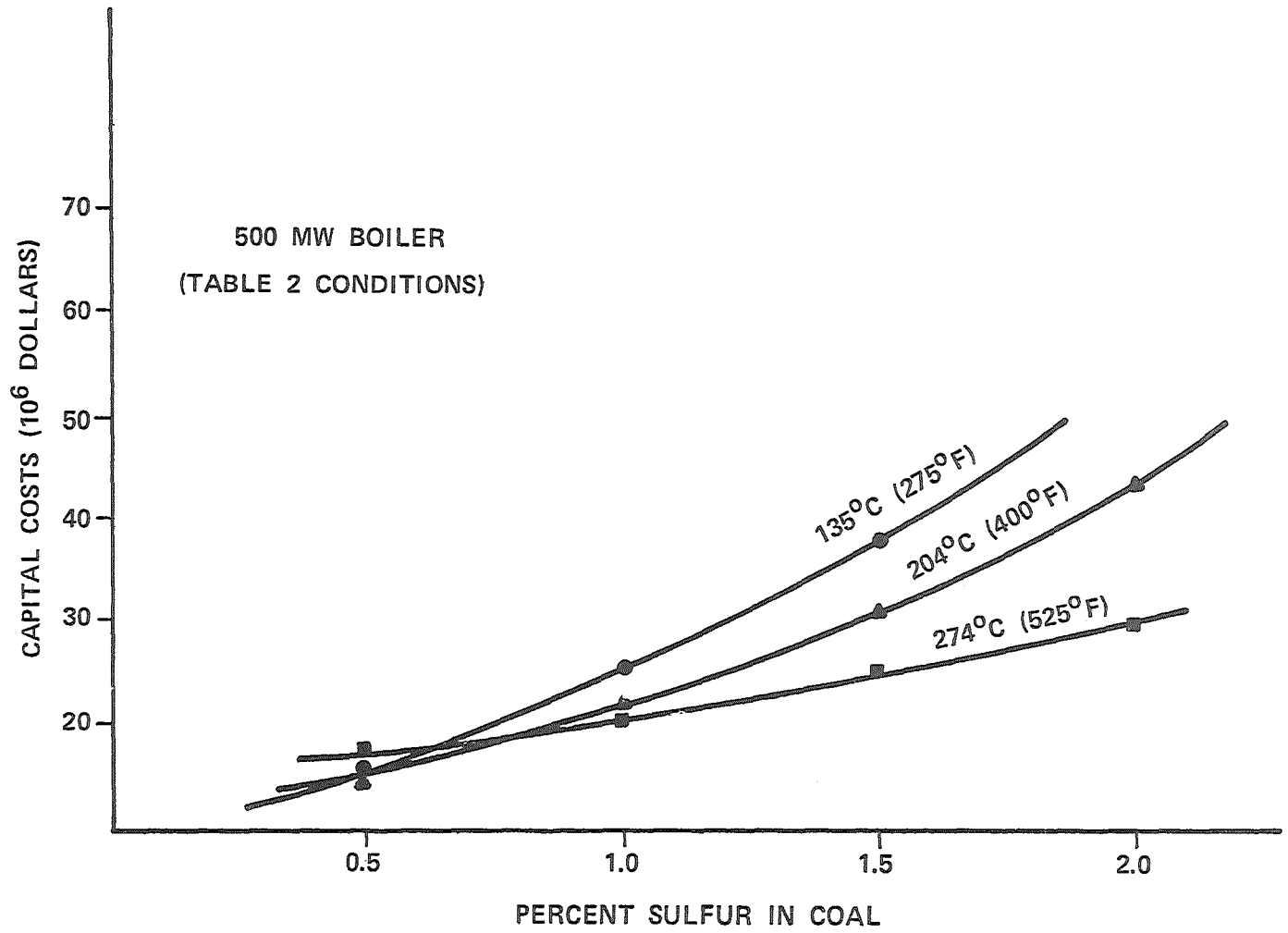


Figure 6. Capital costs versus percent sulfur content [Ref 6].

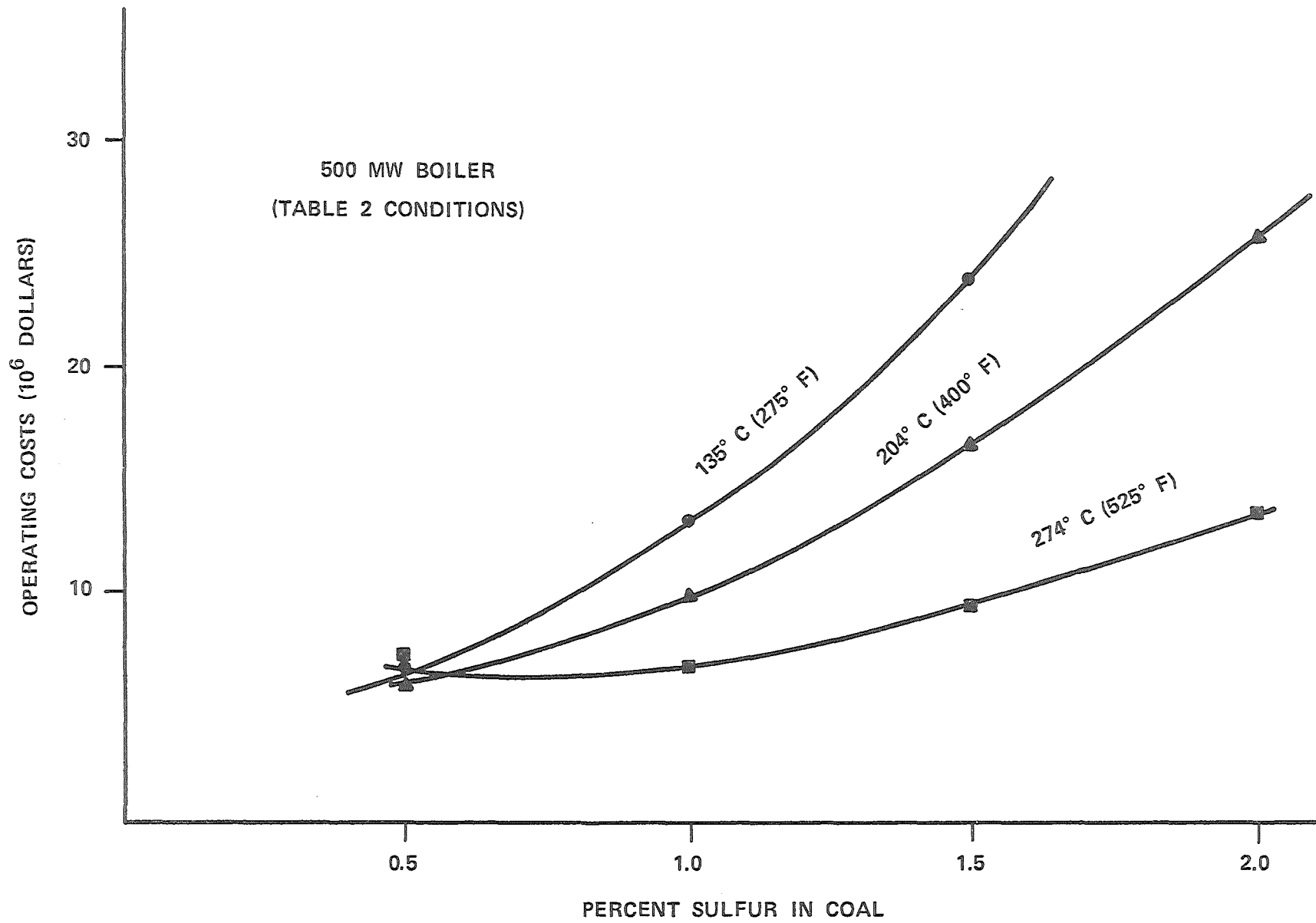


Figure 7. Operating costs versus percent sulfur content [Ref 6].

TABLE 1
CANDIDATE REAGENTS FOR DRY SO₂ SCRUBBING [REFS 1,4,6]

| REAGENT | FLUE GAS TEMP. RANGE | REMARKS |
|-------------------------------------|----------------------|--|
| SLAKED LIME | 371-482°C(700-900°F) | OPTIMUM TEMP. (427°C) TOO HIGH |
| PROMOTED SLAKED LIME (1% NaCl) | " | " |
| SLAKED DOLOMITE LIME | " | " |
| PROMOTED DOLOMITE LIME (1% NaCl) | " | " |
| MANGANESE DIOXIDE | 260-371°C(500-700°F) | HIGH COST REAGENT; NOT VERY TEMP. DEPENDENT OVER THIS RANGE |
| ALKALIZED ALUMINA | 149-260°C(300-500°F) | VERY PROMISING |
| NAHCOLITE | 149°C(300°F) | REACTION PRODUCTS HIGHLY SOLUBLE IN WATER |
| AMMONIA GAS | <88°C(<190°F) | VISIBLE PLUME AND LOW EFFICIENCY ABOVE 88°C; EXCELLENT EFFICIENCY BELOW 88°C |
| MAGNESIA | 135°C-900°C | NOT SUFFICIENTLY REACTIVE AT CONTEMPORARY BAGHOUSE TEMPERATURES |

TABLE 2
CONDITIONS EVALUATED [REF. 6]

500 MW BOILER

WESTERN COAL, 1% SULFUR, 10% ASH

HEATING VALUE: 24.4 MJ/kg (10,500 Btu/lb)

1,200 km RADIUS OF COLORADO DEPOSIT

SEMI-ARID REGION; WATER TABLE 15 m BELOW THE
SURFACE

204° C (400° F) BAGHOUSE TEMPERATURE

70% SO₂ REMOVAL

TABLE 3
COAL PROPERTIES [REF 6]

| STATE | COUNTY | COAL TYPE | S % | ASH % | HEATING VALUE | |
|--------------|------------|-----------|------|-------|---------------|---|
| | | | | | MJ/kg | $\left(\frac{\text{Btu}}{\text{lb}}\right)$ |
| COLORADO | BOULDER | SUBBIT. | 0.27 | 5.4 | 23.3 | (10,000) |
| | GUNNISON | BIT. | 0.43 | 3.4 | 31.4 | (13,500) |
| | LAS ANIMAS | BIT. | 0.70 | 12.8 | 31.4 | (13,000) |
| MONTANA | CARBON | SUBBIT. | 1.1 | 11.2 | 24.4 | (10,500) |
| | VALLEY | LIG. | 1.3 | 9.1 | 15.6 | (6,700) |
| NEW MEXICO | SOCORRO | BIT. | 0.82 | 13.8 | 28.6 | (12,300) |
| SOUTH DAKOTA | PERKINS | LIG. | 1.2 | 9.0 | 14.0 | (6,000) |
| UTAH | CARBON | BIT. | 0.6 | 5.6 | 29.1 | (12,500) |
| WYOMING | LINCOLN | BIT. | 1.0 | 5.5 | 30.9 | (13,300) |
| | SHERIDAN | SUBBIT. | 1.1 | 7.9 | 20.9 | (9,000) |

TABLE 4
SO₂ EMISSION REGULATIONS FOR SELECTED STATES [REF 6]

| STATE | FEDERAL EMISSION REQUIREMENTS, g SO ₂ PER MJ HEAT INPUT (lb SO ₂ PER 10 ⁶ Btu HEAT INPUT) | STATE EMISSION REQUIREMENTS, g SO ₂ PER MJ HEAT INPUT (lb SO ₂ PER 10 ⁶ Btu HEAT INPUT) |
|--------------|--|--|
| ARIZONA | 0.52 (1.2) | 0.34 (0.8) |
| COLORADO | 0.52 (1.2) | 0.13 (0.3) or 150 ppm |
| KANSAS | 0.52 (1.2) | 0.52 (1.2) |
| MONTANA | 0.52 (1.2) | 0.52 (1.2) |
| NEBRASKA | 0.52 (1.2) | 0.52 (1.2) |
| NEVADA | 0.52 (1.2) | 0.090 (0.21) |
| NEW MEXICO | 0.52 (1.2) | 0.15 (0.34) |
| NORTH DAKOTA | 0.52 (1.2) | 0.52 (1.2) |
| SOUTH DAKOTA | 0.52 (1.2) | 0.52 (1.2) |
| TEXAS | 0.52 (1.2) | 0.52 (1.2) |
| UTAH | 0.52 (1.2) | 80% REMOVAL |
| WYOMING | 0.52 (1.2) | 0.09 (0.2) |

TABLE 5
FLUE GAS DESULFURIZATION COST COMPARISON [REF 6]

| PROCESS | CAPITAL COST \$/kW | ANNUALIZED COST Mills/kWh |
|-------------------------|--------------------------|---------------------------------|
| DRY SORBENT BAGHOUSE | 46 | 2.6 |
| LIME SCRUBBING | 49 | 2.8 |
| LIMESTONE SCRUBBING | 55 | 2.8 |

Discussion

In response to Dr. Holighaus' request for further information regarding Figs. 1 and 2 and reaction velocity, Mr. Donovan said that the figures showed measurements in which sodium bicarbonate had been injected into the flue gas of the power plant. Two methods of injection were possible: a single shot or a continuous process. With respect to reaction velocity, residence time was varied by changing the point of injection. Performance correlations were the strongest with temperature and stoichiometric ratio, as shown in Figs. 1 and 2, although more data may show additional, less pronounced dependencies such as residence time.

Dr. Davids asked if the nahcolite technology met State emission standards, and whether compliance depended on the coal's sulphur content. Mr. Donovan answered that compliance depended on both the sulfur content of the coal and the SO_2 standards set by a particular state. He drew attention to the fact that compliance would be achieved in about half the Western states assuming the sulfur content of the coal burnt corresponded to that naturally occurring in that state.

Dr. Hübner mentioned the possibility of formation of bi-sulphide from sodium sulphate; Mr. Donovan replied that the reactions postulated were semiempirical in that reaction products were sampled at various points. No bi-sulphide was detected. Dr. Hübner's second inquiry dealt with differences in the properties of nahcolite and sodium bicarbonate. Mr. Donovan answered that his analysis treated nahcolite and sodium bicarbonate as chemically synonymously except for concentration - - nahcolite was assumed to be 70% sodium bicarbonate and 30% inert material.

PERFORMANCE TESTS OF THE MONTANA POWER COMPANY COLSTRIP STATION FLUE GAS
CLEANING SYSTEM

Joseph D. McCain
Southern Research Institute
2000 - 9th Avenue South
Birmingham, Alabama 35205
U.S.A.

This paper gives a description of a scrubber used for joint collection of sulfur oxides and particulate matter produced by coal combustion at a large coal fired electrical generating station. This novel system utilizes the alkalinity of the flyash produced by the boiler for the major portion of the sulfur dioxide removal. The scrubber was designed and constructed by Combustion Equipment Associates (New York, NY, USA) in cooperation with the Bechtel Power Corporation and A. D. Little, Inc., for the Montana Power Company. The system is currently in commercial operation on units 1 and 2 of the Colstrip Station of the Montana Power Company. Each unit has a generating capacity of 360 MWe.

The scrubber utilizes a variable throat venturi to permit operation at a constant pressure drop (nominally 43 cm w.c.) over the full range of possible boiler gas flow rates. The scrubbing liquor is a recirculating flyash slurry containing 12% solids by weight. The venturi section is followed in order by a spray-type absorber, a washtray system for diluting entrainment, and a chevron-type mist eliminator. Each boiler is equipped with three parallel scrubber modules, each of which is capable of handling 40% of the total, full load gas flow from the boiler.

Performance data are given for both SO₂ and flyash removal by the system.

PERFORMANCE TESTS OF THE MONTANA POWER COMPANY COLSTRIP STATION
FLUE GAS CLEANING SYSTEM

INTRODUCTION

The flue gas cleaning system (Figure 1) now in operation on the two Colstrip 360 MWe units is unique in that a wet scrubbing system is used for both particulate and SO₂ control and that captured ash provides the alkalinity for the SO₂ removal. This paper provides a description of the operation of the scrubber and the results of performance testing carried out to determine the SO₂ and fly ash cleaning efficiencies achieved by the system.

DESCRIPTION OF THE SCRUBBER*

The system currently installed on the two 360 MWe Units 1 and 2 is illustrated in Figures 1 and 2. The hot flue gas leaving the boiler is cooled in the heat recovery air heater and enters the flue gas scrubbing system at about 300°F. Each scrubber module, as shown in simplified drawing in Figure 2, consists of a downflow venturi scrubber centered within an upflow spray tower contactor. The venturi is equipped with a variable throat to maintain constant pressure drop at variable loads. In the venturi the scrubbing liquid is finely dispersed by the high velocity flue gas and serves to efficiently wet and trap the particulate fly ash. In the spray tower the gas contacts a recycle spray of absorption slurry. The slurry from the venturi and the spray contactor is collected and held in the base of the scrubber and recirculated at an L/G ratio 2 ℓ/m^3 (15 gal/1000 ft³) for venturi and 2.4 ℓ/m^3 (18 gal/1000 ft³) for the absorber spray. An agitator in the scrubber base serves to maintain suspension of the fly ash and solid reaction products. Slurry is bled from the recycle to maintain a 12% suspended solids concentration. Slaked quick lime is added as lime slurry only if needed to augment the fly ash alkali and maintain the desired slurry pH.

Each scrubber module is designed to clean 120 MW of equivalent gas flow under normal conditions and 144 MW under emergency conditions (i.e., when one module is down, the two in operation will clean the amount of flue gas generated at 80% of boiler design load.)

*Taken from a paper by C. Grimm, J. Z. Abrams, W. W. Leffmann, I. A. Raben, and C. Lamatia. Presented at the 1977 National Meeting of the AIChE.

THE MONTANA POWER CO. PUGET SOUND POWER & LIGHT
2 - 360 MW COLSTRIP UNITS 1 & 2

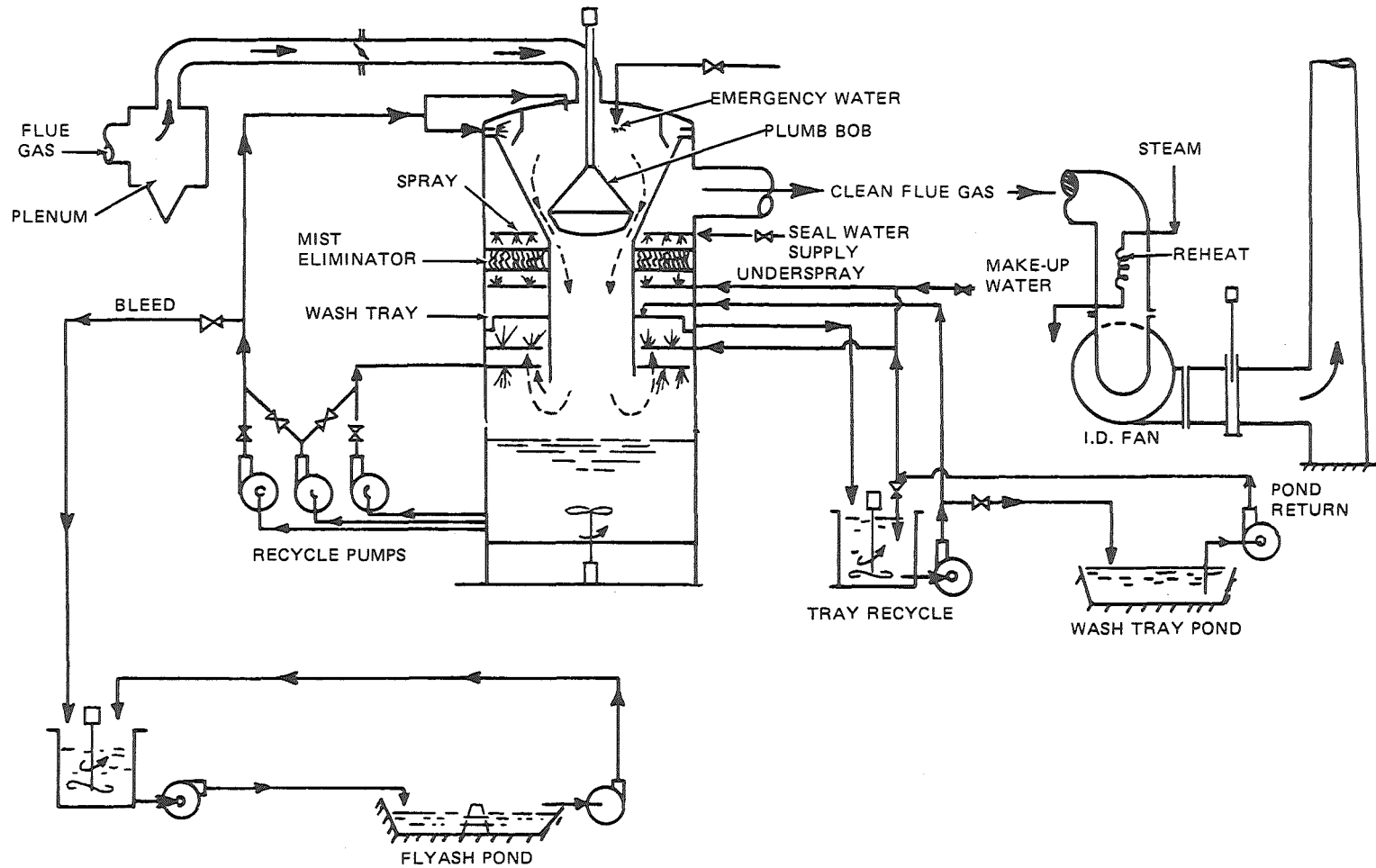


FIGURE 1. THE MONTANA POWER CO. - PUGET SOUND AND LIGHT
COLSTRIP UNITS 1 AND 2 - (360 MW EACH) FLUE GAS CLEANING SYSTEM.

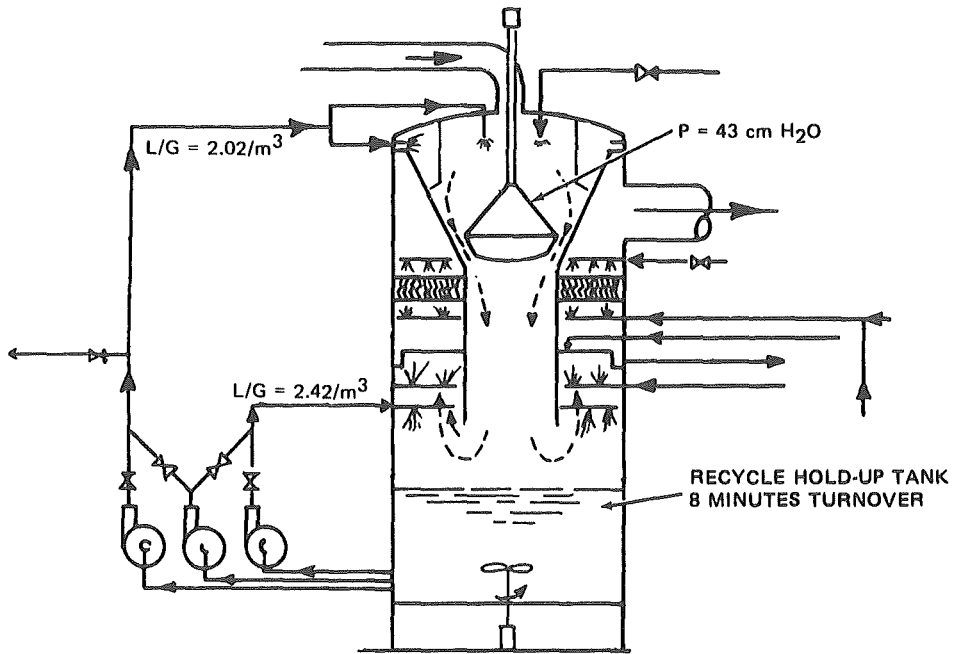


FIGURE 2. COLSTRIP SCRUBBER MODULE.

The treated gas leaving the spray section passes through the water wash-tray which serves to trap and dilute the entrainment. The gas leaving the wash-tray passes through a chevron demister followed by a mesh pad demister and leaves the absorption section water-saturated and cooled to the saturation temperature of about 120°F.

To preclude condensation in the fan and stack, and improve the gas buoyancy, the cooled gas from the scrubber is reheated 50 to 75°F by a steam-heated exchanger. The warmed gas then passes through the dry induced draft fans and is discharged to the atmosphere from the top of a 500 foot stack.

As shown in Figure 1 the slurry discharged from the absorption loop is passed to an intermediate retention pond where the solids settle and from which the clarified water is returned to the absorption system. At intermittent intervals (currently only during the warm summer months), a floating dredge is used to reclaim the settled solids from the intermediate settling pond and transport them as a 30% slurry by pipeline to the remotely located permanent disposal pond. Decanted water (supernate) from the disposal pond is returned, also intermittently, through the same slurry pipeline to the intermediate pond for recycle to the absorption system. No stabilization of the sludge is required and a closed water loop is maintained.

Fresh water is added to the absorption system in an amount equivalent to that evaporated into the warm gas stream plus that retained in the waste sludge. This fresh makeup water is introduced to the system as dilution water for minimizing the calcium saturation level in the mist eliminator washwater. This washwater is trapped by and withdrawn from the washtray and circulated to a small pond where entrained solids are separated. A portion of the water from this pond is returned and used to wash the undersurface of the washtray. Another portion of the flow is diluted with the fresh makeup water, and used for bottom wash of the mist eliminator.

The scrubber has been free of scale while the pH of the recycle liquid remains in the expected range. Corrosion problems in the reheater and demister plugging have not been experienced with the installation.

The successful operation of the Colstrip system as described above represents the culmination of an extensive development program carried out jointly by the architect engineer, Bechtel Power Corporation, the scrubber system supplier, Combustion Equipment Associates, Inc. (CEA), and the power plant owners, Montana Power Company and Puget Sound Power & Light Company.

A study was made by Bechtel of the possible options for meeting particulate and SO₂ removal standards.

A detailed chemical analysis of the fly ash (see Table 1) revealed that it contained alkali metal oxides in an amount theoretically sufficient to react with and adsorb the sulfur dioxide produced by the coal combustion. Laboratory experiments simulating absorption conditions revealed that this alkalinity was only usable under low pH absorption conditions (<5.6). It also revealed that

Table 1

FUEL AND ASH AS DESCRIBED IN SPECIFICATIONS

| COAL: | Average, As Received |
|-----------------|----------------------------------|
| Moisture | 23.87% |
| Volatile Matter | 28.59% |
| Fixed Carbon | 38.96% |
| Ash | 8.59% (Max. 12.58%, Min. 6.1%) |
| Heating Value | 8843 Btu/lb. (Min. 8162 Btu/lb.) |
| Sulfur | .777% (Max. 1.0%, Min. 0.4%) |

ASH: (Estimated composition, sulfur trioxide-free basis)

| | |
|--------------------------------|--------|
| SiO ₂ | 41.60% |
| Al ₂ O ₃ | 22.42% |
| TiO ₂ | 0.79% |
| Fe ₂ O ₃ | 5.44% |
| CaO | 21.90% |
| MgO | 4.95% |
| Na ₂ O | 0.31% |
| K ₂ O | 0.13% |
| P ₂ O ₅ | 0.41% |
| (balance unidentified) | |

Later fly ash data varies slightly from above as follows:

LEACHED IN H₂O (1% Fly Ash)

| | |
|-----------------------------|---------|
| pH | 11.8 |
| Conductivity | 4.150 |
| Total Dissolved Solids | 930 ppm |
| Calcium | 396 ppm |
| Magnesium | 0 ppm |
| Chloride | 15 ppm |
| Sulfate (SO ₄ =) | 30 ppm |

LEACHED IN HCl

| | |
|--|-------|
| % Acid insolubles (SiO ₂) | 57.59 |
| % Calcium as CaO | 22.00 |
| % Magnesium as MgO | 1.27 |
| % Aluminum as Al ₂ O ₃ | 15.59 |
| % Iron as Fe ₂ O ₃ | 4.97 |
| % Sulfate as SO ₄ | 0.71 |
| % Carbonate as CO ₃ | 0.70 |

absorption under these low pH conditions would result in extensive oxidation of the absorbed SO₂ producing calcium sulfate rather than calcium sulfite as the predominant reaction product.

Continued laboratory tests were conducted by Bechtel to determine the process conditions under which the alkalinity of the fly ash could be utilized while at the same time accommodating the scaling potential of the calcium sulfate. The conditions selected were a pH of 5 to 5.6, low enough for alkali utilization and high enough for adequate SO₂ absorption capability. The other, and perhaps the key operating factor, was the use of a high level of suspended solids in the absorption slurry (12 to 15% by weight, of which some 3-4% is calcium sulfate formed in the absorption). This provided a high concentration of calcium sulfate seed crystals to promote desupersaturation. A long residence time for the recycle slurry in a stirred tank external to the scrubber was also proposed to ensure alkali utilization and to provide crystallization of calcium sulfate under controlled and non-scaling conditions. A slurry holdup of 8-10 hours was selected based on bleed rate.

The parameters for the final scrubber design are given in Table 2.

The above two conditions, i.e., low slurry pH and long contact with the oxygen-containing flue gas, provided substantially complete oxidation. This high oxidation was shown to improve the disposal characteristics of the waste sludge produced.

Table 3 compares scrubber availability and plant load for the two units during the time period September 1975 through December 1976. Note the definition of scrubber availability below the table. These generating plants have no bypass capability around the air pollution control system.

PERFORMANCE EVALUATION

The scrubber performance was evaluated by Southern Research Institute (SoRI) for the Industrial Environmental Research Laboratory of the U.S. Environmental Protection Agency during the month of May 1977.

This evaluation was one of a series of studies being conducted by the Industrial Environmental Research Laboratory of the Environmental Protection Agency to identify and test novel devices which are capable of high efficiency collection of particulates. The test methods used may not have been consistent with compliance-type methods, but were state-of-the-art techniques for measuring mass and fractional efficiency using standard mass train and inertial, electrical, and optical methods.

The results of previous testing by other organizations and agencies showed that the scrubber was capable of providing gas cleaning efficiencies substantially in excess of those required to meet both SO₂ and particulate emission standards. The results of some of these tests are summarized in Table 4.

Table 2

DESIGN PARAMETERS FOR THE CEA VARIABLE THROAT VENTURI SCRUBBER
(COLSTRIP APPLICATION)

| | |
|---|---------------------------------------|
| Venturi Pressure Drop | 43.2 cm w.c. (17 in.) |
| Venturi L/G | 2 l/m (15 gal/1000 ACF, saturated) |
| Absorption Spray L/G | 2.41 l/m (18 gal/1000 ACF, saturated) |
| % suspended solids in recirculating slurry, by weight | 12% |
| Residence time in the recycle tank | 8 minutes |
| Gas velocity in mist eliminator zone | 2.65 m/sec (8.7 ft/sec) |
| Wash tray pressure drop | 9.65 cm w.c. (3.8 in.) |
| Mist eliminator pressure drop | 2.5 cm w.c. (1 in.) |
| Reheat pressure drop | 5.6 cm w.c. (2.2 in.) |
| Total system pressure drop (including reheat) | 64.8 cm w.c. (25.5 in.) |
| Total scrubber pressure drop (less reheat) | 55.4 cm w.c. (21.8 in.) |

Table 3

SCRUBBER AVAILABILITY VS. PLANT LOAD

| UNIT | Monthly Capacity Factor % | | No. Days On Line | | Avg. MW for Days On Line | | Scrubber Availability % | |
|------------|------------------------------|------|---------------------|----|--------------------------------|-----|----------------------------|-------|
| | 1 | 2 | 1 | 2 | 1 | 2 | 1 | 2 |
| Sept. 1975 | 0.5 | | 3 | | 50 | | | |
| Oct. | 19.4 | | 19 | | 139 | | | |
| Nov. | 42.2 | | 24 | | 203 | | | |
| Dec. | 59.9 | | 30 | | 239 | | | |
| Jan. 1976 | 63.8 | | 28 | | 265 | | 90.0 | |
| Feb. | 65.4 | | 26 | | 273 | | 98.0 | |
| Mar. | 57.0 | | 24 | | 277 | | 97.6 | |
| Apr. | 49.9 | | 28 | | 219 | | 74.2 | |
| May | 26.0 | 1.3 | 14 | 3 | 210 | 66 | 96.8 | 100.0 |
| June | 0.0 | 23.2 | 0 | 16 | 0 | 171 | - | 99.7 |
| July | 28.0 | 19.5 | 20 | 13 | 167 | 180 | 93.2 | 98.7 |
| Aug. | 37.8 | 13.0 | 23 | 10 | 194 | 162 | 94.7 | 95.8 |
| Sept. | 64.5 | 64.6 | 30 | 30 | 239 | 232 | 88.6 | 98.3 |
| Oct. | 73.1 | 77.0 | 30 | 31 | 281 | 298 | 79.9 | 90.3 |
| Nov. | 55.6 | 79.7 | 30 | 30 | 225 | 303 | 62.7 | 94.7 |
| Dec. | 67.2 | 82.3 | 31 | 31 | 249 | 297 | 73.8 | 92.5 |

Note: Scrubber availability = total module hours available divided by three times the number of hours in month. May through August base is days in operation because of extended scheduled outages.

Table 4

Emission Test Results - EPA Method

| | SO ₂ | | | PARTICULATE | | | NO _x | |
|--|-----------------|-----|----------|-------------|----------|-------|-----------------|----------|
| | LB/HR | PPM | LB/MMBtu | LB/HR | LB/MMBtu | %OPAC | LB/HR | LB/MMBtu |
| 1. Required by NSPS (358 MW) | 4063 | 510 | 1.2 | 339 | 0.10 | 20 | 2370 | 0.7 |
| 2. Scrubber Guarantee (358 MW) | 3386 | 425 | 1.0 | 207 | 0.06 | - | (1) | (1) |
| 3. Projected from Pilot Plant (358 MW) | | | | | | | | |
| a) 0.78%S (760 PPM), 8.19% Ash | 1394 | 185 | 0.41 | 130 | .038 | 20 | 2370 | 0.7 |
| b) 1.0%S (965 PPM), 12.58% Ash | 2071 | 260 | 0.61 | 184 | .054 | 20 | 2370 | 0.7 |
| 4. UNIT 1 TESTS: | | | | | | | | |

COAL AS RECD.

| Date | GEN MW | %Sul. | %Ash | Btu/LB. | LB/HR | PPM | LB/MMBtu | LB/HR | LB/MMBtu | %OPAC | LB/HR | LB/MMBtu |
|-------|--------|-------|------|---------|-------|-----|----------|-------|----------|-------------------|-------|----------|
| 2/76 | 353 | 0.83 | 9.03 | 8638 | 1464 | 197 | 0.44 | 90.1 | .027 | 10 ⁽³⁾ | 880 | 0.26 |
| 4/76 | 210 | 0.71 | 7.79 | 8861 | 420 | 87 | 0.21 | 57.3 | .029 | 14 ⁽²⁾ | 738 | 0.38 |
| 7/76 | 184 | 0.64 | 8.49 | 8807 | 241 | 52 | 0.14 | 53.6 | .031 | 15 ⁽²⁾ | 695 | 0.40 |
| 9/76 | 186 | 0.62 | 7.93 | 8633 | 255 | 56 | 0.14 | 60.5 | .035 | 11 ⁽²⁾ | 646 | 0.37 |
| 12/76 | 223 | 0.94 | 8.54 | 8394 | 898 | 154 | 0.43 | 67.2 | .032 | 15 ⁽²⁾ | 662 | 0.31 |

5. UNIT 2 TESTS:

| | | | | | | | | | | | | |
|-------|-----|------|------|------|------|-----|------|-------|------|-------------------|-----|------|
| 10/76 | 331 | 0.56 | 7.96 | 8368 | 1231 | 178 | 0.39 | 83.4 | .028 | 11 ⁽²⁾ | 862 | 0.28 |
| 11/76 | 327 | 0.59 | 7.86 | 8484 | 664 | 83 | 0.21 | 85.9 | .028 | 10 ⁽²⁾ | 934 | 0.30 |
| 12/76 | 324 | 0.64 | 7.87 | 8690 | 780 | 98 | 0.25 | 105.7 | .034 | 16 ⁽²⁾ | 784 | 0.25 |

- Notes: 1. NO_x Emissions guaranteed by boiler supplier only, equal to NSPS.
 2. Avg. EDC monitor opacity.
 3. Qualified observer.

Figure 3 is a schematic of the power boiler and scrubber systems showing the inlet and outlet sampling locations. The tests were conducted on one of the three identical scrubber modules which are operated in parallel to control SO₂ and particulate emissions from the power boiler. The three modules are independently controlled with respect to liquor flows and venturi pressure drop. Pressure drops across the venturis are regulated by adjusting the position of the "plumb bob" shown in Figure 3, thereby increasing or decreasing the cross sectional area of the venturi throat. Throughout these tests, with the exception of one brief period, the pressure drop across the venturi on the module being tested was held at 46 ± 2 cm w.c.. Gas temperatures at the scrubber inlet ranged from 129°C to 137°C. The scrubber exit gas temperatures ranged from 57°C to 60°C and temperatures at the outlet test plane ranged from 94°C to 99°C. The temperature rise between the scrubber exit and the outlet mass sampling location results from a flue gas reheat system and the action of the fan, both of which are located between the scrubber outlet and the sampling plane. The gas flow handled by the scrubber throughout the tests was approximately 130 DNCM/sec (280,000 DSCFM). A complete summary of the scrubber operating conditions during the tests conducted by SoRI are given in Table 5.

TEST METHODS AND RESULTS

A total of five measurement techniques were used during the tests. These were: (1) electrical mobility techniques using a Thermosystems Model 3030 Electrical Aerosol Analyzer for determining concentrations and size distributions on a number basis for particles having sizes between 0.01 μm and 0.3 μm , (2) optical techniques to determine concentrations and size distributions for particles having diameters between approximately 0.5 μm and 2.0 μm , (3) inertial techniques using cascade impactors for determining concentrations and size distributions on a mass basis for particles giving sizes between approximately 0.5 μm and 5.0 μm , (4) standard mass train (Method 17) measurements for determining total inlet and outlet mass loadings and emission rates, and (5) determinations of SO₂ concentrations by absorption of the SO₂ vapor in a solution of hydrogen peroxide followed by titration for the sulfuric acid reaction product.

The data obtained by Method 17 are summarized in Tables 6 and 7. The overall collection efficiencies for each of the pairs of tests are given in Table 8.

The overall collection efficiency of the scrubber on this source under the conditions of operation tested is thus found to be approximately 99.4 percent.

Inertial sizing was accomplished using modified Brink impactors for inlet measurements and University of Washington Mark III impactors for outlet measurements. Sampling was done in both cases at near isokinetic flow rates, thus errors due to deviations from isokinetic sampling should be of little consequence. All impactors used in this program were calibrated at SoRI using the methods described in EPA publications 600/2-76-280 and 600/2-77-004.

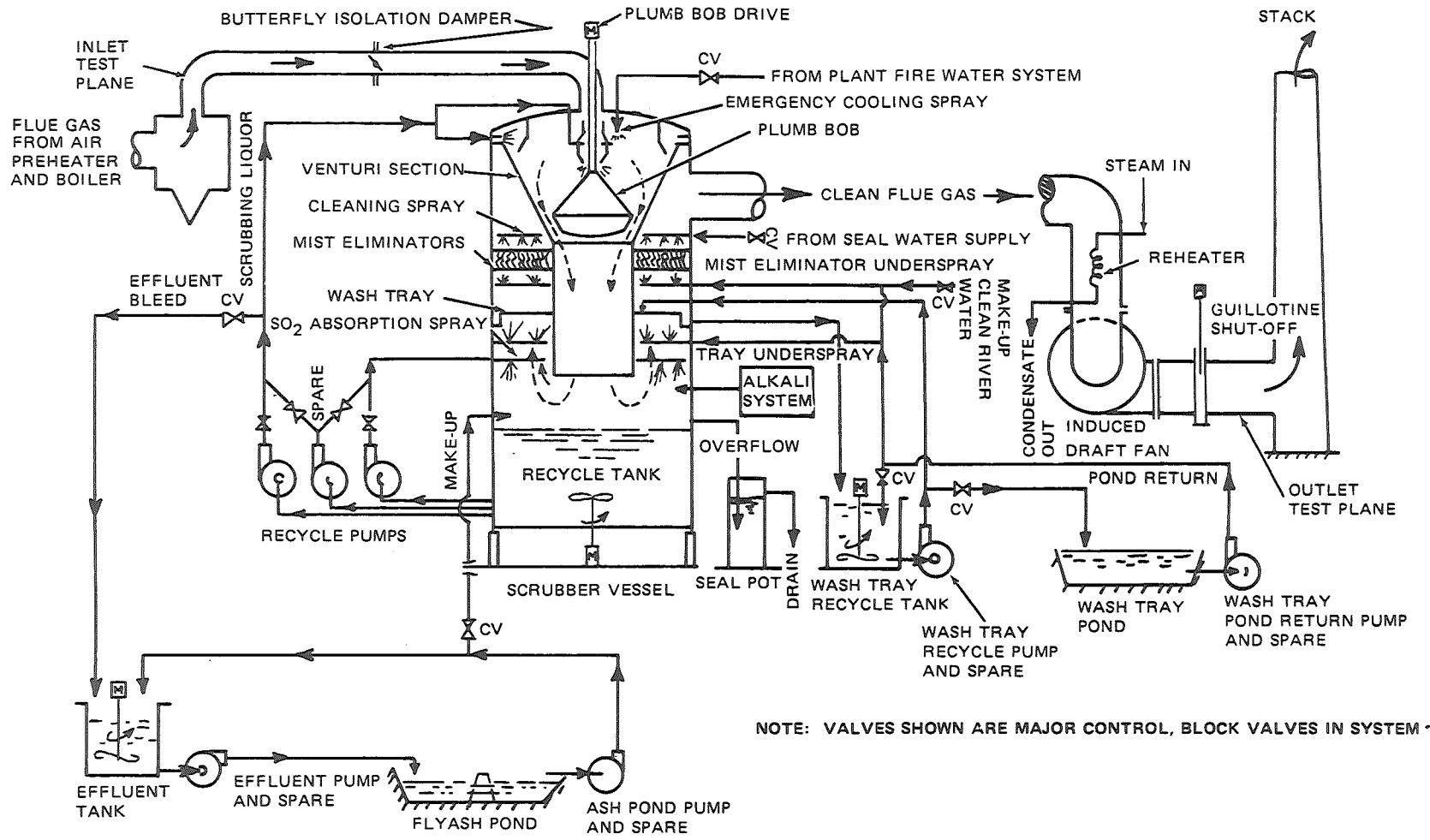


Figure 3. Simplified scrubber flow diagram.

Table 5
Scrubber Operating Conditions

| Date | Unit Load, MW | Measured Gas Flow, DNM/s | | Plumb Bob Position, % of Travel | Venturi P, cm w.c. | Temperatures, °C | | | | Liquor Flows, lpm | | | | | |
|------|------------------|-----------------------------|--------------------|---------------------------------------|--------------------------|-------------------|--------------------|------------------|---------------|-------------------|-----------------|---------------------|-----------------------------|-----------------------------|-------------------|
| | | Inlet | Outlet | | | Scrubber Inlet | Scrubber Outlet | Reheat Outlet | Fan Outlet | Upper Spray | Middle Spray | Absorption Spray | Mist Film Under Spray | Wash Tray Under Spray | Wash Tray Feed |
| 5/17 | 330 | 110 | 128 | 54 | 44.5 | 132 | 60 | 79 | 94 | 15900 | 10200 | 22700 | 570 | 1170 | 3600 |
| 5/18 | 350 | 132 | 140 | 58 | 46.4 | 129 | 58 | 78 | 96 | 15000 | 9370 | 24400 | 570 | 1060 | 2900 |
| 5/18 | 355 | 133 | 162 | 62 | 46.4 | 129 | 57 | 78 | 96 | 18200 | 11360 | 19870 | 570 | 1170 | 2800 |
| 5/19 | 355 | 130 | 137 | 61 | 46.4 | 131 | 59 | 78 | 96 | 17600 | 10790 | 24600 | 625 | 1170 | 3220 |
| 5/19 | 355 | 124 | 139 | 61 | 47.0 | 133 | 57 | 74 | 96 | 17500 | 10600 | 24200 | 625 | 1190 | 2840 |
| 5/20 | 290 | (106) ¹ | (113) ¹ | 53 | 45.7 | 129 | 56 | 82 | 93 | 17800 | 10600 | 25700 | 530 | 1170 | 3220 |
| 5/20 | 348 | (127) ¹ | (136) ¹ | 65 | 45.1 | 129 | 52 | 82 | 93 | 17600 | 11700 | 25000 | 570 | 950 | 3220 |

| | Liquor pH | % Suspended Solids |
|------|--------------|-----------------------|
| 5/17 | 4.3 | 11.4 |
| 5/18 | 4.7 | 15.2 |
| 5/18 | 4.7 | 16.4 |
| 5/19 | 4.7 | 14.3 |
| 5/19 | 4.6 | 13.4 |
| 5/20 | N.A. | N.A. |
| 5/20 | N.A. | N.A. |

¹Based on partial traverse and scaling from previous days.

Table 6

CEA VARIABLE THROAT VENTURI TEST
INLET MASS DATA

| Run Number | 1 | 2 | 3 | 4 | 5 | 6 |
|---|---------|---------|---------|---------|---------|---------|
| Date | 5-16-77 | 5-17-77 | 5-18-77 | 5-18-77 | 5-19-77 | 5-19-77 |
| Time | 1715 | 1455 | 1235 | 1545 | 0825 | 1245 |
| Moisture, % | 10.30 | 11.62 | 10.25 | 10.87 | 11.86 | 12.26 |
| Gas Temperature, °C | 134 | 132 | 129 | 129 | 137 | 133 |
| °F | 274 | 269 | 265 | 264 | 278 | 272 |
| Volumetric Flow, m ³ /sec | 208.6 | 201.3 | 233.9 | 236.9 | 238.8 | 227.6 |
| ACFM | 442,000 | 426,500 | 495,500 | 502,000 | 506,000 | 482,300 |
| Volumetric Flow, DNM/s | 116.5 | 110.3 | 131.9 | 132.9 | 130.1 | 124.4 |
| DSCFM | 247,700 | 233,600 | 279,500 | 281,500 | 275,600 | 263,500 |
| Concentration, grams/ACM | 2.0184 | 2.8325 | 3.3097 | 3.4820 | 3.5145 | 3.5829 |
| Concentration, grams/DNFM | 3.6145 | 5.1701 | 5.8663 | 6.2079 | 6.4512 | 6.5546 |
| Isokinetic, % | 107.62 | 105.85 | 104.23 | 108.62 | 103.79 | 103.56 |

Table 7

CEA VARIABLE THROAT VENTURI
OUTLET MASS TRAIN DATA

| Run Number | 1 | 2 | 3 | 4 | 5 | 6 |
|---|---------|---------|---------|---------|---------|---------|
| Date | 5-16-77 | 5-17-77 | 5-18-77 | 5-18-77 | 5-19-77 | 5-19-77 |
| Time | 1700 | 1315 | | 1500 | 0830 | 1300 |
| Moisture, % | 14.01 | 19.45 | 17.37 | 16.53 | 18.70 | 18.15 |
| Gas Temperature, °C | 99.4 | 94.4 | 96.1 | 96.1 | 96.1 | 96.1 |
| °F | 211 | 202 | 205 | 205 | 205 | 205 |
| Volumetric Flow, m ³ /s | 194.9 | 224.8 | 238.9 | 273.8 | 237.8 | 239.3 |
| ACFM | 413,000 | 476,200 | 506,200 | 579,300 | 503,800 | 507,000 |
| Volumetric Flow, DNM ³ /s | 118.4 | 128.4 | 140.0 | 162.1 | 137.3 | 139.3 |
| DSCFM | 250,800 | 171,100 | 196,700 | 343,500 | 290,900 | 295,200 |
| Concentration, mg/ACM | 26.09 | 25.86 | 19.66 | 21.52 | 24.23 | 19.23 |
| Concentration, mg/DNCM | 42.79 | 45.31 | 33.58 | 36.28 | 41.90 | 33.04 |
| Isokinetic, % | 105.71 | 113.99 | 106.40 | 106.76 | 103.91 | 104.66 |

Table 8

CEA VARIABLE THROAT VENTURI SCRUBBER EFFICIENCIES
FROM MASS TRAIN DATA

| Run No. | Date | Efficiency (%) |
|---------|---------|----------------|
| 1 | 5-16-77 | 98.82 |
| 2 | 5-17-77 | 99.12 |
| 3 | 5-18-77 | 99.43 |
| 4 | 5-18-77 | 99.42 |
| 5 | 5-19-77 | 99.35 |
| 6 | 5-19-77 | 99.50 |

The impactor data are summarized in Figures 4 through 8. Figures 4 and 5 present averaged inlet and outlet size distributions, respectively, on a cumulative percentage (by mass) basis versus aerodynamic particle diameter. Figures 6 and 7 show the same data on a cumulative mass concentration basis. Figure 8 shows the fractional efficiency curve as a function of aerodynamic particle diameter as derived from the inlet and outlet data that were presented in the previous figures. The fractional efficiency curve is shown later in Figure 11 as a function of Stokes diameter together with the efficiency curves derived from the ultrafine particulate data. The scrubber was operating at a venturi pressure drop of about 48 cm w.c. throughout the impactor test periods.

Measurements of the concentration and size distribution of ultrafine particulates were made using a Thermosystems Model 3030 Electrical Aerosol Analyzer (EAA) and a Royco Model 241 Optical Single Particle Counter.

The EAA provides size distribution and concentration data on a number basis for particles having diameters between approximately 0.01 μm and 0.3 μm . The optical counter provides similar data in the range from approximately 0.3 to 2 μm . Both instruments require extensive sample dilution and conditioning when used to sample flue gases. The sample extraction and dilution system used in these tests is described in a forthcoming EPA report on Contract 68-02-2114, Task VIII. Dilution factors of about 150:1 were used at both the inlet and outlet during these tests.

In order to insure that condensation effects were minimal, and that the particles were dry as measured, the diluent air was dried and filtered, and diffusional dryers were utilized in the lines carrying the diluted samples to the instruments.

Because only one set of instruments and dilution system was available it was not possible to obtain simultaneous inlet and outlet data for the ultrafine particulates. The system was first installed at the scrubber inlet and all inlet data were obtained on May 17. The equipment was then moved to the outlet and outlet data were obtained on May 19 and 20. For the purposes of calculating fractional efficiencies the assumption was made that the process was sufficiently stable that the inlet data, as obtained above, were a valid representation of that which would have obtained during the time the outlet measurements were made.

Inlet data were obtained with the optical counter in two size channels-- 0.35 to 0.60 μm and 0.60 to 2.0 μm . However, an instrument malfunction resulted in outlet data being obtained only in the 0.6 to 2.0 μm size interval with this method.

Inlet size distributions on a cumulative concentration by number basis are shown in Figure 9. Outlet size distributions on a similar basis are shown in Figure 10 for the normal scrubber operating condition (48 cm w.c. venturi pressure drop). Figure 11 shows the fractional efficiencies for ultrafine particles. Also shown in Figure 11 are the fractional efficiencies as a function of Stokes diameter, obtained from the impactor data.

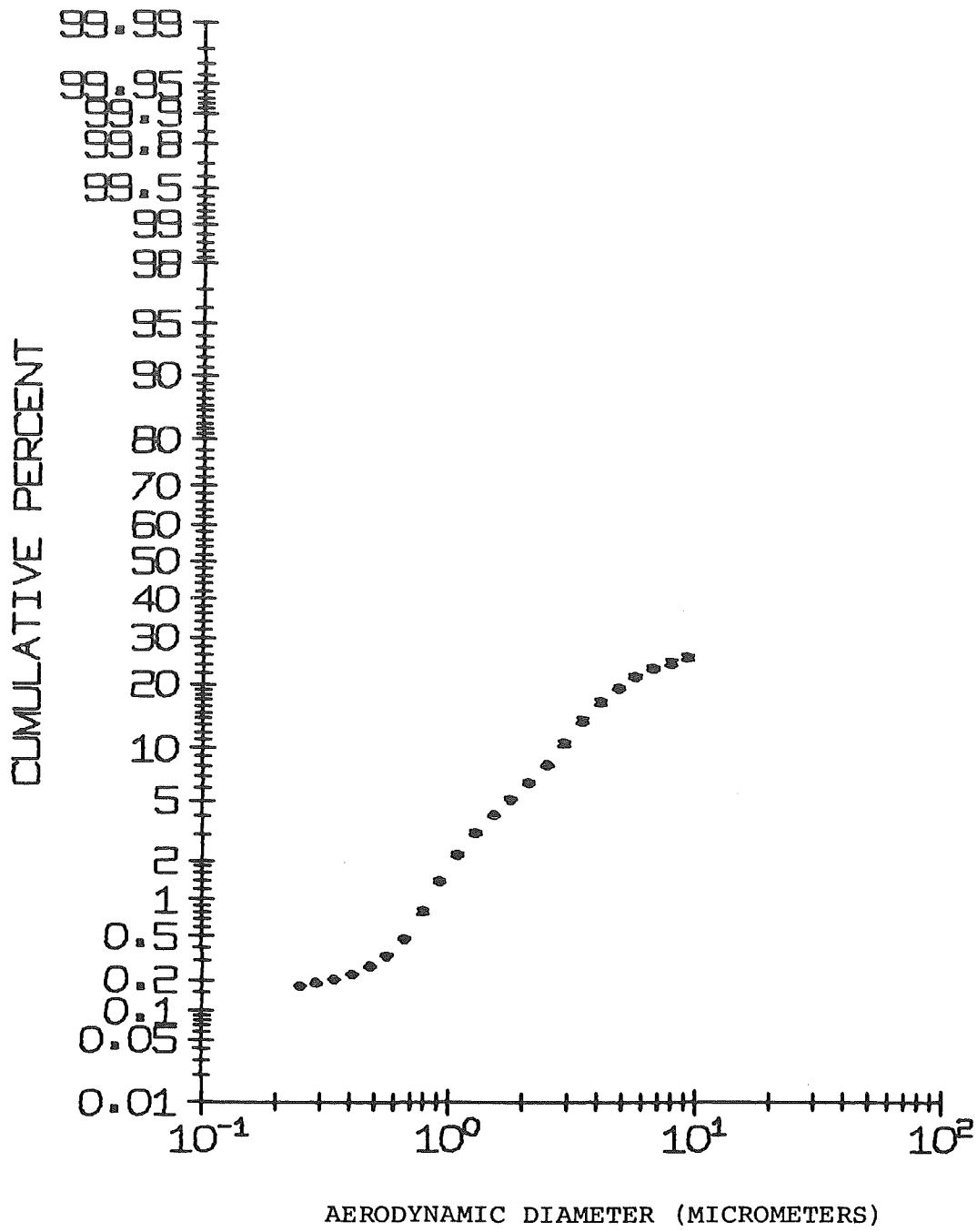


Figure 4. Average inlet particle size distribution from cascade impactor data on a cumulative percent by mass basis.

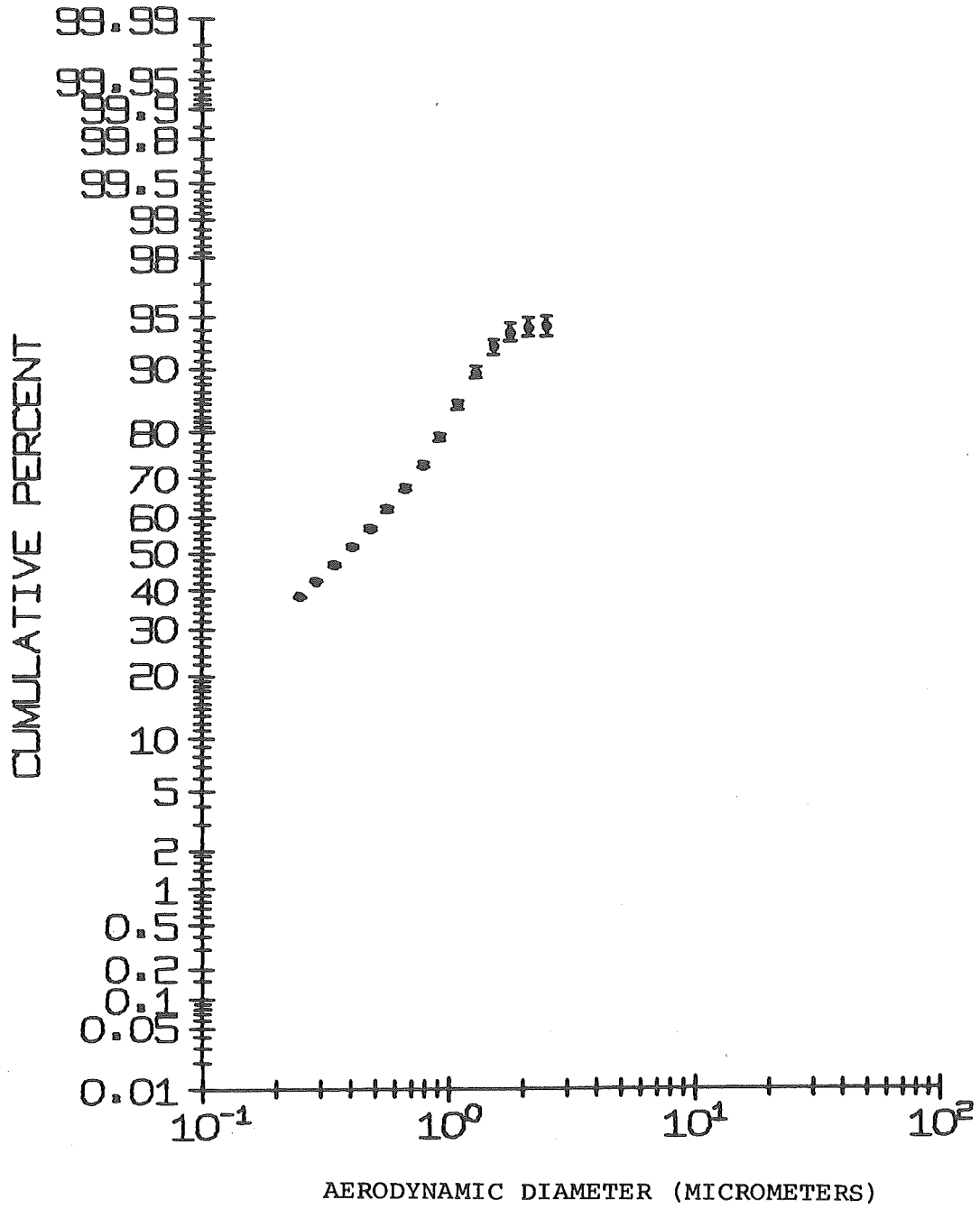


Figure 5. Average outlet particle size distribution from cascade impactor data on a cumulative percent by mass basis.

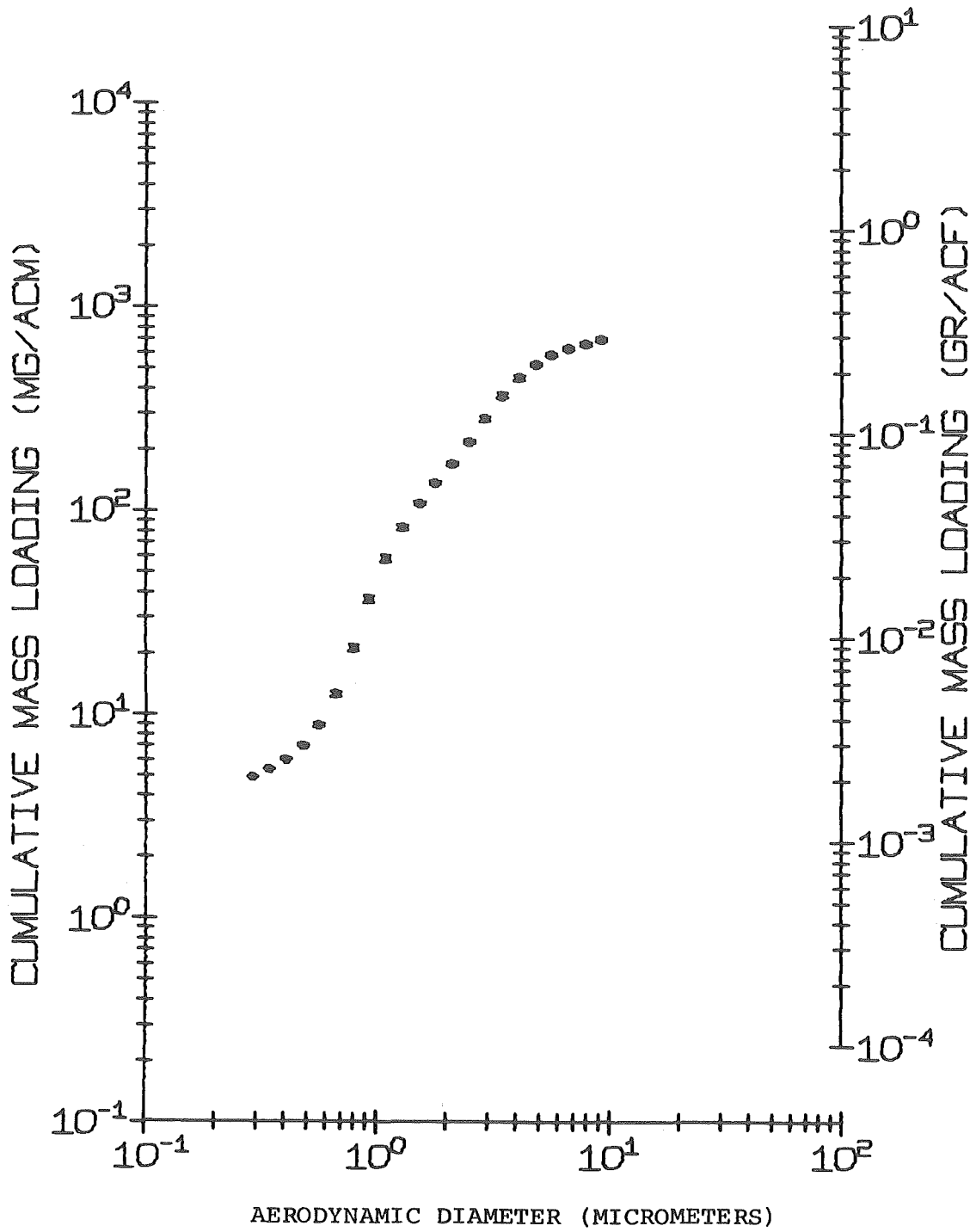


Figure 6. Average inlet particle size distribution on a cumulative mass concentration basis from cascade impactor data.

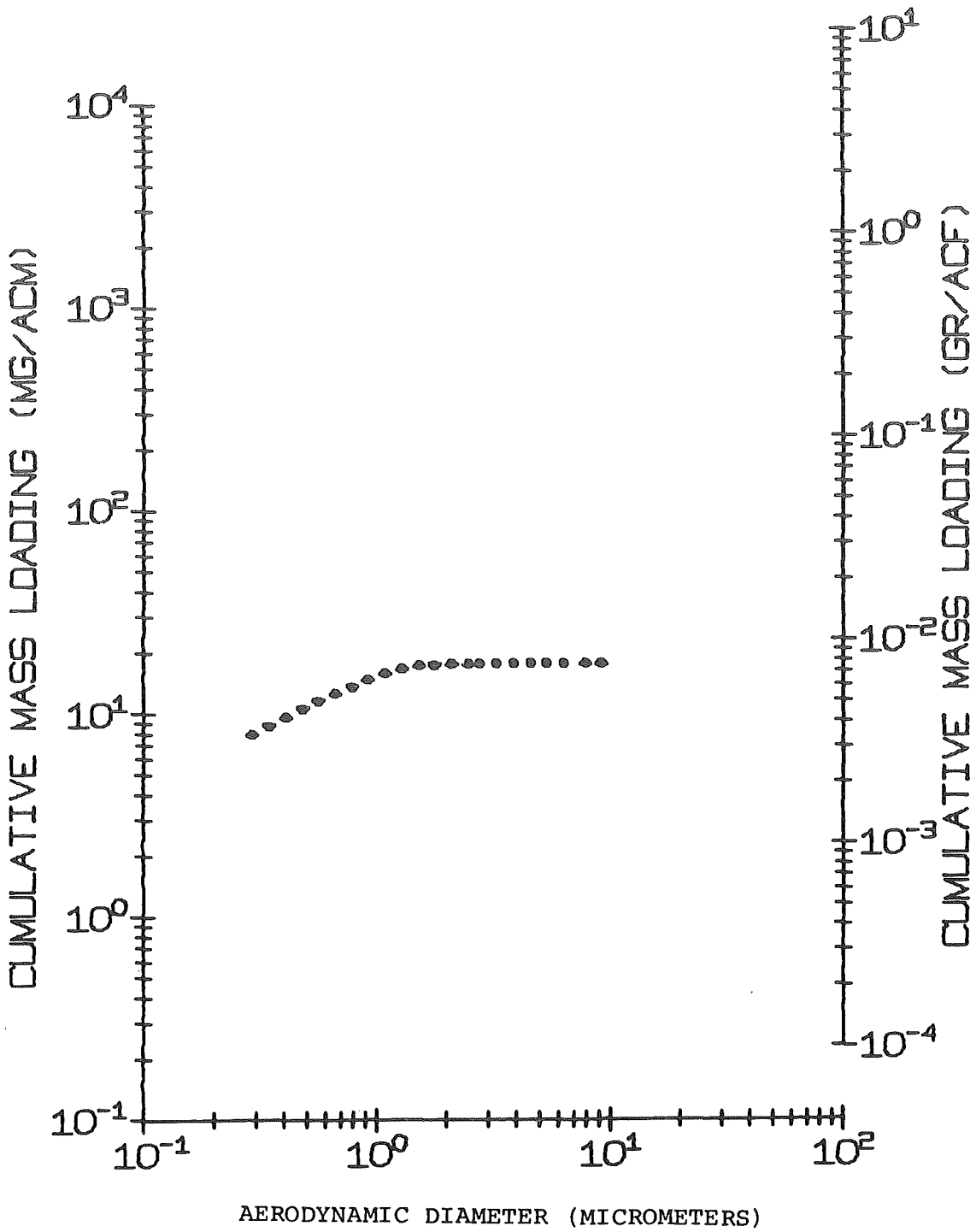


Figure 7. Average-outlet particle size distribution on a cumulative mass concentration basis from cascade impactor data.

PENETRATION-EFFICIENCY

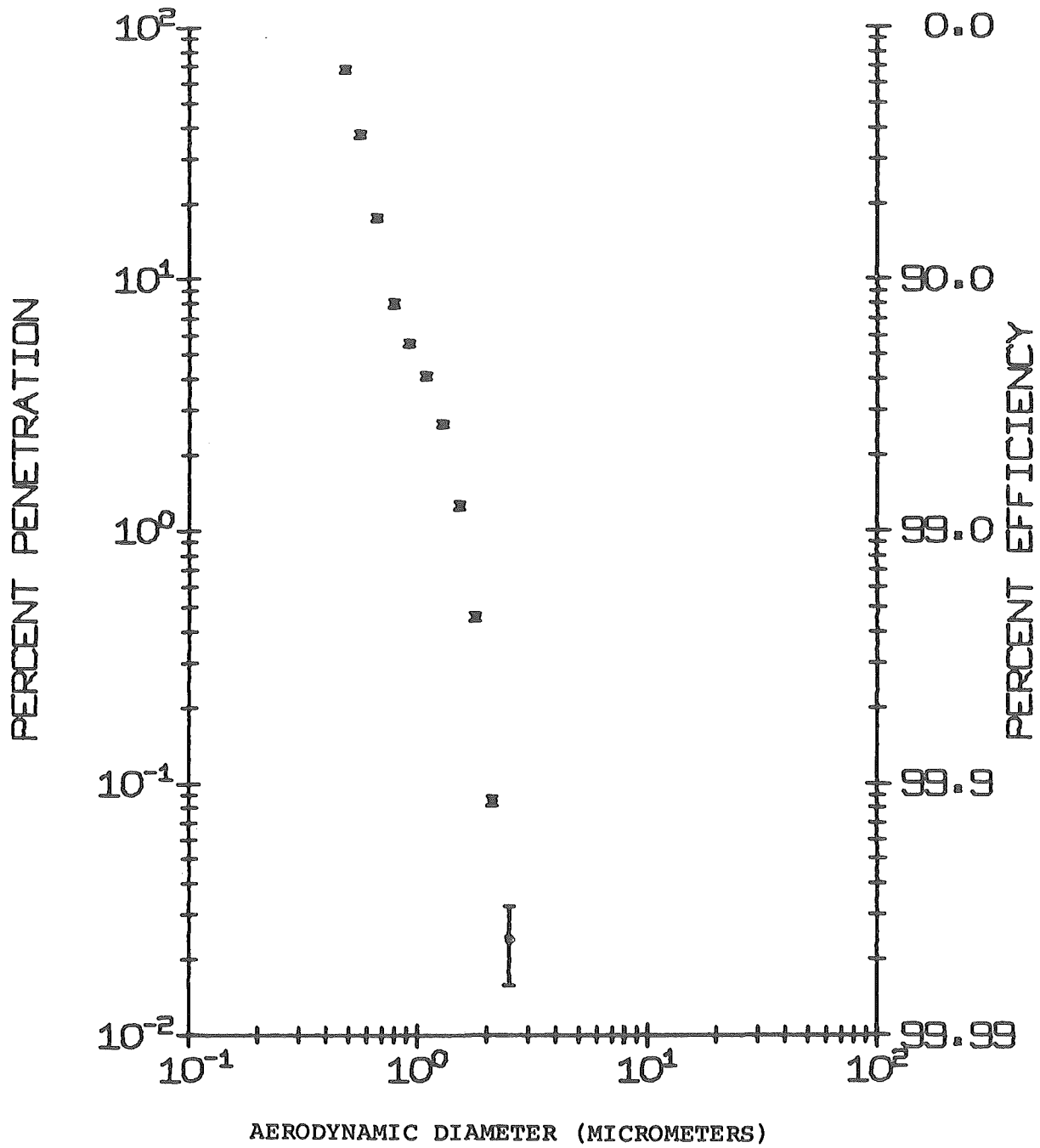


Figure 8. Fractional efficiency curve on an aerodynamic particle diameter basis for the CEA variable throat venturi scrubber operating at a venturi pressure drop of 48 cm (19 in.) w.c..

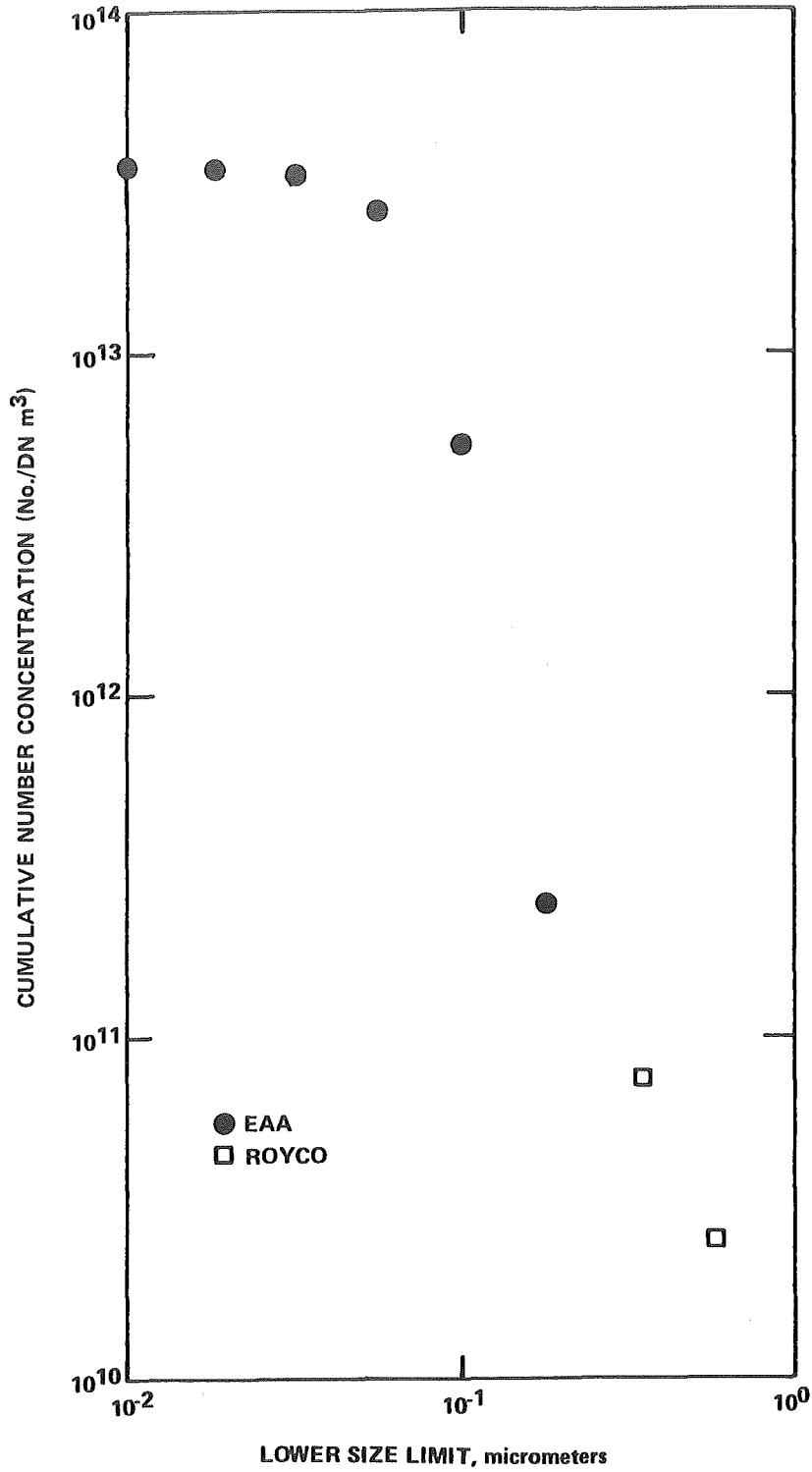


Figure 9. Scrubber inlet particle size distribution from electrical aerosol analyser and Royco optical particle counter data.

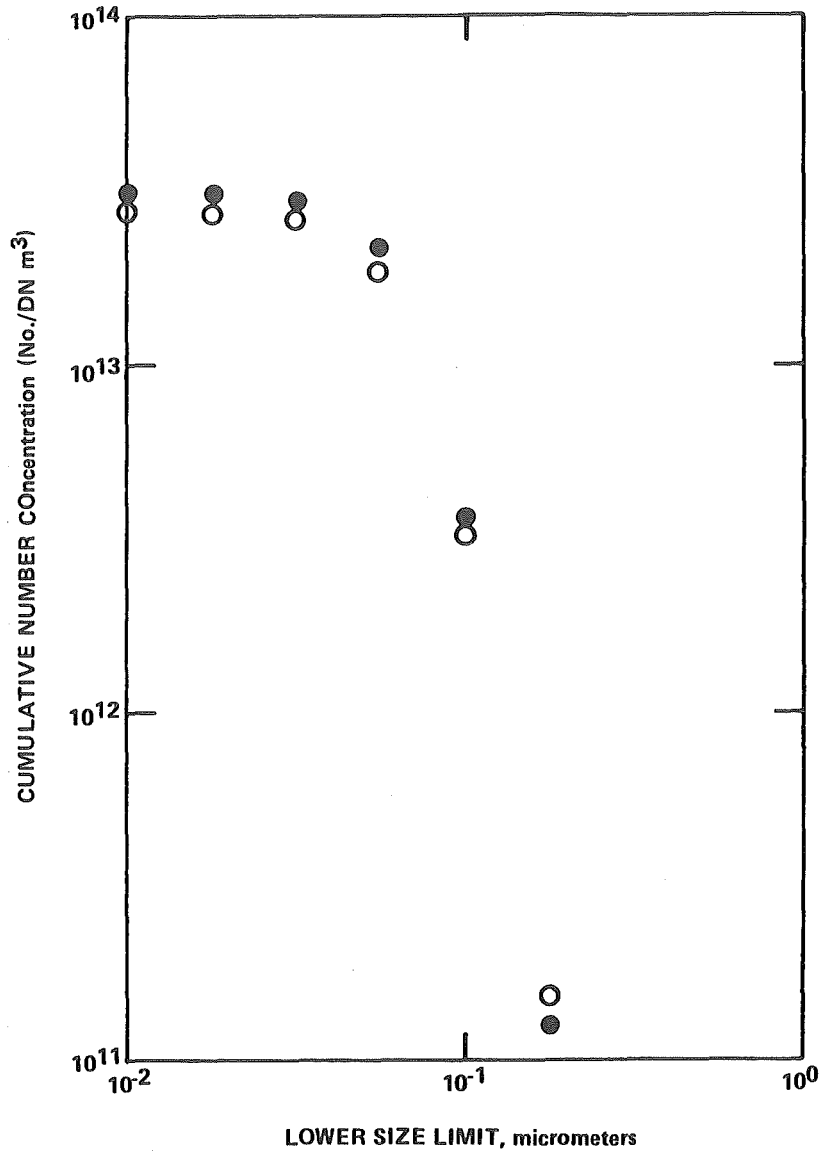


Figure 10. Scrubber outlet particle size distribution from electrical aerosol analyser data.

PENETRATION-EFFICIENCY

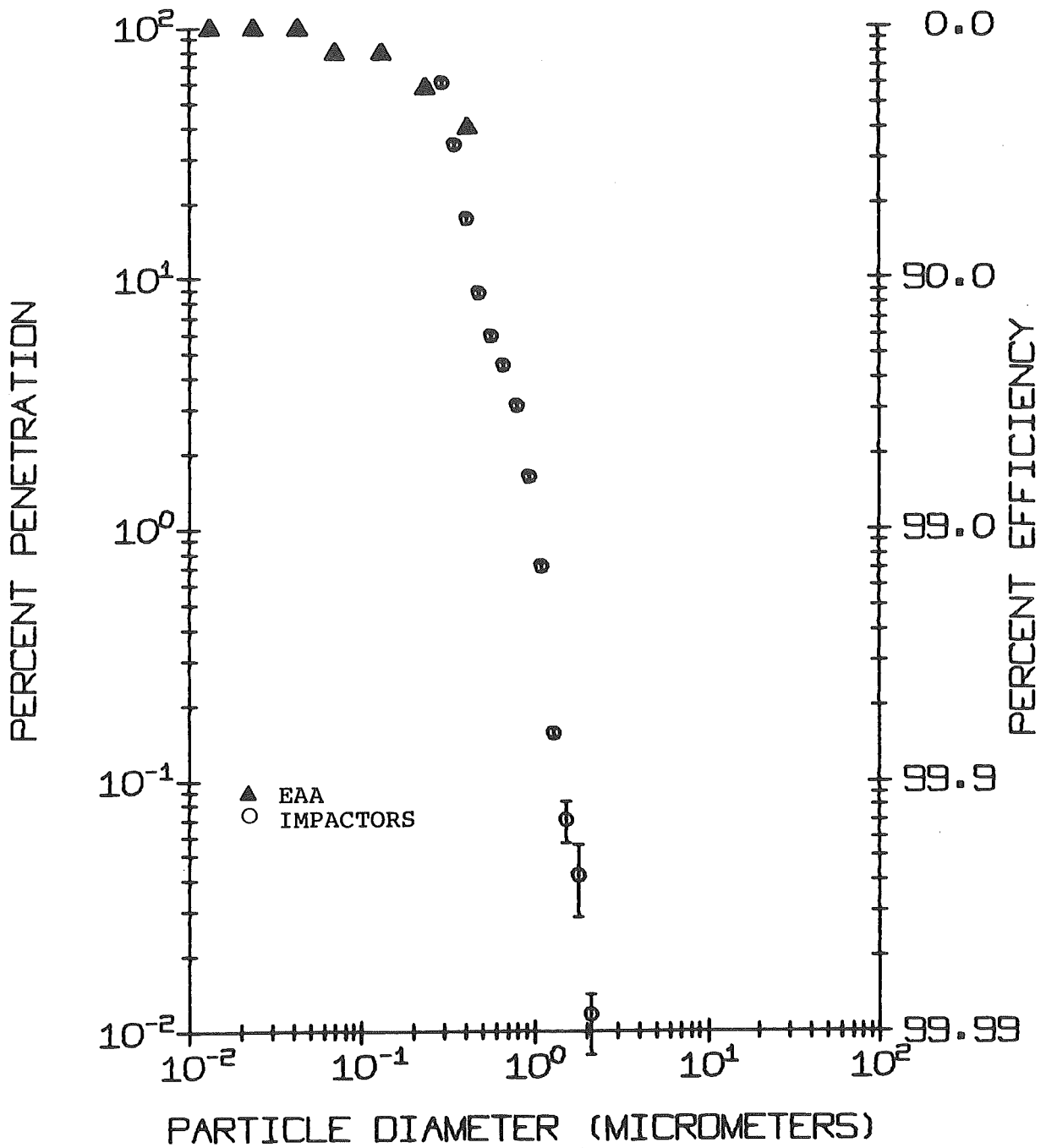


Figure 11. Fractional efficiencies based on electrical mobility and optical methods shown on a "physical" diameter basis. Also shown are fractional efficiencies from the cascade impactor data on a basis of Stokes diameters.

The scrubber was operated at venturi pressure drops of 31, 36, 41, 46, and 51 cm w.c. for a brief period at each condition on May 21, during which time the outlet concentrations were monitored with the EAA and the optical counter. No significant concentration changes were noted in the EAA data over this range of pressure drops, however, the optical counter data did show significant changes. In the 2 μm to 4 μm size interval, a 50% reduction in concentration was obtained by increasing the venturi pressure drop from 31 to 51 cm w.c. and a 35% reduction in concentration occurred in the 0.6 μm to 2.0 μm particle diameter range. These relative concentration changes are shown in Figure 12.

The results of the SO_2 concentration measurements at the scrubber inlet and outlet are given in Table 9. Table 9 also includes SO_2 collection efficiencies derived from the concentration measurements.

SUMMARY

The overall collection efficiency of the CEA variable throat venturi scrubber, determined by conventional (Method 17) techniques on a pulverized coal fired power boiler producing particulate having a mass median diameter of about 20 μm , ranged from 99.12 to 99.50 during three days of testing. The venturi pressure drop ranged from 44.5 cm w.c. to 48.3 cm w.c.. Measured fractional efficiencies were about 5% at 0.06 μm , 25% at 0.1 μm , 40% at 0.20 μm , 50% at 0.5 μm , 98.4% at 1.0 μm , and 99.99% at 2 μm . The system energy usage during the tests was approximately 7200 joules/DNCM. SO_2 collection efficiency ranged from 76.5% to 85.6%.

ACKNOWLEDGEMENTS

Appreciation is expressed to B. Knutson, D. Berube, and C. Grimm of The Montana Power Company for their cooperation during the test program. Appreciation is also expressed to I. A. Raben of Combustion Equipment Associates, Inc. for supplying the information on the design and operation of the scrubber. The test program was conducted under Contract 68-02-2181 for the Industrial Environmental Research Laboratory of the U.S. Environmental Protection Agency. Mr. Dale L. Harmon was the project officer responsible for the technical effort under this contract.

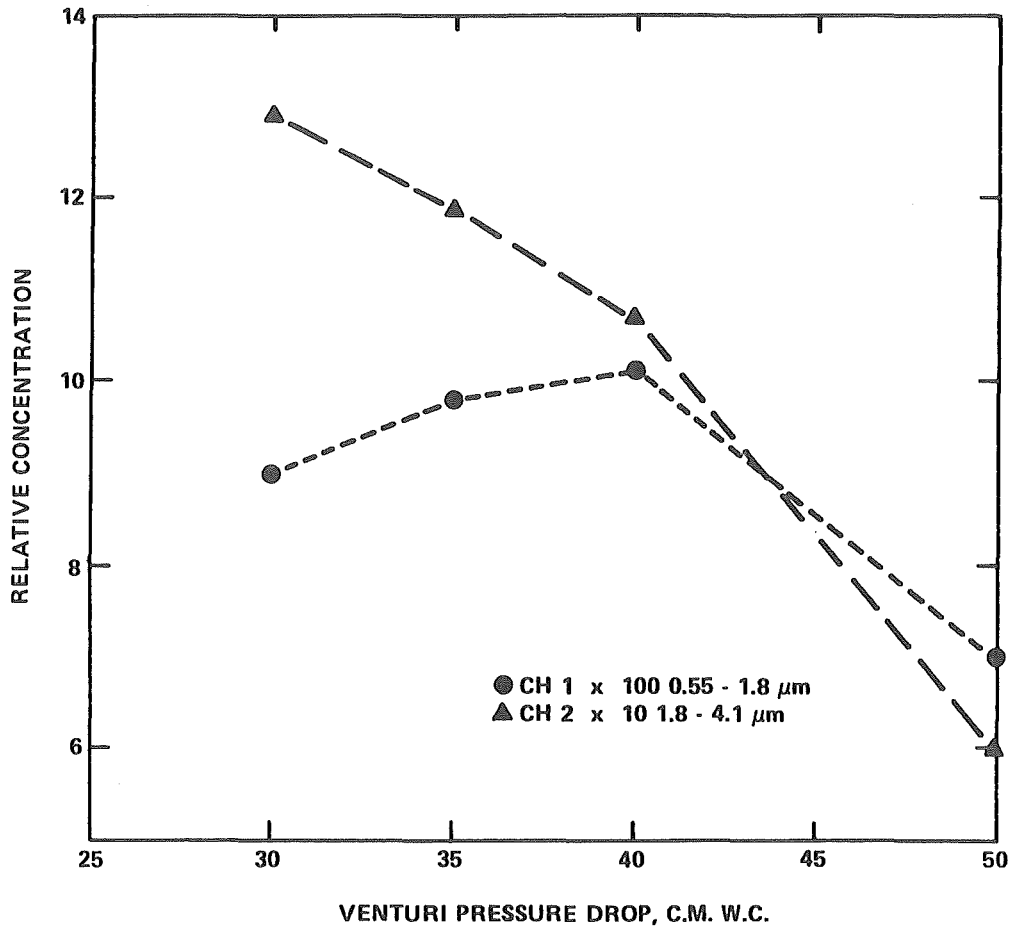


Figure 12. Relative outlet particulate concentrations in two size ranges as functions of venturi pressure drop.

Table 9

COLSTRIP POWER PLANT
SCRUBBER SO₂ REMOVAL EFFICIENCY

| Date | Inlet SO ₂ Concentration (ppm) | Reheater Outlet SO ₂ Concentration (ppm) | SO ₂ Removal Efficiency (%) |
|---------|---|---|--|
| 5-17-77 | 658 | 130 | 80.2 |
| 5-18-77 | 525 | 103 | 80.4 |
| 5-19-77 | 553 | 130 | 76.5 |
| 5-20-77 | 625 | 90 | 85.6 |

Discussion

Dr. Holighaus opened the discussion with a question regarding the difference between using slurry or clean liquid as a cleaning mechanism with view to particle separation. Dr. Calvert maintained that there was little difference; more fundamental was the mass ratio of scrubbing liquid gas. He wondered if the use of a sieve plate would exclude effectively the large particles; a pressure drop of approximately 3-9 ins. would be able to cause removal. Prof. Weber asked what the availability of this kind of plant was, and was told that there was 90% availability.

Dr. Holighaus inquired whether it would separate fly ash and calcium sulphate from the liquid and what happened to water from the ash pond. According to Mr. McCain, separation was unnecessary and water was recirculated. No calcium sulphate was present in the emissions. Mr. Princiotta added that low sulphur coal was suitable for this process.

SIMULTANEOUS SEPARATION OF DUST AND GASEOUS CONSTITUENTS AT
=====

HIGH GAS TEMPERATURES BY THE USE OF MOLTEN METALS AND SALTS.
=====

Prof. Dr.-Ing. E. WEBER
Institut für Mechanische Verfahrenstechnik
Universität Essen GHS
Universitätsstraße 2
Postfach 68 43
D 4300 Essen
Tel. 0201-1832795

Dr.rer.nat. K. HÜBNER
Institut für Mechanische Verfahrenstechnik
Universität Essen GHS
Universitätsstraße 2
Postfach 68 43
D 4300 Essen
Tel. 0201-1832786

SIMULTANEOUS SEPARATION OF DUST AND GASEOUS CONSTITUENTS AT
=====

HIGH GAS TEMPERATURES BY THE USE OF MOLTEN METALS AND SALTS.
=====

K. Hübner, E. Weber

Today the cost and the efficiency of power plants strongly depend on the gas cleaning system. This can be best illustrated for the example of the carbon gasification process. The usual way of handling the generated gas is to cool it down by direct contact to water which is sprayed by nozzles into a spray tower. After that, any conventional gas cleaning system can be employed. This procedure, however, results in an irreversible loss of thermal energy and an unwanted decrease of the power plant's overall energetic efficiency. This difficulty can be avoided by use of a heat exchange system. The gas coming from the gas generator usually contains large amounts of dust and sulfur and in many cases tarry materials causing sticking effects. The properties of the solids to be separated and the wanted high efficiency of the heat exchanger raise great difficulties. It may be necessary to use at least two parallel heat exchange systems.

Using a wet scrubber, a sophisticated regeneration system for the washing liquid is needed. The overall cost of investment and the cost of operation are extremely increased. It seems to be at least doubtful whether the energy spared by the heat exchange system can justify these costs.

The application of fibre filter separators or electrostatic precipitators instead of a Venturi scrubber will raise the cost too, because of the unavoidable additional cleaning system for the gaseous constituents.

It can be summarized that until today, there are no gas cleaning systems allowing the simultaneous separation of gaseous and solid pollutants at elevated temperatures of more than 400 °C without loss of the heat content.

A possible solution for this problem is offered by a high temperature scrubbing process using a suitable washing liquid. The washing medium should be sprayable at elevated temperatures just like water or aqueous solutions in the conventional scrubbing processes. The application of the washing liquid should not lead to additional problems of emission.

For such a gas cleaning system two types of washing media have been developed, the composition of which can slightly be modified according to the given conditions of application. The first type of washing liquid is a melt of inorganic metal compounds having a density of about 1.4 kg/l and a surface tension of about 0.1 N/m. These properties are similar to that of water at room temperature. The other type of washing medium is a mixture of molten metals having a density of about 4.5 to 7 kg/l and a surface tension of about 0.5 N/m.

From the temperature dependence of the vapour pressures (fig. 1) it can be seen that the metal compound melt should not be used at temperatures of more than 1100 K or 800 °C. At this temperature the vapour pressure of this melt is in the 100-Pascals-region, whereas the metal melt has a vapour pressure as low as 1 to 10 Pascals even at 1300 K or 1000 °C. The viscosities of both melts are sufficiently small (fig. 2) in the total given temperature range that means both melts are well sprayable. Whereas the metal melt is only applicable for reductive gases the metal compound melt can be used independently of the oxygen content of the gas. The metal melt allows the separation of a single gaseous pollutant : hydrogen sulfide, which can be removed from the melt by hydrogen rich gas at elevated temperatures to regenerate the melt. The metal melt does not react chemically with solid particles. On the other hand, however, the metal compound melt allows not only the separation of many gaseous constituents with acidic character but even undergoes chemical reaction with solid particles.

Due to its great reactivity the metal compound melt causes material and regeneration problems. The material problems can be solved by the use of nickel alloys. The regeneration of the melt is not necessary

in most cases, since it can operate as a washing medium nearly to the point of chemical saturation with pollutants. The reaction products can be led to disposal after suitable treatment.

Figure 3 shows a scheme of a gas cleaning system using melts as a washing media. After the precipitation of the larger dust particles by a cyclone the gas is scrubbed in a Venturi using the metal-compound melt and then passed to a droplet separator. The melt can be recycled without cleaning to the Venturi for several times because most of the dust particles react with the melt forming a solution which is sprayable without blocking the Venturi's nozzles.

To maintain the melt's reactivity it is necessary that the overall reaction of the melt is basic.

On the other hand it is necessary to neutralize the reacted melt with acidic oxides like SiO_2 or B_2O_3 in order to obtain waste products which can be led to disposal.

Due to the metal-compound melt's low cost and due to its high efficiency this seems the less problematic way, but in principle the melt can be reactivated in the case of the removal of gaseous constituents like SO_2 or H_2S .

In the case of a metal melt, it is necessary to separate the dust particles from the bulk liquid because of the high cost for the metal melt. This can easily be done by the differences in densities between dust and melt. The melt's density is at about 3 times higher than that of the solid particles (e. g. fly ash from a power plant). From the basic laboratory experiments the use of metal and metal compound melts seems practicable for the simultaneous removal of gaseous constituents and solid particles from gases.

Measurements at relatively low gas velocities of less than 10 m/s with a discontinuously operating laboratory plant at temperatures of 400°C have shown that both melts allow the precipitation of dust with an efficiency of more than 95 percent. For the laboratory experiments a metal melt was used which consists of pure tin.

Due to the physical properties of the metal melt it needs high liquid-pressures for spraying when a commercial full cone nozzle is applicated whereas the metal compound melt which consists mainly of alkaline materials can be sprayed like water.

The high liquid-pressures can be avoided by the use of pneumatic atomizers. Figure 4 shows the drop size distribution for a full cone nozzle obtained at a liquid pressure of 12 bars and that for a pneumatic atomizer at 2,5 bars. The drop size distributions have been calculated from sieve analysis of solidified melt droplets which had been chilled by spraying into atmospherical air.

In both cases mean particle sizes of about 300 μm are achieved.

As already mentioned, alkaline melts can be used for the removal of a large scale of gaseous constituents, whereas a tin melt reacts only with hydrogensulphide.

The table gives a comparison of typical reactions between gases and melts at a temperature of 800 K. It can be seen that the reaction of sodium hydroxide, a possible component of an alkaline melt takes place with a relatively large change of the Gibbs-energy, that means the thermodynamic equilibrium is dominated by the removal of the gaseous constituents. In the case of a tin melt the change of the Gibbs-energy is somewhat smaller, but it must be taken into consideration that gases from coal gasitication processes contain simultaneously hydrogen sulfide and hydrogen.

The equilibrium in such gases depends on the ratio of hydrogen partial pressure and the hydrogen sulfide pressure.

Figure 5 shows the Gibbs-energy for the removal of hydrogen sulfide by a tin melt depending on the temperature. It can be seen that for small p_{H_2} to $p_{\text{H}_2\text{S}}$ ratios and comparatively low temperatures the removal of H_2S is favoured, whereas for a hydrogen rich gas and high temperatures the decomposition of the tin sulfide is dominating.

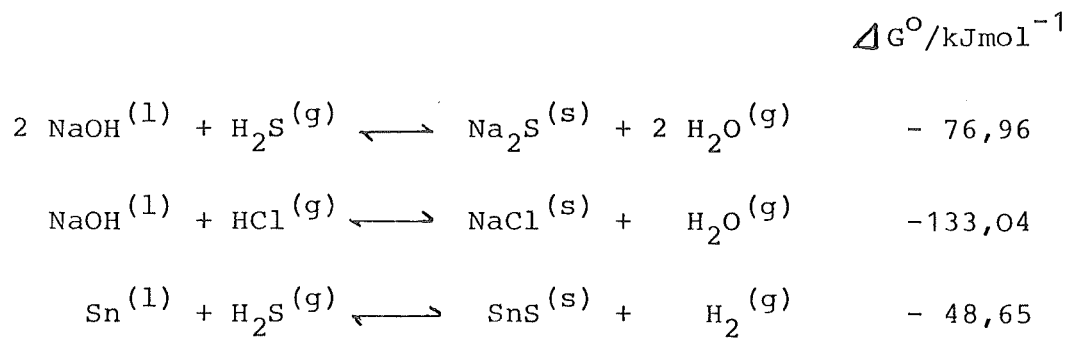
From the viewpoint of the thermodynamic equilibrium both the removal of H_2S and the generation of the tin melt seem possible. Laboratory

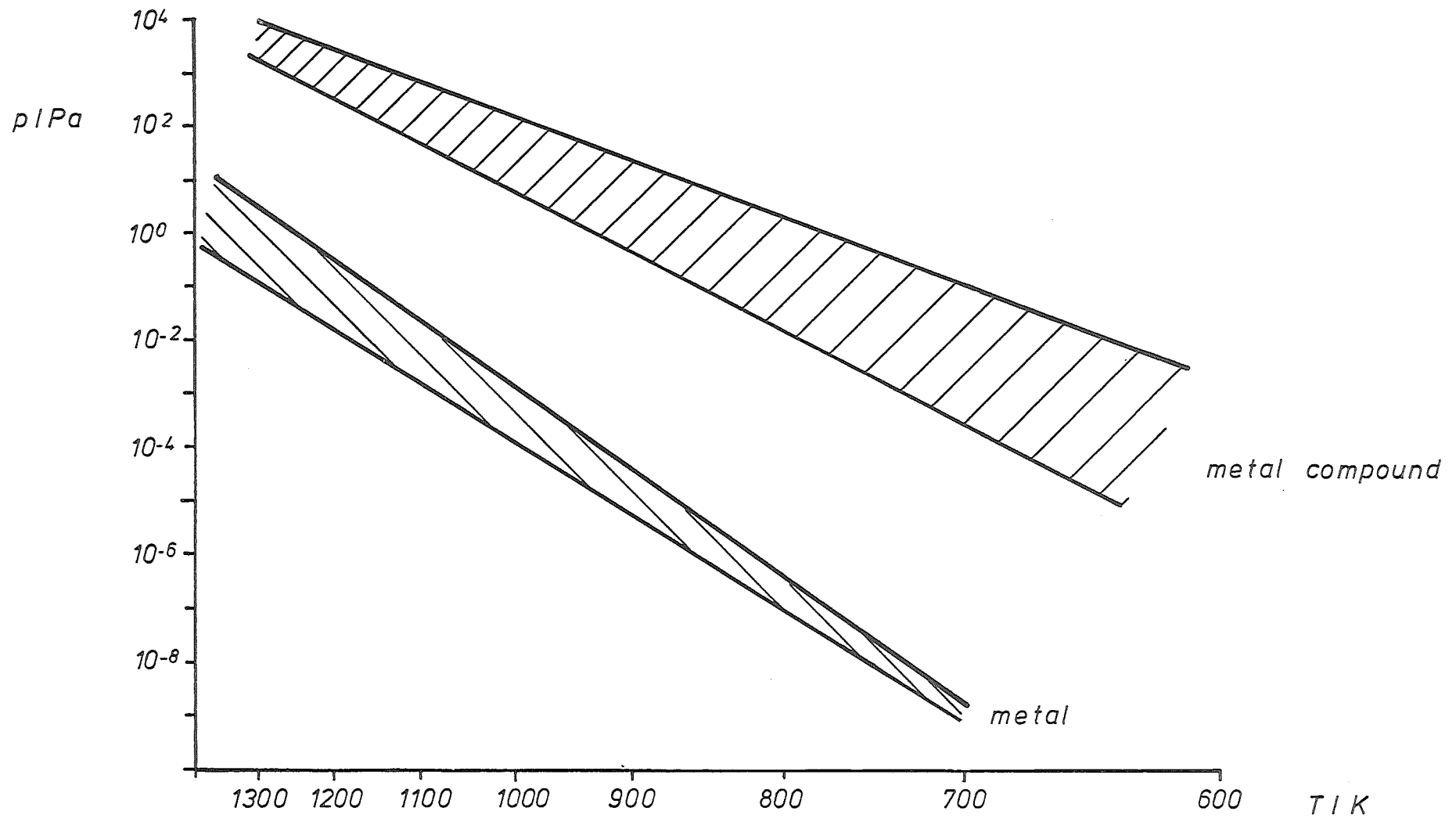
experiments have confirmed these findings showing no severe kinetic hindering at temperatures of more than 400 °C.

At present a continuous pilot plant for 400 m³ gas/h at temperatures of more than 400 °C has been constructed and will operate in a few weeks to complete the experiments of the small discontinuous laboratory plant. The measurements shall be expanded especially into the region of higher gas velocities, in order to optimize the removal of fine particles. Summarizing it can be stated that the application of molten metals or molten salts seems to offer a low cost solution for gas cleaning problems in power plants and in any case where clean gases are needed at high temperatures and pressures.

Table: Standard Gibbs-Energy at 800 K.

Some typical reactions of gases with metal and alkaline compound melts.

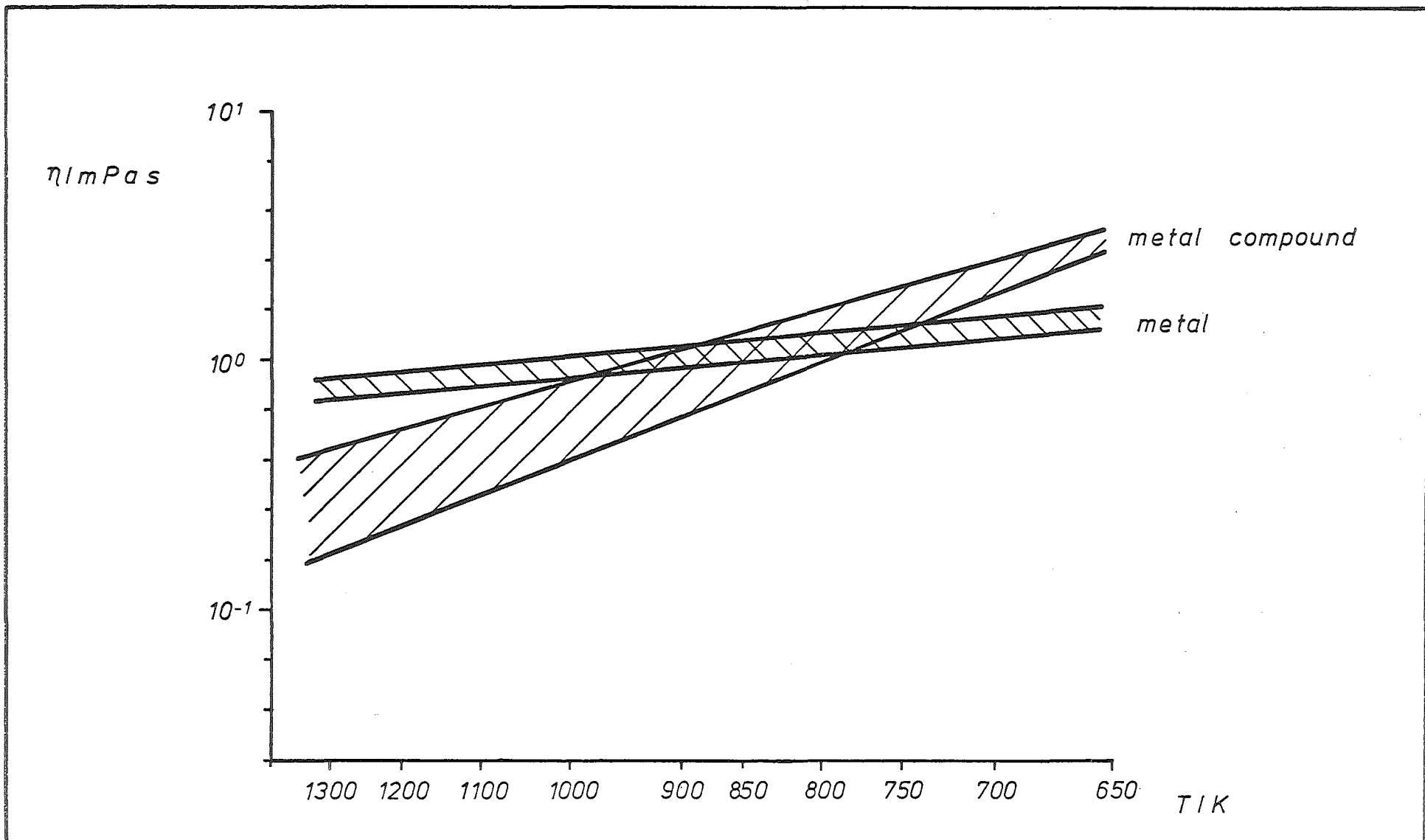




Mechanische
Verfahrenstechnik
Universität Essen

Vapour pressures of melts

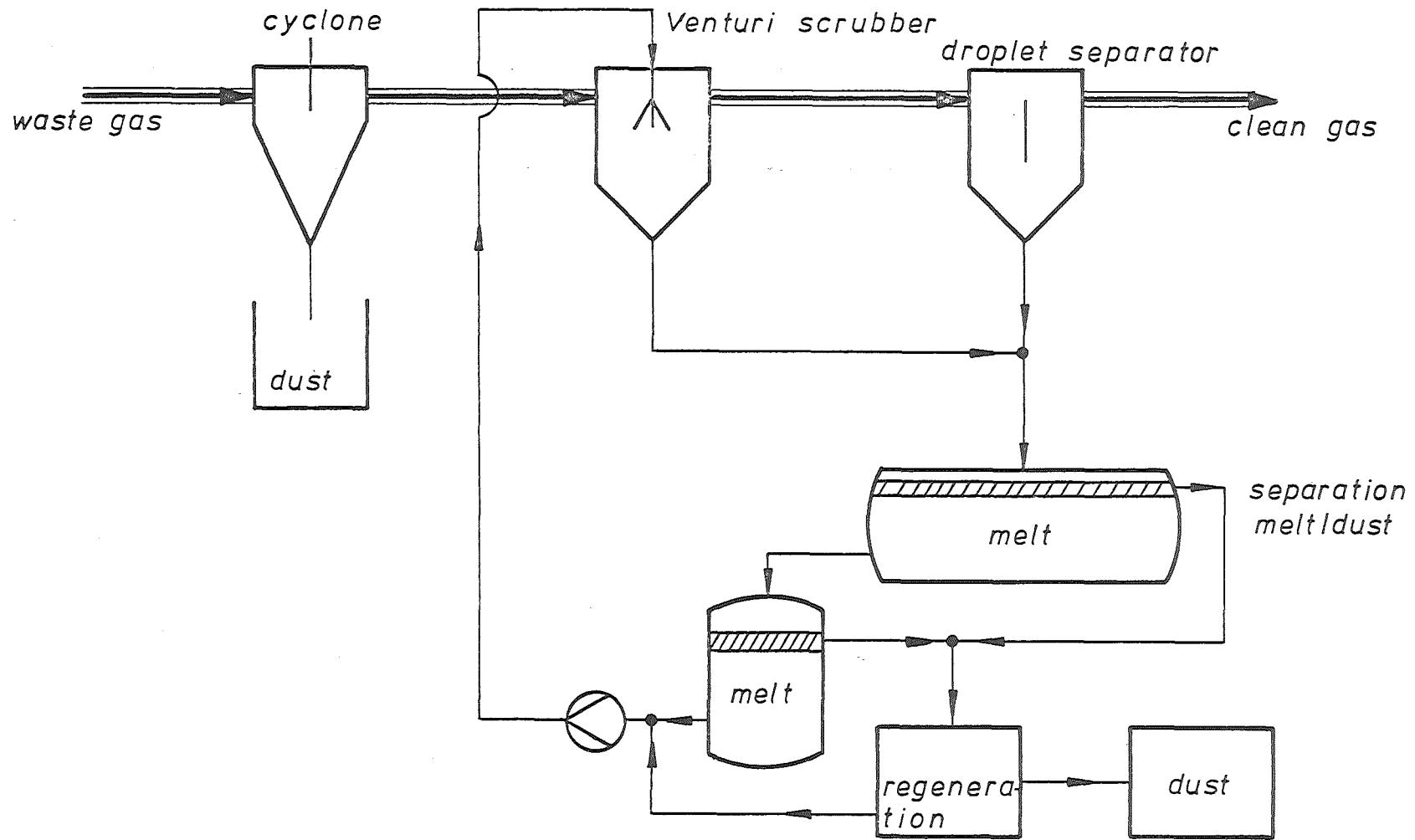
fig.
1

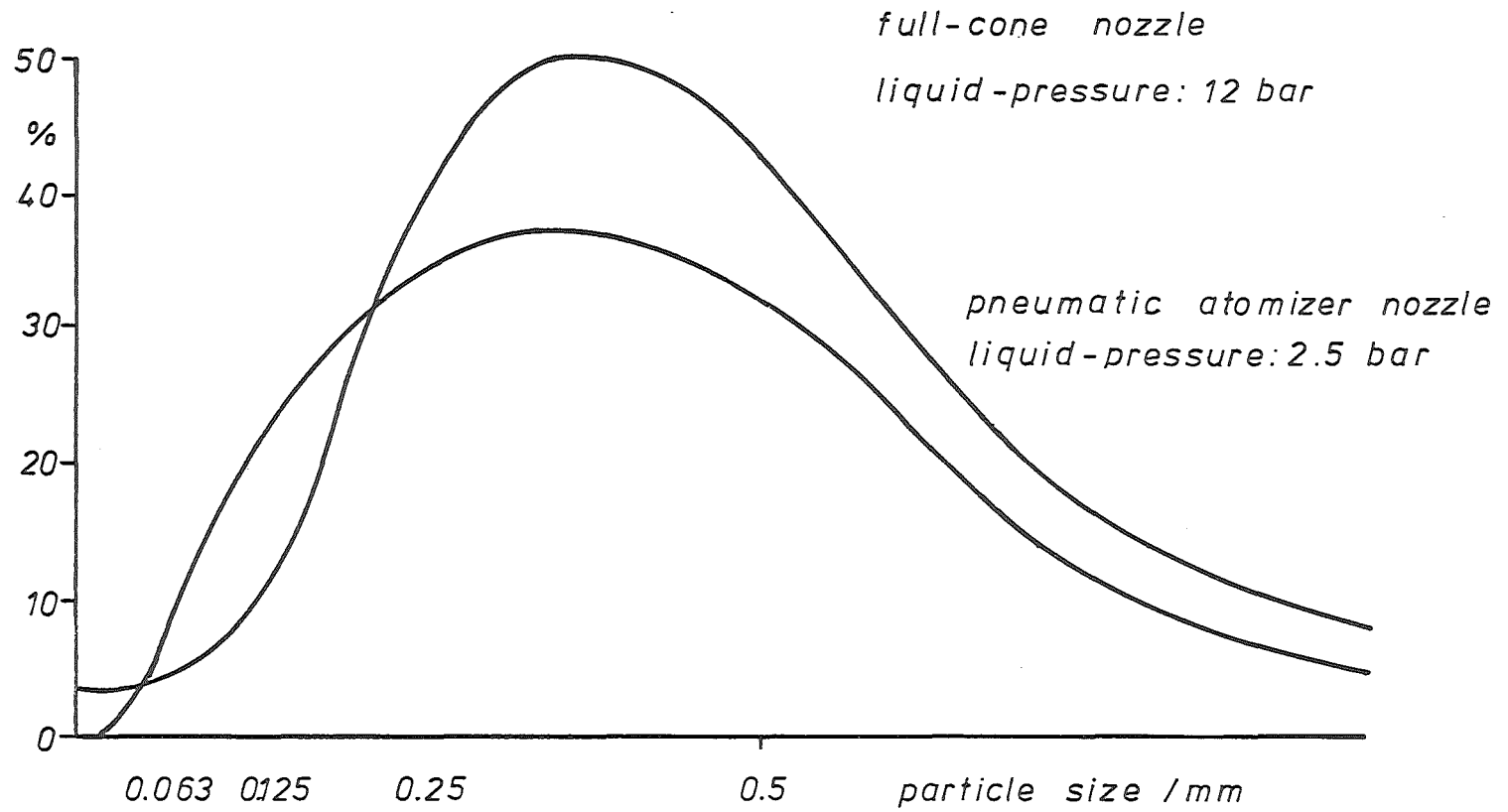


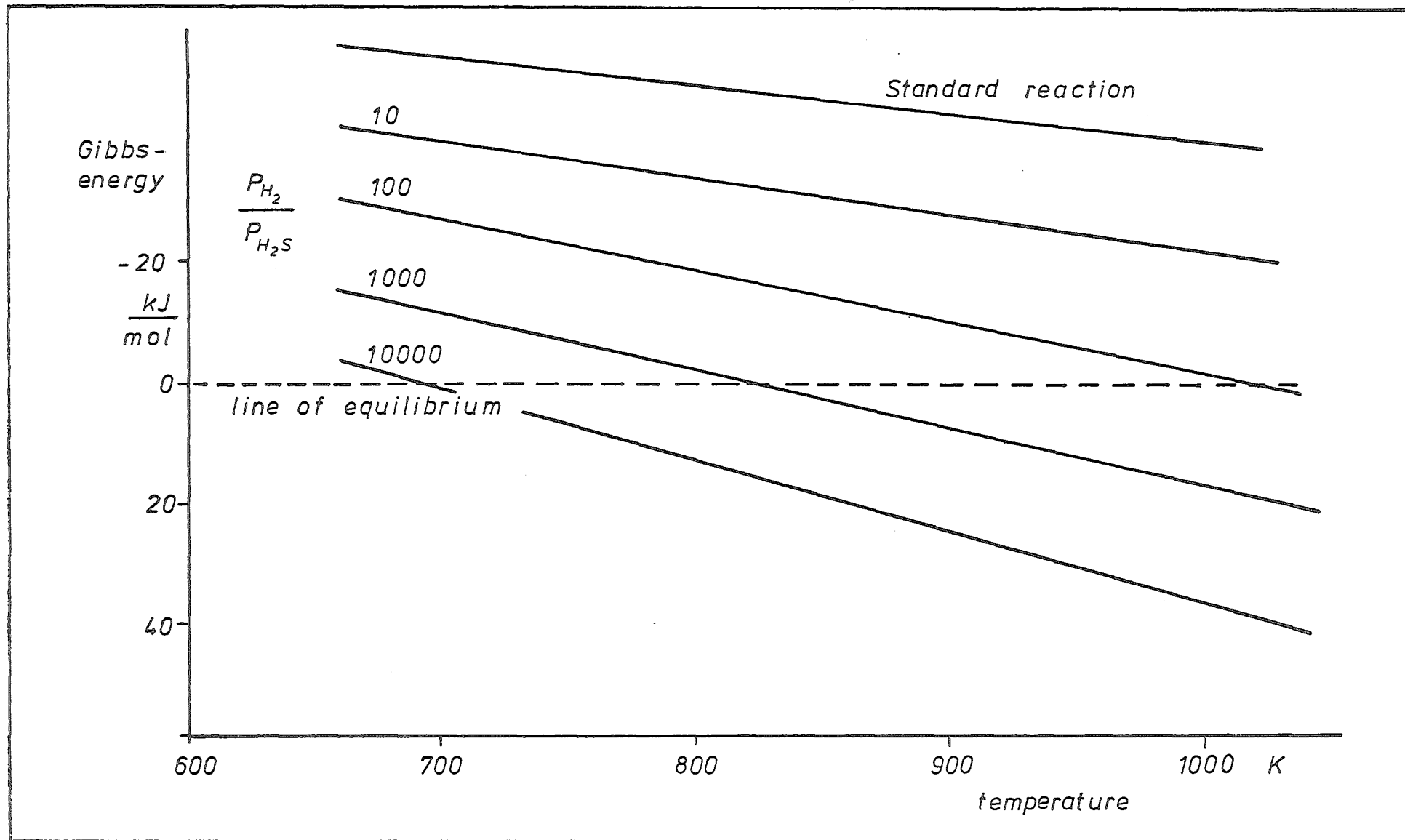
Mechanische
Verfahrenstechnik
Universität Essen

Viscosity of melts

fig.
2







Mechanische
Verfahrenstechnik
Universität Essen



fig.
5

Discussion

Mr. Shackelton asked whether particle collection had been measured and was informed that measurements had been made with flyash from the power plant. A pneumatic atomizer nozzle was used, and the dust collection efficiency was more than 95%. Dr. Holighaus wished to know if there was a sulphur outlet, upon which Dr. Hübner replied that hydrogen rich gas was used at elevated temperatures. This was emitted as a hydrogen sulphate rich gas, which was passed through a cleaning process. The conclusions reached were that the temperature was sufficiently high, and that cleaning could occur at any temperature and in all systems with low energy loss. In reply to Mr. Calvert, Dr. Hübner described the shape of the Venturi Scrubber, which is simply a spray scrubber, 0,1 m in diameter, with an alkali melt full cone. The melt was composed of potash and sodium hydroxide; however, adding a material like limestone or calcium oxide is more economical. (The other type of scrubber described had a pneumatic-atomizer, in order to avoid high pressure). The volumetric flow ratio of liquid: gas was only 1:25 litres m³.

OPTIMIZATION OF WET AND DRY PROCESSES FOR SIMULTANEOUS REMOVAL
OF PARTICULATES AND GASEOUS AIR POLLUTANTS FROM COAL FIRED
POWER STATIONS

by

Peter Davids
Federal Environmental Agency
Berlin

prepared for
A Particulate Workshop
Jülich, Federal Republic of Germany
March 16-17, 1978

1. Emission tendencies

In the Federal Republic of Germany the typical air pollutant emissions from power stations show different tendencies. Fig. 1 presents the trends of NO_x , CO , SO_2 and particulates during the decade from 1965 to 1975 and an estimation for 1980.

The SO_2 -emission could be stabilized to about 4 Mio t/a in spite of increased energy consumption by fuel oil desulfurization, substitution of coal by low sulfur fuels and - at a still very low degree - by flue gas desulfurization. An increase of the contribution of power stations to the total SO_2 -emission from about 30 % in 1965 to about 50 % in 1980 is expected. The total NO_x -emission is increasing from 1.3 to 2.3 Mio t/a permanently; the share of power stations from about 20 % to about one third.

The greatest success in emission control was attained in the field of particulate removal. The total emission could be reduced from about 2 Mio t/a to about 0.5 Mio t/a by application of improved collection techniques. Remarkable is the increasing share of power stations from one fourth to one third of the total emission and the approximately unchanged emission of fine particulates.

At last it can be gathered from Fig. 1 that power stations do not contribute to hydrocarbon emissions significantly.

Fig. 2 presents a map of the Federal Republic of Germany. The territory was divided into squares according to the geographic coordinates. For each square the regional emissions were calculated for 1965, 1970 to an 1975. The results are presented in Fig. 3 to 6.

The SO_2 -emission occurs in the industrialized areas mainly, in particular where power stations are concentrated. Fig. 3 shows the maximum emission in the area around Jülich. In this area we find a concentration of lignite fired power stations with a total capacity of about 15.000 MW. The regional distribution of particulate emissions is similar to the distribution of SO_2 -emissions (Fig. 4), according to the distribution of large power stations. Compared with SO_2 and particulates the NO_x -emission is distributed more uniformly because of the higher share of emissions from motor vehicles (Fig. 5). The most uniform distribution occurs for hydrocarbon emissions because the main sources are motor vehicles and domestic firings (Fig. 6). As above - mentioned power stations do not contribute significantly.

2. Air quality trends

Fig. 7 presents the annual average ground level - concentration of SO_2 at certain places in the Federal Republic of Germany. The recommended air quality standard of the World Health Organization ($60 \mu\text{g SO}_2/\text{m}^3$) is exceeded in the industrialized areas. In the main industrialized region, the Rhine-Ruhr-Area, north-east from Jülich, the ambient SO_2 -concentration even exceeds the national air quality standard of $140 \mu\text{g SO}_2/\text{m}^3$.

The trends of the SO_2 -ground level concentrations from 1970 to 1975 in certain cities are presented in Fig. 8 and 9. The development is not uniform. The concentration is decreasing (e.g. Berlin, Hamburg) or approximately unchanged (e.g. Bochum, Cologne)

or increasing (e.g. Düsseldorf, Saarbrücken).

Fig. 10 presents the development of particulate sedimentation since 1970 in several cities. At most places the values are decreasing. The concentration of suspended particulates is decreasing in most of the cities in the Federal Republic of Germany, too, but at a minor degree than particulate sedimentation (Fig. 11 and 12). In particular the so called "clean air monitoring stations" of the Federal Environmental Agency, far away from industrialized areas, show an unchanged or increasing concentration of suspended particulates due to long range transport of air pollutants.

Altogether, it's of particular importance that the reduction of particulate emissions did not lead to an equivalent reduction of the ambient particulate concentration. The present ground level concentrations require further control measures. In view of the development of emissions and ground level concentrations, the Federal Government has strengthened its efforts to reduce emissions from power stations by use of best available control technologies.

3. Present emission standards

The First General Administrative Regulation under the Federal Air Pollution and Noise Control Law from 1974 contains emission standards for the main air pollutants from power stations:

- the emission of particulates is restricted to 150 mg/m^3 for bituminous coal fired power stations and to 100 mg/m^3 for lignite fired power stations; if using an electrostatic precipitator, the standards also mark the maximum allowable emission even if one electric field of each parallel section is out of service.

- for power stations with a capacity up to 420 MW the sulfur content of coal is limited to 1 %; for larger power stations flue gas desulfurization is required. In 1974 the new source performance standard was set to $3.75 \text{ kg SO}_2/\text{MWh}$; it was reduced to $2.75 \text{ kg SO}_2/\text{MWh}$ in August 1977. For comparison: The Federal US-standard is about $5 \text{ kg SO}_2/\text{MWh}$.

- as to NO_x-control the Administrative Regulation only gives a general recommendation, to reduce emissions as far as possible, for example by two stage combustion or flue gas recirculation.

4. Improvement of control technologies

In view of the emission and air quality - situation in the Federal Republic of Germany in the last years several activities have been introduced to improve existing and to develop new control technologies.

In the field of coal demineralization processes for bituminous coal have been optimized. The available techniques allow a limitation of the ash content to 5 to 10 % for most of German bituminous coal. Thereby the sulfur content can be reduced to about 1 %; heavy metals, chlorine and fluorine can be limited to low levels, too. In the field of NO_x-control in a first step emission reduction by introduction of combustion modification is intended, according to the strategy in the US and in Japan. Optimization of flue gas cleaning processes should offer the largest potential for improvement of emission control, in particular the optimization of flue gas desulfurization processes for simultaneous removal of particulates and gaseous pollutants.

Table 1 presents the range of emission factors for usual fuels in the Federal Republic of Germany. Burning of coal leads to the highest SO₂- and NO_x-emissions and in addition to considerable HCl- and HF-emissions.

Table 1: Emission factors (mg/m³) for power stations in the Federal Republic of Germany

| | bituminous coal | lignite | oil | gas |
|-----------------|-----------------|-----------|-------------|---------|
| SO ₂ | 1,500-5,000 | 500-3,000 | 1,000-5,000 | 100 |
| NO _x | 500-2,000 | 200-1,000 | 200-2,000 | 100-200 |
| HCl | 50- 200 | 20- 100 | - | - |
| HF | 5- 40 | 0.5- 2 | - | - |

Actually the simultaneous removal of SO_2 , NO_x , HCl , HF and fine particulates is being studied with the three desulfurization systems which so far have been developed in the Federal Republic of Germany. These systems are

- the Bischoff (lime/sludge) process
- the Saarberg-Hölter (lime/gypsum) process
- the Bergbauforschung (carbon adsorption) process.

4.1 Bischoff-process

The largest flue gas desulfurization installation in the Federal Republic of Germany is operating at a bituminous coal fired 700 MW power station at Wilhelmshaven. The Bischoff-desulfurization unit has a capacity of about 170 MW (Fig. 13). The scrubber is a combined spray tower and venturi with adjustable throat; the scrubbing liquid is lime slurry; after thickening the process effluent is pumped into a pond.

The inlet particulate concentration to the scrubber is some 50 mg/m^3 , because the boiler flue gas is dedusted first in an electrostatic precipitator. A clean gas particulate concentration below 20 mg/m^3 is expected; the current research program in particular should yield data on the outlet particulate concentration as a function of energy consumption (i.e. pressure drop) to optimize scrubber operation. Variation of pressure drop does not influence SO_2 removal significantly; the efficiency is greater than 90 % independent on pressure drop.

4.2 Saarberg-Hölter process

The particular characteristic of the Saarberg Hölter (lime/gypsum) process is the use of hydrochloric acid and an organic compound as additives; that renders possible a scrubber operation with a clear solution (Fig. 14). A demonstration unit with a capacity of about 40 MW is operating since 1974.

The flue gas is treated in a venturi scrubber. The calcium sulfite in the scrubber effluent is oxidized to sulfate by injection of air into the oxidizer. After thickening and dewatering the byproduct gypsum is sold to the gypsum industry. The operating results have revealed high availability of the system during the last years; the SO_2 removal efficiency is greater than 90 %.

In the current research program removal of fine particulates, HCl, HF and NO_x is being studied. The particulate inlet concentration to the scrubber is about 150 mg/m^3 because the scrubber is connected in series with an electrostatic precipitator; the dust outlet concentration of the scrubber is about 20 mg/m^3 with a pressure drop of about 2000 Pascal.

The removal efficiency for NO_x is poor because more than 90 % of the NO_x occurs as NO. Improvement of NO_x -removal by use of an oxidizing agent in the scrubber is intended. The removal efficiency for HCl and HF is very high, still higher than for SO_2 ; scrubber outlet concentrations of less than 20 mg HCl/m^3 and 5 mg HF/m^3 are achieved.

Objective of the current research program is the further optimization of simultaneous removal of SO_2 , fine particulates and the other gaseous pollutants by systematic variation of the operating parameters, in particular pressure drop, liquid/gas-ratio and composition of the scrubber solution.

4.3 Bergbauforschung - process

The Bergbauforschung-process is a dry process using activated carbon for SO_2 adsorption (Fig. 15). The flue gas is treated in a moving granular bed of carbon grains; the grain size is about 10 mm; the carbon is regenerated at a temperature of about 900 K by mixing with hot sand. The SO_2 -off gas with a concentration of 15 to 20 % SO_2 is processed to elementary sulfur in a Claus furnace.

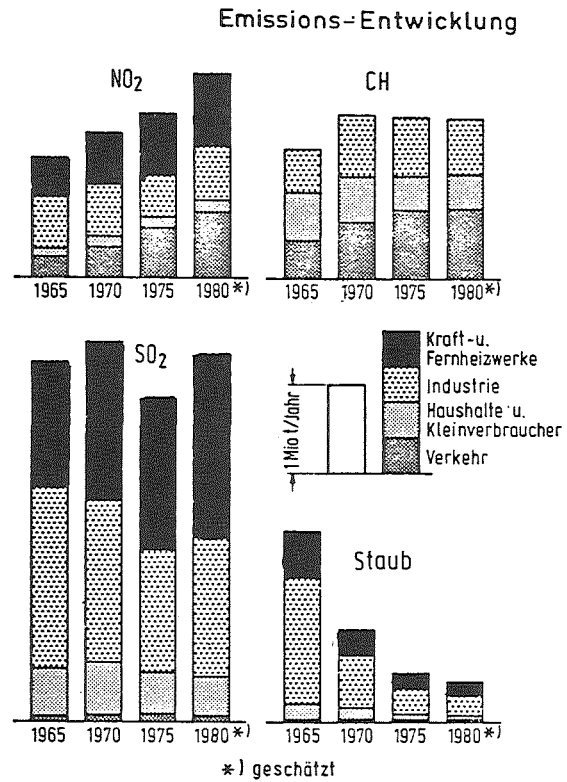
A demonstration unit with a capacity of 50 MW is operating since 1974. Successful results have been attained with the adsorption and desorption section; problems have occurred with the Claus furnace because the desulfurization unit was retrofitted to a peak load power station and the Claus furnace is not very suitable if load changes occur.

With the carbon bed adsorber high removal efficiencies for fine particulates have been achieved, too. The inlet particulate concentration, which is equivalent to the outlet particulate concentration of the electrostatic precipitator, is reduced from about 150 mg/m^3 to about 30 mg/m^3 . The removal efficiency of about 50 % for HCl and HF is poor, compared with wet processes, but NO_x -removal is higher than with wet processes.

Objective of the current research program is the improvement of HCl-, HF- and in particular NO_x -removal with keeping the high efficiencies for SO_2 and fine particulates. Considered measures are optimization of adsorption material and NO_x -reduction by injection of ammonia, using carbon as catalyst.

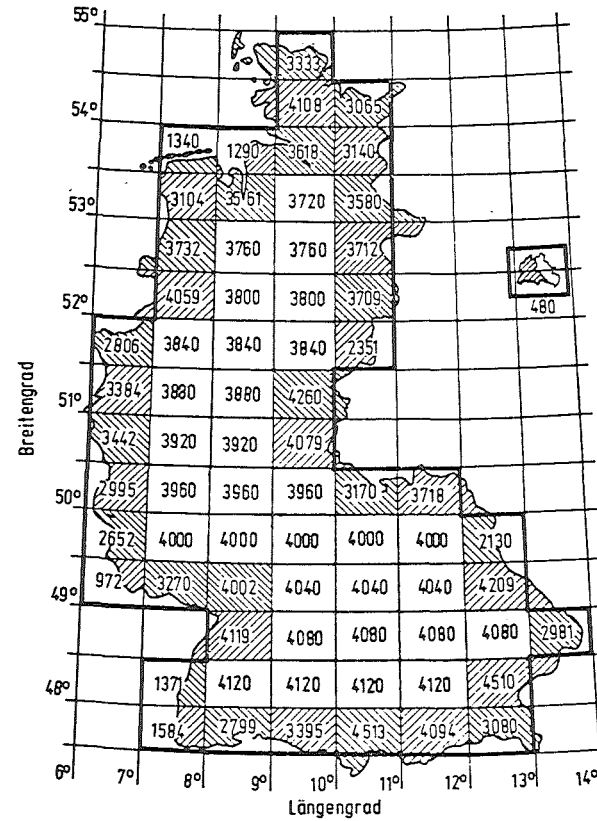
5. Conclusions

The Federal Government intends to update the new source performance standards for power stations within this year. In view of the operating results with the demonstration units in the Federal Republic of Germany and the international experiences, in particular in the US and in Japan, the Federal Environmental Agency has proposed to reduce the emission standards for particulates and SO_2 and to set standards for NO_x , HCl and HF.



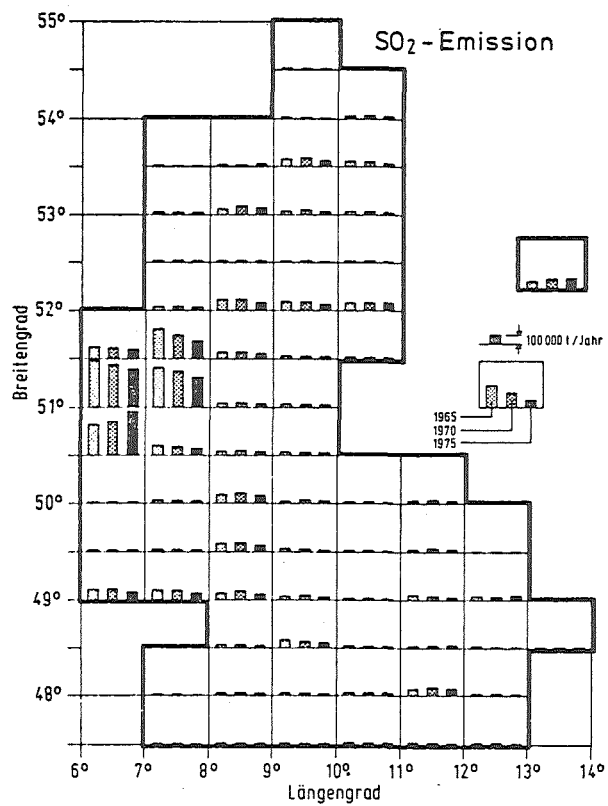
| | | |
|-------------|---|---------------|
| UBA 1977 | Entwicklung der Jahresemission von SO ₂ , NO ₂ , CH und Staub in der Bundesrepublik Deutschland | LU-Emi 123 |
|-------------|---|---------------|

Fig. 1: Annual emissions of SO₂, NO₂, hydrocarbons and particulates in the Federal Republic of Germany



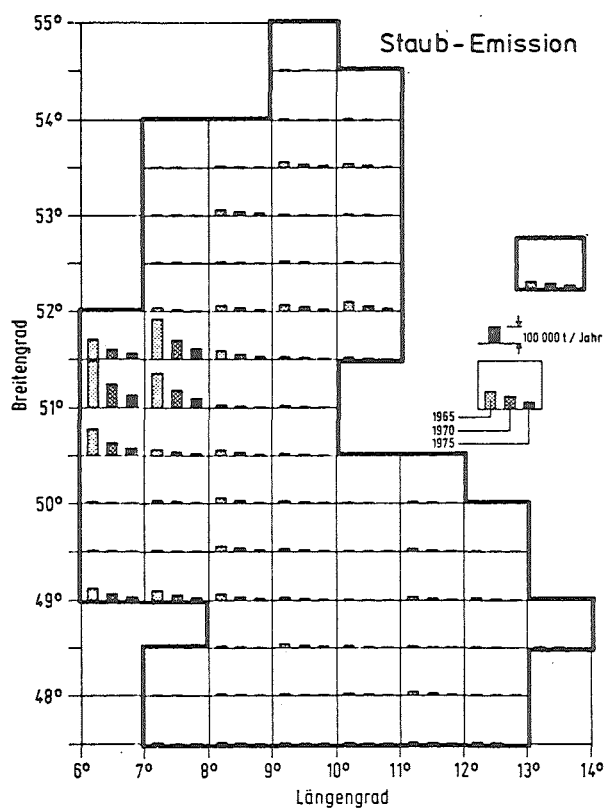
| | | |
|-------------|--|---------------|
| UBA 1977 | Einteilung der Bundesrepublik Deutschland in Erfassungsräume (Flächenangabe in km ²) | LU-All 001 |
|-------------|--|---------------|

Fig. 2: Map of the Federal Republic of Germany



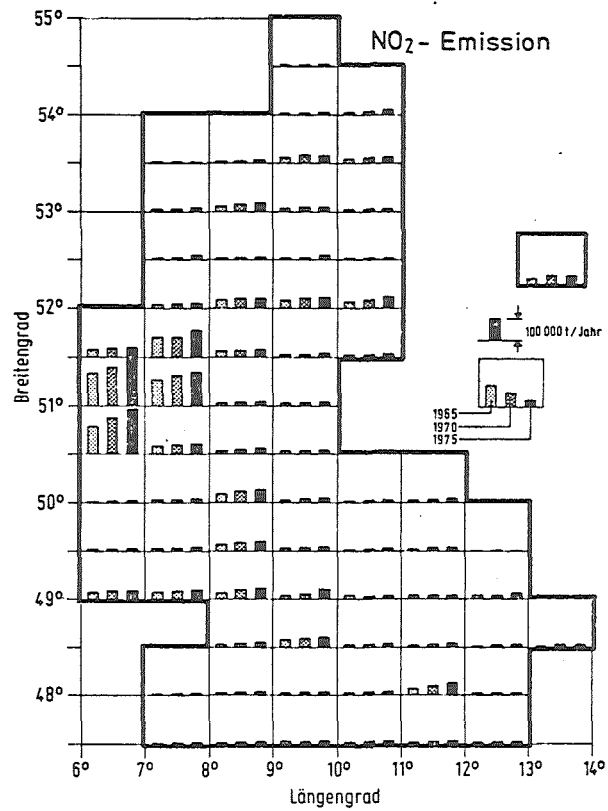
| | | |
|-------------|---|-----------------|
| UBA 1977 | Regionale SO ₂ -Jahresemission | Lu - Emi 003 |
|-------------|---|-----------------|

Fig. 3: Regional SO₂-emission



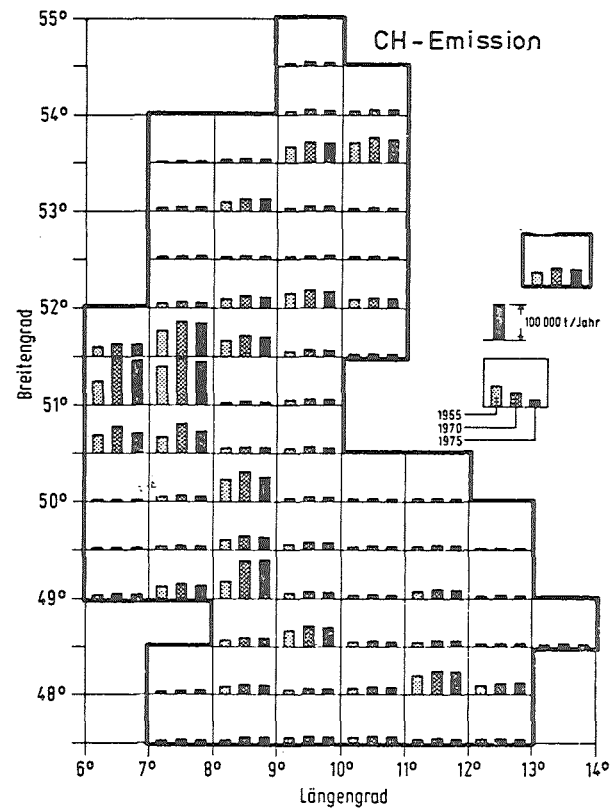
| | | |
|-------------|----------------------------------|-----------------|
| UBA 1977 | Regionale Staub - Jahresemission | LU - Emi 005 |
|-------------|----------------------------------|-----------------|

Fig. 4: Regional particulate emission



| | | |
|-------------|--|-----------------|
| UBA 1977 | Regionale NO ₂ - Jahresemission | Lu - Emi 004 |
|-------------|--|-----------------|

Fig. 5: Regional NO_x-emission



| | | |
|-------------|-------------------------------|-----------------|
| UBA 1977 | Regionale CH - Jahresemission | Lu - Emi 006 |
|-------------|-------------------------------|-----------------|

Fig. 6: Regional hydrocarbon emission

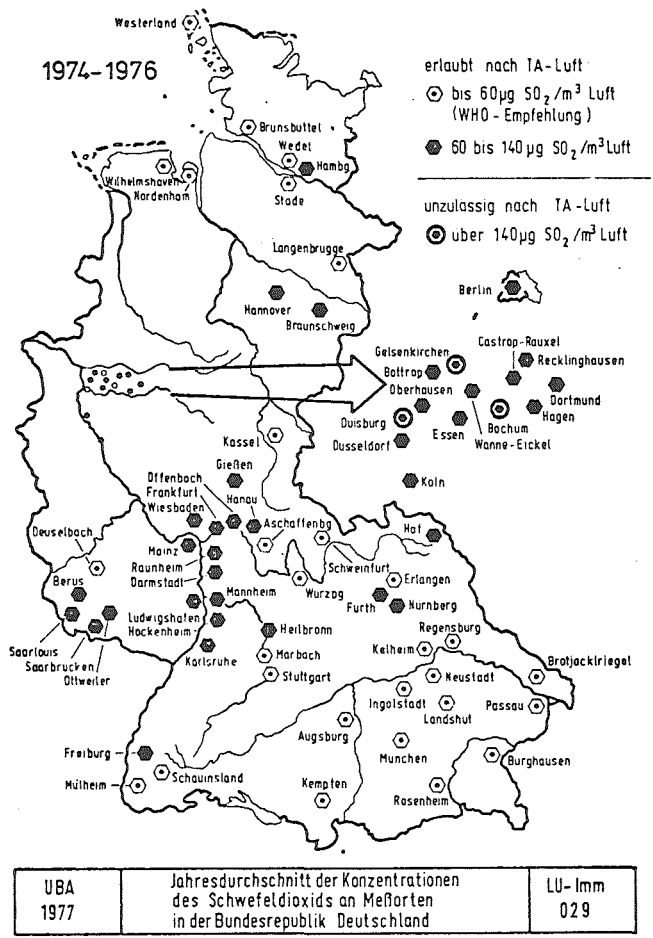


Fig. 7: Annual ambient SO₂-concentration at certain cities in the Federal Republic of Germany

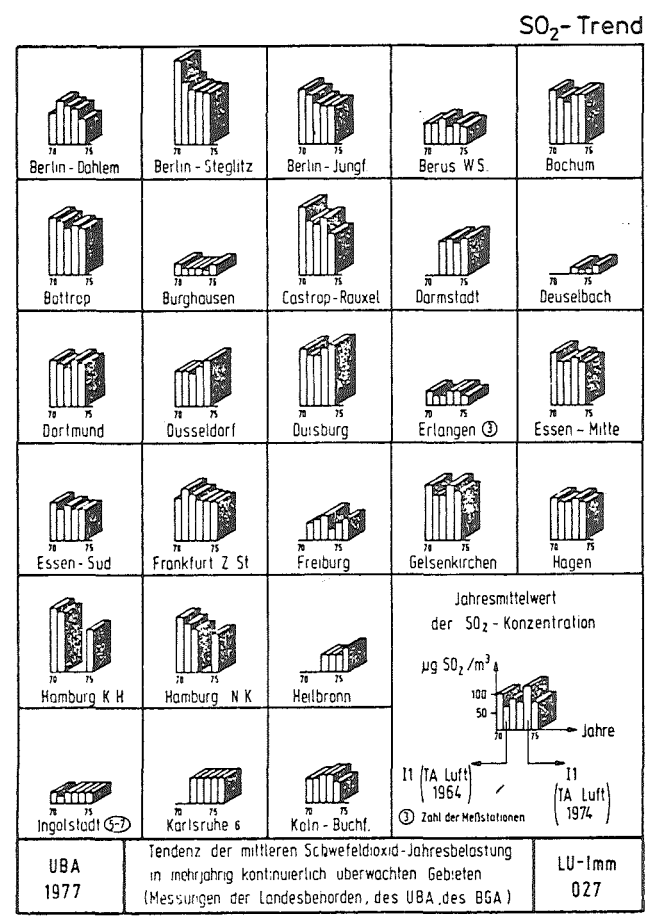


Fig. 8: Trend of ambient SO₂-concentration

SO₂-Trend

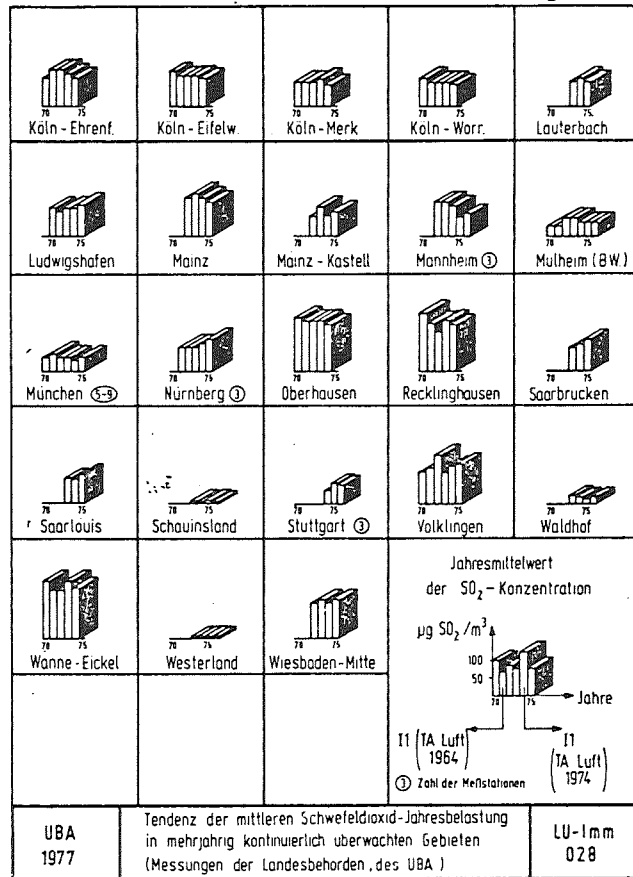


Fig. 9: Trend of ambient SO₂-concentration

Trend Staubniederschlag

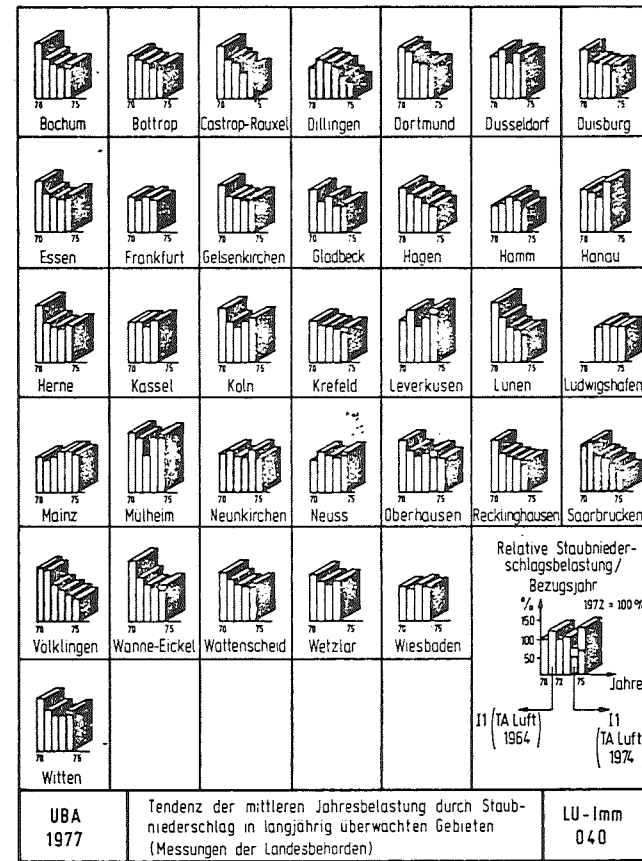


Fig. 10: Trend of particulate sedimentation

Schwebstaubtrend

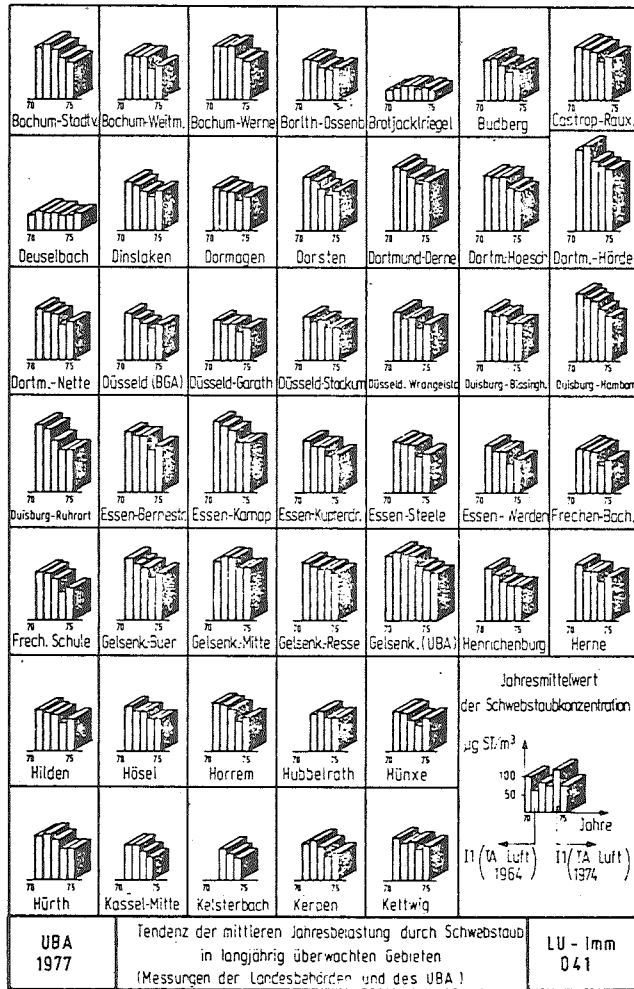


Fig. 11: Trend of suspended particulate concentration

Schwebstaubtrend

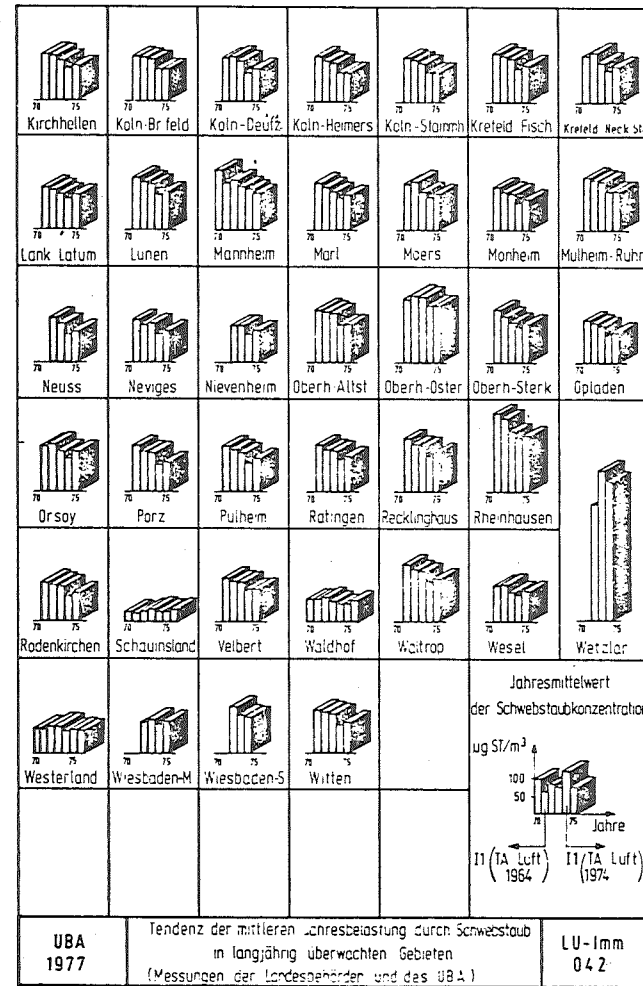
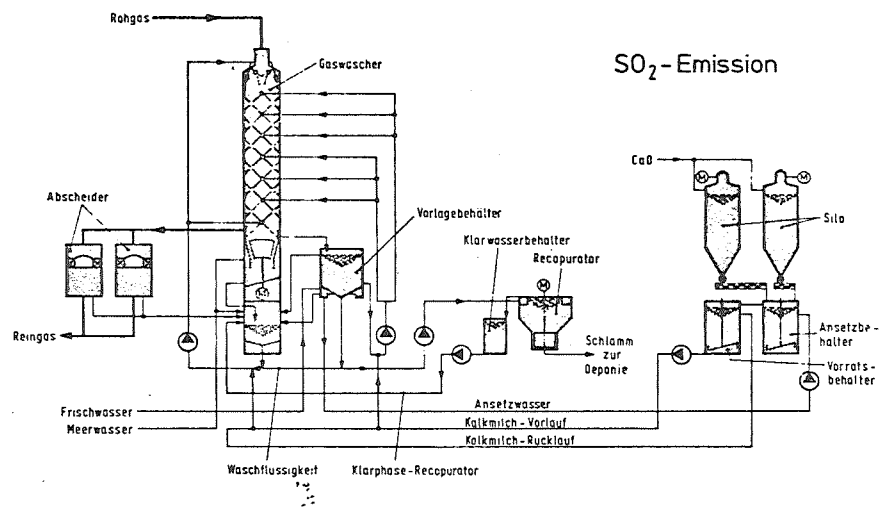


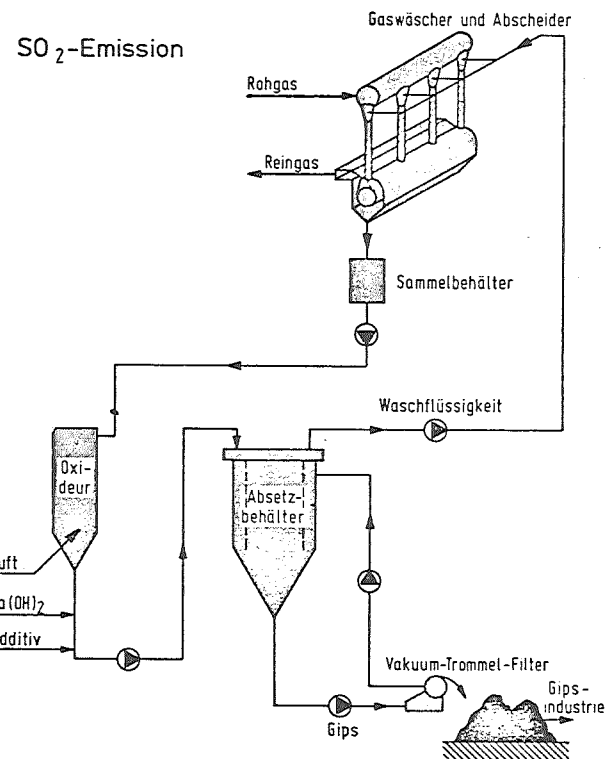
Fig. 12: Trend of suspended particulate concentration



SO₂-Emission

| | | |
|-------------|--|---------------|
| UBA 1977 | Fliebschema der Anlage nach dem Bischoff-Verfahren für 500.000 m ³ /h | LU-Emi 026 |
|-------------|--|---------------|

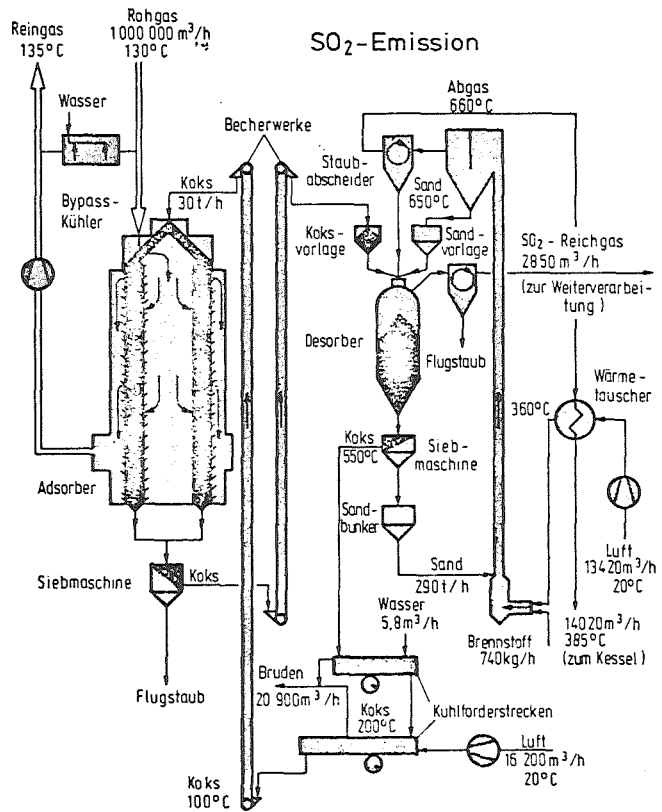
Fig. 13: Bischoff (lime/sludge) flue gas cleaning process



SO₂-Emission

| | | |
|-------------|--|---------------|
| UBA 1977 | Fliebschema d. Anlage nach dem Saarberg-Höller-Verfahren für 125.000 m ³ /h | LU-Emi 025 |
|-------------|--|---------------|

Fig. 14: Saarberg-Höller (lime/gypsum) process for flue gas cleaning



| | | |
|---------------|---|------------------|
| U B A 1977 | Verfahrensschema einer Abgasentschwefelungs-anlage nach dem Bergbau-Forschungs-Verfahren (300 MW) | LU - Emi 0 24 |
|---------------|---|------------------|

Fig. 15: Bergbauforschung (carbon adsorption) process for flue gas cleaning

Discussion

The discussion dealt mainly with these new standards. Dr. Holighaus wished to know whether the standard for SO₂ would be lower than at present (2,75 kg per hour); Mr. Davids replied in the affirmative. He added that new standards would be introduced for HCl and HF, but was unable to describe these at length as the full details had not been finalized at the time. A comparison was then made with standards in the US, which were 5 kg per hour.

SESSION IV: HIGH TEMPERATURE AND PRESSURE PARTICULATE CONTROL

AIR POLLUTION TECHNOLOGY, INC.

4901 MORENA BLVD., SUITE 402 SAN DIEGO, CA 92117 (714) 272-0050

FUNDAMENTALS OF PARTICLE COLLECTION AT HIGH TEMPERATURE AND PRESSURE

by

Dr. Richard Parker and Dr. Seymour Calvert
Air Pollution Technology, Inc.

Presented at the
US/FRG Particulate Workshop

Julich, Germany
March 16-17, 1978



ENGINEERING • CONSULTING • RESEARCH • DEVELOPMENT • DESIGN • EQUIPMENT



ABSTRACT

High temperatures and pressures affect the physical mechanisms by which particles are removed from gas streams. This presentation examines the theoretical basis for predicting high temperature and pressure effects on particle collection mechanisms. In general, particles larger than a few tenths of a micrometer in diameter appear to be more difficult to collect at high temperature and pressure than at standard conditions. Experimental data are needed to confirm these predictions. A U.S. EPA-sponsored project to obtain experimental data is discussed and the test facility is described.

FUNDAMENTALS OF PARTICLE COLLECTION
AT HIGH TEMPERATURE AND PRESSURE

INTRODUCTION

When designing, troubleshooting, or evaluating the performance of particulate control equipment it is important to have a firm understanding of the physical mechanisms by which the particles are removed from the gas stream. This is especially true when the control device is to be used at high temperatures and pressures (HTP) where current design models are unproven. In order to provide a rational basis for design and scale up, a sound theoretical understanding of the HTP effects on particle collection mechanisms is essential.

We have conducted a thorough examination of the literature concerned with HTP effects on particle collection (Calvert and Parker, 1977). Although HTP particle collection has been of interest for over 30 years no fundamental evaluation of the theory has been attempted. In general, conventional models for particle collection (valid at low temperatures and pressures) have been extrapolated to predict performance in HTP situations. Very few performance data are available to evaluate these models at HTP conditions, especially as a function of particle size.

This paper presents a review and evaluation of the theory normally used to describe particle collection mechanisms, and a discussion of the EPA-sponsored experimental program currently under way at A.P.T., Inc.

THEORY

Particle collection devices usually can be characterized by a deposition velocity, u_d , which is related to the particle collection efficiency, η , and the penetration, P_t , as follows:

$$P_t = 1 - \eta = \exp \left\{ \frac{-u_d A_d}{Q_G} \right\} \quad (1)$$

where A_d = deposition area, cm^2
 Q_G = volumetric flow rate, cm^3/s

Particles are kept suspended in a gas stream by the viscous force (drag) of the gas which resists forces tending to precipitate particles. The deposition velocity for any collection mechanism depends on the balance between the driving force (precipitating force) and the resistance force of the gas.

The major difference between the collection of particles at normal conditions and at high temperature and pressure is in the fluid resistance force. The fluid resistance force is generally approximated by Stokes' law modified to allow for non-continuum slip flow effects:

$$F_r = \frac{3 \pi \mu_G d_p u_o}{C'} \quad (2)$$

where F_r = fluid resistance force, dynes
 μ_G = fluid dynamic viscosity, $\text{g}/\text{cm}\cdot\text{s}$
 d_p = particle diameter, cm
 u_o = relative velocity between the particle and the gas, cm/s
 C' = Cunningham slip correction factor, dimensionless

The temperature and pressure dependence of Equation 2 is contained in the terms μ_G and C' . The viscosity of a gas increases with increasing temperature. At extreme pressures, viscosity also increases with pressure. This effect is not significant at pressures below about 20 atm. Adequate theory and experimental data for predicting viscosities at high temperature and pressure are available in the literature.

The Cunningham slip correction factor may be calculated as:

$$C' = 1 + \frac{2\lambda}{d_p} \left[1.257 + 0.40 \exp(-1.1 d_p/2\lambda) \right] \quad (3)$$

where λ = mean free path of gas molecules, cm

The Cunningham slip correction factor is a function of temperature, pressure, and particle diameter. It becomes important for small particles, high temperatures, and low pressures.

Equation 3 is an empirical expression based on Millikan's oil drop experiments (conducted at room temperature and reduced pressure). The constants are dependent on the momentum transfer (and hence accommodation coefficient) between the gas molecules and the particle and may not be accurate at extreme temperatures. Experimental data are needed to resolve this uncertainty.

The particle deposition velocity for most collection mechanisms of interest is inversely proportional to the fluid resistance force, and therefore proportional to the ratio C'/μ_G . The effects of high temperature and pressure on this ratio, plotted as a function of particle diameter, are illustrated in Figure 1. At atmospheric pressure, the ratio decreases with increasing temperature for particles larger than about 0.4 μm . At 15 atm pressure, the ratio decreases with temperature for all particles larger than 0.1 μm . Therefore, the particle deposition velocity will generally be smaller at high temperature and pressure than at normal conditions.

Inertial Impaction

One of the most important mechanisms for the collection of particles larger than a few tenths of a micrometer in diameter is inertial impaction. Inertial impaction takes advantage of the difference in mass between the particles and gas molecules by impinging them on a target. The relative effect of inertial impaction for different particles and flow conditions may be characterized by the inertial impaction parameter, K_p , defined as:

$$K_p = \frac{C' \rho_p d_p^2 u_o}{9 \mu_G d_c} \quad (4)$$

where ρ_p = particle density, g/cm^3

d_c = characteristic diameter for collector, cm

The inertial impaction parameter is equivalent to the ratio of the particle stopping distance, x_s , to $d_c/2$. The particle stopping distance is that distance the particle would travel before coming to rest if injected into a still gas at a velocity, u_o , when only the fluid resistance force acts on the particle. By considering the particle stopping distance divided by u_o , the particle's relative inertia can be characterized by a relaxation time, τ , defined as:

$$\tau = \frac{x_s}{u_o} = \frac{K_p d_c}{2 u_o} = \frac{C' \rho_p d_p^2}{18 \mu_G} \quad (5)$$

From Equation 5 it can be seen that the effects of high temperature and pressure on the particle relaxation time come in through the ratio C'/μ_G . Therefore Figure 1 can be used to illustrate the effects of high temperature and pressure on the particle relaxation time. A longer relaxation time (larger C'/μ_G) implies that the particle can more easily be removed from the gas by inertial impaction. For large particles, therefore, inertial impaction decreases with increasing temperature and pressure.

For small particles (less than about 0.3 μm) at high temperature and atmospheric pressure, Figure 1 indicates that inertial impaction begins to improve with temperature. However, high pressure tends to nullify this beneficial effect of high temperature.

Brownian Diffusion

Small particles can undergo significant Brownian motion resulting from the random bombardment of the particle by gas molecules. The rate of diffusion is characterized by the particle diffusivity, defined as:

$$D = \frac{C' k T}{3 \pi \mu_G d_p} \quad (6)$$

where D = particle diffusivity, cm^2/s

k = Boltzman's constant, $\text{erg}/^\circ\text{K}$

T = absolute temperature, $^\circ\text{K}$

Figure 2 shows the effects of temperature and pressure on particle diffusivity. Smaller particles undergo higher rates of diffusion. High temperature increases the diffusivity for all particle sizes. High pressure decreases the beneficial effect of high temperature because of its effect on the mean free path in C' .

Electrical Migration

The migration of a particle in an electric potential field is proportional to the field strength, the particle charge, and the fluid resistance force.

Electrical migration is generally characterized by a deposition velocity which may be approximated as:

$$u_e = \frac{C' q_p E}{3 \pi \mu_G d_p} (10^7) \quad (7)$$

where u_e = deposition velocity, cm/s
 q_p = particle charge, C
 E = electric field strength, V/cm

For a given field strength and particle charge, the effects of temperature and pressure are contained in the ratio C'/μ_G and are illustrated in Figure 1. The particle charge and electric field strength, however, are also complicated functions of temperature and pressure.

Gravitational Settling and Centrifugal Separation

Using Equation 2 to describe the fluid resistance force, the gravitational settling velocity and the deposition velocity of a particle in a centrifugal force field may be approximated as:

$$u_s = \frac{1}{18} \frac{C' d_p^2 (\rho_p - \rho_G) g}{\mu_G} \quad (8)$$

$$u_c = \frac{1}{18} \frac{C' d_p^2 (\rho_p - \rho_G) u_t^2}{\mu_G} \quad (9)$$

where u_s = gravitational settling velocity, cm/s
 u_c = centrifugal force deposition velocity, cm/s
 g = acceleration of gravity, cm/s²
 u_t = tangential particle velocity at radius R , cm/s
 R = radial position of particle, cm
 ρ_G = density of the gas, g/cm³

In general, even at relatively high pressures (~50 atm), the gas density is much smaller than the particle density and may be neglected in Equations 8 and 9. Therefore the temperature and pressure dependence of Equations 8 and 9 is contained in the ratio C'/μ_G and is illustrated in Figure 1.

Particle Agglomeration

One way to improve the collection efficiency for fine particles is to cause the fine particles to agglomerate into larger aggregates which can be collected more easily.

Particles undergoing random Brownian motion will tend to agglomerate over a period of time. The rate of agglomeration is generally considered to be proportional to the square of the particle number concentration. That is:

$$\frac{d N_p}{dt} = -K_o N_p^2 \quad (10)$$

where N_p = particle number concentration, cm^{-3}

K_o = proportionality constant or agglomeration coefficient, cm^3/s

Using Equation 2 for the gas resistance force, Fuchs (1964) presents the following equation for the agglomeration coefficient of a particle undergoing Brownian motion in a still gas, assuming particles stick together upon touching:

$$K_o = 4 \pi D d_p = \frac{4 C' k T}{3 \mu_G} \quad (11)$$

The agglomeration coefficient is shown as a function of temperature, pressure, and particle diameter in Figure 3. The agglomeration of particles increases with temperature and decreases with pressure. The net effect of high temperature and high pressure (20°C, 1 atm to 1,100°C, 15 atm) is to increase the rate of agglomeration for a 1 μm diameter particle by a factor of 1.5 (K_o increases from $3.5 \times 10^{-10} \text{ cm}^3/\text{s}$ to $5.3 \times 10^{-10} \text{ cm}^3/\text{s}$). For a 0.1 μm diameter particle, the rate of agglomeration remains relatively constant ($K_o = 8.5 \times 10^{-10} \text{ cm}^3/\text{s}$). Therefore it appears that at high pressure and high temperature the rate of agglomeration increases for particles larger than 0.1 μm . At high temperature and atmospheric pressure, the rate of agglomeration of fine particles should increase more substantially.

Particles may also agglomerate as a result of turbulence, particle charge, and sonic disturbances. These agglomeration mechanisms were examined theoretically by Calvert and Parker (1977) and did not appear to offer any

improvement at high temperature and pressure. Sonic agglomeration appeared to increase with temperature but this was countered by a substantial decrease at high pressures.

EXPERIMENTAL PROGRAM

Test Facility

An experimental program to study fundamental particle collection mechanisms at high temperature and pressure is under way at A.P.T., Inc. under EPA sponsorship. The experiments will investigate the collection mechanisms of inertial impaction, Brownian diffusion, and electrical migration at temperatures up to 1,100°C and pressures up to 15 atm. Particles in the general size range of 0.5 to 10 μm will be considered.

A special high temperature and pressure test facility has been designed and constructed. This facility is illustrated in Figure 4. All the high temperature and pressure components are located inside a steel safety barricade. Tests are controlled remotely at the control panel.

High pressure gas is supplied by a manifold of nitrogen gas cylinders. The gas then passes through a high pressure redispersion fly ash dust generator and a cyclone precutter. The dust generator is a batch type high pressure blender. Steady output concentration and size distribution can be maintained for approximately 2 to 4 hours.

The gas and particles are heated in two stages. The first stage uses high temperature heating tapes which can raise the gas temperature to 750°C. The second stage uses resistance heated tube furnaces to increase the gas temperature to a maximum of 1,100°C. Stainless steel type 316, Inconel 600, or Hastelloy X are used for high pressure piping and flanges depending on the maximum temperature anticipated at specific locations.

The high temperature and pressure gas passes through one of three specially designed test sections and is then cooled and returned to the control panel before being vented. The test sections are designed to isolate specific particle collection mechanisms for study at the high temperature and pressure conditions. Specific test sections are discussed in more detail later.

Isokinetic samples are taken at the inlet and outlet of the test section. The samples are collected on sintered metal filters which can be used at

temperatures up to 1,100°C in the nitrogen environment. There is a provision for adding dilution flow before the filters so that low temperature filters can also be used.

The filter samples are removed after each test and are analyzed using an electronic particle counter (Coulter Counter Model TA-II) to determine the mass and size distribution of the fly ash collected on each filter. Also the sample probes are washed after each test and analyzed to determine the amount and size of particles deposited in each probe.

One potential problem using the electronic particle counter is that particles which may have been agglomerates in the test gas stream will be analyzed as single particles. To investigate this problem we have run parallel size distributions using a cascade impactor and a filter (analyzed with the electronic counter). The results were in very close agreement. Also we have used an optical microscope to observe particles collected on a glass slide. There appeared to be very few agglomerates. The dilution line enables us to use cascade impactors at low temperature for comparison with the data we obtain from the sintered metal filters. Also we will examine samples using the microscope as a further check on our analysis.

Inertial Impaction Tests

The inertial impaction test section is illustrated in Figure 5. It is essentially a single stage impactor placed between two flanges. Five separate jet plates are available so that we can look at cut diameters (diameter corresponding to 50% particle collection) ranging from 0.5 μm to 10 μm .

Particles are collected on a ceramic fiber substrate which is used to minimize particle bounce at the impaction plate. The substrate will be removed and analyzed after each test in order to complete the mass balance of particles and to check the efficiency determined from the inlet and outlet samples. We have calibrated this impactor under controlled conditions in the laboratory using monodisperse particles impacting on a greased plate and on the fiber substrates. The agreement between greased and fiber substrates was good.

The data obtained from analysis of the inlet and outlet samples will be used to determine an experimental penetration curve as shown in Figure 6. The penetration curve will be used to determine an experimental cut diameter,

d_{cx} . Experiments will be run at temperatures ranging from 100°C to 1,100°C and pressures from 1 to 15 atm.

Conventional impaction theory will be used to predict a cut diameter, d_{cp} , based on the impactor calibration. The predicted cut diameter will be determined from the following equation:

$$d_{cp} = \left(\frac{9 \mu_G d_h K_{p50}}{\rho_p C' u_h} \right)^{1/2} \quad (12)$$

where K_{p50} = calibrated value for K_p at 50% collection efficiency

d_h = jet diameter, cm

u_h = jet velocity, cm/s

The particle density will be determined by comparing the calibrated cut diameter with the cut diameter measured using fly ash at standard temperature and pressure.

By comparing the experimental and predicted cut diameters at various temperatures and pressures we will be able to evaluate the theory as a function of temperature and pressure. The viscosity of nitrogen gas has been determined at temperatures up to 1,200°C (Saxena, 1971). Therefore any discrepancies between the experimental and predicted cut diameters at high temperatures can be related to the slip correction factor in Stokes' law (Equations 2 and 3).

Brownian Diffusion Tests

The diffusion test section is illustrated in Figure 7. It is basically a screen-type diffusion battery held inside high temperature and pressure pipe. The screens are 120 mesh and made of 316 stainless steel. There will be 50 to 100 screens in the test section.

Particle penetration through the screens will be measured as a function of particle size using the electronic counter for particles down to 0.3 μm diameter. Cascade impactors will also be used to measure particles as small as 0.1 μm . The penetrations will be measured at temperatures ranging from 100°C to 1,100°C and pressures from 1 to 15 atm.

Predictions of penetrations for various temperature and pressure conditions are shown in Figure 8. The predictions were based on the theory presented by Patterson and Calvert (1977). That is:

$$Pt = \exp \left\{ - 6.0 S N_{Pe}^{-0.67} \right\} \quad (13)$$

where S = geometric solidity factor, dimensionless
 N_{Pe} = Peclet number = $u_G d_w / D$, dimensionless
 u_G = superficial gas velocity, cm/s
 d_w = wire diameter of screen, cm

This theory will be confirmed by experimental penetrations at ambient conditions and then used to predict experimental particle diffusivities from penetrations obtained at HTP conditions. The experimental particle diffusivities thus obtained will be compared with theoretical predictions.

Electrical Migration Tests

The electrical migration test section is illustrated in Figure 9. It is basically a laminar flow, concentric cylinder electrical precipitator. Particles will be charged to saturation using a corona charging section at the outlet of the dust generator (before heating). The particle charge collected will be measured using an electrometer. The size distribution collected will be measured using the electronic counter. From the size distribution and total charge collected we will estimate the charge per particle. These data will then enable us to predict a deposition velocity using the expression:

$$u_e = \left(\frac{C' q_p V}{3 \pi \mu_G d_p r_o} \right) 10^7 \quad (14)$$

where V = applied voltage, V
 r_o = radius of outer electrode, cm

The particle penetration through the electrical migration test section will be measured by taking inlet and outlet samples and analyzing them for particle mass and size distribution. Experimental migration velocities will

endless thread.

be determined from the basic equation for a laminar flow electrical precipitator:

$$u_e = \frac{\eta Q_G}{\pi D_c L} \quad (15)$$

where D_c = diameter of outer electrode, cm
 L = length of cylindrical electrodes, cm

The particle saturation charge can be predicted theoretically (White, 1963). Using a charging field strength of 6 kV/cm, particle charges have been predicted and used to estimate the collection efficiency of our test section at various temperatures and pressures. The results are shown in Figure 10. A field strength of 1 kV/cm was assumed for the precipitator with an actual flow rate of 472 cm³/s (1 ACFM).

The comparison between experimental and predicted migration velocities will enable us to evaluate the conventional theory and determine its suitability for use in design models for high temperature electrical precipitation.

CONCLUSIONS

From theoretical considerations it appears that the collection of particles larger than a few tenths of a micron in diameter will be more difficult at high temperature and pressure than at standard conditions. This is largely a consequence of the stronger drag force exerted on particles in high temperature and pressure gas streams.

The theoretical predictions presented in this paper are based on extrapolation of current aerosol theory to high temperature and pressure conditions. Satisfactory theory and experimental data exist for predicting the gas properties at these conditions. However, the available data are insufficient to validate theoretical predictions for particle motion.

To obtain the necessary data, experimental measurements of the fluid resistance force, particle diffusivity and electrical deposition velocity at high temperature and pressure are being made. This experimental research program is scheduled for completion in May of next year.

ACKNOWLEDGEMENT

This work is supported by the U.S. Environmental Protection Agency.

REFERENCES

1. Calvert, S. and R.D. Parker, "Effects of temperature and pressure on particle collection mechanisms: theoretical review," A.P.T., Inc., EPA-600/7-77-002, NTIS PB-264-203, January 1977.
2. Fuchs, N.A., The Mechanics of Aerosols. Pergamon Press, New York, 1964.
3. Saxena, S.C. Transport properties of Gases and Gaseous Mixtures at High Temperatures. High Temp. Sci. 3:168, 1971.
4. Patterson, R.G. and S. Calvert. Screen Diffusion Battery for Monitoring Submicron Aerosols in Stack Gases. Presented at AIHA Conference, New Orleans, Louisiana, May 24, 1977.
5. White, H.J. Industrial Electrostatic Precipitation. Addison-Wesley Publication Company, Reading, Massachusetts, 1963.

LIST OF SYMBOLS

- A_d = deposition area, cm^2
- C' = slip correction factor, dimensionless
- D = particle diffusivity, cm^2/s
- d_c = outer electrode diameter, cm
- D_c = collector diameter, cm
- d_h = jet diameter, cm
- d_p = particle diameter, cm
- d_w = wire diameter, cm
- E = electric field strength, V/cm
- F_r = drag force, dynes
- g = gravitational acceleration, cm/s^2
- k = Boltzman's constant, $\text{erg}/^\circ\text{K}$
- K_o = agglomeration coefficient, cm^3/s
- K_p = inertial impaction parameter, dimensionless
- $K_{p50} = K_p$ at 50% collection efficiency, dimensionless
- L = length of electrode, cm
- N_p = particle number concentration, cm^{-3}
- N_{Pe} = Peclet number, dimensionless
- Pt = penetration, dimensionless
- Q_G = volumetric flow rate, cm^3/s
- q_p = particle charge, C
- R = radial position of particle, cm
- r_o = radius of outer electrode, cm
- S = solidity factor, dimensionless
- T = absolute temperature, $^\circ\text{K}$
- t = time, s

u_c = centrifugal force deposition velocity, cm/s

u_d = deposition velocity, cm/s

u_e = electrical migration deposition velocity, cm/s

u_G = superficial gas velocity, cm/s

u_h = jet velocity, cm/s

u_o = relative velocity between particle and gas, cm/s

u_s = gravitational settling velocity, cm/s

u_t = tangential velocity of gas, cm/s

V = applied voltage, V

x_s = stopping distance, cm

η = collection efficiency, dimensionless

λ = mean free path, cm

μ = gas viscosity, g/cm-s

ρ_G = gas density, g/cm³

ρ_p = particle density, g/cm³

τ = relaxation time, s

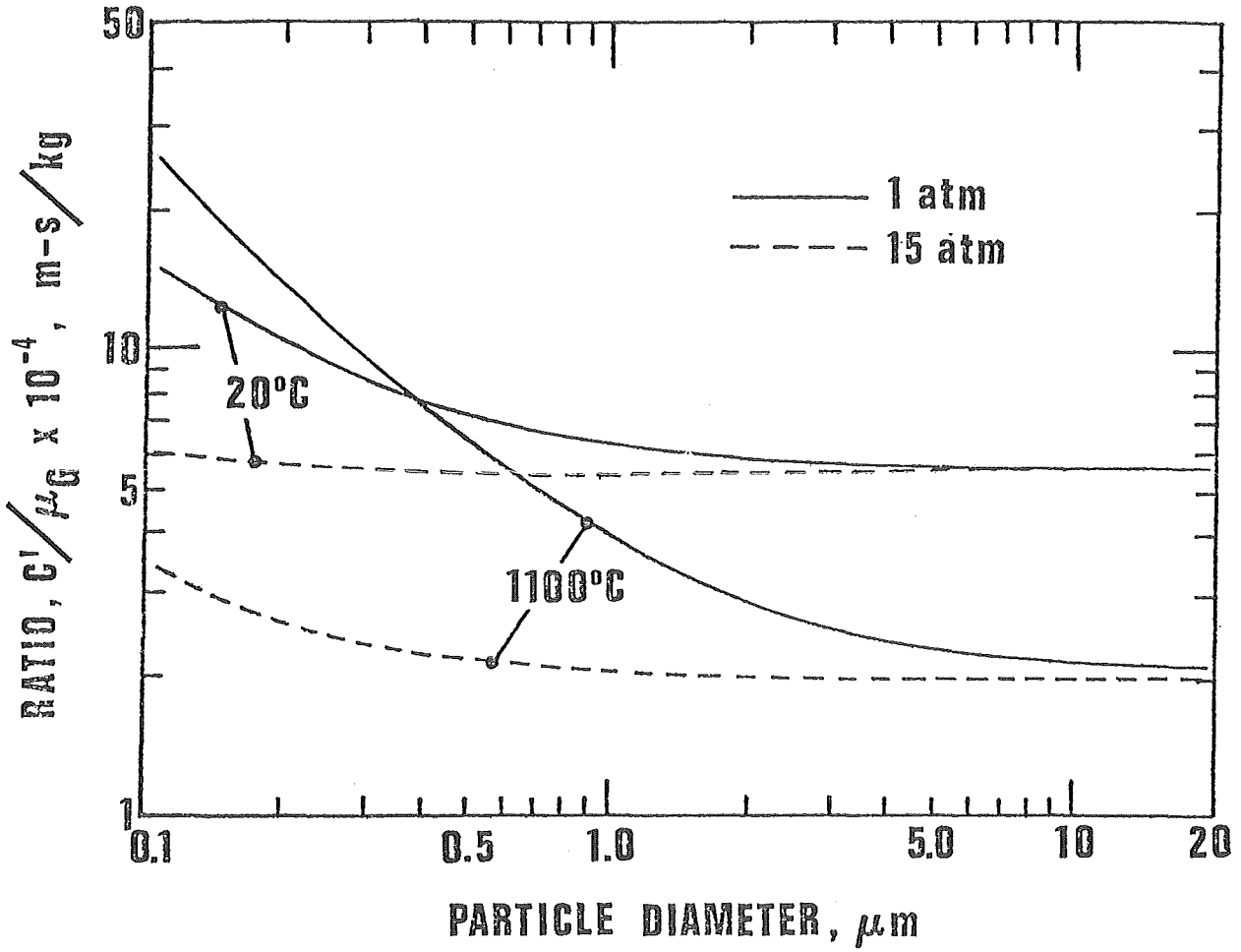


Figure 1. The effect of HTP on the ratio C'/μ_G .

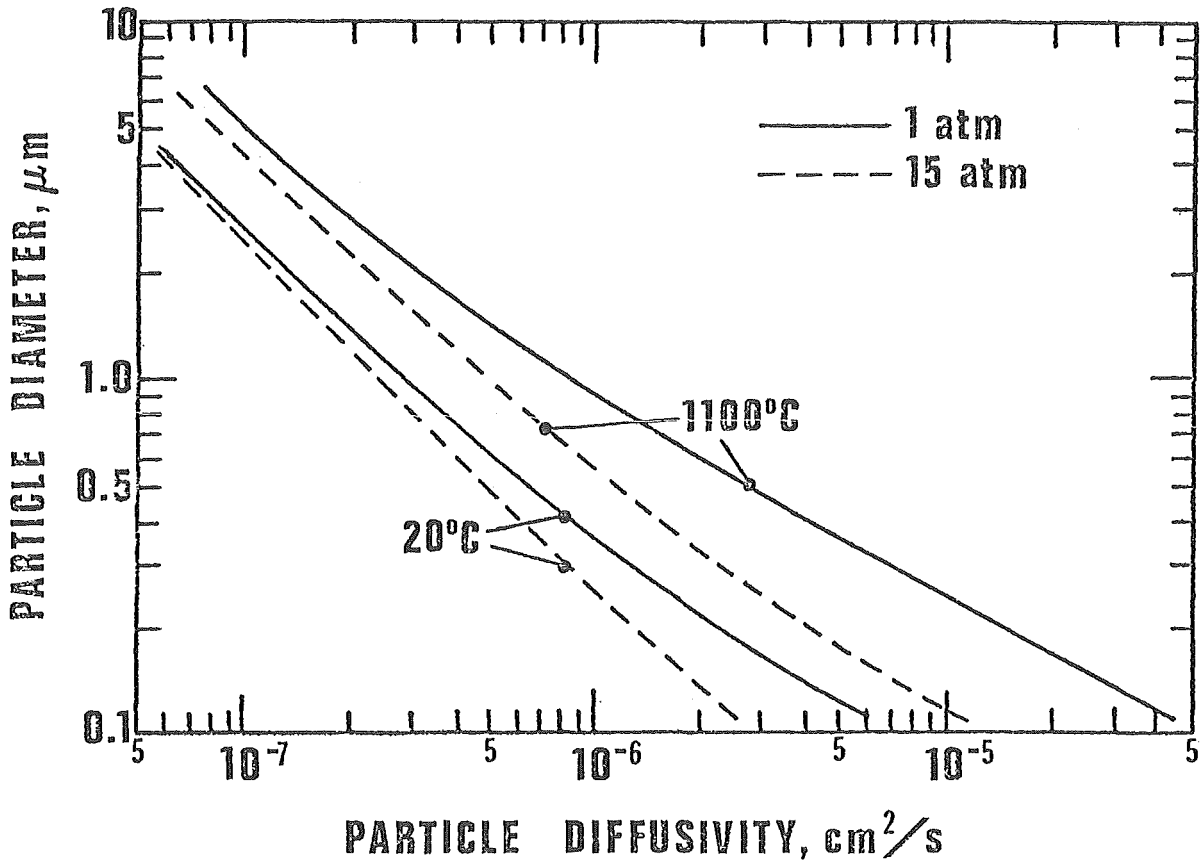


Figure 2. The effect of HTP on particle diffusivity.

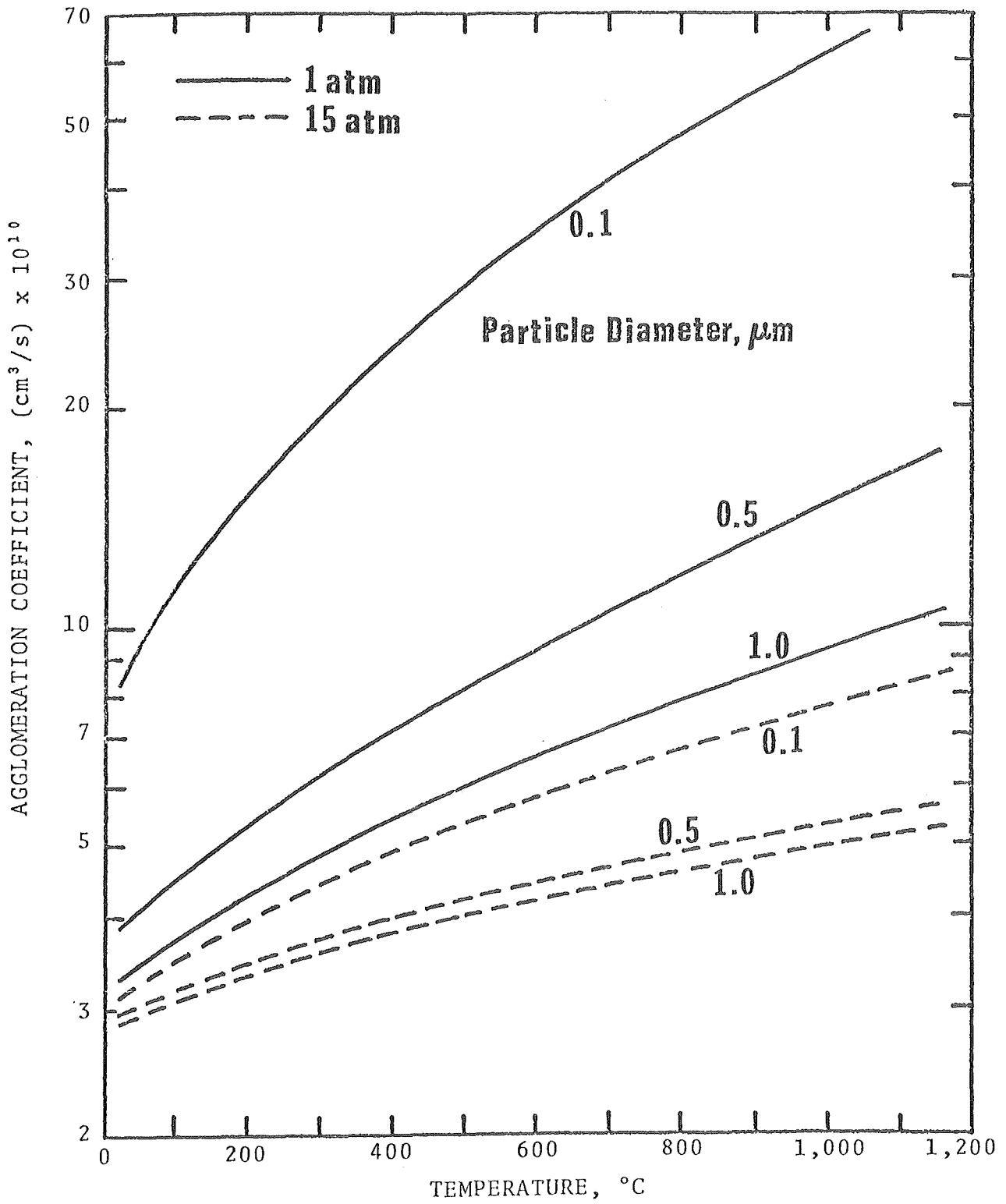


Figure 3. The effect of HTP on Brownian agglomeration.

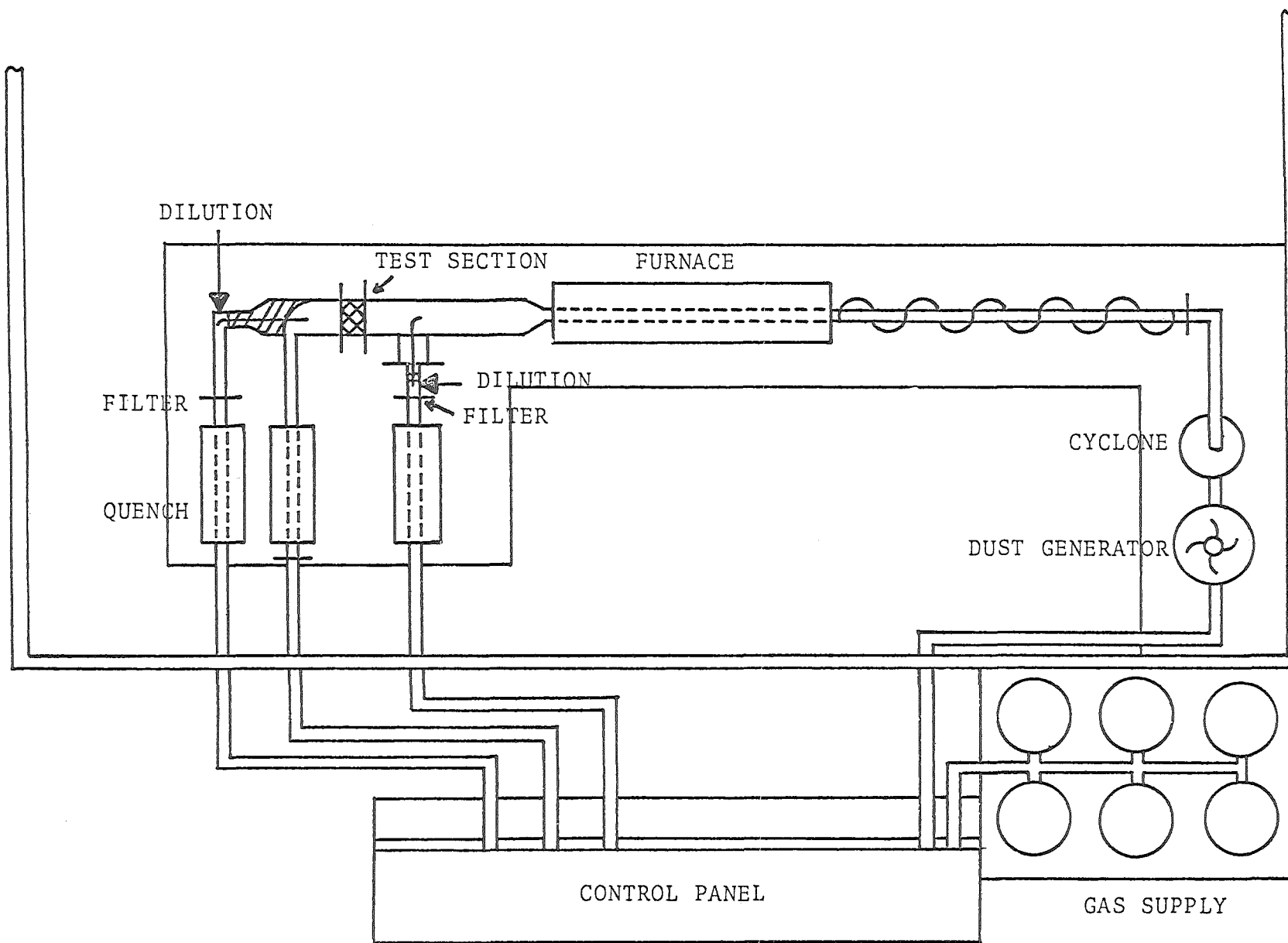


Figure 4. Test facility.

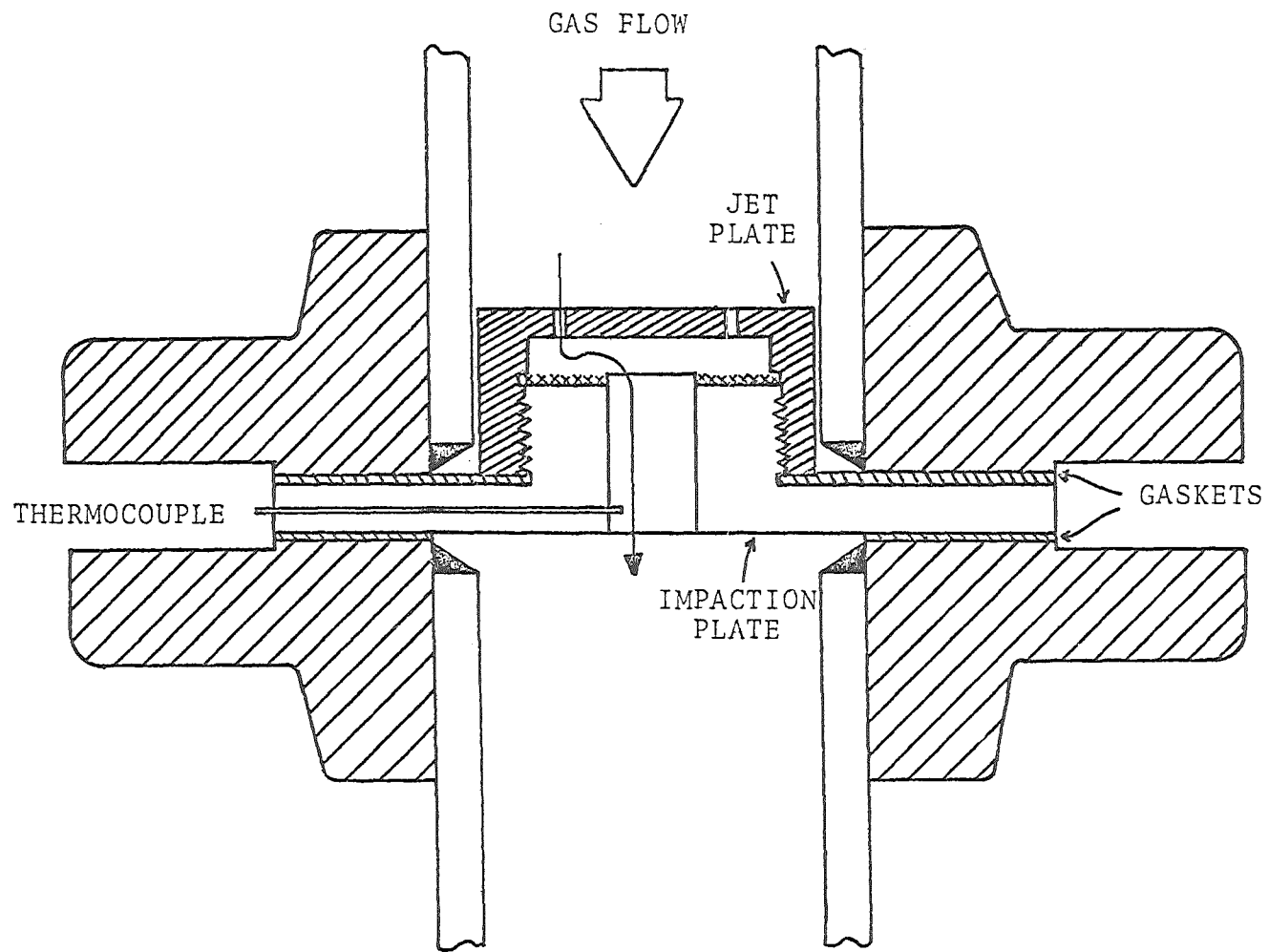


Figure 5. Impaction test section.

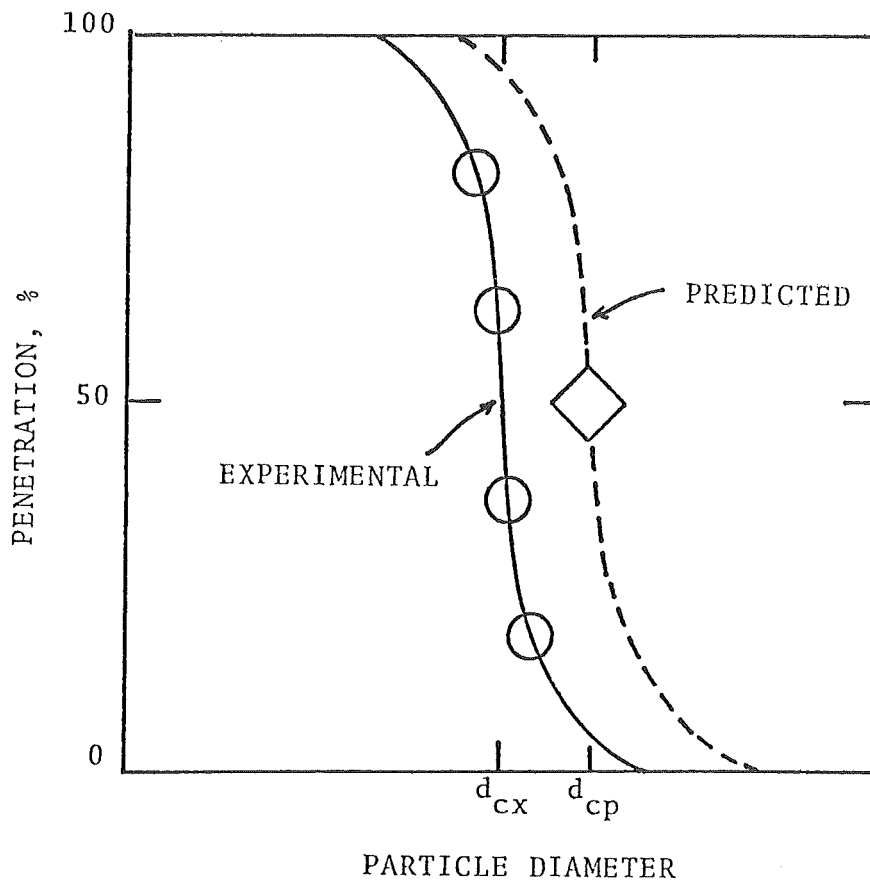


Figure 6. Comparison of Experimental and Predicted Cut Diameters.

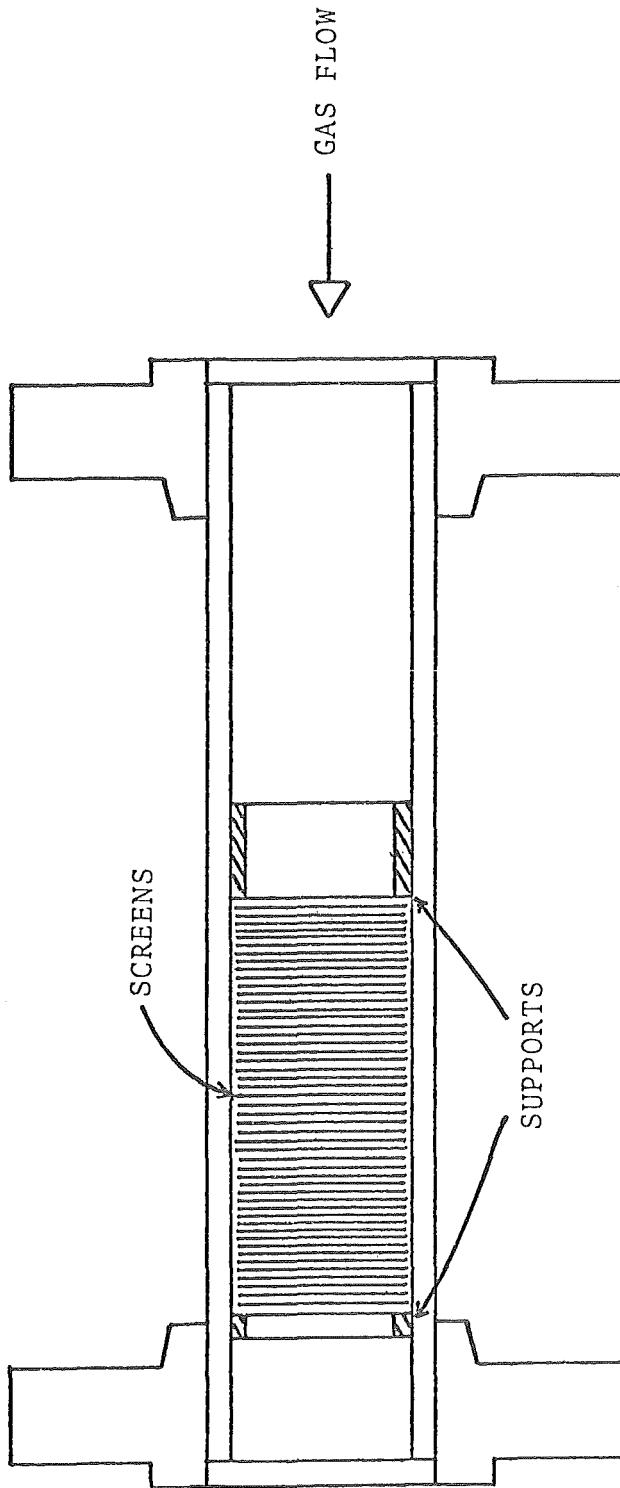


Figure 7. Diffusion test section.

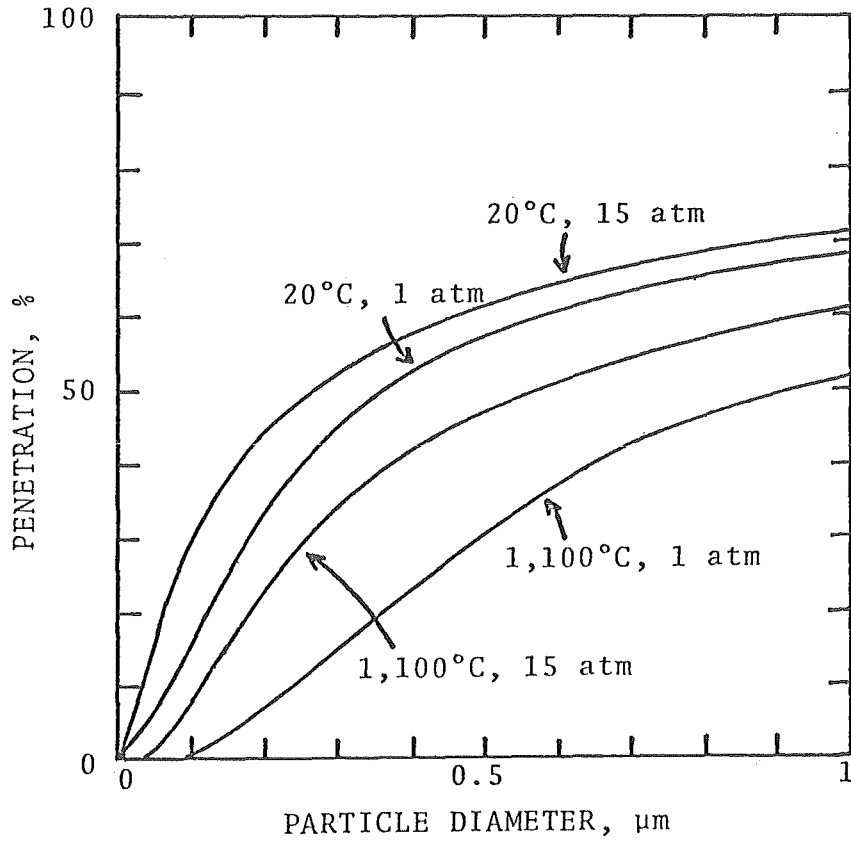


Figure 8. Predicted penetrations for diffusion test section.

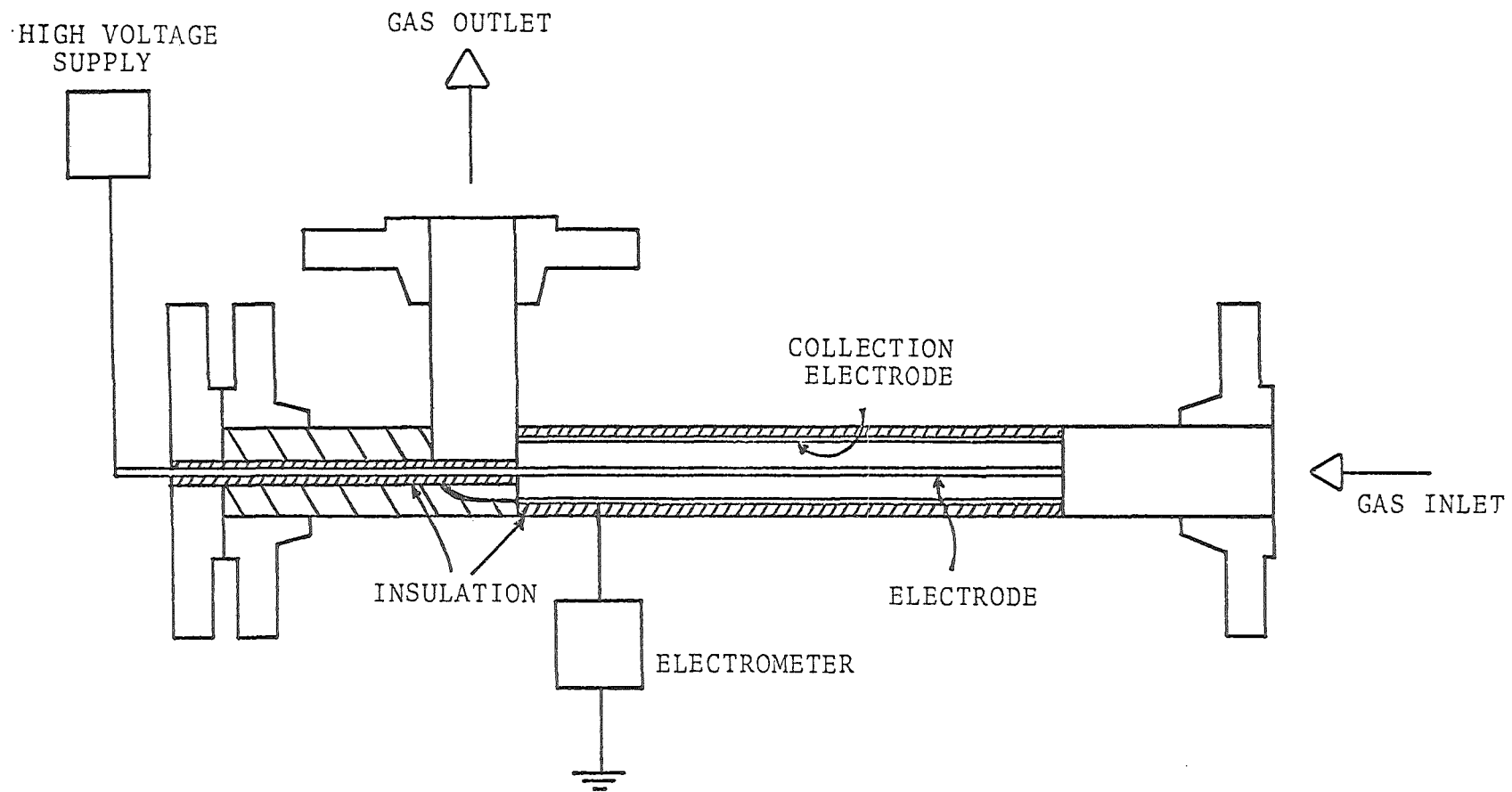


Figure 9. Electrical migration test section.

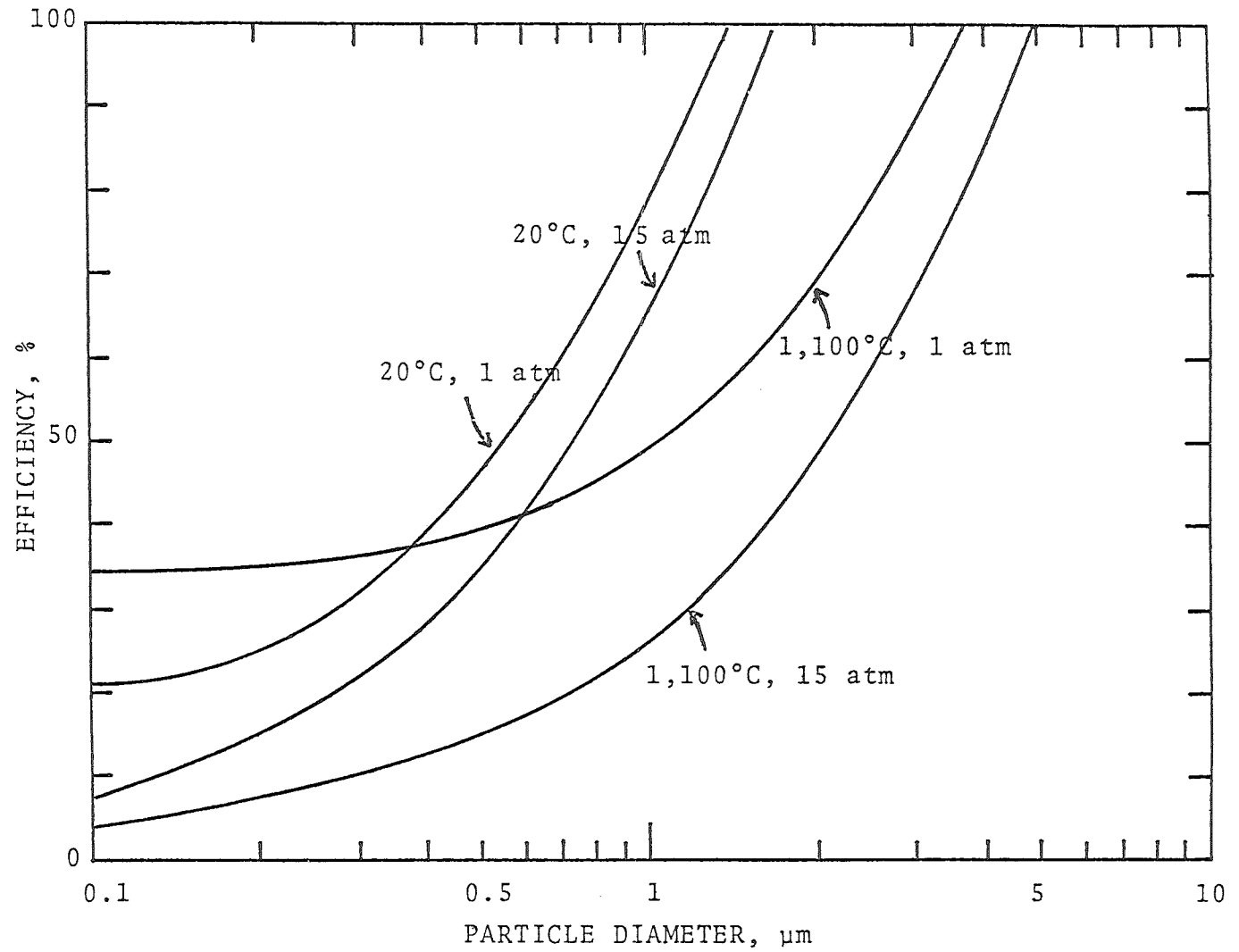


Figure 10. Predicted efficiencies for electrical migration test section.

Discussion

Mr. Gũthner asked whether:

- 1) APT had started measuring collection efficiency in electrostatic precipitators and fabric filters.
- 2) It was really essential to use such expensive alloys.
- 3) Details regarding requirements for new collection techniques in terms of clean gas dust load and pollution load could be given.

Dr. Parker's answers were as follows:

- 1) Work in this field had not been part of the program. U.S.EPA intended to perform tests on baghouses at Exxon Research Company in New Jersey. Our work concerns high temperature and pressure fundamentals as stated in the contract.
- 2) California law requires that pressure vessel code be observed. This necessitated good engineering judgment, and use of the best materials. Steel, nickel and cobalt alloys were chosen, because of the extremely high temperatures and pressures.
- 3) A two-fold requirement existed:
 - a) Similar to that for coal-fired boilers.
 - b) Tolerance of gas turbines for fine particulates.

Erosion damage to the turbine blades occurred when particles larger than 2-3 microns were present. Alkali metals in ash on the blades could also prove hazardous; deposits might build up, impairing performance, or causing further erosion by breaking off. Problems of deposition were important; an outlet concentration of 0.002 grains per std. cu. ft. was desirable.

A controversy existed as to whether more stringent requirements should be introduced to protect the turbine or the environment (Mr. Princiotta). Mr. Parker pointed out the relationship between turbine protection and larger micron particles and environmental protection and sub-micron particles. Further details of U.S. requirements were furnished by Mr. Princiotta. Dr. Holighaus mentioned work being carried out at NASA on damage to blades by small particulates; more research in this area was needed. He also asked whether one could find the best process for separation by using theoretical methods. Dr. Parker replied that operational problems presented the most serious questions. Electrostatic precipitators could be operated at higher voltages in high pressure gases resulting in the possibility of higher collection efficiency. However, practical problems have not been identified, nor have electrostatic precipitators been tested for collecting dust under extreme temperature and pressure conditions.

AIR POLLUTION TECHNOLOGY, INC.

4901 MORENA BLVD., SUITE 402 SAN DIEGO, CA 92117 (714) 272-0050

GRANULAR BED FILTERS AND DRY SCRUBBERS

by

Dr. Richard Parker, Dr. Seymour Calvert,
Mr. Shui Yung, and Dr. Ronald Patterson

Air Pollution Technology, Inc.

Presented at the
US/FRG Particulate Workshop
Julich, Germany

March 16-17, 1978



ENGINEERING • CONSULTING • RESEARCH • DEVELOPMENT • DESIGN • EQUIPMENT



ABSTRACT

This presentation discusses the use of granular bed filters and dry scrubbers for removing particulate matter from high temperature and pressure gas streams. Engineering models are presented and performance predictions are made for high temperature and low temperature applications. Experimental data are presented for verifying the models at low temperature. The primary collection efficiency obtainable using granular bed filters or dry scrubbers is sufficient to meet current environmental regulations. However, there are many operational problems which need to be resolved before these devices will be sufficiently reliable for commercial application.

GRANULAR BED FILTERS AND DRY SCRUBBERS

INTRODUCTION

Granular bed filters and dry scrubbers have been proposed for the removal of particulate matter from high temperature and pressure gases. One such application would be as the tertiary collection device in a pressurized fluidized bed boiler power plant as illustrated schematically in Figure 1. The gas leaves the boiler at a temperature of approximately 900°C and a pressure of about 10 atm. First it passes through a primary cyclone which removes larger particles (including unburnt carbon) and recycles these particles to the combustor. The gas leaves the primary cyclone and passes through a secondary cyclone or multiclone separator. This removes more large particles and reduces the mass loading of particulate to the order of 1 gr/SCF.

A tertiary cleanup device is necessary to reduce the particulate loading sufficiently to protect the gas turbine from excessive erosion and corrosion damage. It is also desirable for the gas at this stage to be sufficiently clean to satisfy all emission regulations. However, if necessary, it is possible to satisfy the emissions regulations by cleaning the gas downstream from the turbine using conventional control technology.

The best available information concerning the size and mass loading of particulate entering the tertiary collection stage of a pressurized fluidized bed process has been reported by Hoke et al. (1977a). The mass loading has been found to be typically about 1 gr/SCF. The size of this particulate is represented in Figure 2. Approximately 30% of the mass is smaller than 2 μm . For this size distribution and loading, approximately 90-95% removal is required to meet U.S. EPA particulate emissions regulations. As much as 99.8% removal may be required to protect the gas turbine, although there is still much debate regarding turbine tolerances for fine particles.

GRANULAR BED FILTERS

Granular bed filters are defined as any filtration system comprised of a stationary or slowly moving bed of separate relatively close-packed granules as the filtration medium. There are three basic approaches to granular bed filtration currently being developed. The first class are referred to as "fixed bed" filters. The bed of granules is kept stationary during filtration. Usually, it is cleaned by a reverse flow of gas which fluidizes the bed and entrains the collected particulate. The principal advantage of the fixed bed approach is that the granules do not have to be recirculated and thus can be used for many filtration cycles. For this reason, fixed beds have potentially lower operating costs.

In a second type of granular bed filter, referred to as the "moving bed" filter, the gas flows through a slowly moving bed of granules. The collected dust particles are carried with the bed and later removed from the granules before the granules are recirculated. Moving beds have the advantage that the granules and dust are separated externally and are free from the problem of particle buildup and bed plugging. An inexpensive but effective means of recirculating the granules could significantly lower operating costs.

The third type of filter, the "intermittently moving" filter, is really a hybrid of the fixed and moving bed filters. This filter uses stationary granules for filtration and causes the granules to move through the system intermittently during the cleaning cycle.

The major problems with each approach are summarized in Table 1. Many of these problems can be resolved through further research and development. Granular bed filters are used successfully to control emissions from clinker coolers in the cement industry and on hog-fuel boilers in the forest products industry. They operate in the range of 100-200°C and near atmospheric pressure. However, applications for controlling fine particulate at elevated temperatures and pressures are very scarce. Granular

bed filters are attractive for these applications because they can be made to withstand high temperature and pressure environments relatively easily. However, more work is needed to determine whether granular bed filters are satisfactory from the point of view of primary collection efficiency, cost, and reliability.

Granular Bed Filter Model

Pressure Drop -

Ergun (1952) proposed the following equations to describe the pressure drop for flow through packed beds:

$$-\Delta P = \frac{f \cdot Z \cdot u_G^2 \cdot (1-\epsilon) \cdot \rho_G}{d_c \cdot \epsilon^3} \quad (1)$$

$$f = \frac{150}{N_{Re}} + 1.75 \quad (2)$$

$$\text{and } N_{Re} = \frac{d_c \cdot u_G \cdot \rho_G}{\mu_G \cdot (1-\epsilon)} \quad (3)$$

Predictions based on these equations agree very well with experimental data (Figure 3). The agreement is so good, in fact, that equation (1) has been used with pressure drop data to determine an experimental "effective bed porosity" for irregular, non-uniform size bed granules.

Collection Efficiency -

No available models were found satisfactory for predicting collection efficiencies for granular bed filters operating at velocities likely to be encountered in practice. We have developed a performance model which has been used to predict collection efficiency for lab-scale and full-scale filters. The model is based on the collection efficiency of a clean granular bed. The collection efficiency would be affected if there were a significant filter cake on the bed surface and within the bed.

The presence of a surface cake, however, has not been noticed by many investigators working with large-scale filters. We feel the clean bed model predicts a conservative estimate of the efficiency attainable by granular filtration and is a satisfactory model for filters which operate primarily without the presence of a filter cake.

The granular bed can be envisioned as a great number of impaction stages connected in series as illustrated in Figure 4. Particle collection is by inertial impaction and is similar to collection in a cascade impactor. The jet openings are the pores in each layer of granules. It is assumed that the jet diameters in the granular bed are of uniform size and are equal to the hydraulic diameter of the void space. The gas velocity in the jet is the average superstitial gas velocity.

If ' η ' is the collection efficiency of one impaction stage, the particle penetration for the granular bed will be,

$$Pt_d = (1-\eta)^N \quad (4)$$

where Pt_d = penetration for particles with diameter, d_p ,
fraction

η = single stage collection efficiency, fraction

N = number of impaction stages

As in some cascade impactors, each layer of granules serves both as the jet plate and as the collection plate. Therefore, each layer is an impaction stage and ' N ' is equal to the number of granular layers in a bed. For a randomly packed bed,

$$N = \frac{3 Z}{2 d_c} \quad (5)$$

where Z = bed depth, cm

d_c = granule diameter, cm

and,

$$Pt_d = (1-\eta)(1.5Z/d_c) \quad (6)$$

The impaction collection efficiency, η , is a function of, K_p , the inertial impaction parameter. The impaction parameter is defined as,

$$K_p = \frac{C' \rho_p d_p^2 u_j}{9 \mu_G d_j} \quad (7)$$

where C' = Cunningham slip factor, dimensionless

ρ_p = particle density, g/cm³

d_p = particle diameter, cm

u_j = jet velocity, cm/s

μ_G = gas viscosity, poise

d_j = jet diameter, cm

since,
$$u_j = u_{Gi} = \frac{u_G}{\epsilon} \quad (8)$$

and,
$$d_j = 4r_H = \frac{2}{3} \left(\frac{\epsilon}{1-\epsilon} \right) d_c \quad (9)$$

where u_{Gi} = average interstitial gas velocity, cm/s

ϵ = bed porosity, fraction

r_H = hydraulic radius, cm

d_c = granule diameter, cm

we have,
$$K_p = \frac{3}{2} \left(\frac{1-\epsilon}{\epsilon^2} \right) \frac{C' \rho_p d_p^2 u_G}{9 \mu_G d_c} \quad (10)$$

The relationship between, η , and, K_p , can be evaluated once the flow field is defined. Flow fields reported in the literature; e.g. Ranz and Wong (1952) and Marple (1970) are adequate for

$K_p > 0.15$. For $K_p < 0.15$, there is no suitable flow field reported in the literature. Therefore, the relationship between, η , and K_p , cannot be calculated analytically from the available literature.

The single stage collection efficiency has been calculated as a function of K_p from equation (6) and experimental data. Figure 5 shows the results. There is scatter in the lower end of the curve. For $K_p < 10^{-2}$, η , is very sensitive to experimental data. A few percent scatter in data will cause, η , to fluctuate greatly. Figure 5 compares the experimentally determined, η , versus, K_p , curve with those reported by Ranz and Wong (1952), Stern et al. (1962), and Mercer and Stafford (1969). All reported curves are for $K_p > 0.15$. As can be seen, the present study is consistent with other researcher's results and is a continuation of their curves into the range most likely to be important for high temperature and pressure filtration.

Paretsky et al. (1971) and Knettig and Beeckmans (1974) studied the collection of monodispersed aerosol particles in granular bed filters. Their data were transformed into, K_p , versus η , plots as shown in Figure 6.

Knettig and Beeckmans (1974) used 425 μm glass beads as granular material. Bed porosity was 0.38. Aerosol particles were 0.8, 1.6, and 2.9 μm in diameter. As can be seen from Figure 6, their data are in close agreement with the results of the present study.

Paretsky et al. (1971) investigated the filtration of 1.1 μm diameter polystyrene latex aerosols by beds of sand. They used a bed of 10-14 mesh (1,200-1,700 μm) angular sand and a bed of 20-30 mesh (500-850 μm) sand at superficial gas velocities between 0.3 and 80 cm/s. Bed porosities were 0.41 and 0.43, respectively. We have calculated single stage collection efficiencies from their data. In the calculation, the granule diameters were assumed to be the arithemtical mean of the smallest and the largest granule size in the bed. The results are plotted in Figure 6. For a given inertial parameter, Paretsky et al.'s data give a higher

collection efficiency than reported in this study. Their data would be close to that of the present study if the smallest granule diameter were used instead of the arithmetic mean.

The design model is based on particle collection by a clean bed. If there is no filter cake formed on the surface and the collected particles are uniformly distributed in the bed, the model should be applicable. The design model has been used to predict the performance of a Rexnord gravel bed filter and of Combustion Power Company "dry scrubber." The predictions are compared with field sampling data taken from the literature.

Rexnord Gravel Bed Filter

McCain (1976) conducted a performance test on a Rexnord gravel bed filter. The gravel bed filter was installed to clean emissions from a clinker cooler in a Portland cement plant.

Samples were taken simultaneously at the filter inlet and outlet with cascade impactors. The operating conditions of the gravel bed were:

Gravel diameter = 4 mm
Face velocity = 73 cm/s
Gas temperature = 175°C
Pressure drop = 25.4 cm W.C.

It was assumed that there was no surface cake and that the pressure drop across the bed was 80% of the overall pressure drop. Ergun's equation was used to estimate a porosity of 0.25. With this bed porosity, the grade penetration curve was calculated for the operating conditions listed above.

Figure 7 is the predicted grade penetration curve along with that measured by McCain (1976). The prediction is in good agreement with the data.

Combustion Power Company Moving Gravel Bed

Hood (1976) reported the evaluation of the Combustion Power Company (CPC) moving gravel bed filter on the control of particulate emissions from a hog-fuel fired boiler. The gravel bed

filter was a prototype unit with suggested capacity of 1,133 Am³/min (40,000 ACFM). The bed was packed with an intermediate-size gravel which was retained on a 3.2 mm (1/8") wire mesh and passed at 6.4 mm (1/4") mesh screen. The bed was a single down-flowing annulus 2.6 m (8.5 ft) O.D. and 1.8 m (6 ft). I.D.

During sampling the unit was operated at a flow rate of 1,558 m³/min (55,000 ACFM). The gas temperature was 177°C (350°F). Figure 8 shows the penetration curves for three sampling runs.

The average granule diameter was assumed to be 4.6 mm and the bed porosity was calculated to be 0.25. The predicted grade penetration curve is shown in Figure 8. The predicted penetration is higher than that measured. Recent data obtained by A.P.T. on the CPC moving bed filter is shown in Figure 9. These data agree well with the model's prediction.

PERFORMANCE PREDICTION FOR HTP APPLICATION

Exxon Research and Engineering Company installed a Ducon granular bed filter at their fluidized bed coal combustor miniplant. The bed is packed with Agsco no. 2 quartz (400 μm mean diameter) to a depth of 3.8 cm (1.5 in.). The temperature of the flue gas from the combustor is 870°C (1,600°F) and the pressure is 10 atm.

According to Hoke (1977b), there is no surface cake formed and the fly ash is uniformly distributed in the bed. For this condition, the clean bed model can be used to predict the performance of the Ducon granular bed in the miniplant.

From the pressure drop data reported by Exxon, the bed porosity was estimated to be 0.24. Figure 10 shows the predicted performance of the miniplant granular bed filter at high temperature and high pressure and at ambient conditions. A particle density of 1.5 g/cm³ was used in the calculation.

If the particle size distribution is known, Figure 10 can be used to estimate the overall collection efficiency of the Ducon granular bed filter. The equation relating the efficiency for collecting one particle diameter to the overall efficiency is:

$$E = 1 - \overline{Pt} = 1 - \int_0^{\infty} Pt_d f(d_p) d(d_p) \quad (11)$$

where E = overall collection efficiency, percent or fraction
 \overline{Pt} = overall penetration, fraction
 Pt_d = penetration for particles with diameter, d_p ,
fraction
 $f(d_p)$ = particle size frequency distribution
 d_p = particle diameter, μm or cm

Hoke (1977a) reported data on the particle size distribution leaving the secondary cyclone (Figure 2). The mass median diameter is $3.5 \mu\text{m}$ and the geometric standard deviation is 2.9. The mass loading is approximately 2.3 g/Nm^3 (1 gr/SCF). The overall collection efficiency for this size distribution was calculated graphically to be 95.1% (2.9% penetration). Experimental efficiencies of 95-97% were reported by Hoke (1977b).

As can be seen from Figure 10, the granular bed filter should be very efficient for all particles larger than 1 to 2 μm in diameter. Whether or not this filter is efficient enough to protect the gas turbine will depend strongly on the turbine's tolerance for submicron particles.

DRY SCRUBBERS

Moving bed filters are sometimes referred to as dry scrubbers. Another type of dry scrubbing system has been developed by A.P.T., Inc. and is called the "PxP" system (particle collection by particles).

The PxP system for fine particle control uses relatively large particles as collection centers for the fine particles in the gas stream. The relatively large particles (collector particles) introduced to the gas stream can collect fine particles by mechanisms such as diffusion, inertial impaction, interception and electrophoresis. The larger size of the collector particles

allows easy separation from the gas stream by methods such as cyclones, and gravitational settling.

Figure 11 is a functional diagram of the process steps for a representative PxP system. The functions represented on this diagram could occur concurrently or separately in several types of equipment.

The first step involves introducing the collectors to the gas stream. This process can involve pneumatic or mechanical injection into the gas stream. The second stage involves contacting the collectors with the gas in order to encourage the movement of the fine particles to the collectors. A venturi device can be used for the contactor which would be analogous to a venturi scrubber except that solid collectors are used instead of liquid drops. Alternative contactors such as a centrifugal scrubber could be used.

The next process step is to remove the collector particles after sufficient exposure in the contactor to cause capture of the initial fine particles present in the gas. At this stage the large size and mass of the collector particles is utilized to separate them from the gas. A cyclone separator could be used for this step. Two streams are shown leaving the separator: the cleaned gas leaves the process at this point and the second stream represents the flow of collector particles to the next step. The final process involves either discarding the collector particles or cleaning them for recycle and disposing of the material collected from the gas stream.

Performance Prediction

The particle collection efficiency and pressure drop for an A.P.T. dry scrubber with cocurrent flow can be predicted with the same relationships that define cocurrent wet scrubber performance. The theoretical performance of the PxP scrubber has been determined based on the venturi scrubber model of Yung et al. (1977). For particle collection in the venturi throat, the penetration for a given particle size is:

$$\begin{aligned}
 P_t = \exp & \left[\left[\frac{B}{K_{po} (1-u_d^*) + 0.7} \right] \left[4 K_{po} (1-u_d^*)^{1.5} \right. \right. \\
 & + 4.2 (1-u_d^*)^{0.5} - 5.02 K_{po}^{0.5} \left((1-u_d^*) + \frac{0.7}{K_{po}} \right) \tan^{-1} \left(\frac{(1-u_d^*) K_{po}}{0.7} \right)^{0.5} \\
 & \left. \left. - \frac{B}{K_{po} \left(1 + \frac{0.7}{K_{po}} \right)} \left[4 K_{po} + 4.2 \right. \right. \right. \\
 & \left. \left. - 5.02 K_{po}^{0.5} \left(1 + \frac{0.7}{K_{po}} \right) \tan^{-1} \left(\frac{K_{po}}{0.7} \right)^{0.5} \right] \right] \quad (12)
 \end{aligned}$$

$$\text{where } K_{po} = \frac{d_{pa}^2 u_{Gt}}{9 \mu_G d_c} \times 10^{-8} \quad (13)$$

$$u_d^* = 2 \left[1 - x^2 + (x^4 - x^2)^{0.5} \right] \quad (14)$$

$$x = \frac{3 l_t C_{Do} \rho_G}{16 d_c \rho_c} + 1 \quad (15)$$

$$\text{and } B = \left(\frac{Q_c}{Q_G} \right) \left(\frac{\rho_c}{\rho_G} \right) \frac{1}{C_{Do}} \quad (16)$$

where u_{Gt} = gas velocity at throat, cm/s
 l_t = throat length, cm
 ρ_c = collector density, g/cm³
 Q_G = gas volumetric flow, m³/s
 Q_c = collector volumetric flow, m³/s
 C_{Do} = drag coefficient for drops at the venturi throat inlet, dimensionless

Particle collection efficiency was predicted for several values of parameters in a cocurrent PxP scrubber using 100 μm diameter collectors and a gas velocity of 57 m/s. Figure 12 is a plot of particle penetration against particle size with collector/gas flow rate ratio as a parameter and with a 20°C gas temperature. Figure 13 is a similar plot with an 820°C gas temperature. To show the effect of temperature on penetration, the curves for a ratio of 0.002 and temperatures of 20°C and 820°C are plotted on Figure 14.

The predicted penetration curves have the following characteristics:

1. For a given set of operating conditions, the penetration decreases with increasing size of fine particles. This is expected since the collection mechanism is inertial impaction of the fine particles upon the collectors.

2. For a given size of collector particle and aerodynamic diameter of fine particle, the penetration decreases with increasing value of $(Q_c \rho_c / Q_G)$.

3. A similar dependence upon the gas velocity is apparent from equation (1).

4. For the 100 μm collectors and a given fine particle aerodynamic diameter, the penetration increases with increasing gas temperature. This is the result of an increase in gas viscosity with temperature which reduces the effective inertia of the fine particles.

It can also be shown that collector particle diameter affects collection efficiency when other factors are held constant. The cut diameter (i.e., the diameter of the particle which is collected at 50% efficiency) decreases as collector diameter decreases. Collection efficiency for particles larger than several microns diameter varies in a more complex way, depending on flow and geometric parameter combinations.

Experimental Program

Experimental work has been performed by A.P.T. to determine fine particle collection efficiency in a PxP scrubber in order to

confirm the predictions obtained from available mathematical models. A dibutylphthalate (DBP) aerosol was used in collection efficiency experiments with 125 μm mean diameter nickel beads and with 100 μm mean diameter sand as collector particles. The DBP aerosol had a mass median aerodynamic diameter of 1.3 μm A and standard deviation, $\sigma_g = 2.0$.

The collectors entered the T-shaped contactor through the branch leg and were entrained by air entering through one of the "run" legs. The length of the 1.1 cm diameter throat varied from 2.5 to 5.1 cm. The throat velocity was 57 m/s and $(Q_c \rho_c / Q_G)$ was around 0.005 g/cm³ for the nickel beads and 0.0017 g/cm³ for the sand.

Test aerosol particle cumulative concentration was measured for each of several diameter increments by means of a Climet light scattering particle analyzer for the experiments with nickel collectors. Cascade impactors were used with the sand collectors. Inlet and outlet cumulative mass distributions were plotted and the particle collection efficiency was computed from the ratio of the curve slopes at several particle diameters.

The resulting penetration data are shown in Figure 15 for DBP collection on sand. The cascade impactor data led to the penetration relationship labeled "experimental curve." The prediction for $(Q_c \rho_c / Q_G) = 0.002$ is also shown in Figure 15 and compares well with the experimental curve.

Particle penetration data for all runs with nickel and sand collectors are represented in Figure 16, a "cut power plot." The cut diameter is plotted against gas pressure drop in Figure 16. The line represents the relationship which is predicted and which has been confirmed by a number of field tests on large wet scrubbers. Agreement between the data points and the line is good.

The experimental data on the primary collection efficiency of the PxP system agree well with predictions based on a mathematical model which was first developed for wet scrubbers. Since the model was derived for the mechanism of particle collection by inertial impaction on spheres in a cocurrent scrubber, it is

reasonable to expect it to fit the data. The PxP A.P.T. dry scrubber system has the same primary collection efficiency/power relationship as a venturi type wet scrubber.

The overall efficiency of the PxP system will depend on the reentrainment characteristics of the specific system in addition to the primary efficiency. Particle and collector properties, system geometry, flow rate, and other parameters will influence reentrainment.

Research is continuing on the experimental evaluation of the PxP system for HTP application.

Table I. Granular Bed Filter Problems

| <u>FIXED BED</u> | <u>MOVING BED</u> | <u>INTERMITTENT BED</u> |
|--|--|--|
| 1. Plugging of retaining grids and possible particle buildup in bed. | 1. Particle re-entrainment in moving bed. | 1. Low gas capacity can cause high capital cost. |
| 2. Particle seepage through bed during cleaning cycles. | 2. Granule recirculation may cause high operating cost. | 2. Granule recirculation may cause high operating cost. |
| 3. Fluidization redisperses fine dust during cleaning. | 3. Difficult to form a cake in moving bed. | 3. Need to form surface cake to avoid plugging problems. |
| 4. HTP valving required for reverse air cleaning. | 4. Erosion of retaining grids and transport systems. | 4. Erosion of retaining grids and transport system. |
| 5. Temperature losses proportional to volume of cleaning air. | 5. Temperature losses proportional to heat capacity of recirculated granules and recirculation rate. | 5. Temperature losses proportional to heat capacity of recirculated granules and recirculation rate. |

LIST OF SYMBOLS

C' = Cunningham slip factor, dimensionless
 C_{Do} = drag coefficient at throat inlet, dimensionless
 d_c = granule diameter, cm
 d_j = jet diameter, cm
 d_p = particle diameter, cm
 d_{pa} = aerodynamic diameter = $d_p (\rho_p C')^{1/2}$, μm
 E = overall collection efficiency, fraction
 f = friction factor, dimensionless
 $f(d_p)$ = particle size frequency distribution
 K_p = inertial impaction parameter, dimensionless
 l_t = throat length, cm
 N = number of impaction stages
 N_{Re} = Reynolds number, dimensionless
 \bar{P}_T = overall penetration, fraction
 P_{T_d} = penetration for particles with diameter, d_p , fraction
 Q_c = collector volumetric flow rate, m^3/s
 Q_G = gas volumetric flow rate, m^3/s
 r_H = hydraulic radius, cm
 u_G = superficial gas velocity, cm/s
 u_{Gi} = average interstitial gas velocity, cm/s
 u_{Gt} = gas throat velocity, cm/s
 u_j = jet velocity, cm/s
 Z = bed depth, cm
 ϵ = bed porosity, fraction
 η = single stage collection efficiency, fraction
 μ_G = gas viscosity, poise
 ρ_c = collector density, g/cm^3
 ρ_G = gas density, g/cm^3
 ρ_p = particle density, g/cm^3

LIST OF REFERENCES

Ergun, S., "Fluid Flow Through Packed Columns," Chem. Eng. Prog., 48: 89-94, 1952.
Hoke, R.C., et al., "A Regenerative Limestone Process for Fluidized Bed Coal Combustion and Desulfurization," Monthly Report 87, 1977a.
Hoke, R.C., "Ducon Gravel Bed Filter Testing," presented at EPA/ERDA Symposium on High Temperature and Pressure Particulate Control, Washington, D.C. September 1977b.
Hood, K.T., "Evaluation of the Combustion Power Company Moving Gravel Bed Dry Scrubber on the Control of Particulate Emissions from a Hog-Fired Boiler," NCASI Special Report, September 1976.
Knettig, P. and J.M. Beeckmans, "Capture of Monodispersed Aerosol Particles in a Fixed and in a Fluidized Bed," Canadian J. of Chem. Eng., 52: 703-706, 1974.
Marple, V., "The Fundamental Study of Inertial Impactors." Ph.D. thesis, University of Minnesota, 1970.
McCain, J.D., "Evaluation of Rexnord Gravel Bed Filter," EPA 600/2-76-164, NTIS PB 225-095, June 1976.
Mercer, T.T. and R.G. Stafford, "Impaction from Round Jets," Ann. Occupational Hygiene, 12: 41-48, 1969.
Paretsky, L., L. Theodore, R. Pfiffer, and A.M. Squires, "Panel Bed Filters for Simultaneous Removal of Fly Ash and Sulfur Dioxide: II Filtration of Diluted Aerosol by Sand Beds," J. APCA, 21: 204-209, 1971.
Ranz, W.E. and J.B. Wong, "Impaction of Dust and Smoke Particles," Ind. Eng. Chem. 44: 1371-1381, 1952.
Stern, A.C., H.W. Zeller, and A.I. Schekman, "Collection Efficiency of Jet Impactors at Reduced Pressures," Ind. and Eng. Fundamentals, 1: 273, 1962.
Yung, S.C., S. Calvert, and H.F. Barbarika, "Venturi Scrubber Performance Model," EPA 600/2-77-172, NTIS PB 271-515/AS, August, 1977.

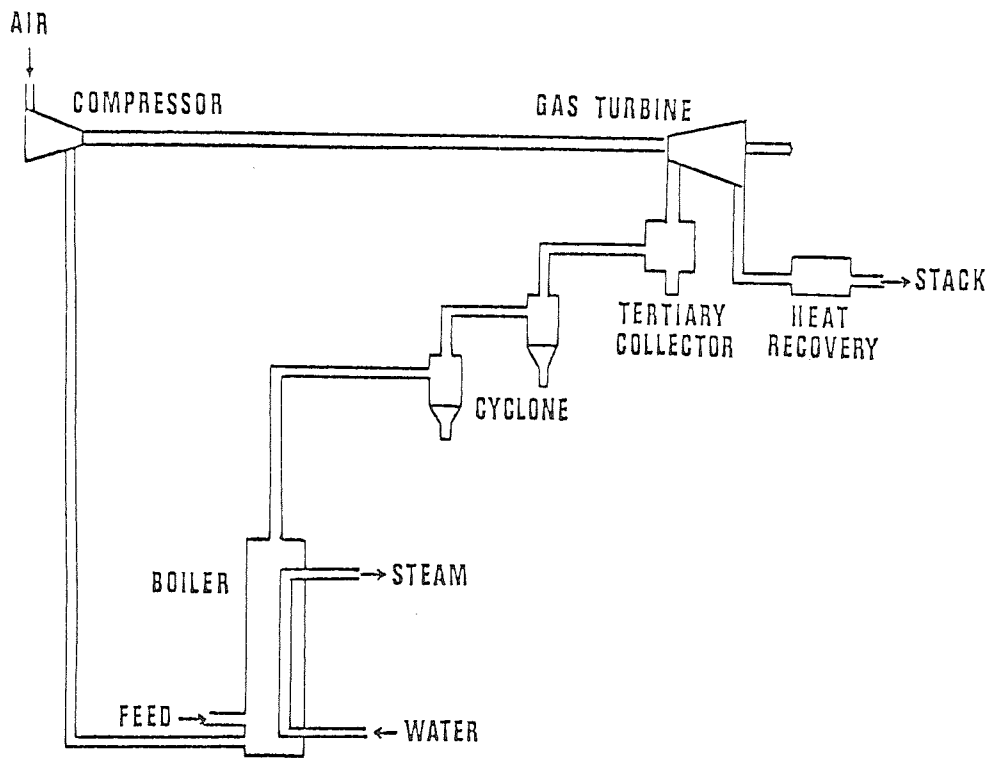


Figure 1. Pressurized fluidized bed boiler

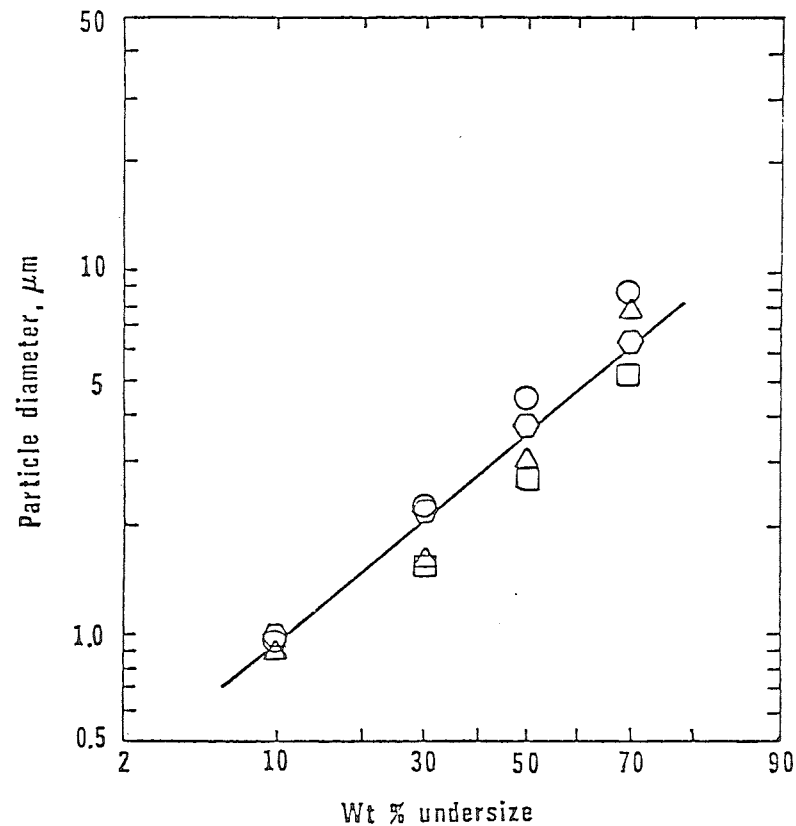


Figure 2. Particle size distribution from Exxon miniplant

AIR POLLUTION TECHNOLOGY, INC.
SAN DIEGO, CALIFORNIA

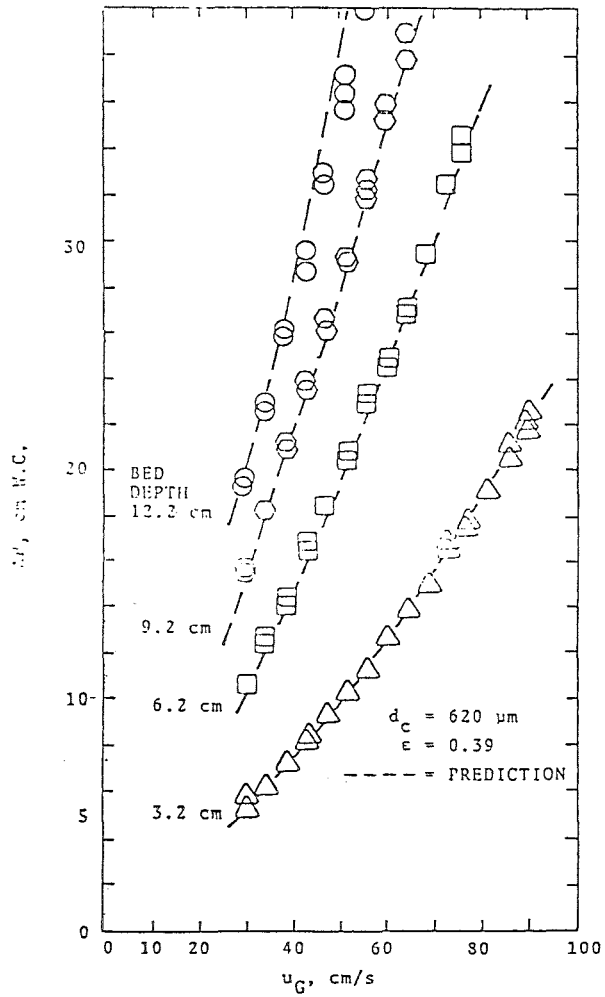


Figure 3. Experimental and predicted pressure drops across granular bed consisting of iron shot.

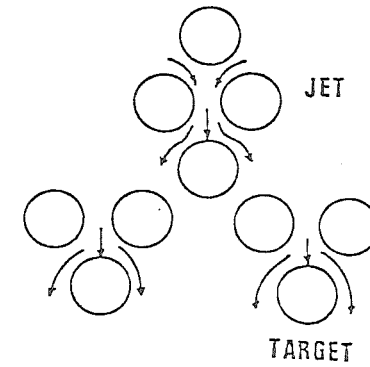


Figure 4. Impaction model

AIR POLLUTION TECHNOLOGY, INC.
SAN DIEGO, CALIFORNIA

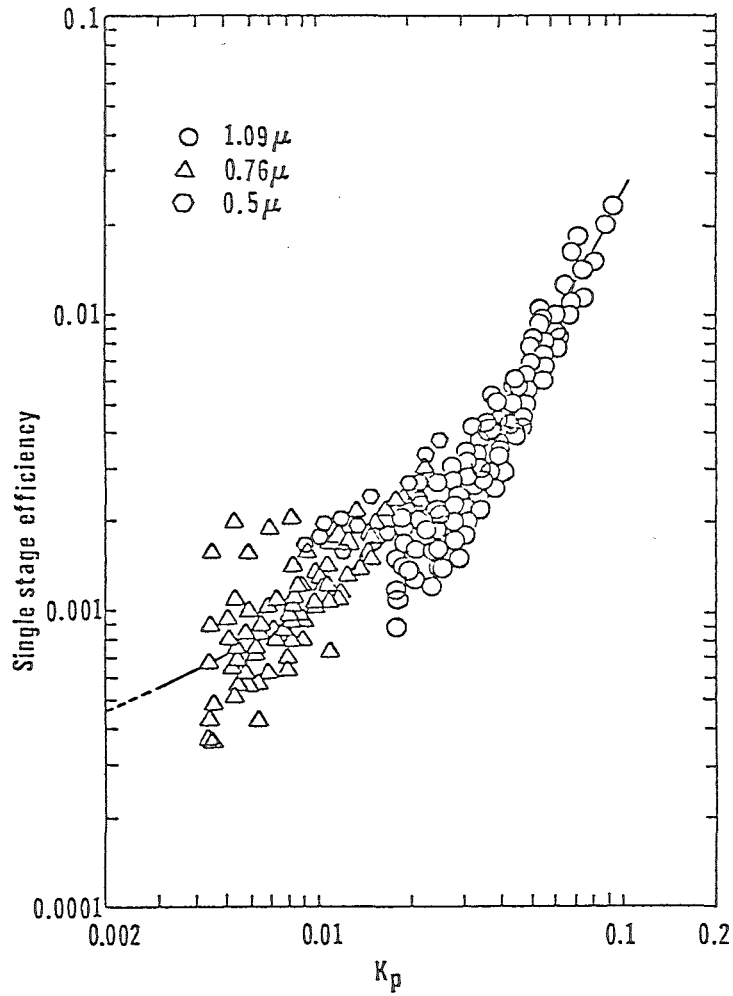


Figure 5. Experimental data

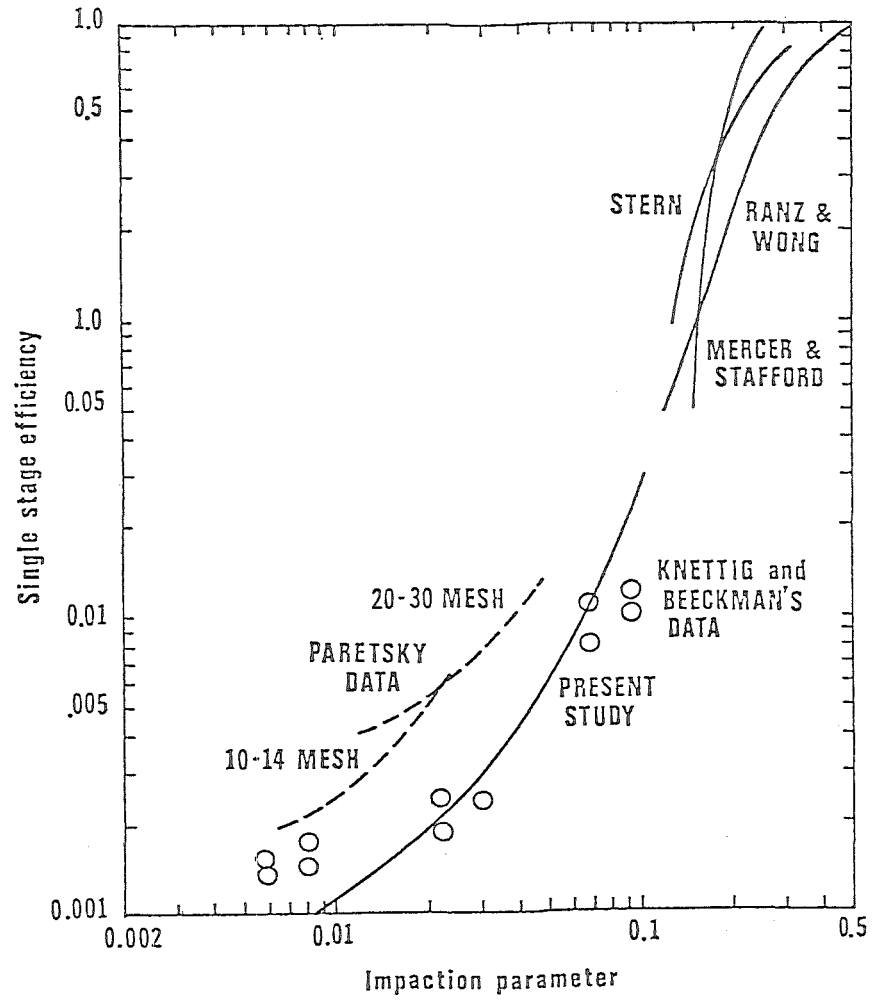


Figure 6. Comparison with previous work

AIR POLLUTION TECHNOLOGY, INC.
SAN DIEGO, CALIFORNIA

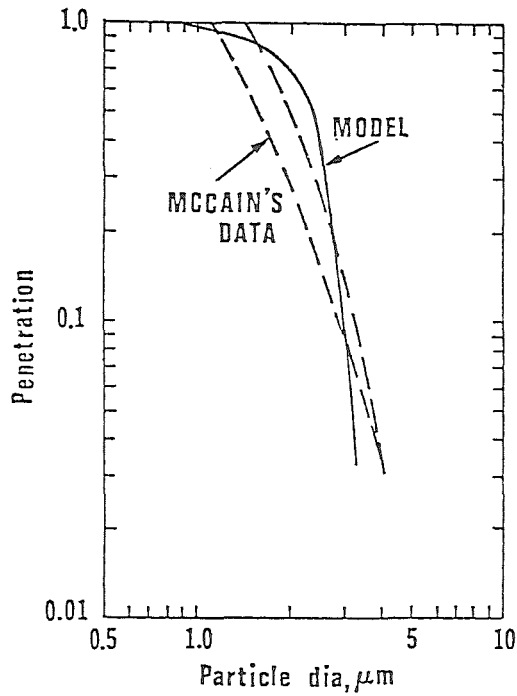


Figure 7. Comparison with data for Rexnord filter

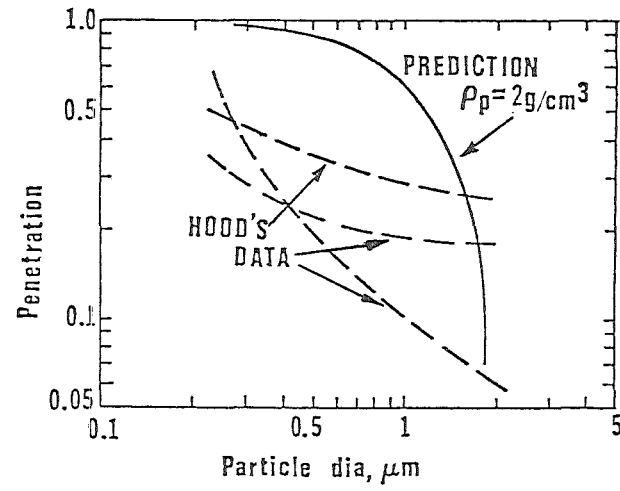


Figure 8. Comparison with data for CPC moving bed filter

AIR POLLUTION TECHNOLOGY, INC.
 SAN DIEGO, CALIFORNIA

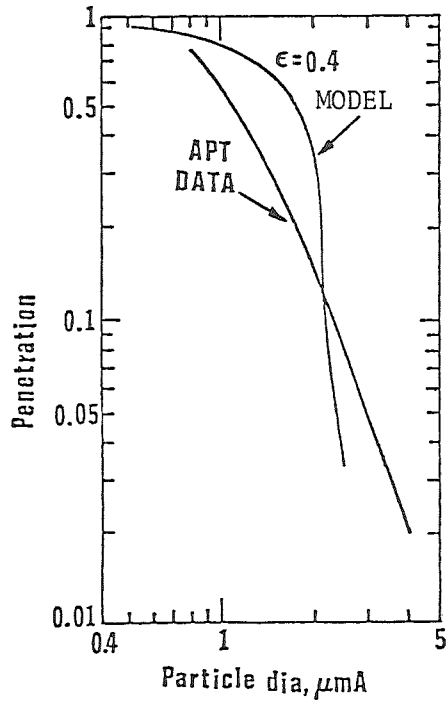


Figure 9 Comparison with CPC moving bed filter

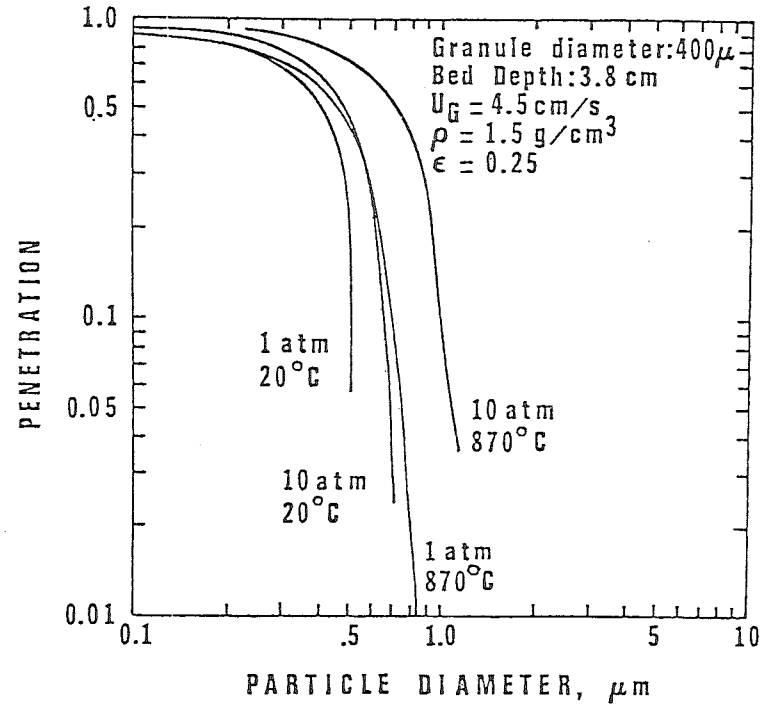


Figure 10: Predicted GBF Performance

AIR POLLUTION TECHNOLOGY, INC.
SAN DIEGO, CALIFORNIA

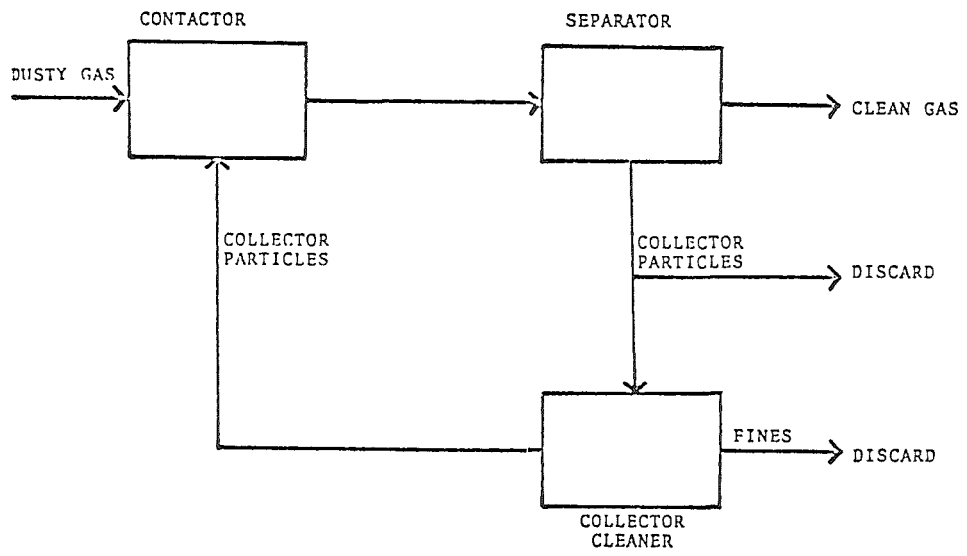


Figure 11. Schematic diagram of A.P.T. dry scrubber system.

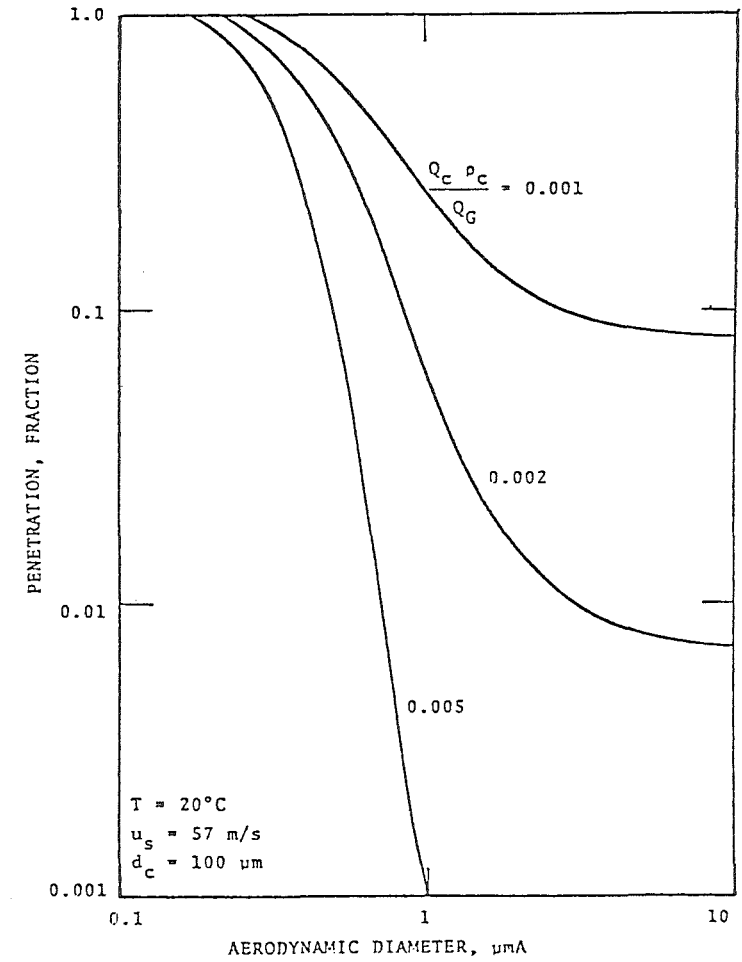


Figure 12. Theoretical particle collection characteristics of the A.P.T. dry scrubber.

AIR POLLUTION TECHNOLOGY, INC.
 SAN DIEGO, CALIFORNIA

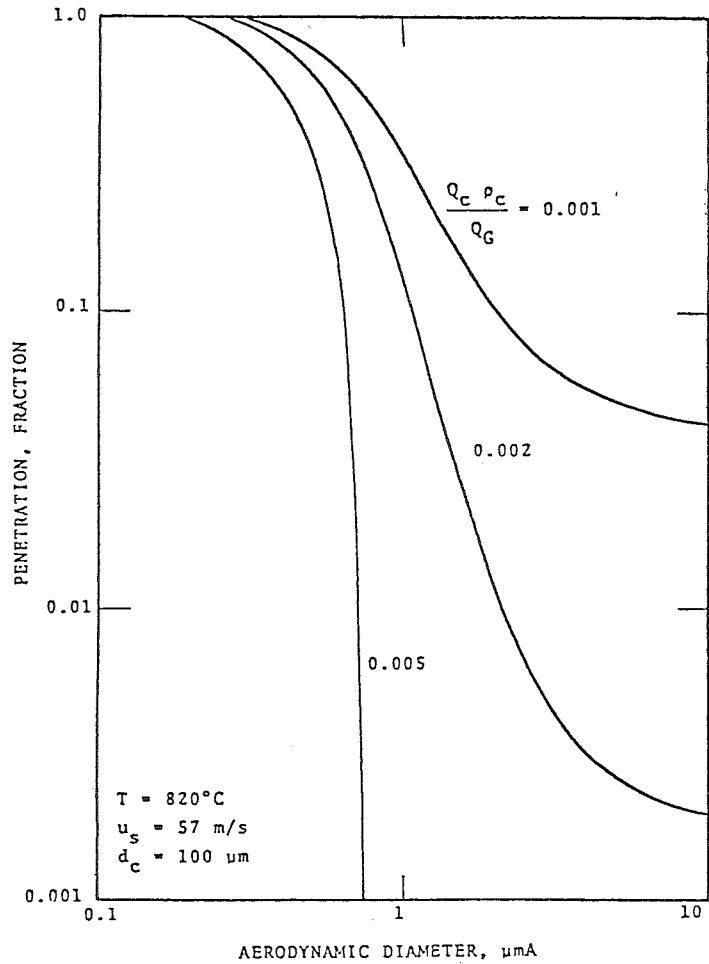


Figure 13. Comparison of the particle collection characteristics of the A.P.T. dry scrubber at 20°C and 820°C.

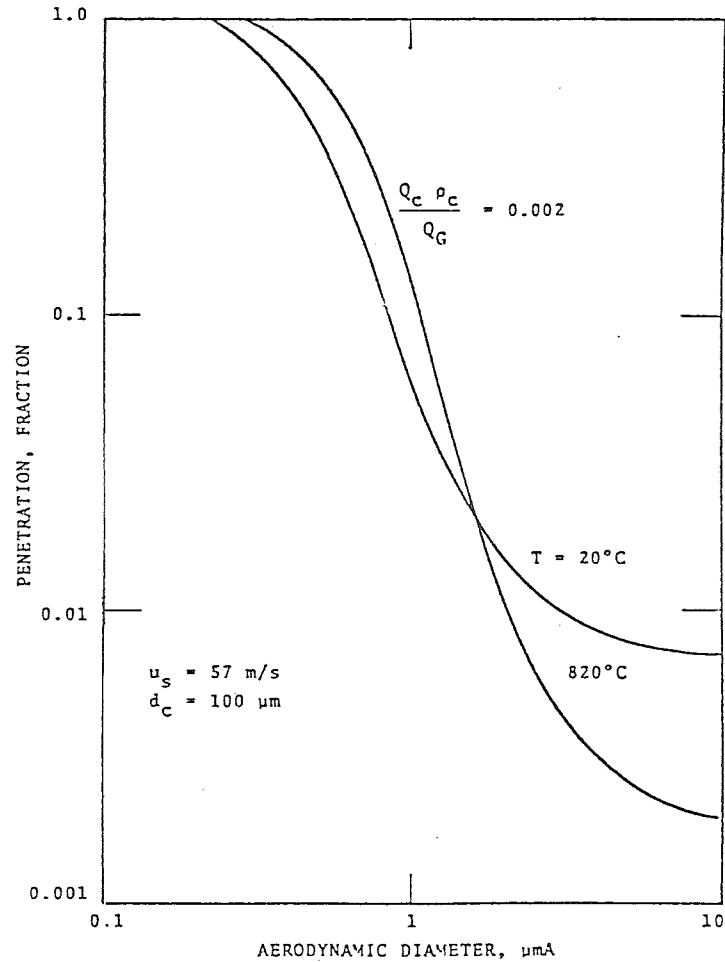


Figure 14. Comparison of the particle collection characteristics of the A.P.T. dry scrubber at 20°C and 820°C.

AIR POLLUTION TECHNOLOGY, INC.
 SAN DIEGO, CALIFORNIA

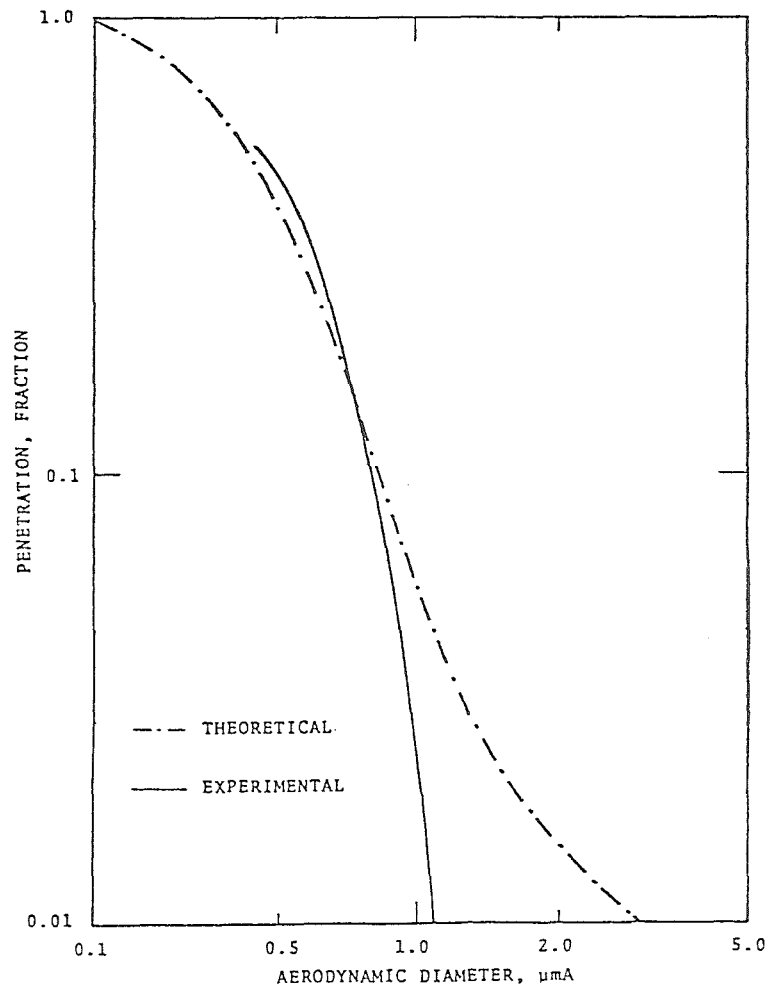


Figure 15. Comparison of experimental with theoretical particle collection characteristics of the A.P.T. dry scrubber.

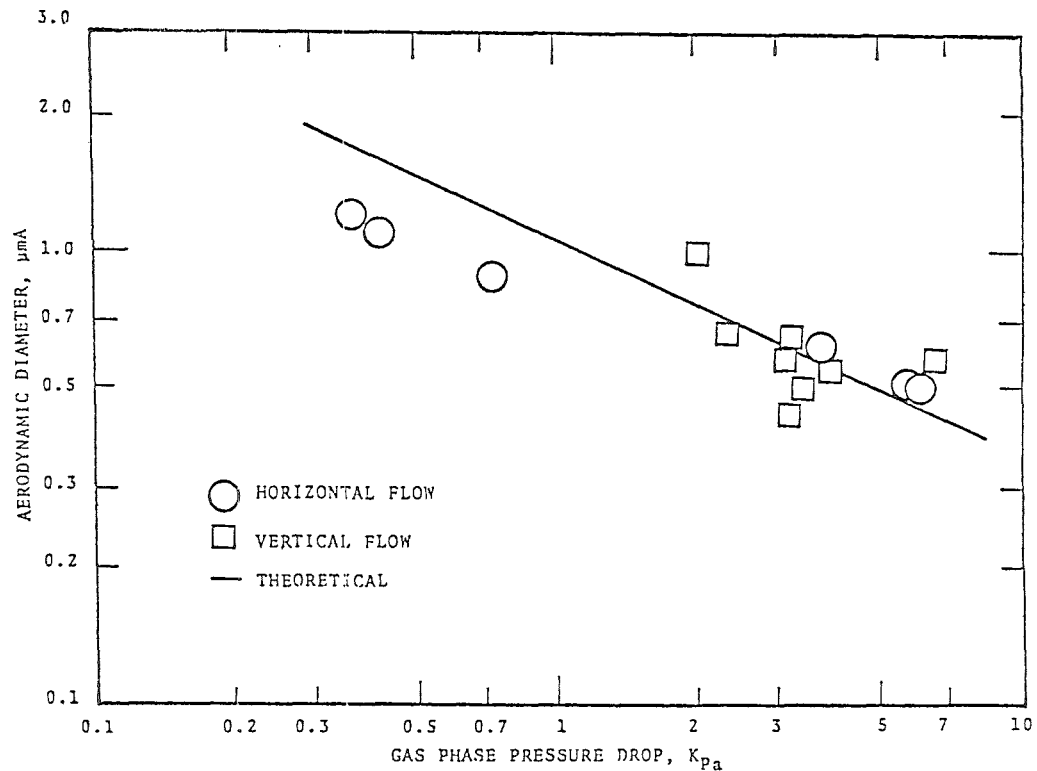


Figure 16. Comparison of particle collection characteristics of the A.P.T. dry scrubber with the A.P.T. cut/power relationship.

AIR POLLUTION TECHNOLOGY, INC.
SAN DIEGO, CALIFORNIA

Discussion

Mr. Cooper mentioned that Acurex had used the same facility but with different equipment and that similar data had been obtained. He wondered which type of equipment had been used in the experiments described by Dr. Parker. The measurements were made at Exxon where a continuous sampling system was used.

Mr. Princiotta asked whether the equipment was capable of cleaning gases, sufficiently to protect the turbine or meet the environmental standards (10-60 mg/m³) and whether it was feasible for these devices to produce sufficient particulate removal. Dr. Parker confirmed the latter point, stating that his talk had been based upon the mechanisms of inertial impaction, which was a feasible although expensive process. Electrostatic augmentation or cake formation on granular bed filters could potentially reduce the expense.

Mr. Wiggers asked for details of the material used in granular filter beds and proposals for recycling process. Alumina, sand, or any substance which could withstand high temperatures was used (Dr. Parker). Pneumatic recirculation took place; particles were fluidized to the top of the bed and were allowed to fall slowly. This achieved more efficient cleaning but was more expensive than a fixed bed. Mr. Wiggers asked whether abrasion occurred; Dr. Parker answered that the moving bed resulted in the attrition of particles and the degradation of the granules themselves.

Mr. Gütthner inquired as to the type of dust for dry scrubbers, what aerosols were used, and whether Dr. Parker could give details of the diameter of scrubber particles. The diameter referred to in the talk was the physical diameter of the collectors, and mono-dispersed aerosol particles were used. The type of collectors used were nickel powder and sand, and an oil aerosol was employed, which eliminated particle bouncing. The venturi scrubber model was validated for the dry scrubber; flyash tests were also carried out with the same results, although attrition problems occurred. The flyash was used as an aerosol, rather than a scrubber collector.

Mr. Finkh requested details of design limits for granular bed filters, particularly maximum pressure in relation to gas turbines. In practice, Dr. Parker answered, the face velocity for granular filters was 40-70 cm/sec. The size needed for a given flow rate could be determined from the velocity.

APPLICATION AND EFFICIENCY OF DRY ELECTROSTATIC PRECIPITATORS

=====

Prof. Dr.-Ing. E. WEBER
Institut für Mechanische Verfahrenstechnik
Universität Essen GHS
Universitätsstraße 2
Postfach 68 43
D 4300 Essen
Tel. 0201-1832795

Dipl.-Ing. H.-G. PAPE
Institut für Mechanische Verfahrenstechnik
Universität Essen GHS
Universitätsstraße 2
Postfach 68 43
D 4300 Essen
Tel. 0201-1832792

APPLICATION AND EFFICIENCY OF DRY ELECTROSTATIC PRECIPITATORS

=====

H.-G. Pape, E. Weber

One of the main problems introducing new technologies of power generation is gas cleaning without energy dissipation. For economical use of fluid bed combustion, and other gas steam processes gas cleaning without great loss of pressure and heat is necessary.

In case of the so called fixed bed gasification for example, the formed lean gas has a temperature of 600 °C and a pressure up to 20 bars. Expansion of that gas by a gas turbine is only possible, if dust and pollution gas are removed.

The gas purification has apart from the necessary desulfurisation to fulfill the following conditions:

Precipitation of the solid components down to dust contents of less than 5 mg/m_n³ gas and dust separation at gas temperatures up to 1000 °C and pressures up to 40 bars.

In addition to fabric filters and wet scrubbers it is possible to use an electrostatic precipitator to reach high degrees of separation. Apart from construction problems, the application of electrostatic precipitators at high pressures and high temperatures is only of interest, if the physical effects of precipitation are not disadvantageously affected. As a consequence the migration velocity, defined by DEUTSCH, would become too small.

The main factors of precipitation are

- 1) the current-voltage-characteristics,
- 2) the corona-starting voltage,
- 3) the sparkover voltage
- 4) the electrical resistivity of the dust.

Up to now electrostatic precipitators are used successfully up to temperatures of 350 °C and pressures up to 3 bars. Publications about high temperature and high pressure electrostatic precipitation are rare. Tests in this line are described sporadically.

Essentially it is written about the relations of voltage, pressure, and temperature, without studying the effectiveness of electrostatic precipitation and the influence of dust resistivity and distance between discharge electrode and collecting electrode.

The studies show in accordance, that electrostatic precipitation at higher temperatures and pressures is possible.

With rising temperatures sparkover voltage and corona-starting voltage decrease, whereas the sparkover voltage decreases more, and the voltages reach the same level. An increase of pressure compensates this decrease, and the difference between sparkover voltage and corona, starting voltage again reaches a value, giving guarantee for a steady filtering process.

From very simplified assumptions the theoretical migration velocity which is at least qualitatively correlated with the effective migration velocity, can be deduced.

Starting from the equation of motion

$$\text{mass force} = \text{electrical force} - \text{power of resistance}$$

it is to obtain

$$V_p \cdot S_p \cdot \frac{dw}{dt} = F - W \quad .$$

The driving electrical force is

$$F = q \cdot E_p$$

with E_p as collecting field intensity.

The power of resistance is to calculate by Stokes law

$$W = 6 \pi \eta_G r_p \cdot W$$

Estimating the time, a single particle needs to reach the final velocity, it is demonstrated, that this time is very short.

So the process of acceleration is to neglect for the calculation of the theoretical migration velocity.

Then

$$q \cdot E_p = 6 \pi \eta_G r_p \cdot W$$

or

$$W_{th} = \frac{q E_p}{6 \pi \eta_G r_p}$$

Assuming, that the partical gets the maximum charge, from the derivatıon of field charging process the factor q is to figure out:

$$q = n_s \cdot e = K E_0 r_p^2$$

E_0 = charging field intensity

n_s = number of particle charge

e = electronic charge

The multiplier K depends upon the dielectric constant of the dust. K is equal to 3 for conductiv particles. So theoretical migration velocity is:

$$W_{th} = \frac{E_0 E_p r_p}{2 \pi \eta_G}$$

As field intensity is proportional to voltage, the theoretical migration velocity among other relations is proportional to the square value of the voltage and inversely proportional to gas viscosity. Attainable voltage, that means sparkover voltage, and gas viscosity decrease by rising temperature. The influence of pressure on gas viscosity is extremly small. But the attainable voltage increases with rising pressure, as given by H.E. Rose and A.J. Wood.

A modification of Peek's equation for corona starting voltage leads to

$$V_0 = K_1 \cdot \delta + K_2 \cdot \sqrt{\delta}$$

K_1, K_2 are fixed by geometry.

δ is the relativ air density.

If this equations hold true, and if in tendency sparkover voltage is behaving like corona starting voltage, the migration velocity might be greater at a pressure of 40 bars and a temperature of 1000 °C than at standard conditions.

But these considerations up to now are not confirmed by experimental investigations in case of very high pressures and temperatures. It seems to be shure, that electrostatic precipitation at high temperatures only is possible, if the pressure at same time is increased.

Another influence on the characteristics of electrostatic precipitation is due to the already mentioned resistivity of dust. As known the resistivity for a good seperation should be between 10^4 and $10^{11} \Omega \text{ cm}$. At high temperatures low dust resistivity, which has negativ influence on separation and especially on adhesion of dust particles on the collecting electrode, is expected. But an extrapolation of test results made by Schütz and Winkel (Abb. 1) seems to disprove these expectations at least for converter dust. Due to these findings the dust resistivity seems to be between 10^6 and $10^7 \Omega \text{ cm}$ at a temperature of 1000 °C. As this extrapolation is not fused by measurements, and these results are restricted to converter dust, the precipitation investigations have to include the determination of dust resistivity at high temperatures and pressures.

By a research project promoted by the ministry of Research and Technology is to examine now, if and under which conditions electrostatic precipitators are to be used succesfully at high temperatures and pressures.

A flow diagramm of the pilot plant, which is built at present, shows picture 2. The gas is led by a compressor (2) about a

pressure tank (4) and a pressure reducing valve (5) to the precipitation tank (1). The compressor permits a pressure up to 35 bars. By heating the precipitator to maximum temperature theoretically the pressure is to increase up to 4.6 fold value. Unaffected by the flow rate the separation pressure is fixed up by the pressure reducing valve. The gas is preheated before reaching the precipitation tank and gas temperature is determined. Dust is blown in behind the heating by slight super pressure. The gas is led off through a watercooled heat exchanger, a regulating valve, permitting a stepless regulation of the flow rate, and a gas-flow meter.

Because of the high pressure the precipitation tank is constructed cylindrical. So the dust separation takes place in a one-tube-electrostatic precipitator. It's intended, to use tubes of different diameters, to determine the influence of the distance of electrodes.

The tubes are heated by resistance wires. The temperature of the wires, being more than 1000 °C is diminished by a heating insulation between the wires and the wall of the precipitation tank.

Measuring the temperature is done by thermocouples.

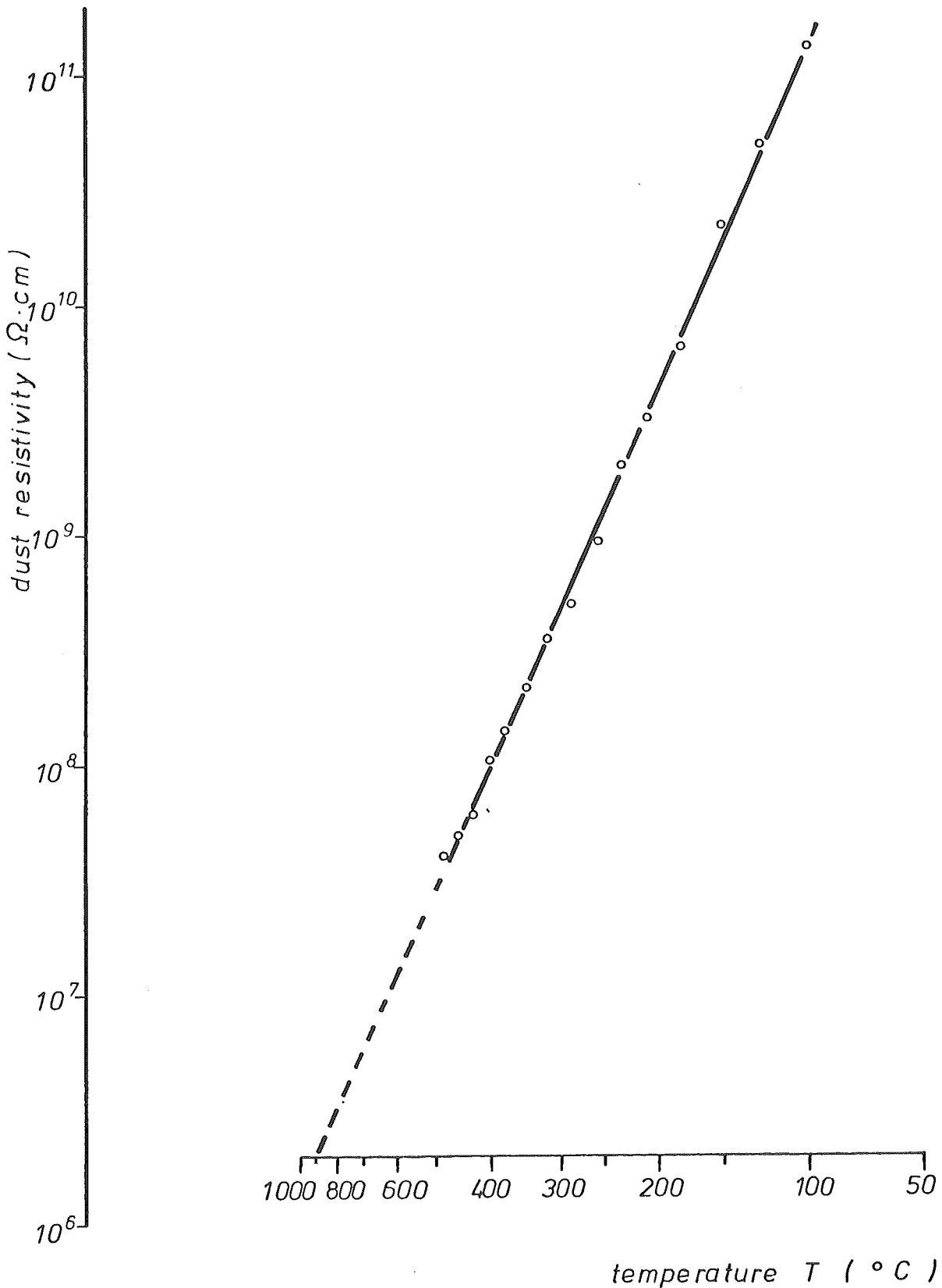
The temperatures of head and bottom of the precipitating tube and of the heating are measured.

The high voltage supply takes place at the top of the precipitation tank. The electrical insulation consists of a pipe made of ceramic, where the discharge electrode is inserted.

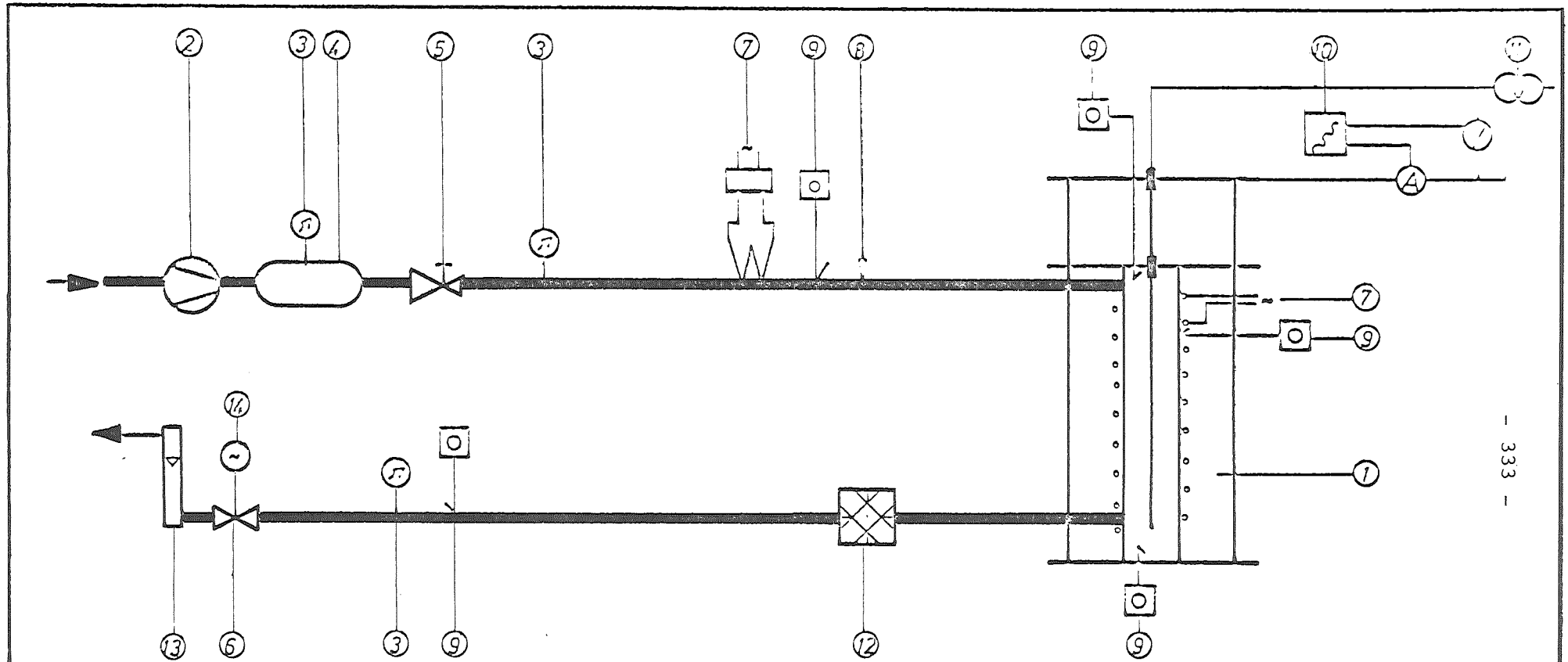
Because of the high pressure during the tests, very high spark over voltages are expected. Therefore a transformer permitting voltages up to 200 kV is used for generating the high voltage.

Heating experiments and pressure tests took a satisfying course. After a short time of heating in the precipitation region a temperature of 1000 °C could be held constantly. An increase of gas pressure up to 45 bars in the precipitation tank didn't show any important leakage.

After contacting all lines of measurement and vontrol the precipitation experiments with various pressures and temperatures can start.



| | | |
|---|---|----------|
| Mechanische Verfahrenstechnik Universität Essen | Resistivity of Converter Dust (from Winkel und Schütz) | UA 11 |
|---|---|----------|



- | | | |
|---------------------------|----------------|------------------|
| ① precipitation tank | ⑥ valve | ⑪ transformer |
| ② compressor | ⑦ el. heating | ⑫ cooling system |
| ③ pressure meter | ⑧ dust feeding | ⑬ flow meter |
| ④ pressure tank | ⑨ thermocouple | ⑭ electric motor |
| ⑤ pressure reducing valve | ⑩ recorder | ○ |

Mechanische
Verfahrenstechnik
Universität Essen

Flow Diagram of a Pilot Plant of a High Pressure and High Temperature Electrostatic Precipitator

Discussion

Mr. Cooper said that it was desirable to remove tar in the coal gasification process. The tar condensed into droplets, which were collected by an electrostatic precipitator. The use of an electrostatic precipitator in coal gasification could perhaps be dangerous (Explosion). Mr. GÜthner added that O_2 in the gas would cause an explosion regardless of temperature. Mr. McCain drew the workshop's attention to a non-explosive mixture used at the Morgantown Coal Gas Plant, which had an electrostatic precipitator. Dr. Gooch asked whether the dielectric strength of the dust could be measured at high temperature, and was told by Dr. Parker that this could be tried; the dielectric strength could be less under certain conditions. Further research is necessary referred to theoretical migration velocity.

Precise details concerning the measurements made during the experiments could be obtained at a later date.

RANGE OF USE FOR FILTERING DUST COLLECTORS

=====

Prof. Dr.-Ing. E. WEBER
Institut für Mechanische Verfahrenstechnik
Universität Essen GHS
Universitätsstraße 2
Postfach 68 43
D 4300 Essen
Tel. 0201-1832795

Dipl.-Ing. R. SCHULZ
Institut für Mechanische Verfahrenstechnik
Universität Essen GHS
Universitätsstraße 2
Postfach 68 43
D 4300 Essen
Tel. 0201-1832788

RANGE OF USE FOR FILTERING DUST COLLECTORS

=====

R. Schulz, E. Weber

With today known filtration collectors it is possible to carry out a gas cleaning only at gas temperatures up to maximal 400 °C. In scope of new energy technologies and energy saving there is an interest in realizing gas purification at high temperatures of about 1000 °C and high pressures up to 40 bar. This should take place without large heat and pressure losses.

Among the known precipitators on principle only the centrifugal separators are applicable for gas cleaning at very high temperatures. But due to their mode of action even a highgrade cyclone cannot reach low dust contents in purified gas, which are for instance necessary for a successful gas turbine process.

At present state of technology very low dust contents in purified gas can be achieved using filtering dust collectors. The particles in the dust loaded gas stream are collected passing through a porous layer of sufficient permeability.

As porous systems are known :

1. different kinds of textile media
2. packed beds of pebbles or sand
3. sintered ceramics

Of these three systems the textile filters play the major roll in the industrial application. Mainly fabrics and needle felts are used of which the needle felts become more and more significant. The advantage of the felts compared with the fabrics is based on its tridimensionality. Its fine pore structure and its high pore volume afford excellent collection grades at high air permeability and low pressure loss.

Fabrics consist of warp and weft. In order to reach a high degree of separation the knit of the fabric has to be tighter. This way the cloth permeability is low and the pressure loss becomes high. Making the knit looser, small openings appear which generate free passages for the dust. These passages will not be closed partly or total before a filter cake is build up.

Whereas for conventional filters the load per filter area in general lies between 80 and 150 $\text{m}^3/\text{m}^2\text{h}$, the needle felt filters can be stressed up to loads of 180 $\text{m}^3/\text{m}^2\text{h}$. This way you can reduce the filter area, save space and energy and finally raise the economy of the filtration plant.

On the other hand filter felts with high collection ability need a thorough cleaning. A tridimensional filter material easier runs the risk of clogging with raising the pressure loss if there is not also a cleaning in the depth of the felt. This can be managed by a strong combined mechanical and pneumatic filter cleaning.

As described above, neither fabric filters nor needle felt filters can be used at gas temperatures above 400 °C. In picture 1a, taken from a paper of H. Dietrich, you can see the heat resistance of present used textile filter materials. The natural fibres wool and cotton do not even resist at temperatures above the vaporization point of water, while organic fibres can be used between 100 and 280 °C. At present inorganic fibres can be applicated up to temperatures of about 400 °C.

On principle also a filtering dust collection at higher temperatures should be possible because fibres are know which can be employed at gas temperatures above 1000 °C (fig. 16). These fibrous materials can be divided into :

1. metallic fibres
2. graphite fibres
3. quartz fibres
4. ceramic fibres

Asbestos fibres should not be used anymore, because asbestos particles are respirable.

Metallic fibres made of inconel meet the requirements with respect to temperature resistance up to 700 °C and mechanic strength. However there is the danger of corrosion and scaling. Another disadvantage are the high costs for metallic fibres of about 800 DM/m².

However leading producers of metallic fibres refer to the high loading capacity of metallic fabrics in comparison to those of meneral materials. It is aspired to get streaming velocities up to 40 cm/s which is equivalent to a filter area loading of about 1400 m³/m²h. Today only loadings of maximal 200 m³/m²h are achieved with common textile filters. A high flow rate would be desirable especially for high temperature filtration because there are large gas volumina due to the high temperature.

Graphite fibres have a high temperature durability in reducing atmosphere. In oxidizing atmosphere however they can be applied only at temperatures up to 350 °C. Therefore these fibres are inapplicable for most cases of high temperature filtration.

Quartz fibres and ceramic fibres are stable at temperatures above 1000 °C. Never the less the mechanical resistance at high temperatures and simultaneous mechanical strain is unknown because the fibres are very brittle. Difficulties must be expected especially at the fixing points of the filter clothes. Outside strengthening at the border of the cloth could be achieved by pasting. Useful adhesives, which are resistant up to temperatures of 1700 °C are offered by several producers. Another possibility is the inside armouring of the filter clothes.

For exsample ceramic fibre felts are armoured by interlacing metallic fibres. But it seems questionable if these armour fibres will withstand the bending stress at high temperatures

which occurs during cleaning the filter clothes. At present one searches for new spinning technologies in order to produce a strong fibre web system also of the short stapled ceramic fibres.

Contrary to filtration at high temperatures there are no problems in fabric filtration at high gas pressure. Independent of the gas pressure only the difference in pressure at the filter material is important for the filtration process. In general this difference amounts between 200 and 4000 Pa. The high gas pressure must be noted only at the construction of the filter chamber.

At present high temperature fibres are offered on the market only for insulation purposes. Talking with the producers it turned out that there are multifarious kinds of high temperature resistant fibres which are already manufactured into fabrics or similar fibre structures. We got already a number of samples.

An unsophisticated pilot plant was built for a first fundamental study of the fabric samples. The schema of this plant is shown in figure 2.

The dust gets over a metering hopper and a funnel into the air stream which is exhausted by a fan at the end of the apparatus. In the first filter cell the dust is collected on the fabric filter. The residual dust content is collected on a paper filter in a second filter cell and can be determined by a gravimetric method. The gas flow rate is kept constant manually with the help of a rotameter and a valve. The change in pressure drop with increasing filter cake on the fabric is registered over a pressure gauge and an amplifier on a chart recorder.

We have got two characteristic pressure drop curves as shown in figure 3. The pressure course according to curve 2 is not suitable for an economical gas cleaning because the pressure drop increases

rapidly in the beginning of the filtering process when the dust loading on the filter cloth is still small. This leads to a higher initial pressure loss after the first filter cleaning. Fortunately most of the investigated fabric samples showed a behaviour according to curve 1.

Concerning dust collection we have got very good results for all fabric samples. For test dust a quartz powder was used with maximal grain size of 63 μm . The dust concentration of the waste gas amounted to 60 g/m^3 . The gas velocity was varied between 3 and 7 cm/s , which corresponds to a load of filter area between 100 and 250 $\text{m}^3/\text{m}^2\text{h}$.

In no case degrees of separation below 99.97 % were noted. The maximal dust load in clean gas was 7 mg/m^3 . Since the used quartz powder showed the trend to agglomerate, it is planned to carry out further measurements with a hydrophobe quartz powder. Then the next step is to investigate the fabrics under extreme temperature conditions.

Until today the general knowledge about high temperature filtration using fabrics or felts, which are made of the described fibres is very low. With financial support of the Ministry for Research and Technology the prototype of a high temperature fabric filter is under construction as shown in figure 4. Three, by pairs parallel filter bags consisting of fleeces, fabrics or mat weaves are used to study the properties of several materials with respect to :

1. Efficiency of dust separation
2. Durability
3. Cleaning

To generate a dust-laden waste gas a pulverized coal firing is used which can be fed additionally with oil in order to obtain higher temperatures. In continuous process waste gas temperatures

between 400 and 700 °C can be achieved with this combustion furnace. Single tests can be carried out also at gas temperatures up to 1000 °C.

The dust load of the furnace gas will be about 1 g/m³_n. If it is necessary a definite increase or a variation of the dust load can be obtained by an additional dust feed. A regulation of the waste gas composition is possible by a variation of the oil rate. The cleaning of the filter bags can be done either by manual knocking, by magnetic generated vibrations or by pneumatic methods.

It can be summarized that due to the quality of the material samples and the results of the first preinvestigations fabric filters should be applicable at low costs for the high temperature gas purification. Since our investigations have started only a few months ago it should be possible to achieve more detailed results in the future.

| | |
|----------------------------|-------------|
| Wool | 70°C |
| Cotton | 70°C |
| Rayon Staple | 70°C |
| Polypropylene | 100°C |
| Polyacrylonitrile | 130°C |
| Polyester | 150°C |
| aliphatic Polyamid (Nylon) | 110 - 120°C |
| aromatic Polyamid (Nomex) | 180 - 200°C |
| Teflon | 260 - 280°C |
| Glass Fibre | 300°C |
| Mineral Fibre | 300 - 350°C |
| Metallic Fibre | 400°C |

Heat Resistance of Textile Filtermedia

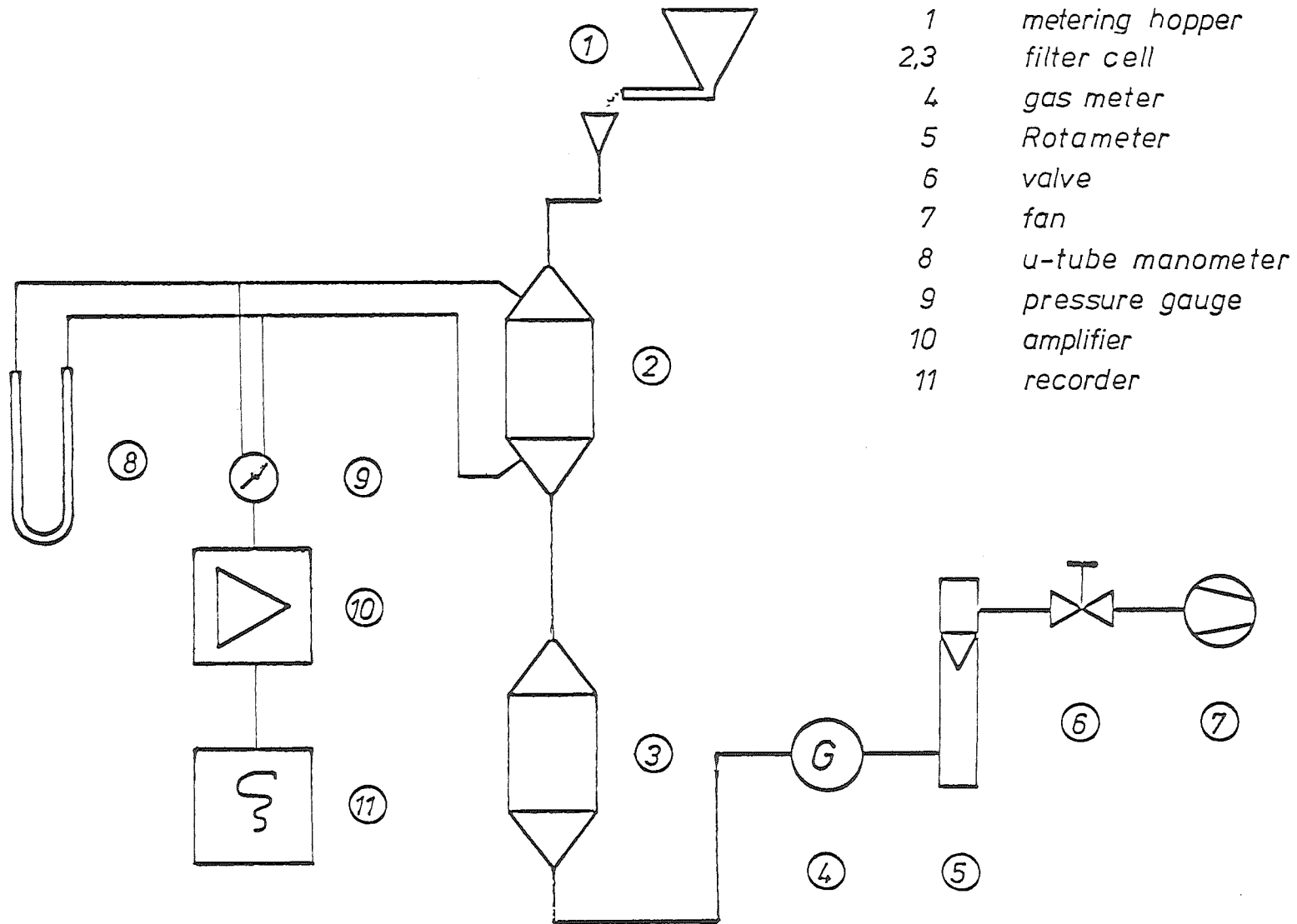
Fig.: 1a

| material | temperature - resisting up to (°C) | manufactured into | lowest dia- meter of the fibres (μm) | chief constituents |
|---|--|--------------------------|---|---|
| glass | 550 | fabric fleece | 2 - 5 | SiO ₂ Al ₂ O ₃ CaO B ₂ O ₃ |
| chrysotile - asbestos | 550 | fabric fleece | 2 - 10 | Mg ₆ [(OH) ₈ Si ₄ O ₁₀] |
| amphibolite- asbestos | 800 | fabric fleece | 2 - 10 | Ca, Na, K, Mg, Fe, Al, Mn, Ti, Si, F |
| quartz | 1200 | fabric fleece | 2 - 5 | SiO ₂ |
| basalt | 1000 | fabric fleece | 10 - 20 | SiO ₂ , Al ₂ O ₃ , CaO, MgO, FeO |
| ceramics | 1200 | fleece | 4 - 20 | SiO ₂ , Al ₂ O ₃ |
| slag | 700 | fleece | 5 - 20 | SiO ₂ , Al ₂ O ₃ , CaO, MgO |
| rock | 700 | fleece | 15 - 30 | SiO ₂ , Al ₂ O ₃ , CaO, MgO |
| graphite oxidizing atmosphere reducing atmosphere | 400 >2000 | felt | 8 - 15 | C |
| metal | 700 | fleece fabric felt | 4 - 10 | C, Cr, Ni, Cu, Mo, Fe |

mineral fibres

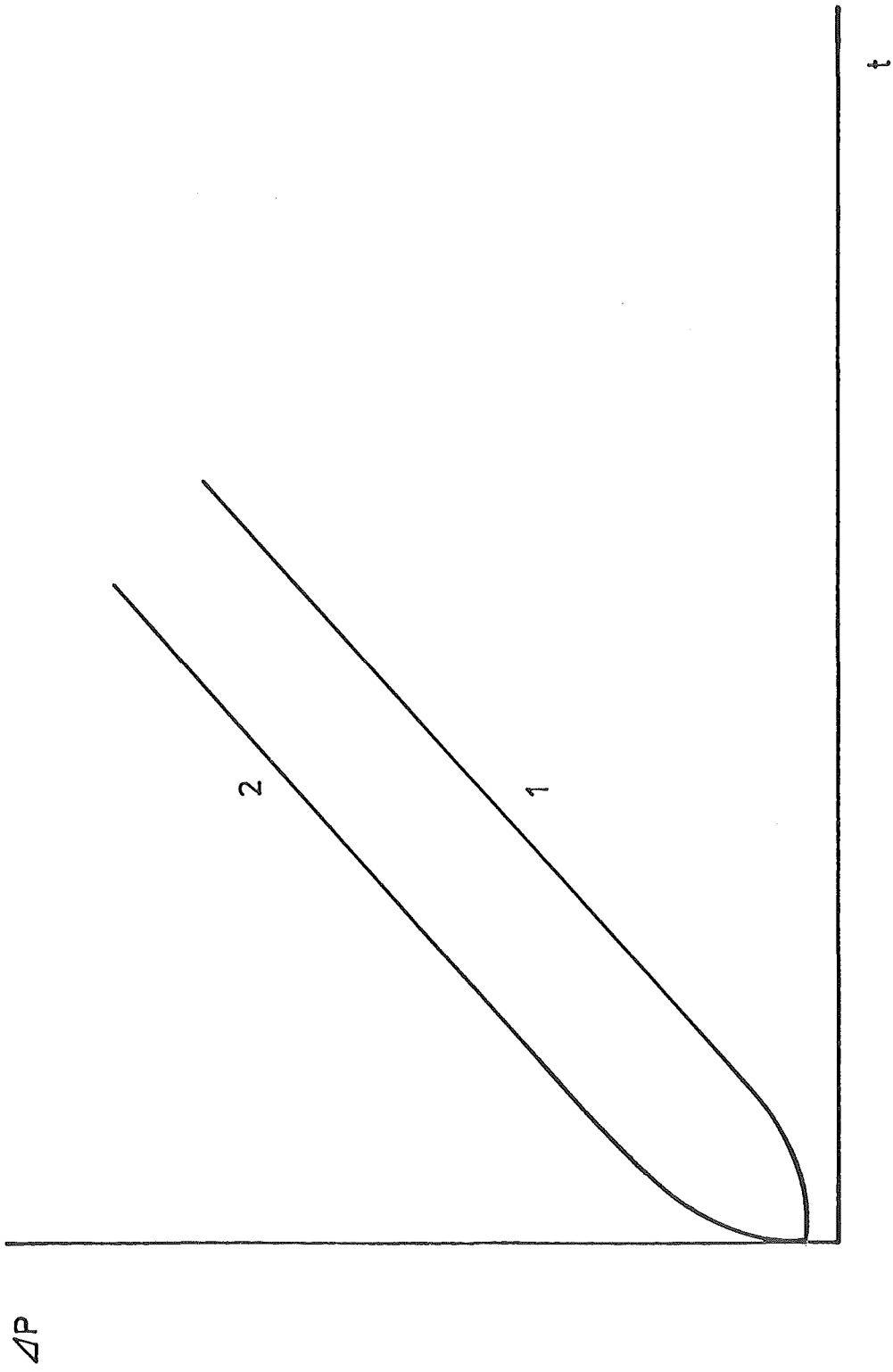
Fibrous Materials for the High Temperature Filtration

Fig. : 1b



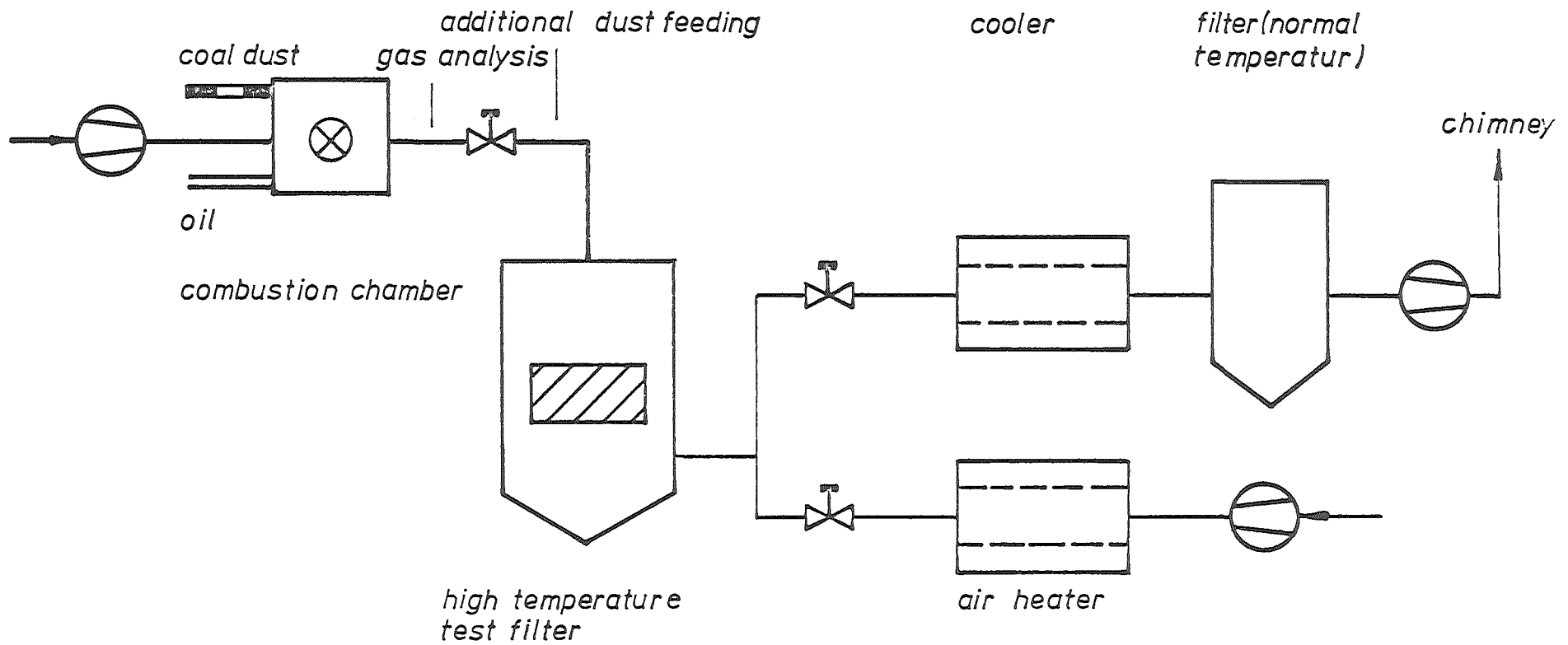
Experimental Arrangement for Fabric Dedusting at Normal Temperatures

Fig. : 2



Pressure Drop-Time Characteristic for High Temperature Fibre Fabrics

Fig.: 3 :



Scheme of the Pilot-Plant for Fabric Dedusting at High Temperatures

Fig. : 4

Discussion

Mr. Princiotta asked for the limitations on gas inlet temperature for a gas turbine. Dr. Holighaus replied that the present temperature limitation is 1000°C. New developments in gas turbine technology will increase the gas inlet temperature to 1250°C.

Mr. Donovan asked if stainless steel fabrics were included in the category "metallic fabrics", and whether all observations made regarding these metallic fabrics were also true for stainless steel fabrics. Mr. Schulz said yes, including the major disadvantage of metallic fabrics--high cost, which means that their use could only be justified in very special filtration application. Prof. Weber added that they were very good at high face velocity (up to 40 cm/sec). Corrosion could occur in metallic fabrics, said Mr. Shackleton. Collection efficiency necessitated a small weave which resulted in a restricted fabric life.

Dr. Glüthner spoke of glass (mineral) fibers, whose life was restricted owing to brittleness. More emphasis should be placed on the fiber finish (rather than the fiber itself) since pulses and other mechanical stresses cause rapid wear.

Glass fibers have a low resistivity to mechanical stress. Mr. Princiotta pointed out that quick heating and cooling could affect this material; silicone was resistant to such sudden changes. Mr. Shackleton said that alumina fibers had been tested at 1800°C and pulsed with unheated air; no problems resulted. In addition, experiments had been performed which showed that fibers did not break even when shocked, said Mr. Wiggers.

HIGH-TEMPERATURE FILTRATION

Dr. Dennis C. Drehmel
U.S. Environmental Protection Agency
Research Triangle Park, N.C. 27711

Michael A. Shackleton
Acurex Corporation
Mountain View, Calif. 94042

Abstract

Research on high temperature particle control using ceramic fiber barrier filtration has shown this technique offers promise of successful development. Results of testing of rigid ceramic membrane structures and of ceramic fiber beds including woven, paper and felt ceramic filters are presented.

HIGH-TEMPERATURE FILTRATION

Introduction

Removal of particles from high temperature gas streams has been studied for many years. Some of the motivation for this research was the desire to operate coal fired gas turbines.¹ Recently there is renewed interest in the utilization of coal. The processes most actively being studied are pressurized fluid bed combustion (PFBC) and gasification combined cycle (GCC) plants. Both processes are called combined cycle since they generate power by means of gas turbines as well as steam turbines.

In the PFBC, coal is burned in a fluid bed of limestone (which removes the SO₂) and heat is transferred to tubes in the fluid bed. Up to 80% of the recoverable heat value of the coal is removed in the fluid bed, and the gas exits at 1500°F and 10 atm pressure. The gas must now be expanded through a gas turbine to recover the remaining energy. However, previous investigations showed that large particles erode turbine blades and small particles cause deposits that choke the turbine. To protect the turbine, some high-temperature particulate control is required. Moreover, since it would not be economical to duplicate particulate control for environmental regulations at another point of the process, high-temperature control must also meet new source performance environmental standards for coal-fired utilities. Currently, this allows emissions to be no greater than 0.1 #/million Btu.

To meet both the environmental and turbine requirements, a system consisting of two cyclones and a filter is being studied. The two cyclones lower the overall particle concentration but fail to remove small particles. Concentrations leaving the second cyclone can be as high as 1.0 grains/scf and have a mass median diameter of 5.0 μm. The filter can be a ceramic bag filter, a ceramic membrane, or a granular bed.

Research to date has concentrated on the granular bed since it has been considered available technology. However, results of tests at the Exxon PFBC Miniplant have been disappointing.² The granular beds tested could barely meet the environmental standard at the beginning of a run and lost efficiency continuously from 95% to as low as 50% within 24 hours. Although granular bed filters may still prove to be a solution to high-temperature particle control, it is now apparent that they will require more developmental work.

Alternative high-temperature filters, using either a ceramic bag or ceramic membrane, are being developed. The remainder of this paper will be devoted to describing ongoing work by the Environmental Protection Agency to assess these high-temperature filters as part of environmental control for the PFBC, although it is expected that results can be extrapolated to the GCC or to high-temperature metallurgical operations.

Ceramic Membrane Filters

Several ceramic materials in many configurations were screened as possible high-temperature filters. One of the most promising materials tested was a ceramic cross flow monolith produced by 3M Company under the trade name of Therma-Comb. This material is composed of alternate layers of corrugations separated by thin filtering barriers. This type of configuration affords a large amount of filter surface in a very small volume. Figure 1 shows a piece of this material illustrating the construction.

Bench side experiments were conducted in the high-temperature ceramic test facility at 970°K. Provisions were made to blow back from the clean side and also down the channels on the dirty side so that various cleaning schemes could be investigated. A sequencer was designed to automatically start and operate the cleaning cycle. A 17 cm diameter by 38 cm deep tubular furnace was used to heat the filter. An additional furnace was added to preheat the dust-laden air.

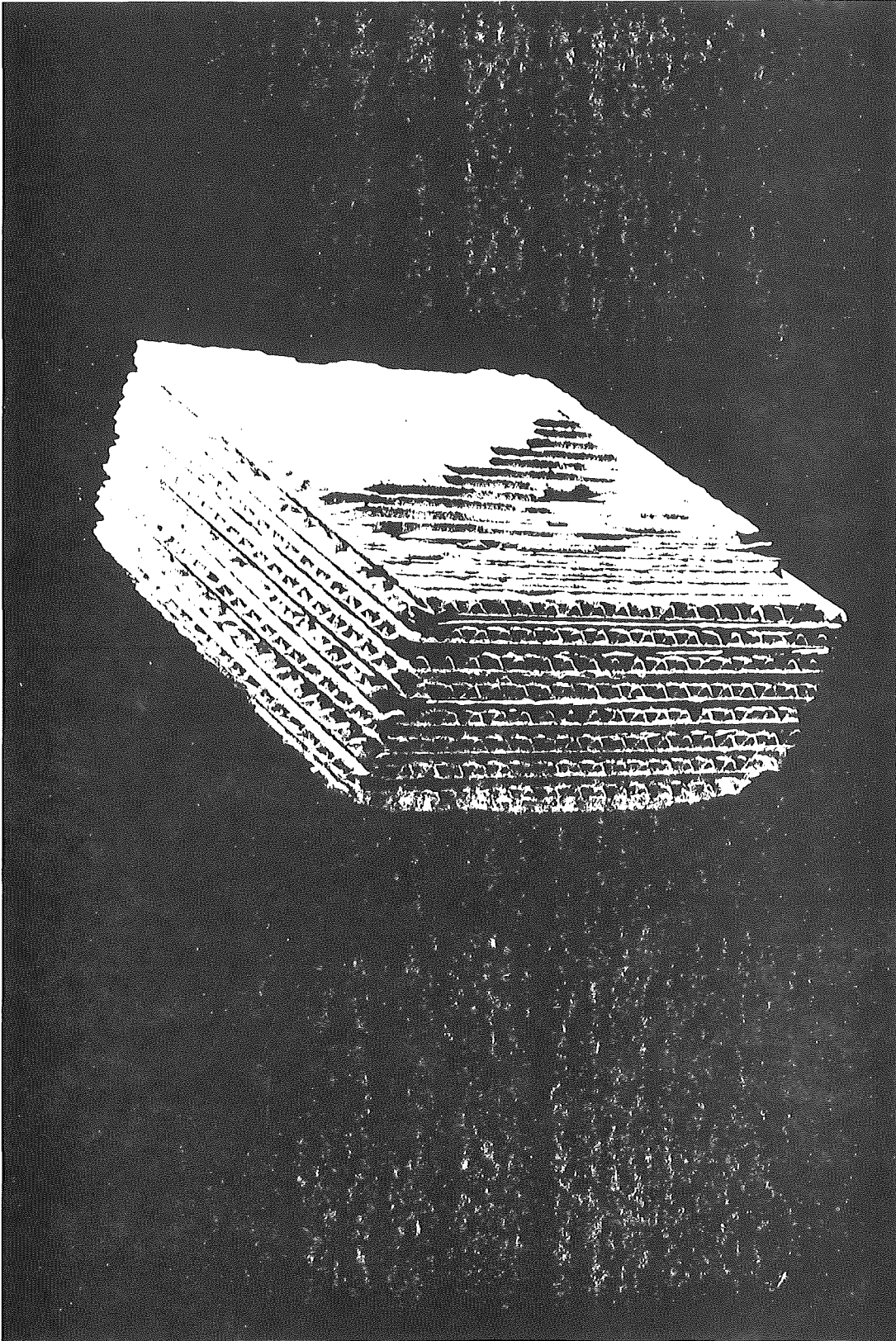


Figure 1. 3-M Company Thermocomb.

Cascade impactors were used to determine the size distribution of the test dust (limestone). The typical mass median diameter was 1.4 μm and the geometric deviation was 3.0 μm . There was some difficulty in maintaining constant feed rate, but dust loadings were maintained at levels from 2 gm/m^3 to 7 gm/m^3 .

Typical results for filtering the limestone test dust with the 3M ThermaComb are summarized in Table 1. Table 2 shows the effect of varying the initial pressure of a 0.6-second pulse. Table 2 also shows the result of a similar set of runs except that the pulse time was increased from 0.6 seconds to 5 seconds. These data show that the length of the pulse does not have much effect on the cleaning results. In both runs the collection efficiency was very high (99.6 to 100%) at a linear velocity of 0.41 m/min (1.33 ft/min). Using the 103.4 kPa pressure pulse for cleaning, it was possible to return to a stable pressure drop across the filter in spite of the relatively high dust loadings which in these two runs were 2.6 and 3.75 gm/m^3 .

Tests using the 3M ThermaComb as a filtering media showed filtering efficiency to be close to 100% even though the test dust had a mass median diameter of 1.4 μm and a significant fraction of sub micron material. Cleanability of the media was verified in experiments evaluating the effect of cleaning pulse intensity and duration. It was determined that the ceramic filter behaved similarly to fabric filters in that the pressure drop could be attributed to a residual pressure drop and that across an incompressible cake.

Ceramic Fiber Barrier Filters

Ceramic fibers are produced by several manufacturers. In general, these materials are sold for refractory insulation applications. Many of these ceramic fiber materials are produced in smaller fiber diameters (3 μm) than are generally

Table 1. Summary of 3M ThermaComb Performance

| | <u>Average</u> | <u>Range Tested</u> |
|--|----------------|---------------------|
| Flow rate m ³ /min | 0.095 | 0.04 - 0.16 |
| Filter area m ² | 0.0227 | - |
| Inlet/Concentration gm/m ³ | 3.6 | 2.2 - 5.4 |
| Temperature °K | 990 | 953 - 1088 |
| Efficiency Percent | 96.6 | 85 - 99.6 |

Table 2. Effect of Changing Cleaning Conditions

| <u>Test Number</u> | <u>Pulse Pressure KPa</u> | <u>Pulse Duration seconds</u> | <u>Cycle Time* minutes</u> | <u>Residual Pressure Drop KPa</u> |
|--------------------|---------------------------|-------------------------------|----------------------------|-----------------------------------|
| 1 | 34.5 | 0.6 | 2 - 4 | 3.5 increasing to limit |
| 1 | 69.0 | 0.6 | 8 | 3.0 increasing to limit |
| 1 | 103.4 | 0.6 | 12 - 20 | 2.8 |
| 2 | 103.4 | 0.6 | 12 | 2.8 |
| 2 | 103.4 | 5 | 12 | 2.8 |

*as required to lower pressure drop away from the upper limit

available for filtration applications at room temperature (20 μm). This smaller fiber diameter, coupled with high temperature and corrosion resistance characteristics, makes these fibers intriguing candidates for high-temperature filtration applications.

Available ceramic fiber configurations can be classified into the following three groups of materials:

- Woven structures - cloth woven from long-filament yarns of ceramic fibers
- Papers - Ceramic structures produced from short lengths of fibers, generally held together with binders.
- Felts - Structures produced to form mats of relatively long fibers. These materials are known as blankets in the insulation industry. They tend to be less tightly packed than conventional felt materials.

Theory

Filtration theory supports the contention that ceramic fiber filters should perform adequately at high temperatures and pressures.

There are three particle collection mechanisms generally considered to account for the performance of a bed of fibers in removing particles from gas streams. These mechanisms are: direct interception, diffusion, and inertial impaction. Examining these mechanisms under high temperature and high pressure (800°C and 10 atm) indicates that direct interception and diffusion will be roughly the same as their performance at room temperatures and ambient pressures, while the inertial impaction mechanism will be slightly less effective at high temperatures and pressures. This statement is true when comparing the performance of a clean filter bed (no dust cake) at low temperature/pressure and at high temperature/pressure. This relatively minor performance reduction can be compensated for in the design of the filter media. For example, using smaller diameter fibers in the filter bed can increase collection efficiency far more than the viscosity effect of high temperature reduces it. A fiber bed consisting of 3 μm diameter

fibers, as compared with 20 μm fibers, can be expected to provide equal collection efficiency with a 3 μm fiber bed weighing only one tenth as much on a weight per unit area basis. Figure 2 presents a calculated prediction of collection efficiency for a 3.0 μm fiber bed, consisting of alumina fibers, collecting a 0.5 μm fly ash particle from an air stream at 815°C and 10 atm pressure. The four curves show that for a decrease in solidity* (α) a reduction in efficiency, for a given basis weight, should be expected. Similarly, an increase in airflow velocity causes a small reduction in collection efficiency for a given filter bed (constant basis weight). Note also that by adding fibers (increasing basis weight), all of these effects can be nullified.

The magnitude of predicted efficiency is also interesting. This analysis shows that for a ceramic fiber bed consisting of 3.0 μm alumina fibers a basis weight of 500-600 g/m^2 should provide 80 to 90 percent collection of a 0.5 μm particle even at the reduced performance levels encountered at high temperatures and pressures.

For comparison, a standard filter media consisting of 20 μm fibers and having a basis weight of 540 g/m^2 (16 oz/yd^2) can be expected to collect only about 20 percent of 0.5 μm particles at room ambient conditions. Thus, to provide collection efficiency performance equal to a conventional filter requires only about one-tenth the weight of fibers for a 3.0 μm fiber bed. Or, put another way, a ceramic fiber bed of equal media weight to a conventional filter, but made from 3.0 μm fibers, will be much more efficient even at high temperatures and pressures than is normally sufficient in the filtration industry.

*Solidity (α) is the fraction of the fiber bed which is solid. A solidity of 0.02 indicates that 2% of the bed is occupied by fibers.

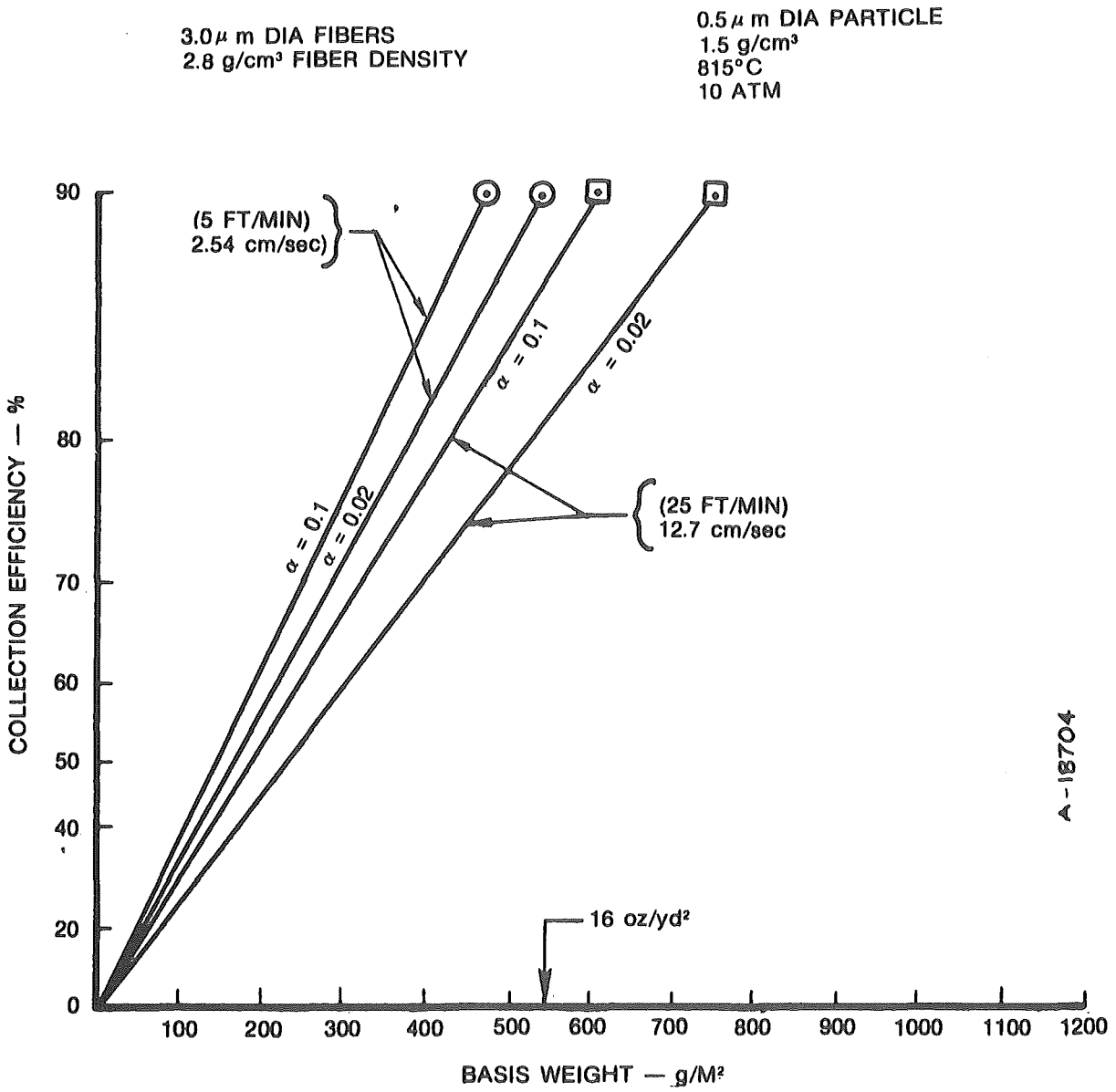


Figure 2. Calculated performance of 3.0 μ m alumina fiber bed.

Room Ambient Filter Media Tests

A large number of ceramic fiber filter media candidates have been subjected to a series of filtration tests at room ambient conditions. These tests included some examples of conventional filter media for comparison. Included among the tests were:

- Dioctylphtalate smoke (D.O.P) penetration as a function of air flow velocity
- Determination of maximum pore size (in micrometers)
- Measurement of permeability
- Flat-sheet dust loading tests using A.C. Fine test dust. Over-all collection efficiency and dust loading required to develop 3.7 KPa (15 in H₂O) pressure drop are determined from this test which is operated at 10 cm/sec (20 ft/min) Air-to-cloth ratio.

Data collected from these tests are summarized on Table 3.

Penetration tests using D.O.P. smoke measure the ability of the clean fiber bed to stop fine particles. The D.O.P. smoke generator is adjusted to provide a nominal particle size of 0.3 μ m diameter which is a "most penetrating" particle size because of the minimal effect of diffusion and inertial impaction at this particle size. The D.O.P. test results should correlate well to the results predicted by analysis since particle collection is provided only by the fibers and not by the dust cake. Figure 3 provides a plot of the DOP efficiency as a function of air flow velocity for all the media tested. Ceramic media data are plotted in solid lines and conventional media in dotted lines. Numbers on the curves refer to those on Table 3. Several interesting observations can be made concerning this data:

- Several of the ceramic materials, especially the ceramic papers and felts, are capable of higher

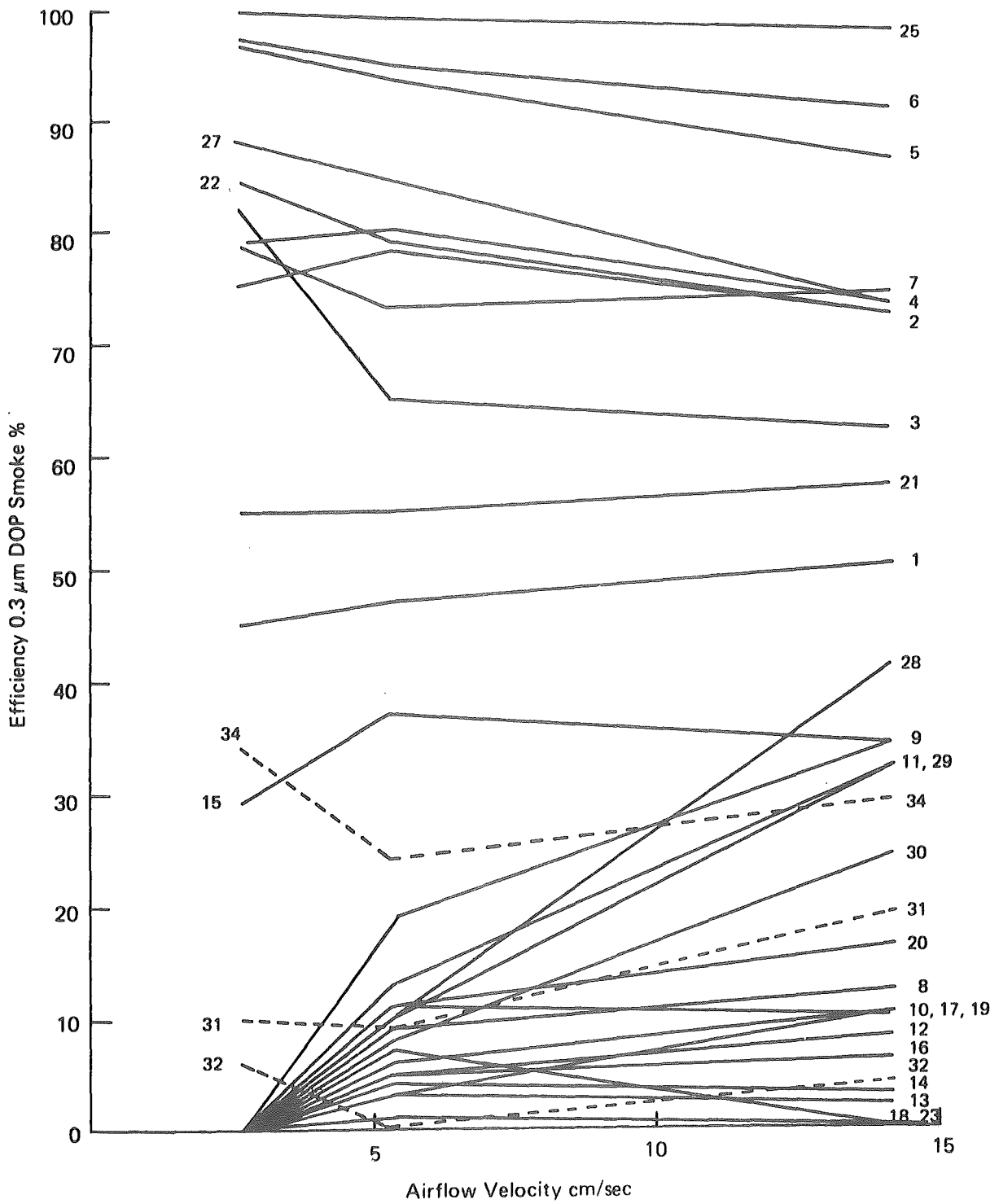


Figure 3. D.O.P. Efficiency fn airflow velocity.

Table 3

SUMMARY ROOM AMBIENT TEST DATA

| | (W) Woven (P) Paper (F) Felt | Basis Weight g/m ² | Percent Efficiency on ACF @ 10 cm/sec (20 ft. min) | Dust Loading g/m² to 5.735 KPa (g/ft ² to 15" H ₂ O) | Permeability cm ³ /sec/cm ² for 0.1245 KPa (ft ³ /min/ft ² for 0.5" H ₂ O ΔP) | Maximum pore size Micrometers | Percent Efficiency on 0.3 μm DOP at cm/sec | | |
|---|------------------------------------|-------------------------------------|--|--|--|-------------------------------------|---|------|-------|
| | | | | | | | 2.68 | 5.35 | 14.22 |
| 1. Carborundum Fiberfrax cloth (W) with nichrome wire insert | | 1366 | 96.55 | .1016 (22.2912) | 8.687 (17.1) | 248.6 | 45 | 47 | 50 |
| 2. Zircar Zirconia felt ZFY-100 (F) | | 615 | 95.64 | Media Fractured | 10.861 (21.38) | 59 | 75 | 73 | 72 |
| 3. ICI Saffil alumina paper (P) with binder | | 165 | 99.805 | .0675 (14.81) | 9.307 (18.32) | 43 | 82 | 65 | 62 |
| 4. ICI Saffil mat (F) | | 355 | 98.74 | Media Fractured | 12.395 (24.4) | 61.1 | 79 | 80 | 73 |
| 5. Babcock & Wilcox Kaowool (F) | | 746 | 98.464 | .0507 (10.980) | 8.067 (15.88) | 66.9 | 96.5 | 93.5 | 86 |
| 6. Carborundum Fiberfrax (F) durablanket | | 1363 | 99.507 | .06225 (13.6523) | 5.583 (10.99) | 68.2 | 97.1 | 94.6 | 90.5 |
| 7. John Mansville Fiberchrome (F) | | 1297 | 99.654 | .1076 (23.59) | 11.897 (23.42) | 112.3 | 78 | 73 | 74 |
| 8. Stevens Astroquartz (W) style 581 | | 283 | 60.77 | Test Stopped - LoF Eff. | 37.236 (73.3) | 248.6 | 0 | 9 | 12 |
| 9. Hitco Refrasil C-100-96 (W) heat cleaned | | 1284 | 81.97 | .00250 (.5482) | 1.240 (2.44) | 112.3 | 0 | 19 | 34 |
| 10. Hitco Refrasil C-100-48 (W) not heat cleaned | | 667 | 83.37 | .00490 (1.074) | 3.099 (6.1) | 133.8 | 0 | 11 | 10 |
| 11. Stevens Astroquartz cloth (W) style 570 | | 677 | 56.83 | Test Stopped Low Eff. | 22.758 (44.8) | 267.7 | 0 | 13 | 32 |
| 12. 3M AB-312 basket weave (W) cloth | | 311 | 51.38 | Test Stopped Low Eff. | 13.553 (26.68) | 870 | 0 | 5 | 8 |

Table 3 (Continued)

| (W) Woven (P) Paper (F) Felt | Basis Weight g/m ² | Percent Efficiency on ACF @ 10 cm/sec (20 ft. min) | Dust Loading g/m² @ 0.735 KPa (g/ft ² to 15" H ₂ O) | Permeability cm ³ /sec/cm ² for 0.1245 KPa (ft ³ /min/ft ² for 0.5" H ₂ O ΔP) | Maximum pore size Micrometers | Percent Efficiency on 0.3 μm DOP at cm/sec | | |
|--|-------------------------------------|--|---|--|-------------------------------------|---|------|-------|
| | | | | | | 2.68 | 5.35 | 14.22 |
| 13. 3M AB-312 twill weave (W) cloth | 231 | 48.55 | Test Stopped Low Eff. (same) | 28.448 (56) | 435 | 0 | 3 | 2 |
| 14. HITCO Refrasil cloth (W) UC-100-48 | 643 | 69.26 | .00903 (1.98024) | 8.687 (17.1) | 193.3 | 0 | 4 | 3 |
| 15. Zircar Zirconia cloth (W) ZFY-30A | 608 | 99.014 | .03733 (8.1853) | 5.791 (11.40) | 248.6 | 29 | 37 | 34 |
| 16. 3M -Stevens Astroquartz (W) cloth crowfoot satin | 352 | 76.19 | .03079 (8.5057) | 16.556 (32.59) | 267.7 | 0 | 5 | 6 |
| 17. 3M AB-312 twill weave (W) cloth coated with 3M coating | 227 | 47.64 | Test Stopped Low Eff. | 65.181 (128.31) | 870 | 0 | 3 | 10 |
| 18. 3M AB-312 basket weave (W) cloth coated with 3M coating | 281 | 45.65 | Test Stopped Low Eff. | 47.595 (93.69) | 580 | 0 | 7 | 0 |
| 19. 3M AB-312 twill weave (W) cloth Menarde coating | 254 | 55.078 | Test Stopped Low Eff. | 51.211 (100.81) | 580 | 0 | 6 | 10 |
| 20. HITCO Refrasil cloth (W) UC-100-96 not heat cleaned | 1249 | 68.46 | .00580 (1.2708) | 3.414 (6.72) | 316 | 0 | 11 | 16 |
| 21. Carborundum Fiberfrax (W) no insert wire L-126TT | 1544 | 99.21 | .07552 (16.1213) | 7.447 (14.66) | 91.6 | 55 | 55 | 57 |
| 22. HITCO Refrasil batt B100-1 (F) | 807 | 99.229 | .0716 (15.706) | 8.900 (17.52) | 64.4 | 84 | 79 | 72 |
| 23. HITCO Refrasil standard (W) not heat cleaned very thin UC-100-28 | 335 | 84.41 | .00969 (2.1257) | 11.897 (23.42) | 139.2 | 0 | 1 | 0 |
| 24. HITCO Irish Refrasil (W) chromized C-1554-48 | 683 | 81.476 | .00507 (1.1116) | 5.121 (10.08) | 124.3 | 2 | 8 | 10 |

Table 3 (Concluded)

| (W) Woven (P) Paper (F) Felt | Basis Weight g/m ² | Percent Efficiency on ACF @ 10 cm/sec (20 ft. min) | Dust Loading g/m² to 3.735 KPa (g/ft ² to 15" H ₂ O) | Permeability cm ³ /sec/cm ² for 0.1245 KPa (ft ³ /min/ft ² for 0.5" H ₂ O ΔP) | Maximum pore size Micrometers | Percent Efficiency on 0.3 μm DOP at cm/sec | | |
|---|-------------------------------------|--|--|--|---|---|------|-------|
| | | | | | | 2.68 | 5.35 | 14.22 |
| 25. Carborundum Fiberfrax (P) paper (with binder) 970J | 604 | 99.99 | 0.5121 (6.8442) | 26.899 (52.95) | 47.7 | 99.5 | 99.0 | 97.6 |
| 26. ICI Saffil Zirconia paper (P) (with binder) | 212 | 93.20 *Probable hole | 0.3483 (7.6374) | 8.692 (17.11) | 37.4 | 83 | 78 | 74 |
| 27. Carborundum Fiberfrax (P) paper (no binder) 970-AH | 152 | 99.91 | 0.3575 (7.8369) | 12.416 (24.44) | 43.5 | 88 | - | 73 |
| 28. 3M AB-312 double thick (W) plain weave | 1035 | 43.86 | Test Stopped Low Eff. | 84.836 (167) | too large to measure with our equipment | 0 | 10 | 41 |
| 29. FMI crowfoot satin cloth (W) astroquartz | 905 | 40.08 | Test Stopped Low Eff. | 62.078 (122.20) | 497 | 0 | 10 | 32 |
| 30. 3M AB-312 12 harness satin (W) weave | 675 | 53.73 | Test Stopped Low Eff. | 75.529 (148.68) | 696 | 0 | 8 | 24 |
| 31. 630 Tuflex fiberglass# (W) | 564 | 93.982 | 0.2015 (4.4187) | 16.038 (31.57) | 174 | 10 | 9 | 19 |
| 32. 15-011-020 woven filament# (W) polyester | 175 | 96.078 | 0.1166 (2.60163) | 6.828 (13.44) | 74 | 6 | 0 | 4 |
| 33. 25-200-070 polyester felt# (F) | 524 | 99.193 | 0.5732 (12.5688) | 11.897 (23.42) | 128.9 | 34 | 24 | 29 |
| 34. HITCO Refrasil cloth (std) (W) not heat cleaned, med. thickness | 637 | 48.40 | 0.1462 (3.2063) | 6.934 (13.65) | - | - | - | - |

#These materials are conventional (not ceramic) media.

efficiency collection of fine particles than are media normally used successively in commercial filter units.

- Many of the woven ceramic materials had zero D.O.P. efficiency at low velocity and higher D.O.P. efficiency at higher velocity.

This is contrary to what theory suggests and to the behavior normally seen in tests of conventional filter materials. A likely explanation for this performance is that it is caused by the presence of many large pores in the media. Examination of the pore size data in Table 3 shows that the woven ceramic materials as a group are characterized by larger pore size than are conventional filter materials. Thus, at low airflow velocity, most of the flow passes through the large pores and little filtration takes place. As velocity is increased, flow through the large pores becomes restricted and some of the flow is caused to pass through smaller pores where more filtration can take place.

- The D.O.P. data also supports the theoretical analysis. Efficiency as a function of basis weight for selected ceramic materials is plotted in Figure 4. The materials selected are ceramic papers and felts. These materials provide a fiber bed similar to that for which the analysis summarized in Figure 2 was based. Figure 4 shows that the nominally 3 μm fibers do indeed provide higher collection efficiency on a weight-per-unit area basis than conventional media produced with larger diameter fibers.

Maximum pore size data shows that many of the woven ceramic materials had pores larger than those characteristic

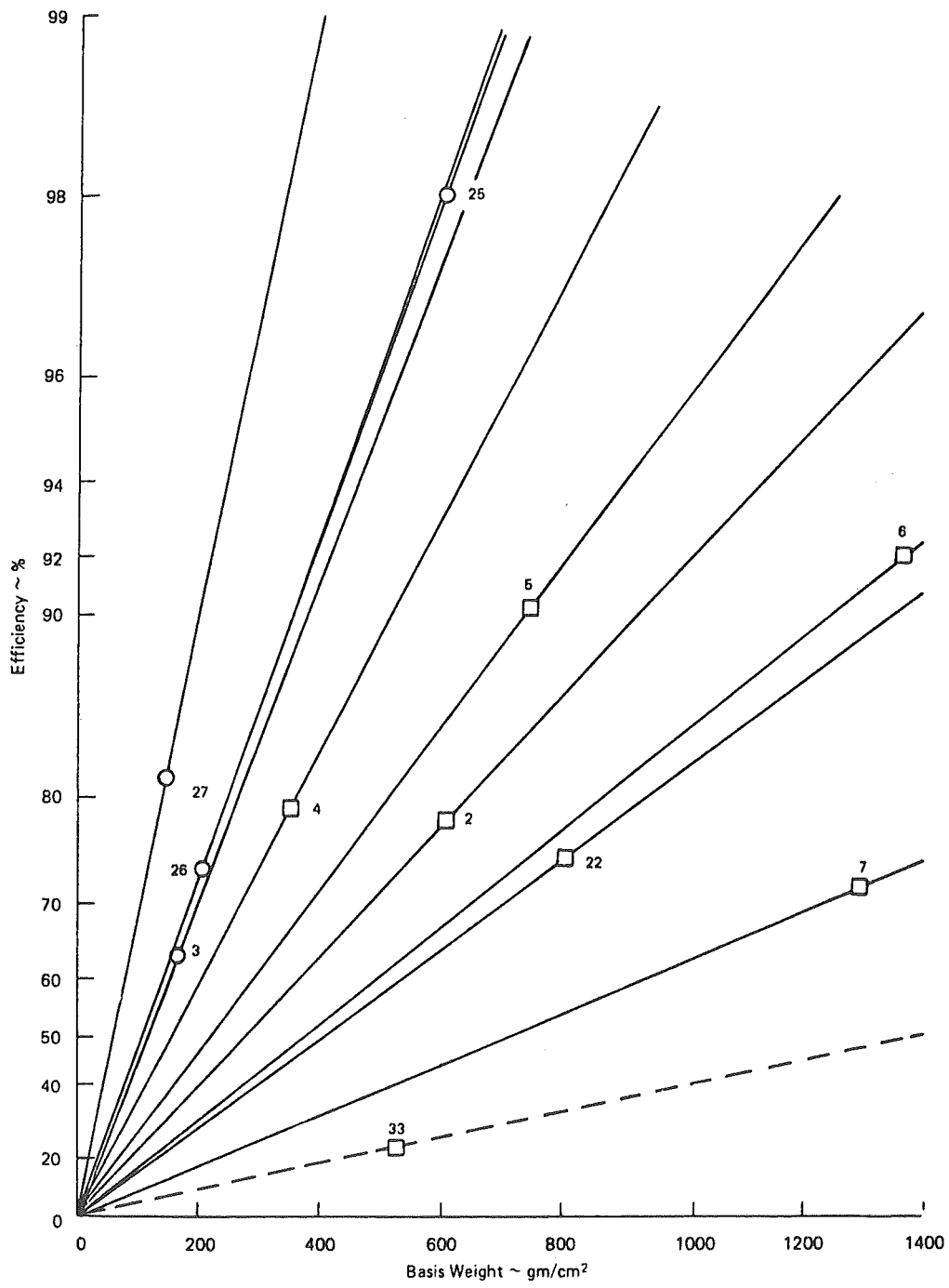


Figure 4. D.O.P. efficiency fn basis weight.

of filter materials. Also, many of the felt and paper materials had pore sizes similar to those of conventional filter materials.

Permeability is measured as the flow per unit area at a constant pressure drop. Thus, a material with low permeability offers a high restriction to gas flow and one with high permeability allows more gas to penetrate for a given pressure drop. Table 3 shows that some ceramic materials are available which have low permeability, while others have high permeability. Some of the woven materials have low permeability and large pore size, while others have high permeability and large pore size. Most of the paper and felt materials have permeability similar to that of commonly used filter materials.

Flat sheet dust loading tests were performed as follows: A 7.62 cm (3 inch) diameter disc of media is suspended across an air stream which is maintained at 10.16 cm/sec (20 ft/min) velocity through the filter media. In this test the media supports itself against the pressure drop (no screen is used). Standard A.C. Fine test dust (0-80 μm silica) was fed to the media at a nominal rate of 0.883 g/m^3 (0.025 g/ft^3) until a pressure drop of 3.735 KPa (15 in H_2O) is reached. Pressure drop as a function of time is monitored during the test. This data is presented in Figures 5, 6, and 7 for selected materials. From the data collected, dust loading (g/m^2) necessary to cause a given pressure drop 3.735 KPa (15 in H_2O) is determined. Examination of this data in Table 3 shows that some of the woven materials reached high pressure drops while collecting only a small weight per unit area of dust. This is true also of the commercial woven materials (items 31 and 32). Other woven ceramics were penetrated so severely that they would not develop a pressure drop of 3.735 KPa (15 in H_2O).

Two of the non-woven samples (which were unsupported) fractured as a result of the pressure drop across them. Several of the ceramic paper and felt materials exhibited dust loading, similar to that which is expected from conventional filter papers and felts.

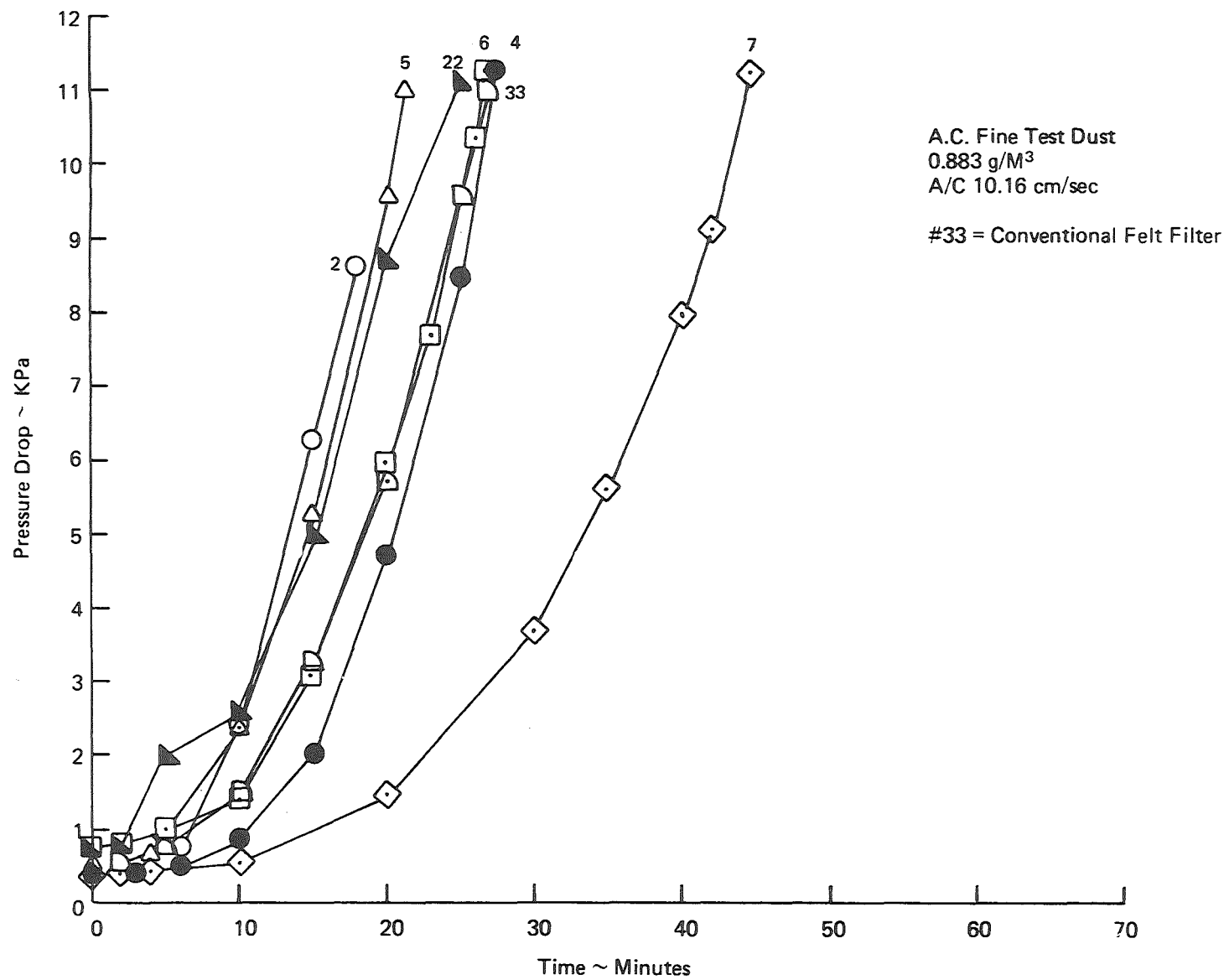


Figure 5. Dust loading of ceramic felts.

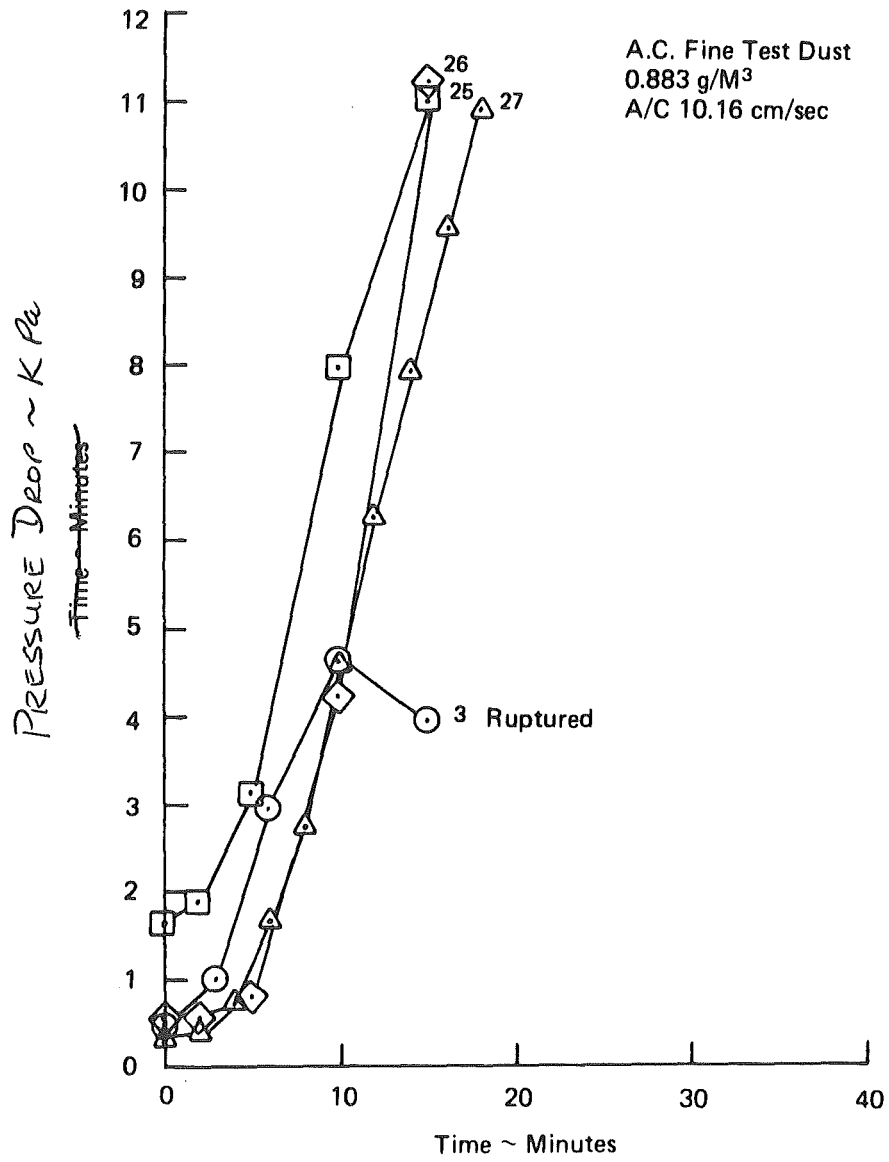


Figure 6. Dust loading of ceramic paper.

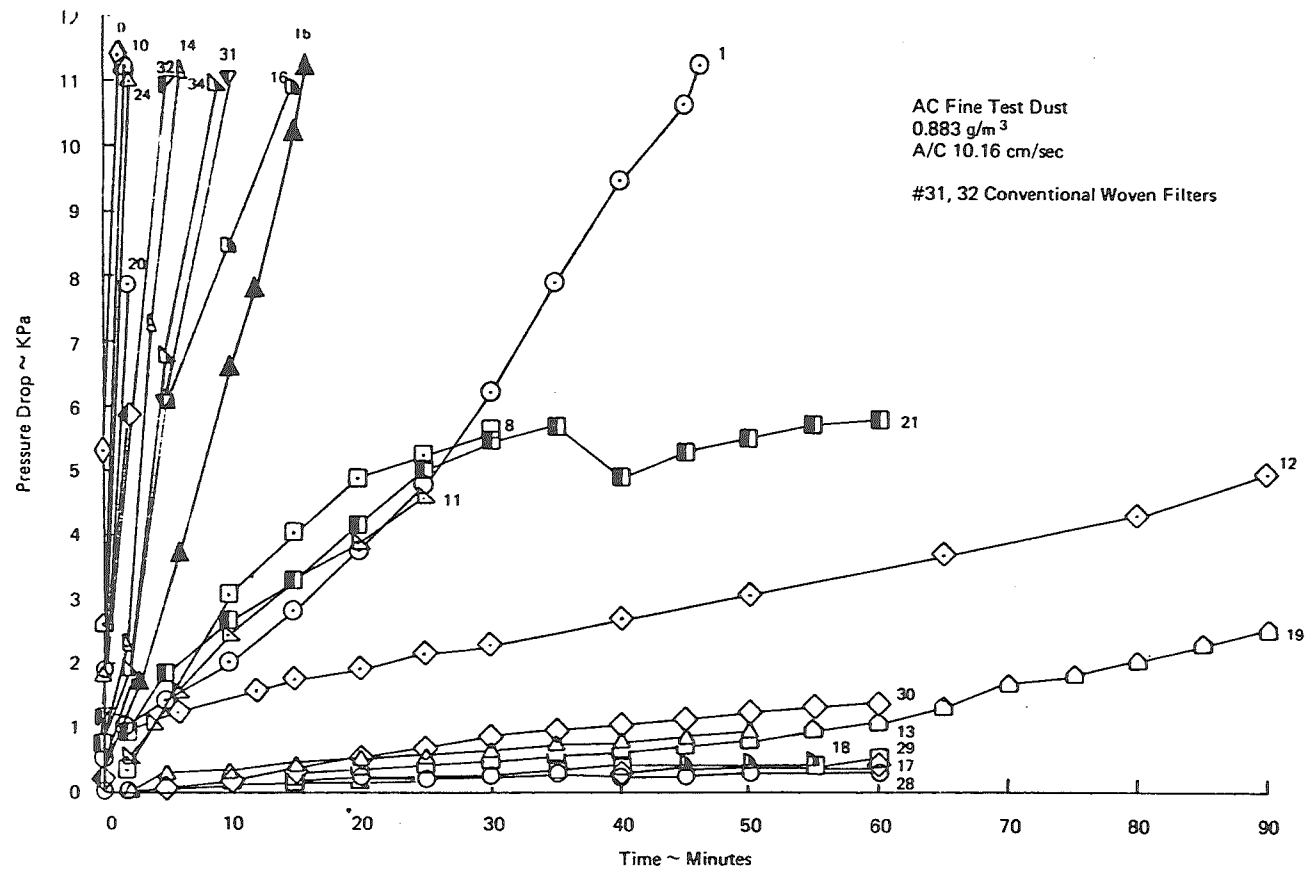


Figure 7. Dust loading of woven ceramic media.

The flat sheet loading tests also provided overall collection efficiency (mass basis) data for the tested materials. Dust penetrating the media was collected in an absolute filter downstream of the test media. Table 3 reveals that most of the woven ceramic materials did not achieve high collection efficiency in this test. On the other hand, woven commercial materials were only moderately efficient. Several of the ceramic paper and felt materials, however, did provide collection efficiency of 99 percent or better. The two materials which fractured would have provided higher efficiency performance had they not fractured. The test was stopped as soon as the fracture was detected.

General Conclusions from Room Ambient Tests

- Several of the ceramic paper and felt materials are capable of removing fine particles at high efficiency without excessive filter weights.
- The ceramic paper and felt materials have filtration characteristics and performed similar to paper and felt commercial filter media in a series of filter media tests.
- The ceramic woven materials in general were characterized by large pores and poor collection efficiency in the dust loading tests. The range of parameters exhibited by the various materials, however, indicate that an acceptable woven ceramic filter media can probably be fabricated, but such a filter media would have the same limitations as currently available woven filters. That is, acceptable performance is only probable at low air-to-cloth ratios.

- "Blanket" ceramic fiber materials (felts) consisting of small diameter fibers (3.0 μm) appear to be the most promising materials for high temperature and pressure tests because of their combination of good filtration performance and relatively high strength.

High Temperature/Pressure Tests

Two major questions concerning the suitability of ceramic fibers for filtration need to be answered. These are:

1. How durable are ceramic fiber structures when subjected to environmental conditions associated with filtration applications.
2. How well do ceramic fibers perform as filters in the HTHP environment.

Some preliminary answers are available concerning the first of these questions.

Three ceramic filter media configurations have survived a test during which the filter elements were subjected to 50,000 cleaning pulses. The objective of these tests was to simulate approximately one year of operation of mechanical loads on the media at high temperature and pressure. Test conditions were as follows:

Temperature - 815°C
Pressure - 930 KPa
Air-to-cloth-ratio - 5 to one (2.54 cm/sec)
Cleaning pulse pressure - 1100 KPa
Cleaning pulse interval - ~10 seconds
Cleaning pulse duration - 100 m second
Dust - recirculated fly ash

The three filter media configurations tested were:

- Saffil alumina mat contained between an inside and an outside layer of 304 stainless steel knit wire screen. Figure 8 shows how easily the residual

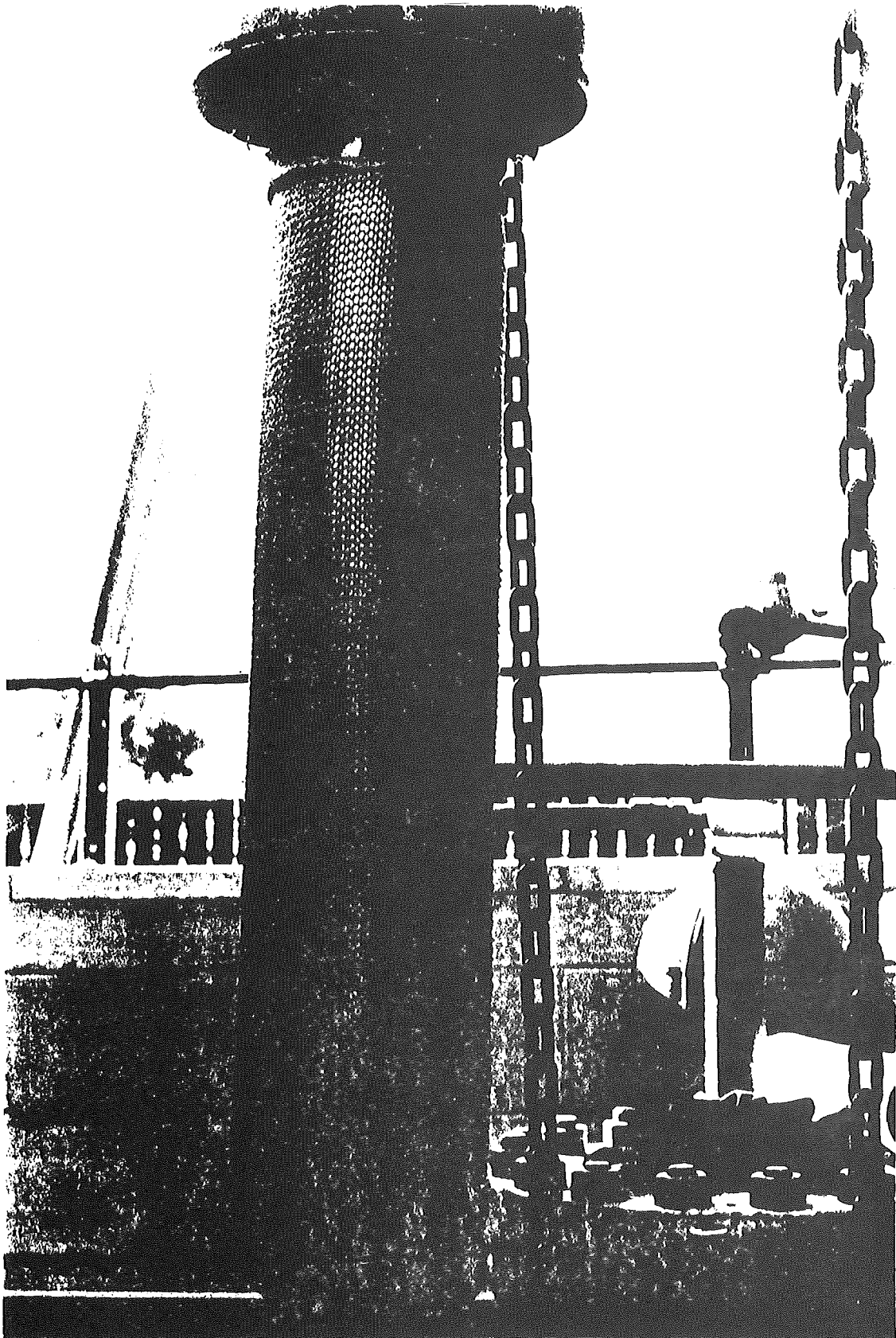


Figure 8.
Saffil Alumina - Post Test Dust Cake
(Clean strip using Vacuum Cleaner)

dust cake was removed from this media after the test.

- Woven Fiberfrax cloth with nichrome wire scrim insert. Figure 9 shows the dust cake following the 50,000 Pulse test.
- Fiberfrax blanket contained between an inside and an outside cylinder of 304 stainless steel square mesh screen similar to common window screen. The ceramic fiber blanket was held in position between the screens with 302ss wire sewn between the screens. This resulted in about 100 penetrations of the ceramic fiber bed. Figure 10 shows the dust cake following the test.

Pressure drop during the tests was controlled by the rapid cleaning pulses and in general remained less than about 5 KPa (20 in H₂O).

Dust penetrating the ceramic test media was collected on a high efficiency filter located downstream (after cooling) of the test chamber. This data is not reported for the Saffil Alumina or for the Woven Fiberfrax Cloth because of a leak discovered in a gasket in the test rig. This problem was corrected before the fiberfrax blanket test was performed. Average outlet loading during this test was 0.0055 g/a m^3 (0.0024 gr/a ft^3). Figure 10 shows that the dust was concentrated near the places where wire penetrated the filter element. This concentration of dust near the wire penetration points could be seen on the inside of the element also. Thus, most of the dust which penetrated apparently did so through the holes made by the wires. It is reasonable to expect that a filter element without holes will experience less penetration. Also a less frequent cleaning pulse interval will reduce penetration. Therefore even better performance than that achieved in this test should result from future tests.

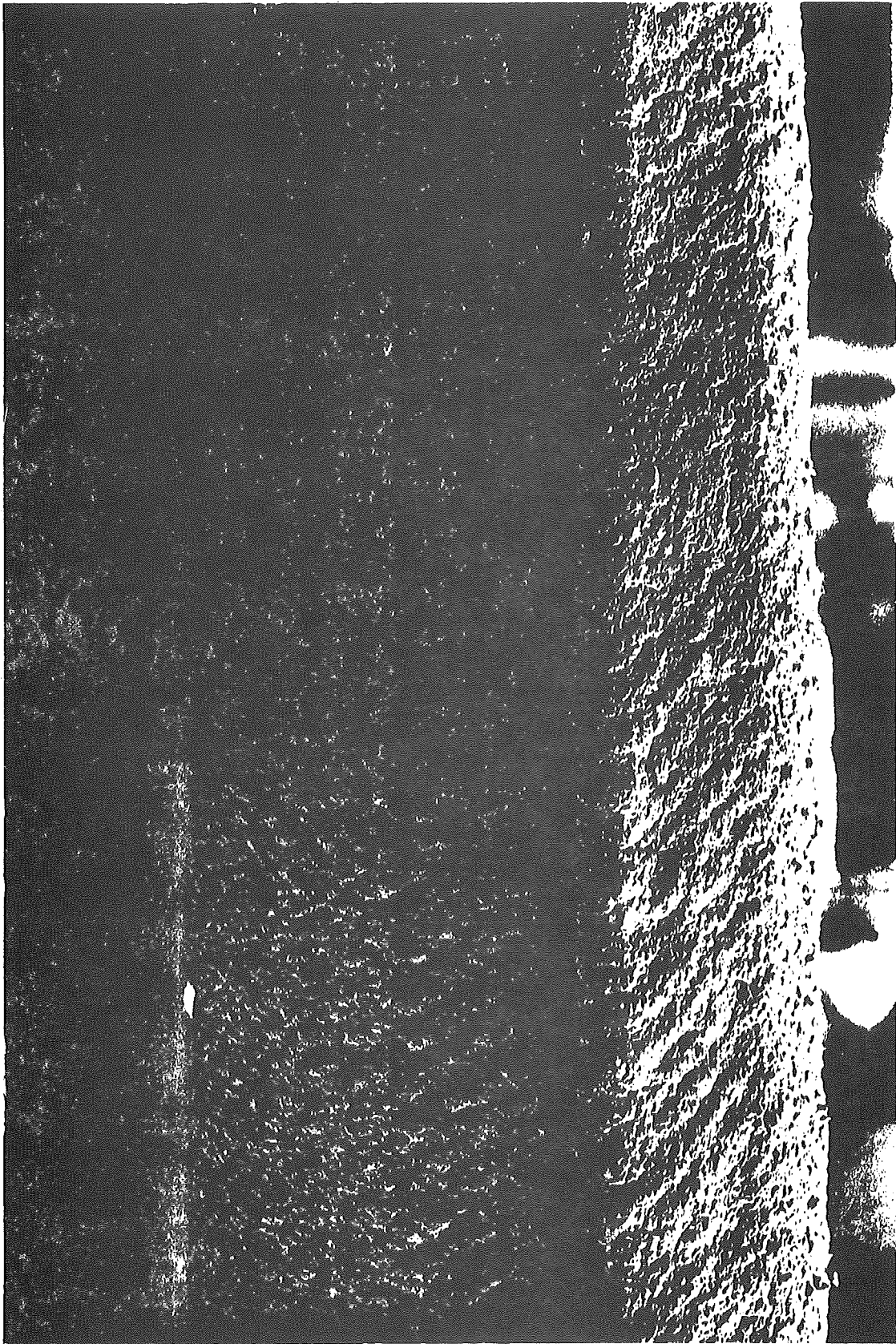


Figure 9.
Woven Fiberfrax - Post Test
Dust Cake

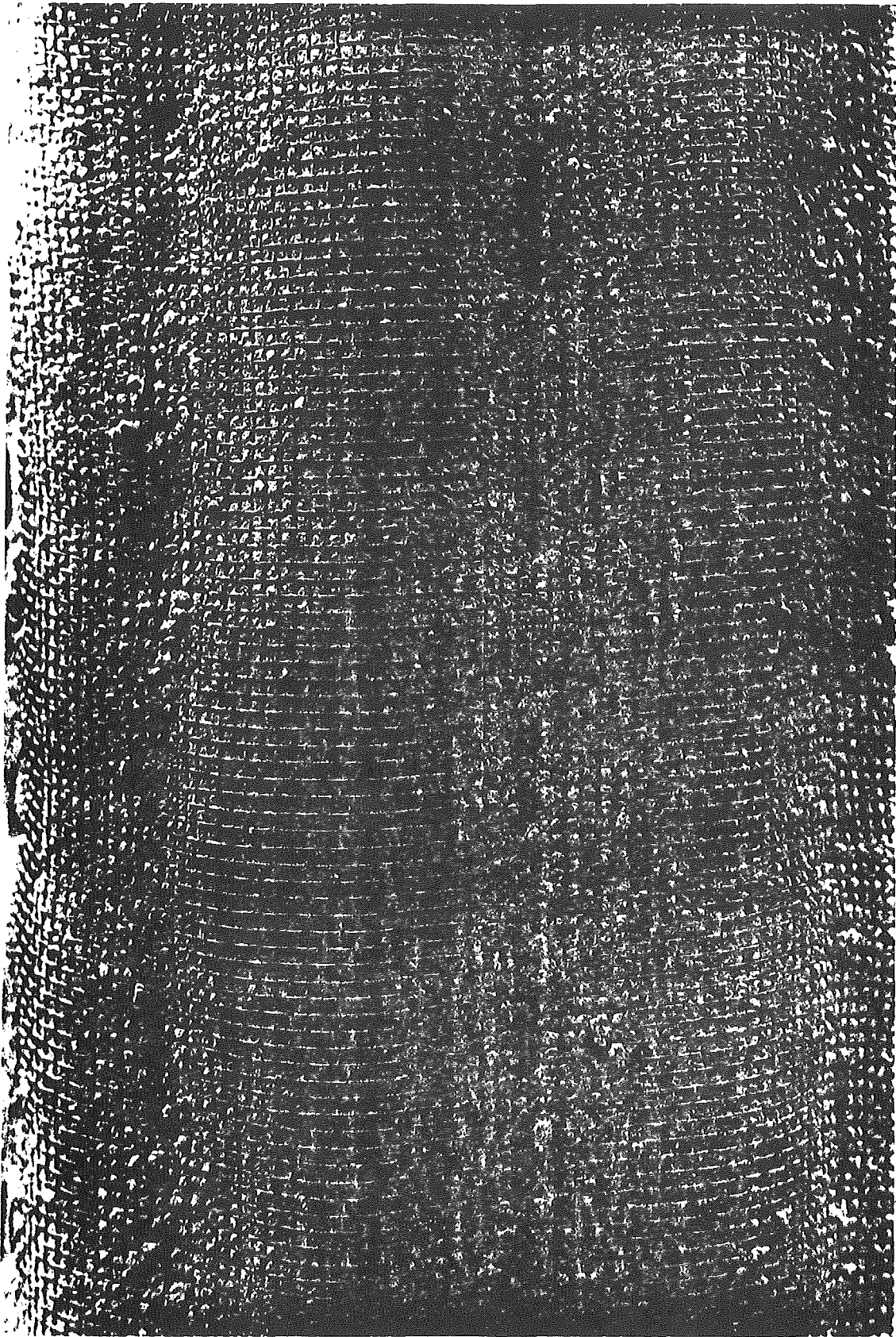


Figure 10.
Fiberfrax Blanket - Post Test
Dust Cake

Conclusions

Research on bench scale indicates that fine particle control at high temperature and pressure can be achieved using barrier filtration by ceramic filter beds. Evidence in support of this contention includes the following:

- A theoretical basis exists for it.
- Room temperature tests show that particles including fine particles are collected at high efficiency.
- Tests at high temperatures and pressures show that several ceramic filter structures are capable of surviving in excess of 50,000 cleaning pulses while maintaining pressure drop at acceptable levels and providing efficiency close to the lowest reported turbine requirements.

REFERENCES

1. Hazard, H. R., "Coal Firing for the Open-Cycle Gas Turbine." Proceedings of the Joint Conference on Combustion, 1955, ATME and IME.
2. Hoke, R., "Ducon Gravel Bed Filter Testing," EPA/ERDA Symposium on High Temperature/Pressure Particle Control, Washington, D.C., Sept. 1977.

Discussion

Mr. Schulz asked whether needle felts were used; Mr. Shackleton replied in the negative. Neither ceramic nor steel needle felts were used. Needling creates holes and defects in the filter. This had been shown by DOP testing. Mr. Guthner inquired whether there had been a steel support cage below the felts and how this was attached. A cage had been used comprising wire screens both inside and outside of the filter. Mr. Shackleton said that the metal screens might have a short life, and that ceramic or quartz-based screens could be employed. Mr. Guthner suspected that the use of metal wire cages for supporting the felts in large installation caused friction and fiber deterioration. Mr. Shackleton referred to proposed work in order to determine suitable cage size, structure and optimization of cleaning systems.

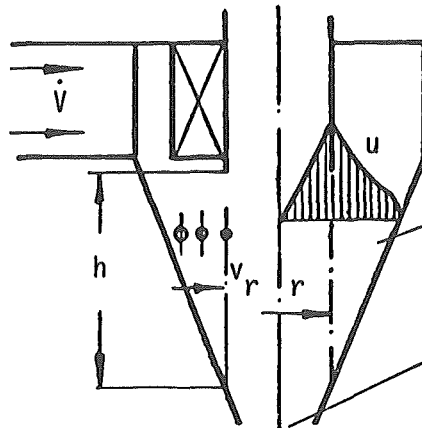
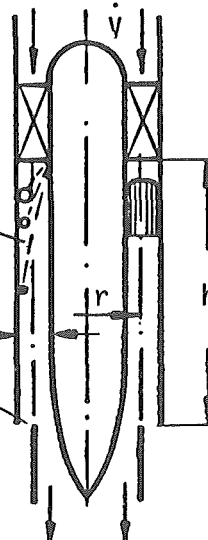
New techniques using fleece (lined on both sides with a screen) as opposed to cloth or needle felts were described by Mr. Shackleton. This type of construction was applicable to all fibers, including organic fibers. Acurex would investigate these novel methods and would also aim to minimize penetration during cleaning.

Mr. Gooding wished to know whether the observations made during the talk were also applicable to cake filtration. One of the reasons for using fine fiber fabric filters was to reduce filter material, said Mr. Shackleton. Fine ceramic fibers occasioned low solidity in the fiber bed and a largely open space with few points of contact.

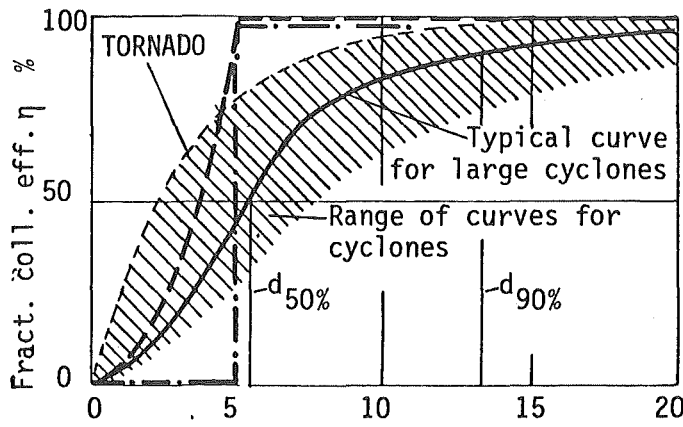
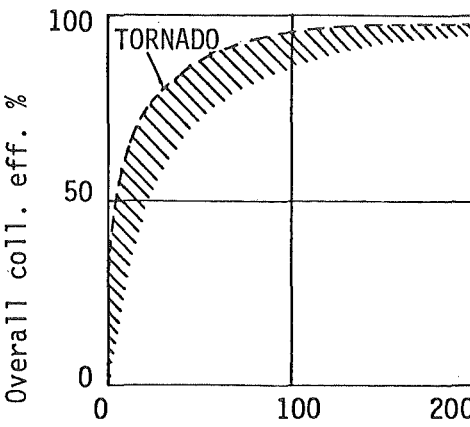
Mr. Finkh asked about the pressure drop after longer periods of filtration, and whether there was a saturation point and a definite period of operation. Mr. Shackleton answered that the tests carried out were not concerned with cleaning, but static loading and were designed to measure filtering capability. A pressure drop did not develop for certain woven ceramic fabrics owing to the number of large pores. One should bear in mind that the materials used were originally developed for insulation, not filtration.

PROBLEMS ON THE APPLICATION OF
CENTRIFUGAL SEPARATORS, ESPECIALLY
OF ROTARY FLOW COLLECTORS

Prof. Dr.-Ing. P. Schmidt,
Dr.-Ing. P. Walzel,
Institut für Apparatechnik
Universität Essen
Unionstr. 2
4300 Essen

| | | | | |
|--|--|--|---|---|
| <p>Reverse flow or radial cyclone</p>  | <p>Straight through flow or axial cyclone</p>  | | | |
| <p>Symbols:</p> <ul style="list-style-type: none"> v_a Axial vel. u Tang. Vel. η Viscosity v_r Rad. Vel. \dot{V} Throughput ρ Density | | | | |
| <p>Smallest particle theoretically collected for laminar flow without agglomeration:</p> <table style="width: 100%; border: none;"> <tr> <td style="width: 33%; text-align: center; border: none;"> <p>reverse flow cyclone</p> $d_{50} = \sqrt{\frac{18 \eta r v_r}{\rho_s u^2}} ;$ </td> <td style="width: 33%; text-align: center; border: none;"> <p>straight through cyclone</p> $= \sqrt{\frac{18 \eta r s v_a}{\rho_s h u^2}}$ </td> <td style="width: 33%; text-align: center; border: none;"> <p>both types of cyclone</p> $= \sqrt{\frac{9 \eta \dot{V}}{\pi \rho_s u^2 h}}$ </td> </tr> </table> | | <p>reverse flow cyclone</p> $d_{50} = \sqrt{\frac{18 \eta r v_r}{\rho_s u^2}} ;$ | <p>straight through cyclone</p> $= \sqrt{\frac{18 \eta r s v_a}{\rho_s h u^2}}$ | <p>both types of cyclone</p> $= \sqrt{\frac{9 \eta \dot{V}}{\pi \rho_s u^2 h}}$ |
| <p>reverse flow cyclone</p> $d_{50} = \sqrt{\frac{18 \eta r v_r}{\rho_s u^2}} ;$ | <p>straight through cyclone</p> $= \sqrt{\frac{18 \eta r s v_a}{\rho_s h u^2}}$ | <p>both types of cyclone</p> $= \sqrt{\frac{9 \eta \dot{V}}{\pi \rho_s u^2 h}}$ | | |
| University Essen Instit. process equipment | Survey of cyclone dust collectors | P. Schmidt 1978 | | |

1. Characterization of efficiency by $d_{50\%}$ or overall efficiency η .
2. In dust collection from hot gases, the largest particle passing through the cyclone often is most dangerous because of later erosion. So effectiveness, f.i. the collection of $d_{99\%}$ -particles, might be more important than efficiency.
3. Efficiency resp. pressure drop or power demand.
4. Efficiency must include removal of dust from the cyclone into the bin.
5. Most important on efficiency, however, is agglomeration.

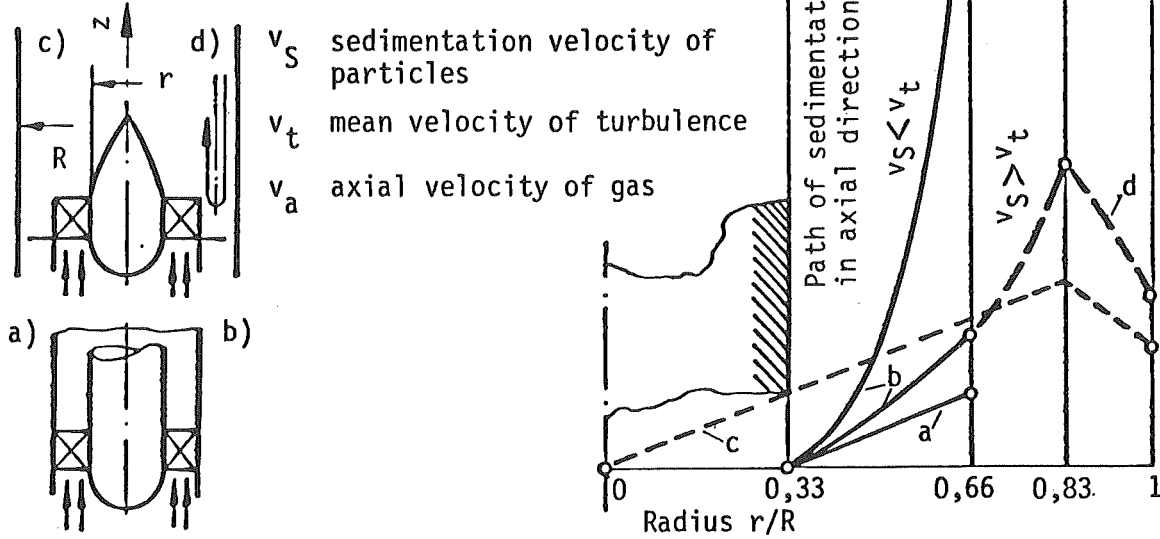
| | |
|---|--|
|  |  |
|---|--|

| | | |
|--|--|--------------------|
| University Essen Instit. process equipment | Problems on efficiency of cyclone dust collectors | P. Schmidt 1978 |
|--|--|--------------------|

| | | |
|---|---|--|
| | <p>1. Unstable vortex flow in reverse cyclones a)</p> <p>2. No constant velocity in radial direction for reverse flow cyclone a)</p> <p>3. Dust strands and wall friction for both types a) and b)</p> <p>4. Disordered flow in the sedimentation chamber a)</p> <p>5. Imperfect dust removal from the settling area, especially in axial flow cyclone b)</p> | <p>6. Changing agglomeration of dust with temperature for both types a) and b)</p> <p>7. To cope with this problems the TORNADO collector has been developed</p> |
| <p>University Essen Instit. process equipment</p> | <p>Problems in cyclone operation</p> | <p>P. Schmidt 1978</p> |

| | | |
|---|---|----------------------------|
| | <p>TORNADO with secondary gas jets from nozzles a) or secondary gas flow through guide vanes b)</p> <p>c) Fresh air circuit, efficiency relatively good only, impossible in hot gas cleaning</p> <p>d) clean gas circuit, high cleaning efficiency</p> <p>e) Flue gas circuit, low power consumption</p> <p>f) Internal fanning circuit, high cleaning efficiency</p> <p>Pressure drop equivalent to cyclone</p> $\Delta p = \frac{\Delta p_1 \dot{V}_1 + \Delta p_2 \dot{V}_2}{\dot{V}_3}$ | |
| <p>University Essen Instit. process equipment</p> | <p>TORNADO dust collector, principle and circuit diagrams</p> | <p>P. Schmidt 1978</p> |

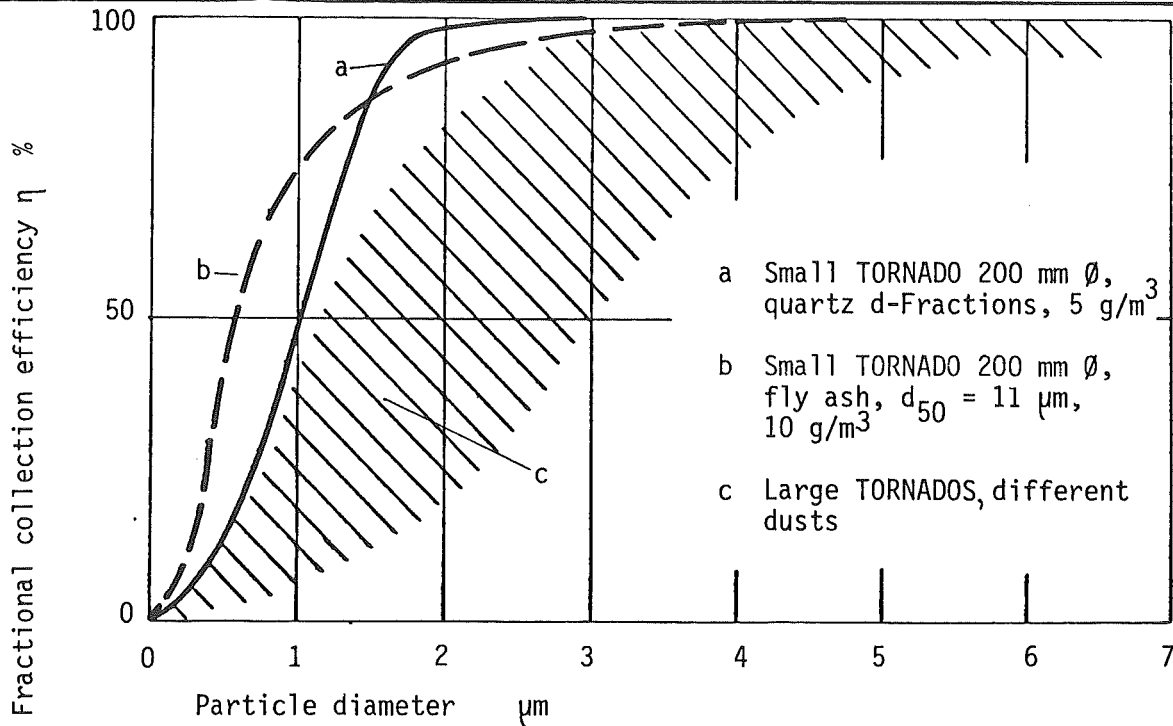
- a) Axial or straight through collector, laminar flow theory
- b) Axial collector, turbulent flow
- c) TORNADO, laminar flow theory
- d) TORNADO, turbulent flow



University Essen
 Instit. process
 equipment

Pathes of comparable particles in axial
 direction for axial and TORNADO collectors

P. Schmidt
 1978



University Essen
 Instit. process
 equipment

Typical collection efficiency curves for
 TORNADO dust collectors

P. Schmidt
 1978

1. In laminar flow it is basically possible to separate all particles from gases by cyclone collectors. However, a practical limit seems to be a diameter of $d \approx 5 \mu\text{m}$ for isolated particles.
2. In turbulent flow particles are totally separable only if their settling velocity is higher than the average velocity of the turbulence. In practice the limit might be $d \approx 15 \mu\text{m}$. The content of smaller particles can be reduced gradually by elutriation, i.e. continuous removal in longer cyclone.
3. In hot gases, the Reynolds number is lower than in air under normal conditions by the factor of about 8. If the pressure is higher, the Re-number however increases by a factor of about 1,1/bar. The use of inserts to build laminar cyclones may be of some interest.
4. When cleaning hot gases a sharp separation limit is essential. - Quite apart from turbulence the overall gas flow should be as homogenous as possible.
5. Dust collection with cyclones is much more efficient in practical operation than in theoretical prediction. In most cases the smallest particle collected with TORNADO collectors really is $d \approx 2 \mu\text{m}$ compared with the stated $15 \mu\text{m}$; this is due to agglomeration. - We know little about agglomeration under normal conditions and less in high temperature gases. Because of its crucial importance in dust collection, investigations are necessary here.

University Essen
Institut. process
equipment

Resumé of dust cleaning hot gases with
cyclone collectors

P. Schmidt
1978

Discussion

Prof. Weber pointed out the relationship between the diameter of the Tornados and its efficiency, an increase in the former resulting in inefficiency. Exact values regarding this relationship could not be provided at the time by the speaker, although an optimum diameter of 1 meter was known. A diagram showed cut size diameter of 50% at 1/2 micron. Mr. Shackelton questioned the source and validity of this curve. Mr. Princiotta said that cyclones were used only for particulate collection in the U.S. and asked for Dr. Walzel's opinion as to whether these could protect turbines.

Information on this could be found in the paper.

Mr. Shackleton described a U.S. modification of a powered cyclone which failed during tests to prove the predictions. An overall particle collection of 80% was inadequate, according to Mr. Princiotta.

Mr. Glüthner, in reply to his question, was informed that the total differential pressure in the cyclone mentioned was 200 mm.

Mr. Bonn (Bergbau-Forschung) discussed the performance of cyclones. General Electric cyclones used in upstream bed combustion failed to reach the predicted standards of efficiency owing to fly ash brittleness and dimisting in conventional cyclone size. Investigation was needed into Tornados, which could be better due to lack of attrition on the walls. Dr. Holighaus said that more information was also needed on high temperature and pressures in the same area. Fluid bed tests were being made at the time in England to compare conventional with Tornado cyclones.

SESSION V: MEASUREMENT TECHNOLOGY

Experience with Continuously Recording Dust Measuring
Instruments

by

Dr. D. W. Laufhütte +)

In accordance with the Federal Republic's Technical Instructions for the Prevention of Air Pollution, solid fuel firing equipment with a heating efficiency above 100 GJ/h must be provided with measuring instruments to control and record dust concentration. At the same time, any equipment emitting more than 15 kg dust/h, must be fitted out with such instruments. The Federal Minister of the Interior publishes suitable measuring instruments and guidelines for the qualification tests, maintenance, installation and calibration of measuring instruments as well as the evaluation of measuring results.

Accordingly the majority of power stations, consuming solid fuels, nowadays are equipped with "smoke meters", following official instructions.

The calibration of these continuously recording measuring instruments is carried out by comparative gravimetric measuring which must cover as many different conditions of firing operation as possible to ensure a safe connection between gravimetric measuring and recording indication. The recording instruments predominantly work on the principle of reflection, i.e. the reflection of a light beam radiated from a lamp. The weakening of the light beam by absorption and diffusion is described by the Lambert-Beer's law. All types of instruments are subjected to laboratory tests prior to admission.

Practical experience with these instruments shows the high dependence on the grain size spectrum and the mineral composition of the available dust types. Fig. 1 (Influence of different fuels at changing coal-fired boiler conditions). This leads inevitably to the question for the extent of error which may result from fluctuations of the material composition of flue dust and the grain spectrum of these dust types.

In order to get an idea on the fluctuation spectrum of the particle size distribution which may occur, the Institute for Mechanical Processing Technique of the Karlsruhe University (TMM), in an initial test series with approx. 80 samples of flue dust from different lignite power stations, carried out particle size analysis. Moreover, the absorbance was measured on fractions of different solid materials with a known particle size distribution and predetermined values of concentration to estimate the influence of the grain spectrum on the integral (mean) scattering cross section determined experimentally. The goal of this test series was to have new lights on how the particle size distribution and composition of flue dust may vary in the course of time, for, as already mentioned, the temporal constancy of the scattering cross section is a precondition for the future validity of a calibration curve once determined.

In the scope of the first test series, absorbance was measured on homogenous substances, such as limestone, quartz, graphite and four samples of flue dust from lignite power stations. From all samples, fractions were made for absorbance measuring and their distribution determined by photographic sedimentation analysis and wet mechanical analysis.

For absorbance measuring, the Sick instrument RM 4 was used. The test equipment was arranged in such a way that small amounts of material could be used for measuring at a relatively long measuring distance of 2.50 m. Not only the position of the distribution with regard to the median value substantially influences the absorbance but also the width. The fraction with the higher content of fine particles, as a rule will result in a higher specific absorbance, as indicated in Fig. 2. The distribution curve with a higher content of fine particles shows a steeper line of absorbance at an almost equal median value.

The trials with homogenous substances served as an example for demonstrating the basic connections of the photometric determination of mass concentration, whereby it could be proven that a simple physical connection between absorbance and mass concentration does not exist.

The respective connections flue dust are reflected by the absorbance results of four dust samples in conjunction with the grain size analyses conducted.

The four dust samples from crude gas dust were first converted to two fractions each with particles below 18 μ m and below 50 μ m. The resultant distribution curves are given in the upper diagram of Fig. 3. The dependence of the absorbance as a function of dust concentration can be taken from the lower diagram.

Compared to the fine fractions, the coarse fractions clearly show the more gently rising straight lines with the lower absorbance values.

Additional density tests with the 52 pure gas dust samples drawn in the summer 1976 show the trend that the density increases with diminishing dust particles.

As random sample analyses showed, normally the density within a complete fraction can be expected to rise with a reduction in grain size, too.

On the whole, absorbance tests with the fractionated crude gas dust show the considerable range of fluctuation of the specific absorbance by changes in grain size and density. The absorbance differences at equal dust concentration for the coarse fractions (below 50 μ m) amounted to more than 100 % and for the fine fractions (below 18 μ m) still 25 %.

The results of particle size analyses by the Technical University of Karlsruhe indicate in Fig. 4 the considerable scattering range which may occur in the distribution of

flue dust samples from lignite fire places. The demonstrated scattering range reflects the results of 17 pure gas dust samples from one power plant block. The median values extend from about $3.5\ \mu\text{m}$ to almost $40\ \mu\text{m}$.

The median values determined in the second test series from 52 pure gas dust samples even ranged between $3\ \mu\text{m}$ and $65\ \mu\text{m}$.

Establishing a relation between the considerable fluctuations of the pure gas dust sample distributions and the results from measuring the absorbance of fractionated crude gas dust, differences in the specific absorbance of far more than 100% cannot be excluded.

Related to the use of smoke meters, this means that concentration errors to the same extent must be expected, when basing a medium calibration curve. Strictly speaking, this is only applicable to the photometric determination of dust concentration behind lignite fire places. Errors to the same extent are, however, also likely with coal fire places and mixed fire places, as for instance imported coal of different origin and composition is used in power stations. Even the local coal varies in composition from mine to mine, resulting in deviations in the grain spectrum and the physical features of flue dust. Respective absorbance tests of the Technical University of Munich with flue dust from coal fire places demonstrated the possibility of errors occurring to a similar extent.

Practical effects

After the principle clarification of the possible error extent in the photometric determination of dust concentration, the question arises whether the aforementioned errors actually appear.

The first example in Fig. 5 shows three calibrations within one and a half years behind a lignite fire.

What is noted immediately is the fact that no calibration result approaches the other; three absorbance values extremely deviating from one another are coordinated to the same dust concentration in the range of 100 mg/m^3 , the maximum difference of which is 150%.

A great portion of deviations in the calibration curves is caused by changes in the material properties of the pure gas dust, as indicated by the following example.

Fig. 6 also shows two calibration results determined behind a lignite fire which heavily differ despite identical conditions of operation and the use of the new instrument type, practically excluding datum errors by instrument shifting. The measurement of both calibrations did not result in a statistical connection between absorbance and specific dust content, the straight regression lines having a vertical course. The left hand measuring series is a TÜV calibration from 1973, the right hand series an operator's calibration from 1975. The recalibration was carried out, following the request of the competent supervisory office.

Although in both calibrations a statistical connection between absorbance and dust concentrations could not be found due to an unfavourable arrangement of measuring points, both results may be considered as a proof for the displacement of the measuring series by a change in the grain spectrum on account of the same characteristics (vertical regression line despite identical fluctuations in the dust content). At the same medium dust concentration, the change of the corresponding absorbance values averaging 0.08 to 0.12 amounts to nevertheless 50%. For reasons of completeness, it should be mentioned that an instrumental defect could not be detected by the supplier.

Both practical examples give an impression to the fact that a temporal constancy of the specific scattering cross section substantially determining the calibration curve of the metering equipment, due to the fluctuations in the compo-

sition of material of the pure gas dust from lignite fire places cannot on principle be presupposed. Therefore, even errors in the specific absorbance of more than 100% cannot be excluded.

Conclusions

The practical control of dust emissions by the photometric instruments is carried out according to the evaluation method stipulated by the Federal Minister of the Interior's circular letter dated 3-3-1975.

The confidence areas of the calibration curves and tolerance ranges of the individual values calculated in the scope of the statistical evaluation form the basis for the assessment of whether a margin has been surpassed or not. These tolerance ranges already include measuring errors of more than 10%, resulting from gravimetric determinations of the dust content. On principal the operator may only utilize the closer confidence area for himself because exceeding a mean absorbance value - formed from 10 to 15 individual values - beyond the confidence area means that a marginal value according to the evaluation method has not been met (Fig. 7).

On account of the incomplete registration of the variation range of the grain spectrum during calibration, the confidence and tolerance ranges are too close to ensure a sufficient security in the evaluation of the calibration curve. Under these aspects, the practiced evaluation method may result in misinterpretations regarding a surpassing of a marginal value inspite of the tolerances allowed.

Particularly in old plants the surpassing of a marginal value simulated by the absorbance reading cannot be excluded because their electric filters work in the marginal range due to the tightening restrictions for dust emission values. In such cases instructions of the competent supervisory office may be expected, requiring cost-intensive reconstruction or new construction of additional plant parts of the power station on account of tightening legal regulations.

In this connection the use of integrators intended by authorities must be seen, resulting in a shutting down of a power station concerned by an automatic cut-off when a predetermined absorbance value is surpassed. In this way, integrators are already used in the cement industry, however, under the prerequisite of calibration results beyond doubt by completely registering the grain spectrum of dust.

The use of photometric instruments and consequently of integrators in conjunction with the evaluation method practiced at present seems to be rather delicate when the dust properties show temporally heavy fluctuating features.

A trouble-free use of photometric instruments behind lignite and coal fire places with considerable fuel fluctuations and without errors in the concentration reading is only possible by additional information on the grain spectrum of pure gas dust, continuously correcting the photometric values, i.e. the absorbance values. A unique analysis of grain size distribution even of all types of flue dust occurring in praxis is of no use if the type of coal used cannot be predetermined. In praxis such a predetermination will hardly be possible, as the operational analyses (e.g. of sulphur, ashes and water content) normally do not permit conclusions concerning the material properties and the grain spectrum of flue dust.

+) Dr. rer. nat. D.W. Laufhütte, Saarbergwerke AG
department Environmental Protection and commissioner
for emission protection, Saarbrücken

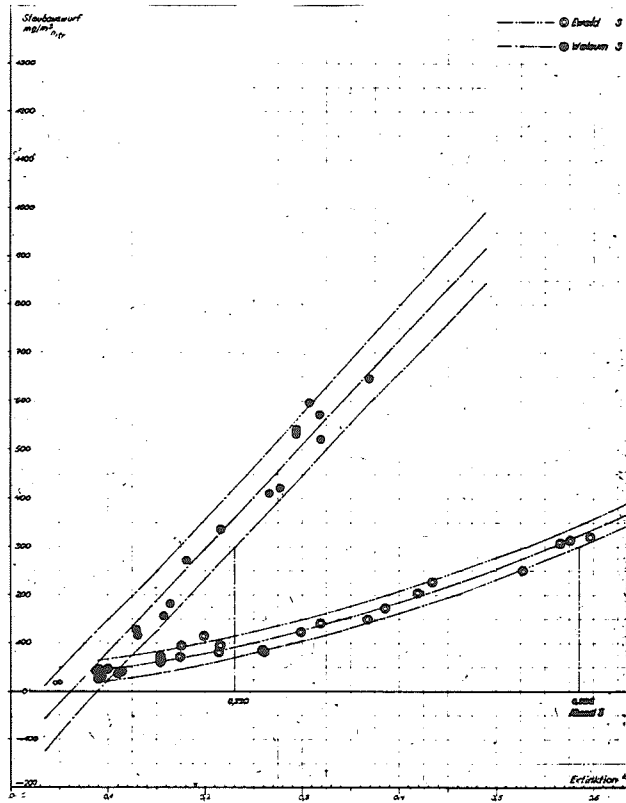


Fig. 1

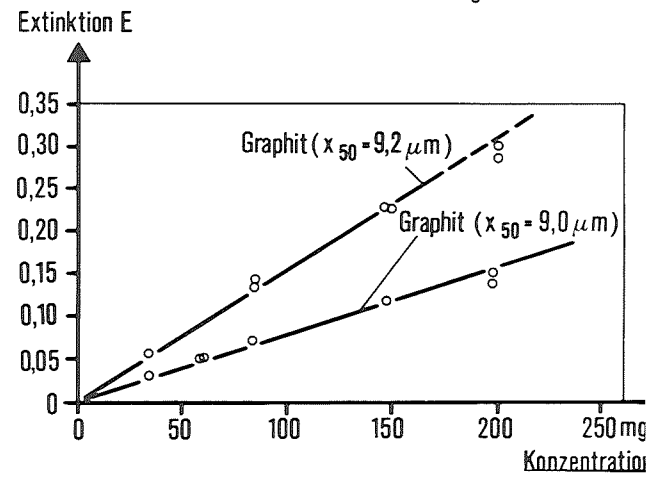
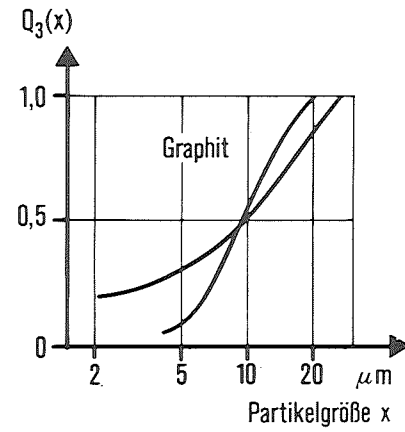


Fig. 2

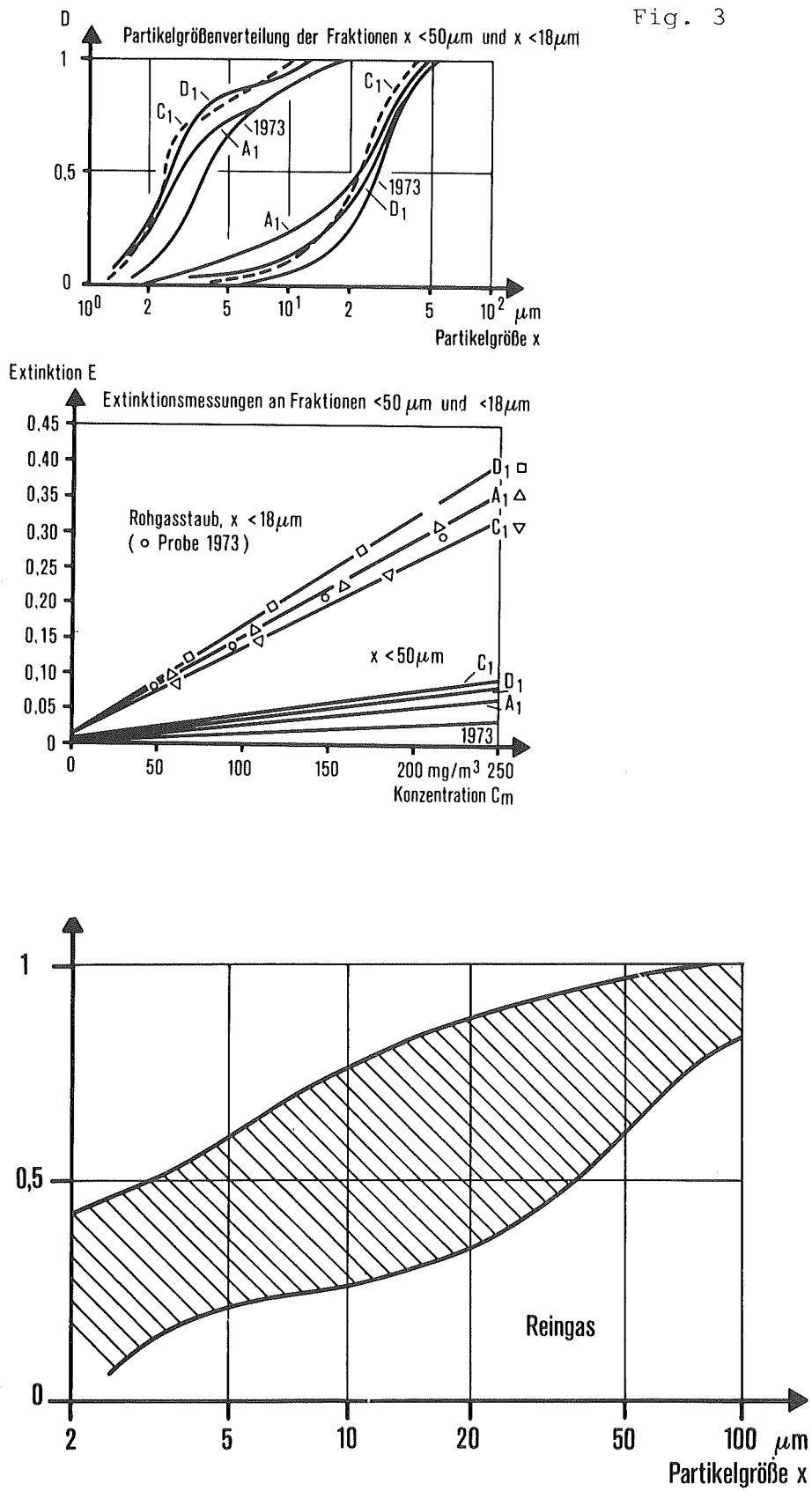


Fig. 4

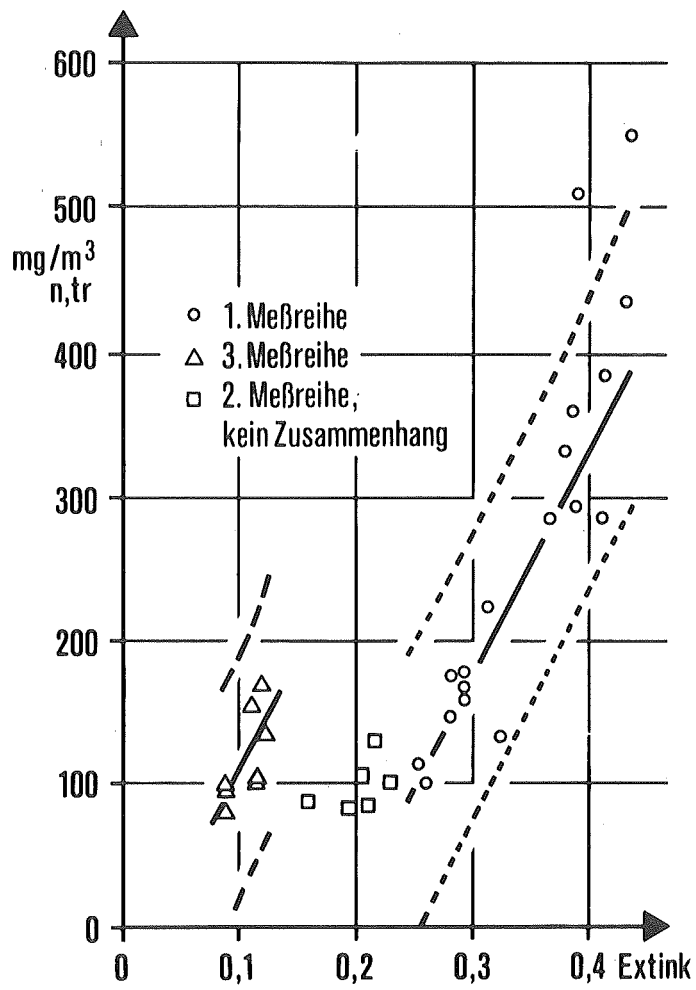


Fig. 5

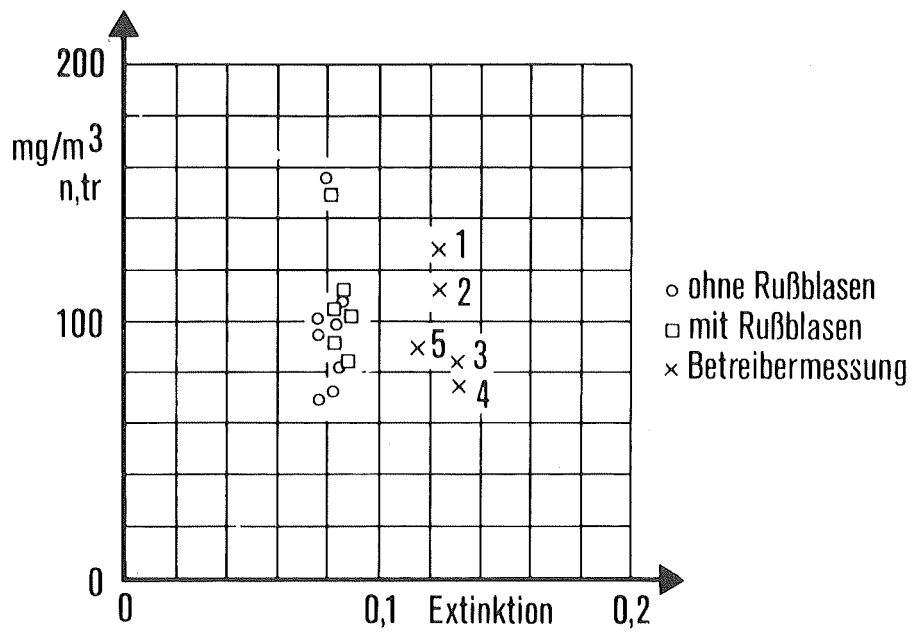


Fig. 6

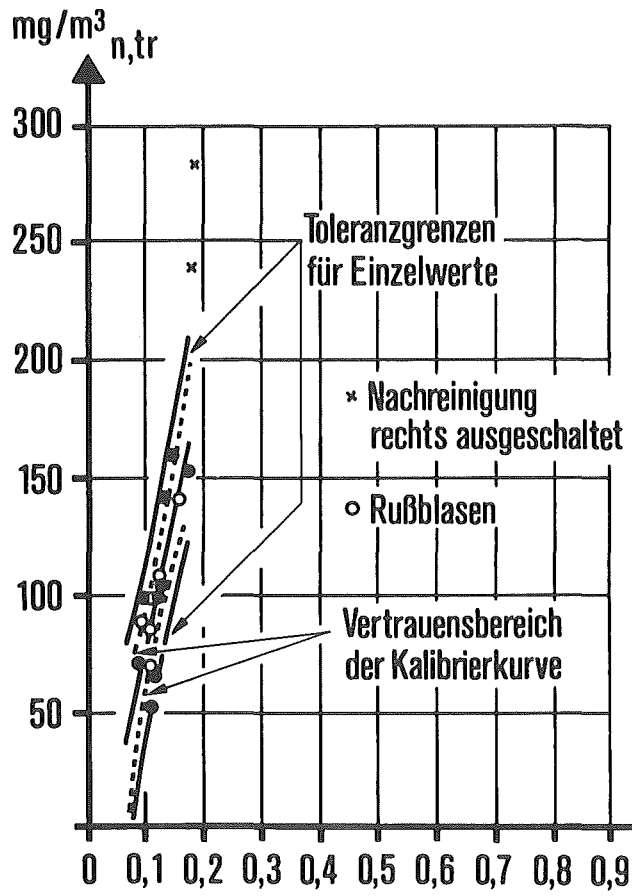


Fig. 7

Discussion

Dr. Holighaus drew attention to the fact that the techniques described in the talk were the same as those in the US. Mr. Kuykendal reported that work had been carried out there with transmissometers. Good correlations between mass and opacity had been found during tests carried out in certain North Carolinian industries. The operation range was limited and there was no regulation requirement. Questions were posed regarding new regulations, including those concerning opacity. This was not to exceed 20%, according to Mr. Kuykendal, although the limit could be exceeded for brief periods of time. Continuous monitoring of dust concentration and visible emission was carried out. Dr. Calvert referred to an opacity study which had been performed at a coal-fired power plant. Investigations showed a good relationship between predictions and measurements regarding concentration, particle size distribution and refractive index. In the case of multiple scattering, 40% extinction was found and charges occurred (More information on this could be obtained from a paper by Wei et al.) The work was based on 6 m tubing on Western coal.

CONTINUOUS CONTROL OF THE DUST CONTENT IN STACK GASES
=====

WITH LASER DEVICES.
=====

Prof. Dr.-Ing. E. WEBER
Institut für Mechanische Verfahrenstechnik
Universität Essen GHS
Universitätsstraße 2
Postfach 68 43
D 4300 Essen
Tel. 0201-1832795

Dipl.-Phys. H. WIGGERS
Institut für Mechanische Verfahrenstechnik
Universität Essen GHS
Universitätsstraße 2
Postfach 68 43
D 4300 Essen
Tel. 0201-1832788

CONTINUOUS CONTROL OF THE DUST CONTENT IN STACK GASES
=====

WITH LASER DEVICES.
=====

H. Wiggers, E. Weber

It is one of the most important demands for any control of the dust content of stack gases that the measuring data are continuously available. For this reason sampling devices are not usable. With these procedures an immediate and continuous measurement is not feasible because each sample has to be collected during a longer period. Nevertheless the sampling procedures are up to now the essential basis for any calibration of the light, x-ray, or β -ray measuring devices.

All these three procedures offer the potentiality of a continuous measurement. Mostly the transmission ratio is measured to get informations about the dust content. If a beam with an initially power S_0 penetrates an aerosol and if the power at the outlet is S , the ratio of these powers is defined as the transmission ratio τ :

$$\tau = \frac{S}{S_0}$$

If the dust concentration is not too high, the law of " Lambert-Beer " predicts the power at the outlet :

$$S = S_0 \cdot e^{-\alpha z c}$$

Here z is the optical path length of the beam through the aerosol and c is the value of the dust concentration. α depends upon the type of the dust and it is also affected by the particle size distribution if the problematic x-rays are not taken into account. This law is indeed valid only for low dust concentrations, but also at higher values the emerging power is always a strict monotonic

function of c . That is, the measurement of the transmission ratio is by all means an appropriate method for controlling the dust content, at least so long as one can assure a constant type and particle size distribution of the dust.

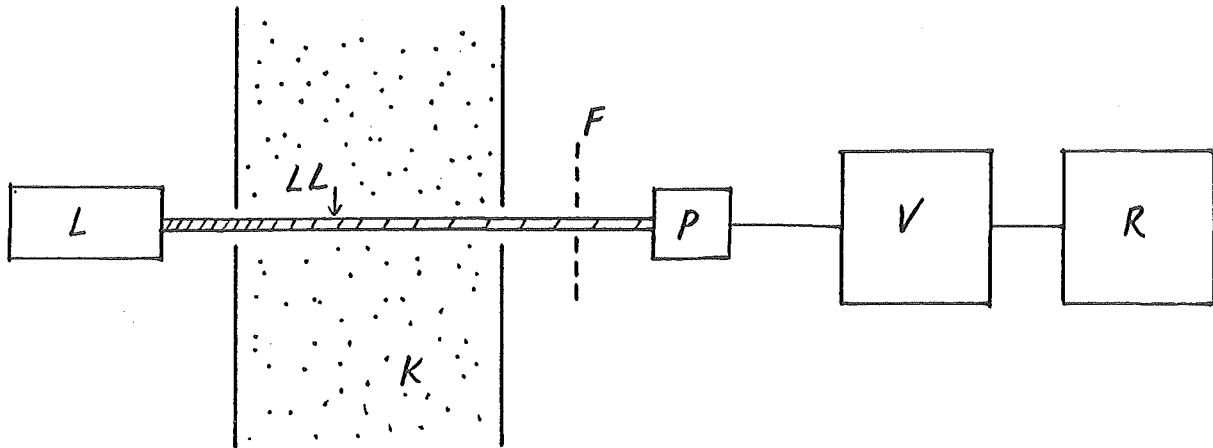
For monitoring the emission of dust, for instance that of fossil fueled power stations, it is up to now customary to use devices that measure the transmission ratios of white light. These measurements are done at relative low dust concentrations. Higher dust contents, for instance those in the flue duct before the precipitator, cannot be determined with these devices. But for a research project such a control has become necessary. The extreme conditions, a dust concentration of about 30 g m^{-3} at normal conditions and a duct width of 4.5 m, seemed to require complex measurements. (A measurement across the total width of the duct has been aspired) The problem was solved utilizing consequently the characteristics of a laser beam. The successfully tested device is a surprising plain construction and it recorded immediately each variation of the operating conditions in the combustion chamber, so that a permanent application is considered now.

For a better understanding the typical characteristics of a laser beam should be mentioned :

1. The light of the used Helium-Neon-Laser is monochromatic, i. e. the bandwidth of the light is less than 1 nm.
2. The radiant intensity of the Laser beam is high.
3. The beam divergence is extremely low. Even in a distance of many meters the beam diameter is practically the same.
4. The light of a laser is highly coherent.

The principle assembly is plain :

As the light transmitter a laser L is used, any system of lenses can be discarded.



The laser light LL penetrates the flue duct K. As the pressure of the flue gas is lower than normal two little holes are sufficient as lead - in and outlet. Before the laser - light, more or less weakened by the dust in the duct, can reach a photo-sensible cell P it has to pass a laserline-filter F. This linefilter can be transmitted only by such a radiation that has precisely the wavelength of the laser light. That means the photo-sensible cell is blocked from any other light that could disturb. The photocell converts the striking laser-light to a corresponding electrical potential. Appropriately amplified the voltage can be recorded.

With this device the first three of the previously mentioned characteristics of a laser beam are utilized. Because of the low beam divergence a single photoelement is enough and no focusing system of lenses or mirrors is necessary. The effects are a simple procedure for adjustment and also a good resolution of low light intensities. The monochromatic light of the laser permits the use of the linefilter. With its bandwidth of 1 nm the filter blockades about 99.7 % of any accidentally incoming white light. The high

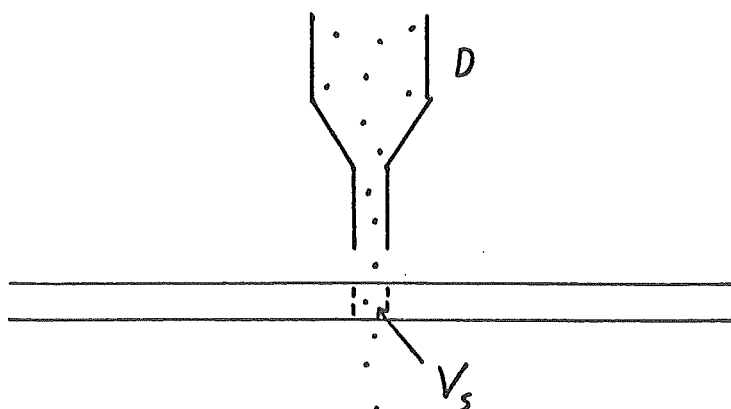
energy density of the laser beam provides that also under the mentioned extreme conditions enough light attains the photocell.

To give some figure data: The output of the used Helium-Neon laser is 5 mW. Under the extreme conditions of a dust concentration of about 30 g m^{-3} and a duct width of 4.5 m the radiant flux was weakened with a factor of about 10^{-5} . The remaining radiant power could be determined perfectly. As modern photocells have a sensitivity range of 7 and more magnitudes the limitation of the described measuring instrument was certainly not reached. It should be added that the instrument is also appropriate for the measurement of low dust contents. At present it is used to record dust concentrations of less than 10 mg m^{-3} in the duct of an electrostatic precipitator.

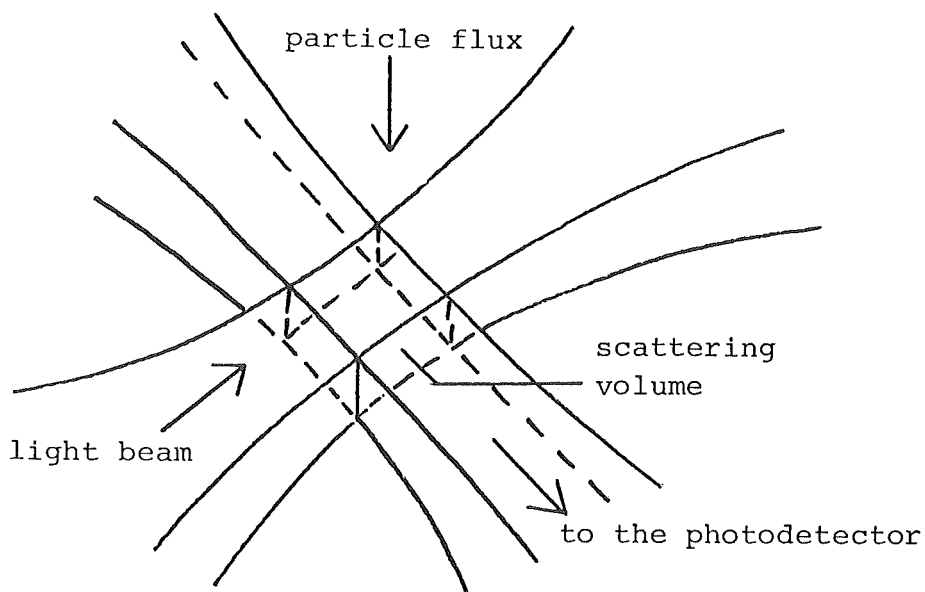
The measurements of the transmission ratio with light have a cardinal disadvantage that should be emphasized also: The transmission ratio depends upon the particle size distribution, too. At the same concentration a dust with smaller particles entails a lower outgoing radiant power of the light beam.

Also therefor one exerts since some years on the problem how to get continuously particle size distributions with optical methods. Two different ways for the solution are known:

The first method consists in determining the size of the single dust particles. The measured and then classified particles are to count. To measure their size the particles are let individually into a light beam and their scattered light is observed. The scattering volume, where the single particles are exposed to the light, can be fixed mechanically or optically. To localized the scattering volume V_s mechanically the dust particles are led through the light beam at one location. This can be done for instance with a nozzle D :



To localize the scattering volume optically one has to use a system of lenses and slits. The intensity of a light beam is made constant relative to its width and only from a certain location the scattered light can get to a photodetector. One proceeds from the assumption that the particles come accidentally into the scattering volume and that they are therefore representative:



Indeed, at both methods of fixing a scattering volume an upper limit of the measurable dust concentration exists. For to avoid an obstruction the mentioned nozzle should have no diameter smaller than 0.2 mm, respectively the extension of the optically fixed scattering volume should not be lower than 0.15 mm due to statistical reasons. Both methods demand therefore a scattering

volume of at least $3 \cdot 10^{-3} \text{ mm}^3$. From that one gets the maximum of the particle number per m^3 as $3 \cdot 10^{11}$. Taking the mean particle diameter as $3 \mu\text{m}$ the highest dust volume per m^3 is about

$$3 \cdot 10^{11} \cdot \frac{\pi}{6} \cdot (3 \cdot 10^{-4} \text{ cm})^3 \approx 4 \text{ cm}^3$$

The upper limit of the dust concentration is therefore at a few grams per m^3 . As a result the optical methods of particle counting are applicable mainly at clean gases.

As light both, white and laser light, can be used. But with this application of a laser the typical characteristics of the laser light are hardly used. Only the high power density brings an advantage that enables to determine also particles in the range below $1 \mu\text{m}$.

For the second optical method to get particle size distributions the laser light should be used. Because here not only a high power density but also monochromatic light is necessary. If a laser beam strikes on a particle that is in front of a screen, a diffraction pattern depending on the size of the particle is generated on the screen. If this screen is a multi-element-photodetector then it is possible to compute from many simultaneous existing patterns the particle size distribution.

Discussion

Discussion was opened by Dr. Cooper, who asked whether the techniques described offered promising prospects for process stream measurements. Mr. Wiggers answered that these measurements could be performed with a Brewster window, cleaned by a jet. No interference by the luminescence of the high temperature stream occurred. Nor was there any window surface on which obscuration could occur. The problem of dust building up on the optic filter was raised by Mr. Kuykendal. Experiments in this had been performed, but further work was necessary, according to Dr. Wiggers. It was important for the laser output to be constant. Two mirrors with low transmittance could be employed and the beam emitted could be used with a photocell to correct charges in output. Dr. Holighaus asked whether results obtained from tests with this equipment were comparable with other measurements made. Mr. Wiggers replied in the affirmative, that experiments had been carried out with white light at power stations. It had been shown that lasers unlike other devices, could measure dust concentrations before electrostatic precipitators.

MANUAL METHODS FOR THE DETERMINATION OF PARTICULATE CONCENTRATION, RESISTIVITY,
AND PARTICLE SIZE DISTRIBUTIONS IN INDUSTRIAL FLUE GASES

Joseph D. McCain
Southern Research Institute
2000 - 9th Avenue South
Birmingham, Alabama 35205
U.S.A.

Descriptions are given of manual sampling and analytical techniques used for determining particulate concentrations and size distributions in the U.S.A.. The methods described include those used for verifying compliance with applicable particulate emission standards, for establishing attainment of control device performance guarantees, and for research purposes on control device performance.

The techniques used for particulate concentration and emission rate determinations are all based on filtration, either internal or external to the duct. The actual sampling protocol depends on the gas conditions and the intended use of the data. Particle size distributions are obtained using a variety of inertial methods for particles having diameters between about 0.5 and 30 μm . Various optical, diffusional, and electrical mobility methods are employed for determinations of particle size distribution and concentration in near real time. The optical techniques provide information over the size range from about 0.3 μm to 50 μm while the diffusional and electrical mobility techniques provide concentration and size distribution information over the size range from about 0.01 μm to 0.3 μm .

In addition, methods for the determination of dust resistivity will be described. One is a field method which provides in situ data, while the second is a laboratory method.

MANUAL METHODS FOR THE DETERMINATION OF PARTICULATE CONCENTRATION, RESISTIVITY,
AND PARTICLE SIZE DISTRIBUTIONS IN INDUSTRIAL FLUE GASES

Design and assessment of the performance of industrial particulate emission control equipment require the measurement of a number of properties of the particulate emissions. Among these are mass emission rates, mass concentrations, particle size distributions, and, in some cases, particulate resistivity. Methods for determining these properties can be divided into two broad classes - manual and automatic. In the context of this discussion automatic methods are those which are used for unattended, continuous, on-line data acquisition while manual methods are those which require continuous or periodic operator intervention and are normally used only on a sporadic basis. This presentation will cover only manual methods.

MASS CONCENTRATION AND MASS EMISSION RATE

Gravimetric methods using filtration for obtaining samples are used for determinations of mass concentration and mass emission rates. Samples are obtained by withdrawing measured gas volumes from the process stream for equal time intervals at a series of points across the duct. These traverse points are located at the centers of zones which divide the duct into a number of zones of equal area. The number of zones into which the duct is divided depends on the distances to upstream and downstream flow disturbances and the duct dimensions. All samples are taken under isokinetic conditions.

One of two general types of sampling systems is used for these determinations depending on the test conditions and the purposes for which the data are being acquired. The simpler system, illustrated in Figure 1, utilizes a filter holder and attached sampling nozzle which are introduced directly into the gas stream. The filtration medium may be a flat glass fiber filter, a glass fiber thimble or an alundum (ceramic) thimble. The choice depends on gas temperature, the concentration of the particulate matter, and the intended use of the data. A pitot tube and thermocouple located adjacent to the sampling nozzle make it possible to continuously monitor the gas velocity and permit correction of the sample flow rate as required to maintain isokinetic sampling conditions. On those occasions when the velocity field within the duct is stable over long periods of time separate traverses may be made for determination of velocity and dust sampling, in which case the pitot tube on the sampling probe may be omitted. This system is frequently used for determining whether a control device is meeting performance guarantees and for some research purposes, but in most instances cannot be used for determining compliance with applicable air pollution regulations in the United States of America.

Testing for compliance with air pollution regulations, with few exceptions, must be done with the system shown in Figure 2. This system, known as the U.S. Environmental Protection Agency's Method 5 sampling train, uses a nozzle and heated probe to withdraw the sample from the duct to a filter located within a temperature controlled oven.

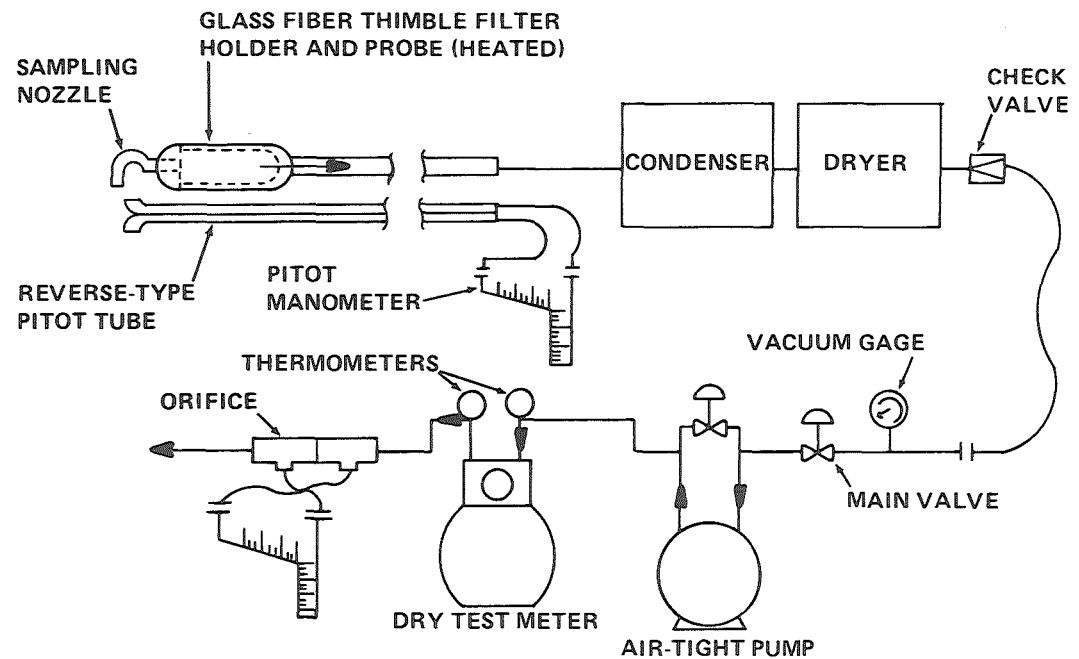


Figure 1. American Society For Testing and Materials' Particulate Sampling Train.

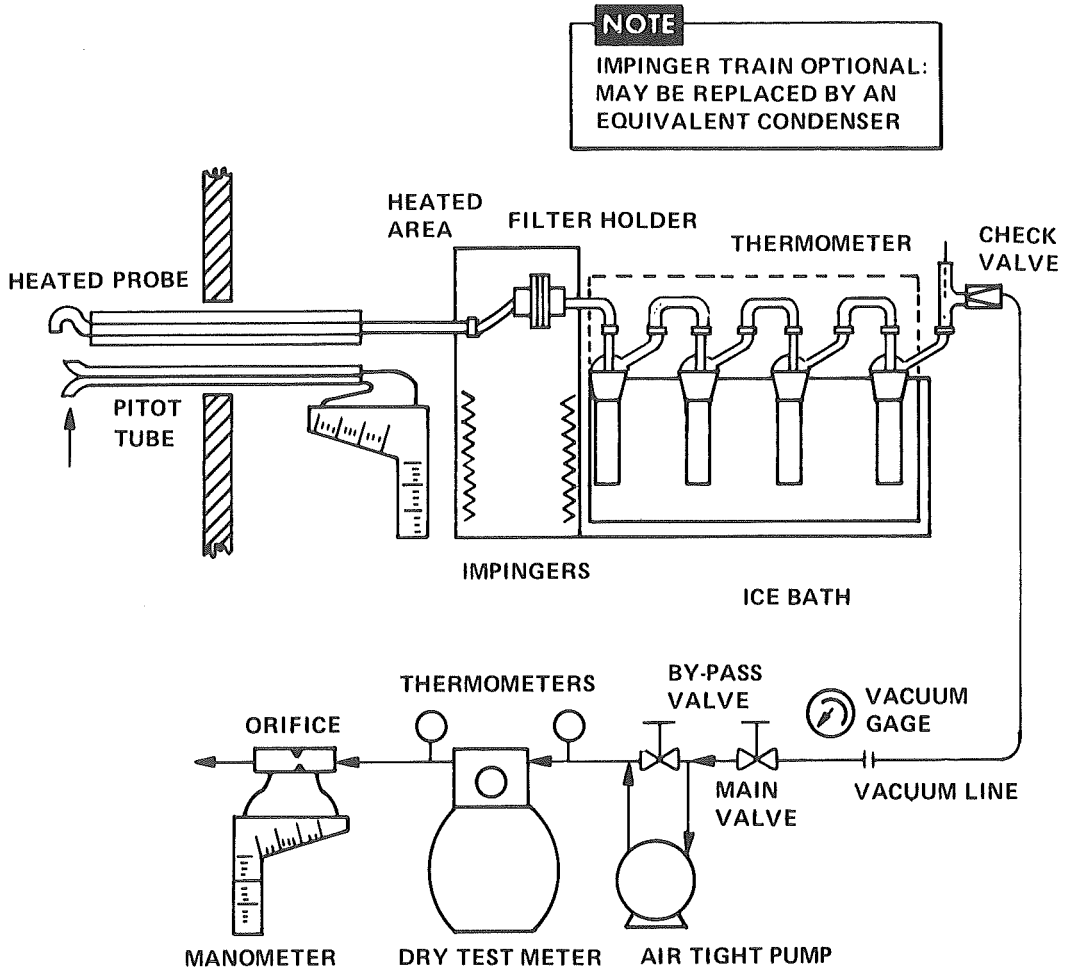


Figure 2. U.S. Environmental Protection Agency's Method 5 Particulate Sampling Train.²

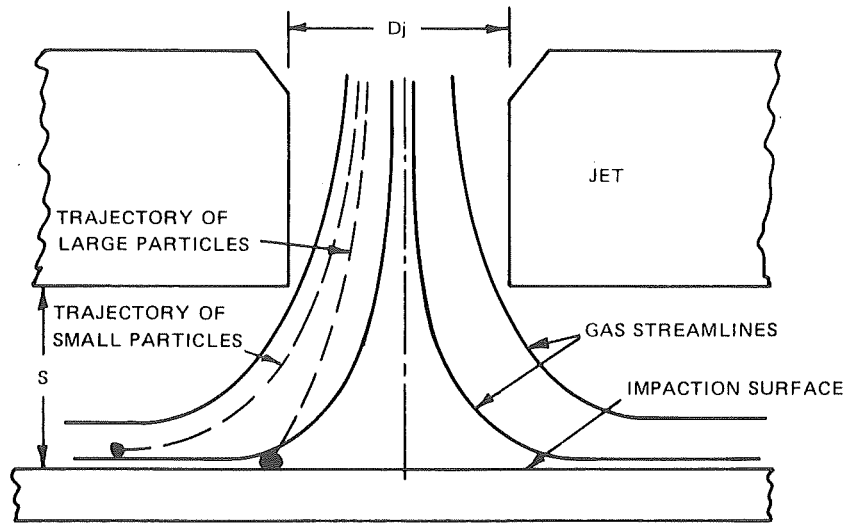
The filter may be followed by either a condenser and moisture absorbent or by a series of impingers and an absorbent. A leakless pump is used to provide the necessary suction downstream of which are located a dry gas meter and an orifice-type flow meter. The latter is used for monitoring and setting the sampling rate during a test. This system provides for simultaneous determinations of volumetric gas flows within the duct being tested, mass emission rate, mass concentration, and moisture content. The use of appropriate reagents in the impinger portion of the train permits simultaneous determination of one or more vapor phase components of the flue gas as well (e.g., SO_3 , SO_2). The probe connecting the nozzle and filter housing must be glass lined or, if longer than 2.5m, may be stainless steel or Incolloy. With the exception of tests of fossil fuel utility boilers the temperatures may be raised to 165 C to prevent or minimize the addition of sulfuric acid condensate to the particulate catch. Sampling rates range from 20 ℓpm to 200 ℓpm .

PARTICLE SIZE DISTRIBUTIONS

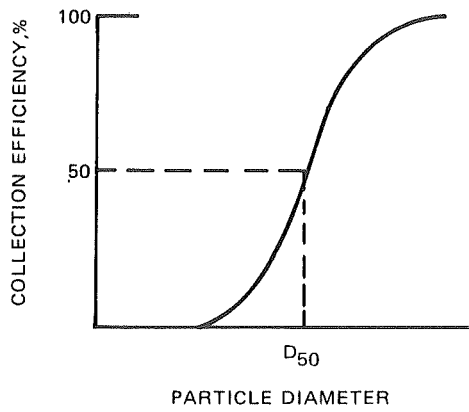
The methods most widely used in the U.S.A. for the determination of particle size distributions of industrial flue gas particulate matter are based on inertial separation. The separators include cascade impactors, cyclone separators, and other forms of air elutriators, including the Bahco "microparticle classifier." Because of the lack of resolution in the fine particle end of the size spectrum and the problems inherent in the redispersion of collected aerosols, the use of laboratory devices such as the Bahco are generally being discarded in favor of other devices which perform the size separation during the sampling operation.

The cascade impactor is the device most commonly used at this time for determining particle size distributions. The operation of an impactor stage is illustrated in Figure 3. An aerosol sample is withdrawn isokinetically from the gas stream and passed sequentially through a series of impingement stages like that shown in Figure 3. Each succeeding stage operates at higher jet velocities than the previous stage thereby removing successively smaller particles at each stage. Determinations of the amount of particulate matter collected on each stage is then made either by gravimetric or chemical analysis. The particle size range spanned by an impactor is usually from about 0.50 μm to 10 μm . The number of stages ranges from about 6 to 13 and flow rates range from about 0.6 ℓpm to 30 ℓpm . Prototypes of impactors providing size distribution information to diameters as small as 0.02 μm have been constructed and successfully tested at industrial sites. Figures 4 and 5 show two of the more popular conventional (0.5 μm to 10 μm) impactors in use today.

The cyclone separator is a second type of inertial separator which is in fairly wide use at the present time. Small cyclones have been demonstrated to provide rather sharp particle size selection characteristics as illustrated in Figure 6. This shows calibration data obtained using monodisperse aerosols for a "cascade cyclone" designed and constructed by Southern Research Institute for the U.S. Environmental Protection Agency. The system operates at a nominal flow rate of 28 ℓpm and provides particle size information from about 0.3 μm to 7.0 μm . Figure 7 illustrates the cyclone system itself. Cyclonic type collectors

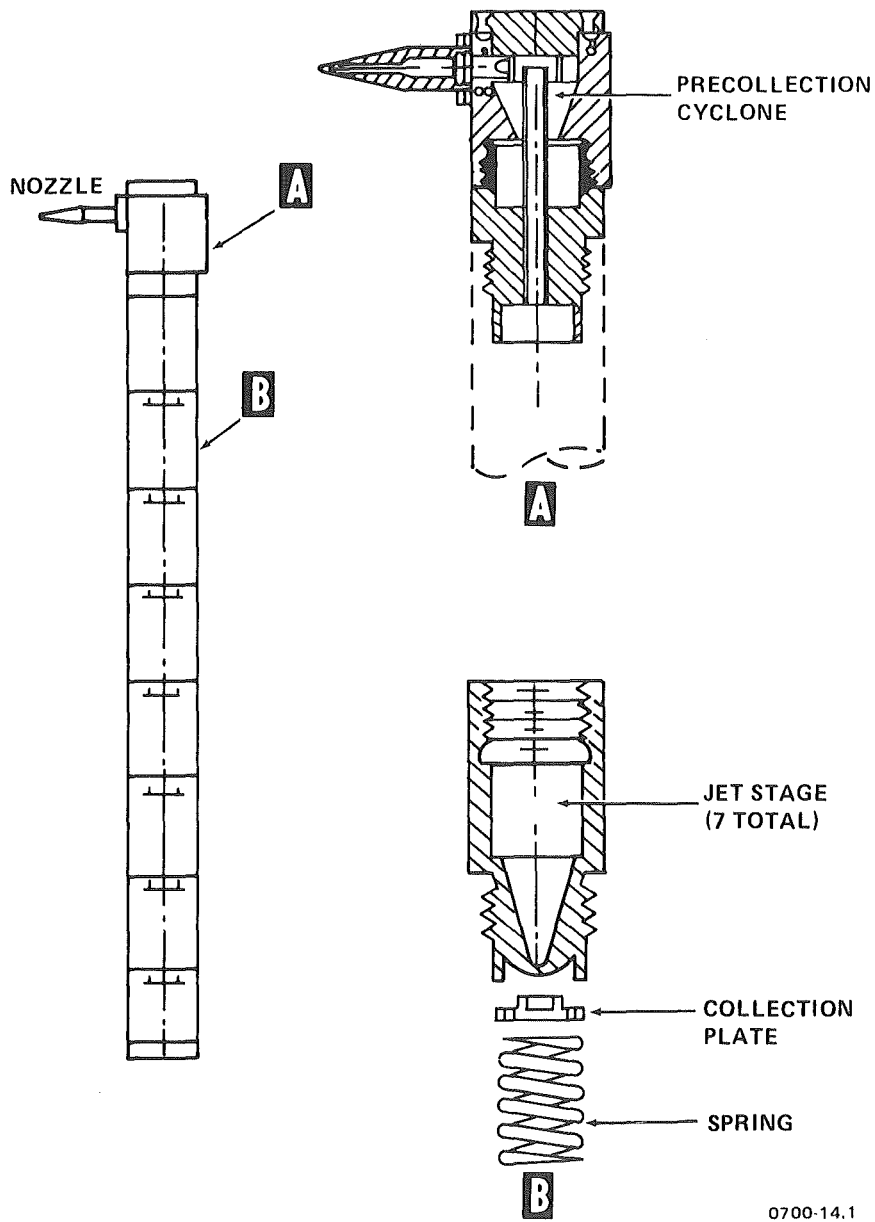


A. TYPICAL IMPACTOR JET AND COLLECTION PLATE



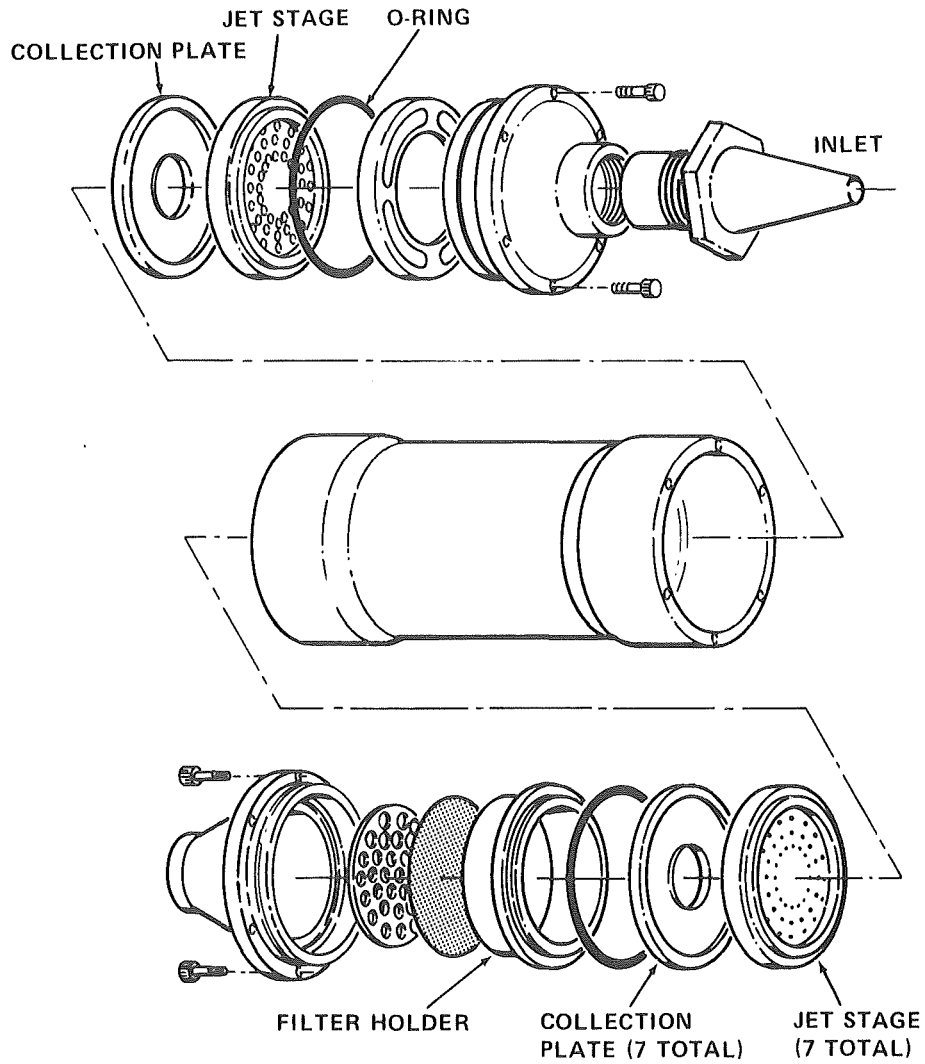
B. GENERALIZED STAGE COLLECTION EFFICIENCY CURVE

Figure 3. Operation principle and typical performance for a cascade impactor.



0700-14.1

Figure 4. Modified Brink Model BMS-11 Cascade Impactor.



0700-14.2

Figure 5. University of Washington Mark III Source Test Cascade Impactor.

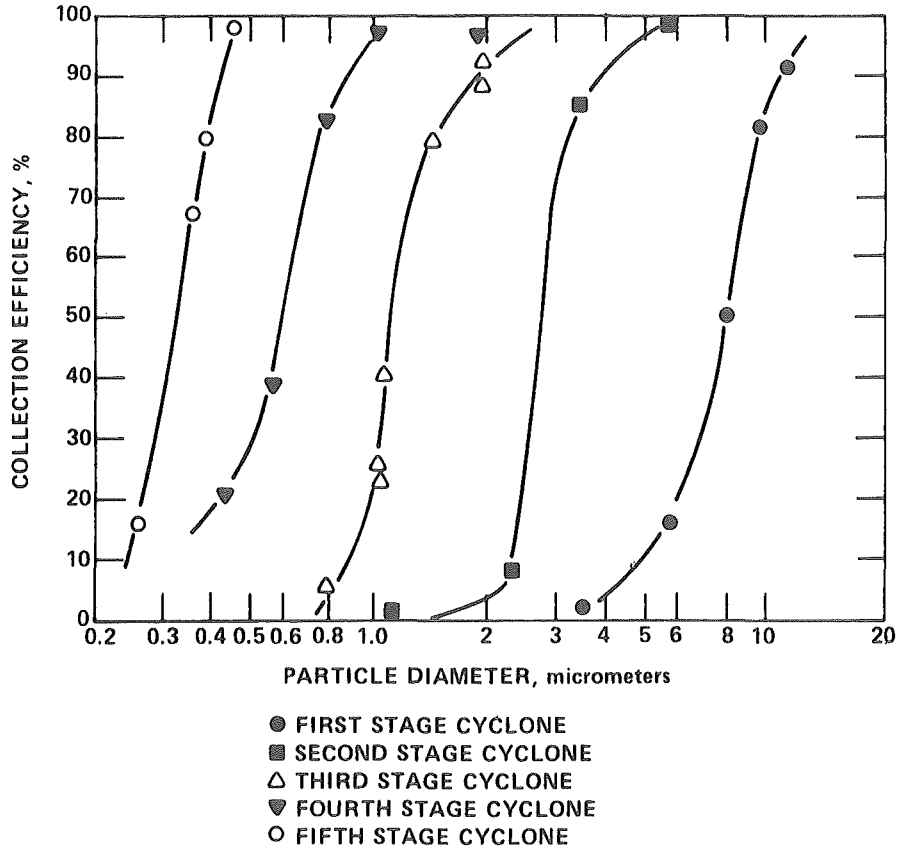


Figure 6. Laboratory Calibration for the Five Stage Series Cyclone System. (472 cm³/sec, particle density--1.0 gm/cm³).³

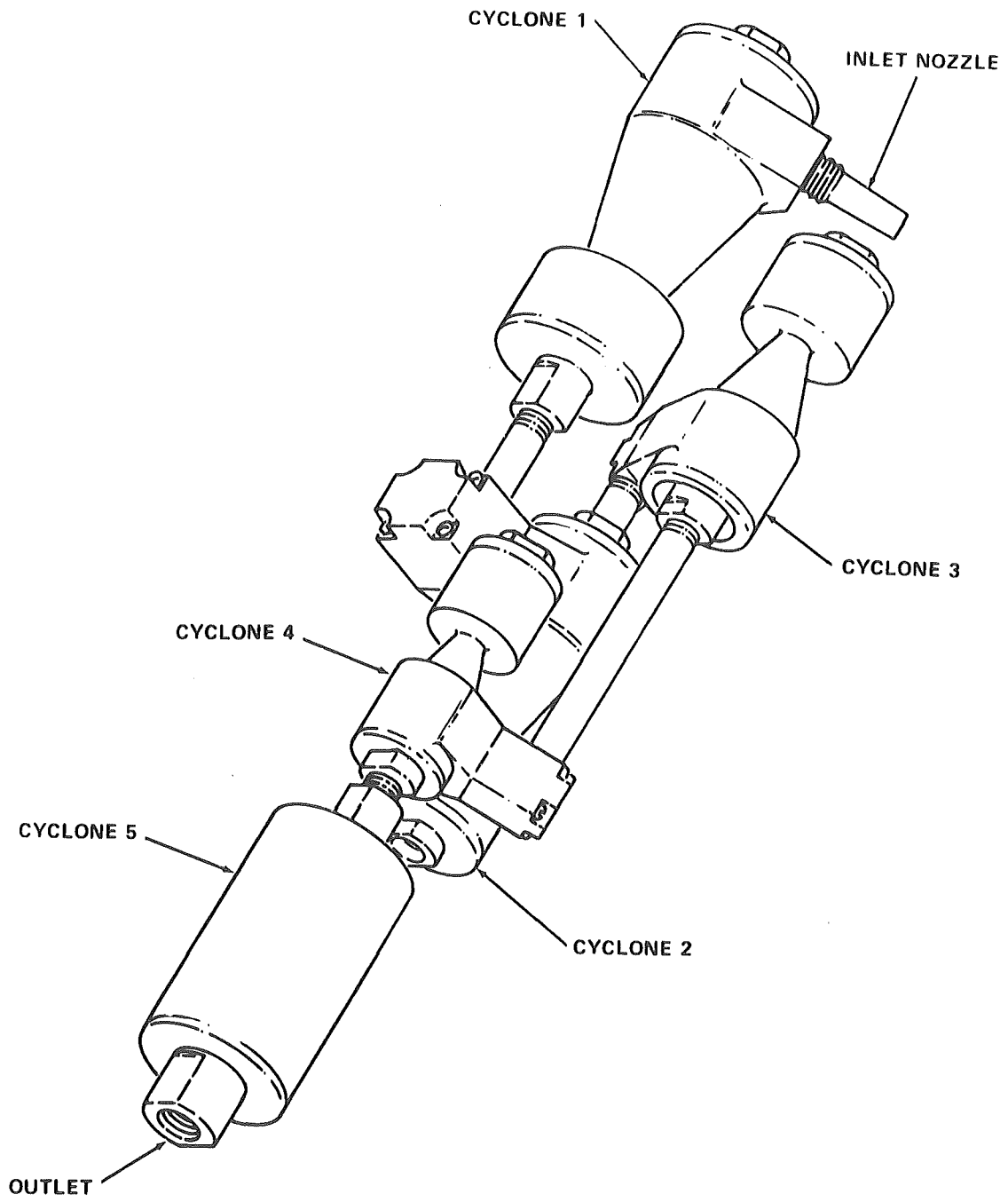


Figure 7. Five Stage Series Cyclone System.³

are particularly useful when sampling gas streams having high dust concentrations, which tend to lead to rapid overloading of impactors, and when large samples are needed for chemical or toxicological studies. They may also be a valuable tool for determining size distributions in high temperature process streams (600°C to 1100°C) such as those associated with coal gasifiers and fluidized bed combustors for combined cycle electrical generating stations. Cascade impactors may not be suitable for high temperature studies because of a lack of a suitable substrate on which to collect the particles. Small cyclonic separators are also frequently used as precollectors upstream of cascade impactors to eliminate rapid overloading of the first impaction stage. Figure 4 shows one application of a cyclone precollector.

A three-stage "cascade cyclone" operating at a flow rate of 140 sLpm is in routine use today as a part of the Source Assessment Sampling System (SASS). The SASS, illustrated in Figure 8, is used for providing semiquantitative information on the form, nature, and composition of pollutants emitted from industrial processes for the purpose of assessing their potential impact on the environment. The system provides size segregated samples of particulate matter in four size ranges (greater than 10 μm , 3 μm to 10 μm , 1 μm to 3 μm , and smaller than 1 μm), usually in sufficient quantities for chemical analysis and for toxicological studies to determine their potential impact on human health and terrestrial and aquatic ecosystems. In addition to the particulate samples, the system also provides samples of organic and inorganic vapors for similar analyses.

Optical and electron microscopy are also used occasionally for determining particle size distributions but difficulties in obtaining unagglomerated samples at suitable surface densities on the collection media while still collecting a truly representative sample make the use of microscopy infrequent.

Size distributions are measured rather frequently using inertial techniques to provide information for particles larger than 0.5 μm . Details of particle size distributions from about 0.01 μm to about 0.5 μm (ultrafine particles) are desired or needed occasionally, but far less frequently than for the larger particles. Electron microscopy is sometimes used to provide information on the ultrafine particulate size distribution. Here again, difficulties in obtaining suitable representative, uncontaminated, unagglomerated samples make this an infrequently chosen method. The methods most frequently used for the determination of the concentrations and size distributions of ultrafine particles are diffusional and electrical mobility analyses.

Diffusional methods generally use condensation nuclei counters for measurement of particle concentrations and diffusion batteries for providing the necessary particle size discrimination. The condensation nuclei counter, illustrated in Figure 9, operates by causing a sample of the aerosol being measured to become supersaturated in the concentration of some condensible vapor--usually water or alcohol. The supersaturated vapor will condense on any particles present in the sample having diameters larger than some critical diameter which is determined by the particle solubility and the amount of supersaturation achieved.

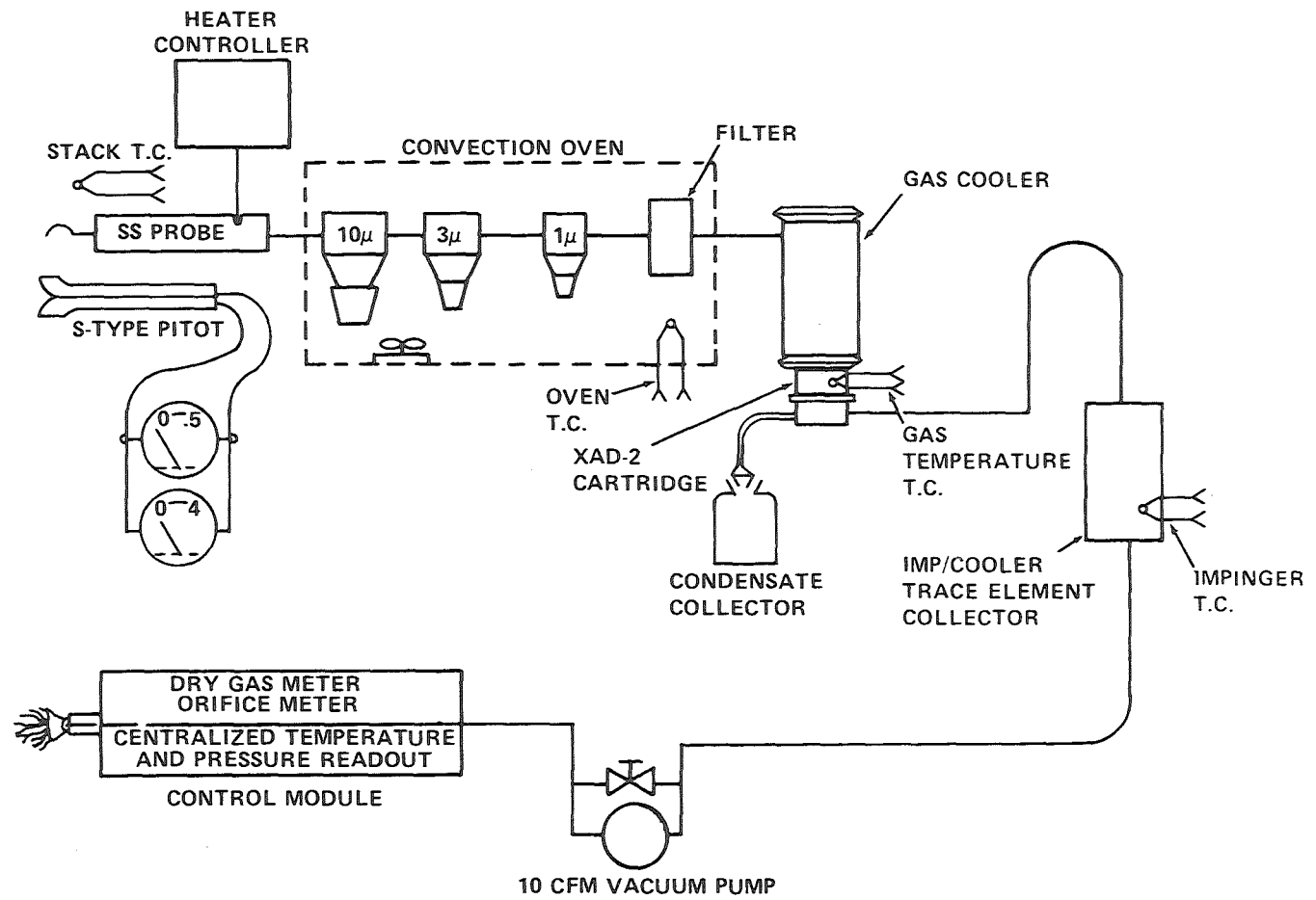
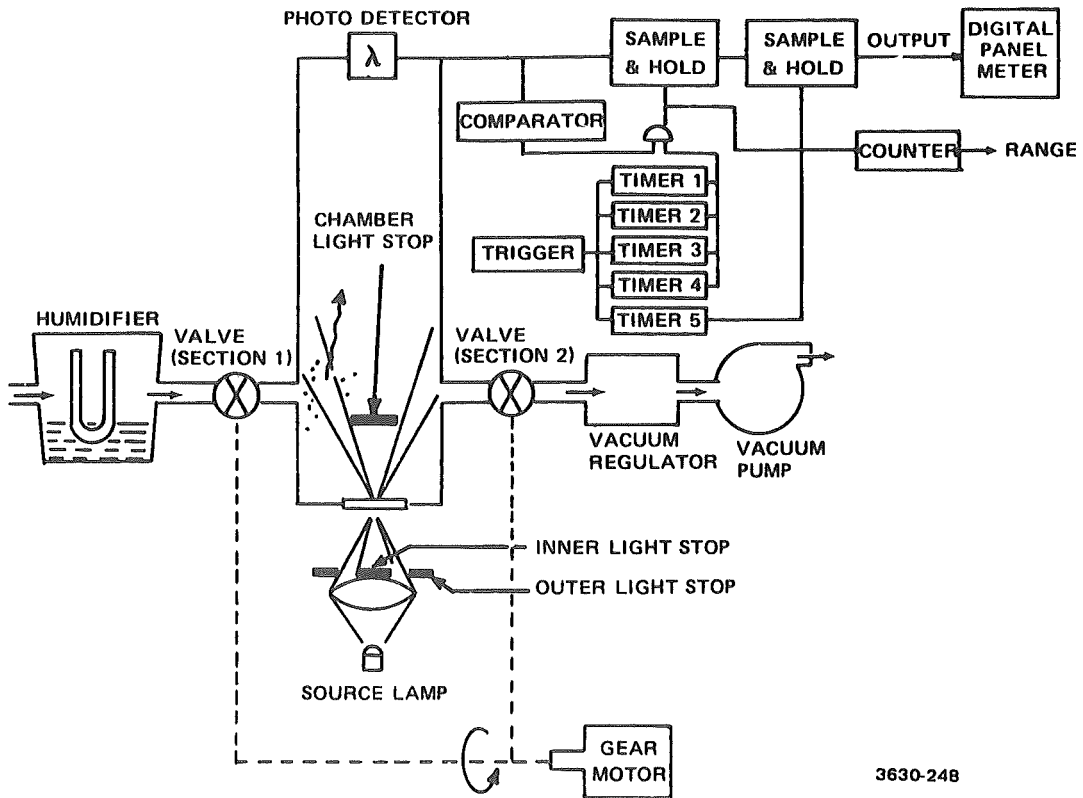


Figure 8. Schematic of the Source Assessment Sampling System.⁴



3630-248

Figure 9. Diagram of a condensation nuclei counter. After Haberl and Fusco.⁵

This critical diameter is typically about $0.002 \mu\text{m}$. The condensation of the vapor results in the formation of a rather homogeneous, monodisperse fog containing one fog droplet for every particle in the sample which had a diameter larger than the critical nucleation diameter. Light scattering techniques are then used to determine the concentration of the fog droplets and hence the original concentration of the particles whose diameters were larger than the critical size. Size distributions are then determined by measuring the concentrations of a sample gas stream upstream and downstream of a series of tubes, narrow parallel rectangular channels, or screens for which losses resulting from particle diffusion (resulting from Brownian motion) to the internal surfaces can be predicted as functions of particle size. Figure 10 illustrates a typical diffusion battery of the parallel rectangular channel type and penetration curves for a particular set of flow conditions. The condensation nuclei counters require samples which are essentially at ambient pressure and temperature and which have much lower particle concentrations than those typically found in industrial flue gases. Therefore extractive sampling is required followed by extensive dilution and sample conditioning to remove undesirable condensable vapors. A schematic diagram of a complete system used for such analyses by Southern Research Institute is shown in Figure 11. Dilutions from 10:1 to 4000:1 can be provided with the system. Diffusional analyses typically provide data over the size range from about $0.01 \mu\text{m}$ to $0.2 \mu\text{m}$.

Electrical mobility techniques provide an alternative to the diffusional techniques for making measurements of ultrafine particles. In this technique the particles are charged to predictable levels whereupon they are passed through a mobility analyzer in which particles having progressively lower mobilities are removed by making step increases in the applied electric field in the mobility analyzer section of the instrument. Figure 12 illustrates a commercial instrument of this type. Because there is a monotonic relationship between particle mobility and size in the size range of interest, sorting the particles by mobility leads to size separation of the particles. Concentrations are determined by measuring the current carried by the particles which are not collected in the mobility analyzer portion of the device. This current coupled with the known (predicted) charge per particle permits the calculation of the particle concentration at the exit end of the analyzer. This device, like the condensation nuclei counter, also requires that the sample be at or near ambient temperature and pressure and that the particle concentrations be much lower than those found in most flue gases. Thus a dilution and conditioning system like that used for diffusional analyses is required. The electrical mobility technique, like the diffusional technique, is capable of providing near real time output for monitoring process variations.

Optical single particle counters such as those illustrated in Figure 13 are sometimes used to provide real time data on the concentration and size distributions of particles larger than about $0.3 \mu\text{m}$ (a new counter has recently been introduced with detection and sizing capabilities down to a diameter of about $0.08 \mu\text{m}$ but this device has not been utilized in flue gas sampling to date). These counters operate by sensing the light scattered by individual particles

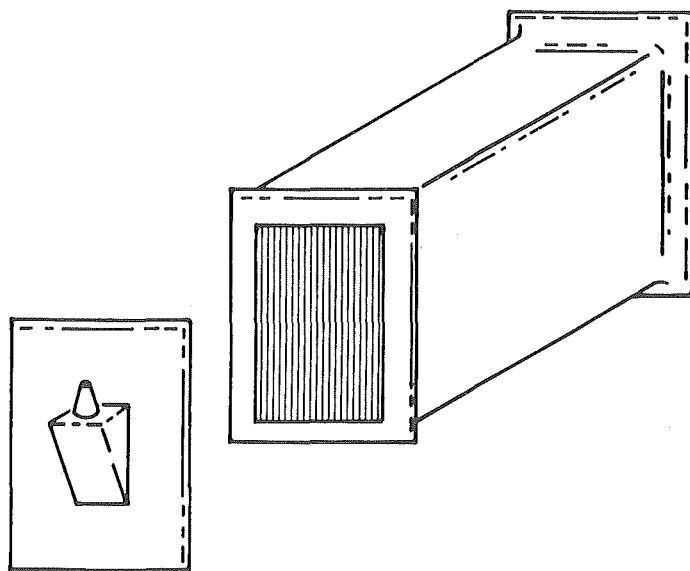


Figure 10a. Parallel plate diffusion battery.

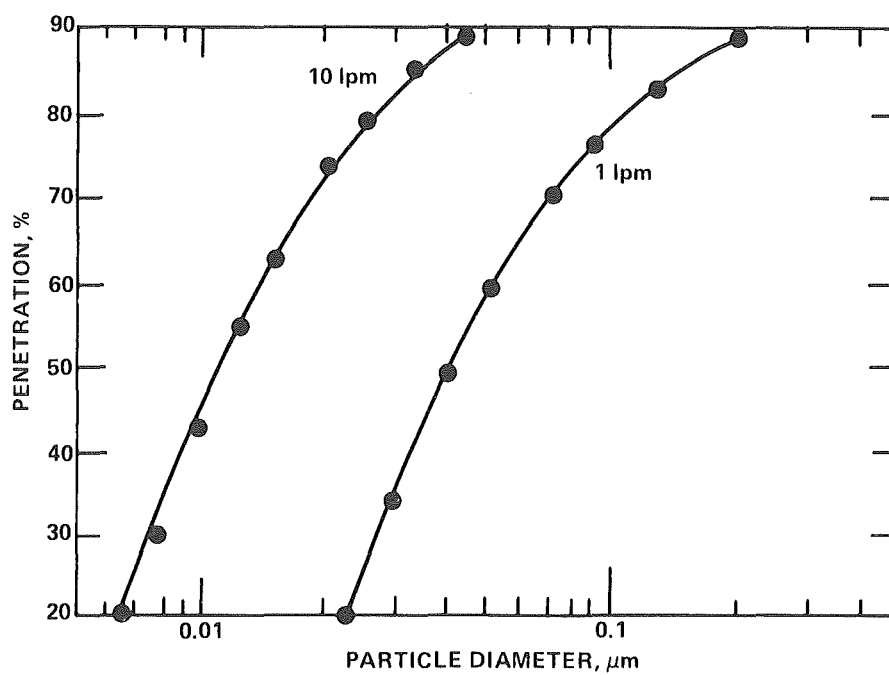
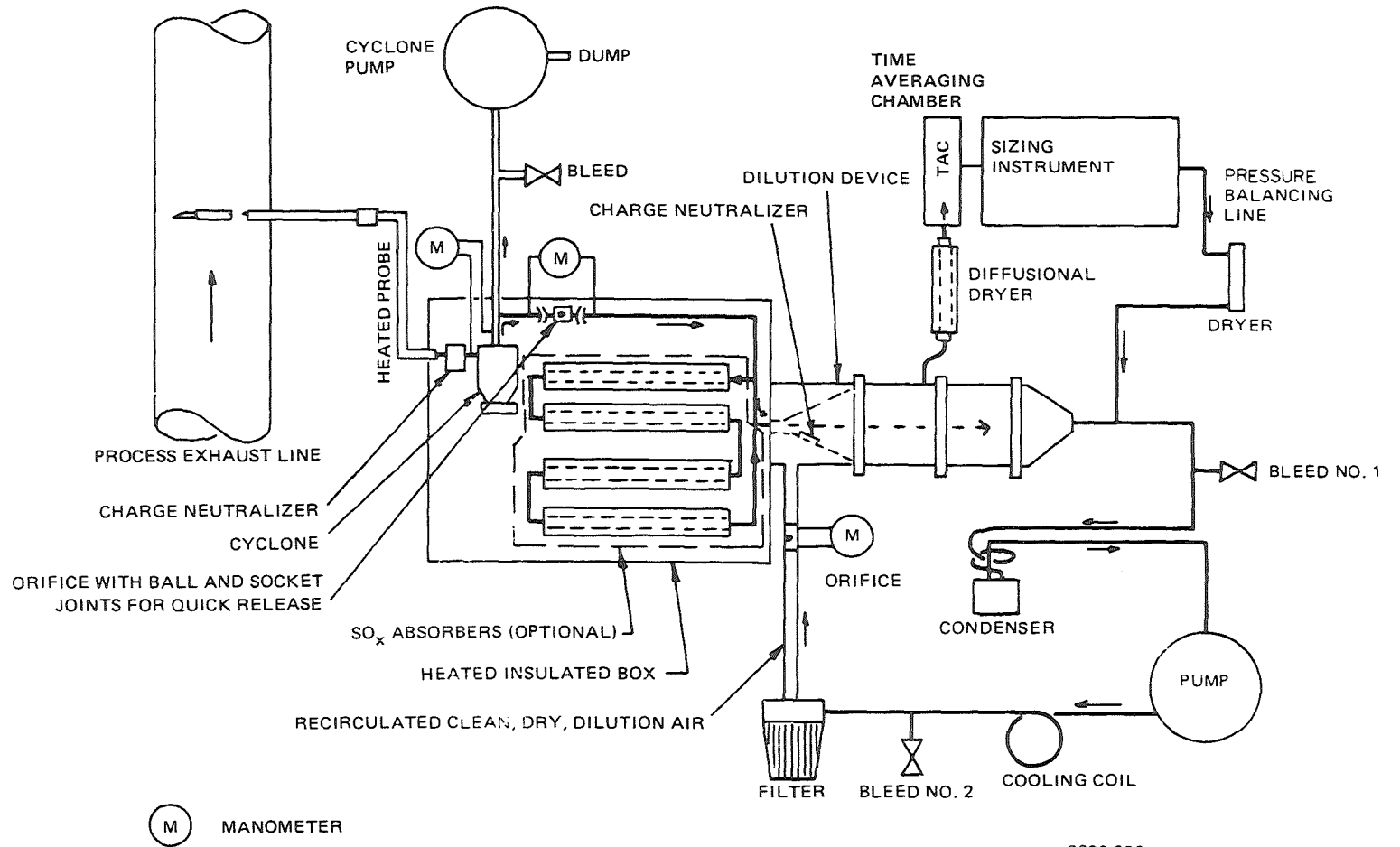


Figure 10b. Parallel plate diffusion battery penetration curves for monodisperse aerosols (12 channels, 0.1 x 10 x 48 cm).⁴



3630-036

Figure 11. Sample Extraction-Dilution System (SEDS).⁴

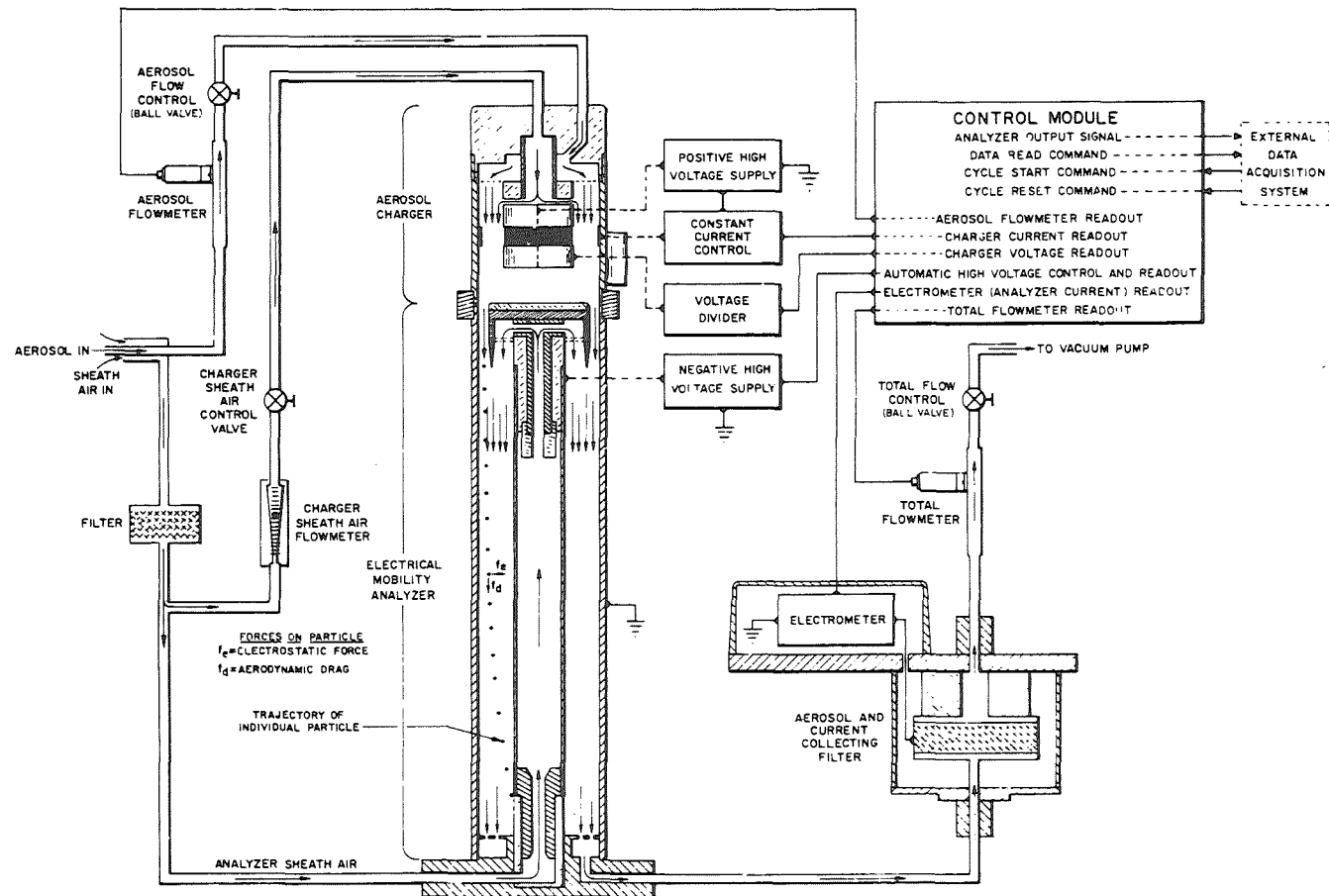


Figure 12. Flow schematic and electronic block diagram of the Electrical Aerosol Analyzer. Liu and Pui.⁶

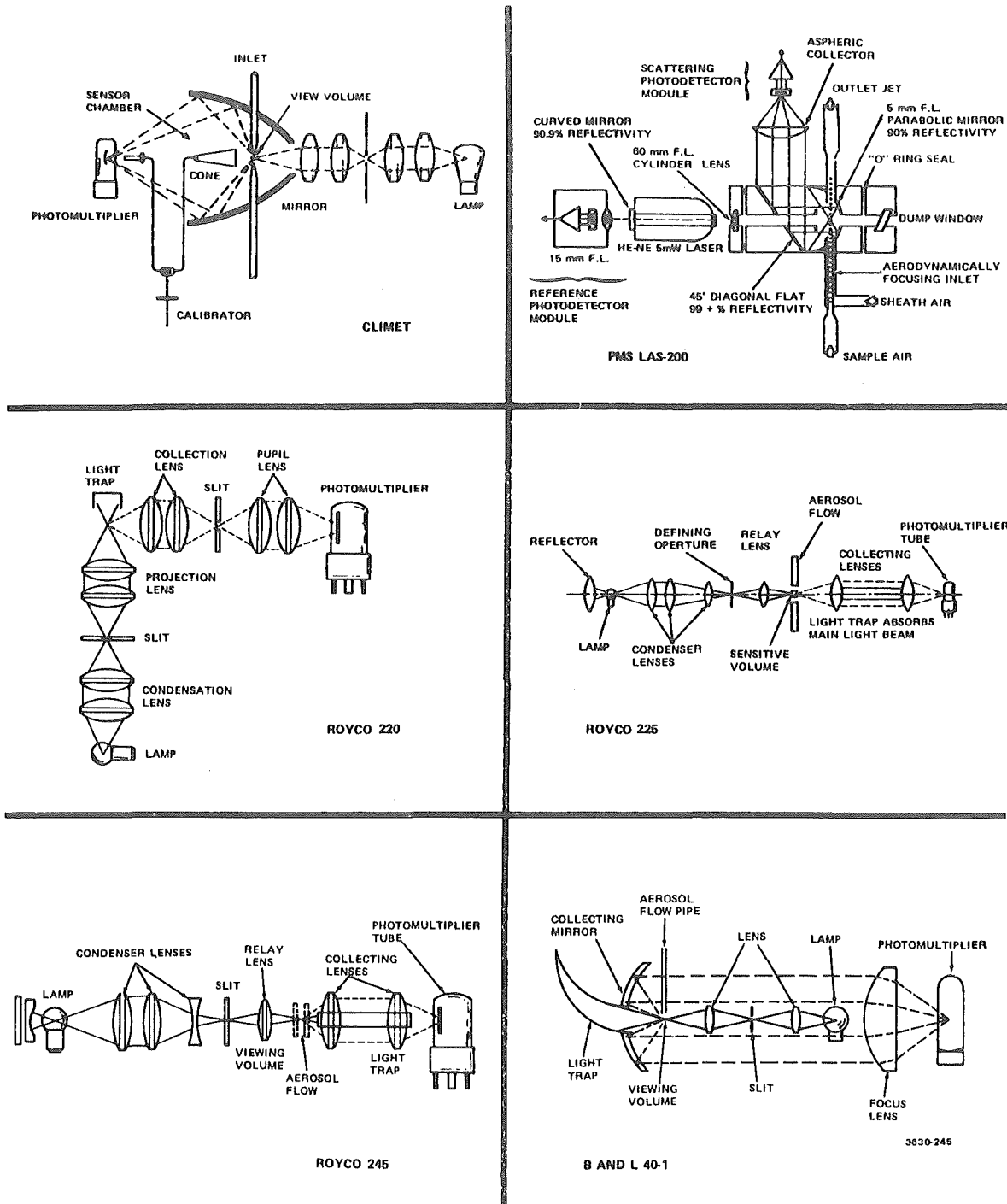


Figure 13. Optical configurations for six commercial particle counters.

as they pass through a small sensing zone. The intensity of the scattered light from the particle provides a measure of its size while the rate at which the particles pass through the sensing zone provides a measure of particle concentration. Typical counting rates are 5000 to 10000 particles per second. These devices also require extensive dilution and sample conditioning for use in measuring industrial process streams. They can provide very useful information regarding process variations and for control device diagnostics (e.g., characterizing emissions from dry electrostatic precipitators resulting from the cleaning of the collecting electrodes).

DUST RESISTIVITY

Because of the widespread use of dry electrostatic precipitators for the control of industrial particulate emissions the resistivity of the dust to be collected can be of great importance. A dust having a high resistivity ($>2 \times 10^{10}$ ohm-centimeters) can tend to limit the maximum operating currents in an electrostatic precipitator because of electrical breakdown within the collected dust layer and the resultant back corona. Resistivity determinations can be made using either in situ or laboratory techniques. Because of possible changes in the surface chemistry of the dust particles when a sample is extracted and cooled for transport to the laboratory the in situ analysis is preferred. The in situ resistivity probe, illustrated in Figure 14, uses a point-plane precipitator to deposit a dust layer on a collection disk. The voltage and current of the precipitator are monitored during the sample deposition phase as the difference between clean plate and dirty plate voltage-current curves provides one means of resistivity determination. After the dust layer is collected a movable pad is lowered by means of a micrometer actuated system to simultaneously measure the thickness of the deposited layer and to provide a second disk electrode. Voltage-current characteristics are then measured across the dust layer which is now contained between the two disks. This then provides the necessary information for a second means of the determination of the resistivity. The second method is more reliable.

A similar, but much larger, cell is used for the laboratory determination. However, in this case the dust sample is a bulk sample previously taken from the gas stream which is simply poured and tamped into the cell until a certain surface bearing strength is reached. The cell is then placed in an oven, in simulated flue gas conditions, and the voltage-current characteristics of the dust layer are measured at the required temperature(s).

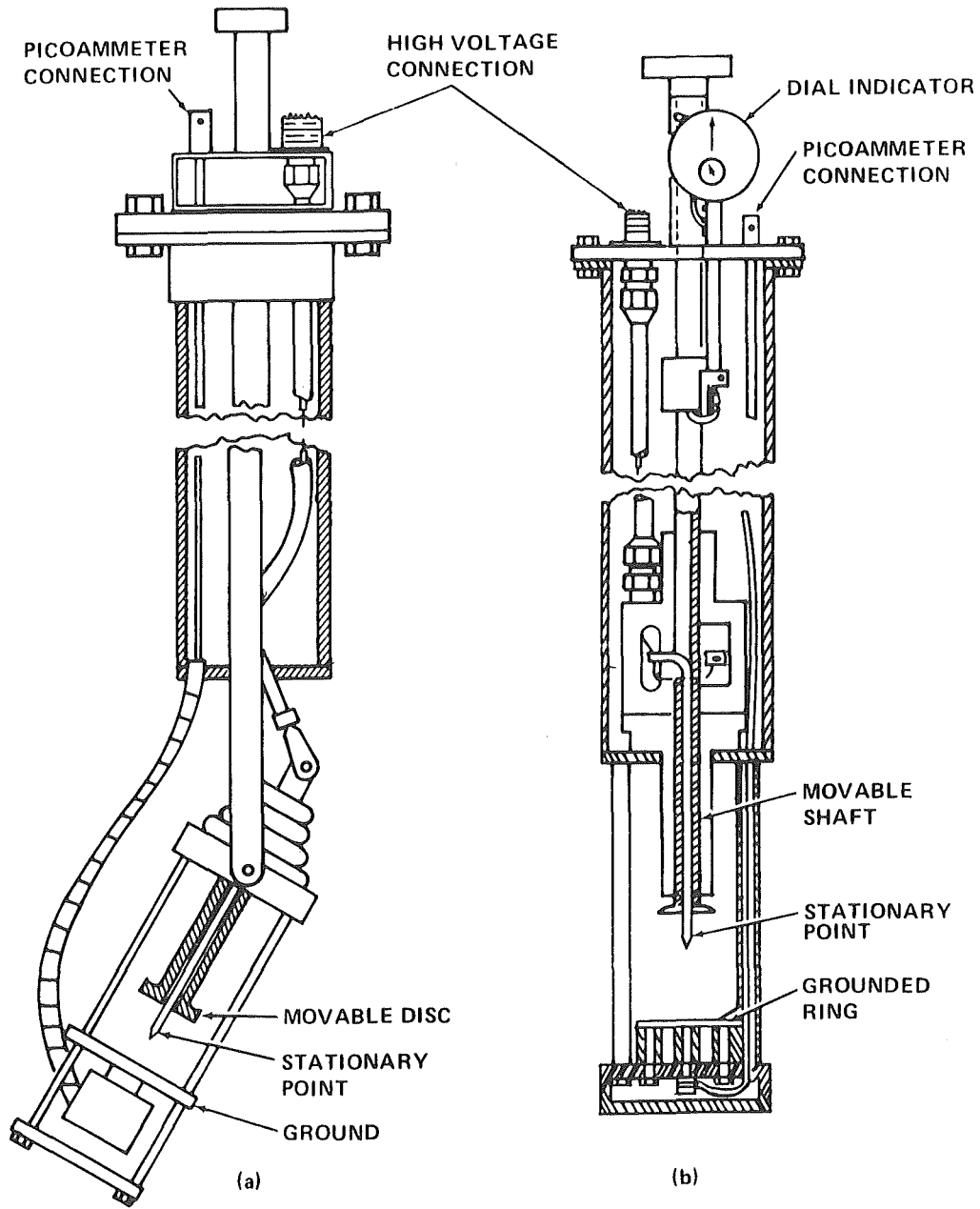


Figure 14. Two types of point-to-plane resistivity probes.⁴

REFERENCES

1. American Society For Testing and Materials. Standard Method For Sampling Stacks For Particulate Matter. Designation D2928-71, Annual Book of ASTM Standards, 1977.
2. Federal Register. Standards of Performance For New Stationary Sources: Revision to Reference Methods 1-8. Volume 42, Number 160, Thursday, August 18, 1977, pp. 41753-41789.
3. Smith, Wallace B. and R. R. Wilson, Jr. Development and Laboratory Evaluation Of A Five-Stage Cyclone System. Interagency Energy-Environment Research and Development Program Report, EPA-600/7-78-008, January, 1978. U.S. Environmental Protection Agency, Office of Research and Development, Research Triangle Park, NC 27711.
4. Smith, W. B., K. M. Cushing, and J. D. McCain. Procedures Manual For Electrostatic Precipitator Evaluation. Interagency Energy-Environment Research and Development Program Report, EPA-600/7-77-059, June, 1977. U.S. Environmental Protection Agency, Office of Research and Development, Research Triangle Park, NC 27711.
5. Haberl, J. B. and S. J. Fusco. Condensation Nuclei Counters: Theory and Principles of Operation. General Electric Technical Information Series, No. 70-POD 12 (1970).
6. Liu, B. Y. H., and D. Y. H. Pui. On the Performance of the Electrical Aerosol Analyzer. J. Aerosol Science, 6, pp. 249-64 (1975).

Discussion

Mr. G^uthner asked what the upper dust concentration limit was for cascading impactors. Mr. McCain answered that a maximum load to each stage was more significant than the dust concentration. Dust loadings up to 10 mg per impactor stage are usually acceptable. Reasonable sampling times (15-30 min) are usually possible with dust concentrations of 2 to 10 g/m³. At the precipitator inlet, the use of a small cyclone before the impactor was usual. Large particles with high momentum could rebound, biasing the findings. These could be removed by a cyclone however. (more information on Cascade measurement techniques could be obtained from EPA; National Technical Information Center).

Mr. Gooding asked whether a test using in situ resistivity had been done. Mr. McCain said that one very inconclusive preliminary test (at a high temperature) had been carried out. Further investigations had also met with little success. Dr. Gooch added that two measurements had been made at the plant, before this self-destructed. Data corresponded to laboratory temperature data (300°C).

In reply to a question by Mr. Wiggers, Mr. McCain said that resistivity was measured by a plate with electrical contact; a small voltage existed between a pad and a collection plate. Both voltage and current were measured. The dust package count charged slightly and clean plates became necessary as dust was collected.

INSTRUMENTAL TECHNIQUES FOR SIZING INDUSTRIAL SOURCE PARTICULATE

William B. Kuykendal
Process Measurements Branch
Industrial Environmental Research Laboratory
Environmental Protection Agency
Research Triangle Park, North Carolina

Introduction

Over the past several years there has been an active interest within the Environmental Protection Agency, as well as within other organizations, to develop instrumentation that can measure particle sizes in industrial sources. This interest stems, for the most part, from a desire to develop engineering data which will allow for the development, evaluation, and refinement of particulate control devices.

Ideally an instrument should size the particulate without disturbing it or its flow field yet obtain a sample of the particulate for subsequent chemical and toxicological analysis. Such an instrument should have real time output and two or more sensors so that particulate control devices could be evaluated on line. The particle size range of interest for control device evaluation would be 0.01 to 10 micrometers. The preferred sizing parameter would be the aerodynamic diameter, although the optical diameter is also of interest.¹ Clearly some of the items on this ideal list are very optimistic while others appear to be unachievable. For example, it would be most difficult to obtain a sized particulate sample for subsequent analysis and not disturb the particle.

The purpose of this paper is to present recent and current work in summary form so that the reader may obtain a concise picture of the direction of EPA's research in the area of particle sizing instrumentation. Seven instruments will be discussed. The first three are optical instruments which make use of light scattering techniques to give an optical particle size. The next three instruments all use inertial impaction to size segregate the particles. Various schemes are used to detect the particles to yield the aerodynamic particle diameter. The final instrument uses an acoustic approach to aerodynamically size the particulate. Table 1 presents a summary of these instruments.

PILLS IV

The Particulate Instrumentation by Laser Light Scattering (PILLS) family of instruments has been developed by Environmental Systems Corporation of Knoxville, Tennessee. The PILLS IV is the fourth instrument in the series and was designed specifically to size particulate in industrial stacks at temperatures up to 200°C. The instrument schematic

in Figure 1 shows how the instrument operates. The light source of the PILLS IV is a GaAs diode laser with a lens system that focuses the beam to a very small cross-section of the order of tens of microns across. There are three photo detectors at angles of 14° , 7° , and 0° from the incident beam. The detector at 0° is used to monitor the undeviated beam to establish a reference for the 14° and 7° detector signals. When the laser is pulsed (10^3 times/sec), the 14° and 7° detectors respond to the scattered light from a particle in the view volume. If the ratio of these two signals (7° - to 14° -signal) is greater than 1.1, then a particle size is inferred from its value. If the ratio is less than 1.1, the signal from the 14° detector is used to determine particle size.

The output of the PILLS IV is the number of particles per channel in two series of channels, one series corresponding to values of the signal ratio and one series to values of the 14° -signal. The upper and lower limits of each channel can be varied by the operator, who then relates particle size to each channel from calibration curves. One curve gives the 14° detector signal versus particle size, and the other gives the ratio of the 7° -signal to the 14° -signal versus particle size.²

The entire optical assembly is housed in an air cooled probe which can be inserted through a standard 10 cm sampling port. The cooling air doubles as purge air to keep the optics clean.

The PILLS IV was evaluated in a wind tunnel test to compare its results with those from other particle sizing techniques. Figure 2 shows the results from this study. It can be seen that the output from the PILLS IV differs considerably from the results obtained by cascade impactors represented by the solid curve.³ The anomalous response of the PILLS IV at the low end of the size range is of particular concern. This problem appears to result in changes in the sizing volume caused by the two different size ranges used by the instrument. This problem could perhaps be overcome by modifying the instrument. Future development of this instrument is uncertain and awaits results from ongoing research on other techniques discussed below. A report on the evaluation of the PILLS IV should be published in April 1978.

Fine Particle Size Spectrometer

Work on the Fine Particle Size Spectrometer (FPSS) was initiated in October 1977 by Particle Measuring Systems, Inc. of Boulder, Colorado. The instrument uses a He-Ne laser as shown in Figure 3 as the illumination source for the forward scattering technique. The input beam is directed to the condensing mirror which focuses the beam to a 150 micrometer diameter sensing volume at the object plane. The object plane is defined by the combination of the condensing mirror and the prime objective lens. The prime objective gathers the total light scattered over the forward angles 2° to 11° . The secondary objective magnifies the 150 micrometer object

plane by a factor of twenty to increase the object area on the paired photodiodes. A beam splitter is used to divide the image on to each photodiode. One photodiode has a mask which obscures a portion of the object plane. This is done to limit the response of the instrument to only those particles that are in the uniformly illuminated portion of the input beam. In order for a signal to be processed, it must appear on the unmasked photodiode and not on the masked photodiode. All of the optical components except for the condensing mirror are housed in a water cooled enclosure. The condensing mirror protrudes from this housing on two support rods. The condensing mirror will be cleaned by a purge of dry air or nitrogen. The entire assembly can be inserted through a 10 cm sampling port.

The scattering signal from the photodiodes is then electronically compared with the theoretical Mie scattering curve shown in Figure 4 to yield the particle size data. This curve exhibits the characteristic oscillation in the Mie scattering below about 3 micrometers for the range of index of refraction considered. However, it should be noted that if a best fit calibration curve is used at no point is the uncertainty greater than $\pm 20\%$. Laboratory calibration tests conducted with Latex spheres indicate that the actual uncertainty is less than the maximum. Present data indicates that sizing accuracy of $\pm 10\%$ seems reasonable.

This instrument is in the field prototype stage and will be tested in a wind tunnel and then in a coal fired power plant. The current assessment of the instrument is very positive. It appears that it will function well and yield reliable real time data. No major development problems are anticipated. A report is expected in October 1978.

Optical Particle Sizer

The Optical Particle Sizer is currently being developed by Leeds and Northrup Company of North Wales, Pennsylvania. This instrument differs from the two previous instruments by determining the particle size by measuring the signal from an ensemble of particles rather than from single particles. The optical schematic of Figure 5 shows the basic layout of the major components. A xenon arc lamp is used as the multiwavelength illumination source. The 0.3 to 10 micrometer sizing range is divided into two ranges. Particles larger than 1.0 micrometer are sized by forward scattering. Three scattering angles (10° , 5° , 3.5°) are measured simultaneously and the signal is compared to a theoretical response curve to give the particle size. Particles less than 1.0 micrometer are sized using the depolarization ratio of the light scattered at 90° and at the wavelengths of 0.421 micrometers and 0.850 micrometers. This ratio is electronically compared with a theoretical response curve to yield particle size. Because this instrument makes use of the scattered signal from a volume of particles it is limited to relatively low particle concentrations to avoid multiple scattering effects. In most applications it is expected that the instrument would function properly after an efficient particulate control device, but not before one.

The instrument is housed in a probe much like the one used by the PILLS IV. This probe can then be inserted into the stack. Optical fibers are used to transmit the light from both the forward scatter and side scatter optics to the photodetectors located outside of the stack as shown in Figure 6.

The assessment at the present time for this instrument is quite good. It is in the prototype stage and wind tunnel and stack tests are planned. The final report is expected in July 1978.

Beta Impactor

Work on the Beta Impactor was initiated in 1974 by GCA Corporation of Bedford, Massachusetts. This prototype instrument uses an inertial cascade impactor to aerodynamically size classify the particulate coupled with a beta radiation detector to sense the mass of particulate on each impactor collection stage. The attenuation of beta radiation has been shown to be a linear function of the mass of collected particulate without regard to the chemical composition of the particulate. This useful phenomenon had been used in stack particulate mass instruments and therefore seemed reasonable for use in the Beta Impactor. It was also desirable to size the particulate as nearly in situ as possible and the decision was made to locate the impactor with beta sources and detectors in the stack.

The particle sizing is exactly the same as with a conventional cascade impactor. The particulate laden gas stream enters the impactor nozzle and is directed on to the impaction surface. Particles larger than the size cut point for the stage impact on the stage surface, while the smaller particles follow the gas stream to the next stage. The Beta Impactor uses a moving impaction substrate which collects the sized particulate. Two source-detector pairs are used to measure the mass of the substrate before and after impaction and the real time particulate mass per stage is computed by difference. Carbon 14 was used as the beta source while geiger-müller tubes were used for detectors.

A very serious development problem was encountered during the program which was never overcome. Since the device was designed to operate at stack conditions it was necessary that the beta detectors should be capable of operation at the 200°C stack temperature. No beta detectors were located or developed that could achieve this design requirement.

The instrument was tested in a wind tunnel to evaluate its operational characteristics at ambient temperature.³ These results are shown in Figure 7. This figure compares the output of the Beta Impactor with the same reference impactor curve presented in Figure 2. Subsequent analysis of the wind tunnel test configuration revealed that there was an obstruction between the reference impactor and the Beta Impactor. This obstruction had the net effect of diverting approximately 80% of the flow away from the Beta Impactor. If this correction is applied to the Beta Impactor data, the data points fall more nearly on the reference curve. However,

the same degree of scatter in the data results and the first impaction stage remains well below the reference curve.

These discrepancies with the reference impactor could probably be minimized with a refined design. However, when coupled with the beta detector problems discussed earlier, it was decided that further development of this technique was not warranted. A report on this work was published in April 1977.

Differential Pressure Impactor

As the development problems of the Beta Impactor became apparent, a second program was initiated with GCA Corporation to develop an in stack impactor with real time data presentation. Under this program a simpler sensor was selected from several candidates. The system schematic is presented in Figure 8. This instrument utilizes virtual impaction on to a stationary gas rather than the more conventional impaction on to a surface employed by the Beta Impactor. With virtual impaction the separated sized particles settle into a collection chamber where a small portion of the total flow is extracted. The particles are collected on a filter and the differential pressure across the filter is measured. The change in the differential pressure is proportional to the weight gain of the filter and the real time particle size can be calculated.

Because a sample is collected on a filter several advantages result. The differential pressure/mass calibration can be verified for each test by weighing the filters. Likewise, because a sample is collected, subsequent chemical and toxicological analysis can be performed.

The experimental results on this technique, however, were disappointing. Figure 9 shows a typical test using fly ash. It is quite apparent from this data that the instrument suffers from a lack of sensitivity. Minimum time response can be up to 10 minutes depending on source characteristics. Although the technique offers more promise than the Beta Impactor, further development would be required before a useable instrument could result. EPA has no plans for further work on this instrument. The program results were published in a report in August 1977.

Light Scattering Impactor

Meteorology Research, Inc. of Altadena, California, was selected in October 1977 to develop an impactor based instrument utilizing a light scattering data readout. Although the final design has not been selected, Figure 10 shows the basic concept. A conventional inertial impactor, possibly employing virtual impaction, will be used to separate the particulate by their aerodynamic diameter. Each impactor stage will be followed by a detector module. The active optical elements (light source, photo-detectors, and associated electronics) will be located outside of the stack and connected to the in-stack impactor with optical fibers. The

detection scheme can be seen in Figure 11. It employs forward scattering over a fairly large angular range from the total ensemble of sized particles. It is recognized that this method of sensing is dependent on the index of refraction of the particles. However, because the size of the particles is known from the impactor characteristics, and because it is only necessary to measure the particle concentration, the approach appears reasonable.

Although no experimental work has been performed to date, the approach is quite straightforward and no serious problems are foreseen. Future testing, if warranted, calls for evaluation of the instrument in a wind tunnel followed by a field evaluation in a coal fired power plant. The Light Scattering Impactor will be compared with conventional impactors in each test. A report is expected in May 1979.

Acoustical Particle Sizing Instrument

Work on the Acoustical Particle Sizing Instrument was begun in February 1978 by KLD Associates, Inc. of Huntington Station, New York. The instrument computes the aerodynamic particle size by measuring the change in the speed of sound at various audio frequencies. When a particle is exposed to a sound wave in a gaseous medium, the particle will either oscillate in the gaseous medium at the frequency of the sound wave or it will be unaffected. The particles' aerodynamic drag and mass are the parameters that determine whether or not the particle will oscillate. For each size particle there is a unique frequency above which the particle will no longer oscillate. If the particle oscillates with the gas then the apparent density of the gas is increased by the addition of the mass of the particle to the mass of the gas. If the particle does not oscillate with the gas then no change is observed in the gas density. Since the speed of sound is a function of the density of the transmitting medium, then by measuring a change in the speed of sound the change in apparent gas density can be calculated.

The application of this useful relationship can be seen in Figure 12. Two known frequencies F_X and F_R are passed through the particulate laden gas medium. The reference frequency, F_R , is chosen sufficiently high so that none of the particles of interest will oscillate. Therefore, the velocity of sound at F_R will remain constant. When the velocity of sound at F_X is measured it is found to be different than the sonic velocity at F_R . The difference in sonic velocity represents the addition of the total mass of particles in the gas stream that oscillate between frequencies F_X and F_R . A useful instrument would result if the frequency F_X is varied to cover the full range of particle sizes of interest as shown in Figure 13. Curve (A) represents the case when no particles are present in the gas stream. The sonic velocity remains constant across the audio spectrum. When a monodispersed aerosol is introduced curve (B) results. In this case sonic velocity is constant until the critical frequency for the monodispersed particles is reached. The speed of sound changes by an amount ΔC as the particles start to oscillate and then assumes a constant but different value. If a polydispersed aerosol is introduced then curve

(C) will result. There is an initial reduction in the sonic velocity (ΔC_A) caused by the total mass of particles present in the gas stream that oscillate above the initial frequency. As the frequency is changed from point A to point B the sonic velocity changes by ΔC_{AB} . This represents the total mass of particles that oscillate between frequency A and frequency B. The particle size distribution can be determined by differentiating curve (C) to obtain the mass at any desired size.

Although the concept appears quite promising, no experimental work has been done. There are a number of potential problems dealing with acoustic transducers that have not been addressed. This instrument may prove useful, but considerable research will be required. A technical report is scheduled to be published in June 1979.

Assessment

Past work to develop in situ real time particle sizing instruments has been largely unsuccessful. Current work, however, seems to hold considerable hope for success. It appears that both the Fine Particle Size Spectrometer and the Optical Particle Sizer have excellent chances of working well and developing reliable data in industrial sources. Likewise, the Light Scattering Impactor offers promise of success. The Acoustical Particle Sizing Instrument will represent a major advance in particle sizing technology if it is successful. Current research should answer these questions.

It is the author's opinion that within one year practical, if not optimum, real time particle sizing instruments will be available.

References

1. Harris, D. B. and W. B. Kuykendal. Problems in Stack Sampling and Measurement. Proceedings of the Symposium on Fine Particles, Minneapolis, MN. EPA-600/2-75-059. October 1975.
2. Shofner, F. M., G. Kreikebaum, H. W. Schmitt, and B. E. Barnhart. In Situ, Continuous Measurement of Particulate Size Distribution and Mass Concentration Using Electro-Optical Instrumentation. Presented at the Fifth Annual Industrial Air Pollution Control Conference, Knoxville, TN. April 1975.
3. Gooding, C. H. Wind Tunnel Evaluation of Particle Sizing Instruments. EPA-600/2-76-073. March 1976.
4. Lilienfeld, P., D. P. Anderson and D. W. Cooper. Design, Development, and Demonstration of a Fine Particulate Measuring Device. EPA-600/2-77-077. April 1977.
5. Lilienfeld, P., D. P. Anderson, and D. W. Cooper. Study on the Feasibility and Design of Automatic Particulate Size Distribution Analyzer for Source Emissions. EPA-600/2-77-050. August 1977.

Table 1

INSTRUMENT SUMMARY

| INSTRUMENT | OPERATING PRINCIPLE | SIZING RANGE, micrometers | DEVELOPMENT COSTS, \$ | ESTIMATED UNIT COST, \$ | STATUS |
|---------------------------------------|--|---------------------------|-----------------------|-------------------------|---------------------|
| PILLS IV | FORWARD LIGHT SINGLE PARTICLE SCATTERING | 0.2 - 3 | UNKNOWN | 30,000 | EVALUATION COMPLETE |
| FINE PARTICLE SIZE SPECTROMETER | FORWARD LIGHT SINGLE PARTICLE SCATTERING | 0.4 - 10 | 155,000* | 35,000 | ACTIVE DEVELOPMENT |
| OPTICAL PARTICLE SIZER | FORWARD LIGHT VOLUME SCATTERING/SIDE SCATTERING POLARIZATION RATIO | 0.3 - 10 | 150,000 | 25,000 | ACTIVE DEVELOPMENT |
| BETA IMPACTOR | INERTIAL IMPACTION BETA ATTENUATION SENSING | 0.2 - 5 | 175,000 | NOT APPLICABLE | RESEARCH TERMINATED |
| DIFFERENTIAL PRESSURE IMPACTOR | INERTIAL IMPACTION PRESSURE BUILD-UP SENSING | 0.2 - 5 | 90,000 | NOT APPLICABLE | RESEARCH TERMINATED |
| LIGHT SCATTERING IMPACTOR | INERTIAL IMPACTION LIGHT SCATTER SENSING | 0.5 - 5.0 | 265,000* | 40,000 | ACTIVE DEVELOPMENT |
| ACOUSTICAL PARTICLE SIZING INSTRUMENT | CHANGE IN SONIC VELOCITY VS AUDIO FREQUENCY | 0.5 - 5.0 | 140,000* | 30,000 | ACTIVE DEVELOPMENT |

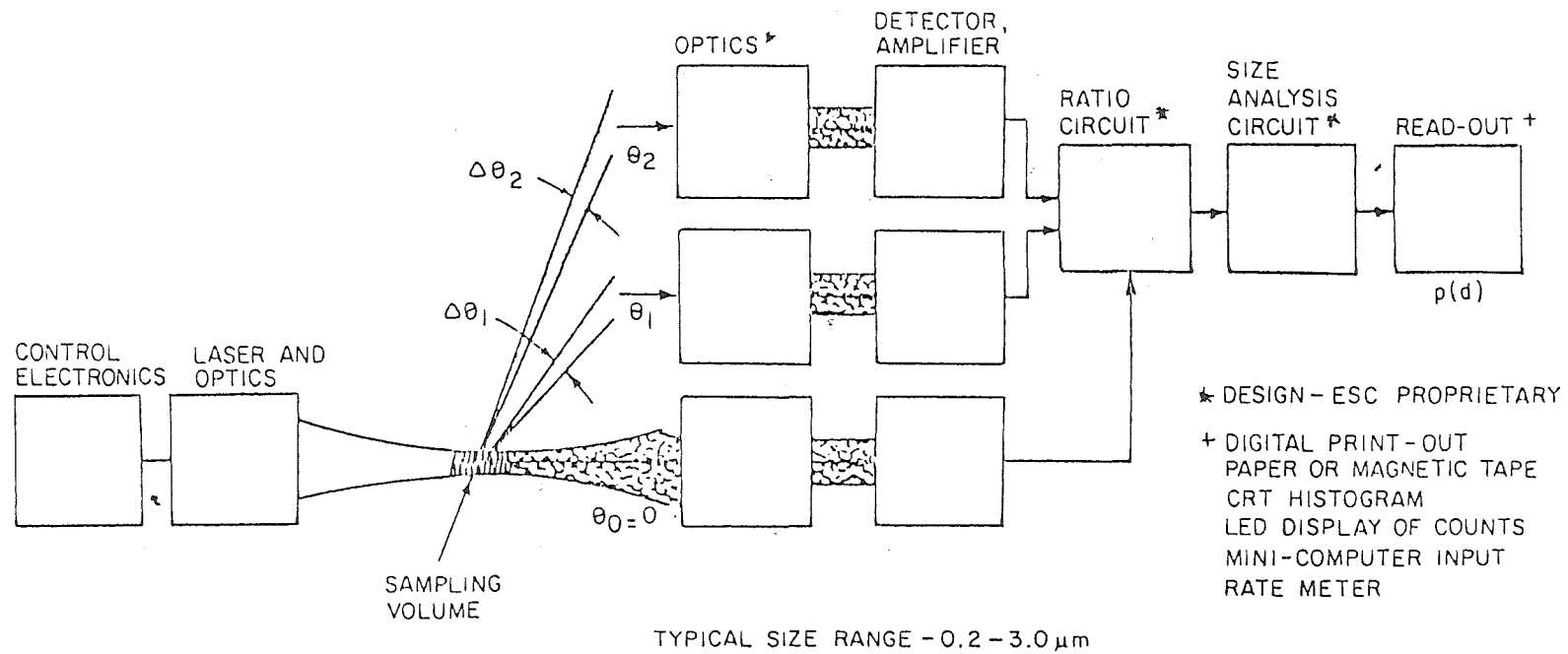


Figure 1. PILLS IV Optical Particle Counter.

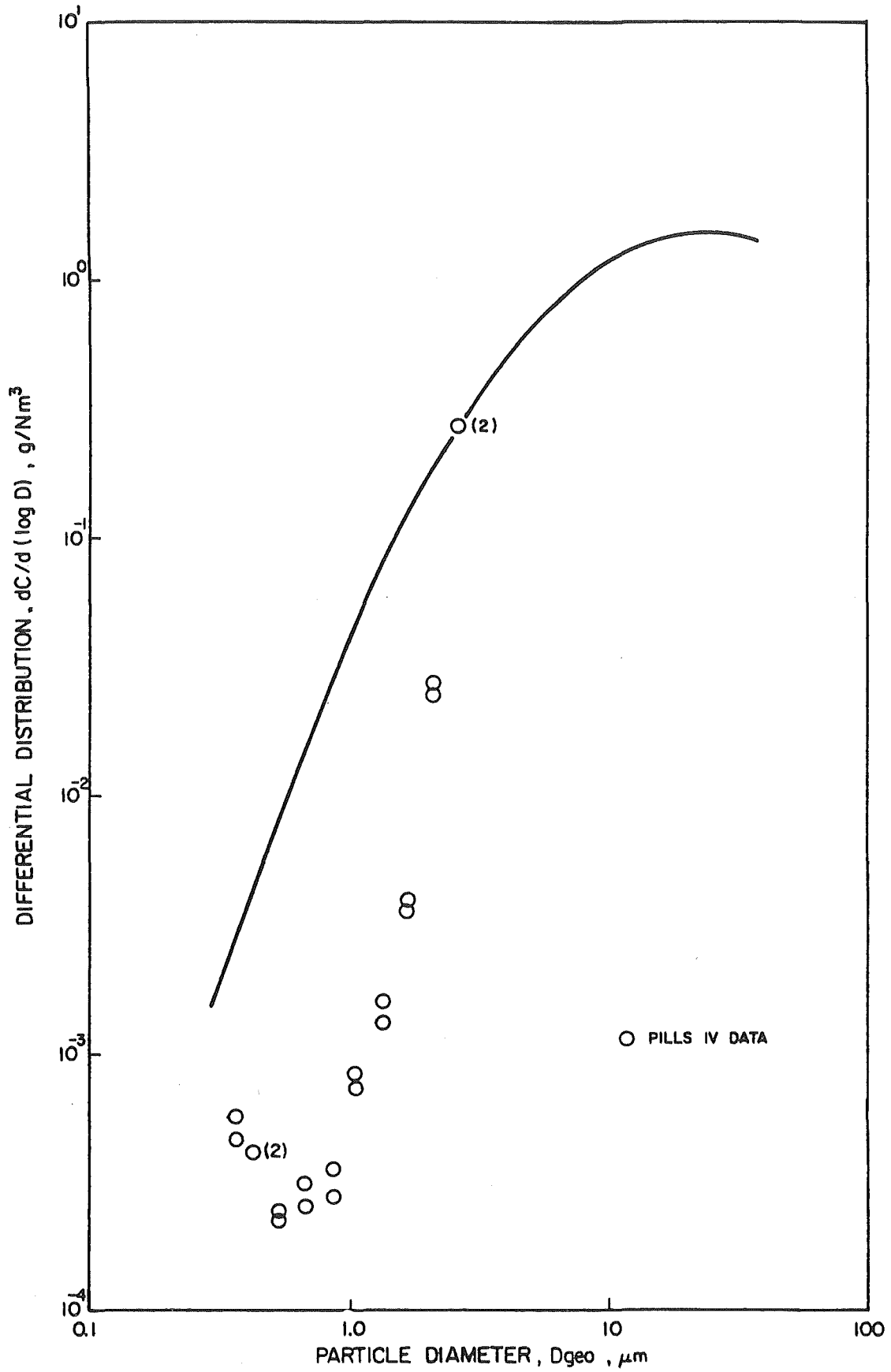


Figure 2. Comparison of PILLS IV data with impactor curve (concentration = 0.955 g/Nm³).

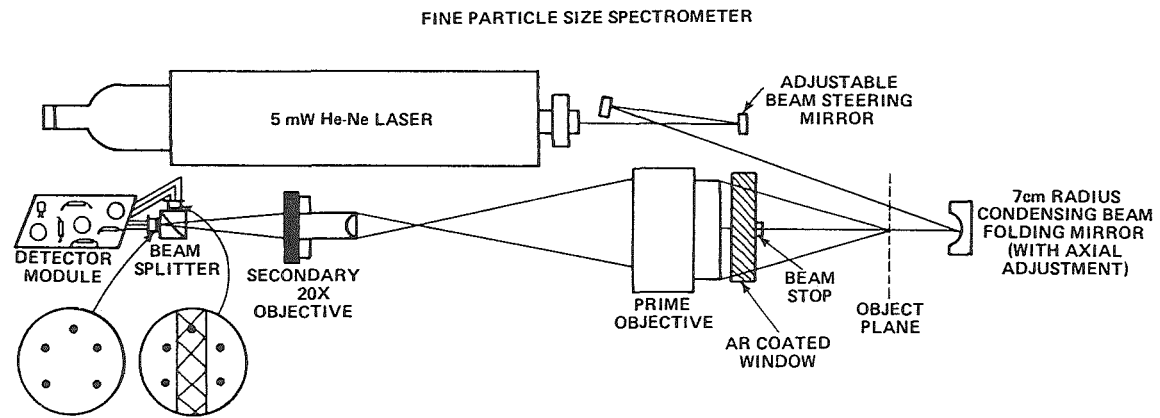


Figure 3

FINE PARTICLE SIZE SPECTROMETER

THEORETICAL MIE SCATTERING FOR 2-11° REAL INDICES 1.4, 1.5, 1.6, & 1.7

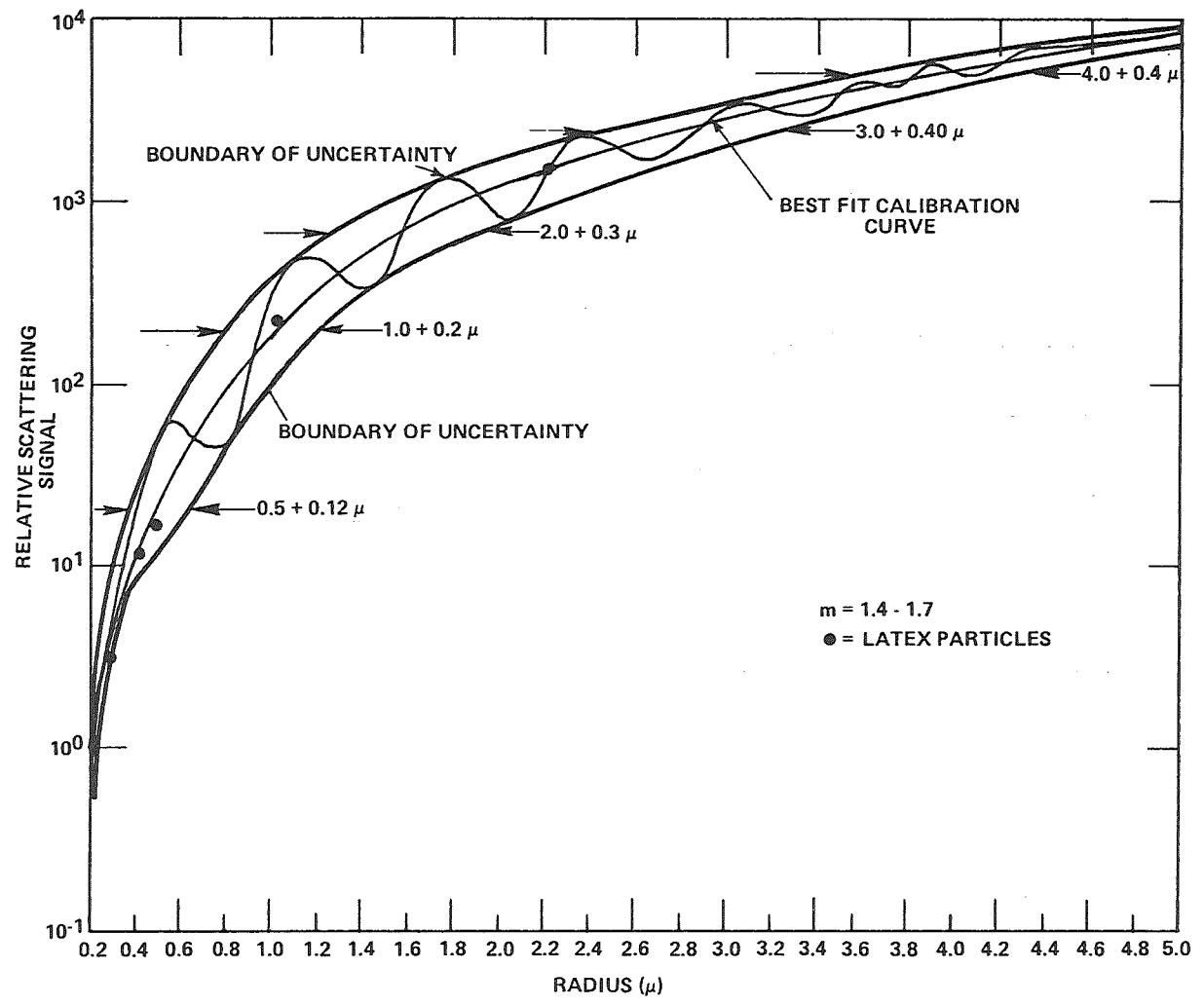


Figure 4

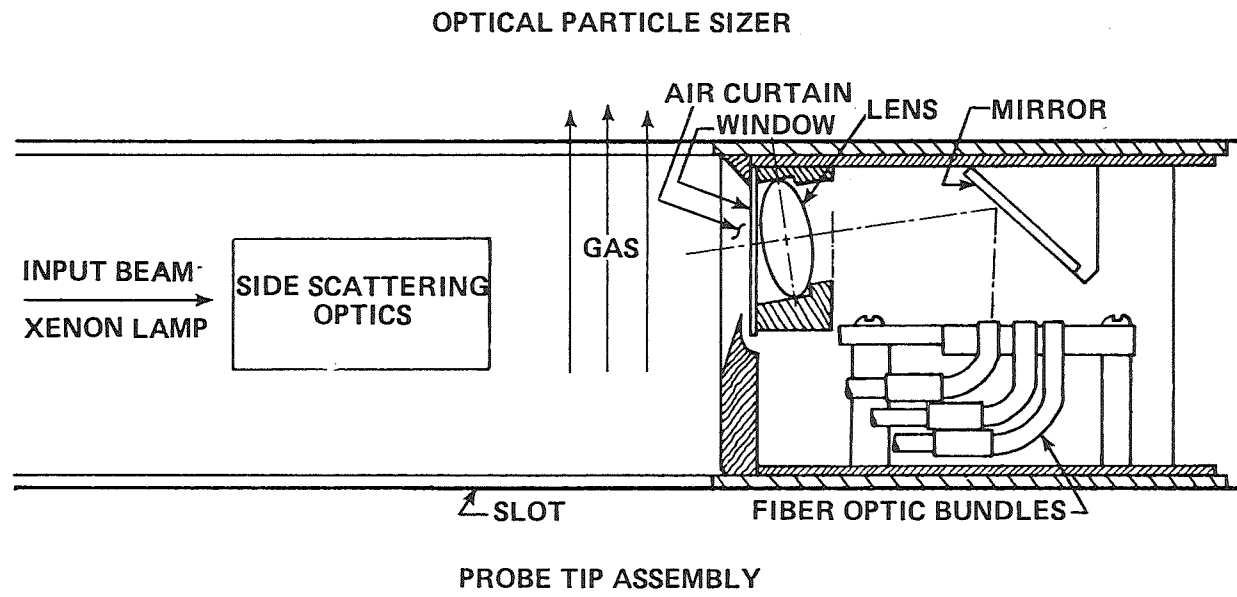


Figure 5

OPTICAL PARTICLE SIZER

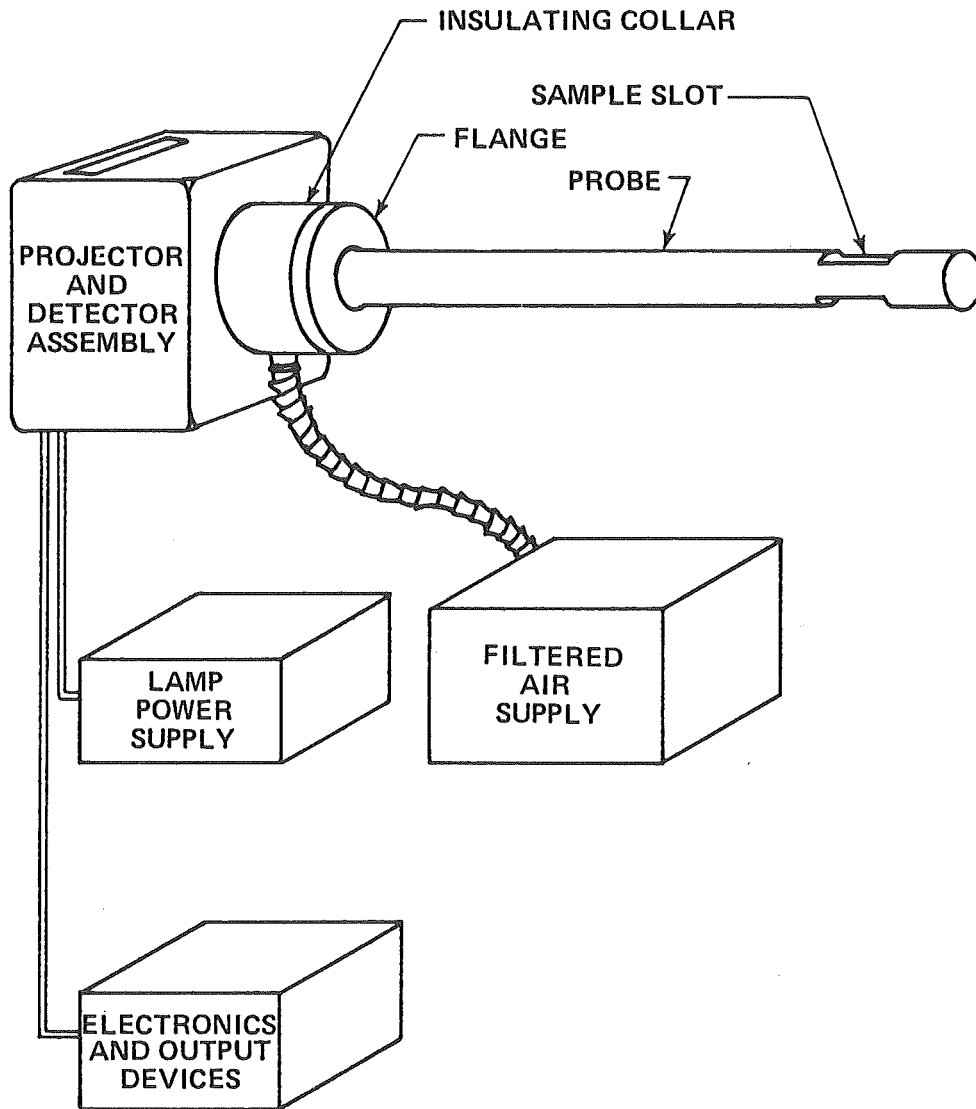


Figure 6

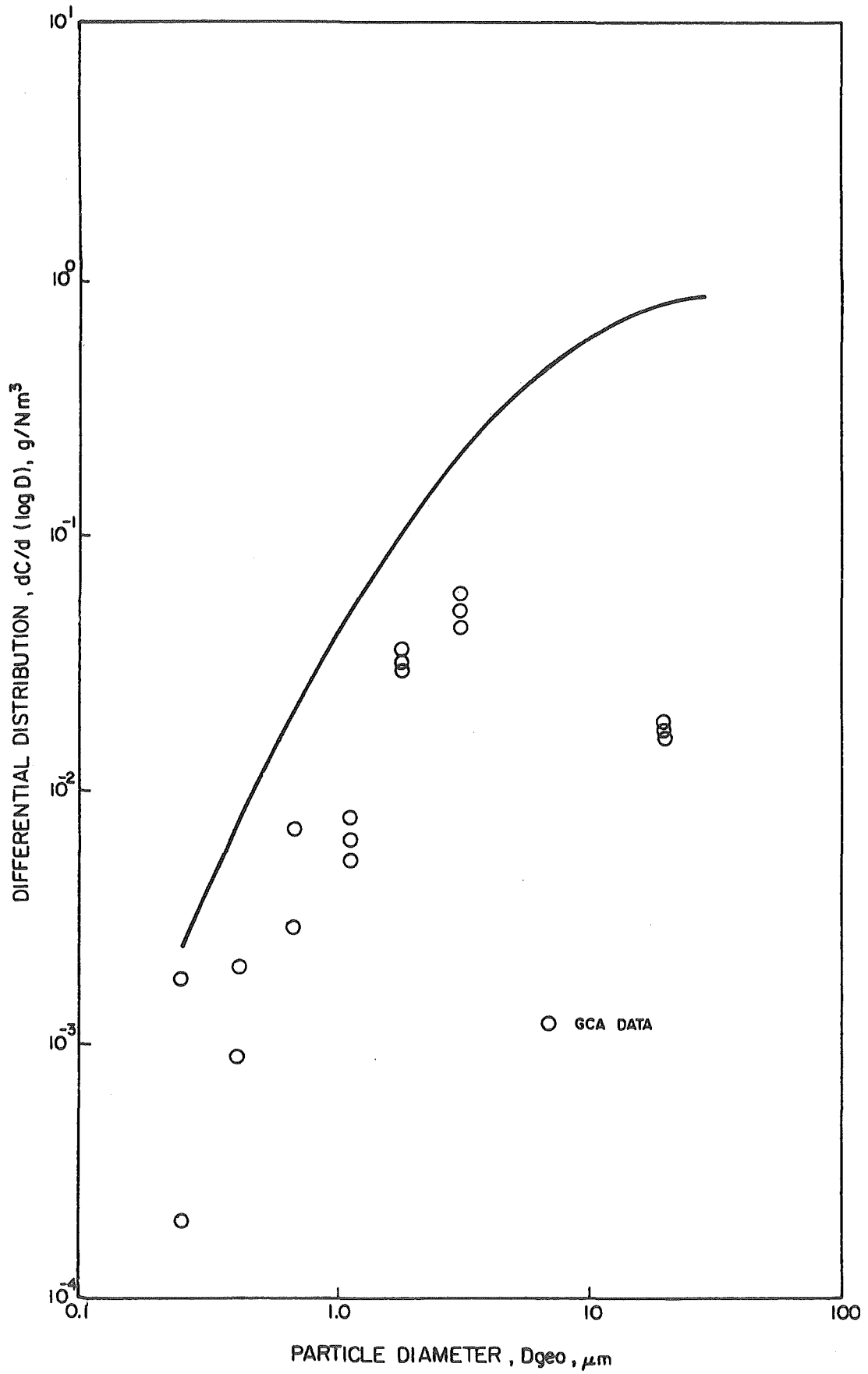


Figure 7. Comparison of Beta Impactor data with impactor curve (concentration = 0.955 g/Nm³).

DIFFERENTIAL PRESSURE IMPACTOR SCHEMATIC.

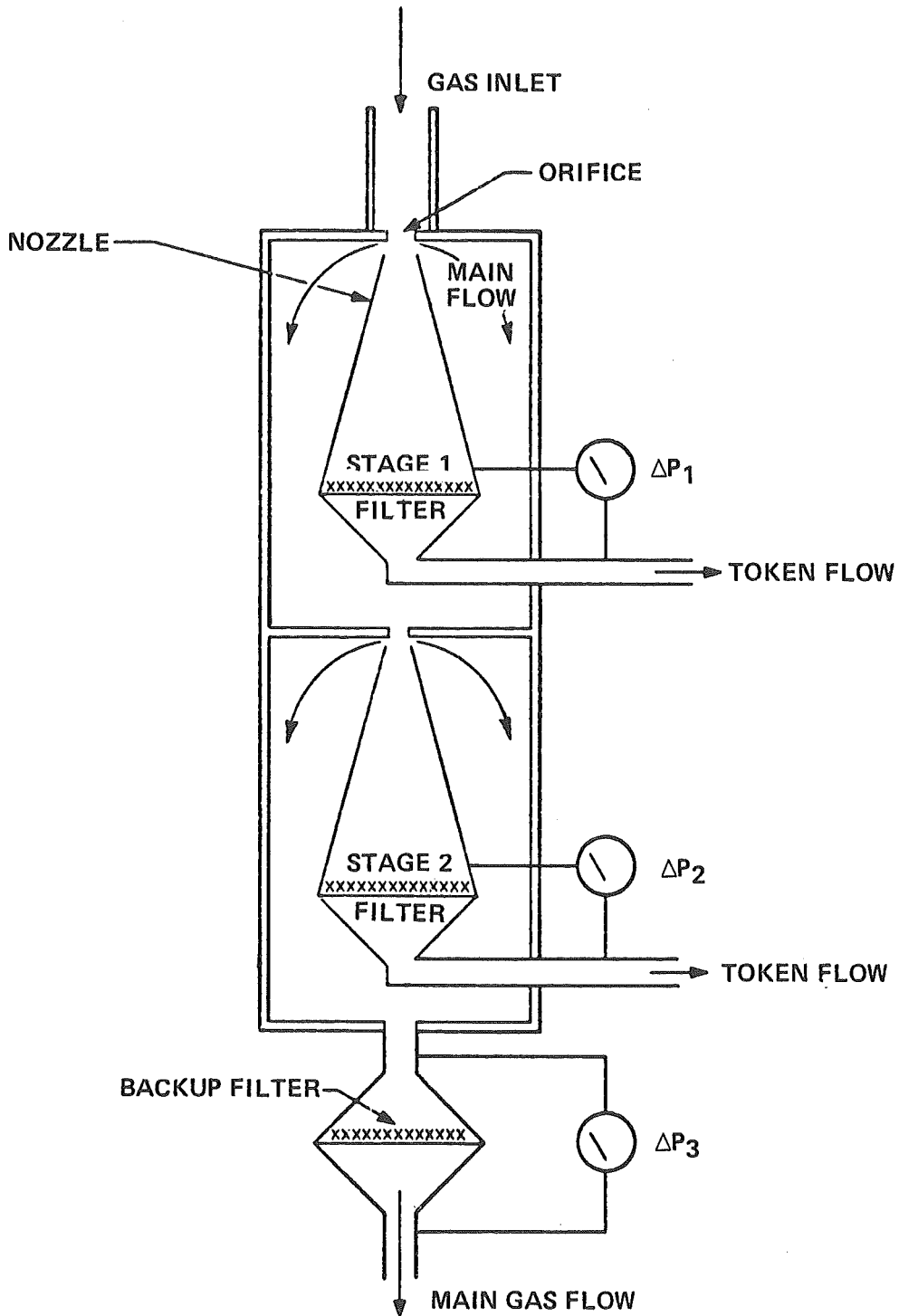
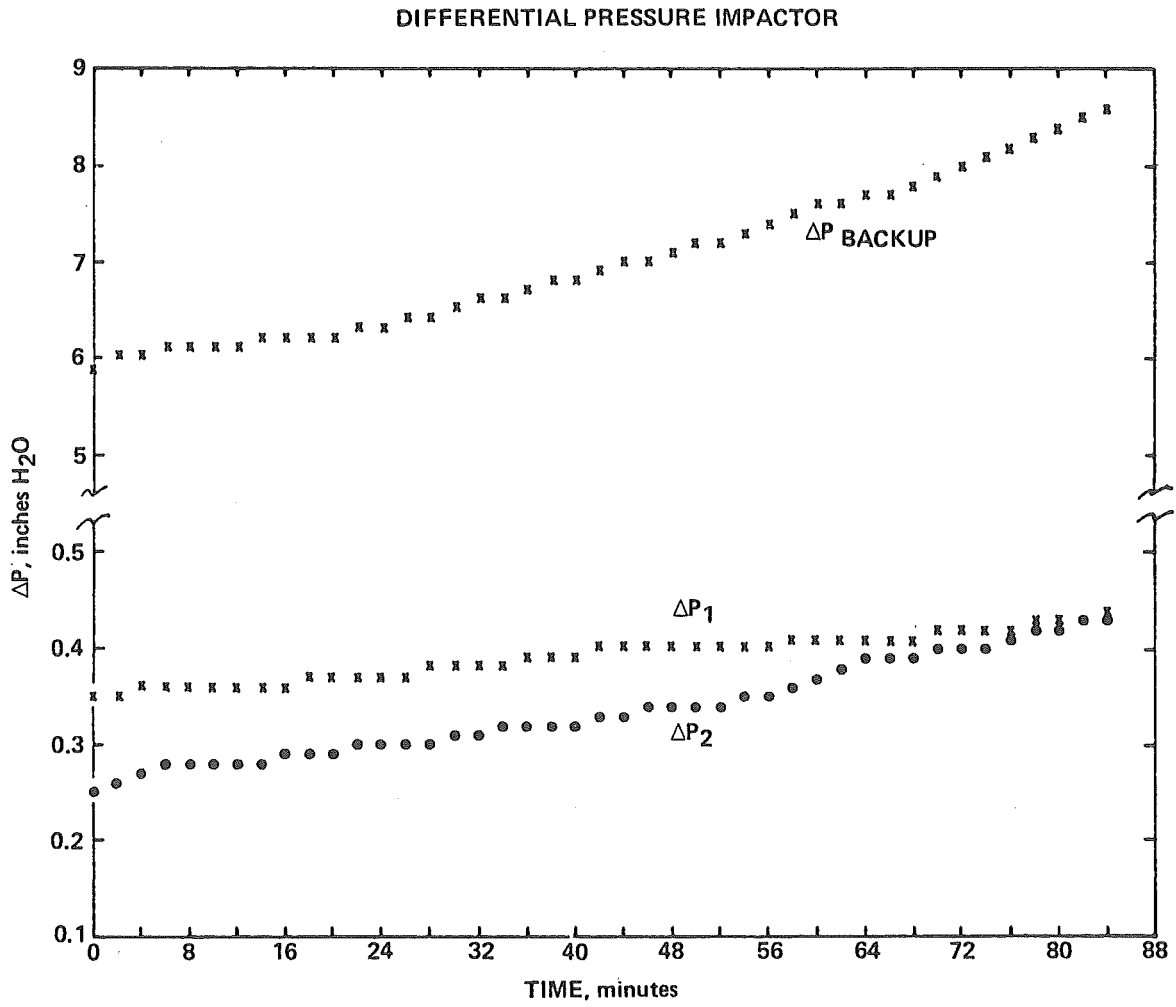


Figure 8



TEST NUMBER 29, FLY ASH.

Figure 9

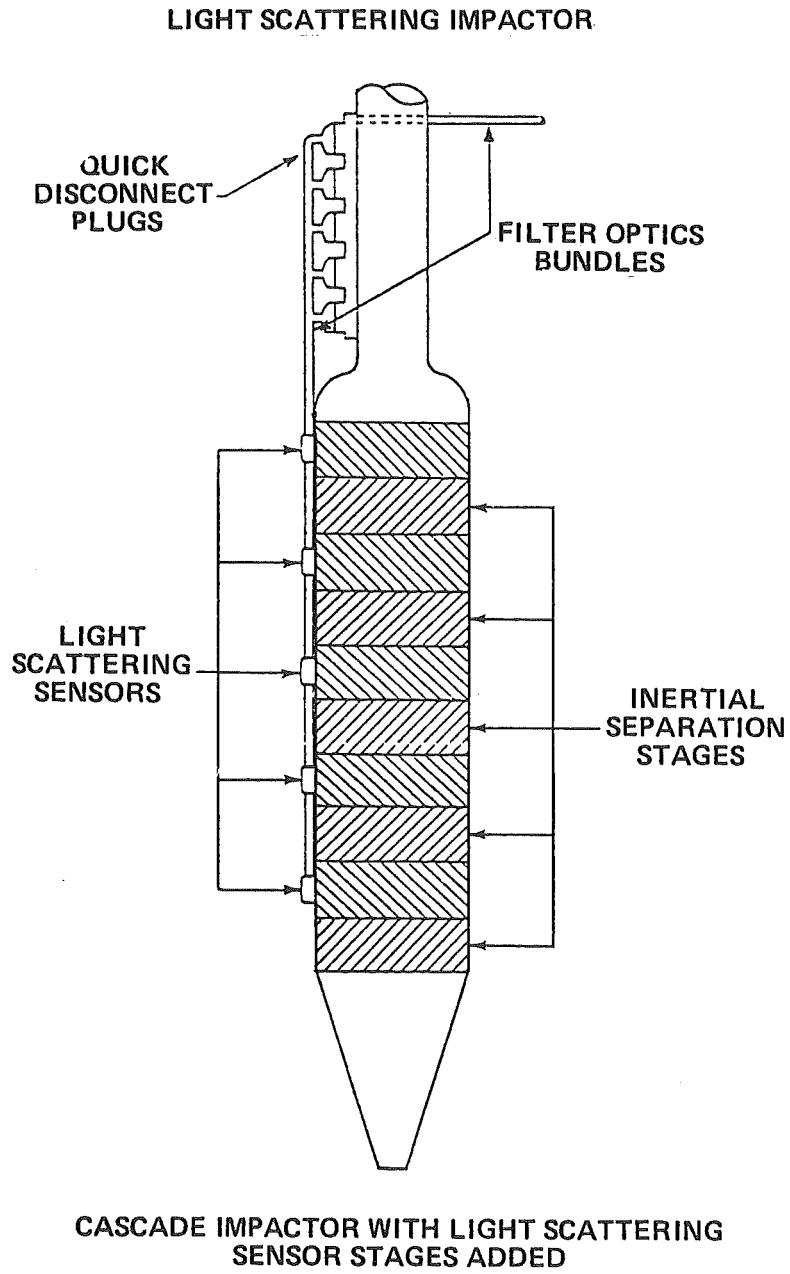


Figure 10

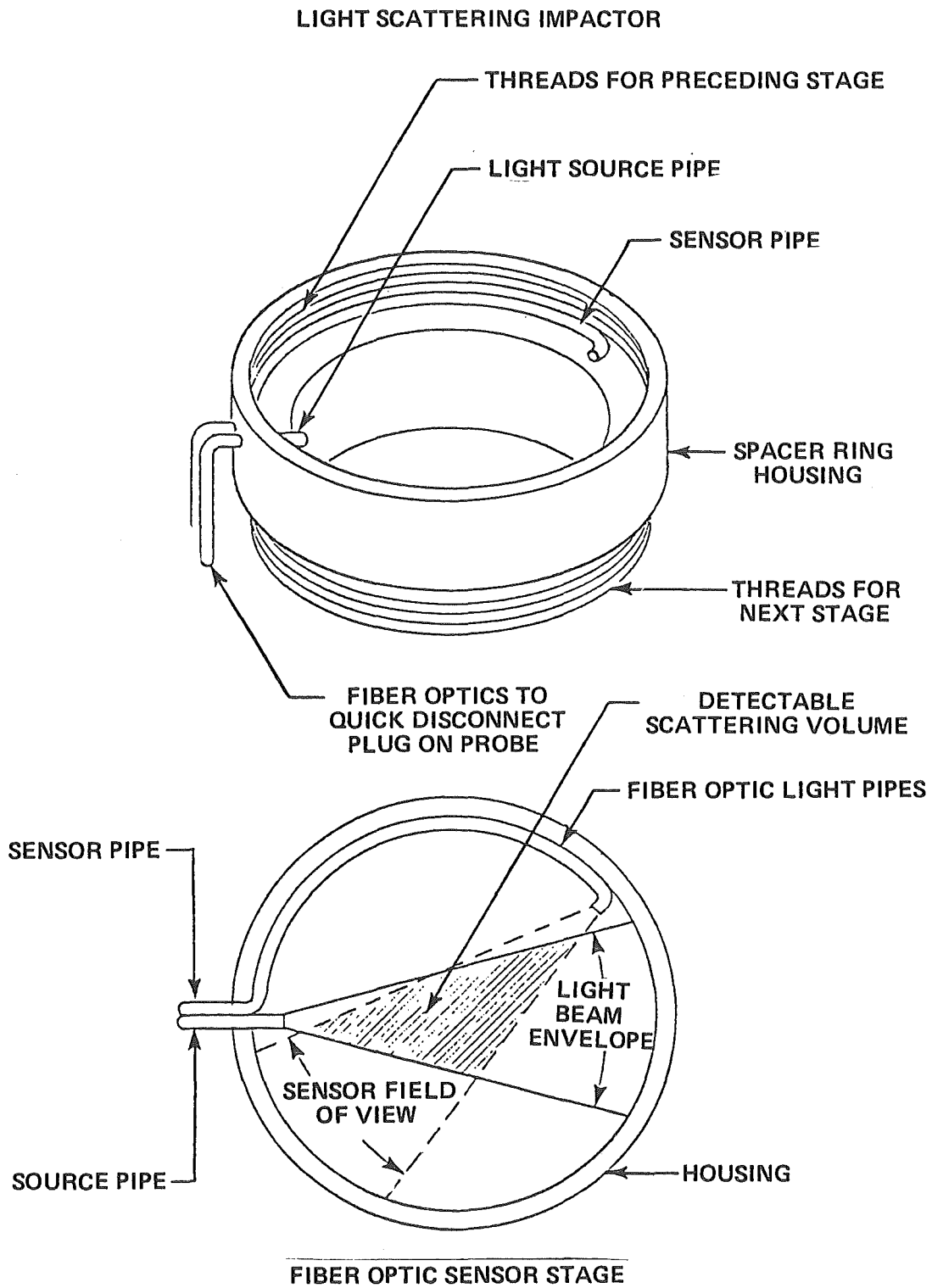
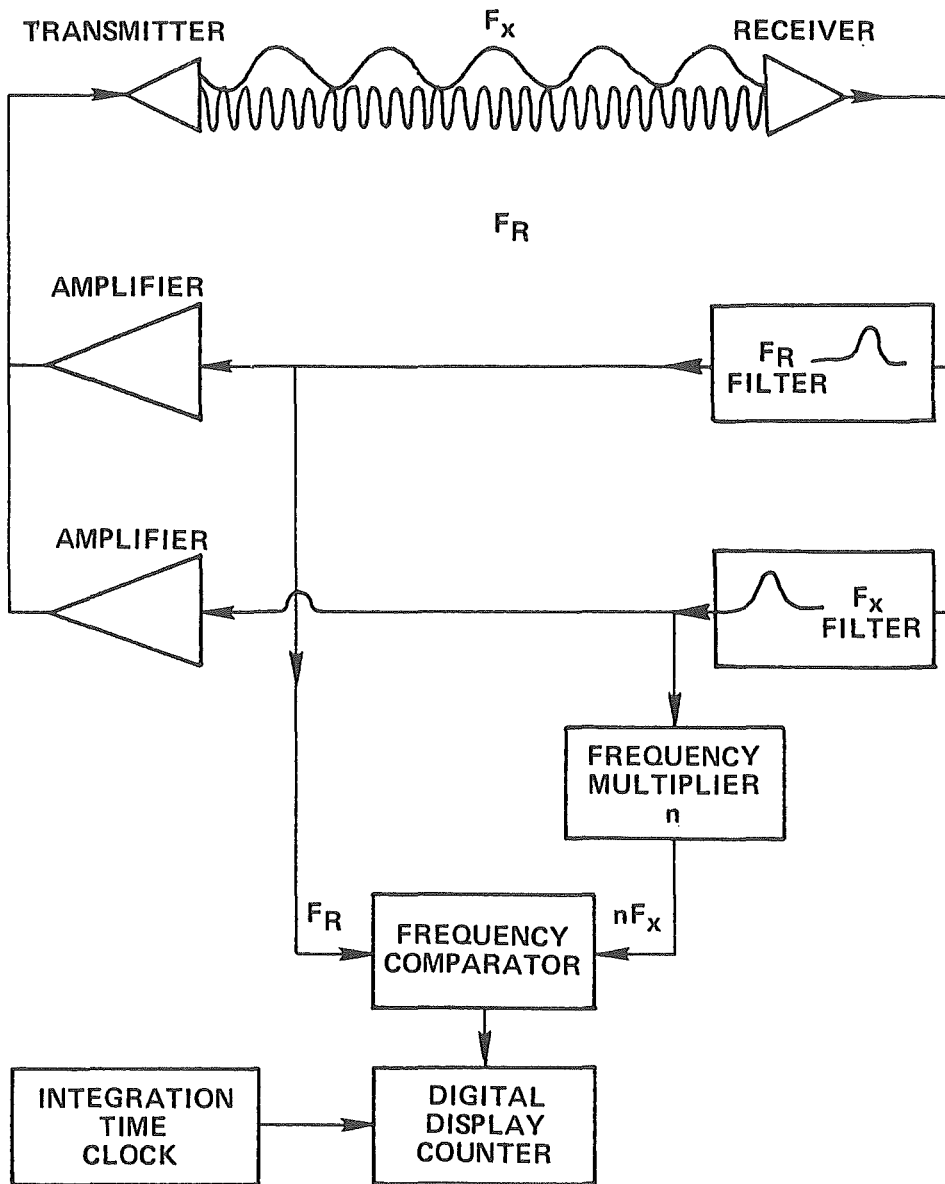
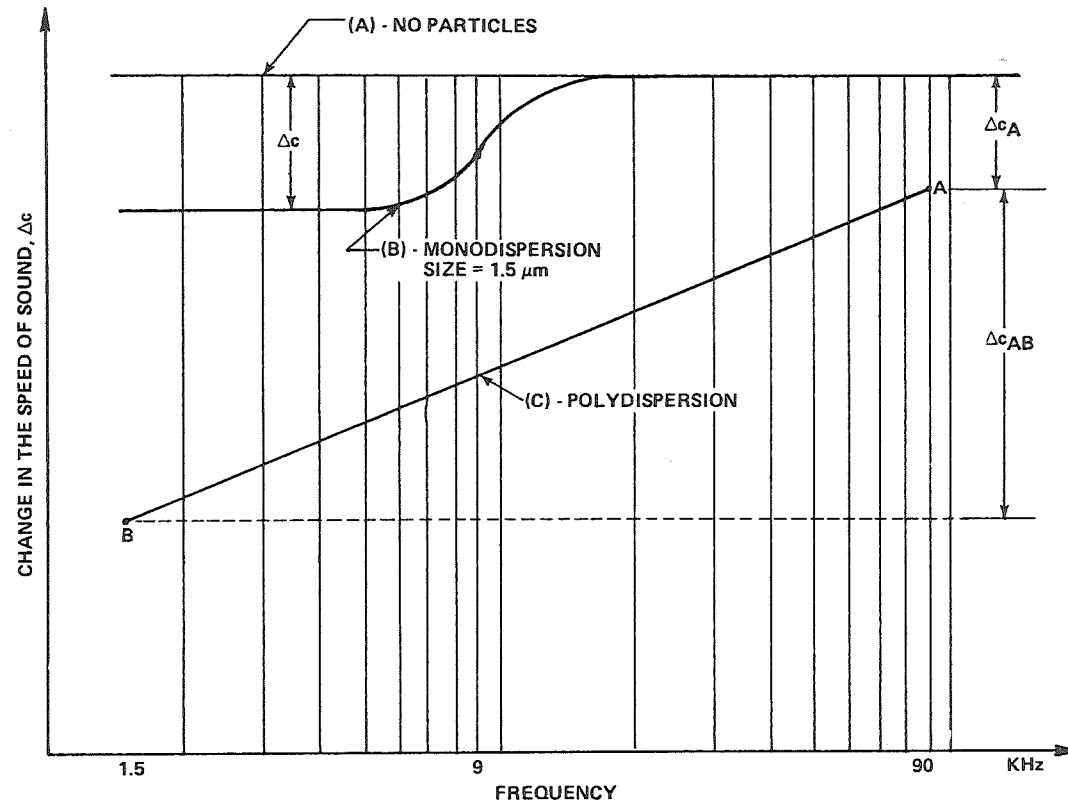


Figure 11



SCHEMATIC OF THE ACOUSTICAL PARTICLE SIZING INSTRUMENT FOR MEASUREMENTS AT FREQUENCY, F_x , WITH RESPECT TO THE REFERENCE FREQUENCY, F_R

Figure 12



TYPICAL OUTPUT TRACES FROM THE ACOUSTICAL PARTICLE SIZING INSTRUMENT

- (A) NO PARTICLES IN SIZE RANGE
- (B) MONODISPERSION: SIZE = 1.5 μm
- (C) POLYDISPERSION

Figure 13

Discussion

Mr. Kuykendal stated that all devices described required physical insertion into the gas stream. In reply to Mr. Wiggers, he said that the PILLS IV instrument functioned well apart from a response problem and that a trained technician (not necessarily a specialist) was well able to handle the data obtained.

Evaluation of Particle Size Distributions by Means of
Particle Counters

H.J. FiBan

C. Helsper

Vortrag auf dem Workshop "Particulate Control",
Kernforschungsanlage Jülich, 16.03. - 17.03.1978

Bericht Nr. 33

Evaluation of Particle Size Distributions by Means of
Particle Counters

Prof. Dr.-Ing. H. Fißan; Dipl. Ing. C. Helsper
Institut für Aerosolmeßtechnik
Gesamthochschule Duisburg

Introduction

The emission of particulate matter is usually described by its total mass concentration, or, as a function of particle size, by its mass distribution.

The mass of a single aerosol particle decreases rapidly with decreasing particle size. Therefore, the determination of the particle mass concentration or the particle mass distribution of an aerosol with particle diameters in the submicron range by gravimetric methods yields certain difficulties like long sampling times and a loss in accuracy.

For submicron particles it is easier, and more precise to count the particles in order to get parameters, describing the aerosol. Another advantage is, that most of the particle counters allow near real-time measurement, so that the aerosol parameters can be obtained in time intervals of a few minutes. Then it is possible to determine changes in the aerosol as a function of time.

Mass distributions can be calculated starting from particle number distributions under the assumption of spherical particle shape, if the density of the particle material is known.

Instrument description

In our laboratory a set of two instruments has been used to determine size distributions of aerosols emitted by combustion processes in the particle diameter range between 0.01 and 10 microns.

For the diameter range below one micron an Electrical Aerosol Analyzer (E A A, TSI, Model 3030) was used. Fig. 1 shows a schematic diagram of this instrument. The aerosol particles are charged in the upper section of a tube by unipolar gaseous ions produced by a corona discharge. These charged particles enter a cylindrical condenser through a narrow annular slot near the inner wall of the outer tube. A flow of clean air near the center electrode is necessary to obtain a laminar flow. With a negative voltage at the center electrode the particles are deflected through the air stream towards the electrode. The particles, which are not precipitated on the center electrode, are collected on a filter downstream the precipitator. The particle charge flow is measured by an electrometer sensor. If the voltage at the center electrode is increased by a certain amount, the electrometer current will decrease, because particles of less electric mobility are precipitated with the higher voltage in the condenser. The difference in current for a defined voltage step is a measure for the number concentration in a certain particle mobility range. Thus, by varying the precipitating voltage, the electric mobility distribution of an aerosol can be determined. The relation between particle size and particle mobility depends on the number of elementary charges per particle. Because of the random nature of the charging procedure this relation can be described only statistically. This is the reason for a non-ideal instrument behaviour which causes systematic errors in the measured size distribution. The instrument response for monodisperse aerosols has been determined by Liu and Pui in 1974. Based on their results a correction of these errors is possible.

For the measurement of the larger particles an Optical Particle Counter (O P C, Royco, Model 225) has been used. Fig. 2 explains the principle of the instrument. A beam of white light is focussed by a set of lenses and is then caught by a light trap.

The aerosol stream, focussed by clean sheath air crosses the focus of the light beam. The amount of light, that is scattered by a particle going through this volume, is a function of particle size. The light pulse in forward direction is led to a photomultiplier. The output pulse of the photomultiplier is amplified and transformed in a square shaped pulse of the same amplitude. The pulses are stored according to their amplitude by a multi-channel-analyzer.

Automatic instrument control and data reduction is done by a PDP 11/10 computer. Fig. 3 shows a block diagram of the whole system. The EAA and the OPC are complemented by a Condensation Nuclei Counter (C N C) for the determination of the total number concentration in the size range below 0.8 micron, and a piezoelectric microbalance, which determines the total mass concentration. By specific interface circuits the data are modified and transferred to the processor unit, from where they can be stored on a magnetic storage device. Data output is available on a graphic plotter or on a teletype.

The two instruments were designed for ambient air measurement and have certain limits concerning the maximum particle number concentration as well as the temperature and pressure of the gas.

Emission aerosols exceed these limits in many cases. Therefore it is necessary to modify these aerosols by dilution and cooling. For dilution a certain amount of the aerosol flow is led through a filter. The particle-free gas is then mixed again with the rest of the aerosol flow. Dilution ratios of 50 to 1 can be obtained with this method without altering the shape of the size distribution.

Cooling of aerosols is much more critical because condensation processes can alter the properties of an aerosol considerably.

Data reduction and correction

The data of the EAA and to some extent that of the OPC, too, are not free from systematic errors. Fig. 4 and 5 show the effects, caused by these errors. The continuous curve in Fig. 4 shows a model number distribution similar to the size distribution of atmospheric aerosols. It was obtained by the superposition of two log-normal distributions and is represented by the full line. The instruments' response to that model aerosol was simulated numerically and is represented by the histogram. The solid lined blocks represent the EAA data and the broken lined the OPC data. Practically all particles lie in the size range below one micron. A considerable part of the distribution lies even below 0.01 micron, which means, that no direct information can be obtained about this part of the distribution with these instruments. The differences between the measured data and the model distribution are not very large at first sight because of the logarithmic scale which ranges over six orders of magnitude for the number concentration axis. But in the upper size channels the values differ by a factor of nearly five.

These differences become more obvious, if the number distribution is transformed into a volume distribution, which corresponds to the mass distribution for unit density of the particles. This transformation has been done under the assumption of spherical particles. Its results are shown in Fig. 5.

One can see, that nearly ninety percent of the particle mass is concentrated in the size range below one micron. The largest differences between the model distribution and the measured data lie now near the maximum of the distribution, so that, for example, their effect for the total mass concentration is much greater than for the total number concentration.

Besides the intention to correct the measured data it would be convenient to describe the whole distribution by a mathematical model distribution with a limited number of parameters. This reduces the amount of data necessary to describe the aerosol and allows an extrapolation over the limits of the size range covered by the instruments. A superposition of two or three log-normal distributions has found to be consistent with most of the experimental data.

A computer program has been developed, which determines for such a model distribution a set of parameters that fits the measured data best, taking into account the non-ideal instrument behaviour. Based on the measured data a set of start parameters for the model distribution is estimated. The measuring procedure is then simulated numerically for the distribution represented by these start parameters.

The result of this operation is a set of simulated data, which is compared with the measured data to estimate the goodness of fit. An optimization algorithm now varies the distribution parameters according to a certain strategy in order to minimize the deviation between the measured and the simulated data. If the deviations fall within the range of the instruments accuracy, the iteration stops. The model distribution, found in this way represents the measured data within the accuracy range of the measurement, which is about twenty percent.

Experimental results

As an example for the application of the instruments for the determination of the size distribution of combustion aerosols the result of a measurement at the exhaust gas of an internal combustion engine shall be discussed. In order to compare the results of the particle counting technique with those of gravimetric methods we used a

six stage cascade impactor.

All instruments took their samples downstream a model exhaust system which cooled the exhaust gases below fifty degrees centigrade. To compare the results of the different methods, mass concentrations were calculated from the number concentration values, assuming a density of the aerosol material of 1 g/cm^3 .

The resulting mass distribution, which is based on uncorrected data is shown in Fig. 6. The solid points represent the data calculated from the EAA - measurement. The open circles show the results of the cascade impactor and the two squares result from the OPC measurement. Even with the uncorrected data the fit between the different methods is reasonably well.

The total mass concentration for that measurement was about 15 mg/m^3 .

Nearly eighty percent of the particle mass lies in the size range covered by the EAA.

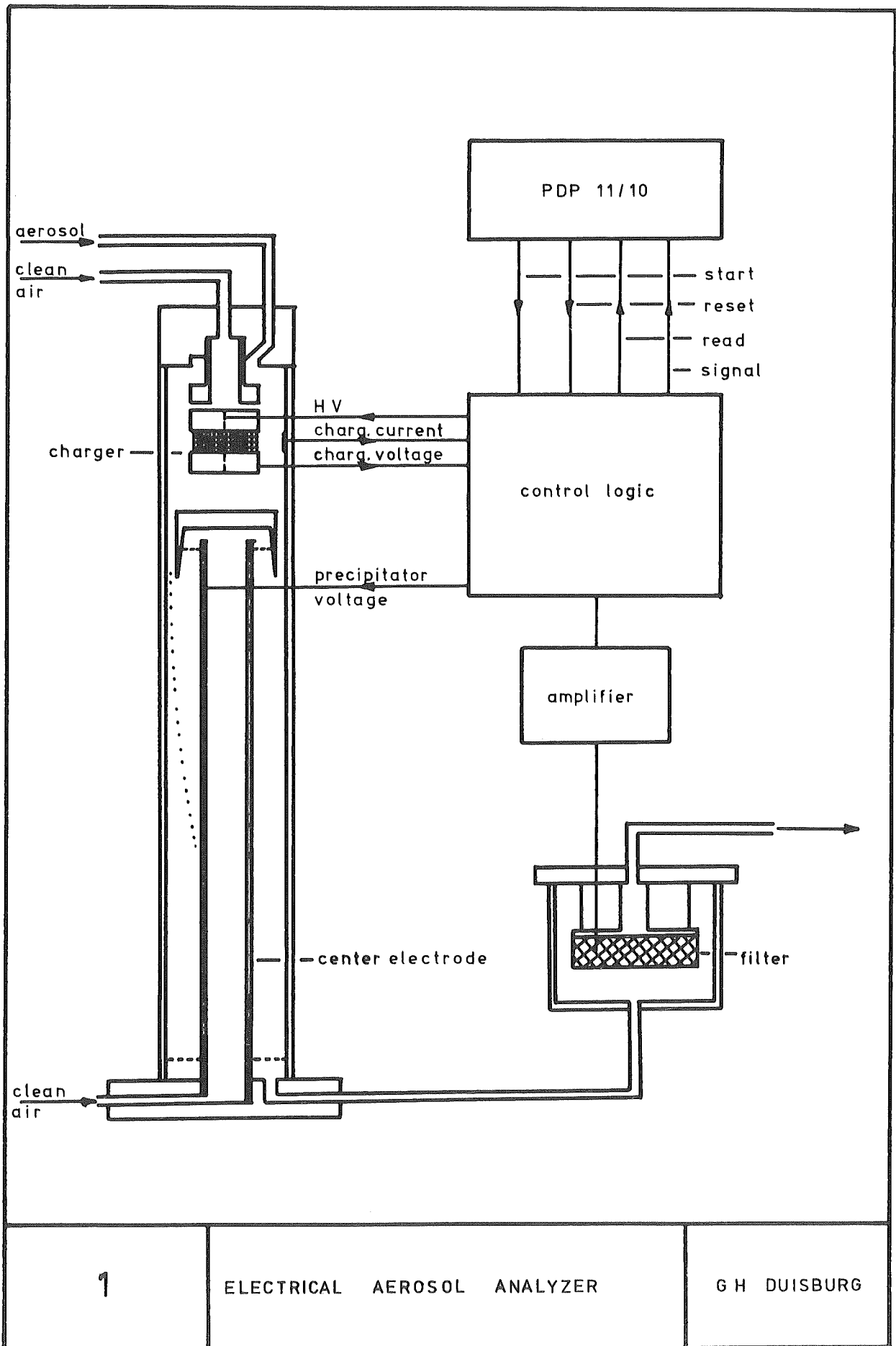
Summary:

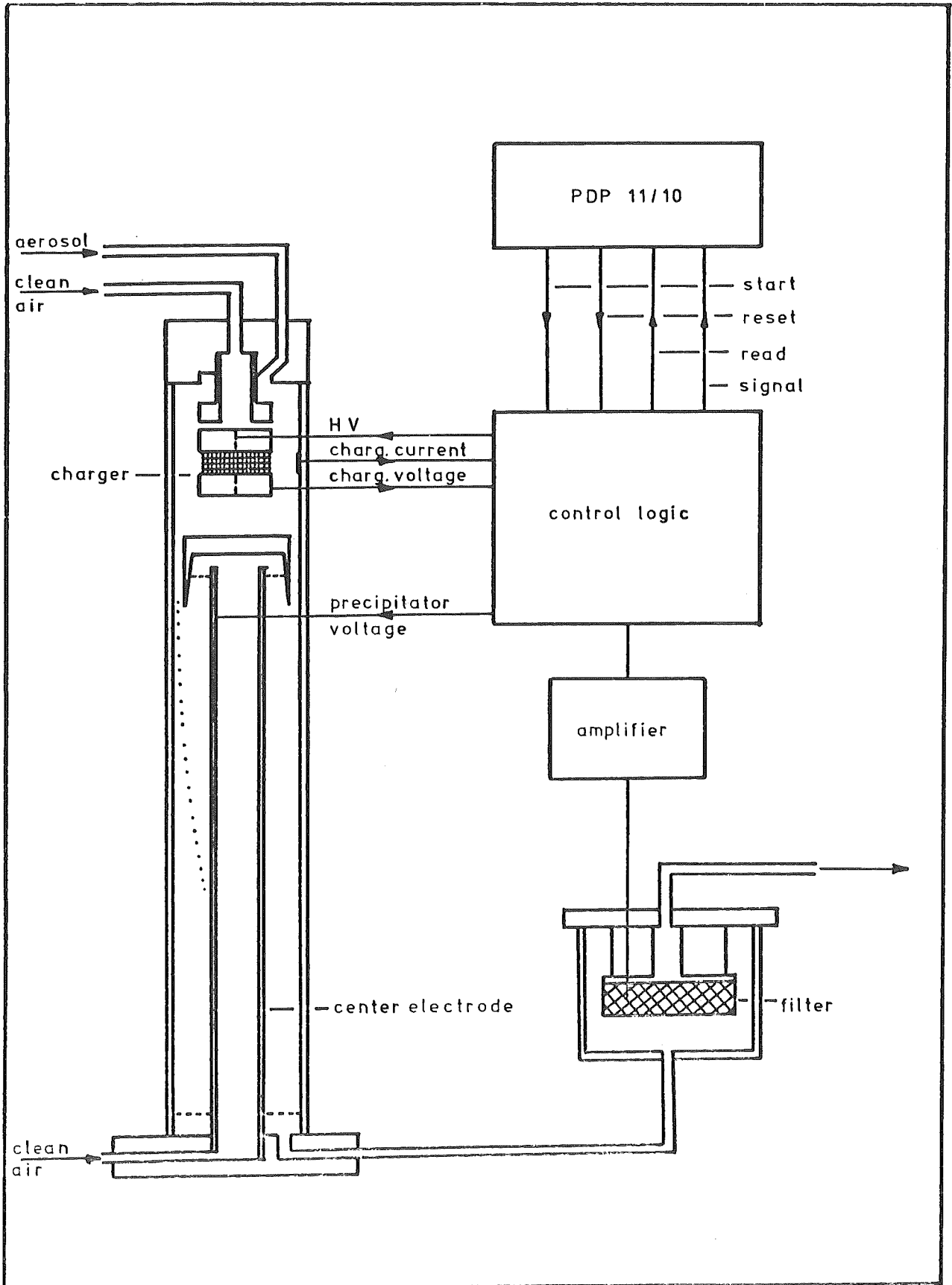
In the submicron size range the determination of aerosol parameters by particle counting techniques has several advantages compared with gravimetric methods. The instruments used cover a size range from 0.01 to 10 microns. As these instruments were designed for atmospheric aerosol measurements, emission aerosols have to be diluted in most cases to fit the limits of the instruments. Certain systematic errors based on the principle of operation can be corrected to a great extent if necessary by a special correction algorithm.

The comparison of the particle counting techniques with a gravimetric method shows a rather good agreement.

List of figures

1. Electrical aerosol analyzer
2. Optical particle counter
3. Aerosol measuring system
4. Instrument behaviour for a number distribution
5. Instrument behaviour for a volume distribution
6. Mass distribution of an exhaust aerosol

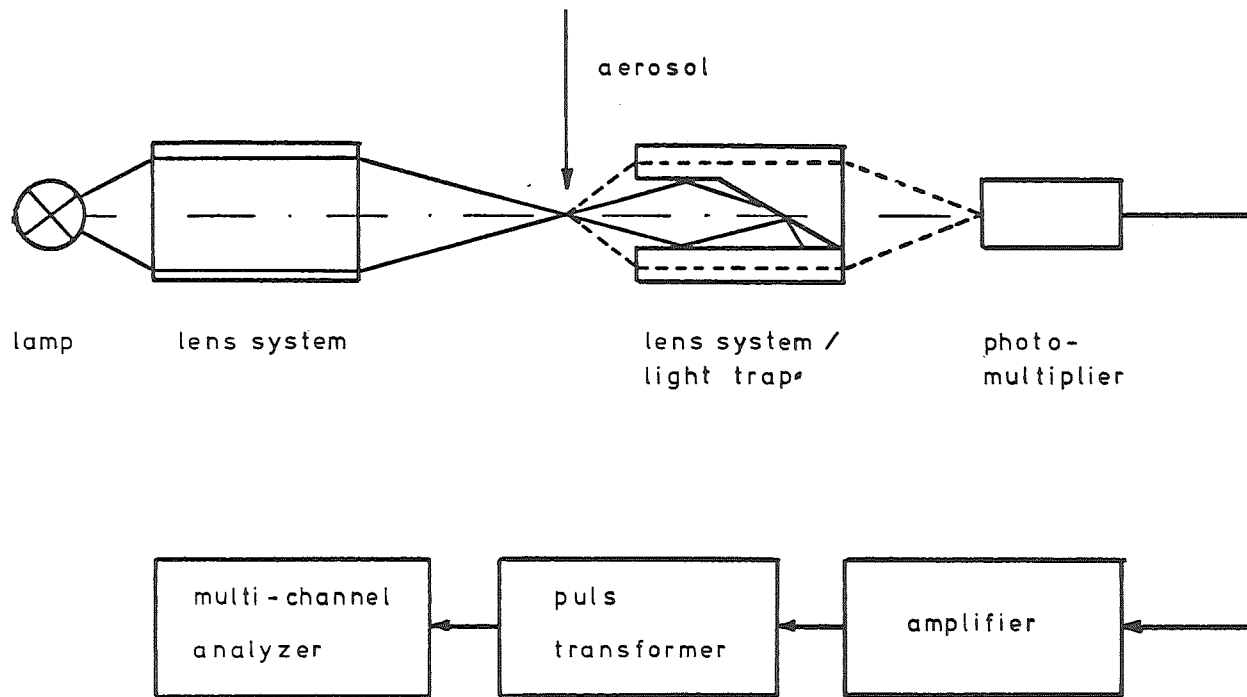


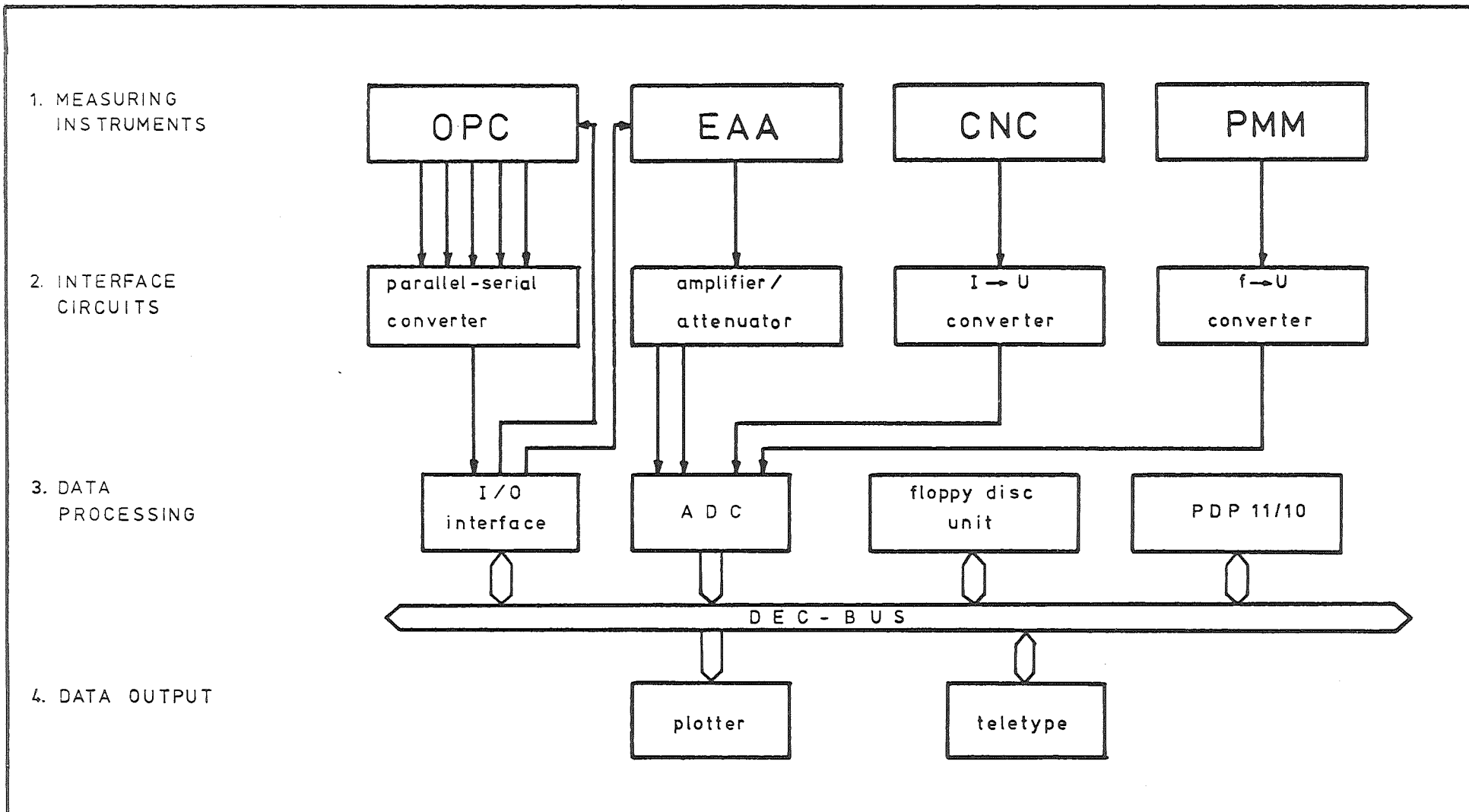


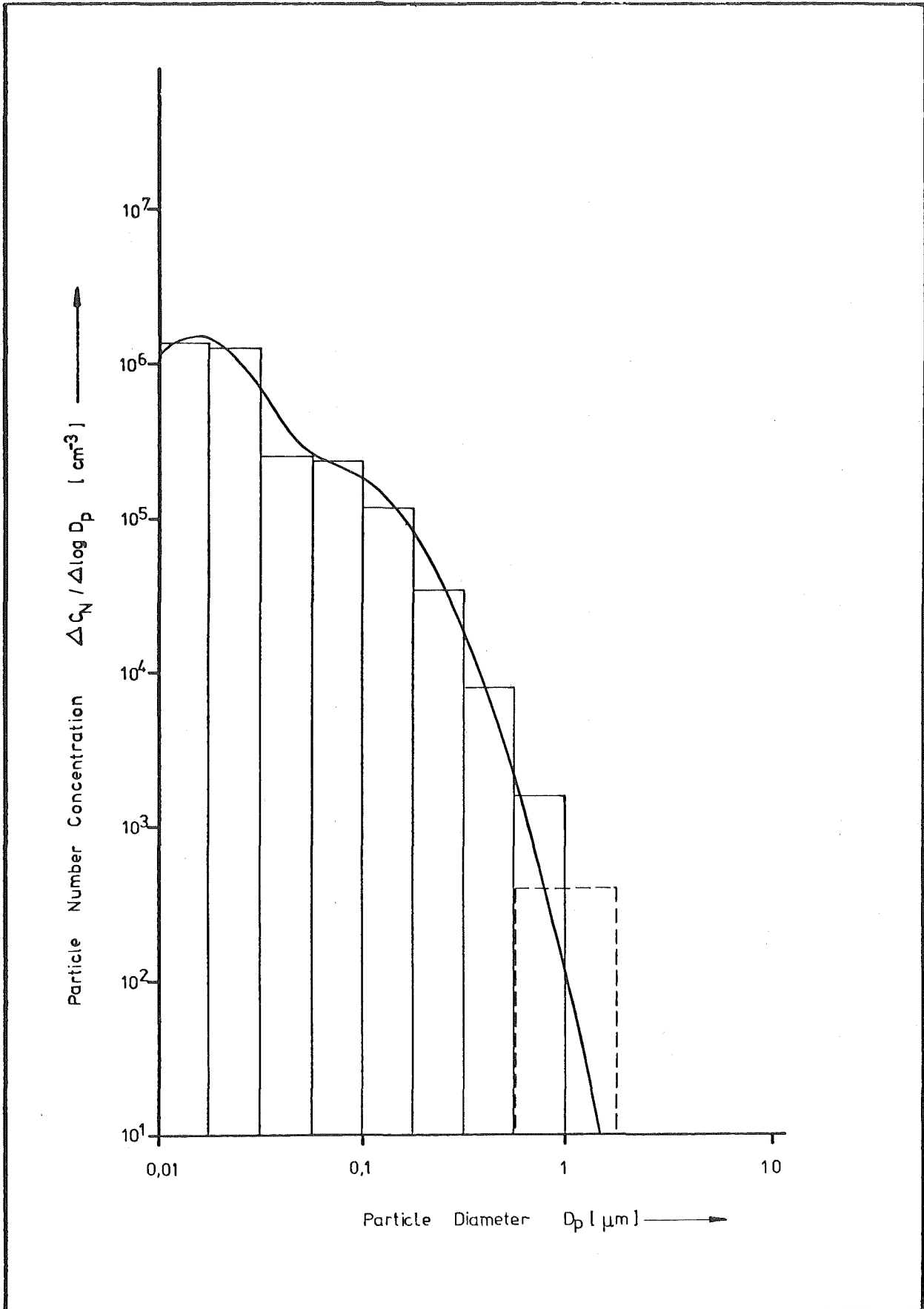
1

ELECTRICAL AEROSOL ANALYZER

G H DUISBURG



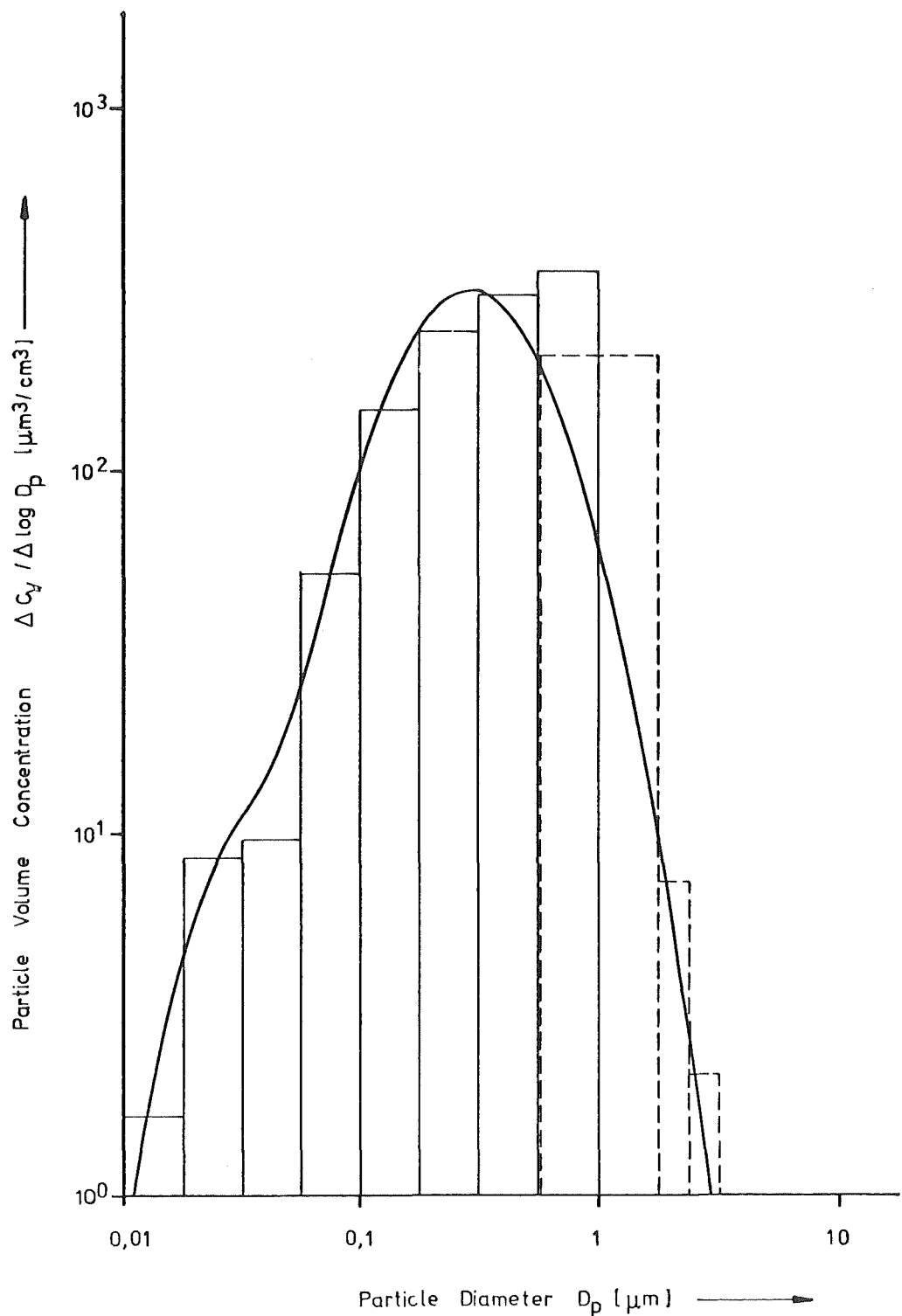




4

INSTRUMENT BEHAVIOUR FOR A
NUMBER DISTRIBUTION

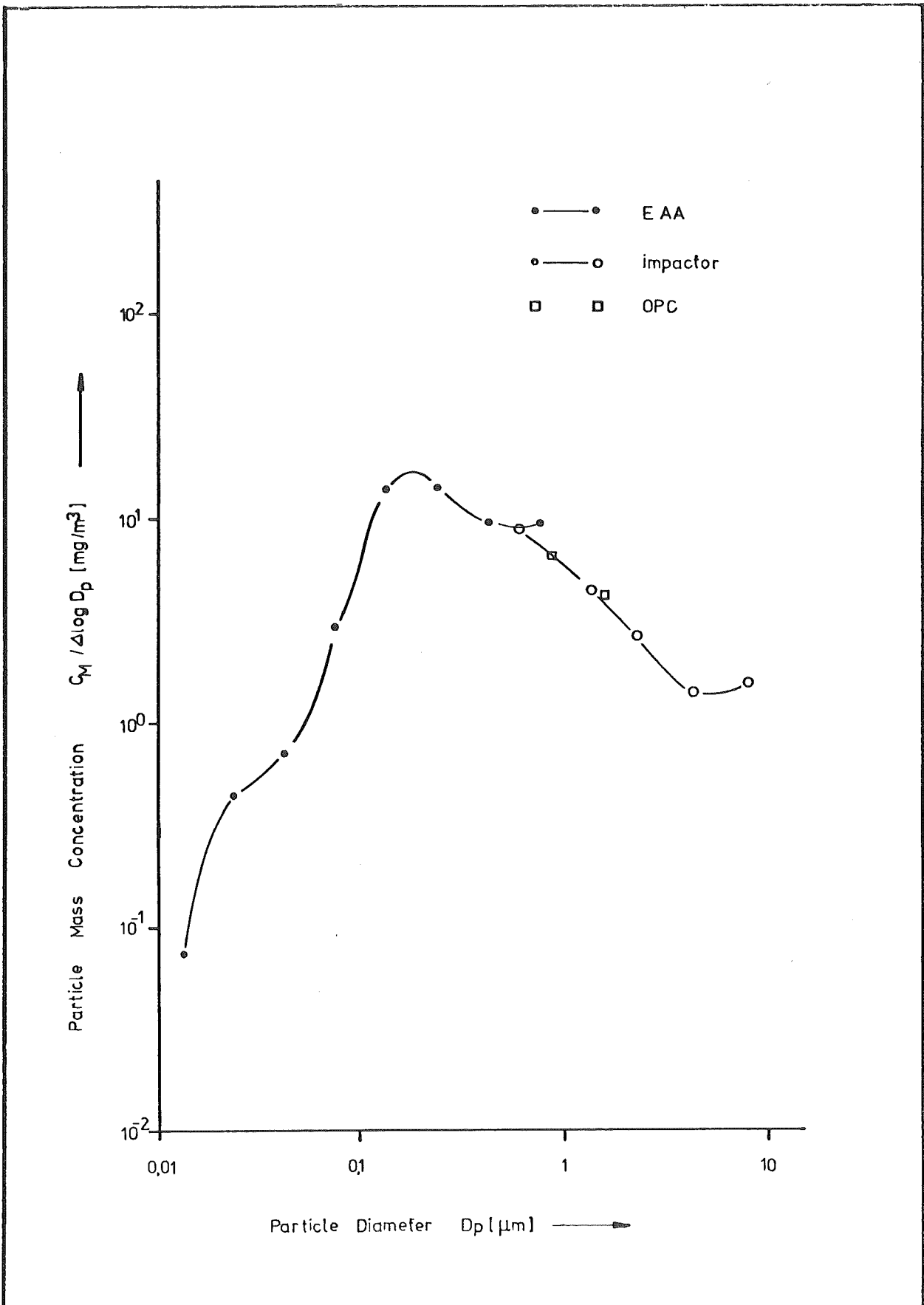
G H DUISBURG



5

INSTRUMENT BEHAVIOUR FOR A
VOLUME DISTRIBUTION

G H DUISBURG



A PARTICULATE SAMPLING SYSTEM
FOR PRESSURIZED FLUIDIZED BED COMBUSTORS

By:
William Masters, Robert Larkin, and Larry Cooper

Acurex Corporation

ABSTRACT

A particulate sampler for high-temperature, high-pressure processes has been developed and successfully demonstrated. The system uses an extractive approach, removing samples from the process stream for complete analysis of particulate size distribution, morphology, and chemical composition. System capabilities have been demonstrated by sampling a pressurized fluidized bed combustor. This paper describes the extractive sampling approach, the HTHP sampler design, and the data obtained from sampling operations.

INTRODUCTION

Advanced coal conversion processes present new problems in particulate sampling, including severe environments beyond the capabilities of conventional equipment. This paper describes a newly developed sampling system, specifically designed for the high temperatures and pressures found in pressurized fluidized bed combustors. The system uses an extractive sampling approach, withdrawing samples from the process stream for complete analysis of particulate concentration, shape, size, and chemical composition. The capabilities of the new system have been demonstrated in two phases of sampling operations at a pilot-scale fluidized bed combustor owned and operated by Exxon Corporation. The first phase of testing was performed with the sample probe in its basic configuration. The second test phase utilized modified probe internals designed to investigate possible condensation of alkali metals. The system performed successfully in a variety of operating modes, producing sample data from both test series.

The following sections of this paper discuss the extractive sampling concept, the HTHP sampler design, and sampling operations that have been performed with the new system.

Extractive Sampling

In extractive sampling, a quantity of particle-laden product gas is drawn out of the process for analysis. Once extracted, the sample can be thoroughly examined by conventional methods. If proper care is taken to obtain and maintain a representative sample, the extractive approach will provide complete, accurate information on process constituents.

The sample is typically extracted through a probe inserted into the process duct. The sample withdrawal rate at the probe nozzle must be matched to the duct velocity to avoid biasing particle size distribution measurements (isokinetic sampling). The error in measured particle content as a function of an isokinetic velocity mismatch can be estimated analytically (see Figure 1). For fine particles at low velocities the error is negligible, but for larger particles or high velocities, serious errors result.

Sample temperature is also a consideration in the extractive approach. Ideally, the temperature would be maintained at process conditions during particulate separation and analysis. In practice, however, the sample is usually cooled to temperatures compatible with analysis equipment.

The major advantage of the extractive method is that the sample can be analyzed by conventional techniques. For example, particulate removal and size classification

*Acurex Corporation has developed the HTHP sampler for the Industrial Environmental Research Laboratory of the Environmental Protection Agency. The work is part of a broad program investigating new sampling technology for advanced coal conversion processes (Contract 68-02-2153). The EPA Project Officer for the contract is William Kuykendal.

devices, trace element collectors, and chemical analysis techniques are all highly developed (References 1 to 5). Extractive sampling is commonly used in emissions measurement and combustion studies.

Access to the pressurized duct is the main difficulty in extending extractive sampling technology to high-pressure, high-temperature processes. The hardware requirements for entering a pressurized process are much more complex than for ambient pressure applications. The selected design for the HTHP sampler is described in the following section.

HTHP SAMPLER DESIGN

The new sampler design adapts conventional sampling technology to high-temperature, high-pressure environments. Key system components are:

- A traversing sample probe that can be inserted or withdrawn during process operation
- A probe housing that contains process pressure during sampling
- A cascade impactor to both collect and size particulate -- interchangeable with a bulk filter (Phase I tests)
- An in-stack scalping cyclone and backup filter followed by a "cold" final filter (Phase II tests)
- Conventional trace element collectors (organics trap and impingers)
- Measurement and control instrumentation to assure isokinetic conditions

A schematic diagram of the Phase I sampler is shown in Figure 2. The sample probe is mounted within a pressure-containment housing. The probe can be inserted into the stream through valves that connect the housing assembly to the process duct. Sample flow in the probe passes through a cooler and particulate collector (cascade impactor). Flowrate is controlled by a throttle valve at the probe exit. After leaving the probe, sample gases are conducted through the trace element collectors, and vented.

The sampling system is shown in Figure 3. In addition to the probe and housing assembly, controls, and sample collectors, the system includes a portable hydraulic pump.

One of the basic decisions in designing the sampler was the choice between fixed and translating probe configurations. A translating probe (one that is insertable and removable during process operation) is more complex than a stationary probe, but offers several operating advantages:

- Particulate deposition losses in the probe can be recovered
- Nozzles can be changed to maintain isokinetic conditions
- The probe can traverse the duct to measure flow variations
- Probe exposure to erosive/corrosive conditions is minimized
- Inspection and maintenance are possible during process operations

Based on these advantages, the translating probe design was selected for the HTHP sampler. The sample probe and particle collector are shown in Figure 4.

Selecting the particulate collection temperature was a second major design decision. A number of well-characterized devices are available for use below 500°F, but, high-temperature particulate collectors are in an early stage of development. Based on this practical limitation, a collection temperature of 450°F was selected with the awareness that possible changes in particulate composition would have to be considered. Major changes in composition are not likely above the sulfuric acid dewpoint. However, changes in trace element concentration are a potential concern. The HTHP sampler has

been used in an experiment investigating the effect of collection temperature on particulate composition, as described in a later section of this paper. The impactor used with the HTHP sampler is a Mark III, University of Washington Source Test Cascade Impactor, Model D.

The cascade impactor has several advantages over other particle collectors. The device provides many stages of size classification in a small volume. Also, impactors classify particle size based on inertial and aerodynamic properties that relate directly to the performance of particulate removal devices. Impactor performance is well characterized for moderate temperature, ambient pressure operation. The effect of high pressure on sizing performance can be estimated using theoretical correction factors. For fine particles at moderate temperatures, even large pressure increases have little effect on impactor performance. Collection temperature, however, can affect measurements more significantly. Variations in cut size with temperatures have been calculated by the impactor supplier for temperatures up to 500°F.

In the selected sampler design, the sample probe enters the pressurized process through 4-inch diameter full-opening valves while process pressure is contained by a surrounding housing assembly. The housing, shown in Figure 5, consists of two telescoping cylinders which move the probe into and out of the process. Hydraulic cylinders connect the two parts of the housing. Their function is to accurately position the probe, and withstand the large forces from process pressure. Sealing at the joint between the housing cylinders is critical, so redundant seals are used. The telescoping housing is the most complex part of the sampling system and consequently required the most design and development effort.

The HTHP sampling system also includes the instruments and controls necessary for accurate sampling. Sample flowrate is one of the important parameters that is monitored and controlled. Flow must be both isokinetic at the probe nozzle and within the operating limits of the particle collector. For proper control, flow conditions in both the process stream and sample probe must be measured. A pitot tube and thermocouple are mounted on the probe to measure process stream conditions, and a calibrated orifice and thermocouple check the sample flow. The flowrate is adjusted to particle collector requirements by a valve near the probe exit. Nozzle entrance velocity is varied by selecting larger or smaller nozzles. The sampling system includes other controls for sample temperature, probe traverse, trace element collector flow, and other key operating parameters. System controls are housed in two portable enclosures, shown in Figure 6.

The trace element collection equipment included in the sampling system consists of an organics module and impinger train (see Figure 7). Both units are identical to those used in the Source Assessment Sampling System that is commercially available from Acurex. The organic module cools the sample gas to 70°F and traps organic vapors in a porous polymer granular bed. The polymer used in this test series is Rohm & Haas XAD-2 gas chromatographic packing material. The impinger train has four high-volume glass impingers, three filled with oxidizing solutions and one with silica gel moisture absorbant. The oxidizing reagents in the impingers collect volatile trace elements by oxidative dissolution. The reagents are:

| <u>Impinger</u> | <u>Solution</u> |
|-----------------|--|
| No. 1 | 6M H ₂ O ₂ |
| No. 2 | 0.2M (NH ₄) ₂ S ₂ O ₈ + 0.02M AgNO ₃ |
| No. 3 | 0.2M (NH ₄) ₂ S ₂ O ₈ + 0.02M AgNO ₃ |
| No. 4 | Silica gel |

The peroxide solution in Impinger No. 1 collects reducing gases such as sulfur dioxide which would lessen the oxidative capability of Impingers Nos. 2 and 3. The ammonium sulfate and silver nitrate solutions serve as the trace element collectors in the impinger train (Reference 3).

PFBC Facility

The new HTHP sampler has been demonstrated in operations at the Exxon Miniplant PFBC. The PFBC facility is described in this section.

The Miniplant is a pilot-scale pressurized fluidized bed combustor operated for the EPA by the Exxon Research and Engineering Company in Linden, New Jersey. The PFBC process, shown in Figure 8, is a combined-cycle coal combustion process. Combustion occurs under pressure in a limestone bed that is fluidized by incoming air. Fluidization gives good mixing for efficient combustion, and the limestone bed removes much of the sulfur released during the combustion process. Added useful energy can be produced by expanding high-pressure flue gases in a gas turbine, if particulate loading can be reduced to the levels (0.0002 to 0.002 gr/scf) required to protect turbine blades. The Exxon Miniplant facility is being used to investigate fluidized bed combustion, gas cleanup devices, and particulate effects on turbine components. At the time of sampling, the facility did not include a gas turbine or final cleanup device.

For the sampler demonstration and condensation tests, the sampling location is downstream of the primary cyclone as indicated in Figure 8. At this location, there is a specially constructed duct section with a sampling port (4-inch, 300-pound pipe flange) which interfaces with the sampling system access valves. Measured process conditions were 1350°F and 118 psig.

The Miniplant facility is a four-story structure, with platforms at each level (see Figure 9). The sampling location is physically located at the top of the combustor tower. When installed, the probe assembly is horizontal, about 4 feet above the platform (see Figure 10). The coolant console and hydraulic pump are also placed on the top platform, near the probe assembly. The control consoles and gas train equipment are set up one floor below, where a partial enclosure gives some weather protection.

Systems Operations and Test Data

The new HTHP sampler has been used in two series of operations at the Miniplant PFBC. One series was a field test of system capabilities, the other an investigation of the effect of sample handling temperature on particulate collection, in particular, possible condensation effects. The sampler operated successfully in both tests series. These operations and some of their results are described in this section.

Phase I -- Demonstration Tests

The first series of sampling operations investigated system performance under field conditions. These operations successfully demonstrated a variety of system capabilities. Three sampling runs were made: one using a filter to collect total particulate, and two using a cascade impactor for particle sizing into eight fractions. Trace element and organic collection equipment was operated during the filter run. The tests produced the following data:

- Particulate size distribution
- Particulate chemical composition
- Particulate shape
- Particulate concentration
- Process temperature and pressure
- Moisture content
- Structure temperatures (valves and probe housing)
- Trace element samples (not yet analyzed)
- Organic samples (not yet analyzed)

Particle size distributions from cascade impactor data are plotted in Figure 11. The effect of pressure and temperature on impactor size cuts was estimated using Reference 5. At the relatively low collection temperatures used, increased pressure had little effect on impactor performance for particles larger than 1 micrometer.

The impactor substrates are shown in Figure 12. Generally, the patterns are regular indicating normal impactor operation. Stage 7, however, shows evidence of

several plugged jets. The substrates from Run 2 are lightly loaded. Those from Run 3 show heavier, three-dimensional deposits.

Examples of particulate photomicrographs, showing particle size and shape, are shown in Figures 13 and 14. These plots were made by a scanning electron microscope. The irregular appearance is typical of flyash from lower temperature combustion processes (Reference 8). The photos show the trend of decreasing physical size from Stage 1 to Stage 6, although irregular shape and possible agglomeration make visual interpretation of particle size very difficult.

The chemical composition of the collected particulate was analyzed by dispersive X-ray fluorescence. Spectra of X-ray emissions from impactor Stage 1 and Stage 6 are shown in Figure 15. The peaks in the spectra correspond to the number of emissions detected at characteristic wavelengths of various elements. Results show the presence of aluminum, silicon, sulfur, potassium, calcium, titanium, iron and copper.

Comparing the relative height of the peaks in two spectra can give a rough indication of the relative quantities of elements present in two samples. The comparison of Stage 1 and Stage 6 spectra shows no apparent difference in bulk composition between the coarse particles collected (D₅₀ of about 30 microns) and the finer particles (D₅₀ of about 0.6 micron).

Data from the system demonstration tests are discussed more extensively in a test report submitted to EPA IERL (Reference 9).

Phase II -- Condensation Tests

Following the system demonstration tests, a second series of sampling operations was conducted at the Exxon Miniplant. The purpose of these tests was to investigate the effect of sample cooling on measured particulate mass and composition. We were specifically concerned that trace elements might condense between process temperature and conventional particulate collection temperature (about 450°F). Of particular interest were the alkali metals, primarily sodium and potassium. For these tests, the sampler was set up to collect particulate at process temperature, so trace element condensation could be investigated in two ways. First, the trace element content of particulate collected at 450°F (from the demonstration test series) could be compared with the content of particulate collected at duct temperature to see if any significant differences result. Second, after the particulate was removed at process temperature, the sample gasses could be cooled and filtered to collect condensation products.

The probe configuration for the condensation tests is shown in Figure 16. A scalping cyclone and a high-temperature filter are mounted on the front of the probe to remove particulate at process conditions. After a series of choked orifices, used to gradually reduce sample gas pressure, a final filter removes condensed material as well as breakthrough particulate. The cyclone is a Southern Research Institute model, designed for much less severe operating temperatures. This cyclone was readily available, was small enough for insertion into the duct, and had a very efficient 0.6-micron cut-point. During the tests, however, the cyclone's protective gold plating blistered and fell off, leaving titanium surfaces exposed to heavy oxidation. Chemical analysis of the particulate samples showed significant gold contamination in the cyclone and front filters but none in the rear filter. Titanium contamination was not evident in any of the samples.

The high-temperature filter following the scalping cyclone is made of saffil alumina, a material that Acurex is currently testing for high-temperature baghouse filters. This material seems to offer excellent temperature resistance and effective filtration, but its performance hasn't yet been fully characterized. Its performance in the condensation tests was quite good, particularly with a two-filter "sandwich." The estimated filter efficiency was well over 90 percent of the fine particulate passed by the scalping cyclone.

The final filter at the sample probe exit is a standard Gelman "microquartz" type with high efficiency and low trace element content. It is possible to use conventional filter materials at this location because sample gas temperatures are substantially reduced by the probe cooler section and by sonic throttling in the orifice section.

Four sampling runs were completed in the condensation test series. Conclusions have been drawn on the available data regarding condensation of trace metals, particularly the more common alkali metals, sodium and potassium.

The original intention of the Phase II tests was to compare the elemental concentrations found in the filtered material of the in-stack scalping cyclone and backup filter with the material caught on the rear filter. If the system worked ideally, one could assume all the material on the rear filter was in a gaseous state at stream conditions and would thereby pass through the hot cyclone filter combination and thus be indicative of condensation products produced within the probe. Unfortunately, the rear (or cold) filter could not be reliably analyzed. Carryover of glass fiber filter material during sample preparation, the small amount of the sample available on the cold filter and additional contaminations, yielded poor detection limits with the spark source mass spectrometer (SSMS). Moreover, the values reported for this filter were in mass units rather than concentration units because a net filter collection weight was not determined. This made any direct comparisons of cold and hot catches from Phase II results alone difficult.

Samples of the probe wash were analyzed by Arthur D. Little, Inc., to determine the source of the suspected contamination of the rear filter. A sample from each test was analyzed by thermal gravimetric analysis (TGA), infrared analysis (IR), X-ray fluorescence (XRF), and low resolution mass spectra (LRMS). Results indicated there were three sources of contamination. They were: (1) approximately 30 percent particulate -- attributed to hot, in-stack filter breakthrough, (2) approximately 25 percent sulfuric acid and sulfate condensate -- attributed to localized cold spots (measured at 200°F) below the H₂SO₄ condensation temperature, and (3) approximately 40 percent organics -- attributed to the disintegration of packing material from a valve located just upstream of the rear filter. The evidence of breakthrough particulate contamination was supported by photomicrographs, which showed similar appearance between material on the front and rear filters, and by dispersive fluorescent X-ray spectrum which shows a similarity in chemical composition. The sulfur content did, however, increase on the rear filter, apparently as a result of sulfate condensation.

An alternate approach was taken to resolve the question of trace metal condensables. During the Phase I demonstration tests at Exxon, a test run was made at essentially the same operating and stream conditions as the Phase II tests. A total mass filter was used in place of the cascade impactor and was maintained near 400°F. Northrop Services, Inc. performed a SSMS analysis of the bulk filter catch, as they did with the Phase II cyclone and backup filter samples. Table I presents the results for these analyses. The measured elemental content is similar to common flyash. A partial, nondimensionalized comparison of these two sets of results, Phase I and Phase II, is presented in Table II. Reference quantities Fe and Mg, have been chosen to nondimensionalize the results because they exist in significant concentrations in each sample and are not likely to be present as a result of contamination. Nondimensionalizing was done because there appeared to be a diluent in the Phase I filter catch. The Si concentrations indicate that the filter material itself may be the diluent in the sample. In fact, the sample analyst acknowledged some difficulty in separating the sample from the filtering media.

Aside from the Si results, comparison of the other quantities shown indicates that there was no detectable change in the concentration of Na or K from the hot to cold particulate catches. This limited data would indicate that particulate collection at low-pressure and 400°F yields accurate results for particulates.

CONCLUSIONS

The sampling system described in this paper demonstrates that extractive sampling is a feasible approach for sampling high-temperature, high-pressure processes. Furthermore, the Phase II condensation test data indicates that sample filtration at reduced pressure and low temperature (400°F) yields accurate results for particulates. Technology for sampling pressurized fluidized bed combustors is now developed and available. Future development also will be required, however, to make useful application of this technology and extend it to other advanced coal conversion processes.

One of the remaining issues for PFBC high-temperature, high-pressure sampling, is system cost/performance trade-offs. Process developers seem to be interested in both upgraded and downgraded versions of the sampling system. Upgraded versions offer

longer sampling durations, quicker turnaround and better operating convenience. Downgraded versions, such as fixed-probe designs, are cheaper, but give less information.

The next objective for extractive sampling is to develop technology for coal gasifiers. Particulate measurement is also important for developing these processes, and environmental difficulties are even more severe than for FPBC's.

REFERENCES

1. Lundgren and Calvert, "Aerosol Sampling with a Side Port Probe," Amer. Ind. Hyg. Ass. J., 28:213 (1967).
2. Calvert and Parker, "Collection Mechanisms at High Temperature and Pressure," Symposium on Particulate Control in Energy Process, EPA-600/7-76-010, Sept. 1976.
3. Hamersma, et al., IERL-RTP Procedures Manual: Level 1 Environmental Assessment, EPA-600/2-76-106a, June 1976.
4. Blake, D. E., Operating and Service Manual -- Source Assessment Sampling System, Aerotherm Report UM-77-80, March 1977.
5. Gooding, C. H., Wind Tunnel Evaluation of Particle Sizing Instruments, EPA-600/2-76-073, March 1976.
6. Operation Manual, Mark III University of Washington Source Test Cascade Impactor (Model D), Pollution Control Systems Corporation, Renton Washington, March 1974.
7. Hoke, R. C., "FBC Particulate Control Practice and Future Needs: Exxon Miniplant," Symposium on Particulate Control in Energy Processes, EPA-600/7-76-010, Sept. 1976.
8. Hoke, R. C., Exxon Research and Engineering Company, Linden, New Jersey, Personal Communication.
9. Masters, W. Z., "Field Testing of a Sampling System for High-Temperature/High-Pressure Processes," Annual Report, Measurements of High-Temperature/High-Pressure Processes, Aerotherm Report TR-77-55, July 1977.

Table I. Concentration of Elements in Flyash SSMS Analysis (Partial)

| Element | Test No. 3 -- Phase II | | | | Phase I |
|---------|------------------------|----------------|---------------|---------------------|----------------------|
| | Cyclone (ppm) | Front (ppm) | Rear (ppm) | Rear Blank (ppm) | Bulk Filter (ppm) |
| K | 8,200 | 8,850 | 15.1 | 5.4 | 16,260 |
| Na | 1,310 | 2,500 | <135.0 * | 91.0 | 3,560 |
| Rb | <70 | <68 | <0.43* | 0.13 | 866 |
| Cs | 6.7 | 0.23 | <0.62 | -- | 8.8 |
| Al | 164,000 | 94,000 | 64.2 | 6.4 | Major |
| Si | 94,000 | 82,600 | <2510.0 | 1210 | 310,000 |
| Fe | 30,000 | 13,400 | 60.0 | 2.36 | 36,300 |
| Ca | 20,000 | 19,000 | <6.6 * | 7.3 | 44,700 |
| Mg | 11,400 | 17,800 | 38.0 | 5.9 | 28,600 |
| Ti | 2,430 | 1,950 | 7.1 | 3.1 | 10,600 |
| Sr | 810 | 555 | 0.6 | 1.15 | 1,320 |
| Ba | 710 | 694 | <5.0 * | 1.5 | 1,080 |
| Au | 650 | 118 | <1.4 | -- | 13 |
| P | 276 | 223 | <224.0 * | 68.0 | 1,880 |
| Cu | 248 | 165 | <1.5 * | 0.91 | 142 |
| Zr | 160 | 140 | <2.1 * | 0.64 | 334 |
| Ni | 120 | 100 | 5.8 | 0.29 | 348 |
| Cr | <90 | <140 | <13.1 | 6.4 | 366 |
| Pb | 85 | 75 | <4.0 * | 1.2 | 86 |

Notes: < - Natural background limited defection limit.

<* - Blank limited detection limit.

Table II. Partial Comparison of Front and Rear Particulate Catches from Exxon Test Series I and II

| | Phase I Tests Bulk Filter | Cyclone | Phase II Tests Front Filter | Avg. | Ratio |
|-----------------|------------------------------|---------|--------------------------------|------|-------|
| $\frac{K}{Fe}$ | 0.45 | 0.26 | 0.66 | 0.47 | 0.96 |
| $\frac{Na}{Fe}$ | 0.10 | 0.04 | 0.19 | 0.12 | 0.83 |
| $\frac{Si}{Fe}$ | 8.54 | 3.13 | 6.16 | 4.65 | 1.84 |
| $\frac{Ca}{Fe}$ | 1.23 | 0.67 | 1.42 | 1.05 | 1.17 |
| $\frac{Mg}{Fe}$ | 0.79 | 0.38 | 1.33 | 0.86 | 0.92 |
| $\frac{Sr}{Fe}$ | 0.04 | 0.03 | 0.04 | 0.04 | 1.00 |
| $\frac{Ba}{Fe}$ | 0.03 | 0.02 | 0.05 | 0.04 | 0.75 |
| $\frac{K}{Mg}$ | 0.57 | 0.72 | 0.50 | 0.61 | 0.93 |
| $\frac{Na}{Mg}$ | 0.12 | 0.11 | 0.14 | 0.13 | 0.92 |
| $\frac{Si}{Mg}$ | 10.84 | 8.25 | 4.64 | 6.45 | 1.68 |
| $\frac{Fe}{Mg}$ | 1.27 | 2.63 | 0.75 | 1.69 | 0.75 |
| $\frac{Ca}{Mg}$ | 1.56 | 1.75 | 1.07 | 1.41 | 1.11 |
| $\frac{Sr}{Mg}$ | 0.05 | 0.07 | 0.03 | 0.05 | 1.00 |
| $\frac{Ba}{Mg}$ | 0.04 | 0.06 | 0.04 | 0.05 | 0.80 |

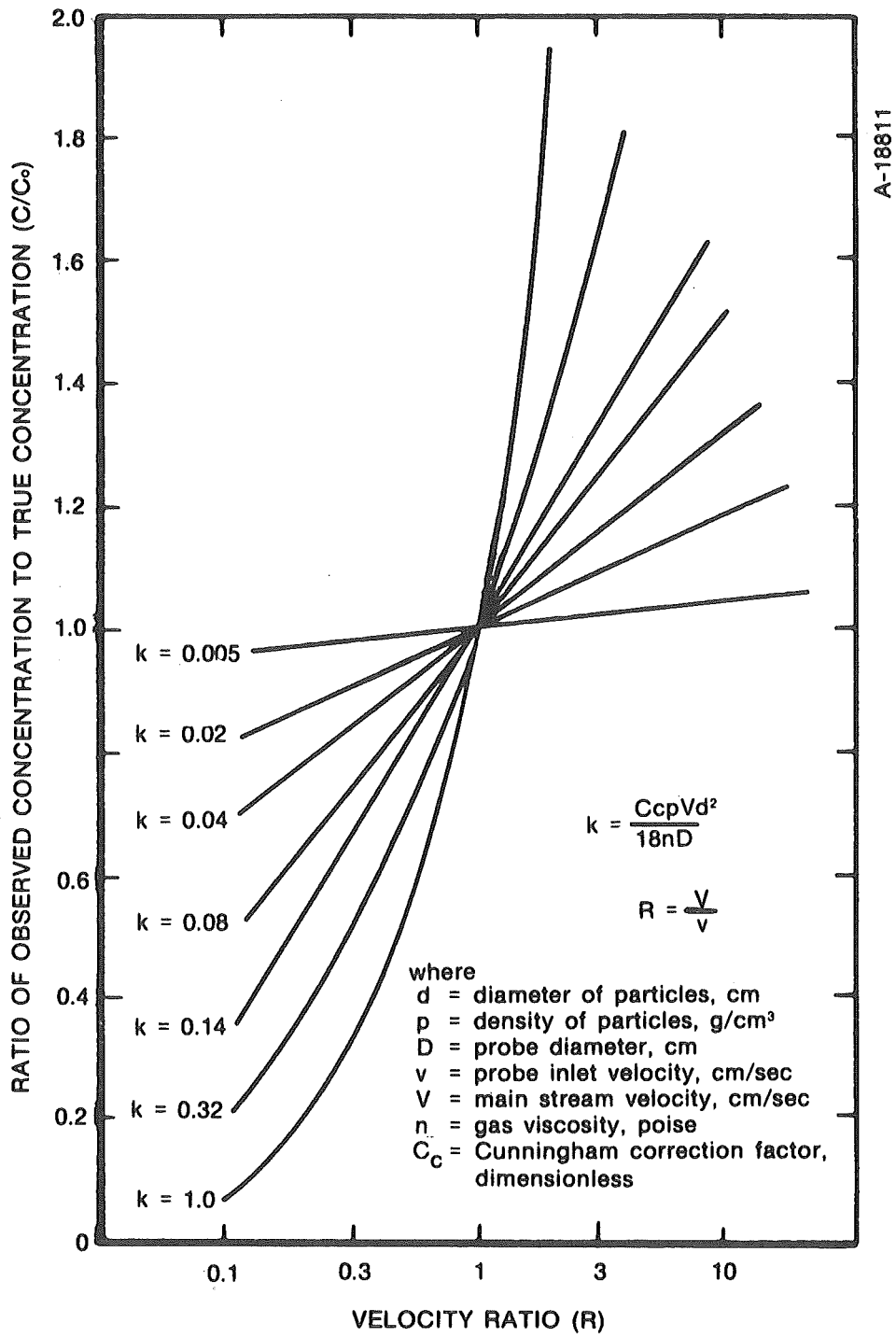


Figure 1. Probe Inlet Bias (from Reference 1)

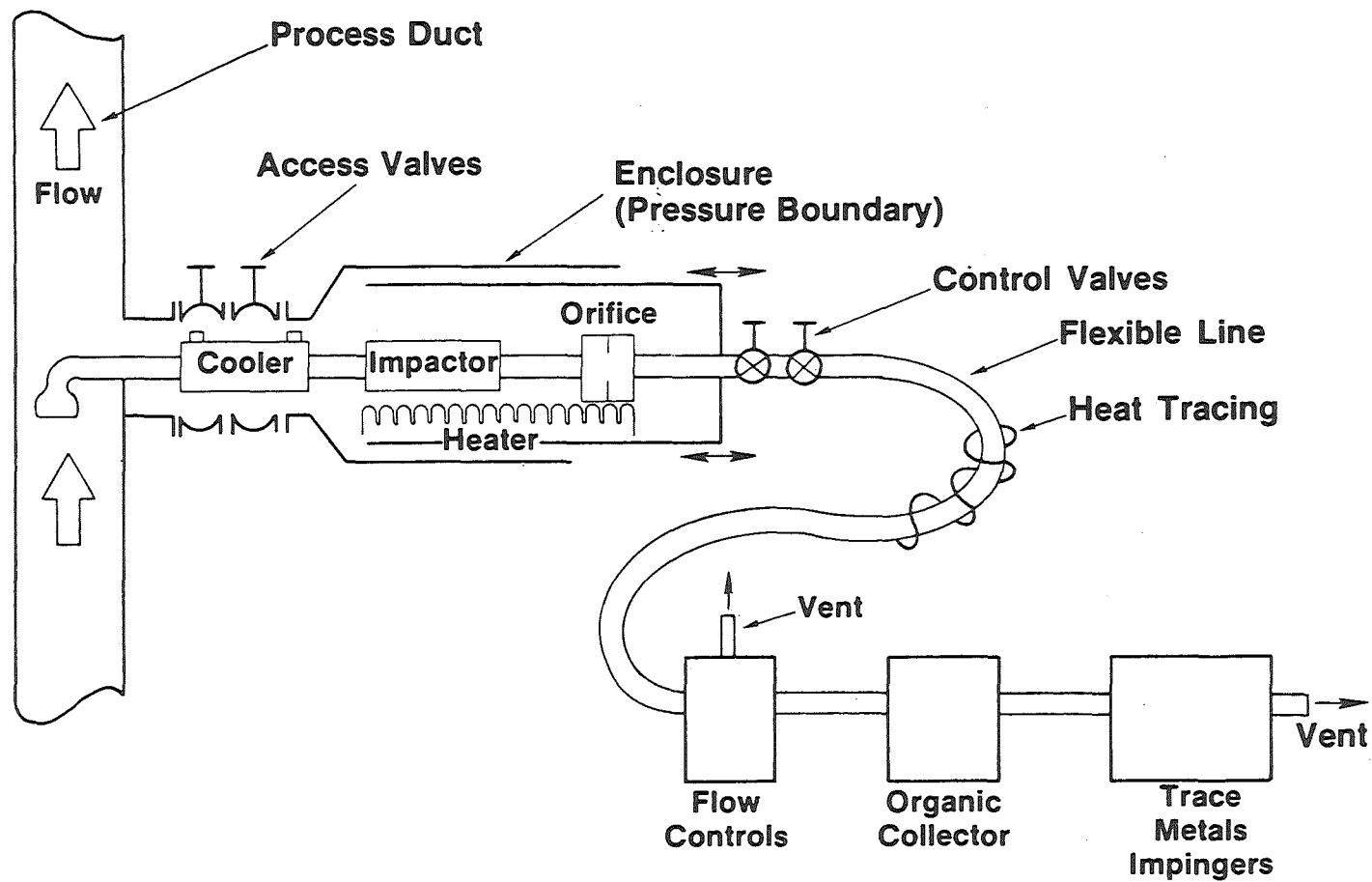


Figure 2. System Schematic

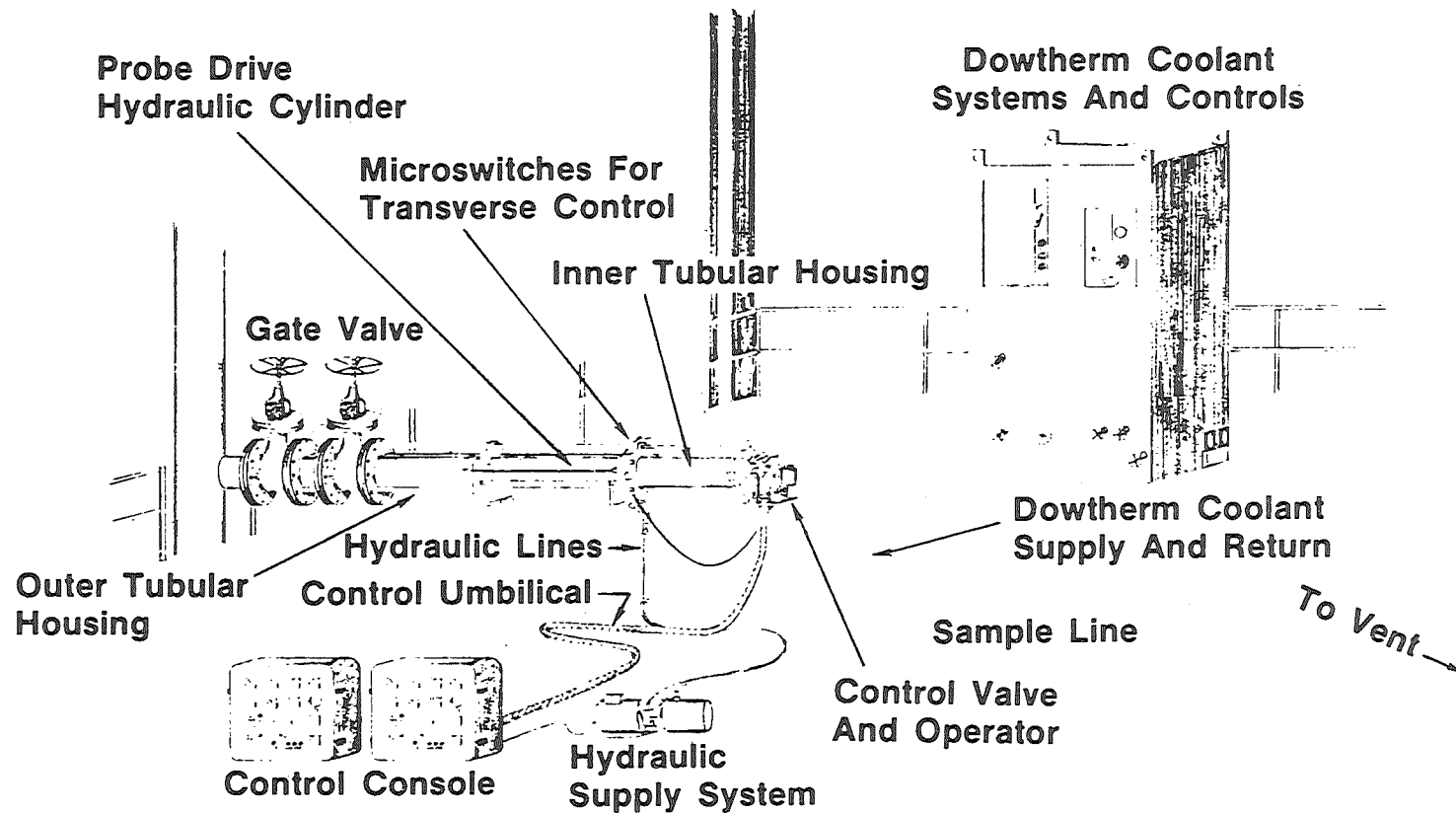


Figure 3. High-Temperature, High-Pressure Sampling System

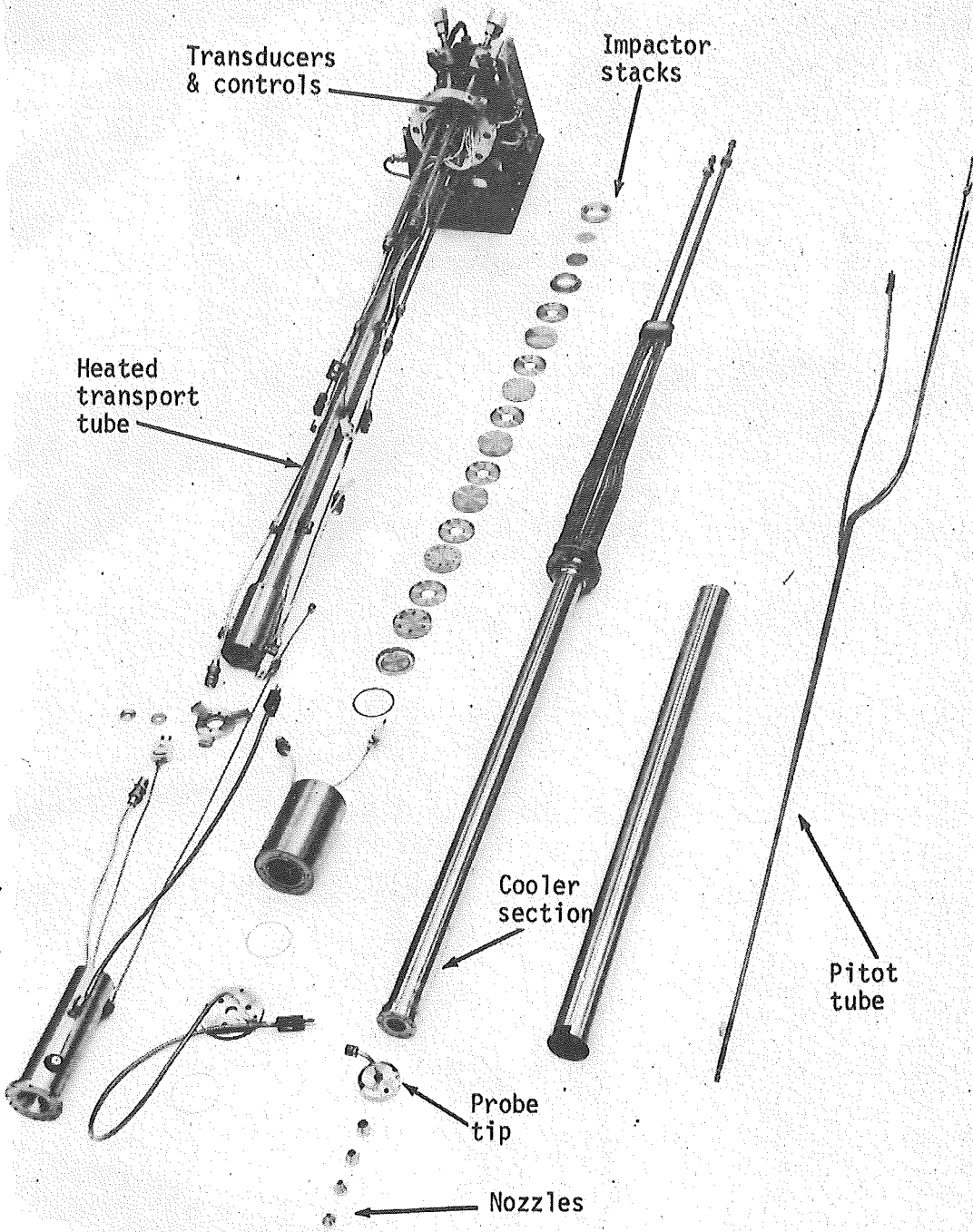


Figure 4. Exploded view of HTHP probe.

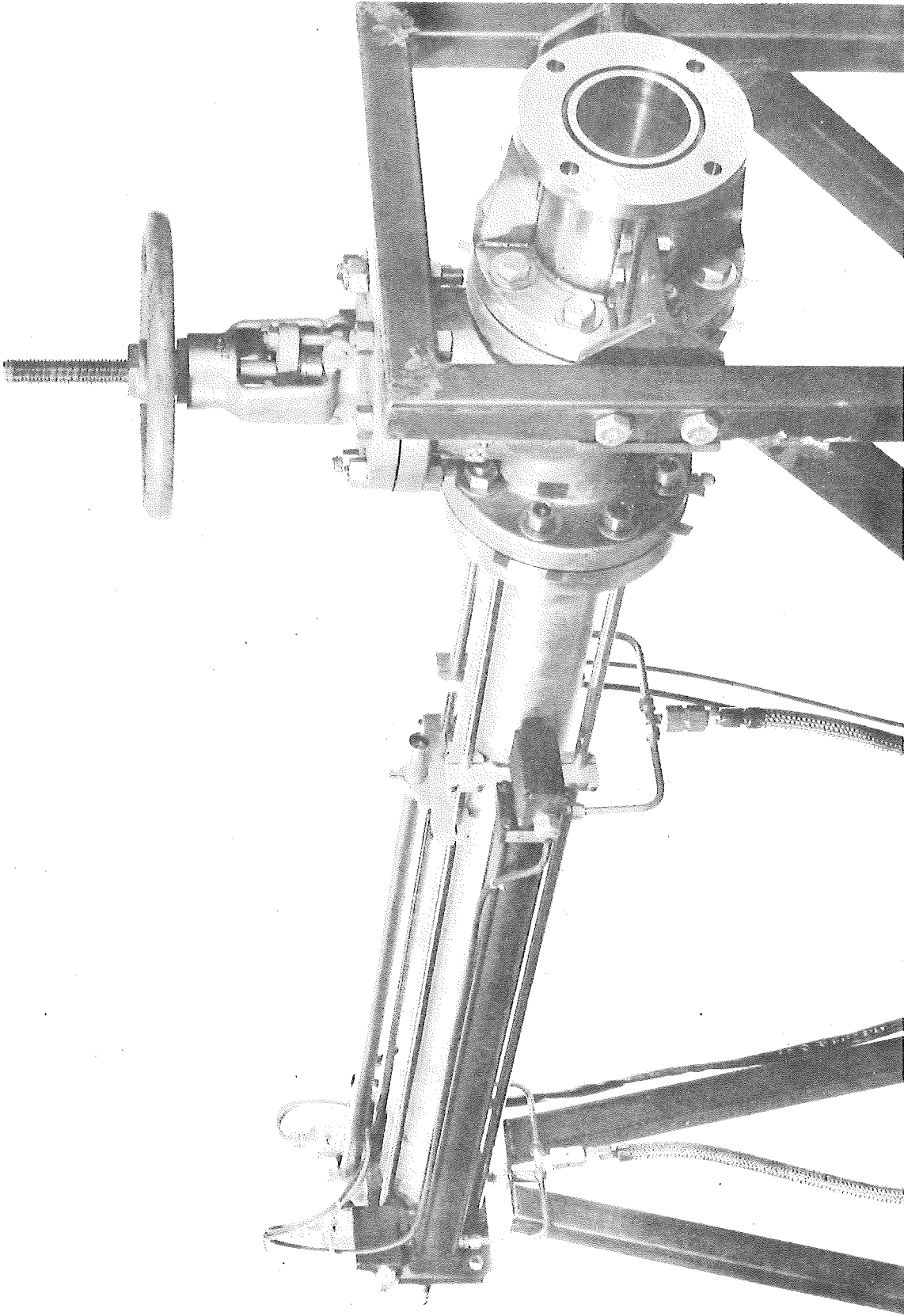


Figure 5. Aerothem HTHP sampling probe and duct interface valve.

9980-H

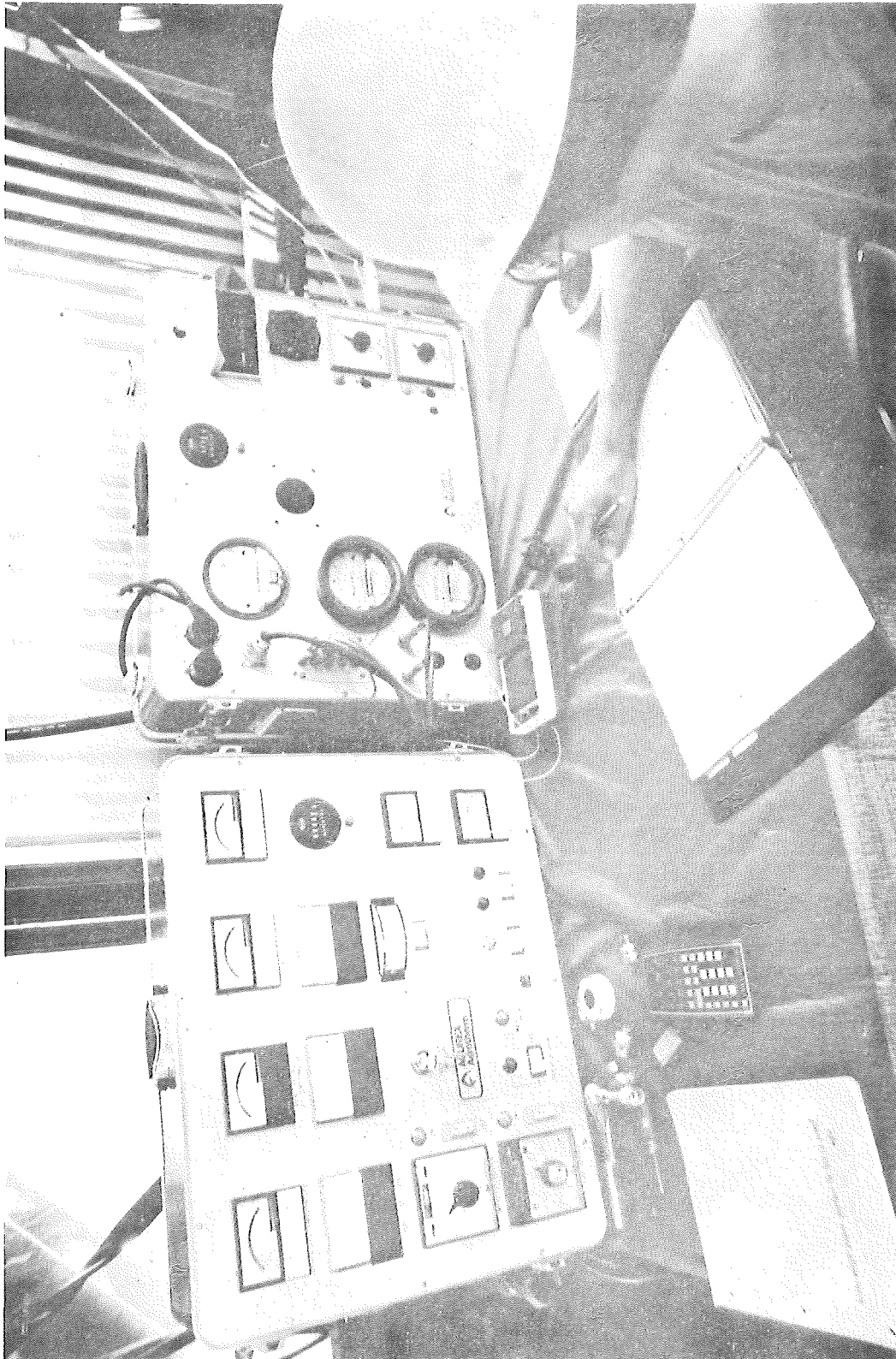


Figure 6. Control consoles.

H-037b

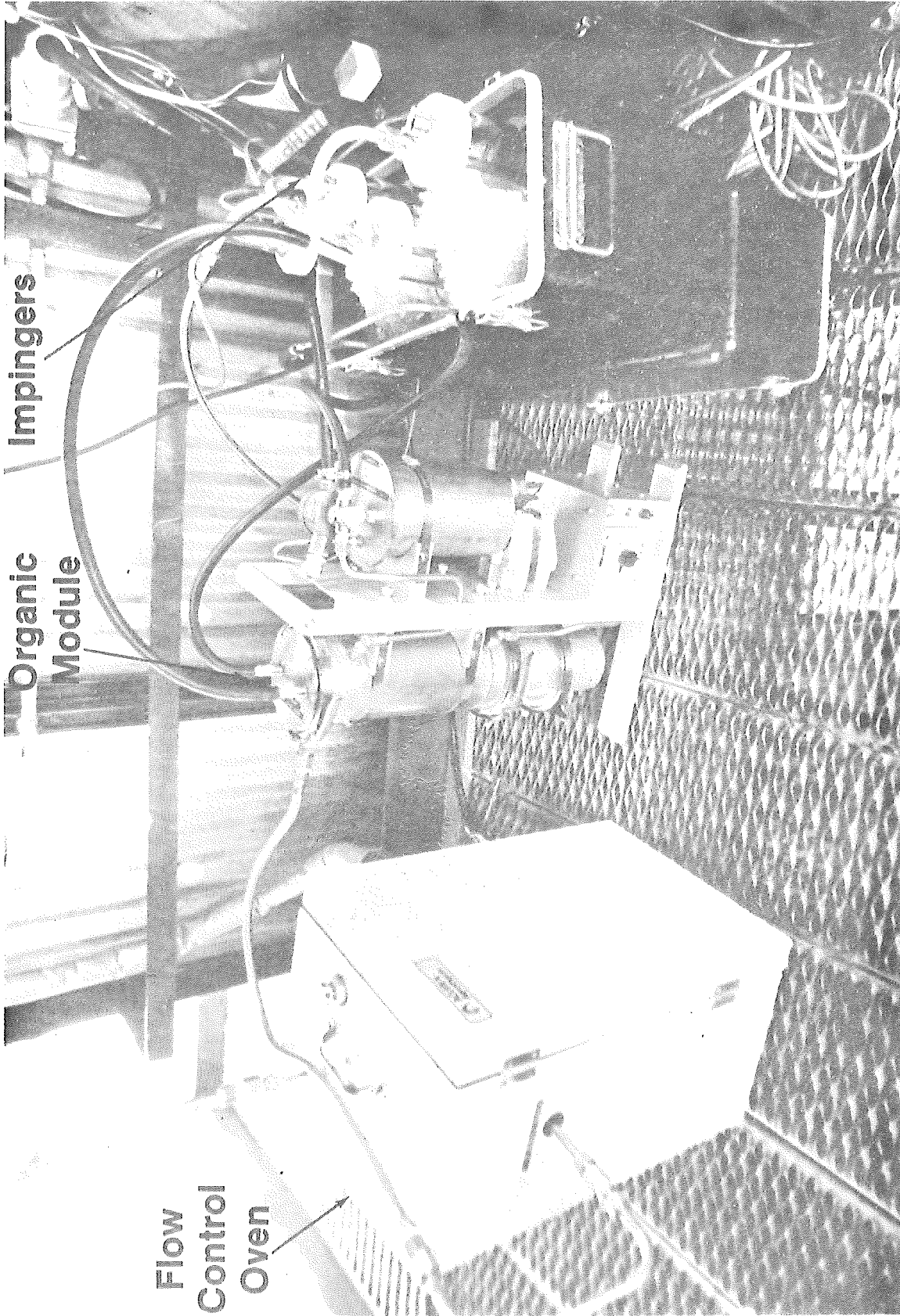


Figure 7. Flow Control Oven and Gas Train

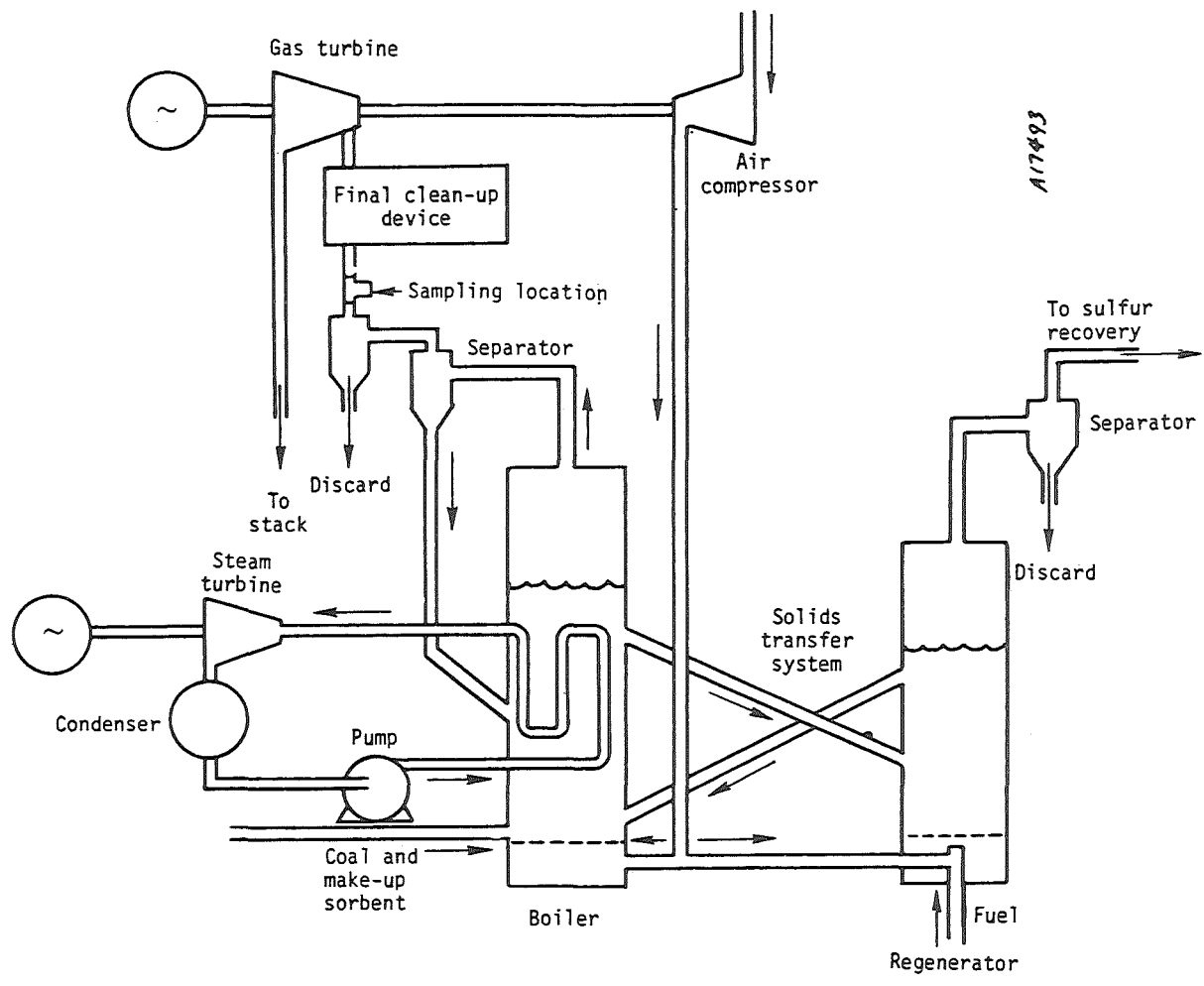


Figure 8. Pressurized Fluidized Bed Coal Combustor System

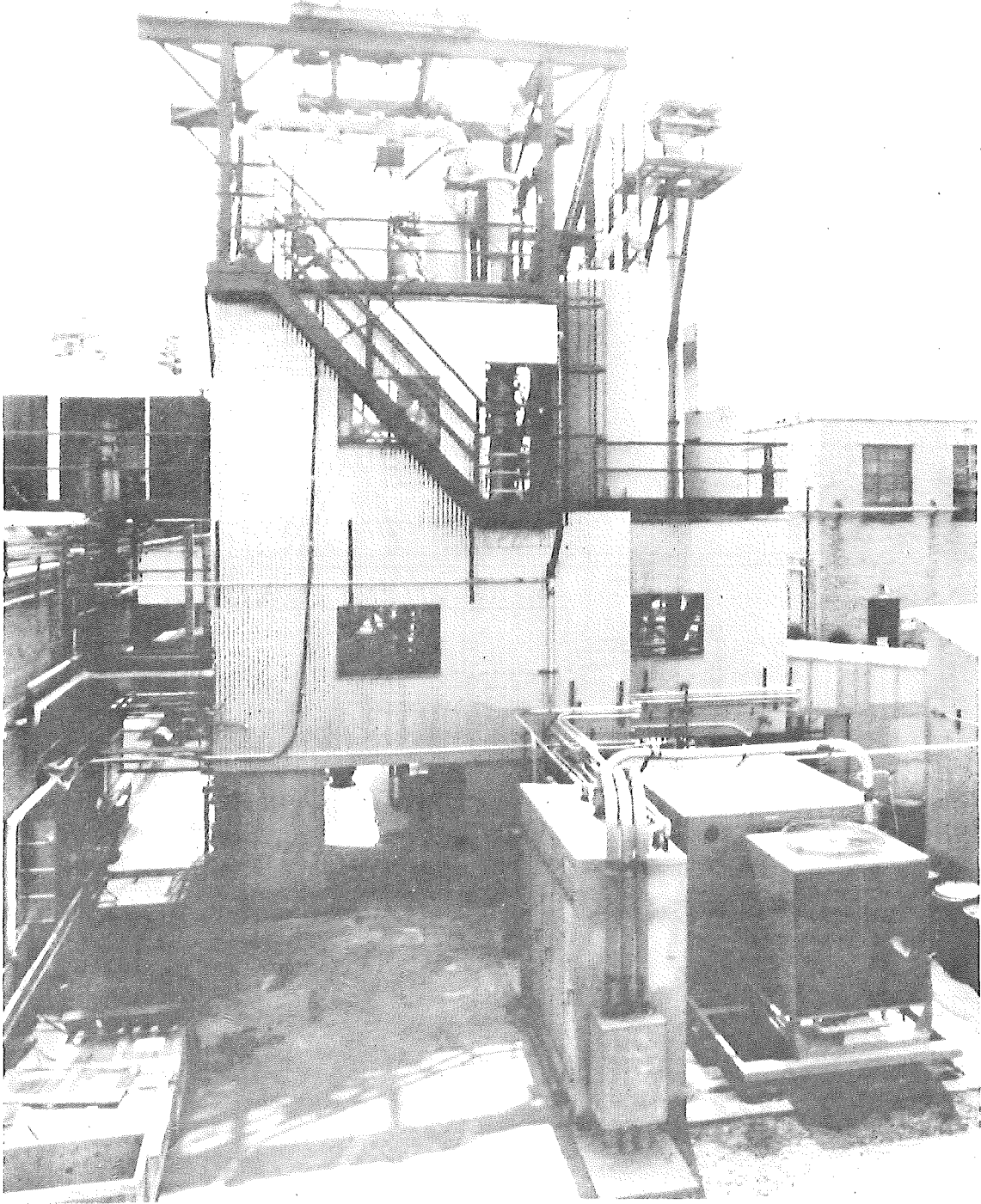


Figure 9. Miniplant PFBC.

H-032b

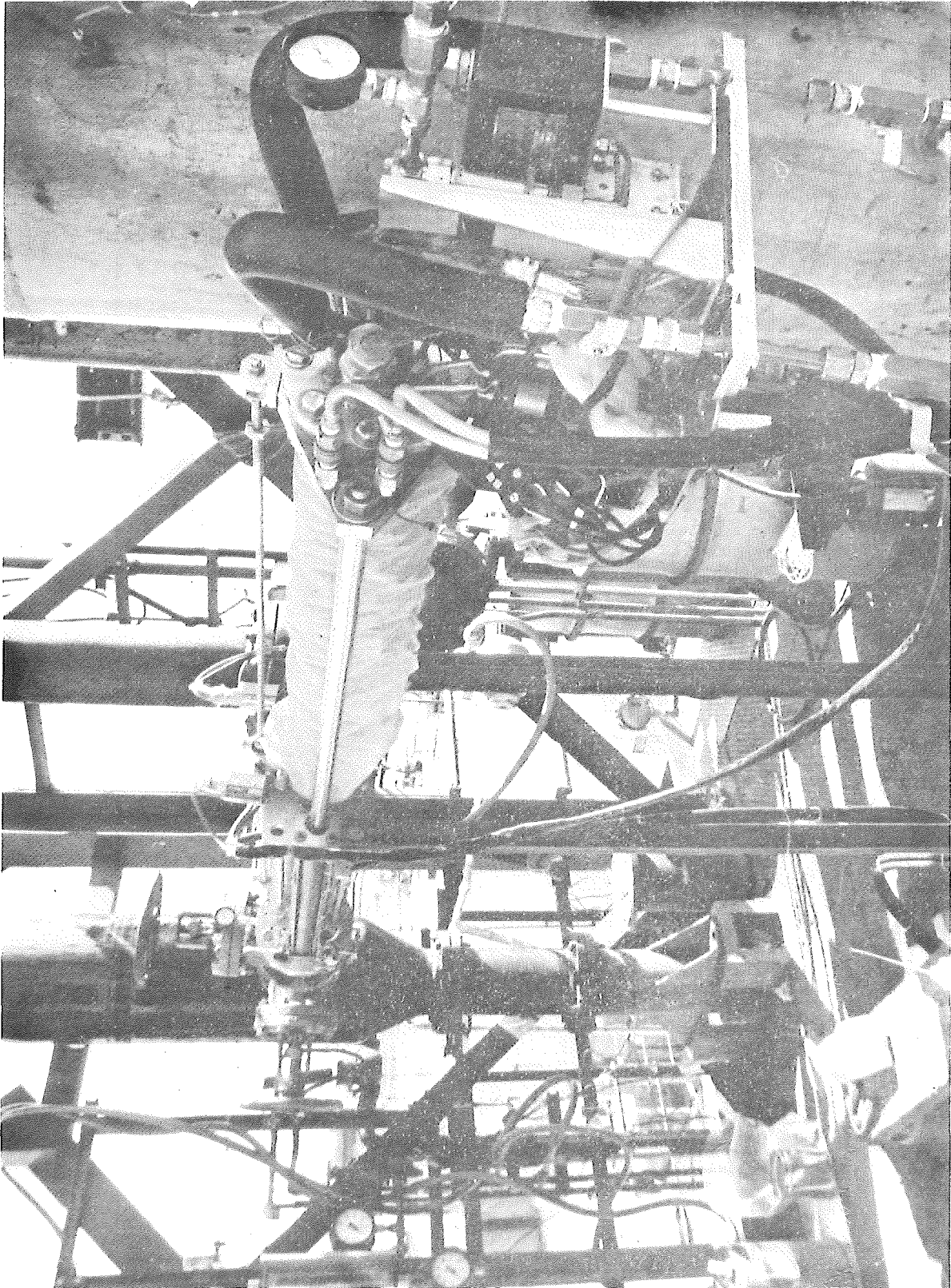


Figure 10.
HTHP probe assembly
installed at Exxon miniplant.

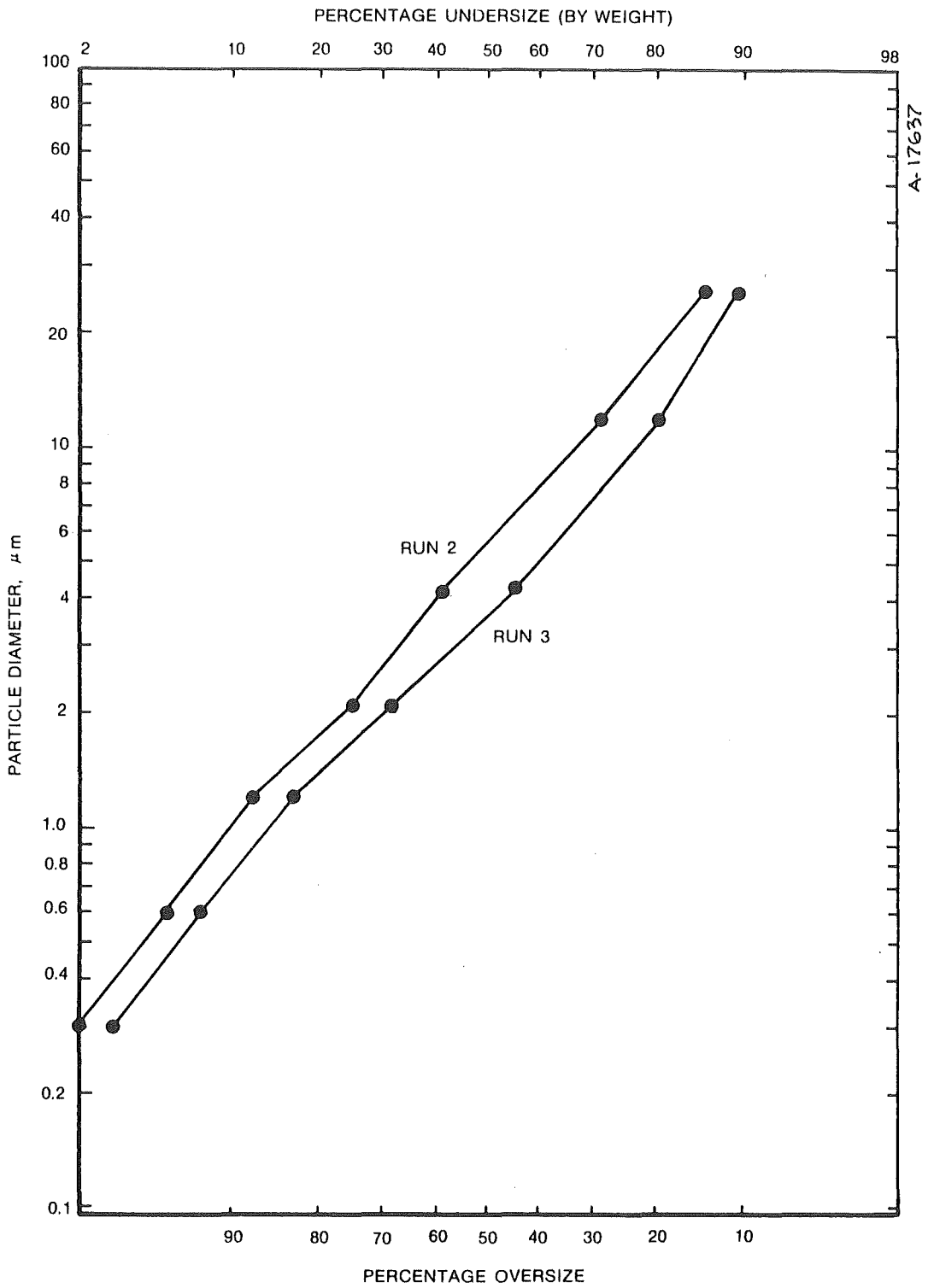


Figure 11. Particle Size Distribution

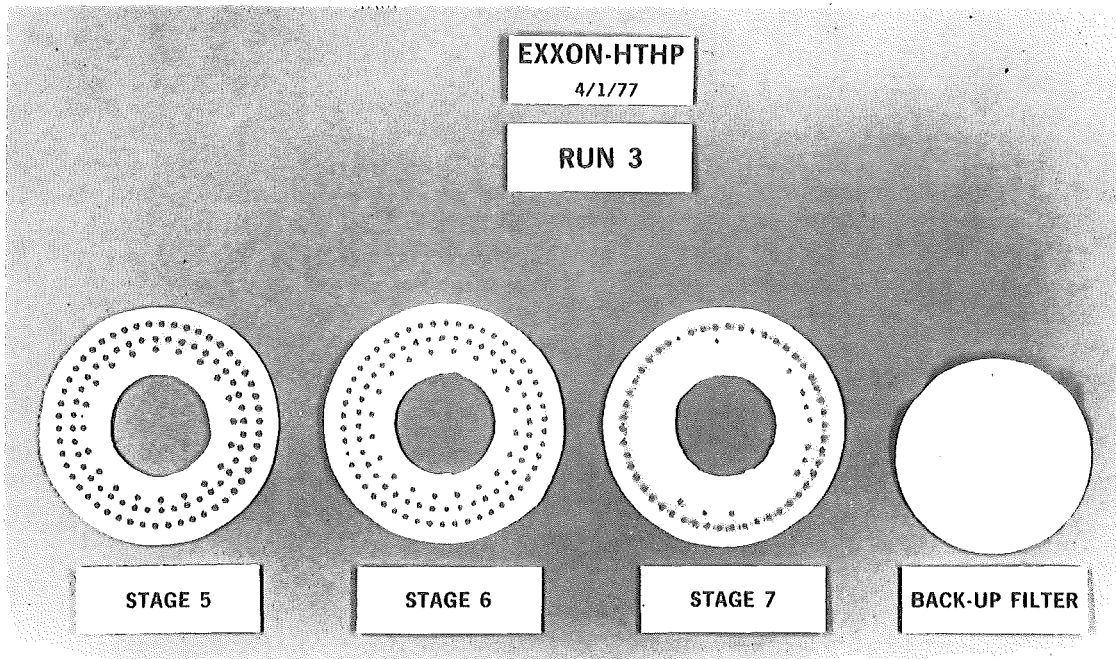
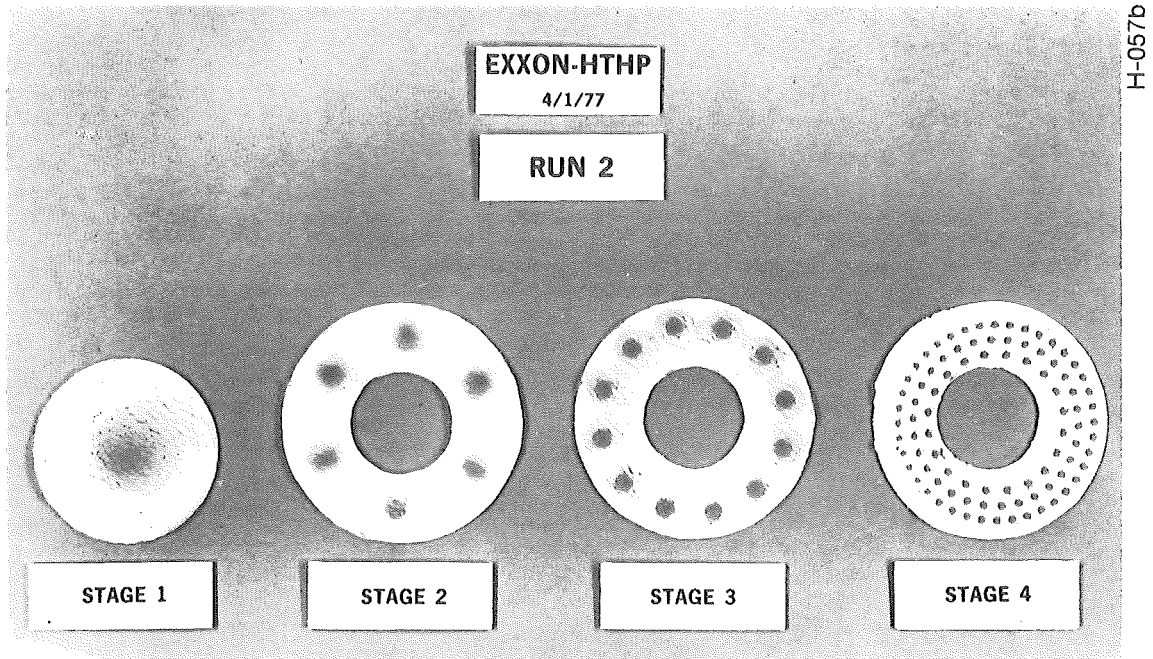
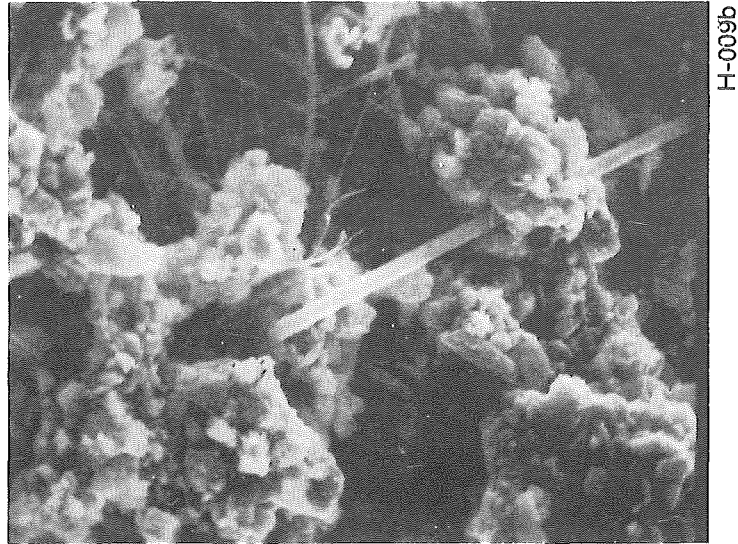
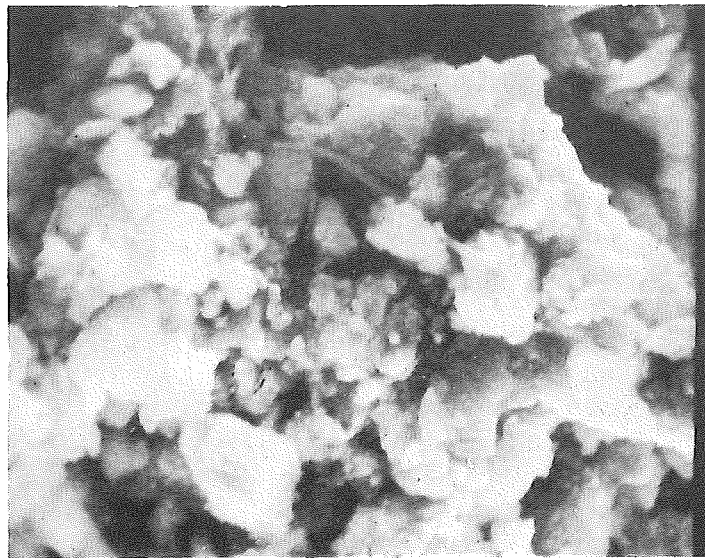


Figure 12. Impactor substrates.



1000X

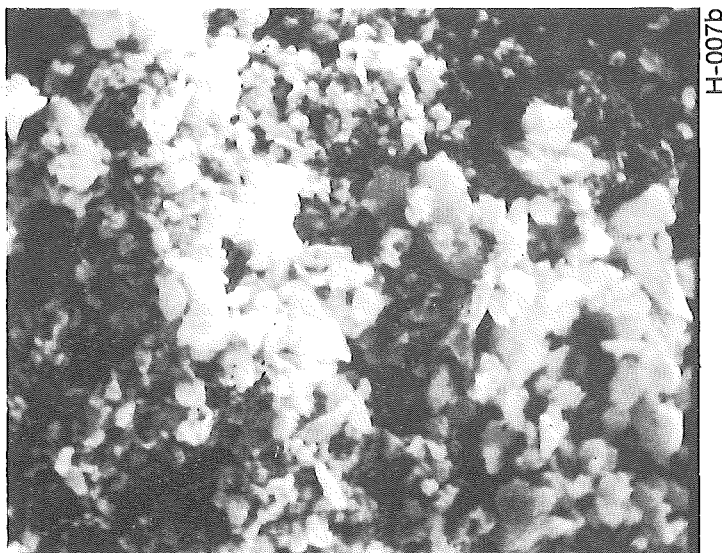
↔ 10 Microns



3000X

↔ 3 microns

Figure 13.
Particle photomicrographs Stage 1.



H-007b

3000X

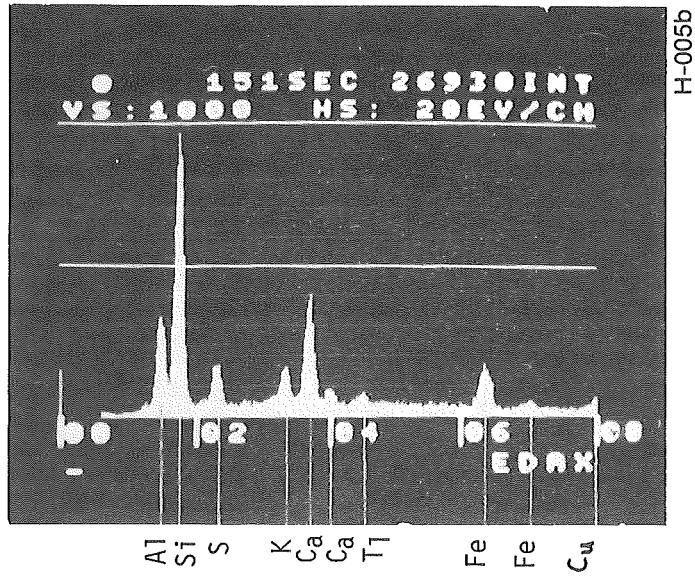


10000X

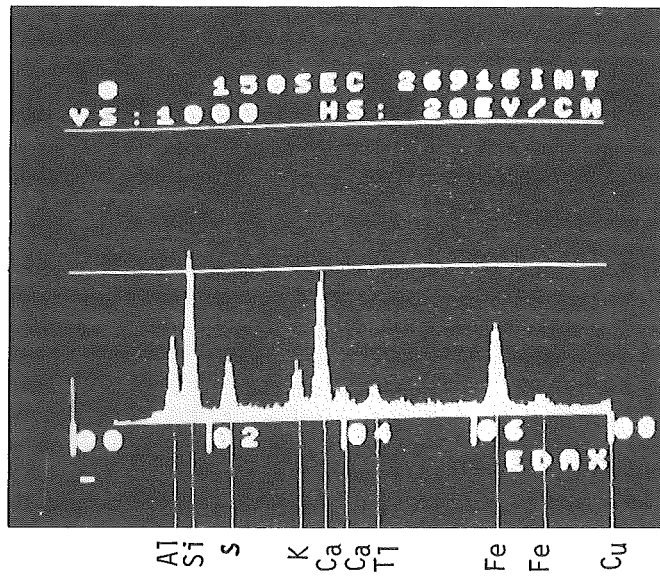
↔ 1 micron

Figure 14.

Particle photomicrographs Stage 6.



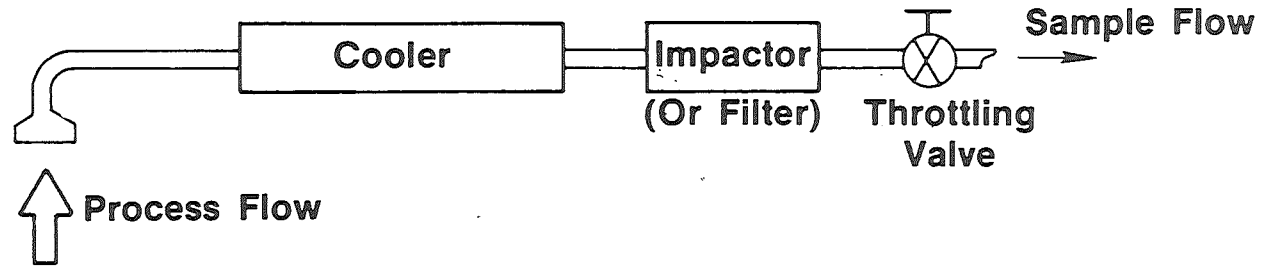
Stage 1, Run 2



Stage 6, Run 2

Figure 15. Particle Chemical Composition - Demonstration Tests

Normal



Condensation Test

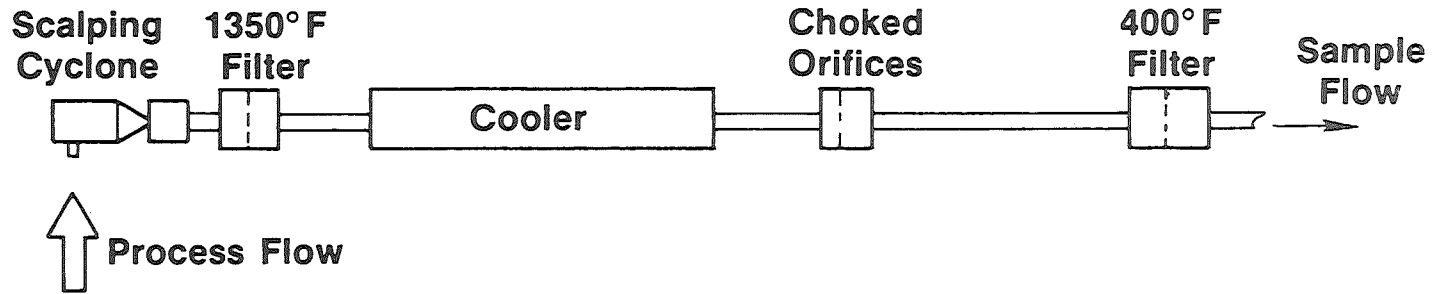


Figure 16. Probe Configuration

Discussion

In reply to Dr. Holighaus, Dr. Cooper said that the difficult techniques described in his talk could not be used in a fluidized bed, which was characterized by chaotic motion. Mr. Kuykendal asked if a sample after the first cyclone were possible, and Dr. Cooper answered that particulate loadings were heavy and that a series of impactors would become overloaded. Impactors could be replaced by cyclones, however.

Work on fluidized bed combustion would be transferred in the future from EPA to the Department of Energy. Inside probes on the fluidized bed would be an interesting, but expensive, basis for West German/US cooperation. Such work could eventually encourage the production of new equipment.

Mr. Bonn requested details of the measurement technique's influence on the fly ash, adding that impactors could break up the granules. Dr. Cooper said evidence of fracture and agglomeration of particles existed. A more comprehensive program using various sampling techniques was needed.

Mr. Princiotta mentioned that a two cyclone series owned by EPA came close to providing the total required protection. In answer to Dr. Holighaus Dr. Cooper said that the type of measuring equipment to be used with fluidized beds had not been determined at the time the study was initiated.

Final Discussion

Dr. Cooper, seconded by Mr. Princiotta, thanked the KFA for its hospitality.

Possibilities regarding West German/US Co-operation were then discussed. Mr. Parker raised the question of West German involvement in the fluidized bed combustion program. Dr. Holighaus said that DM 200 million could be spent on the project, and drew attention to the advanced investigations on fluid bed combustion and gas turbines at the Bergbauforschung. Feasibility of combustion using existing equipment would be tested (end of 1979). The main interest was in the pressurized bed for power stations. Atmospheric beds were applicable to smaller industries. Three projects would take place:

6 kcl p.h. steam generated
30 MW Combination of atmospheric fluid bed and
a normal power station
low quality coal would be used in 1) and high
quality in 2)

An extensive project dealing with 200 MW of electricity was planned for 1981. Also, a joint pressure/fluidized bed project was being carried out in co-operation with the United Kingdom. Other work, financed by the German government and companions, was also being carried out. Two-thirds of the funds came from the public, and a third from the companions. Outside technology would not be used, nor did a project exist at the time dealing with SO₃ additives to electric precipitators.

Mr. G uthner mentioned that one power station had a license to introduce SO₃. Obtaining agreements with the authorities to carry out such work constituted a problem. Use of US produced additives was then discussed. Herr Kastner mentioned the abandonment of a scheme to add NH₃ at two power plants, owing to trouble with fly-ash recycling.

Dr. Holighaus added that all additives could be tested.

Mr. Princiotta referred to a combined wet and dry scrubber program which had been discussed six months before the workshop; no further developments had been made in this direction. Mr. Kastner pointed out that using a wet scrubber for flyash collection was disadvantageous, as it was limited to this function and had few discarding facilities.

Dr. Holighaus stressed the need for US/West German co-operation regarding measurement techniques. More information on new developments would be available in August 1978.

The Umweltbundesamt will provide reports which would be available to EPA.

The workshop ended with vote of thanks for those who had read papers.

List of Participants

1. Mr. Robert Donovan
Research Triangle Institute
Research Triangle Park, N.C.
2. Dr. Richard Parker
Air Pollution Technology, Inc.
San Diego, California
3. Dr. John Gooch
Southern Research Institute
Birmingham, Alabama
4. Mr. Dale L. Harmon
Particulate Technology Branch
Industrial Environmental Research Laboratory
Environmental Protection Agency
Research Triangle Park, N.C.
5. Mr. Seymour Calvert
Air Pollution Technology, Inc.
San Diego, California
6. Mr. Charles Gooding
Research Triangle Institute
Research Triangle Park, N.C.
7. Mr. Joseph McCain
Southern Research Institute
Birmingham, Alabama
8. Mr. Michael Shackleton
Aeotherm-Acurex Corporation
Mountain View, California

.....

.....

9. Mr. William Kuykendal
Process Measurements Branch
Industrial Environmental Research Laboratory
Environmental Protection Agency
Research Triangle Park, N.C.

10. Mr. Larry Cooper
Aerotherm-Acurex Corporation
Mountain View, California

11. Dr. Steven Gage
Assistant Administrator
for Research and Development
Environmental Protection Agency
Washington D.C. 20460

12. Mr. Frank Princiotta
Director of Energy Processes Division
Particulate Technology Branch
Research Triangle Park, N.C.

13. Dipl.-Ing. G. Helsper
Institut für Aerosolmeßtechnik
Gesamthochschule Duisburg
Bismarckstr. 81
D-4000 Duisburg 1

14. Dr. Laufhütte
Saarbergwerke AG
Postfach 10 30
6600 Saarbrücken

15. Dr. Kelleter
Kernforschungsanlage Jülich GmbH
Postfach 1913
5170 Jülich

.....

.....

16. Dr.-Ing. P. Walzel
Institut für Apparatechnik
Universität Essen
Unionstr. 2
4300 Essen

17. Prof. Dr.-Ing. E. Weber
Institut für Mechanische Verfahrenstechnik
Universität Essen
Unionstr. 2
4300 Essen

18. Dr. rer. nat. K. Hübner
Institut für Mechanische Verfahrenstechnik
Universität Essen
Unionstr. 2
4300 Essen

19. Dipl.-Ing. H.-G. Pape
Institut für Mechanische Verfahrenstechnik
Universität Essen
Unionstr. 2
4300 Essen

20. Dipl.-Ing. R. Schulz
Institut für Mechanische Verfahrenstechnik
Universität Essen
Unionstr. 2
4300 Essen

21. Dipl.-Phys. H. Wiggers
Institut für Mechanische Verfahrenstechnik
Universität Essen
Unionstr. 2
4300 Essen

.....

.....

22. Dr.-Ing. P. Davids
Umweltbundesamt
Bismarckplatz
1000 Berlin 33
23. Dipl.-Ing. G. GÜthner
Umweltbundesamt
Bismarckplatz
1000 Berlin 33
24. Dr. Reissmann
Lurgi Umwelt und Chemotechnik GmbH
Postfach 11 91 81
6000 Frankfurt/M. 2
25. Dr. Ziegler
Bundesministerium für Forschung
und Technologie
Postfach 20 07 06
5300 Bonn 2
26. Dr. Dr.-Ing. H.J. Stöcker
Kernforschungsanlage Jülich GmbH
Projektleitung Energieforschung
Postfach 1913
5170 Jülich
27. Dr.-Ing. R. Holighaus
Kernforschungsanlage Jülich GmbH
Projektleitung Energieforschung
Postfach 1913
5170 Jülich
28. Frau D. Ermisch
Kernforschungsanlage Jülich GmbH
Projektleitung Energieforschung
Postfach 1913
5170 Jülich

.....

29. Dipl.-Ing. Grabenhorst
 Kraftwerk Siersdorf GbR
 Roermonderstr. 63
 5120 Herzogenrath-Kohlscheid
30. Dr.-Ing. Finkh
 Kraftwerk Union
 Hammerbachstr. 12/14
 8520 Erlangen
31. Dr. rer. nat. Schilling
 Bergbau-Forschung GmbH
 Franz-Fischer-Weg 61
 4300 Essen 13

